KORESPONDENSI JURNAL INTERNASIONAL BEREPUTASI

Eastern-European Journal of Enterprise Technologies (Q3)

SJR: 0.247 H-Index: 42

SYNGAS QUALITY IMPROVEMENT IN CORNCOB UPDRAFT GASIFICATION USING CAO/ACTIVATED CARBON PALM FIBER CATALYST

Penulis Pertama dan Corresponding author:

Purbo Suwandono

Anggota:

Widya Wijayanti

Nova Risdiyanto Ismail

Dzulfikar Johan Akbar

Muhammad Reza

SUBMIT JURNAL

14 Februari 2026

Purbo Suwandono <purbo@widyagama.ac.id>

[EEJET] Submission Acknowledgement

1 message

Frolova Liliia <eejet@entc.com.ua> Sat, Feb 14, 2026 at 2:19 PM
To: Purbo Suwandono <purbo@widyagama.ac.id>

Purbo Suwandono:

Thank you for submitting the manuscript, "SYNGAS QUALITY IMPROVEMENT IN CORNCOB UPDRAFT GASIFICATION USING CAO/ACTIVATED CARBON PALM FIBER CATALYST" to Eastern-European Journal of Enterprise Technologies. With the online journal management system that we are using, you will be able to track its progress through the editorial process by logging in to the journal web site:

Submission URL: https://journals.uran.ua/eejet/authorDashboard/submission/352281
Username: purbo

If you have any questions, please contact me. Thank you for considering this journal as a venue for your work.

Frolova Liliia
_____ Sincerely edition of
Eastern-European journal of enterprise technologies

Submission Files

Search

816712-1 purbo, SYNGAS QUALITY IMPROVEMENT IN CORNCOB UPDRAFT GASIFICATION USING CAOACTIVATED CARBON PALM FIBER CATALYST.docx	February 14, 2026	Article Text

Download All Files

Pre-Review Discussions

Add discussion

Name	From	Last Reply	Replies	Closed

No Items

UDC

ПОКРАЩЕННЯ ЯКОСТІ СИНТЕЗ-ГАЗУ ПРИ ВИСХІДНІЙ ГАЗИФІКАЦІЇ КУКУРУДЗЯНИХ КАЧАНІВ З ВИКОРИСТАННЯМ КАТАЛІЗАТОРА НА ОСНОВІ CAO/АКТИВОВАНОГО ВУГІЛЛЯ НА ПАЛЬМОВОМУ ВОЛОКН

Purbo Suwandono, Widya Wijayanti, Nova Risdiyanto Ismail, Dzulfikar Johan Akbar, Muhammad Reza

SYNGAS QUALITY IMPROVEMENT IN CORNCOB UPDRAFT GASIFICATION USING CAO/ACTIVATED CARBON PALM FIBER CATALYST

Purbo Suwandono, Widya Wijayanti, Nova Risdiyanto Ismail, Dzulfikar Johan Akbar, Muhammad Reza

Анотація:
Це дослідження зосереджується на поліпшенні якості синтез-газу, отриманого в результаті газифікації кукурудзяних качанів за допомогою висхідного потоку, з використанням подвійної каталітичної системи на основі CaO та активованого вугілля, отриманого з пальмового волокна (AC-PF). Основними досліджуваними робочими змінними були коефіцієнт еквівалентності (ER), навантаження каталізатора та співвідношення CaO/AC-PF (0:1, 1:0, 1:1 та 2:1). Характеристика каталізатора показує, що AC-PF забезпечує пористу структуру, яка покращує контакт газу з твердою речовиною та сприяє вторинним реакціям, тоді як включення CaO утворює композит із модифікованою структурою пор та поверхневими речовинами, пов'язаними з функцією сорбції CO_2. Експериментальні результати показують, що збільшення ER загалом підвищує частки H_2 та CH_4, одночасно зменшуючи CO_2, тоді як CO демонструє оптимальний результат при середньому ER, а потім зменшується при найвищому ER. Навпаки, більш високе навантаження каталізатора, як правило, зменшує H_2 і CH_4, але збільшує CO, що свідчить про зміну селективності вторинної реакції при більш інтенсивному каталітичному контакті. З енергетичної точки зору, LHV синтез-газу збільшується з ER, але може знижуватися при більш високих навантаженнях каталізатора через зменшення внеску CH_4.

Ключові слова: Газифікація висхідним потоком; Кукурудзяні качани; Синтетичний газ; Каталізатор CaO; Активоване вугілля

Abstract:
This study focuses on improving syngas quality from corncob updraft gasification using a dual catalyst system based on CaO and palm-fiber-derived activated carbon (AC-PF). The main operating variables investigated were the equivalence ratio (ER), catalyst

loading, and the CaO/AC-PF ratio (0:1, 1:0, 1:1, and 2:1). Catalyst characterization indicates that AC-PF provides a porous structure that enhances gas–solid contact and promotes secondary reactions, whereas CaO incorporation forms a composite with modified pore texture and surface species associated with CO_2 sorption functionality. Experimental results show that increasing ER generally raises the H_2 and CH_4 fractions while reducing CO_2, whereas CO exhibits an optimum at intermediate ER before decreasing at the highest ER. In contrast, higher catalyst loading tends to decrease H_2 and CH_4 but increase CO, suggesting a shift in secondary-reaction selectivity under more intensive catalytic contact. From an energy perspective, the syngas LHV increases with ER but may decline at higher catalyst loadings due to a reduced CH_4 contribution.
Key words: Updraft gasification; Corncob; Syngas; CaO catalyst; Activated carbon

1. Introduction

Indonesia is one of the largest corn producers in Southeast Asia, with national production reaching more than 18 million tons of dry kernels per year. Of this amount, about 15-20% is cobs after the kernel removal process, resulting in a very large amount of corn cob waste, estimated at 2.5-3.5 million tons annually[1]. Until now, most corn cobs have only been used to a limited extent, for example as traditional fuel, small amounts of animal feed, or even burned directly on post-harvest land, which has the potential to cause air pollution. Most of the rest are simply piled up or left to rot on the land, posing a risk of becoming a source of plant disease[2].

Corn cobs have quite promising chemical and energy characteristics. Their composition is dominated by cellulose, hemicellulose, and lignin, with a calorific value of around 15–17 MJ/kg, making them very suitable as raw materials in various biomass-based energy conversion technologies [3]. Their hard and fibrous nature also makes them suitable for processing into biochar, activated charcoal, or direct use in pyrolysis and gasification processes. This significant potential indicates that corn cobs are not merely waste but a renewable resource that can be optimized to support energy security and reduce dependence on fossil fuels.

Biomass gasification is a promising thermochemical technology for converting renewable resources into syngas consisting of H_2, CO, CH_4, and CO_2. Of the various types of biomass, corn cobs are a potential candidate due to their abundant availability in Indonesia and lignocellulose content that supports the energy conversion process [4]. However, the biomass gasification process still faces several obstacles, particularly the low hydrogen fraction in syngas and the formation of significant amounts of tar. Tar can cause reactor clogging, reduced thermal efficiency, and increased purification costs.

To overcome these problems, the use of catalysts is an important strategy. A number of studies have proven that metal catalysts such as Ni [5], Ca[6], and K[7] can increase hydrogen yield while suppressing tar formation. On the other hand, activated carbon is also widely used as a catalyst support because it has a high surface area, porous structure, and good chemical stability. The use of agricultural waste, particularly palm

fiber, as raw material for activated carbon is not only economically valuable but also supports the concept of a circular economy in plantation waste management. In addition, calcium oxide (CaO) is known to have a dual role, namely as a catalyst in the tar decomposition reaction and as a CO_2 absorber that promotes sorption-enhanced gasification to increase the hydrogen fraction in syngas[8].

Although various studies have examined the role of metal catalysts and activated carbon separately, research focusing on the combination of biomass bases catalyst such as palm fiber-based activated carbon with CaO in corn cob gasification is still limited. The uniqueness of this study lies in the integration of two catalyst, which is expected to provide a synergistic effect: activated carbon with high porosity increases catalyst dispersion and activity, while CaO simultaneously breaks down tar and absorbs CO_2. This approach has the potential to significantly increase hydrogen production and reduce carbon emissions.

However, there are several research gaps that remain unanswered. First, the optimal composition and ratio of activated carbon and CaO in corn cob gasification have not been extensively studied. Second, the synergistic mechanism using two catalyst in increasing syngas quality not yet fully understood. In addition, a systematic and statistically robust approach is required to disentangle the coupled effects of key operating and catalyst variables.

Based on this background and research gaps, this study aims to investigate the performance of a composite catalyst based on activated carbon from palm fiber combined with CaO in the corn cob gasification process. The main focus is on increasing hydrogen production, reducing tar, and evaluating the potential synergistic effects between materials. This research is expected to contribute to the development of low-cost, locally sourced, and sustainable catalyst systems that are relevant to supporting the clean energy transition and practical applications of biomass-to-hydrogen in the future.

2. Literature review and problem statement

A study by Tosuli [9] explored Sago-based foods are staple in eastern Indonesia. Al_2O_3 (5–10 wt%) added to sago-dregs pellets in a TULD gasifier enhances syngas: H_2 is highest at 5% (31.65%), while CO (4.33%) and CH_4 (26.45%) peak at 10%. The H_2/CO ratio remains favorable (1.65–1.51) with low tar, indicating potential for internal combustion engine fuel.

A research by Tuan [10] explored an updraft gasifier processed 3 kg of dried rice husk using air, steam–air, and air with dolomite at varied conditions. Among the tested agents, catalytic air gasification (air + dolomite) gave the best results, producing the highest H_2 (15.4 mol%) and LHV (5.1 MJ/Nm^3), compared with steam–air (7.08 mol%, 3.6 MJ/Nm^3) and air only (3.6 mol%). The optimum setting was an airflow of 3 m^3/h with 15% dolomite.

A research by Yousef [11] explored Cigarette butts are hazardous urban waste rich in cellulose acetate and volatile matter, making them a potential renewable feedstock for hydrogen production. This study valorized as-received cigarette butts via continuous updraft gasification (700–900 °C; ER 0.15–0.25), followed by steam catalytic reforming over KATALCO™ 57-4GQ at 900 °C. Gasification alone produced high syngas yields (82.3–89.7%) but limited H_2 (<20.84 vol% at 900 °C, ER 0.15). The reforming step increased H_2 to 30.27 vol% and reduced tar from 18.15 to 13.38 g/m³, improving fuel quality (HHV from 11,038 to 11,528 kJ/kg).

A research by Bilbao [12] explored slumgum suitability as a gasification fuel. Slumgum and slumgum–pine sawdust pellets were produced (ISO 17225 tests) and gasified in a modified updraft reactor while measuring gas composition and LHV. Pure slumgum pellets showed very high durability (99.98%) and HHV (27.66 MJ/kg), likely due to high fat content, but high sulfur (2.17%) and nitrogen (3.52%) prevented ISO compliance. In gasification, adding sawdust increased LHV, reaching 7.62 MJ/Nm³ at a 50:50 blend, although ER stayed very low (0.0125–0.0204) because higher airflow raised fuel consumption.

A research by Yesilova [13] examined catalyst effects on biomass-mixture gasification using lab-scale updraft and modifiable-downdraft fixed-bed reactors. Red mud (RM) and an Al–Ni alloy were tested at high temperature, where H_2 levels of 51–65 vol% were obtained at 900 °C in both systems. The Al–Ni catalyst showed the strongest enhancement, achieving 65 vol% H_2 in the updraft reactor at 900 °C with 0.05 L/min dry air, and widening the H_2/CO range from 2–4 (no catalyst) to 1.6–7. RM generally increased H_2 in the updraft reactor by about 1–7 vol% at 900 °C, but in the modifiable-downdraft reactor it reduced H_2 by roughly 2–6%.

A research by Jancauskas [14] examined three MSW fractions (FDS, SRF, and plastic packaging mixture/PPM) from mechanical–biological treatment plants were gasified in an allothermal fixed-bed updraft reactor at 800 °C using air at ER ≈ 0.15 and 0.21. All feeds showed similar volatile-release peaks (~330 and ~500 °C). Lowering ER increased the heating value of combustible gases; PPM produced the highest H_2 (11.39%). SRF generated the most tar (47.44 g/m³), dominated by aromatic compounds.

A research by Junga [15] examined co-gasifying laying hens manure (LHM) with common litter such as wheat straw remains limited, particularly across a wide range of air–fuel equivalence ratios (AFER). This laboratory study used a fixed-bed updraft reactor to gasify straw–LHM blends (25–75% LHM) under low (0.12–0.28) and high (0.30–0.45) AFER to assess how LHM affects producer-gas quality and process efficiency. At higher AFER, the producer-gas LHV stayed around 3.3–3.4 MJ/m³ (depending on blend), with cold gas efficiency 60% and carbon conversion efficiency of 82–94%.

A study by Tezer [16] evaluated the gasification of olive pomace in fixed-bed updraft and downdraft systems. Dried olive pomace obtained from an olive-oil soap plant in Izmir (Türkiye) was characterized and gasified at 700–900 °C using dry air at 0.05–0.4 L/min, with additional tests using pure oxygen (0.01 L/min). With dry air, the syngas

reached 48 vol% H_2 in the updraft and 45 vol% in the downdraft, with a heating value of about 12.4 MJ/Nm^3. Under oxygen, H_2 increased to ~53 vol% in the updraft but was ~39 vol% in the downdraft.

A study by Isik [17] gasified MDF wood-waste in a 2100 kg/h updraft fixed-bed system (tested at 1500–2100 kg/h) using oak chips as a reference. Syngas yield was 2.5 Nm^3/kg with LHV 6.0–7.0 MJ/Nm^3, and the gas composition at full-load MDF was similar to oak. Hot syngas (430 °C) containing tar/soot was burned directly in a retrofitted thermal-oil heater (7 MWh) to supply an ORC turbine generating 955 kW electricity, converting 88 wt% of MDF residue into syngas.

Based on the above literature, it is evident that syngas quality in fixed-bed updraft gasification is primarily governed by catalytic strategy such as Al_2O_3, dolomite, Al/Ni, red mud, oxidant selection, and equivalence ratio, while secondary upgrading can further suppress tar and enrich H_2. However, most published studies still emphasize single catalyst systems or isolated additives, and comparatively few have investigated dual catalyst synergy in updraft configurations using a systematic, design-of-experiments optimization framework.

In this context, the present study on Syngas Quality Improvement in Corncob Updraft Gasification Using a CaO/Activated Carbon Palm-Fiber Catalyst addresses a clear research gap. The CaO-activated carbon combination is expected to deliver a dual-synergistic function: CaO acts as an in-situ CO_2 sorbent that can shift gasification equilibria toward higher H_2 formation, whereas palm-fiber-derived activated carbon provides high-surface-area catalytic sites to promote tar cracking and reforming of volatiles, thereby reducing condensable by-products while enhancing the combustible gas fraction. Consequently, this work is positioned to contribute both mechanistic and practical advances by demonstrating a scalable dual-catalyst route to produce cleaner, H_2-richer, and higher-LHV syngas from corncob waste in an updraft reactor.

3. The aim and objectives of the study

The aim of the study is to enhance syngas quality from corncob updraft gasification by developing and optimizing a dual-synergy CaO/palm-fiber-derived activated carbon (CaO/AC-PF) catalytic system.

Objectives of the study:

- To synthesize and characterize the CaO and palm-fiber activated carbon catalysts using FTIR, SEM, and BET
- To investigate the effects of operating parameters, particularly equivalence ratio (ER), catalyst loading, and CaO/AC ratio, on syngas composition H_2, CO, CH_4, CO_2 and LHV

4. Materials and methods

4.1 Catalyst Preparation

Approximately 6 grams of ground palm fiber was mixed with 60 mL of distilled water and stirred for 10 minutes. The mixture was then placed in an autoclave and heated to 200 °C at a rate of 5 °C per minute for 6 hours in an electric oven. After that, the reactor is allowed to cool naturally to room temperature. The resulting solid hydrocarbon product (hydrochar) is then separated using Whatman No. 42 filter paper. The filtered product is then dried at 105 °C for 24 hours and stored in a glass vial. The next stage is the activation process. The hydrochar is immersed in a 3 M KOH solution with a weight ratio of 1:3 (Hydrochar:KOH) for 16 hours, then dried at 85 °C for 6 hours. Spectroscopic evidence indicates that KOH preferentially reacts with oxygenated sites and can increase the relative abundance of C–OH functionalities, while higher KOH ratio and activation temperature significantly enhance porosity and BET surface area [18][19]. To obtain the CaO/AC mixture, CaO powder and activated carbon (AC) were mixed in specific proportions using a grinder until a homogeneous mixture was obtained. Next, CaO, AC, and CaO/AC were activated using a tube furnace at a temperature of 700 °C for 1 hour with a continuous flow of nitrogen during the activation process. The resulting product was then washed using distilled water until it reached a neutral pH. This stage produced activated carbon that was ready for use in research.

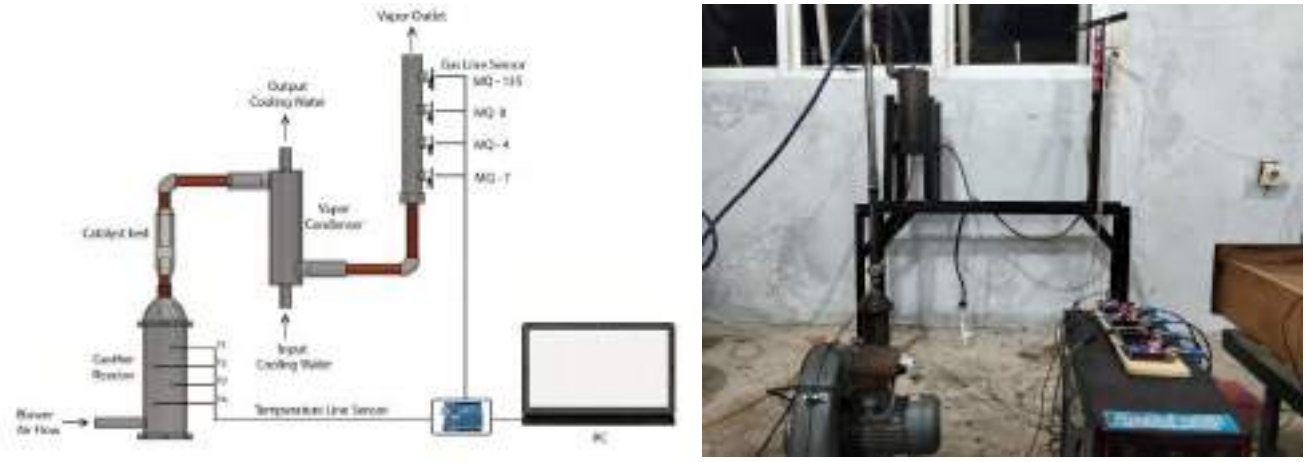
4.2 Experimental Setup

Corncob biomass was obtained from farmers in the South Malang region of East Java. Before use, the biomass was cleaned of impurities and dried in an oven for 6 hours at 100 °C to remove moisture (water vapor) content. The ultimate and proximate test results are as follows:

Table 1

Ultimate And Proximate Test Corn Cob

Parameter	Units	Corn cobs
Moisture	%	6.3
Volatile matter	%	90.65
Fixed carbon	%	25.44
Ash	%	2.28
C	%	43.6
H	%	6.3
O	%	46.8
N	%	9.5
HHV	kJ/kg	17.61



a b

Fig. 1. Updraft Gasifier: a – Schematic Experiment; b - Experimental Setup

This study used an updraft gasification reactor designed with a total height of 20 cm. The lower part of the reactor consisted of an ash container with a height of 5 cm, while the active reactor had a height of 15 cm and a diameter of 3 inches. The reactor was equipped with a 1-inch diameter air inlet pipe connected to a blower. The blower was modified with a potentiometer so that the air speed could be adjusted as needed. To monitor the thermal conditions inside the reactor, four 3 cm long type K thermocouples were installed at several different points so that the temperature profile in the gasification zone could be observed in more detail. Each test was conducted with a fixed biomass mass, a mixture of corn cobs weighing 80 grams. The reactor was made of iron and equipped with a gas seal to prevent leaks during the gasification process.

The gas produced by the reactor was fed into a condenser, which cooled the hot gas so that the water vapor components could be separated. The condenser was made of a copper spiral pipe with a diameter of ½ inch and a height of 30 cm. Cooling water was circulated from the bottom of the condenser and exited through the top to ensure efficient heat transfer. This cooling system was driven by a 60-watt water pump, ensuring stable water flow and optimal condensation. The catalyst was positioned downstream after the reactor, where it was supported on steel wool and wrapped with an 80-µm wire mesh to secure the catalyst and prevent particle carryover with the gas flow

To analyse the gas composition, four types of MQ gas sensors were used. The MQ-8 sensor was used to detect H_2, MQ-4 for CH_4, MQ-135 for CO2 and MQ-7 for CO. Each gas sensor was calibrated according to the manufacturer's datasheet, specifically by determining the Ro value, which is the sensor resistance in clean air conditions. This Ro value is used as a reference in calculating the measured gas concentration during the process[20][21].

All data from the gas sensors and thermocouples were acquired using an Arduino Uno microcontroller. Each gas sensor is connected to a separate Arduino Uno to facilitate the calibration process and reduce the possibility of interference between sensors. Arduino is also used to record temperature data from four thermocouples installed in the reactor,

so that gas composition and temperature distribution data can be obtained simultaneously.

The ER range of 0.2, 0.25, 0.3 and 0.35. The catalyst load was between 4%, 6%, 8% and 10% from the mass of input feedstock. The CaO/AC-PF ratio was varied between 0:1, 1:0, 1:1, and 2:1. Design of experiment can be seen in table 2.

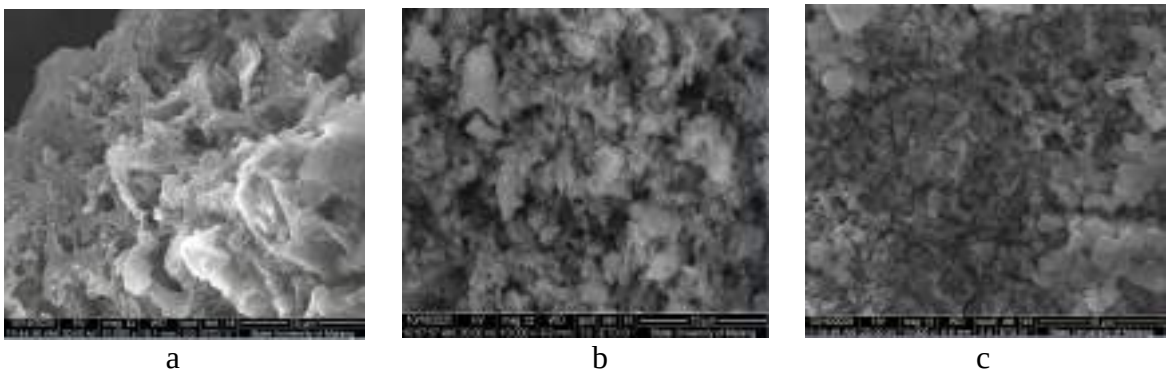
Table 2

Design of Experiment using

Run	Equivalence Ratio (E.R)	Catalyst Load %	CaO/AC
1	0.2	4	1:0
2	0.2	6	0:1
3	0.2	8	1:1
4	0.2	10	2:1
5	0.25	4	0:1
6	0.25	6	1:0
7	0.25	8	2:1
8	0.25	10	1:1
9	0.3	4	1:1
10	0.3	6	2:1
11	0.3	8	1:0
12	0.3	10	0:1
13	0.35	4	2:1
14	0.35	6	1:1
15	0.35	8	0:1
16	0.35	10	1:0

5. Results

5.1 SEM Catalyst Result



a b c

Fig. 2. SEM Catalyst Result: a-SEM AC-PF, b-SEM CaO:AC;1:1, c-SEM CaO:AC;2:1

Figure 2 (a) shows the image obtained from a Scanning Electron Microscope (SEM) with a magnification of 10,000× shows the surface morphology of palm fiber-based

activated carbon (AC-PF). The surface structure appears porous and irregular, with a combination of void areas and layered surfaces. This characteristic indicates that the activation process that using KOH has successfully formed micropores and mesopores, which play an important role in increasing the specific surface area of activated carbon.
The rough and textured surface indicates that most of the material has undergone lignocellulose cell wall exfoliation, resulting in numerous interparticle gaps[22]. This porous structure greatly supports gas adsorption and diffusion capabilities when used as a catalyst in gasification or thermochemical reactions.
The presence of 1–5 μm voids indicates that most pores are in the mesopore category, supporting the adsorption of gas molecules such as H_2, CO, and tar during the gasification reaction[23].
The morphology of AC-PF shows the characteristics of porous activated carbon with a heterogeneous pore distribution, where the pores allow increased contact between gas reactants and active sites on the material surface, thereby increasing catalytic efficiency and the ability to absorb tar or CO_2 in biomass-based energy applications[24].
Figure 2 (b) shows the surface morphology of the CaO:AC-PF catalyst with a ratio of 1:1. Visually, it can be seen that the surface of this material consists of fine particles ranging in size from microns to submicrons that stick together to form a layered and slightly agglomerated structure.
The presence of fine, light-colored grains indicates an even distribution of CaO particles impregnated on the surface of activated carbon (AC-PF). This CaO distribution fills some of the pores of the carbon, resulting in a denser surface compared to pure AC-PF. However, there are still small gaps and voids between the grains, indicating that the microporous and mesoporous structures are still formed and can support catalytic activity[25].
This morphology illustrates the success of the CaO impregnation process on activated carbon from palm fiber, where the interaction between CaO and the carbon pore walls produces a composite material that is more thermally and chemically stable. This structure is highly conducive to catalyst applications in biomass gasification processes, as CaO particles can function as CO_2 absorbers while accelerating the tar reforming reaction[26].
Figure 2 (c) shows the surface morphology of the CaO:AC-PF (2:1) catalyst. The image shows that the surface of the material is dominated by agglomerations of fine, round, and irregular particles ranging in size from microns to submicrons. Compared to the CaO:AC-PF (1:1) sample, this structure appears denser and tighter, indicating that an increase in the CaO ratio causes partial closure of the activated carbon surface pores by CaO particles.
The distribution of CaO particles appears more uniform and covers the carbon surface, indicating the successful impregnation of a larger amount of CaO. The light color in some areas indicates the presence of a calcium oxide phase that is strongly attached to the activated carbon matrix[27]. This structure indicates a strong interaction between CaO and AC-PF, forming a thermally stable composite.

Although some pores are covered, there are still microscopic gaps between the CaO grains that allow gas diffusion to occur, so that the catalyst retains its good adsorption capacity. The combination of the active area of CaO and the porous carbon structure makes this material very promising for biomass gasification or tar reforming applications, as CaO can act as a CO_2 absorber and increase the conversion of carbon to hydrogen gas.

5.2 FTIR Catalyst Result

The FTIR analysis results shown in the figure 3 reveal clear spectral differences between the AC-PF, CaO, and their mixtures (CaO:AC-PF) with ratios of 2:1 and 1:1. In the AC-PF spectrum, the absorption band at 2926 cm^{-1} is associated with the stretching vibration of the C–H group from –CH2 or –CH3 (methylene/methyl stretching), which indicates the presence of hydrocarbon chain residues from the lignocellulose structure. The peak at 1577 cm^{-1} indicates the presence of aromatic C=C or C=O stretching, while the band at 1056 cm^{-1} represents C–O stretching from alcohol or ether groups. In addition, the –OH group that appears in the 3500–3600 cm^{-1} region is identified as the result of AC-PF activation using a KOH solution, which causes the formation of hydroxyl groups on the activated carbon surface. This –OH group plays an important role in increasing the surface activity and adsorption capacity of AC-PF as a catalyst support medium [28][29].

In pure CaO, the intense band at 3639 cm^{-1} is associated with the stretching of the O–H group from $Ca(OH)_2$, which is formed due to the partial hydration of CaO when exposed to humid air. Meanwhile, the absorption bands at 1426 cm^{-1} and 876 cm^{-1} are associated with C–O stretching and CO_3^{2-} bending, respectively, indicating the formation of $CaCO_3$ due to CO_2 adsorption from the air. This shows that CaO is highly reactive to moisture and carbon dioxide in the environment.

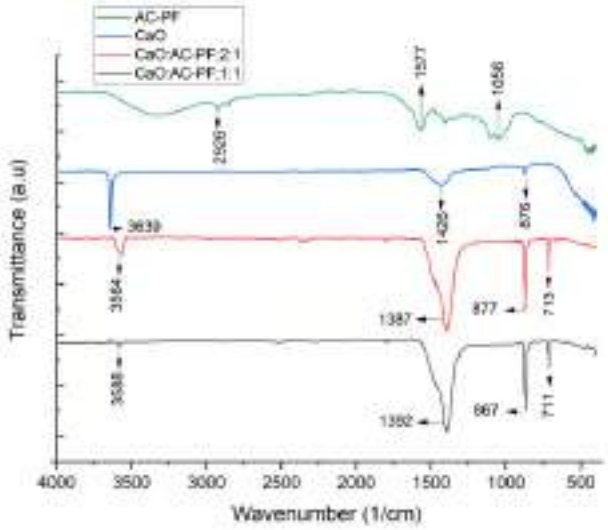


Fig. 3. FTIR Catalyst Result

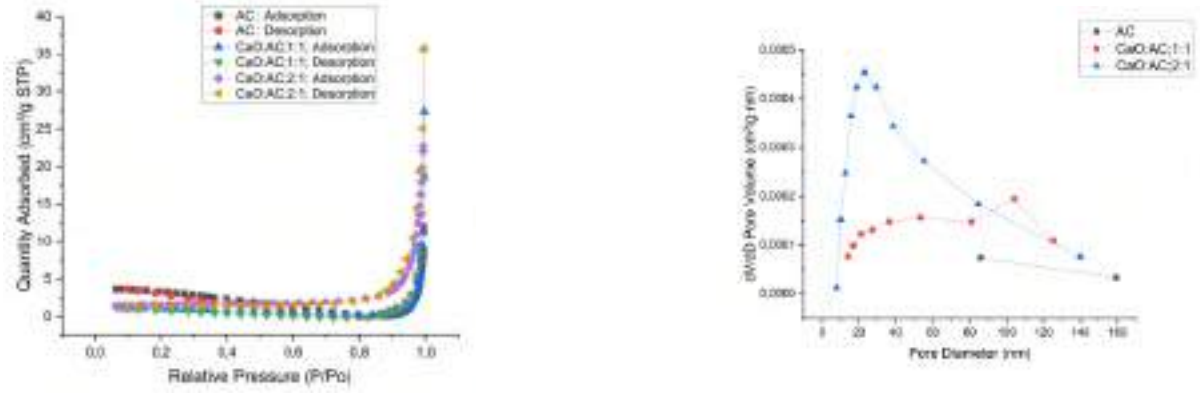
For the CaO:AC-PF (2:1), the main absorption bands were detected at 3564 cm^{-1} (O–H stretching from $Ca(OH)_2$ and the –OH group in AC-PF), 1387 cm^{-1} (C–O stretching), and 877 cm^{-1} and 713 cm^{-1} (bending vibration of CO_3^{2-}). This combination of bands indicates the formation of carbonate compounds ($CaCO_3$) due to the interaction between CaO and the oxygen groups of activated carbon. The presence of –OH groups from KOH activation also strengthens the basic properties on the surface, which can increase the chemical interaction between CaO and AC-PF[30].

At a CaO:AC-PF ratio of 1:1, the absorption bands at 3588 cm^{-1}, 1392 cm^{-1}, 867 cm^{-1}, and 711 cm^{-1} show a similar pattern, indicating the presence of hydroxyl (O–H) and carbonate (CO_3^{2-}) groups. The difference in peak intensity compared to the 2:1 ratio indicates variations in the level of interaction between CaO and the –OH groups resulting from KOH activation on AC-PF, which affects the formation of carbonate-hydroxide complexes on the material surface[31].

5.3 BET Catalyst Result

Figure 4 shows the adsorption–desorption isotherm curves for nitrogen for the AC, CaO:AC (1:1), and CaO:AC (2:1) samples are shown in Figure 4. All three samples exhibit type IV isotherms with clear hysteresis loops at relatively high pressures (P/Po > 0.9). Based on the IUPAC classification, this characteristic indicates that the material has a mesoporous structure formed through capillary condensation within the pore channels. The difference between the adsorption and desorption pathways indicates that the pore shape is not perfectly cylindrical, but rather tends to be irregular or slit-like, which is commonly found in modified activated carbon materials[32].

The pure activated carbon (AC) sample showed a relatively low nitrogen adsorption volume with a specific surface area of 24.51 m^2/g and an average pore diameter of 0.74 nm, indicating a predominance of microporous structures. In the CaO:AC (1:1) composite, the surface area did not change significantly compared to pure AC, indicating that the addition of a moderate amount of CaO did not cover the carbon pores much, but only adhered to the external surface of the carbon matrix [33].



a b

Fig. 4. BET Result: a-AC Surface Analysis Adsorption Desorption Isotherm; b-BJH Adsorption Pore Size Distribution

Conversely, in the CaO:AC (2:1) mixture, there was a sharp increase in adsorption volume at relatively high pressure (P/Po > 0.9) to around 35 cm^3/g STP, while the BET surface area decreased dramatically to 5.06 m^2/g, and the pore diameter increased to 22.87 nm.

These changes in isotherm shape and pore size increase indicate that CaO impregnation not only modifies the surface chemistry but also significantly alters the pore structure of activated carbon. This transformation is positive in the context of catalytic applications in biomass gasification processes, as the mesoporous structure can enhance gas diffusion and accessibility to active sites during the tar reforming and water–gas shift reactions. Thus, even though the specific surface area decreases, the increase in mesoporousness and pore connectivity can actually improve catalyst performance in hydrogen gas production[34].

Figure 4.b shows the BJH pore size distribution curves that provide further insight into the textural evolution of the palm-fiber-based activated carbon after CaO impregnation. The pristine AC exhibits a relatively low dV/dD value and a broad contribution only at large pore diameters (>60 nm), indicating that its pore system is dominated by macropores with a limited amount of mesopores. Such a texture is less favourable for gas–solid reactions because the accessible surface area in the mesopore range (2–50 nm) is relatively small.

After CaO loading, the shape and intensity of the BJH curves change markedly. For CaO:AC = 1:1, the distribution shifts toward smaller pore diameters with a pronounced contribution in the mesopore region of approximately 15–60 nm. This behaviour shows that CaO impregnation partially reconstructs the carbon matrix, enlarging existing micropores and opening blocked pores to generate additional mesoporosity. The effect becomes even more evident at CaO:AC = 2:1, where the curve displays the highest dV/dD values and a distinct maximum centred at about 30–40 nm. The strong peak in this range confirms that a higher CaO loading promotes the development of well-defined mesopores while reducing the relative fraction of very large macropores.

Overall, the BJH analysis demonstrates that CaO acts not only as a reactive sorbent but also as a textural promoter for the palm-fiber AC. The increase in mesopore volume and the shift of the dominant pore size toward 20–40 nm are expected to facilitate the diffusion of gasifying agents and tar molecules, as well as to improve the accessibility of CaO active sites for CO_2 capture and reforming reactions. These features are therefore beneficial for enhancing the catalytic performance of the CaO/AC composite in biomass gasification toward H_2-rich syngas production.

5.4 Effect of ER on Syngas Product

The composition of syngas from updraft gasification is greatly influenced by the Equivalence Ratio (ER), which is the ratio of the mass flow rate of air compared to the mass flow rate of corncob in the experiment compared to the stoichiometry of air

required for complete combustion of corncob. In this study, the ER used was 0.2–0.35 with the following formula:

$$ER = \frac{(\dot{m}_a/\dot{m}_{cc})_{exp}}{(\dot{m}_a/\dot{m}_{cc})_{stc}}$$

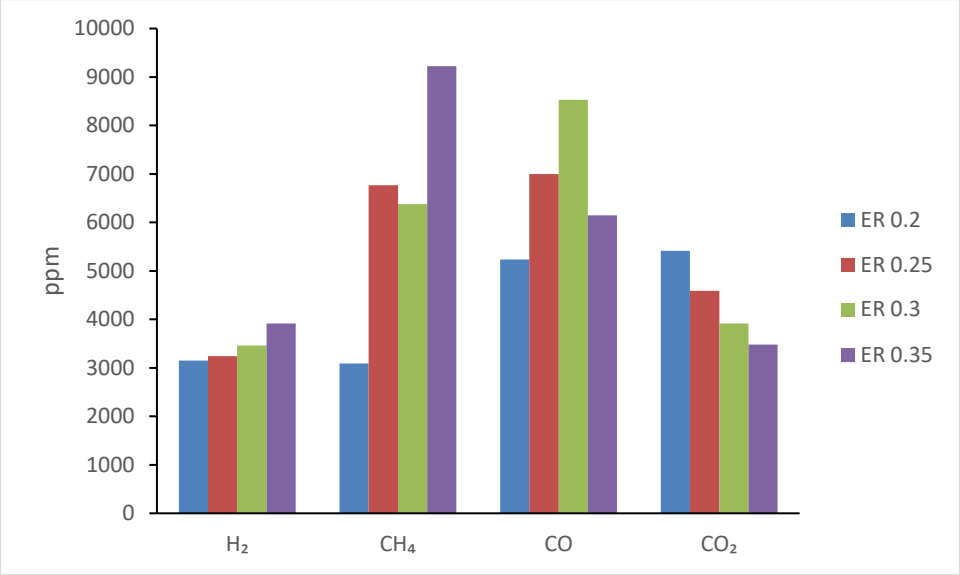


Fig. 5. Syngas Composition with Different ER

The graph above shows that the higher the ER, the higher the hydrogen composition produced. At ER 0.2, the ppm is 3150 ppm, at ER 0.25 it is 3241 ppm, at ER 0.3 it is 3457 ppm, and at ER 0.35 it is 3914 ppm. A higher oxidant supply promotes the formation of more stable autothermal conditions and higher reaction temperatures due to partial oxidation. This increase in temperature accelerates hydrogen-forming reactions, particularly the gasification of active carbon catalyst interactions with steam ($C + H_2O \rightarrow CO + H_2$), the reforming of volatile compounds/light hydrocarbons ($CxHy + H_2O \rightarrow CO + H_2$), and the cracking of tar/volatile into lighter gas species. At low ER, some volatiles tend to be incompletely converted and still have the potential to escape as condensable components, while increasing ER increases heat availability, making the conversion of volatiles into gas fractions (including H_2) more effective.

The higher the ER, the higher the CH4 composition produced. At ER 0.2, 3093 ppm was obtained, at ER 0.25 6767 ppm, ER 0.3 6377 ppm, and ER 0.35 9221 ppm. This trend indicates that the supply of oxidants not only increases autothermal conditions and the rate of devolatilization, but also shifts the reaction pathway towards the formation of light hydrocarbons through hydrogenation and/or methanation reactions in the reactor zone where the temperature still supports CH_4 formation. In particular, increased H_2 at higher ERs can promote the methanation reaction of CO ($CO + 3H_2 \rightleftharpoons CH_4 + H_2O$), so that CH_4 increases along with a tendency for CO to decrease at the highest ER. In addition, more intensive fragmentation of volatiles and tar at high ERs has the potential to produce light gas precursors which are then hydrogenated to CH_4.

CO formation increased up to an ER of 0.3 and decreased at an ER of 0.35. At an ER of 0.2, 5238 ppm was obtained, at an ER of 0.25, 6999 ppm, at an ER of 0.3, 8532 ppm, and decreased at an ER of 0.35 to 6145 ppm. At low ER (0.20–0.25), limited oxygen supply resulted in relatively low heat release, so that the reaction zone temperature and char reactivity were not sufficient to intensify CO formation reactions, especially the Boudouard reaction ($C + CO_2 \rightleftharpoons 2CO$) and char gasification with steam ($C + H_2O \rightleftharpoons CO + H_2$). When the ER is increased towards 0.30, the increase in autothermal heat strengthens these reduction reactions, causing CO formation to increase and reach its peak. However, at higher ERs (0.35), the CO fraction tends to decrease because some CO can be converted to CH_4.

CO_2 formation continues to decrease as ER increases. At ER 0.2, 5412 ppm is obtained; at ER 0.25, 4592 ppm; at ER 0.3, 3916 ppm; and at ER 0.35, 3479 ppm. The increase in oxidant supply at this ER does not promote complete combustion, but rather strengthens the CO_2 reduction mechanism. At higher ERs, the heat generated from partial oxidation increases the temperature of the reduction zone, thereby accelerating the Boudouard reaction ($C + CO_2 \rightleftharpoons 2CO$), in which CO_2 is reduced by char to CO. This mechanism is consistent with the increase in CO until it reaches a maximum at an ER of 0.30, while also explaining the decrease in CO_2 under the same conditions. Interestingly, at an ER of 0.35, CO_2 remains at its lowest level even though CO decreases, indicating that the CO formed is not completely accumulated at the outlet but has the potential to undergo further conversion along the gas flow path.

5.5 Effect of Catalyst Loading on Syngas Product

The catalyst load or amount of catalyst in this study was 4%, 6%, 8%, and 10% of the total biomass weight. The figure 6. shows that the composition of H_2 and CH_4 increases as the catalyst load decreases. The H_2 gas composition at catalyst loads of 4%, 6%, 8%, and 10% is 3742 ppm, 3471 ppm, 3372 ppm, and 3176 ppm, respectively. As the catalyst load increases, the reaction pathways that consume H_2 tend to strengthen, particularly the reverse water–gas shift ($CO_2 + H_2 \rightarrow CO + H_2O$) and H_2 interactions on the catalyst surface during the conversion of gasification compounds. As a result, even though reforming occurs, the measured net H_2 decreases because more H_2 is used for CO formation and surface reactions. The CH_4 gas composition at catalyst loads of 4%, 6%, 8%, and 10% was 7031 ppm, 6476 ppm, 6206 ppm, and 5746 ppm, respectively. An increase in catalyst load increases the number of active sites and gas-catalyst contact, so that methane/light hydrocarbon cracking and reforming occur more intensely. CH_4 then acts as a reactant that is converted into more reactive syngas components, causing the CH_4 concentration to decrease at higher catalyst loads.

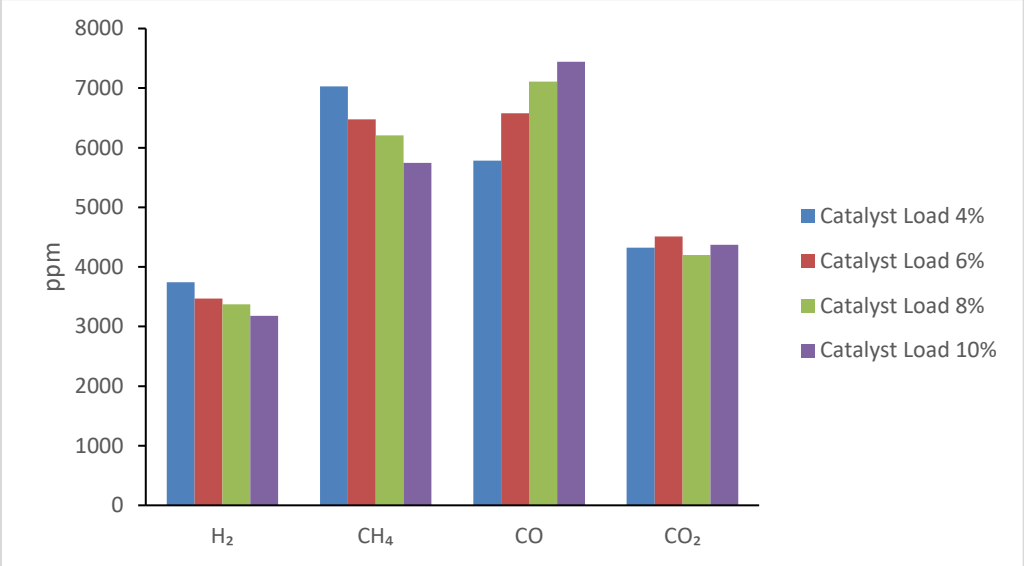


Fig. 6. Syngas Composition with Catalyst Load Variation

The CO gas composition increases with increasing catalyst load, namely for catalyst loads of 4%, 6%, 8% and 10% at 5782 ppm, 6576 ppm, 7111 ppm and 7445 ppm, respectively. The increase in catalyst loading strengthens the CO-forming reactions, particularly dry reforming ($CH_4 + CO_2 \rightarrow 2CO + 2H_2$), char–$CO_2$ reaction ($C + CO_2 \rightarrow 2CO$), and reverse water–gas shift. This combination shifts the product selectivity towards CO, so that the CO fraction increases consistently as the catalyst is increased. The CO_2 gas composition tends to stagnate with increasing catalyst loading, at catalyst loads of 4%, 6%, 8%, and 10% at 4322 ppm, 4510 ppm, 4198 ppm, and 4369 ppm, respectively. CO_2 shows minor changes because it is in a searching for a chemical equilibrium between the partial oxidation and the dry reforming. When the catalyst load increases, the rate of CO_2 consumption may rise, but this is often offset by CO_2 formation in the reaction zone, so that the CO_2 value appears stable or only fluctuates.

5.6 Effect of Catalyst Ratio on Syngas Product

At a catalyst load of 4%, the CaO/AC ratio changes the gasification reaction through differences in the dominance of tar cracking/reforming and CO_2 capture by CaO, so that the gas composition is highly dependent on the number of active sites and the effectiveness of gas-catalyst contact. At 0:1 (AC), CH_4 and CO are relatively high because AC promotes volatile/tar cracking, but CO_2 remains high because there is no absorption. At 1:0 (CaO), CH_4 decreases but CO_2 is highest, indicating that CO_2 capture is not yet effective due to limited surface area/carbonate layer formation. The 1:1 ratio produces the highest CO with moderate CO_2, indicating CaO–AC synergy that increases the conversion of volatiles into reactive gases. Meanwhile, the 2:1 (CaO-rich) ratio provides the highest H_2 and lowest CO_2 due to the sorption-enhanced effect of CaO, but CH_4 remains high due to the smaller contribution of AC, so methane reforming/cracking is not yet optimal.

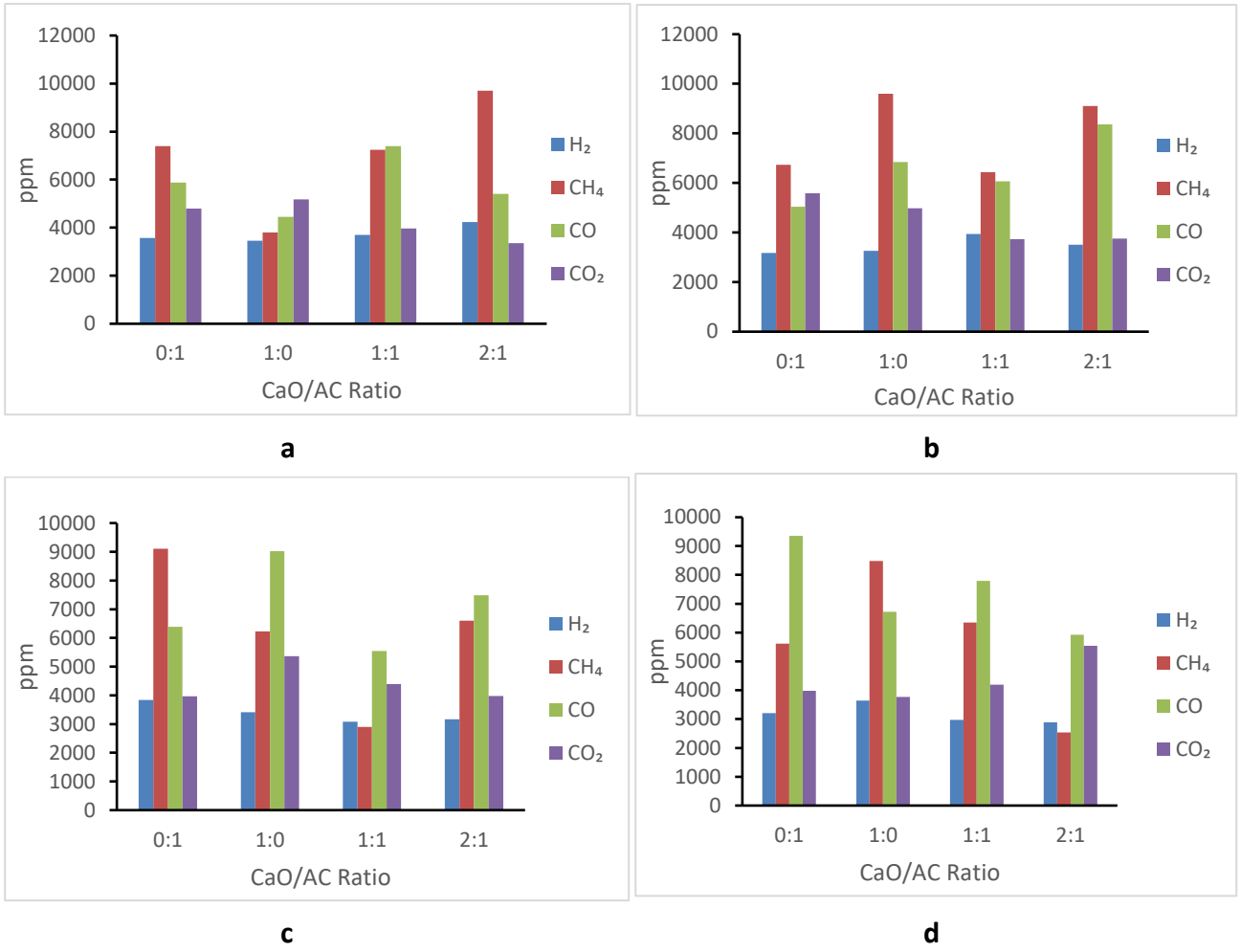


Fig. 7. Effect CaO/AC ratio with various catalyst load: a – 4%, b – 6%, c – 8%, d – 10%

At a catalyst load of 4%, the CaO/AC ratio changes the gasification reaction through differences in the dominance of tar cracking/reforming and CO_2 capture by CaO, so that the gas composition is highly dependent on the number of active sites and the effectiveness of gas-catalyst contact. At 0:1 (AC), CH_4 and CO are relatively high because AC promotes volatile/tar cracking, but CO_2 remains high because there is no absorption. At 1:0 (CaO), CH_4 decreases but CO_2 is highest, indicating that CO_2 capture is not yet effective due to limited surface area/carbonate layer formation. The 1:1 ratio produces the highest CO with moderate CO_2, indicating CaO–AC synergy that increases the conversion of volatiles into reactive gases. Meanwhile, the 2:1 (CaO-rich) ratio provides the highest H_2 and lowest CO_2 due to the sorption-enhanced effect of CaO, but CH_4 remains high due to the smaller contribution of AC, so methane reforming/cracking is not yet optimal.

At a catalyst load of 6%, the CaO/AC ratio mainly shifts the selectivity of secondary reactions (tar cracking/reforming and CO_2 capture), where AC enhances the conversion of volatiles/light hydrocarbons, while CaO reduces CO_2 through carbonation ($CaO + CO_2 \rightarrow CaCO_3$) and changes the reaction equilibrium. At 0:1, CH_4 and CO_2 remain high

because there is no CO_2 capture and methane reforming is not yet optimal, so volatiles still escape as CH_4. At 1:0, CO_2 tends to decrease, but CH_4 becomes the highest due to the absence of AC's role in cracking/reforming. The most favorable conditions occur at 1:1, with the highest H_2 and lowest CO_2, indicating CaO–AC synergy that promotes sorption-enhanced reforming and increases the conversion of hydrocarbons into syngas components. At 2:1, CO is highest and CO_2 remains low, but CH_4 rises again and H_2 is not maximized because excess CaO has the potential to rapidly carbonate/cause contact limitations, thereby reducing the contribution of AC in cracking/reforming.

At a catalyst load of 8%, the CaO/AC ratio significantly shifts the selectivity of the syngas reaction. At 0:1 (AC), CH_4 is still high because some light hydrocarbons have not been fully converted even though the tar cracking process is already active. At 1:0 (CaO), CO increases the most, but CO_2 also tends to be high, indicating that CaO in this condition is more dominant in promoting the CO formation pathway, while the CO_2 capture function is not yet optimal due to contact limitations or carbonation saturation. The 1:1 ratio produces the lowest CH_4, indicating the most effective CaO–AC synergy for cracking/reforming light hydrocarbons so that more methane is converted into reactive gas. At 2:1, CO increases again but CH_4 also rises, indicating that a smaller AC fraction reduces the intensity of methane reforming/cracking, while the decrease in CO_2 remains dependent on the effectiveness of CaO sorption.

At a catalyst load of 10%, the increase in total catalyst makes secondary reactions (tar cracking/reforming, solid-gas heterogeneous reactions, and equilibrium shifts) very dominant, so that the CaO/AC ratio mainly determines the direction of product selectivity. At 0:1 (AC), CO formation tends to be strongest because the porous carbon surface accelerates the cracking/reforming of volatiles and the conversion of tar into reactive gases. At ratios involving CaO (1:0, 1:1, 2:1), CaO can retain CO_2 through carbonation, but at high loads the effect is often non-linear because CaO rapidly carbonates/diffusion limitations and pore blocking occur, so that under CaO-rich conditions (2:1) CH_4 can decrease, but CO_2 may increase and H_2 is not maximized due to reaction competition. Overall, at a 10% load, a trade-off is observed: AC-dominant increases CO, while CaO-dominant suppresses light hydrocarbons but has the potential to trigger non-ideal conditions (saturation/mass transport) that reduce the benefits of H_2 and CO_2.

5.7 LHV Syngas

To calculate the LHV of syngas, it must first be converted from ppm to % volume of gas. The formula is $\%vol_i = \frac{ppmv_i}{10^4}$. To calculate the LHV, use the formula:

$$LHV_{mix}\left(\frac{MJ}{Nm^3}\right) = \frac{10{,}8(\%H_2) + 12.63(\%CO) + 35.8(\%CH_4)}{100}$$

LHV H_2 = 10.8 MJ/Nm^3

LHV CO = 12.63 MJ/Nm^3

LHV CH_4 = 35.8 MJ/Nm^3

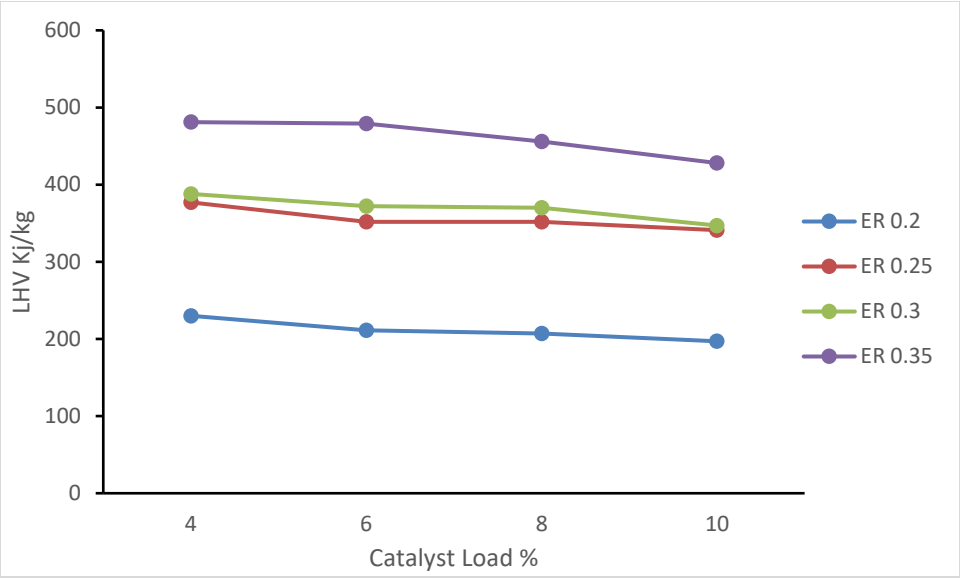


Fig. 8. LHV syngas with various ER

Figure 8 shows that the LHV value increases with the ER, where a higher ER produces more intense autothermal conditions, causing the reactor temperature to rise. This increase in temperature accelerates the decomposition of volatiles and tar cracking, and promotes more complete gasification and reforming reactions, thereby increasing the fraction of permanent gases that contribute to the calorific value (mainly CO and CH_4, as well as some H_2). In addition, the increase in temperature is also associated with more effective hydrogen formation, because H_2 formation reactions (e.g., through steam-water and reforming reactions) are generally more optimal at high temperatures, with the temperature range often reported to be most conducive to H_2 formation being 800–1000 °C.

However, all ER values show that LHV tends to decrease when the catalyst load is increased from 4% to 10%. This decrease indicates that excessive catalyst addition under these operating conditions does not always improve gas energy quality, because the catalyst can shift the reaction selectivity towards the conversion of high calorific components especially CH_4 into CO and H_2 through reforming, while at the same time the fraction of diluent gases such as CO_2 (and steam) may increase due to reaction. Since CH_4 has a very large calorific value contribution in the syngas mixture, the decrease in its fraction is often more dominant than the increase in CO/H_2, so that the total LHV tends to decrease.

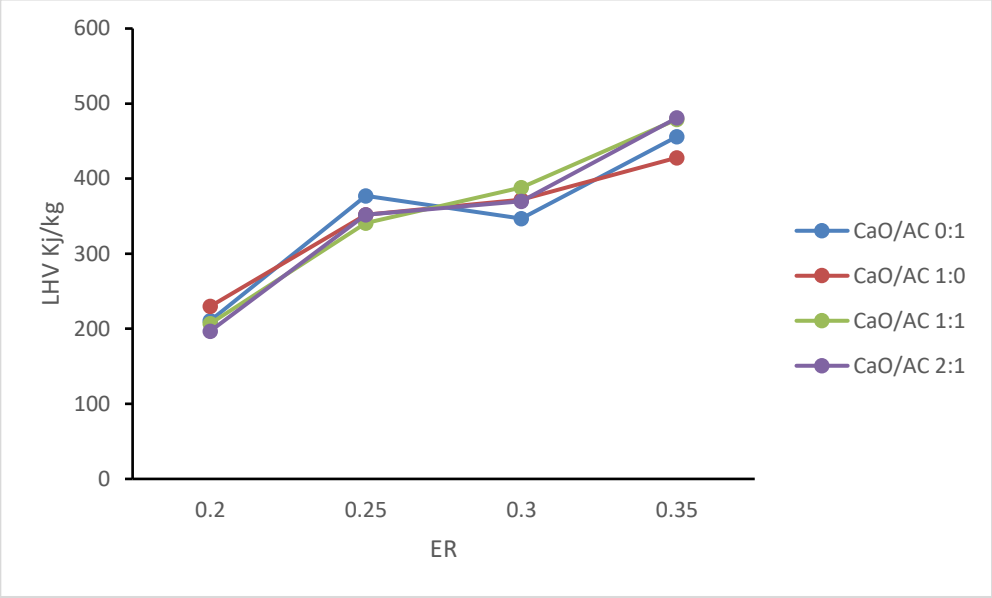


Fig 9. LHV Syngas with Various CaO/AC Ratio

Figure 9 shows that the LHV of syngas increases consistently with the increase in ER 0.2 to 0.35 for all CaO/AC ratios, indicating that a higher ER strengthens autothermal conditions so that the reaction temperature increases and the conversion of volatiles into syngas becomes more complete. At low ER (0.2), the difference in LHV between ratios is still small because secondary reactions such as cracking, reforming and heterogeneous reactions are not yet dominant; the system is still relatively influenced by incompletely converted volatiles. When the ER is increased to 0.25–0.30, the effect of the catalyst ratio becomes apparent: compositions involving AC tend to produce higher LHV because they accelerate tar cracking and increase the fraction of calorific gas, while the contribution of CaO can shift the reaction equilibrium through a decrease in CO_2. At the highest ER (0.35), the LHV reaches its maximum at all ratios, with CaO/AC 2:1 and 0:1 showing peak values, indicating that at high temperatures, the reactive gas formation pathway (via cracking/reforming on the carbon surface and/or CaO-rich-promoted heterogeneous reactions) becomes dominant. Overall, ER acts as the main controlling factor for LHV increase through the temperature effect, while the CaO/AC ratio modulates LHV through the balance between cracking/reforming (AC) and CO_2 control (CaO), especially at medium–high ER.

6. Discussion

The characteristics of AC-PF-based catalysts (activated carbon from palm fiber) show a rough, porous surface that supports tar/volatile adsorption and increases the chances of heterogeneous reactions (cracking/reforming) on the catalyst surface. This porous structure is crucial in updraft gasification because pyrolysis gases and volatiles move through the bed, so the presence of porous media has the potential to strengthen secondary reactions before the gas exits to the condenser. After the addition of CaO, CaO particle dispersion was observed on the carbon surface; however, at high CaO

ratios (e.g., 2:1), the structure became denser, indicating that some of the micropores were closed. Nevertheless, BET data reveal an important phenomenon: the surface area decreases, but the pore diameter increases to the mesopore scale, which can improve the accessibility of tar/volatiles to active sites and improve mass transport in the reforming reaction. From a surface chemistry perspective, FTIR indicates the presence of –OH groups and Ca carbonate, confirming that CaO acts not only as a base catalyst but also as a CO_2 sorbent, enabling a sorption-enhanced mechanism that modulates the gasification reaction equilibrium [35].

On the process side, ER emerges as the dominant variable governing autothermal conditions, primarily through increases in effective temperature and secondary reaction intensity. An increase in ER from low to high levels consistently increases H_2, which can be explained by the acceleration of H_2 formation reactions such as char gasification with steam ($C + H_2O \rightarrow CO + H_2$) [36], light hydrocarbon reforming, and more intense tar cracking at higher temperatures. At the same time, CH_4 also increases sharply at high ER, indicating that in updraft autothermal systems, increased temperature and changes in gas composition can facilitate the formation of light gases. Meanwhile, CO tends to peak at medium ER and then decreases at higher ER, consistent with competition between CO formation against CO consumption through subsequent reactions such as methanation [37]. The decrease in CO_2 at high ER indicates the role of high temperatures in enhancing the CO_2 reduction reaction by char (Boudouard) and/or the role of CaO sorption when available.

The effect of catalyst loading shows that adding catalyst does not always increase H_2. An increase in catalyst loading from low to high levels tends to decrease H_2 and CH_4 but increase CO. Mechanistically, this condition can occur when the catalyst strengthens pathways that increase CO and/or promotes RWGS ($CO_2 + H_2 \rightarrow CO + H_2O$)[38], which consumes H_2 so that net H_2 decreases. Additionally, at high catalyst loading, the possibility of diffusion/agglomeration penalties increases, so that selectivity may shift and some active sites become less effective. Thus, the target of H_2-rich syngas in this reactor is more dependent on ER adjustment and the selection of moderate/lower catalyst loading, rather than simply increasing the loading.

The CaO/AC-PF ratio exhibits synergistic but non-linear behaviour. AC-PF primarily acts as a porous medium that enhances cracking/reforming of volatiles, while CaO provides both basic sites and CO_2 sorbents to shift the equilibrium. At high CaO ratios, the sorption and base effects may increase, but the risk of micro-pore closure and diffusion pathway changes also increases. This explains why certain compositions are optimal at certain catalyst loads: the best performance arises from a balance between pore accessibility the role of AC-PF and sorption/base strength the role of CaO.

From an energy quality perspective, the LHV value of syngas is highly sensitive to changes in CH_4. Therefore, high ER conditions that increase CH_4 tend to increase LHV. However, the interpretation of LHV needs to be read in conjunction with the process objective, because an increase in LHV is not always synonymous with an increase in syngas quality for all applications.

However, there are several limitations. First, the gas composition is obtained from ppm-based MQ sensors, so absolute accuracy can be affected by cross-sensitivity, humidity, sensor drift, and gas sampling temperature; this can affect %vol and LHV estimates, especially when CO and CH_4 changes occur simultaneously. Second, catalyst characterization (SEM–FTIR–BET) already supports the role of surface texture and chemistry, but has not yet quantified active phase changes during operation. carbonation levels, and activity decline due to fouling/pore closure

Based on these limitations, several directions for future work are recommended. Perform gas composition calibration/validation using GC-TCD/GC-FID or micro-GC to convert sensor readings into more accurate %vol and include LHV uncertainty analysis. Evaluate catalyst stability and regeneration, particularly for easily carbonated CaO, through carbonation-calcination cycle tests and post-reaction characterization (XRD/TGA/SEM-EDX) to assess phase changes and activity loss. Develop experimental designs towards ANOVA interactions or RSM so that interaction effects and predictive models can be obtained and validated through replication confirmation tests. Add process performance metrics such as gas yield (Nm^3/kg), cold gas efficiency, pressure drop, and air consumption so that "syngas quality improvement" can be demonstrated on the basis of mass-energy balance and operability, not just composition.

7. Conclusion

1. AC-PF with rich -OH group acts as a porous catalytic medium that facilitates volatile cracking and supports the reduction of condensable by-products, while CaO contributes to absorb CO_2. The BJH analysis confirms that CaO plays a dual role as a reactive sorbent and a textural promoter in palm-fiber activated carbon by enlarging mesopores (20–40 nm), thereby enhancing gas diffusion and improving access to CaO active sites, which ultimately strengthens catalytic performance.
2. Increasing ER to 0.35 enhances the combustible gas fraction H_2 and CH_4 and suppresses CO_2, whereas CO typically peaks at intermediate ER due to competing CO formation and consumption reactions along the updraft reaction zones. Increasing catalyst loading shifts syngas composition: CO increases, while H_2 and CH_4 decrease, indicating changes in dominant secondary reactions and possible diffusion or agglomeration limitations at higher loadings. Increasing ER lead to increase LHV syngas, but it can decrease at high catalyst loading. An increase in the CaO/AC ratio to 2:1 resulted in a higher syngas LHV, with a maximum value of 481 kJ/kg.

Conflict of interest

The authors declare that they have no conflict of interest in relation to this research, whether financial, personal, authorship or otherwise, that could affect the research and its results presented in this paper.

Financing
The authors sincerely thank the Ministry of Education, Culture, Research and Technology, Republic of Indonesia for fully supporting this research through the DRTPM Research Grant under Fundamental Research, Universitas Widyagama Malang, Indonesia 2025 (Grant Number:128/C3/DT.05.00/PL/2025;023/LL7/DT.05.00/PL/2025;010/ Kontrak/PT/PTS.030.7/PN/V/2025).

Data availability
Manuscript has no associated data.

Use of artificial intelligence
The authors declare that generative artificial intelligence tools were used exclusively for language editing, grammar checking, and technical formatting of the manuscript under full human control. Artificial intelligence was not used to generate, process, or interpret scientific data, form conclusions, or other ele-ments of the scientific results in the paper. Tool used: ChatGPT (OpenAI GPT-5.2, version 2026). The authors bear full responsibility for the content, reli-ability, and scientific correctness of the submitted material.

Acknowledgements
We as the Research Team would like to thank Ministry of Education, Culture, Research and Technology, Republic of Indonesia (Kemendiktisaintek Indonesia) for financing research activities.

References
[1] ASEAN Statistical Brief, "Role of Agriculture , Forestry , and Fishing Industry in ASEAN Economy," vol. VII, no. June 2023, p. 511191, 2024.
[2] V. K. Yadav *et al.*, "Emerging trends in the valorization of agricultural waste and their utilization in agricultural, pharmaceuticals, and environmental cleanup," *Waste and Biomass Valorization*, pp. 1–55, 2025.
[3] W. M. Lewandowski, M. Ryms, and W. Kosakowski, "Thermal biomass conversion: A review," *Processes*, vol. 8, no. 5, p. 516, 2020.
[4] D. Ariyanti *et al.*, "Valorization of corn cob waste for furfural production: A circular economy approach," *Biomass and Bioenergy*, vol. 194, p. 107665, 2025.
[5] A. Raizada, A. Shukla, S. Yadav, P. Katiyar, and R. Kumar, "Enhancement of H2 production via catalytic steam gasification of food waste as feedstock and its ash as a support and promoter for Ni catalyst," *Int. J. Hydrogen Energy*, vol. 60, pp. 272–281, 2024.
[6] Y. Dai *et al.*, "Co-gasification characteristics of Ca-rich sludge and Fe-rich sludge under CO2 atmosphere, and potential utilization of gasification residues as renewable catalyst in biomass pyrolysis," *Renew. Energy*, vol. 224, p. 120118, 2024.

[7] H. Sun *et al.*, “Three-stage behaviors of K2CO3 catalyst during CO2 catalytic gasification of coal,” *Fuel*, vol. 367, p. 131149, 2024.
[8] J. Zhang, Z. Chu, R. Cao, X. Wu, and K. Han, “A review of resource recovery from waste plastics via pyrolysis and gasification,” *Fuel*, vol. 404, p. 136319, 2026.
[9] Y. Tangke Tosuli, Cahyadi, H. Dafiqurrohman, R. Hermawan, and A. Surjosatyo, “Gasification of sago dreg waste in a top-lit updraft fixed bed gasifier: Syngas composition and its effect with additional Al2O3 as catalyst,” *Energy Convers. Manag. X*, vol. 24, no. October, p. 100775, 2024, doi: 10.1016/j.ecmx.2024.100775.
[10] P. Dinh *et al.*, “Enrichment of hydrogen in product gas from a pilot-scale rice husk updraft gasification system,” *Carbon Resour. Convers.*, vol. 5, no. 3, pp. 231–239, 2025, doi: 10.1016/j.crcon.2022.07.003.
[11] S. Yousef and J. Eimontas, “International Journal of Hydrogen Energy Oxygen updraft gasification-catalytic reforming of cigarettes butts for hydrogen-rich syngas production,” vol. 171, no. May, 2025, doi: 10.1016/j.ijhydene.2025.150650.
[12] D. Contreras, E. Blanco, and D. Travieso, “Experimental assessment of the energy potential of pellets produced from beekeeping wastes by updraft gasification,” vol. 343, no. January, 2025, doi: 10.1016/j.enconman.2025.120206.
[13] N. Yesilova, O. Tezer, A. Ongen, and A. Ayol, “International Journal of Hydrogen Energy Enhancing biomass gasification : A comparative study of catalyst applications in updraft and modifiable-downdraft fixed bed reactors,” *Int. J. Hydrogen Energy*, vol. 76, no. April, pp. 290–303, 2024, doi: 10.1016/j.ijhydene.2024.05.075.
[14] R. Skvor and A. Jan, “Experimental investigation of sorted municipal solid wastes producer gas composition in an updraft fixed bed gasifier,” vol. 289, no. August 2022, 2024, doi: 10.1016/j.energy.2023.130063.
[15] R. Junga, M. Tańczuk, S. Sobek, M. Chabiński, and Ł. Ziółkowski, “Effect of the addition of laying hens manure to the straw on gasification efficiency in updraft gasifier under air atmosphere,” *Appl. Therm. Eng.*, vol. 226, no. February, p. 120269, 2023, doi: 10.1016/j.applthermaleng.2023.120269.
[16] A. Ongen and A. Ayol, “ScienceDirect Gasification performance of olive pomace in updraft and downdraft fixed bed reactors,” vol. I, 2023, doi: 10.1016/j.ijhydene.2023.02.088.
[17] K. Ertas, “Gasification of MDF residue in an updraft fixed bed gasifier to produce heat and power via an ORC turbine,” vol. 169, no. February, pp. 43–51, 2023, doi: 10.1016/j.wasman.2023.06.025.
[18] S. Gorthy, S. Verma, N. Sinha, S. Shetty, H. Nguyen, and M. Neurock, “Theoretical Insights into the Effects of KOH Concentration and the Role of OH– in the Electrocatalytic Reduction of CO2 on Au,” *ACS Catal.*, vol. 13, no. 19, pp. 12924–12940, 2023.

[19] X. Wang, W. Zeng, C. Xin, X. Kong, X. Hu, and Q. Guo, “The development of activated carbon from corncob for CO2 capture,” *RSC Adv.*, vol. 12, no. 51, pp. 33069–33078, 2022, doi: 10.1039/d2ra05979g.
[20] D. Ali, H. Fakra, D. Armel, and S. Andriatoavina, “A simple and low-cost integrative sensor system for methane and hydrogen measurement,” vol. 1, no. August, 2020, doi: 10.1016/j.sintl.2020.100032.
[21] S. V. Co-digestion and H. Ram, “Assessment of a Low-Cost Hydrogen Sensor for Detection and Monitoring of Biohydrogen Production during Sugarcane,” pp. 479–490, 2024.
[22] H. Du *et al.*, “Lignocellulosic Films: Preparation, Properties, and Applications,” *Chem. Rev.*, 2025.
[23] S. De, A. M. Balu, J. C. Van Der Waal, and R. Luque, “Biomass-derived porous carbon materials: synthesis and catalytic applications,” *ChemCatChem*, vol. 7, no. 11, pp. 1608–1629, 2015.
[24] C. Li *et al.*, “Importance of oxidation reactions in creating pores in physical activation of biomasses,” *Chem. Eng. J.*, vol. 474, p. 145748, 2023.
[25] B. Zhou *et al.*, “Insights into effects of grain boundary engineering in composite metal oxide catalysts for improving catalytic performance,” *J. Colloid Interface Sci.*, vol. 653, pp. 1177–1187, 2024.
[26] Y. Zhu *et al.*, “Preparation of hierarchically porous carbon ash composite material from fine slag of coal gasification and ash slag of biomass combustion for CO2 capture,” *Sep. Purif. Technol.*, vol. 330, p. 125452, 2024.
[27] Y. Y. García-Guel, E. M. Múzquiz-Ramos, J. C. Ríos-Hurtado, A. Moreno-Santos, S. E. Flores-Villaseñor, and G. B. Escalante-Ibarra, “Surface modification of activated carbon cloth with calcium silicate and hydroxyapatite: bioactive composite material,” *Heliyon*, vol. 8, no. 11, 2022.
[28] M. Ilić *et al.*, “Surface functional groups and degree of carbonization of selected chars from different processes and feedstock,” *PLoS One*, vol. 17, no. 11, p. e0277365, 2022.
[29] R. Ali, Z. Aslam, R. A. Shawabkeh, A. Asghar, and I. A. Hussein, “BET, FTIR, and RAMAN characterizations of activated carbon from waste oil fly ash,” *Turkish J. Chem.*, vol. 44, no. 2, pp. 279–295, 2020.
[30] K. J. Stanienda-Pilecki, “The importance of Fourier-Transform Infrared Spectroscopy in the identification of carbonate phases differentiated in magnesium content,” 2019.
[31] F. Dai, Q. Zhuang, G. Huang, H. Deng, and X. Zhang, “Infrared spectrum characteristics and quantification of OH groups in coal,” *ACS omega*, vol. 8, no. 19, pp. 17064–17076, 2023.
[32] E. M. de Salazar Martínez, M. F. Alexandre-Franco, A. J. Nieto-Sanchez, and E. M. Cuerda-Correa, “Exploring the role of surface and porosity in CO2 capture by CaO-based adsorbents through response surface methodology (RSM) and artificial neural networks (ANN),” *J. CO2 Util.*, vol. 83, p. 102773, 2024.

[33] J. A. Tavizón-Pozos, H. Cervantes-Cuevas, G. G. Garcia-Camacho, G. Chavez-Esquivel, and D. R. Acosta-Najarro, “Biodiesel Production Using K–Sr/CaO and CaO Catalysts Derived from Eggshells by Canola Oil Transesterification,” *ACS omega*, vol. 10, no. 7, pp. 6827–6838, 2025.
[34] W. Koo-Amornpattana, P. Phadungbut, N. Kunthakudee, W. Jonglertjunya, S. Ratchahat, and M. Hunsom, “Innovative metal oxides (CaO, SrO, MgO) impregnated waste-derived activated carbon for biohydrogen purification,” *Sci. Rep.*, vol. 13, no. 1, p. 4705, 2023.
[35] C. Quan, M. Wang, N. Gao, T. Yang, and R. Li, “In situ adsorption of CO2 to enhance biomass gasification for hydrogen production using Ca/Ni based composites,” *J. Energy Inst.*, vol. 108, p. 101229, 2023, doi: https://doi.org/10.1016/j.joei.2023.101229.
[36] F. Micheli, E. Mattucci, C. Courson, and K. Gallucci, “Bi-Functional Catalyst/Sorbent for a H2-Rich Gas from Biomass Gasification,” 2021. doi: 10.3390/pr9071249.
[37] M. Zhu, Q. Wang, and S. Wang, “Recent Advances and Future Perspectives in Catalyst Development for Efficient and Sustainable Biomass Gasification: A Comprehensive Review,” 2025. doi: 10.3390/su17167370.
[38] N. Cerone, F. Zimbardi, L. Contuzzi, J. Baleta, and D. Cerinski, “Experimental investigation of syngas composition variation along updraft fixed bed gasifier,” *Energy Convers. Manag.*, vol. 221, no. July, p. 113116, 2020, doi: 10.1016/j.enconman.2020.113116.

REVIEW EDITOR TAHAP 1

KELENGKAPAN DOKUMEN, COVER LETTER, LICENSE AGREEMENT

20 Februari 2026

Purbo Suwandono <purbo@widyagama.ac.id>

from "Eastern-European Journal of Enterprise Technologies" (confirm receipt)_Suwandono P. _No. 2 (140).2026 - acknowledge receipt

5 messages

Oksana Nikitina <0661966nauka@gmail.com> Fri, Feb 20, 2026 at 12:10 PM
To: purbo@widyagama.ac.id

Good day!

The article was accepted for consideration of the possibility of publication in No. 2 (140).2026.

Invoice No **29/1-102-2026** on **50 euro** (type of payment: article processing charges (APCs) № 29/102).

Attention, payment only in EUR, we do not accept dollars, be careful!

Please be sure to indicate invoice number - No 29/1-102-2026 - THIS IS NECESSARY AND IMPORTANT! Otherwise, the amounts without specifying the invoice number are sent before clarification and the clarification period is up to 2 weeks. By this, either the article is removed, because the advance payment or the amount for the publication was not paid on time, or is transferred to another issue of the journal.

Bank information (check the payment details carefully):
Beneficiary: NIKOLAIEVA YULIIA PRIVATE ENTREPRENEUR
IBAN: UA313052990000026003045904406
Beneficiary's bank: JSC CB "PRIVATBANK"
Bank Address: 1D HRUSHEVSKOHO STR., KYIV, 01001, UKRAINE
SWIFT code: PBANUA2X

Pay immediately (as soon as you receive the receipt). Payment must be made strictly on your behalf. As soon as you have made the payment, you can send us a scanned receipt by e-mail. We warn you that the payment should be made within 1-3 days. The advance payment will be deducted from the total amount at the 6-th stage if your article will be accepted, but if you are refused - the deposit will not be refunded (detailed information on the journal's website http://jet.com.ua/en/publication-terms/rules-for-submitting). We warn you immediately that at this stage you confirm that the payment will be made by an individual (on your behalf) and not by a legal entity, according to the details that will be provided to you upon acceptance of the article. **We expect payment from you no later than February 23, 2026.**

A package of documents that we ask you to prepare and send a scanned copy to e-mail 0661966nauka@gmail.com no later than 23.02.2026 is attached:
1. The license agreement (see attachment) to the article can be drawn up in electronic form and signed by all authors. ID Card - such identifiers can be the number of any identity card, or the date of birth with the registration address.
2. The agreement for payment **№ 29/102-c10-2026** (see attachment) must be signed by the author by the correspondent and sent electronically along with the payment.
3. Cover letter (see attachment, please sign only the author, the contact person must be indicated in clause 10.2. of the License Agreement).
4. The official letter of permission in the attachment "Before submitting the manuscript", please fill out and send on behalf of the author (the contact person must be specified in clause 10.2. of the License Agreement).

We work 24/7 and are ready to help you around the clock!

With best regards, Manager Yu. Prylutska
TECHNOLOGY CENTER GROUP LTD
Viber/ WhatsApp/ Telegram: +380 (50) 3033801
Editorial staff of the "Eastern-European Journal of Enterprise Technologies"
Website: https://jet.com.ua/en/, http://journals.uran.ua/eejet/

PAYMENT INSTRUCTIONS: Important, please pay attention!
When paying for services by bank transfer (international payment in the SWIFT system), please use the OUR* code (All bank charges and commissions are charged from your account).
To do this, in the payment order, in field 71A "Details of Charges", check: OUR*.
**OUR ("Payer pays all fees" or "Sender bears all transaction fees"): All fees are charged to the sender of the transfer, and the recipient receives the full amount provided by the sender. These fees include fees charged by the sending*

bank and any fees applied by intermediary banks (correspondent banks).



Відвідати сайт



Відвідати сайт

Attention! The author (team of authors) submitting the manuscript to the editorial office of the journal **«Eastern-European Journal of Enterprise Technologies»** agrees with all requirements for registration, submission of the manuscript of the article and payment and be responsible in case of violation of these requirements.

Our company may rely on your freely given consent at the time you provided your personal data to us replying on this email then the lawfulness of such processing is based on that consent under EU GDPR 2016/679. You have the right to withdraw consent at any time.

Subscribe

5 attachments

Before submitting the manuscript_2026.doc
28K

Surname_Cover Letter EEJET_2026.doc
36K

2_AGREEMENT_GRUP_Suwandono P. _ukr_eng.pdf
713K

Suwandono P. _License_Agreement_ENG_EEJET_2026.pdf
3277K

invoice_ClubSience_Suwandono P. _29_102.pdf
12355K

Purbo Suwandono <purbo@widyagama.ac.id> Fri, Feb 20, 2026 at 10:24 PM
To: Oksana Nikitina <0661966nauka@gmail.com>

Dear Oksana,

Good day.

Thank you for your email and the detailed instructions.

I would like to inform you that I have completed all the requested documents and have signed/prepared them as required. I have also made the payment for **Invoice No. 29/1-102-2026** in the amount of **50 EUR** from my personal account, as instructed. Track the transfer using this link:

https://wise.com/en/track/b7ff363344084d798ab6496588dba3dc?utm_medium=rmt&utm_source=android&utm_content=activity-page

I am attaching the scanned payment receipt and the requested scanned documents to this email for your verification:

Please let me know if there is any incorrect information in the completed documents and whether you have received the transferred payment.

Thank you for your assistance.

Best regards,
Purbo Suwandono

[Quoted text hidden]

4 attachments

2_AGREEMENT_GRUP_Suwandono P. _ukr_eng.pdf
852K

Suwandono_Cover Letter EEJET_2026.doc
40K

Suwandono P. _License_Agreement_ENG_EEJET_2026_fix.pdf
1777K

Suwandono_Before submitting the manuscript_2026.doc
28K

Oksana Nikitina <0661966nauka@gmail.com> Sat, Feb 21, 2026 at 3:07 AM
To: Purbo Suwandono <purbo@widyagama.ac.id>

Good day!
Thanks! Payment receipt has been received.
As soon as the payment is credited to the account, I will inform you.
I accept the license agreement and all documents, thank you very much.
If you have any questions, please call or write, we will be happy to answer them.
Best regards, Oksana

пт, 20 февр. 2026 г. в 17:24, Purbo Suwandono <purbo@widyagama.ac.id>:
[Quoted text hidden]

--
[Quoted text hidden]

Oksana Nikitina <0661966nauka@gmail.com> Mon, Feb 23, 2026 at 2:10 PM
To: purbo@widyagama.ac.id

ДОГОВІР № 29/102-c10-2026

надання послуг інформаційно-технологічного супроводження наукового рукопису

м. Харків, Україна

20/02/2026 р

Фізична особа нерезидент України *Suwandono Purbo* який діє від імені усіх співавторів *Purbo Suwandono, Widya Wijayanti, Nova Risdiyanto Ismail, Dzulfikar Johan Akbar, Muhammad Reza* з одного боку, надалі «Замовник» , та ТОВАРИСТВО З ОБМЕЖЕНОЮ ВІДПОВІДАЛЬНІСТЮ «ТЕХНОЛОГІЧНИЙ ЦЕНТР ГРУП», в особі директора Дьоміної Олени Борисівни, який діє на підставі Статуту, з іншого боку, іменоване в подальшому **«**Виконавець», уклали цей Договір про представлення Виконавцем інтересів Замовника перед Видавцем періодичних наукових видань в частині надання послуг інформаційно-технологічного супроводження наукового рукопису Замовника (далі по тексту – Договір).

ОСНОВНІ ТЕРМІНИ І ВИЗНАЧЕННЯ

Рукопис – наукова стаття, яка запропонована для опублікування у Виданні до моменту прийняття до публікації;

Твір – наукова стаття, яка пройшла повний Регламент інформаційно-технологічного супроводження та яка готова до опублікування чи опублікована Видавцем у Виданні;

Періодичне наукове видання – журнал або інше періодичне видання наукового змісту, яке має власний міжнародний номер ISSN;

Видавничий процес – сукупність усіх робіт по перетворенню Рукопису в Твір;

Регламент видавничого процесу – порядок та умови виконання видавничого процесу, визначений Видавцем;

Регламент інформаційно-технологічного супроводження – сукупність усіх робіт, передбачених видавничим процесом, регламентованим Видавцем, зокрема редагування, перекладу Рукопису англійською чи перевірки наданого англомовного варіанту Рукопису, підготовки графічних зображень, оформлення таблиць та формул, оформлення літератури згідно до обраного Видавцем стандарту тощо (додрукарська підготовка рукопису до публікації), оплати відповідних послуг для подальшого опублікування Твору за умови виконання вимог прийняття до публікації;

Прийняття до публікації – успішно завершений процес розгляду Рукопису, що базується на висновку редакції щодо можливості опублікування після перетворення Рукопису в Твір, за умови позитивної рекомендації рецензентів та реалізації у повному обсязі Регламенту видавничого процесу;

Публікація – оприлюднення результатів наукових досліджень у Періодичному науковому виданні в Електронних ресурсах наукового спрямування в електронному варіанті та/чи друкованому варіанті у вигляді Твору, за умови виконання повного Регламенту

AGREEMENT № 29/102-c10-2026

for the provision of information and technological support services of a scientific manuscript

Kharkiv, Ukraine

20/02/2026 p

A person, non-resident of Ukraine *Suwandono Purbo* acts on behalf of all co-authors *Purbo Suwandono, Widya Wijayanti, Nova Risdiyanto Ismail, Dzulfikar Johan Akbar, Muhammad Reza* one party, hereafter referred to as "Customer", and TECHNOLOGY CENTER GROUP LTD, represented by Director, Olena Domina, acting on the basis of the Charter, hereafter referred to as "Contractor", concluded this Agreement on the Contractor's representation of the Customer's interests before the Publisher of periodical s cientific publications in terms of providing information and technological support services to the Customer's scientific manuscript (hereinafter referred to as the Agreement).

BASIC TERMS AND DEFINITIONS

Manuscript is a scientific paper that is proposed for publication in the Publication until acceptance for publication;

Work is a scientific paper that has passed the full Regulations on information and technological support and which is ready for publication or published by the Publisher in the Publication;

Periodical scientific publication is a journal or other periodical of scientific content, which has its international number ISSN;

Publishing process is a set of all activities on the transformation of the Manuscript into a Work;

Regulations of the publishing process are the procedure and conditions for executing the publishing process determined by the Publisher*;*

Regulations of information and technological support is a set of all activities included in the publishing process regulated by the Publisher, in particular editing, translating the Manuscript into English or checking the English version of the Manuscript provided, preparing graphic images, drawing up tables and formulas, reference materials submitted in accordance with the standard chosen by the Publisher, etc. (prepress preparation of the manuscript for publication), payment for the relevant services for further publication of the Work, subject to compliance with acceptance requirements for publication;

Acceptance for publication is a successfully completed process of consideration of the Manuscript, based on the conclusion by the editorial board on the possibility of publication after the transformation of the Manuscript into the Work, subject to a positive recommendation from reviewers and the implementation in full of the Rules of publishing;

Publication is the publication of the results of scientific research in the Periodical scientific publication on electronic resources of scientific direction in electronic version and/or printed version in the form of a Work, subject to the implementation of the full Regulations of

видавничого процесу та Прийняття до публікації, та за наявності метаданих та DOI;
Електронний ресурс наукового спрямування – електронний ресурс, на сайті якого наведена інформація про наукові видання. Такими ресурсами можуть бути електронні бази даних, наукометричні бази даних, репозитарії, каталоги, бібліотеки, сайти Видавця.
Метадані – фрагмент бази даних, який містить блок описових даних про Твір.
DOI (від англ. *digital object identifier*) – цифровий ідентифікатор для унікального об'єкта інтелектуальної власності, який надається опублікованому документу і не залежить від місця його знаходження. DOI є унікальною алфавітно-цифровою послідовністю (літери латинські, великі і малі літери не розрізняються). Складається з двох частин (Префіксу DOI та Суфіксу DOI) і має вигляд 10.pppp/ssssss, де 10.pppp – префікс DOI, а ssssss – суфікс DOI.
DOI ® є зареєстрованим товарним знаком фонду International DOI Foundation.
Видавець – фізична чи юридична особа, яка є видавцем або видавничою організацією у термінах Закону України "Про видавничу справу" (№318/97-ВР від 05.06.1997 р.), здійснює видання Творів наукового змісту, в тому числі на електронних носіях;
Редакція – підрозділ Видавця, який має повноваження здійснювати усі необхідні дії щодо окремого періодичного наукового видання, відповідає за коректність, актуальність і достовірність даних, які представляються на веб-сайті періодичного наукового видання;
Автор – фізична особа, яка своєю творчою працею створила Рукопис;
Співавтори – особи, спільною творчою працею яких створено Рукопис.

1. Предмет договору

1.1. Предметом цього договору є надання Замовнику інформаційно-технологічного супроводження наукового рукопису *SYNGAS QUALITY IMPROVEMENT IN CORNCOB UPDRAFT GASIFICATION USING CAO/ACTIVATED CARBON PALM FIBER CATALYST* поданого для опублікування в періодичному науковому виданні Eastern-European Journal of Enterprise Technologies», (ISSN (print) 1729-3774, ISSN(on-line) 1729-4061, а також вчинення Виконавцем в інтересах Замовника усіх дій, передбачених Регламентом видавничого процесу Видавця.

1.2. Виконавець зобов'язується особисто, або із залученням третіх осіб, надати Замовнику послуги у визначеному цим договором і чинним законодавством порядку, а Замовник зобов'язується оплатити ці послуги.

2. Порядок надання послуг

2.1. Надання послуг та вчинення в інтересах Замовника усіх необхідних дій здійснюється у відповідності до необхідних термінів згідно Регламенту видавничого процесу, передбаченого політикою Видавця в періодичному науковому виданні, обраному Замовником.
2.2. Для надання послуг за цим договором Виконавець

the publishing process and acceptance for publication, and in the presence of metadata and DOI;
Electronic resource of scientific direction is an electronic resource whose website provides information about scientific publications. Such resources include electronic databases, scientometric databases, repositories, catalogs, libraries, Publisher websites.
Metadata are a fragment of the database that contains descriptive data about a Work.
DOI (Digital Object Identifier) is a digital identifier for a unique intellectual property object that is provided to a published document and does not depend on its location. DOI is a unique alphanumeric sequence (Latin letters, uppercase and lowercase letters do not differ). It consists of two parts (DOI prefix and DOI suffix) and takes the form 10.pppp/ssssss, where 10.pppp is the DOI prefix, and ssssss is the DOI suffix. DOI ® is a registered trademark of the International DOI Foundation.

Publisher is a person or a legal entity who/which is a publisher or a publishing organization in the terms of the Law of Ukraine "On Publishing" (No. 318/97-BP as of 05.06.1997) and publishes works of scientific content, including on electronic media;
Editorial office is a division of the Publisher, which has the authority to carry out all necessary activities in relation to a separate periodical scientific publication, and is responsible for the correctness, relevance, and reliability of the data provided on the website of the periodical;
Author is an individual who created the Manuscript by his/her creative work;
Co-authors are persons whose joint creative work produced the Manuscript.

1. Subject of Agreement

1.1. The subject of this agreement is to provide the Customer with information and technological support of a scientific manuscript *SYNGAS QUALITY IMPROVEMENT IN CORNCOB UPDRAFT GASIFICATION USING CAO/ACTIVATED CARBON PALM FIBER CATALYST* submitted for publication in a periodical scientific publication Eastern-European Journal of Enterprise Technologies», (ISSN (print) 1729-3774, ISSN(on-line) 1729-4061, as well as the Contractor's activities in the interests of the Customer provided for by the Publishing Process Regulations of the Publisher.
1.2. The Contractor undertakes to personally, or with the involvement of third parties, provide the Customer with services in accordance with the procedure established by this agreement and the current legislation, and the Customer undertakes to pay for these services.

2. The procedure for the provision of services

2.1. The provision of services and the execution of all necessary activities in the interests of the Customer is carried out in accordance with the necessary terms in accordance with the Rules of the publishing process provided for by the Publisher's policy in the periodical scientific publication chosen by the Customer.
2.2. To render services under this agreement, the

має право залучати (на свій розсуд і за рахунок своєї винагороди) третіх осіб.
2.3. Порядок, способи і методи надання послуг і вирішення конкретних завдань, методика здійснення діяльності Виконавця визначаються Виконавцем самостійно, а Замовник за необхідності залучається до доопрацювання рукопису.
2.4. Остаточний варіант рукопису узгоджується Замовником в термін не пізніше 5 днів з моменту надання Виконавцем Замовнику електронного варіанту рукопису, готового до передачі в редакцію Видавця.

3. Обов'язки та права сторін

3.1. Обов'язки та права Виконавця
3.1.1. Виконавець зобов'язаний надавати Замовнику всю інформацію про поточний стан виконання послуг за цим договором у формі усних звітів, а на вимогу Замовника – в письмовій формі.
3.1.2. Виконавець зобов'язаний своєчасно, не пізніше однієї доби, сповіщати Замовника про всі дії і заходи, в яких необхідна участь представників Замовника.
3.1.3. Виконавець зобов'язується повернути Замовнику в цілості й схоронності документацію, передану йому Замовником в рамках цього Договору.
3.1.4. Виконавець зобов'язується надати Замовнику рахунок на оплату за здійснення послуг інформаційно-технологічного супроводження наукового рукопису згідно п.4 Договору.
3.1.5. Виконавець має право вимагати від Замовника своєчасного надання необхідних документів та інформації, що стосується структури та змісту рукопису.
3.1.6. Виконавець має право на свій розсуд планувати конкретні заходи і дії в процесі виконання послуг за цим договором.
3.2. Обов'язки та права Замовника
3.2.1. Замовник зобов'язаний підписати Ліцензійний договір з Видавцем обраного періодичного наукового видання та надати Виконавцю скан-копію в термін не пізніше 3 діб з дати підписання цього договору.
3.2.2. Замовник зобов'язаний своєчасно оплачувати послуги Виконавця в порядку, визначеному цим договором.
3.2.3. Замовник зобов'язаний своєчасно надавати Виконавцю усе необхідне (документи, додаткові матеріали, що стосуються підтвердження результатів досліджень, що викладаються в рукописі, дорученнями і т.д.) для якісного та оперативного виконання своїх функцій.
3.2.4. Замовник зобов'язаний відшкодовувати Виконавцю всі витрати, пов'язані з виконанням доручень Замовника в рамках цього Договору (поточні витрати), але лише за їх наявності.
3.2.5. Замовник має право вимагати від Виконавця надання всієї необхідної інформації про хід надання послуг за цим Договором.

4. Розмір та порядок оплати послуг

4.1. Оплата здійснюється:

Contractor has the right to attract (at its discretion and at the expense of its remuneration) third parties.
2.3. The procedure, techniques, and methods of providing services and solving specific tasks, the methodology of the Contractor's activities are determined by the Contractor independently, and the Customer, if necessary, is involved in the revision of the manuscript.
2.4. The final version of the manuscript is agreed by the Customer within a period not later than 5 days from the date of submission by the Contractor to the Customer of an electronic version of the manuscript ready for transfer to the Publisher's editorial office.

3. Obligations and rights of the parties

3.1. Obligations and rights of the Contractor
3.1.1. The Contractor is obliged to provide the Customer with all information about the current state of execution of services under this contract in the form of oral reports, and, at the request of the Customer, in writing.
3.1.2. The Contractor is obliged to notify the Customer in a timely manner, no later than one day, of all actions and measures in which the participation of the Customer's representatives is necessary.
3.1.3. The Contractor undertakes to return to the Customer in entirety and safety the documents transmitted to him by the Customer within the framework of this Agreement.
3.1.4. The Contractor undertakes to provide the Customer with an invoice for payment for the implementation of information and technological support services of the scientific manuscript in accordance with chapter 4 of the Agreement.
3.1.5. The Contractor has the right to demand from the Customer the timely provision of the necessary documents and information relating to the structure and content of the manuscript.
3.1.6. The Contractor has the right, at its discretion, to plan specific measures and activities in the process of rendering services under this contract.
3.2. Obligations and rights of the Customer
3.2.1. The Customer is obliged to sign the License Agreement with the Publisher of the selected periodical scientific publication and provide the Contractor with a scanned copy within a period not later than 3 days from the date of signing this agreement.
3.2.2. The Customer is obliged to pay for the Contractor's services in a timely manner in the manner prescribed by this agreement.
3.2.3. The Customer is obliged to provide the Contractor with everything necessary in a timely manner (documents, additional materials relating to the confirmation of the results of research taught in the manuscript, instructions, etc.) for the qualitative and prompt execution of their functions.
3.2.4. The Customer is obliged to reimburse the Contractor for all costs associated with the execution of the Customer's orders under this Agreement (current expenses), but only if any.
3.2.5. The Customer has the right to require the Contractor to provide all necessary information on the progress of the provision of services under this Agreement.

4. The amount and procedure for payment for services

4.1. Payment is effected:

– за додрукарську підготовку – в термін не пізніше двох днів з моменту підписання цього Договору,
– за послуги інформаційно-технологічного супроводження наукового рукопису в разі прийняття рукопису до публікації в термін не пізніше 3 робочих днів з моменту отримання електронного листа на адресу Виконавця від редакції з позитивним рішенням щодо можливості опублікування.

В разі, якщо рукопис відхилений редакцією, відкликання автором (авторами) рукопису з власної ініціативи до моменту його прийняття до публікації, відмови автора (авторів) вносити виправлення, спрямовані на усунення невідповідності вимог рукопису за структурою та змістом статті вимогам обраного Замовником періодичного наукового видання, оплата за додрукарську підготовку не повертається та покриває послуги додрукарської підготовки. В разі, якщо рукопис приймається редакцією, сума оплати за додрукарську підготовку враховується як аванс за послуги інформаційно-технологічного супроводження.

4.2. Фактом виконання робіт та надання послуг в повному обсязі, їх прийняття є прийняття рукопису до опублікування, про що Виконавець направляє лист на електронну пошту Замовника. Цей лист одночасно є Актом наданих послуг.
4.3. Оплата послуг Виконавця за цим договором здійснюється Замовником на підставі рахунків Виконавця.

5. Відповідальність сторін

5.1. За порушення зобов'язань за цим Договором, сторони несуть відповідальність відповідно до чинного законодавства України.
5.2. Виконавець звільняється від відповідальності за невиконання або неналежне виконання своїх зобов'язань за договором, якщо причиною цьому послужила прострочення виконання або невиконання Замовником зобов'язань, визначених у пп.3.2.1.–3.2.4. цього Договору.

5.3. У разі порушення Замовником умов оплати, визначених в п. 4.1 Договору, Виконавець повідомляє редакцію наукового видання про порушення Замовником умов цього Договору та зупиняє будь-які дії з Рукописом, щодо якого здійснювалося інформаційно-технологічне супроводження, до моменту здійснення Замовником відповідної оплати. Виконавець не несе відповідальності за будь-які подальші рішення або дії редакції, що виникли внаслідок такого повідомлення.

6. Форс-мажор

6.1. Сторони звільняються від відповідальності за невиконання або неналежне виконання зобов'язань за цим Договором, якщо це невиконання стало наслідком обставин непереборної сили, що виникли після укладання Договору в результаті подій надзвичайного характеру, які Сторона не могла не передбачати не запобігти розумними заходами.

– for pre-printing preparation – within a period not later than two days from the date of signing this Agreement,
– for the services of information and technological support of the scientific manuscript in the case of acceptance of the manuscript for publication within a period not later than 3 working days from the date of receipt of the e-mail to the Contractor from the editorial office with a positive decision on the possibility of publication.
In the event that the manuscript is rejected by the editorial board, the author(s) withdraw the manuscript on their own initiative before it is accepted for publication, or the author(s) refuse to make corrections aimed at eliminating the inconsistency of the manuscript requirements for the structure and content of the article with the requirements of the periodical scientific publication chosen by the Customer, the payment for pre-print preparation is not refunded and covers the prepress services. If the manuscript is accepted by the editorial board, the amount of payment for prepress services is taken into account as an advance payment for the services of information and technological support.
4.2. The fact of performing the work and providing the services in full, their acceptance is the acceptance of the manuscript for publication, about which the Contractor sends a letter to the Customer's email. This letter is also an Act of the services provided.
4.3. Payment for the Contractor's services under this agreement is made by the Customer based on the Contractor's invoices.

5. Responsibility of the parties

5.1. For violation of obligations under this Agreement, the parties are liable in accordance with the current legislation of Ukraine.
5.2. The Contractor shall be released from liability for non-fulfillment or improper performance of its obligations under the contract if the reason for this was the delay in the fulfillment or non-fulfillment by the Customer of the obligations specified in chapters 3.2.1.–3.2.4 of this Agreement.
5.3. In the event of a violation by the Customer of the payment terms specified in clause 4.1 of the Agreement, the Contractor shall notify the editorial office of the scientific publication of the Customer's violation of the terms of this Agreement and shall suspend any actions with the Manuscript for which information and technological support was provided until the Customer makes the appropriate payment. The Contractor shall not be liable for any further decisions or actions of the editorial office resulting from such notification.

6. Force Majeure

6.1. The Parties shall be released from liability for non-fulfillment or improper performance of obligations under this Agreement if this non-fulfillment was the result of force majeure circumstances arising after the conclusion of the Treaty as a result of events of an extraordinary nature, which the Party could not but foresee not to prevent by reasonable measures.

6.2. До обставин непереборної сили відносяться події, на які Сторона не може вплинути й за виникнення яких не несе відповідальності, а саме: воєнні дії, стихійні лиха, громадські безладдя, що прямо перешкоджають Стороні або Сторонам виконанню обов'язків за цим Договором. Факт настання обставин форс – мажору повинен бути підтверджений висновком Торгівельно-промислової палати України.

6.3. Сторона, для якої створилася неможливість виконання зобов'язання за цим Договором, повинна на протязі трьох робочих днів в письмовій формі сповістити іншу Сторону про дату припинення зобов'язань у зв'язку з настанням обставини непереборної сили й про передбачувану дату припинення даних обставин.

6.4. Якщо невиконання зобов'язань за цим Договором триває більше двох місяців, то кожна Сторона має право розірвати даний Договір в односторонньому порядку, сповістивши про це іншу Сторону.

7. Термін дії договору

7.1. Цей договір діє з моменту його підписання до моменту прийняття рукопису до публікації чи відмови в публікації з боку редакції.

8. Зміна і розірвання договору

8.1. Кожна зі сторін має право в будь-який час відмовитися від договору в порядку визначеному чинним законодавством України. У разі відмови від договору з ініціативи Замовника, він зобов'язаний оплатити послуги, пропорційно виконаному обсягу на момент розірвання договору, а також оплатити фактично понесені Виконавцем на момент розірвання витрати. До складу фактичних витрат включаються витрати Виконавця по виплаті винагород третім особам, залученим їм в якості субпідрядників в рамках надання послуг за цим договором. У разі односторонньої відмови від виконання договору Виконавцем він відшкодовує Замовнику збитки в повному обсязі.

8.2. Всі зміни і доповнення цього договору повинні оформлятися письмово.

9. Прикінцеві положення

9.1. Цей договір складено двома мовами (українська та англійська) в двох примірниках, які мають однакову силу, по одному примірнику для кожної сторони.

9.2. Договір набирає законної сили з моменту його підписання сторонами.

9.3. У всіх інших питаннях, що не врегульовані цим Договором, сторони керуються чинним законодавством України.

9.4. Замовник надає Виконавцю право використовувати дані, які потрібні для виконання ним умов цього Договору та затребувані Видавцем для публікації Твору в друкований та/чи електронний спосіб та розміщення Твору в електронних ресурсах наукового спрямування. Зокрема до них відносяться усі необхідні метадані, ORCID, інформація для зв'язку з автором (співавторами) з боку зацікавлених читачів для можливого налагодження професійних зв'язків та створення сумісних науково-дослідницьких колективів.

6.2. Force majeure circumstances include events which a Party cannot influence and for the occurrence of which is not responsible, namely: military actions, natural disasters, public disorders that directly impede the Party or the Parties from fulfilling the obligations under this Agreement. The fact of occurrence of force majeure circumstances must be confirmed by the conclusion of the Chamber of Commerce and Industry of Ukraine.

6.3. The Party for which the impossibility of fulfilling the obligation under this Agreement has been created shall notify the other Party within three working days in writing of the date of termination of obligations in connection with the occurrence of a force majeure circumstance and the expected date of termination of these circumstances.

6.4. If the non-fulfillment of obligations under this Agreement lasts more than two months, each Party has the right to terminate this Agreement unilaterally by notifying the other Party.

7. Term of Agreement

7.1. This agreement is valid from the moment of its signing until the acceptance of the manuscript to the publication or refusal to publish by the editorial board.

8. Change and Termination of Agreement

8.1. Each party has the right at any time to withdraw from the contract in accordance with the procedure established by the current legislation of Ukraine. In the case of refusal of the contract at the initiative of the Customer, he is obliged to pay for services in proportion to the amount performed at the time of termination of the contract, as well as to pay the costs actually incurred by the Contractor at the time of termination. The actual expenses include the Contractor's expenses for the payment of remuneration to third parties involved in them as subcontractors in the framework of the provision of services under this agreement. In the case of unilateral refusal to execute the contract by the Contractor, he reimburses the Customer for losses in full.

8.2. All changes and additions to this agreement must be made in writing.

9. Final provisions

9.1. This agreement is drawn up in two languages (Ukrainian and English) in two copies, which have the same force, one copy for each party.

9.2. The agreement comes into force from the moment of its signing by the parties.

9.3. In all other matters not regulated by this Agreement, the parties are guided by the current legislation of Ukraine.

9.4. The Customer grants the Contractor the right to use the data necessary for the fulfillment of the terms of this Agreement and are requested by the Publisher for the publication of the Work in a printed and/or electronic way and the placement of the Work in electronic scientific resources. In particular, these include all the necessary metadata, ORCID, information for communication with the author (co-authors) from interested readers for the possible establishment of professional connections and for setting up compatible research teams.

9.5. Відносно цього Договору і будь-яких відомостей, наданих у зв'язку з цим Договором та помічених як конфіденційні, їх одержувач зобов'язується:
(А) зберігати конфіденційність відомостей обґрунтованим і адекватним чином або відповідно до професійних нормами; (Б) використовувати конфіденційні відомості тільки з метою виконання зобов'язань за цим Договором; і (в) відтворювати конфіденційні відомості тільки в разі потреби для виконання своїх зобов'язань за цим Договором.
9.6 Положення п.п. 9.5. не застосовується до відомостей, які:
(А) є загальновідомими;
(Б) вже відомі одній зі сторін на неконфіденційної основі від іншого джерела, ніж інша сторона;
9.7 Виконавець має право розкривати конфіденційні відомості державним органам, уповноваженим запитувати такі відомості відповідно до чинного законодавства України, на підставі належним чином оформленого запиту на надання таких відомостей, при цьому Виконавець не несе відповідальності за таке розкриття.
9.8. З урахуванням дотримання обмежень, які стосуються конфіденційності, Виконавець має право надавати аналогічні послуги будь-яким третім особам, навіть якщо такі особи конкурують з Замовником, за умови, що в разі, якщо Замовник направив Виконавцю попереднє письмове повідомлення про обставини, потенційно викликають конфлікт інтересів, Виконавець або отримує від обох сторін підтвердження про відсутність конфлікту (причому надання такого підтвердження не повинно необґрунтовано затримуватися або відхилятися), або утримується від надання послуг (або частин послуг) тільки щодо таких обставин.

9.5. With respect to this Agreement and any information provided in connection with this Agreement and marked as confidential, their recipient undertakes:
(A) maintain the confidentiality of information in a reasonable and adequate manner or in accordance with professional standards; (B) use confidential information only for the purpose of fulfilling the obligations under this Agreement; and (C) reproduce confidential information only if necessary to fulfill its obligations under this Agreement.
9.6. Chapter 9.5. does not apply to information that:
(A) is well-known;
(B) is already known to one of the parties on a non-confidential basis from a source other than the other party;
9.7. The Contractor has the right to disclose confidential information to state authorities authorized to request such information in accordance with the current legislation of Ukraine, based on a duly executed request for such information, while the Contractor is not responsible for such disclosure.
9.8. Subject to confidentiality restrictions, the Contractor has the right to provide similar services to any third parties, even if such persons compete with the Customer, provided that if the Customer has sent the Contractor a preliminary written notice of the circumstances that potentially cause a conflict of interest, the Contractor either receives confirmation from both parties of the absence of a conflict (and the provision of such confirmation should not unreasonably be delayed or refrains from providing services (or parts of services) only with respect to such circumstances.

10. Реквізити сторін

Виконавець
ТОВ «ТЕХНОЛОГІЧНИЙ ЦЕНТР ГРУП »
Адреса: вул. Шатилова Дача, буд.4, м. Харків, 61165
Bank information:
Beneficiary: **TECHNOLOGY CENTER GROUP LTD**
IBAN: UA943052990000026009025905645
Beneficiary's bank: JSC CB "PRIVATBANK",
Bank Adress: 1D HRUSHEVSKOHO STR., KYIV, 01001, UKRAINE
SWIFT code : PBANUA2X

BY:
Дьоміна О. Б / Olena Domina
Директор/ Director
Date signed: 20/02/2026

10. Details of Parties

Contractor
TECHNOLOGY CENTER GROUP LTD
Address: 4 Shatilova Dacha Street, Kharkov, Ukraine, 61165

TECHNOLOGY CENTER GROUP LTD
ТОВ "ТЕХНОЛОГІЧНИЙ ЦЕНТР ГРУП" №44446240
UKRAINE • KHARKIV

Замовник /Customer

Suwandono Purbo
Department of Mechanical Engineering
Widya Gama University
Borobudur Street No. 35, Mojolangu, Lowokwaru District, Malang City, East Java, Indonesia, 65142
E-mail: purbo@widyagama.ac.id
Contact phone: +6282132697144

BY: _____

Фізична особа/ Person
Date signed: 20/02/2026

signature

Purbo Suwandono

Widya Wijayanti

Nova Risdiyanto Ismail

Dzulfikar Johan Akbar

Muhammad Reza

Cover Letter

[Purbo Suwandono, Widya Wijayanti, Nova Risdiyanto Ismail, Dzulfikar Johan Akbar, Muhammad Reza]
[Universitas Widyagama Malang]
[Borobudur Street No.35, Mojolangu, Lowokwaru, Malang City, East Java, Indonesia]

[02.20.2026]
To the Editor of the Eastern-European Journal of Enterprise Technologies

I, Purbo Suwandono, confirm that I have been familiarized with the authorship identification policy and act on behalf of the entire author team on any issues of interaction with the editorial office, and am also responsible for ensuring that all agreements are reached regarding the Publisher's regulations on converting a manuscript into an article and its subsequent publication, as well as at the stage after publication of the article, if such a need arises.

We are sending for consideration for publication the original scientific and research manuscript " SYNGAS QUALITY IMPROVEMENT IN CORNCOB UPDRAFT GASIFICATION USING CAO/ACTIVATED CARBON PALM FIBER CATALYST" of the authors Purbo Suwandono, Widya Wijayanti, Nova Risdiyanto Ismail, Dzulfikar Johan Akbar, Muhammad Reza.

All authors have read and approved this version of the manuscript. The authors confirm that this manuscript (as well as its parts) is original and has not been previously published, and has not been sent for consideration to other journals.

In this article, the authors consider the improvement of syngas quality from corncob updraft gasification using a dual-synergy CaO and palm-fiber-derived activated carbon (AC-PF) catalyst system. This is important because the introduction of this hybrid catalyst into the gasification process significantly alters the dominant reaction pathways and kinetics of volatile cracking, tar reforming, and CO_2 capture. However, there are objective difficulties associated with determining the optimal catalyst composition and loading in the system, because there is still uncertainty regarding the non-linear synergistic effects of CaO and AC-PF on pore structure evolution, gas–solid contact, and secondary reaction selectivity during biomass gasification..

The authors believe that this manuscript is suitable for publication in the "Technology audit and production reserves" journal, because within the framework of the research described in this article, the mechanisms governing syngas quality enhancement through catalyst-assisted corncob updraft gasification have been systematically investigated. This allows a rational approach to determining the optimal catalyst composition and operating conditions to obtain targeted improvements in syngas composition and energy performance. In particular, the productivity and efficiency of biomass gasification processes can be improved while operational costs and downstream gas-cleaning requirements can be reduced.
This article meets the goals and objectives of the journal, because it contains materials of a completed scientific research in the field of thermochemical biomass conversion and catalytic materials engineering related to the determination of syngas formation and upgrading mechanisms. The results obtained in the article provide a sound basis for potential implementation in real industrial biomass-to-energy and syngas upgrading processes.
The scientific novelty of this study is as follows. Usually, in conventional updraft gasification systems, single-function catalysts or inert bed materials are used. However, the application of such components is often effective only within limited temperature windows and gas–solid contact conditions. When attempting to intensify the process to further enhance syngas quality

and hydrogen enrichment, objective difficulties arise due to uncertainties in dominant reaction pathways and mass-transfer limitations governing syngas formation and upgrading under updraft gasification conditions. Within the framework of the study described in this article, an approach for overcoming these difficulties is proposed. It is based on the synergistic integration of CaO as an in-situ CO_2 sorbent with palm-fiber-derived activated carbon as a porous reforming and tar-cracking catalyst. This approach enables the establishment of a more stable and effective catalytic environment under high-temperature gasification conditions. This means that the obtained scientific results, in the form of a mechanistic interpretation of syngas formation and upgrading pathways, are of clear theoretical interest. From a practical point of view, the identified synergistic mechanism enables the determination of suitable operating conditions and catalyst formulations for application in practical biomass gasification systems. Thus, the applied significance of the obtained scientific results lies in the potential to improve typical biomass-to-syngas technological processes in terms of gas quality, energy efficiency, and operational stability. This creates the prerequisites for transferring the proposed technological solutions to pilot-scale and industrial biomass gasification applications.

The authors Purbo Suwandono, Widya Wijayanti, Nova Risdiyanto Ismail, Dzulfikar Johan Akbar, Muhammad Reza, submitting the manuscript for consideration for publication in the "Technology audit and production reserves" journal, confirm that they are familiar with and agree with all the requirements for the design, submission of the manuscript of the article, payment, the Main Provisions of the Publishing Policy, the Editorial Policy and bear full responsibility in case of violation of these requirements.

The authors propose the following reviewers:

Muji Setiyo
Prof. Dr. ST., MT.
Mechanical Engineering
Universitas Muhammadiyah Magelang
Tidar Street No.21, Magersari, Magelang City, Central Java, Indonesia
E-mail: setiyo.muji@ummgl.ac.id
Contact tel.: +6281328648046
ORCID: http://orcid.org/0000-0002-6582-5340

Nurkholis Hamidi
Prof. Dr. Eng. ST., M. Eng.
Mechanical Engineering
Universitas Brawijaya
Veteran Street No.10-11, Ketawanggede, Lowokwaru, Malang City, East Java, Indonesia
E-mail: hamidy@ub.ac.id
Contact tel.: +6281259293165
ORCID: https://orcid.org/0000-0003-2910-2353

Please direct all correspondence regarding this manuscript to the corresponding author Purbo Suwandono at the address purbo@widyagama.ac.id

Thank you for considering this manuscript.
Sincerely,
Purbo Suwandono

Ліцензійний договір / License Agreement № 29/2-2026
про надання невиключної ліцензії на використання Твору /
on granting a non-exclusive license to use the Work

м. Харків, Україна / Kharkiv, Ukraine '20" 02 2026 р.

Purbo Suwandono, Widya Wijayanti, Nova Risdiyanto Ismail, Dzulfikar Johan Akbar, Muhammad Reza

(П.І.Б. автора, співавторів) / (Full name, Author, Co-authors)

(що надалі іменується Ліцензіар (Ліцензіари)) з одного боку та Видавець ПРИВАТНЕ ПІДПРИЄМСТВО «ТЕХНОЛОГІЧНИЙ ЦЕНТР» в особі директора Дьоміна Дмитра Олександровича, що діє на підставі Статуту (надалі іменується Ліцензіат), уклали даний договір про таке:

(hereinafter referred to as Licensor (Licensors)), and the Publisher, TECHNOLOGY CENTER PRIVATE COMPANY, represented by Director Dmytro Domin, acting on the basis of the Charter (hereinafter referred to as Licensee), concluded this Agreement on the following:

Визначення термінів

Терміни, що використовуються в цьому Договорі, вживаються у такому значенні:

Ліцензіар – автор (співавтори);

Ліцензіат – видавець;

Автор – фізична особа, яка своєю творчою працею створила Рукопис;

Співавтори – особи, спільною творчою працею яких створено Рукопис;

Рукопис – наукова стаття, редакція якої схвалена всіма авторами/співавторами, яка запропонована Ліцензіаром для опублікування у Виданні до моменту прийняття до публікації;

Видання – «Eastern-European Journal of Enterprise Technologies» ISSN (print) 1729-3774, ISSN (on-line) 1729-4061;

Регламент – сукупність усіх робіт, передбачених видавничим технологічним процесом, включно з процедурами подвійного сліпого рецензування, редагування, перекладу Рукопису англійською чи перевірки наданого англомовного варіанту Рукопису, для подальшого опублікування Твору за умови виконання вимог прийняття до публікації;

Твір – наукова стаття, яка пройшла повний Регламент та яка готова до опублікування чи опублікована Ліцензіатом у Виданні;

Прийняття до публікації – успішно завершений процес розгляду Рукопису, що базується на висновку редакції щодо можливості опублікування після перетворення Рукопису в Твір, за умови позитивної рекомендації рецензентів;

Авторське право – право на оригінальний результат у вигляді продукту творчої діяльності, існуючого в об'єктивній формі як повний Рукопис / Твір чи певна його частина. Такий продукт є оригінальним, якщо він є результатом інтелектуальної творчості автора (співавторів);

Невиключне право на використання твору – право використовувати Твір певним способом і у межах, встановлених даним Договором, що передається Ліцензіаром Ліцензіату. При цьому за Ліцензіаром, який передає невиключне право, зберігається право на використання твору і на передачу невиключного права

Definition of terms

The terms used in this Agreement are used in the following meaning:

Licensor: Author (Co-authors);

Licensee: Publisher;

Author: an individual who created the Manuscript with his/her creative work;

Co-authors: persons whose joint creative work produced a Manuscript;

Manuscript: is a scientific article, the editing of which is approved by all authors/co-authors, which is proposed by the Licensor for publication by the Publisher before the moment of acceptance for publication;

Journal: "Eastern-European Journal of Enterprise Technologies" ISSN (print) 1729-3774, ISSN (on-line) 1729-4061;

Regulation: a set of all activities implied by the publishing technological process, including procedures of double blind peer review, editing, translating the Manuscript into English or checking the provided English version of the Manuscript, for further publication of the Work, subject to the requirements of acceptance for publication;

Work: a scientific paper that fully complies with Regulation and which is ready for publication or published by Licensee in Journal;

Acceptance for publication: a successfully completed process of consideration of the Manuscript, based on the conclusion by the editorial board on the possibility of publication after the transformation of the Manuscript into a Work, subject to a positive recommendation from reviewers;

Copyright: the right to the original result in the form of a product of the creative activity, existing in an objective form as a complete Manuscript / Work, or a certain part of it. Such a product is original if it is the result of the intellectual creativity of the author (co-authors);

Non-exclusive right to use the work: the right to use a Work in a certain way and within the limits established by this Agreement, transferred by Licensor to Licensor. At the same time, the Licensor that transfers a non-exclusive right retains the right to use the work and to transfer the non-exclusive right to use the work to other persons;

Представник ліцензіарів Representative of licensors Suwandono Purbo

Підпис Signature

на використання твору іншим особам; Виключне право на використання твору – право дозволяти використання Твору і право перешкоджати неправомірному використанню Твору, у тому числі забороняти таке використання;

Creative Commons CC BY – міжнародна публічна ліцензія;

COPE – комітет з етики публікацій. Детальніше про комітет тут – https://publicationethics.org/.

Інші терміни, що використовуються в Договорі, визначаються згідно з нормами чинного законодавства України.

1. Предмет договору

1.1. Ліцензіар на весь час дії майнових авторських прав безоплатно передає Ліцензіату невиключну Ліцензію на використання Рукопису, викладеного англійською мовою з робочою назвою

Exclusive right to use the work: the right to allow the use of the Work and the right to impede the misuse of the Work, including prohibiting such use;

Creative Commons CC BY: an international public license.

COPE: publication ethics committee. Read more about the Committee at https://publicationethics.org/

Other terms used in the Agreement are determined in accordance with the norms of the acting legislation of Ukraine.

1. Subject of the Agreement

1.1. Licensor grants a non-exclusive License to use the Manuscript, written in English, with a working title

SYNGAS QUALITY IMPROVEMENT IN CORNCOB UPDRAFT GASIFICATION USING CAO/ACTIVATED CARBON PALM FIBER CATALYST

Purbo Suwandono, Widya Wijayanti, Nova Risdiyanto Ismail, Dzulfikar Johan Akbar, Muhammad Reza

під авторством / authored by

1.2 Ліцензіат виконує видавничий процес в повному обсязі відповідно до Регламенту для перетворення Рукопису в Твір, викладений англійською мовою та прийняття Твору до публікації та опублікування у Виданні.

1.3. За цим договором Ліцензіар на весь час діх майнових авторських прав надає Ліцензіату дозвіл на використання Твору на веб-сторінках Видавництва та інших Інтернет-ресурсах на умовах публічної ліцензії *Creative Commons* CC BY.

2. Запевнення та Гарантії Ліцензіара та Ліцензіата

2.1. Ліцензіар гарантує, що володіє усіма авторськими правами на Рукопис, вказаний в п. 1.1. цього Договору на момент надання Ліцензії Ліцензіату та не порушував авторських прав інших осіб, переданий Ліцензіату Рукопис не містить плагіату, незаконного використання інформації, в тому числі у вигляді перекладу інформації без дозволу її автора.

2.2. Ліцензіар гарантує, що:

– він є автором (співавтором) Рукопису / Твору;

– авторські права на Рукопис / Твір не передавались раніше третім особам;

– на момент укладення Договору права Ліцензіара на Рукопис / Твір не оскаржені, не закладені, не надані за ліцензійними договорами іншим особам;

– Рукопис / Твір не переданий іншим особам;

– Рукопис / Твір не були раніше опубліковані у будь-якому іншому виданні до публікації його Ліцензіатом;

– він не порушив права інтелектуальної власності інших осіб. Якщо в Рукопису / Творі наведені матеріали інших осіб, за виключенням випадків цитування в обсязі, виправданому науковим, інформаційним або критичним характером Рукопису / Твору, використання таких матеріалів здійснюється Ліцензіаром з дотриманням норм законодавства;

– він отримав усі необхідні дозволи на використання результатів, фактів та інших перейнятих матеріалів, правовласником яких він є;

1.2. The Licensee executes the publishing process in full in accordance with the Regulations in order to convert the Manuscript into a Work set forth in the English language and accept the Work for publication and publish it in the Journal.

1.3. Under this agreement, the Licensor for the entire duration of the proprietary copyright grants the Licensee permission to use the Work at the web pages of the Publisher and other Internet resources under the terms of the Creative Commons CC BY.

2. Assurances and Guarantees of Licensor and Licensee

2.1. Licensor guarantees that s/he owns all copyrights to the Manuscript specified in p. 1.1. of this Agreement at the time of granting the Licensee and did not violate the copyright of other persons; the Manuscript transferred to the Licensee does not contain plagiarism, illegal use of information, including in the form of translation of information without the permission of his/her author.

2.2. Licensor guarantees that:

– s/he is the author (co-author) of the Manuscript / Work;

– the copyright to the Manuscript / Work was not previously transferred to third parties;

– at the time of conclusion of the Agreement, Licensor's rights to the Manuscript / Work are not disputed, not pledged, not granted under license agreements to other persons;

– the Manuscript / Work was not transferred to other persons;

– the Manuscript/ Work was not previously published in any other publication before its publication by Licensee;

– s/he did not infringe the intellectual property rights of others. If the Manuscript / Works contains materials by other persons, except for cases of citation to the extent justified by the scientific, informational, or critical nature of the Manuscript / Work, such materials are used by the Licensor in compliance with the norms of the law;

– s/he received all the necessary permits to use the results, facts, and other adopted materials, the right holder of which is not her/him;

Представник ліцензіарів
Representative of licensors Suwandono Purbo

Підпис
Signature

– Рукопис / Твір не містить відомості, заборонені до відкритої публікації згадно чинного законодавства України та його друк і/або розповсюдження Ліцензіатом не призведуть до розголошення секретної (конфеденційної) інформації (включаючи державну, службову таємницю);

– Рукопис / Твір не будуть опубліковані у будь-якому іншому виданні до публікації його Ліцензіатом.

2.3. Ліцензіар гарантує, що Рукопис/Твір не містить фальсифіковані, сфабриковані дані та/або маніпуляцію із даними.

2.4. Ліцензіар гарантує, що Відомості про автора (співавторів) Рукопису є достовірними та подані в повному обсязі згідно п. 14 «Вимоги до оформлення статті» (посилання).

2.5. Ліцензіат гарантує, що в разі відмови в опублікуванні Рукопис не буде переданий іншим особам та видаляється, а зміст його не використовується

3. Майнові права, що передаються Ліцензіату

3.1. Ліцензіар надає Ліцензіату на весь строк дій майнових авторських прав на Рукопис наступні права**:**

3.1.1. право переробляти, адаптувати, редагувати або іншим чином змінювати Рукопис без порушення суті змісту, задля забезпечення виконання в повному обсязі Регламенту для перетворення Рукопису в Твір;

3.1.2. право перекладати Рукопис у випадку, коли Рукопис викладений мовою іншою, ніж мова, якою передбачена публікація у Виданні, або виконувати перевірку якості англомовного варіанту Рукопису, якщо його подано англійською мовою, та, за необхідності, переробляти, адаптувати, редагувати або іншим чином змінювати Рукопис без порушення суті змісту, задля забезпечення виконання в повному обсязі Регламенту для перетворення Рукопису в Твір;

3.1.3. право на зміну робочої назви Рукопису на остаточну, яка публікується у Виданні;

3.1.4. право на розміщення електронного варіанту Рукопису, після прийняття його до опублікування, мовою оригіналу на веб-сторінках журналу з водяним знаком «For reading only. Not a reprint».

3.2. Ліцензіар надає Ліцензіату на весь строк дій майнових авторських прав на Твір наступні права:

3.2.1. право на відтворення Твору: опублікування у Виданні англійською мовою, оприлюднення, дублювання, тиражування або інше розмноження Твору без обмеження тиражу примірників. При цьому кожен екземпляр Твору повинен містити ім’я (імена) Ліцензіара;

3.2.2. право на використання Твору під комерційним найменуванням та/або торговою маркою Ліцензіата із зазначенням знаку охорони авторського права;

3.2.3. право на розповсюдження Твору будь-яким способом, включаючи сайти Ліцензіата, будь-які світові бази даних, в тому числі наукометричні, агрегатори баз даних, бібліотеки, репозиторії та інші Інтернет-ресурси, що відносяться до наукової або науково-прикладної сфери, а також будь-яким іншим не забороненим законом способом без обмеження території;

3.2.4. право на включення Твору чи його частин до Видання, збірок, довідників, електронних довідників;

3.2.5. право на доведення до загального відома, у т.ч. розміщення Твору повністю або частково в мережі

– the Manuscript / Work does not contain information prohibited for open publication in accordance with the acting legislation of Ukraine and its printing and/or dissemination by the Licensee will not lead to the disclosure of classified (confidential) information (including state, official secrets);

– the Manuscript / Work will not be published in any other publication prior to its publication by the Licensee;

2.3. Licensor guarantees that the Manuscript / Work does not contain falsified, fabricated data and/or data manipulation

2.4. Licensor guarantees that Information about the author (co-authors) of the Manuscript is reliable and submitted in full in accordance with p. 14 "Requirments for article forming" (link).

2.5. Licensee guarantees that in case of refusal to publish it, the Manuscript will not be transferred to other persons and will be deleted, and its content is not to be used by Licensee in any way.

3. Property rights transferred to Licensee

3.1. Licensor grants the Licensee the following rights to the Manuscript for the entire duration of the proprietary copyright:

3.1.1. the right to re-work, adapt, edit, or otherwise modify the Manuscript without violating the essence of the content, in order to ensure the full implementation of the Regulations for the conversion of the Manuscript into a Work;

3.1.2. the right to translate the Manuscript in the event that the Manuscript is written in a language other than the language implied for publication in the Journal, or to verify the quality of the English version of the Manuscript if submitted in English, and, if necessary, to re-work, adapt, edit, or otherwise modify the Manuscript without violating the essence of the content, in order to ensure the full implementation of the Regulations for the conversion of the Manuscript into a Work;

3.1.3. the right to change the working title of the Manuscript to the final one, which is published in the Journal;

3.1.4. the right to host an electronic version of the Manuscript, after its adoption for publication, in the original language on the web pages of the Journal, with a watermark "For reading only. Not a reprint».

3.2. Licensor grants the Licensee the following rights to the Work for the entire duration of the proprietary copyright:

3.2.1. the right to reproduce the Work: publish in the Journal in English, make public, duplicate, or reproduce the Work without limiting the circulation of copies. In this case, each copy of the Work must contain the name (names) of the Licensor;

3.2.2. the right to use the Work under the commercial title and/or trademark of Licensee indicating the copyright protection mark;

3.2.3. the right to distribute the Work in any way, including Licensee's websites, any global databases, including scientometric, database aggregators, libraries, repositories, and other Internet resources, related to the scientific or scientific and applied fields, as well as in any other non-prohibited way without the restriction of the territory;

3.2.4. the right to include the Work or its parts in the Journal, collections, references, electronic directories;

3.2.5. the right to draw general attention, including the placement of the Work in whole or in part on the Internet on

Інтернет на веб-сторінках журналу та інших інформаційних ресурсах;

3.2.6. право на експорт Твору;

3.2.7. право переробляти, адаптувати або іншим чином змінювати Твір без порушення суті змісту;

3.2.8. право перекладати Твір іншими мовами у випадку, коли цього вимагають дії, спрямовані на реалізацію заходів з поширення представленості Твору в світових ресурсах індексації наукового контенту;

3.2.9. право на використання метаданих (назва, ім'я автора (правовласника), анотації, бібліографічні матеріали, e-mail, робоча адреса тощо) Твору шляхом росповсюдження і доведення до загального відома, обробки та систематизації, а також включення в різні бази даних та інформаційні системи;

3.2.10. право на використання Твору на умовах публічної ліцензії Creative Commons Atribution у відкритому або закритому доступуі на некомерційній або комерційній основі на веб-сайтах Ліцензіата та інших Інтернет-ресурсах;

3.2.11. право розкривати будь-яку інформацію, яка розумно необхідна для забезпечення законності і захисту прав та інтересів залучених сторін, якщо цього вимагають обставини, відповідно до чинного законодавства, з метою захисту прав та інтересів користувачів Видання. або відповідно до юридичних запитів державних органів або відповідо до політики конфіденційності та авторських прав;

3.2.12. інші права, передбачені законом для даного виду договорів.

4. Права та обов'язки Ліцензіара та Ліцензіата

4.1 Права Ліцензіара

Ліцензіар має право використовувати Рукопис/Твір тільки після опублікування Твору Ліцензіатом, будь яким способом в межах закону, якщо обраний Лацензіаром спосіб використання Твору не порушує умов цього Договору.

4.2. Обов’язки Ліцензіара

4.2.1. Ліцензіар погоджується при поданні Рукопису до Видання Ліцензіата з усіма вимогами до оформлення, подачі Рукопису та оплати, що викладені на офіційному сайті Видання, та несе повну відповідальність у разі порушення цих вимог.

4.2.2. Ліцензіар зобов’язується не передавати Рукопис іншим видавцям, якщо його подано до Видання Ліцензіата до моменту опублікування Твору Ліцензіатом;

4.2.3. Ліцензіар зобов’язується при використанні Твору шляхом його переопублікування будь-якою мовою, поширення через будь-які ресурси, тощо вказувати усі дані, які в повному обсязі ідентифікують Ліцензіата як первинного володаря невиключних майнових прав на Твір та свідчать про факт первинного опублікування Твору у Виданні Ліцензіата.

4.2.4. Ліцензіар зобов’язується не використовувати Твір у випадку відмови з власної ініціативи публікувати Твір у Ліцензіата після затвердження Твору до публікації.

4.2.5. Ліцензіар зобов’язується відшкодувати витрати, пов’язані з підготовкою Рукопису до опублікування у вигляді Твору, якщо Ліцензіар з власної ініціативи відкликає Твір, прийнятий Ліцензіатом для

the web pages of the Journal, and other information resources;

3.2.6. the right to export the Work;

3.2.7. the right to rework, adapt, or otherwise modify the Work without violating the essence of the content;

3.2.8. the right to translate the Work into other languages if it is required by activities aimed at implementing measures to disseminate the representation of the Work in the global resources for indexing scientific content;

3.2.9. the right to use metadata (title, name of the author (copyright holder), abstracts, bibliographic materials, e-mail accounts, work address, etc.) of the Work by dissemination and bringing to general attention, processing, and systematization, as well as inclusion in various databases and information systems;

3.2.10. the right to use the Work under the terms of a Creative Commons Attribution Public License in open or closed access on a non-commercial or commercial basis on Licensee's websites and other Internet resources;

3.2.11. the right to disclose any information that is reasonably necessary to ensure the legality and protection of the rights and interests of the parties involved, if required by circumstances, in accordance with the current legislation, in order to protect the rights and interests of users of the Journal, or in accordance with legal requests by state authorities, or in accordance with the privacy and copyright policy;

3.2.12. other rights implied by law for this type of Agreements.

4. Rights and obligations of Licensor and Licensee

4.1. Licensor's rights

Licensor has the right to use the Manuscript/Work only after Licensee has published the Work, in any way, within the limits of the law, unless the method chosen by Licensor to use the Work does not violate the terms of this Agreement.

4.2. Responsibilities of Licensor

4.2.1. When submitting a Manuscript to the Licensee's Publication, the Licensor agrees with all the requirements for registration, submission of the Manuscript and payment set out on the official Publisher’s website, and bears full responsibility in case of violation of these requirements;

4.2.2. Licensor undertakes not to transfer the Manuscript to other publishers if it is submitted to the Licensee's Journal before the publication of the Work by Licensee;

4.2.3. Licensor undertakes, when using the Work by republishing it in any language, dissemination through any resources, etc., to indicate all data that fully identify the Licensee as the primary owner of non-exclusive proprietary rights to the Work and indicate the fact of the original publication of the Work in the Licensee's Journal;

4.2.4. Licensor undertakes not to use the Work in case of refusal on its own initiative to publish the Work with Licensee after approval of the Work for publication;

4.2.5. Licensor undertakes to reimburse the costs associated with the preparation of the Manuscript for publication in the form of a Work, if the Licensor on its own initiative withdraws the Work adopted by Licensee for

опублікування, згідно п. 7.5, чи Рукопис, до етапу перекладу чи перевірки перекладу, згідно п.7.4.

4.2.6. Ліцензіар зобов’язується не вчиняти оманливих/несправедливих/маніпуляційних дій, що спрямовані на отримання позитивного результату розгляду Рукопису або його опублікування у вигляді Твору.

4.3. Права Ліцензіата

4.3.1. Ліцензіат має право встановлювати умови прийому і опублікування Твору в журналі. Редакції Видання належить виняткове право відбору або відхилення Рукопису. Редакція в листування з питань відхилення Рукопису не вступає, дані рецензентів не розголошуються.

4.3.2. Ліцензіат має право виконувати в повному обсязі Регламент.

4.3.3. Ліцензіат має право на розміщення електронного варіанту Рукопису, після прийняття його до опублікування, мовою оригіналу на веб-сторінках журналу з водяним знаком "For reading only. Not a reprint", та розмыщення електронного варіанту Твору повністю або частково в мережі Інтернет на веб-сторінках журналу та інших інформаційних ресурсах.

4.3.4. Ліцензіат має право на відтворення та поширення Твору будь-яким способом, якщо не порушує умов цього Договору.

4.3.5. Ліцензіат має право на включення Твору до Видання або інших складених творів.

4.3.6. Ліцензіат має право переробляти, адаптувати або іншим чином змінювати Твір без порушення суті змісту в разі включення Твору до інших складених творів.

4.3.7. Ліцензіат має право перекладати Твір іншими мовами у випадку, коли цього вимагають дії, спрямовані на реалізацію заходів з поширення представленості Твору в світових ресурсах індексації наукового контенту.

4.3.8. Ліцензіат має право на використання метаданих (назва Рукопису/Твору, прізвище, ім’я по батькові автора (співавторів), дата народження, відомості про освіту, вчене звання та науковий ступінь, відомості про місце роботи і посаду, анотації, бібліографічні матеріали, e-mail, робоча адреса тощо) Твору шляхом розповсюдження і доведення до загального відома, обробки та систематизації, а також включення в різні бази даних та інформаційні системи.

4.3.9. Ліцензіат має право на власний розсуд визначати форму та спосіб доступу до Твору читачів.

4.3.10. Ліцензіат має право вимагати від Ліцензіара відшкодування витрат, пов'язаних з підготовкою Рукопису до опублікування у вигляді Твору, якщо Ліцензіар з власної ініціативи відкликає Твір, прийнятий Ліцензіатом для опублікування.

4.3.11. Ліцензіат має право розкривати будь-яку інформацію, яка розумно необхідна для забезпечення законності і захисту прав та інтересів залучених сторін, якщо цього вимагають обставини, відповідно до чинного законодавства, з метою захисту прав та інтересів користувачів Видання, або відповідо до юридичних запитів державних органів або відповідно до політики конфіденційності та авторських прав.

publication, pursuant to p. 7.5, or the Manuscript, prior to the stage of translation or verification of translation, pursuant to p.7.4.

4.2.6. The Licensor undertakes not to commit misleading/unfair/manipulative actions aimed at obtaining a positive result of the Manuscript review or its publication in the form of a Work.

4.3. Licensee's rights

4.3.1. The Licensee has the right to establish the conditions for admission and publication of the Work in the Journal. The Editorial Board of the Journal has the exclusive right to select or reject the Manuscript. The Editorial Board does not enter into correspondence on the rejection of the Manuscript; the data on reviewers are not disclosed;

4.3.2. Licensee has the right to comply in full with the Regulations;

4.3.3. Licensee has the right to place an electronic version of the Manuscript, after its acceptance for publication, in the original language on the web pages of the Journal with a watermark "For reading only. Not a reprint", and hosting an electronic version of the Work in whole or in part on the Internet on the web pages of the Journal and other information resources;

4.3.4. Licensee has the right to reproduce and disseminate the Work in any way unless it violates the terms of this Agreement;

4.3.5. The Licensee has the right to include the Work in the Journal or other composite works;

4.3.6. Licensee has the right to rework, adapt, or otherwise modify the Work without violating the essence of the content in the event of inclusion of the Work in other composite works;

4.3.7. Licensee has the right to translate the Work in other languages in the event that it is required by activities aimed at implementing measures to disseminate the representation of the Work in the global resources for indexing scientific content;

4.3.8. Licensee has the right to use metadata (Manuscript/Work title, surname, patronymic name of the author (co-authors), date of birth, information about education, academic rank and scientific degree, information about the place of work and position, abstracts, bibliographic materials, e-mail accounts, working address, etc.) of the Work by distribution and bringing to general knowledge, processing, and systematization, as well as inclusion in various databases and information systems;

4.3.9. The Licensee has the right, at its sole discretion, to determine the form and method of accessing the Work by readers;

4.3.10. The Licensor has the right to demand from the Licensor reimbursement of costs associated with the preparation of the Manuscript for publication in the form of a Work, if the Licensor on his/her own initiative withdraws the Work adopted by the Licensee for publication;

4.3.11. Licensee has the right to disclose any information that is reasonably necessary to ensure the legality and protection of the rights and interests of the parties involved, if required by circumstances, in accordance with applicable law, in order to protect the rights and interests of users of the Journal, or in accordance with legal requests by state authorities or in accordance with the privacy and copyright policy;

4.3.12. Усі майнові авторські права на переклад Твору та Твір, що ще не опублікований, але готовий для опублікування, залишаються за Ліцензіатом.

4.4. Обов'язки Ліцензіата

4.4.1. Ліцензіат зобов'язується не передавати Рукопис третім особам, за виключенням тих, діяльність яких передбачена Регламентом.

4.4.2. Ліцензіат зобов'язується в разі відмови в опублікуванні не передавати Рукопис іншим особам та видалити його, а зміст його не використовувати в будь-який спосіб.

4.2.3 Ліцензіат зобов'язується виконувати Регламент з повним дотриманням норм академічної доброчесності та норм етики відповідно до COPE.

5. Територія використання

5.1. Територія, на якій допускається використання Ліцензіатом прав на Твір, не обмежена**.**

6. Термін дії Договору

6.1. Договір є чинним з дати його підписання та укладається на весь термін дії майнових авторських прав.

7. Відповідальність сторін договору

7.1. Ліцензіат зобов'язується дотримуватися передбачених чинним законодавством авторських прав Ліцензіара, а також приймати всі можливі заходи для попередження порушення авторських прав третіми особами.

7.2. В разі виявлення на етапі роботи з Рукописом факту порушення п. 2.1. та п. 2.2. цього Договору з боку Ліцензіарів Ліцензіат відхиляє Рукопис та запроваджує штрафні санкції в розмірі EUR 100,00 (сто євро 00 євроцентів).

7.3. В разі виявлення після опублікування Твору факту порушення п. 2.1. та п. 2.2. цього Договору з боку Ліцензіарів, незалежно від того, хто виявив цей факт, та в разі пред'явлення претензії стосовно порушення авторських прав з боку третьої сторони, відповідальність несе відповідний Ліцензіар. Ліцензіат може запровадити штрафні санкції в розмірі EUR 2000,00 (дві тисячі євро 00 євроцентів).

7.4. В разі, якщо Ліцензіари з власної ініціативи відкликають Рукопис до етапу перекладу чи перевірки перекладу, після виконання процедур редагування та рецензування, за підсумками якого прийнято позитивне рішення щодо опублікування Твору, Ліцензіат може запровадити штрафні санкції в розмірі EUR 500,00 (п'ятсот євро 00 євроцентів).

7.5. В разі відмови Ліцензіара з власної ініціативи від опублікування Твору, прийнятого Ліцензіатом для опублікування, Ліцензіат може запровадити штрафні санкції в розмірі EUR 1000,00 (одна тисяча євро 00 євроцентів).

7.6. Виплата штрафу не звільняє Ліцензіара від покриття збитків в натурі.

7.7. Ліцензіат не бере на себе будь-яку відповідальність за будь-які незаконні, несправедливі або шахрайські дії, вчинені Ліцензіаром в рамках цього Договору, наслідком яких є порушення авторських прав та прав інтелектуальної власності інших осіб.

7.8. В разі виявлення на будь-якому етапі виконання Регламенту факту порушення п. 2.3 цього Договору з боку Ліцензіара Ліцензіат може запровадити штрафні санкції у розмірі EUR 500 (п'ятсот євро 00 євроцентів).

4.3.12. All proprietary copyrights for the translation of the Work, and the Work that has not yet been published but is ready for publication, remain with the Licensee.

4.4. Licensee's duties

4.4.1. The Licensee undertakes not to transfer the Manuscript to third parties, except those whose activities are implied by the Regulations;

4.4.2. The Licensee undertakes, in case of refusal to publish, not to transfer the Manuscript to other persons and delete it, and the content is not to be used in any way;

4.2.3. The Licensee undertakes to comply with the Regulations in full compliance with academic integrity and ethical standards in accordance with COPE.

5. Territory of use

5.1. The territory in which Licensee may use the rights to the Work is not limited.

6. Term of the Agreement

6.1. The Agreement is valid from the date of its signing and is concluded for the entire term of property copyright.

7. Liability of the parties to the Agreement

7.1. The Licensee undertakes to comply with the copyright laws of the Licensor, in accordance with acting law, as well as to take all possible measures to prevent copyright infringement by third parties.

7.2. In case of discovery at the stage of work with the Manuscript of the fact of violation of Clause 2.1. and Clause 2.2. of this Agreement on the part of the Licensors, the Licensee rejects the Manuscript and imposes fines in the amount of EUR 100.00 (one hundred euros 00 eurocents).

7.3. In case of discovery after the publication of the Work of the fact of violation of Clause 2.1. and Clause 2.2. of this Agreement by the Licensors, regardless of who discovered this fact, and in the case of a claim regarding copyright infringement by a third party, the respective Licensor shall be responsible. The licensee may impose fines in the amount of EUR 2000.00 (two thousand euros 00 euro cents).

7.4. In the event that the Licensors, on their own initiative, withdraw the Manuscript before the stage of translation or translation verification, after the completion of the editing and review procedures, as a result of which a positive decision was made regarding the publication of the Work, the Licensee may introduce fines in the amount of EUR 500.00 (five hundred euros 00 euro cents).

7.5. In the case that the Licensor, on its own initiative, refuses to publish the Work accepted by the Licensee for publication, the Licensee may impose fines in the amount of EUR 1000.00 (one thousand euros 00 eurocents).

7.6. Payment of the fine does not release the Licensor from covering damages in kind.

7.7. The Licensee does not assume any liability for any illegal, unfair, or fraudulent actions committed by the Licensor under this Agreement, which result in infringement of copyright and intellectual property rights of other persons.

7.8. If at any stage of the implementation of the Regulations a violation of clause 2.3 of this Agreement by the Licensor is detected, the Licensee may impose penalties in the amount of € 500.00 (five hundred euros).

Представник ліцензіарів
Representative of licensors Suwandono Purbo

Підпис
Signature

7.9. В разі виявлення після опублікування Твору факту порушення п. 2.3. цього Договору з боку Ліцензіара, незалежно від того, хто виявив цей факт, Ліцензіат може запровадити штрафні санкції у розмірі EUR 1 500 (одна тисяча п'ятсот євро 00 євроцентів).

7.10 Сторона, яка неналежним чином виконала або не виконала свої обов'язки за цим Договором, зобов'язана відшкодувати збитки, завдані іншій Стороні, включаючи упущену вигоду.

7.11. У всьому, що не передбачено цим Договором, Ліцензіар та Ліцензіат керуються нормами чинного законодавства України.

7.12. У випадку виявлення Ліцензіатом фактів вчинення Ліцензіаром оманливих/несправедливих/ маніпуляційних дій, що були спрямовані на отримання позитивного рішення про опублікування Рукопису у вигляді Твору на сайті Видання на будь-якому етапі розгляду Рукопису, Ліцензіат може запровадити штрафні санкції в розмірі EUR 750 (сімсот п’ятдесят євро).

7.13. Цей Договір складений в 6 примірниках, що мають однаковий зміст і рівну юридичну силу, по одному для кожного з підписантів.

8. Умови розірвання договору

8.1. Договір може бути розірваний у випадках:

– коли Рукопис не прийнято до публікації через негативне рішення рецензентів, через відмову Ліцензіара вносити виправлення, спрямовані на усунення невідповідності Рукопису за структурою та змістом вимогам Видання, або через відмову Ліцензіара вносити виправлення, спрямовані на усунення зауважень рецензентів, які унеможливлюють публікацію через невідповідініть рівню наукової новизни Рукопису,

– в разі, якщо Ліцензіар відкликав Рукопис з власної ініціативи до початку робіт згідно Регламенту;

– в разі, якщо Ліцензіар відкликав Твір з власної ініціативи та відшкодував усі збитки пов’язані з підготовкою до публікації;

– за взаємною письмовою згодою сторін.

9. Форс-мажорні обставини

9.1. Сторони не несуть відповідальності за невиконання або неналежне виконання умов Договору за умов виникнення форс-мажорних обставин.

9.2. По завершенні таких обставин Сторона, яка не виконала свої зобов’язання за Договором, повинна виконати їх у терміни, на які було призупинено виконання зобов’язань.

9.3. Сторона не має права посилатися на форс-мажорні обставини у випадку, коли вони розпочалися у момент прострочення нею виконання її обов’язків за Договором.

9.4. Форс-мажорні обставини повинні бути підтверджені висновком компетентного органу.

10. Інші умови

10.1. Ліцензіар надає Ліцензіату згоду на передачу, зберігання та обробку його персональних даних без обмеження терміну з метою включення їх до бази даних відповідно до Закону України No. 2297-VI "Про захист персональних даних" від 01.06.2010:

– прізвище, ім’я, по батькові;

– реєстраційний номер облікової картки платника податків (РНОКПП);

– відомості про наукову кваліфікацію (науковий ступінь, вчене звання);

– відомості про місце роботи та посаду;

– контактні дані авторів (контактний телефон, e-mail);

7.9. In case of discovery after the publication of the Work of the fact of violation of Clause 2.3 of this Agreement by the Licensors, regardless of who discovered this fact, the Licensee may impose fines in the amount of € 1 500 (one thousand five hundred euros).

7.10. A party that improperly performed or failed to perform its obligations under this Agreement is obliged to reimburse the damages caused to the other Party, including the lost benefit.

7.11. In everything not provided for by this Agreement, Licensor and Licensee are guided by the norms of the acting legislation of Ukraine.

7.12. In the case that the Licensee discovers facts of the Licensor committing deceptive/unfair/manipulative actions aimed at obtaining a positive decision to publish the Manuscript as a Work on the Publisher's website at any stage of the Manuscript review, the Licensee may impose penalties in the amount of up to EUR 750.00 (seven hundred fifty).

7.13. This Agreement is drawn up in 6 copies that convey the same meaning and have equal legal force, one for each of the Signers.

8. Terms of termination of the Agreement

8.1. The Agreement may be terminated in the following cases:

– when the Manuscript is not accepted for publication due to the negative decision by reviewers, due to Licensor's refusal to make corrections aimed at eliminating the inconsistency of the Manuscript with the requirements as regards the structure and content of the by the Journal, or due to Licensor's refusal to make corrections aimed at eliminating the comments of reviewers, which makes it impossible to publish due to the inconsistency with the level of scientific novelty of the Manuscript,

– in case the Licensor withdrew the Manuscript on his/her own initiative before the onset of activities in accordance with the Regulations;

– in the event that the Licensor withdrew the Work on his/her own initiative and reimbursed all losses related to the preparation for publication;

– by mutual written consent of the parties.

9. Force majeure

9.1. The Parties shall not be liable for non-fulfillment or improper fulfillment of the terms of the Agreement in case of force majeure circumstances.

9.2. Upon completion of such circumstances, the Party that has not fulfilled its obligations under the Agreement shall fulfill them within the time frame for which the performance of obligations has been suspended.

9.3. A party has no right to refer to force majeure circumstances in the event that they have begun at the time of its delay in fulfilling its obligations under the Agreement.

9.4. Force majeure circumstances must be confirmed by the conclusion of the competent authority.

10. Other terms

10.1. The Licensor gives the Licensee consent to the transfer, storage, and processing of his/her personal data without limitation of the term in order to include them in the database in accordance with the Law of Ukraine No. 2297-VI "On Personal Data Protection" as of 01.06.2010:

– surname, first name, patronymic;

– identity card number;

– information about the scientific qualification (scientific degree, academic rank);

– information about the place of work and position;

– authors' contact details (contact phone, e-mail account);

Представник ліцензіарів
Representative of licensors Suwandono Purbo

Підпис
Signature

– відомості про наявність друкованих творів у загальнодержавних та міжнародних базах даних наукової літератури з метою їх подальшої обробки для здійснення пошукових операцій у цих базах даних.

Персональні дані і метадані статті надаються для їх зберігання і обробки в різноманітних базах даних і інформаційних системах, включення їх в аналітичні і статистичні звітності, створення обгрунтованих взаємозв'язків об'єктів творів науки, літератури і мистецтва з персональними даними і т.п. на території, яка не обмежена. Ліцензіат має право передати зазначені дані для обробки та зберігання третім особам за умови повідомлення про такий факт з наданням відомостей про третю особі (найменування та адреса) Ліцензіару. Відкликання згоди на зберігання та обробку персональних даних проводиться Ліцензіаром шляхом направлення відповідного письмового повідомлення Ліцензіату.

10.2. Для організації оперативної взаємодії в рамках цього Договору сторона «Ліцензіари» повинна призначити зі свого числа представника по цьому Договору.

– information about the availability of published works in national and international databases of scientific literature for the purpose of its further processing for search operations in these databases.

Personal data and metadata of the paper are provided for their storage and processing in various databases and information systems, for including them in analytical and statistical reports, creating reasonable relationships between objects of works of science, literature, art and personal data, etc. in the territory that is not limited. The Licensee has the right to transfer the specified data for processing and storage to third parties, subject to notifying the Licensor about such a fact with the provision of information about a third party (name and address). Withdrawal of consent to the storage and processing of personal data is carried out by Licensor by sending the relevant written notice to the Licensee.

10.2. In order to organize operative interaction within the framework of this Agreement, the party "Licensors" must appoint a representative under this Agreement.

Така особа є / This person is Suwandono Purbo ,

конт.тел. / contact tel. +6282132697144 e-mail purbo@widyagama.ac.id

10.3. Поштова адреса для відправки Видання (Mailing address for sending the Journal):

та отримувач Видання (the Journal is to be received by):

(П.І.Б. повністю ((Full Name))).

10.4. Підписаний договір, який відправлений факсом чи електронною поштою, має повну юридичну силу до моменту обміну оригіналами, породжує права та обов'язки для сторін, може бути поданий в судові інстанції в якості належних доказів і не може заперечуватись стороною, від імені якої він був відправлений.

10.4. The signed Agreement, which is sent by fax or e-mail, is valid until the originals are exchanged; it generates rights and obligations for the parties: it can be submitted to the courts as proper evidence and cannot be objected to by the party on whose behalf it was sent.

Українська мова є основною та офіційною мовою цього Договору. Англійський текст Договору включено виключно для зручності сторін.

The Ukrainian language text is the official text of the Agreement. English text in this Agreement is included for the convenience of the parties.

11. Реквізити і підписи сторін / Bank details and signatures of the parties

Ліцензіар (Ліцензіари) (ПІБ повністю) / Licensor (Licensors) (Full Name)

_____(Suwandono Purbo)(3573051207870005)	
ПІБ / Full name РНОКПП / ID card	
_____(Widya Wijayanti)(3573044208750006)	
ПІБ / Full name РНОКПП / ID card	
_____(Nova Risdiyanto Ismail)(3507242711750006)	
ПІБ / Full name РНОКПП / ID card	
_____(Dzulfikar Johan Akbar)(3507240705020003)	
ПІБ / Full name РНОКПП / ID card	
_____(Muhammad Reza)(7402192106040001)	
ПІБ / Full name РНОКПП / ID card	
_____(_____)(_____)	
ПІБ / Full name РНОКПП / ID card	
_____(_____)(_____)	
ПІБ / Full name РНОКПП / ID card	
_____(_____)(_____)	
ПІБ / Full name РНОКПП / ID card	
_____(_____)(_____)	
ПІБ / Full name РНОКПП / ID card	
_____(_____)(_____)	
ПІБ / Full name РНОКПП / ID card	

Ліцензіат / Licensee

ПРИВАТНЕ ПІДПРИЄМСТВО "ТЕХНОЛОГІЧНИЙ ЦЕНТР"
Україна, 61165, Харківська обл., місто Харків, вул. Шатилова дача, будинок 4
ЄДРПОУ 31886700

TECHNOLOGY CENTER PRIVAT COMPANY
Ukraine, 61165, Kharkiv region, Kharkiv, Shatylova dacha str., 4
Company registration no. 31886700

Директор/ Director — Дьомін Д.О. Dmytro Domin

Представник ліцензіарів Representative of licensors Suwandono Purbo

Підпис Signature

Dear Editors!

Please find attached the original research article " SYNGAS QUALITY IMPROVEMENT IN CORNCOB UPDRAFT GASIFICATION USING CAO/ACTIVATED CARBON PALM FIBER CATALYST" written by authors Purbo Suwandono, Widya Wijayanti, Nova Risdiyanto Ismail, Dzulfikar Johan Akbar, Muhammad Reza for your kind consideration for publication.
All authors have read and approved this variant of the paper. No part of it has been published or presented elsewhere. The authors have no conflicts of interest related to the research described in the manuscript. The authors Purbo Suwandono, Widya Wijayanti, Nova Risdiyanto Ismail, Dzulfikar Johan Akbar, Muhammad Reza, submitting a manuscript to the editors of the "Eastern-European Journal of Enterprise Technologies", are familiar with and agree to all the requirements for registration, submission of the article manuscript, payment, which are on the official website of the journal via links, and bear full responsibility in case of violation of these requirements.

We look forward to receiving comments from reviewers.

On behalf of all the authors of this manuscript,

_____

This contact person must be specified in clause 10.2. of the License Agreement

TAHAP 2

REVIEW EDITOR TAHAP 2

21 Februari 2026

Purbo Suwandono <purbo@widyagama.ac.id>

from "Eastern-European Journal of Enterprise Technologies" - Suwandono P. (stage 2, No. 2(140).2026 (April))

6 messages

Oksana Nikitina <0661966nauka@gmail.com> Sat, Feb 21, 2026 at 3:51 AM
To: purbo@widyagama.ac.id, "Widya Wijayanti, ST.,MT" <widya_dinata@ub.ac.id>, nova@widyagama.ac.id, johanakbar@student.ub.ac.id, muhapanjangreza@gmail.com

Good afternoon, dear authors.

The article was accepted for consideration of the possibility of publication in (No. 2(140).2026).

At the 2nd stage of editing, please take into account the comments of the editor (article in the application, color notes are highlighted).

We ask you to right strictly in the option which is in the attachment (see attachment).

We ask you not to delete the comments so that we can see all your edits. All corrections by the author, please highlight in green.

Please provide an edited version of the article **by 25.02.2026.**

If you have any questions, please call or write; we will be happy to answer them.

With best regards, Manager Yu. Prylutska
TECHNOLOGY CENTER GROUP LTD
Viber/ WhatsApp/ Telegram: +380 (50) 3033801
Editorial staff of the "Eastern-European Journal of Enterprise Technologies"
Website: https://jet.com.ua/en/, http://journals.uran.ua/eejet/



Відвідати сайт



Відвідати сайт

Attention! The author (team of authors) submitting the manuscript to the editorial office of the journal **«Eastern-European Journal of Enterprise Technologies»** agrees with all requirements for registration, submission of the manuscript of the article and payment and be responsible in case of violation of these requirements.

Our company may rely on your freely given consent at the time you provided your personal data to us replying on this email then the lawfulness of such processing is based on that consent under EU GDPR 2016/679. You have the right to withdraw consent at any time.

Subscribe

Suwandono 22-ап-(1).doc
1063K

Purbo Suwandono <purbo@widyagama.ac.id> Wed, Feb 25, 2026 at 9:12 PM
To: Oksana Nikitina <0661966nauka@gmail.com>

Dear Editor,

Good afternoon, and thank you for your email and for accepting our article for consideration for publication in No. 2(140).2026.

We have received the edited file and the editor's comments, and we understand the instructions.

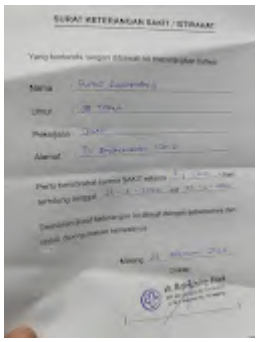
However, I would like to kindly inform you that I am currently still unwell and my doctor has advised me to rest for several days. Therefore, I respectfully ask for your kind understanding and a short extension of the revision deadline for a few more days.

I will do my best to complete and submit the revised version as soon as possible.

Thank you very much for your understanding and support.

Best regards,
Purbo Suwandono

[Quoted text hidden]



Doctors Note.jpeg
119K

Oksana Nikitina <0661966nauka@gmail.com> Wed, Feb 25, 2026 at 9:18 PM
To: Purbo Suwandono <purbo@widyagama.ac.id>

Don't worry and get well soon, I'm waiting for the article on March 2, 2026.

ср, 25 февр. 2026 г. в 16:12, Purbo Suwandono <purbo@widyagama.ac.id>:
[Quoted text hidden]

--
[Quoted text hidden]

Oksana Nikitina <0661966nauka@gmail.com> Thu, Mar 5, 2026 at 2:18 AM
To: Purbo Suwandono <purbo@widyagama.ac.id>

Good afternoon, dear authors,
This is a friendly reminder that we expect the corrected version of your article **by March 06, 2026.**
Please feel free to reach out if you need any assistance.
We are always happy to help!
Best regards, Oksana

ср, 25 февр. 2026 г. в 16:18, Oksana Nikitina <0661966nauka@gmail.com>:
[Quoted text hidden]
[Quoted text hidden]

Purbo Suwandono <purbo@widyagama.ac.id> Fri, Mar 6, 2026 at 2:26 AM

To: Oksana Nikitina <0661966nauka@gmail.com>

Dear Editor,

Good afternoon.

Thank you for your reminder. I would like to inform you that the revised version of the manuscript has now been completed and attached to this email.

Please accept my sincere apologies for the slight delay in submitting the revision, as I have only recently recovered from a medical condition over the past few days. Thank you very much for your understanding.

I have carefully addressed the comments and suggestions provided by the editor and reviewers. I hope the revised manuscript meets the requirements.

Thank you for your kind assistance and support.

Best regards,
Purbo Suwandono

[Quoted text hidden]

Suwandono 22-ап-(1)_Revision.doc
1176K

Oksana Nikitina <0661966nauka@gmail.com> Fri, Mar 6, 2026 at 12:23 PM
To: Purbo Suwandono <purbo@widyagama.ac.id>

Good day!
The article has been sent to the editor for checking.
If you have any questions, please call or write. We will be happy to answer them.
We wish you a great day and a good mood!
Regards, Oksana

чт, 5 мар. 2026 г. в 21:27, Purbo Suwandono <purbo@widyagama.ac.id>:
[Quoted text hidden]
[Quoted text hidden]

Received date: 20.02.2026
Accepted date:

UDC

ПОКРАЩЕННЯ ЯКОСТІ СИНТЕЗ-ГАЗУ ПРИ ВИСХІДНІЙ ГАЗИФІКАЦІЇ КУКУРУДЗЯНИХ КАЧАНІВ З ВИКОРИСТАННЯМ КАТАЛІЗАТОРА НА ОСНОВІ CAO/АКТИВОВАНОГО ВУГІЛЛЯ НА ПАЛЬМОВОМУ ВОЛОКН

Purbo Suwandono, Widya Wijayanti, Nova Risdiyanto Ismail, Dzulfikar Johan Akbar, Muhammad Reza

SYNGAS QUALITY IMPROVEMENT IN CORNCOB UPDRAFT GASIFICATION USING CAO/ACTIVATED CARBON PALM FIBER CATALYST

Purbo Suwandono, Widya Wijayanti, Nova Risdiyanto Ismail, Dzulfikar Johan Akbar, Muhammad Reza

Це дослідження зосереджується на поліпшенні якості синтез-газу, отриманого в результаті газифікації кукурудзяних качанів за допомогою висхідного потоку, з використанням подвійної каталітичної системи на основі CaO та активованого вугілля, отриманого з пальмового волокна (AC-PF). Основними досліджуваними робочими змінними були коефіцієнт еквівалентності (ER), навантаження каталізатора та співвідношення CaO/AC-PF (0:1, 1:0, 1:1 та 2:1). Характеристика каталізатора показує, що AC-PF забезпечує пористу структуру, яка покращує контакт газу з твердою речовиною та сприяє вторинним реакціям, тоді як включення CaO утворює композит із модифікованою структурою пор та поверхневими речовинами, пов'язаними з функцією сорбції CO_2. Експериментальні результати показують, що збільшення ER загалом підвищує частки H_2 та CH_4, одночасно зменшуючи CO_2, тоді як CO демонструє оптимальний результат при середньому ER, а потім зменшується при найвищому ER. Навпаки, більш високе навантаження каталізатора, як правило, зменшує H_2 і CH_4, але збільшує CO, що свідчить про зміну селективності вторинної реакції при більш інтенсивному каталітичному контакті. З енергетичної точки зору, LHV The abbreviations must be decrypted *синтез-газу збільшується з ER, але може знижуватися при більш високих навантаженнях каталізатора через зменшення внеску CH_4.*

Ключові слова: Газифікація висхідним потоком; Кукурудзяні качани; Синтетичний газ; Каталізатор CaO; Активоване вугілля

The sum of summary + keywords= should be 1800-1900 characters with spaces.

The summary should contain the following information:
- object of research
- problem that was solved
- results obtained
- brief interpretation of the results (what explains them)
- features and distinctive features of the results obtained, thanks to which they allowed to solve the problem under study
- the scope and conditions of practical use of the results obtained

This study focuses on improving syngas quality from corncob updraft gasification using a dual catalyst system based on CaO and palm-fiber-derived activated carbon (AC-PF). The main operating variables investigated were the equivalence ratio (ER), catalyst loading, and the CaO/AC-PF ratio (0:1, 1:0, 1:1, and 2:1). Catalyst characterization indicates that AC-PF provides a porous structure that enhances gas–solid contact and promotes secondary reactions, whereas CaO incorporation forms a composite with modified pore texture and surface species associated with CO_2 sorption functionality. Experimental results show that increasing ER generally raises the H_2 and CH_4 fractions while reducing CO_2, whereas CO exhibits an optimum at intermediate ER before decreasing at the highest ER. In contrast, higher catalyst loading tends to decrease H_2 and CH_4 but increase CO, suggesting a shift in secondary-reaction selectivity under more intensive catalytic contact. From an energy perspective, the syngas LHV increases with ER but may decline at higher catalyst loadings due to a reduced CH_4 contribution

Keywords: updraft gasification, corncob, syngas, CaO catalyst, activated carbon
10 words

Keywords are used to index jobs on electronic systems and the Internet. The better the keywords are chosen, the more people will be able to find the paper by typing in the same keywords as in the paper. This will increase the readability of the paper, and therefore the likelihood that the paper will be cited.

The main purpose of keywords is to allow you to quickly find an article on the desired topic.

Replace hyphens (-) with dashes (–) by text (except word combinations)

1. Introduction

Indonesia is one of the largest corn producers in Southeast Asia, with national production reaching more than 18 million tons of dry kernels per year. Of this amount, about 15-20% is cobs after the kernel removal process, resulting in a very large amount of corn cob waste, estimated at 2.5-3.5 million tons annually [1]. Until now, most corn cobs have only been used to a limited extent, for example as traditional fuel, small amounts of animal feed, or even burned directly on post-harvest land, which has the

potential to cause air pollution. Most of the rest are simply piled up or left to rot on the land, posing a risk of becoming a source of plant disease [2].

Corn cobs have quite promising chemical and energy characteristics. Their composition is dominated by cellulose, hemicellulose, and lignin, with a calorific value of around 15–17 MJ/kg, making them very suitable as raw materials in various biomass-based energy conversion technologies [3]. Their hard and fibrous nature also makes them suitable for processing into biochar, activated charcoal, or direct use in pyrolysis and gasification processes. This significant potential indicates that corn cobs are not merely waste but a renewable resource that can be optimized to support energy security and reduce dependence on fossil fuels.

Biomass gasification is a promising thermochemical technology for converting renewable resources into syngas consisting of H_2, CO, CH_4, and CO_2. Of the various types of biomass, corn cobs are a potential candidate due to their abundant availability in Indonesia and lignocellulose content that supports the energy conversion process [4]. However, the biomass gasification process still faces several obstacles, particularly the low hydrogen fraction in syngas and the formation of significant amounts of tar. Tar can cause reactor clogging, reduced thermal efficiency, and increased purification costs.

To overcome these problems, the use of catalysts is an important strategy. A number of studies have proven that metal catalysts such as Ni [5], Ca [6], and K [7] can increase hydrogen yield while suppressing tar formation. On the other hand, activated carbon is also widely used as a catalyst support because it has a high surface area, porous structure, and good chemical stability. The use of agricultural waste, particularly palm fiber, as raw material for activated carbon is not only economically valuable but also supports the concept of a circular economy in plantation waste management. In addition, calcium oxide (CaO) is known to have a dual role, namely as a catalyst in the tar decomposition reaction and as a CO_2 absorber that promotes sorption-enhanced gasification to increase the hydrogen fraction in syngas [8].

Although various studies have examined the role of metal catalysts and activated carbon separately, research focusing on the combination of biomass bases catalyst such as palm fiber-based activated carbon with CaO in corn cob gasification is still limited. The uniqueness of this study lies in the integration of two catalyst, which is expected to provide a synergistic effect: activated carbon with high porosity increases catalyst dispersion and activity, while CaO simultaneously breaks down tar and absorbs CO_2. This approach has the potential to significantly increase hydrogen production and reduce carbon emissions.

However, there are several research gaps that remain unanswered. First, the optimal composition and ratio of activated carbon and CaO in corn cob gasification have not been extensively studied. Second, the synergistic mechanism using two catalyst in increasing syngas quality not yet fully understood. In addition, a systematic and statistically robust approach is required to disentangle the coupled effects of key operating and catalyst variables.

Based on this background and research gaps, this study aims to investigate the performance of a composite catalyst based on activated carbon from palm fiber combined with CaO in the corn cob gasification process. The main focus is on increasing hydrogen production, reducing tar, and evaluating the potential synergistic effects between materials. This research is expected to contribute to the development of low-cost, locally sourced, and sustainable catalyst systems that are relevant to supporting the clean energy transition and practical applications of biomass-to-hydrogen in the future.

2. Literature review and problem statement

How this section should be built: The paper [.] presents the results of research ..., Shown, that..., But there were unresolved issues related to ..., The reason for this may be (objective difficulties associated with ..., fundamental impossibility ..., cost part in terms of ..., which makes relevant research impractical, etc.). A way to overcome these difficulties can be ..., This approach was used in [.], however ..., All this suggests that it is advisable to conduct a study on ...

Names are not mentioned in scientific articles, references to works are enough

A study by ~~Tosuli~~ [9] explored Sago-based foods are staple in eastern Indonesia. Al_2O_3 (5–10 wt%) added to sago-dregs pellets in a TULD gasifier enhances syngas: H_2 is highest at 5% (31.65%), while CO (4.33%) and CH_4 (26.45%) peak at 10%. The H_2/CO ratio remains favorable (1.65–1.51) with low tar, indicating potential for internal combustion engine fuel.

A research by ~~Tuan~~ [10] explored an updraft gasifier processed 3 kg of dried rice husk using air, steam-air, and air with dolomite at varied conditions. Among the tested agents, catalytic air gasification (air + dolomite) gave the best results, producing the highest H_2 (15.4 mol%) and LHV (5.1 MJ/Nm^3), compared with steam-air (7.08 mol%, 3.6 MJ/Nm^3) and air only (3.6 mol%). The optimum setting was an airflow of 3 m^3/h with 15% dolomite.

A research by ~~Yousef~~ [11] explored Cigarette butts are hazardous urban waste rich in cellulose acetate and volatile matter, making them a potential renewable feedstock for hydrogen production. This study valorized as-received cigarette butts via continuous updraft gasification (700–900 °C; ER 0.15–0.25), followed by steam catalytic reforming over KATALCO™ 57-4GQ at 900 °C. Gasification alone produced high syngas yields (82.3–89.7%) but limited H_2 (<20.84 vol% at 900 °C, ER 0.15). The reforming step increased H_2 to 30.27 vol% and reduced tar from 18.15 to 13.38 g/m^3, improving fuel quality (HHV from 11,038 to 11,528 kJ/kg).

A research by ~~Bilbao~~ [12] explored slumgum suitability as a gasification fuel. Slumgum and slumgum-pine sawdust pellets were produced (ISO 17225 tests) and gasified in a modified updraft reactor while measuring gas composition and LHV. Pure slumgum pellets showed very high durability (99.98%) and HHV (27.66 MJ/kg), likely due to high fat content, but high sulfur (2.17%) and nitrogen (3.52%) prevented ISO

compliance. In gasification, adding sawdust increased LHV, reaching 7.62 MJ/Nm³ at a 50:50 blend, although ER stayed very low (0.0125–0.0204) because higher airflow raised fuel consumption.

A research by ~~Yesilova~~ [13] examined catalyst effects on biomass-mixture gasification using lab-scale updraft and modifiable-downdraft fixed-bed reactors. Red mud (RM) and an Al–Ni alloy were tested at high temperature, where H_2 levels of 51–65 vol% were obtained at 900 °C in both systems. The Al–Ni catalyst showed the strongest enhancement, achieving 65 vol% H_2 in the updraft reactor at 900 °C with 0.05 L/min dry air, and widening the H_2/CO range from 2–4 (no catalyst) to 1.6–7. RM generally increased H_2 in the updraft reactor by about 1–7 vol% at 900 °C, but in the modifiable-downdraft reactor it reduced H_2 by roughly 2–6%.

A research by ~~Jancauskas~~ [14] examined three MSW fractions (FDS, SRF, and plastic packaging mixture/PPM) from mechanical–biological treatment plants were gasified in an allothermal fixed-bed updraft reactor at 800 °C using air at ER ≈ 0.15 and 0.21. All feeds showed similar volatile-release peaks (~330 and ~500 °C). Lowering ER increased the heating value of combustible gases; PPM produced the highest H_2 (11.39%). SRF generated the most tar (47.44 g/m³), dominated by aromatic compounds.

A research by ~~Junga~~ [15] examined co-gasifying laying hens manure (LHM) with common litter such as wheat straw remains limited, particularly across a wide range of air–fuel equivalence ratios (AFER). This laboratory study used a fixed-bed updraft reactor to gasify straw-LHM blends (25–75% LHM) under low (0.12–0.28) and high (0.30–0.45) AFER to assess how LHM affects producer-gas quality and process efficiency. At higher AFER, the producer-gas LHV stayed around 3.3–3.4 MJ/m³ (depending on blend), with cold gas efficiency 60% and carbon conversion efficiency of 82–94%.

A study by ~~Tezer~~ [16] evaluated the gasification of olive pomace in fixed-bed updraft and downdraft systems. Dried olive pomace obtained from an olive-oil soap plant in Izmir (Türkiye) was characterized and gasified at 700–900 °C using dry air at 0.05–0.4 L/min, with additional tests using pure oxygen (0.01 L/min). With dry air, the syngas reached 48 vol% H_2 in the updraft and 45 vol% in the downdraft, with a heating value of about 12.4 MJ/Nm³. Under oxygen, H_2 increased to ~53 vol% in the updraft but was ~39 vol% in the downdraft.

A study by ~~Isik~~ [17] gasified MDF wood-waste in a 2100 kg/h updraft fixed-bed system (tested at 1500–2100 kg/h) using oak chips as a reference. Syngas yield was 2.5 Nm³/kg with LHV 6.0–7.0 MJ/Nm³, and the gas composition at full-load MDF was similar to oak. Hot syngas (430 °C) containing tar/soot was burned directly in a retrofitted thermal-oil heater (7 MWh) to supply an ORC turbine generating 955 kW electricity, converting 88 wt% of MDF residue into syngas.

Based on the above literature, it is evident that syngas quality in fixed-bed updraft gasification is primarily governed by catalytic strategy such as Al_2O_3, dolomite, Al/Ni, red mud, oxidant selection, and equivalence ratio, while secondary upgrading can further suppress tar and enrich H_2. However, most published studies still emphasize single

catalyst systems or isolated additives, and comparatively few have investigated dual catalyst synergy in updraft configurations using a systematic, design-of-experiments optimization framework.

In this context, the present study on Syngas Quality Improvement in Corncob Updraft Gasification Using a CaO/Activated Carbon Palm-Fiber Catalyst addresses a clear research gap. The CaO-activated carbon combination is expected to deliver a dual-synergistic function: CaO acts as an in-situ CO_2 sorbent that can shift gasification equilibria toward higher H_2 formation, whereas palm-fiber-derived activated carbon provides high-surface-area catalytic sites to promote tar cracking and reforming of volatiles, thereby reducing condensable by-products while enhancing the combustible gas fraction. Consequently, this work is positioned to contribute both mechanistic and practical advances by demonstrating a scalable dual-catalyst route to produce cleaner, H_2-richer, and higher-LHV syngas from corncob waste in an updraft reactor.

Please add a summary of the section on literary data analysis and problem statement. All this allows us to conclude that it is expedient to conduct research devoted to...

The purpose of the study (section 3) should follow from the unresolved problem formulated at the end of section 2.

3. The aim and objectives of the study

The purpose statement should include two components: scientific (The purpose of the study is...) and practical (This will allow...). The scientific part should correspond to the title of the article, the practical part should indicate what the scientific results obtained will give to practice (i.e., the achievement of the scientific component of the research goal)

The aim of the study is to enhance syngas quality from corncob updraft gasification by developing and optimizing a dual-synergy CaO/palm-fiber-derived activated carbon (CaO/AC-PF) catalytic system.

Objectives of the study:

It is strictly prohibited to use an automatic list. All lists are marked in manual mode!

- to synthesize and characterize the CaO and palm-fiber activated carbon catalysts using FTIR, SEM, and BET The abbreviations must be decrypted

- to investigate the effects of operating parameters, particularly equivalence ratio (ER), catalyst loading, and CaO/AC ratio, on syngas composition H_2, CO, CH_4, CO_2 and LHV.

4. Materials and methods

Section 4 should begin with the following:

The object of study (this is the practical physical object or process on which the results of the study will be used and, as a result, something will increase or decrease),

The research hypothesis is what underlies the achievement of the research goal, i.e., what was tested and had to be accepted or refuted.

Assumptions made before the start of the research.

Simplifications made in the course of the research.

4. 1. Catalyst Preparation

Approximately 6 grams of ground palm fiber was mixed with 60 mL of distilled water and stirred for 10 minutes. The mixture was then placed in an autoclave and heated to 200°C at a rate of 5°C per minute for 6 hours in an electric oven. After that, the reactor is allowed to cool naturally to room temperature. The resulting solid hydrocarbon product (hydrochar) is then separated using Whatman No. 42 filter paper. The filtered product is then dried at 105°C for 24 hours and stored in a glass vial. The next stage is the activation process. The hydrochar is immersed in a 3 M KOH solution with a weight ratio of 1:3 (Hydrochar:KOH) for 16 hours, then dried at 85°C for 6 hours. Spectroscopic evidence indicates that KOH preferentially reacts with oxygenated sites and can increase the relative abundance of C–OH functionalities, while higher KOH ratio and activation temperature significantly enhance porosity and BET surface area [18, 19]. To obtain the CaO/AC mixture, CaO powder and activated carbon (AC) were mixed in specific proportions using a grinder until a homogeneous mixture was obtained. Next, CaO, AC, and CaO/AC were activated using a tube furnace at a temperature of 700°C for 1 hour with a continuous flow of nitrogen during the activation process. The resulting product was then washed using distilled water until it reached a neutral pH. This stage produced activated carbon that was ready for use in research.

4. 2. Experimental Setup

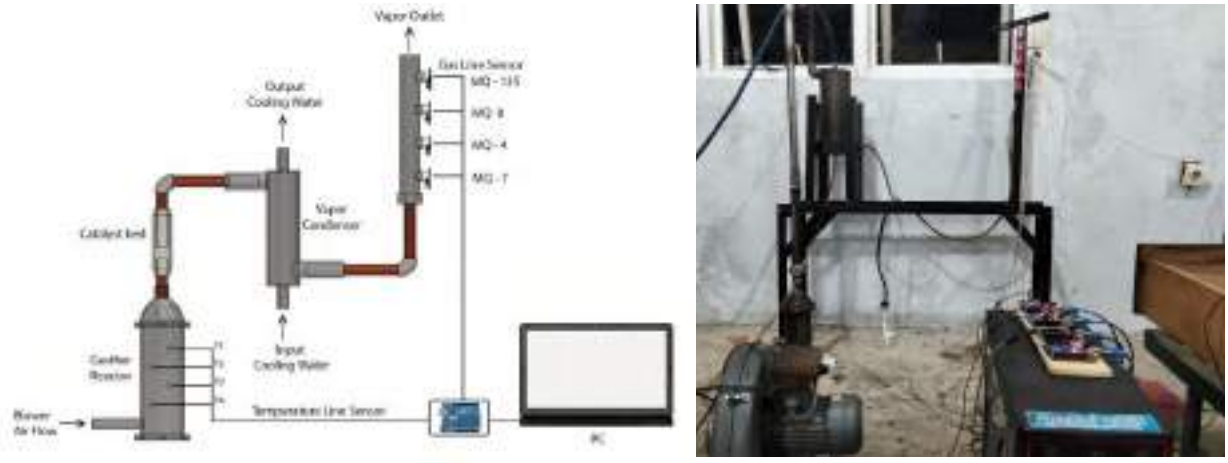
Corncob biomass was obtained from farmers in the South Malang region of East Java. Before use, the biomass was cleaned of impurities and dried in an oven for 6 hours at 100°C to remove moisture (water vapor) content. The ultimate and proximate test results are as follows.

There must be a reference to the table in the text before the table

Table 1
Ultimate And Proximate Test Corn Cob

Parameter	Units	Corn cobs
Moisture	%	6.3
Volatile matter	%	90.65
Fixed carbon	%	25.44
Ash	%	2.28
C	%	43.6

H	%	6.3
O	%	46.8
N	%	9.5
HHV	kJ/kg	17.61



a *b*

Fig. 1. Updraft gasifier: *a* – schematic experiment; *b* – experimental setup

This study used an updraft gasification reactor designed with a total height of 20 cm. The lower part of the reactor consisted of an ash container with a height of 5 cm, while the active reactor had a height of 15 cm and a diameter of 3 inches. The reactor was equipped with a 1-inch diameter air inlet pipe connected to a blower. The blower was modified with a potentiometer so that the air speed could be adjusted as needed. To monitor the thermal conditions inside the reactor, four 3 cm long type K thermocouples were installed at several different points so that the temperature profile in the gasification zone could be observed in more detail. Each test was conducted with a fixed biomass mass, a mixture of corn cobs weighing 80 grams. The reactor was made of iron and equipped with a gas seal to prevent leaks during the gasification process.

The gas produced by the reactor was fed into a condenser, which cooled the hot gas so that the water vapor components could be separated. The condenser was made of a copper spiral pipe with a diameter of ½ inch and a height of 30 cm. Cooling water was circulated from the bottom of the condenser and exited through the top to ensure efficient heat transfer. This cooling system was driven by a 60-watt water pump, ensuring stable water flow and optimal condensation. The catalyst was positioned downstream after the reactor, where it was supported on steel wool and wrapped with an 80-µm wire mesh to secure the catalyst and prevent particle carryover with the gas flow

To analyse the gas composition, four types of MQ gas sensors were used. The MQ-8 sensor was used to detect H_2, MQ-4 for CH_4, MQ-135 for CO_2 and MQ-7 for CO. Each gas sensor was calibrated according to the manufacturer's datasheet, specifically by determining the Ro value, which is the sensor resistance in clean air conditions. This

Ro value is used as a reference in calculating the measured gas concentration during the process [20, 21].

All data from the gas sensors and thermocouples were acquired using an Arduino Uno microcontroller. Each gas sensor is connected to a separate Arduino Uno to facilitate the calibration process and reduce the possibility of interference between sensors. Arduino is also used to record temperature data from four thermocouples installed in the reactor, so that gas composition and temperature distribution data can be obtained simultaneously.

The ER range of 0.2, 0.25, 0.3 and 0.35. The catalyst load was between 4%, 6%, 8% and 10% from the mass of input feedstock. The CaO/AC-PF ratio was varied between 0:1, 1:0, 1:1, and 2:1. Design of experiment can be seen in Table 2.

Table 2
Design of Experiment using

Run	Equivalence Ratio (E.R)	Catalyst Load %	CaO/AC
1	0.2	4	1:0
2	0.2	6	0:1
3	0.2	8	1:1
4	0.2	10	2:1
5	0.25	4	0:1
6	0.25	6	1:0
7	0.25	8	2:1
8	0.25	10	1:1
9	0.3	4	1:1
10	0.3	6	2:1
11	0.3	8	1:0
12	0.3	10	0:1
13	0.35	4	2:1
14	0.35	6	1:1
15	0.35	8	0:1
16	0.35	10	1:0

IT IS NOT CORRECT TO END THE SECTION WITH THE TABLE. WE NEED SOME KIND OF INTERPRETATION

5. Results (which one, what one?)

The title of the section should be specific and correspond to the essence of the article

Structure the "Research Results" section according to the objectives (Section 3).

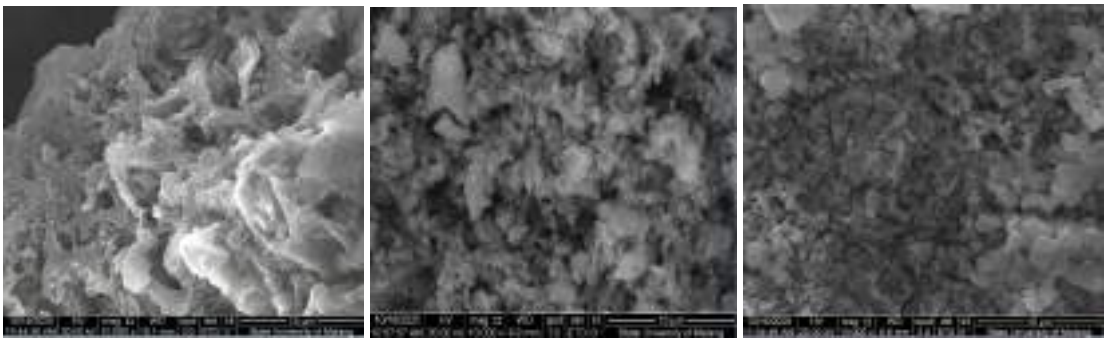
5. 1

5. 2

Each subsection should correspond to a specific task, showing exactly where each task begins and where each task ends.

5. 1. SEM Catalyst Result abbreviations in section names are not allowed

Fig. 2, *a* shows the image obtained from a Scanning Electron Microscope (SEM) with a magnification of 10,000× shows the surface morphology of palm fiber-based activated carbon (AC-PF). The surface structure appears porous and irregular, with a combination of void areas and layered surfaces. This characteristic indicates that the activation process that using KOH has successfully formed micropores and mesopores, which play an important role in increasing the specific surface area of activated carbon.



a *b* *c*

Fig. 2. SEM Catalyst Result: *a* – SEM AC-PF; *b* – SEM CaO:AC;1:1; *c* – SEM CaO:AC;2:1

abbreviations in the names of figures are not allowed

The rough and textured surface indicates that most of the material has undergone lignocellulose cell wall exfoliation, resulting in numerous interparticle gaps [22]. This porous structure greatly supports gas adsorption and diffusion capabilities when used as a catalyst in gasification or thermochemical reactions.

The presence of 1–5 μm voids indicates that most pores are in the mesopore category, supporting the adsorption of gas molecules such as H_2, CO, and tar during the gasification reaction [23].

The morphology of AC-PF shows the characteristics of porous activated carbon with a heterogeneous pore distribution, where the pores allow increased contact between gas reactants and active sites on the material surface, thereby increasing catalytic efficiency and the ability to absorb tar or CO_2 in biomass-based energy applications [24].

Fig. 2, *b* shows the surface morphology of the CaO:AC-PF catalyst with a ratio of 1:1. Visually, it can be seen that the surface of this material consists of fine particles

ranging in size from microns to submicrons that stick together to form a layered and slightly agglomerated structure.

The presence of fine, light-colored grains indicates an even distribution of CaO particles impregnated on the surface of activated carbon (AC-PF). This CaO distribution fills some of the pores of the carbon, resulting in a denser surface compared to pure AC-PF. However, there are still small gaps and voids between the grains, indicating that the microporous and mesoporous structures are still formed and can support catalytic activity [25].

This morphology illustrates the success of the CaO impregnation process on activated carbon from palm fiber, where the interaction between CaO and the carbon pore walls produces a composite material that is more thermally and chemically stable. This structure is highly conducive to catalyst applications in biomass gasification processes, as CaO particles can function as CO_2 absorbers while accelerating the tar reforming reaction [26].

Fig. 2, c shows the surface morphology of the CaO:AC-PF (2:1) catalyst. The image shows that the surface of the material is dominated by agglomerations of fine, round, and irregular particles ranging in size from microns to submicrons. Compared to the CaO:AC-PF (1:1) sample, this structure appears denser and tighter, indicating that an increase in the CaO ratio causes partial closure of the activated carbon surface pores by CaO particles.

The distribution of CaO particles appears more uniform and covers the carbon surface, indicating the successful impregnation of a larger amount of CaO. The light color in some areas indicates the presence of a calcium oxide phase that is strongly attached to the activated carbon matrix [27]. This structure indicates a strong interaction between CaO and AC-PF, forming a thermally stable composite.

Although some pores are covered, there are still microscopic gaps between the CaO grains that allow gas diffusion to occur, so that the catalyst retains its good adsorption capacity. The combination of the active area of CaO and the porous carbon structure makes this material very promising for biomass gasification or tar reforming applications, as CaO can act as a CO_2 absorber and increase the conversion of carbon to hydrogen gas.

5. 2. FTIR catalyst result abbreviations in section names are not allowed

The FTIR analysis results shown in the Fig. 3 reveal clear spectral differences between the AC-PF, CaO, and their mixtures (CaO:AC-PF) with ratios of 2:1 and 1:1. In the AC-PF spectrum, the absorption band at 2926 cm^{-1} is associated with the stretching vibration of the C–H group from –CH2 or –CH3 (methylene/methyl stretching), which indicates the presence of hydrocarbon chain residues from the lignocellulose structure. The peak at 1577 cm^{-1} indicates the presence of aromatic C=C or C=O stretching, while the band at 1056 cm^{-1} represents C–O stretching from alcohol or ether groups. In addition, the –OH group that appears in the 3500–3600 cm^{-1} region is identified as the result of AC-PF activation using a KOH solution, which causes the formation of

hydroxyl groups on the activated carbon surface. This –OH group plays an important role in increasing the surface activity and adsorption capacity of AC-PF as a catalyst support medium [28, 29].

In pure CaO, the intense band at 3639 cm^{-1} is associated with the stretching of the O–H group from $Ca(OH)_2$, which is formed due to the partial hydration of CaO when exposed to humid air. Meanwhile, the absorption bands at 1426 cm^{-1} and 876 cm^{-1} are associated with C–O stretching and CO_3^{2-} bending, respectively, indicating the formation of $CaCO_3$ due to CO_2 adsorption from the air. This shows that CaO is highly reactive to moisture and carbon dioxide in the environment.

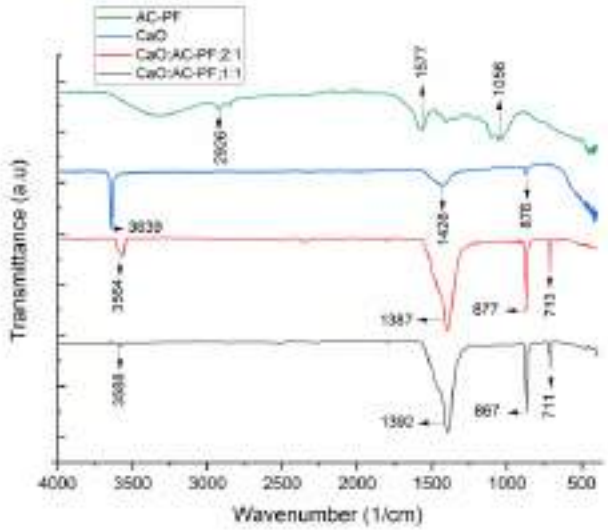


Fig. 3. FTIR Catalyst Result

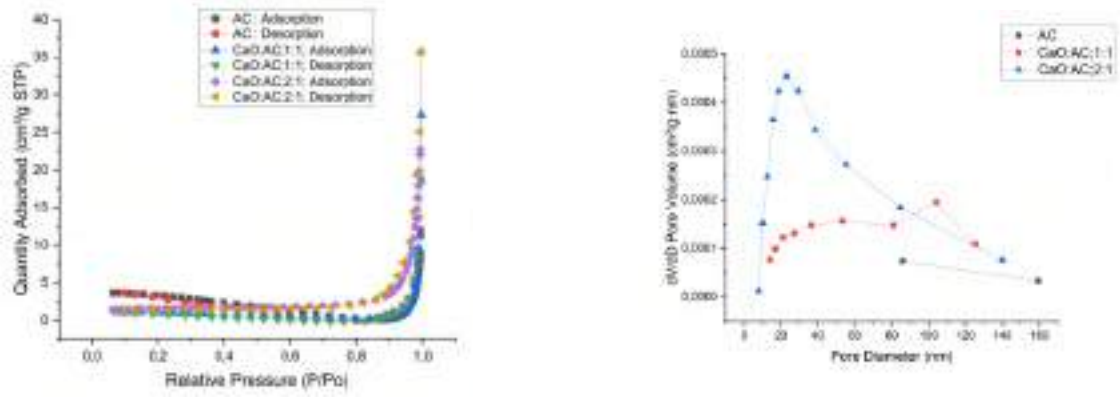
For the CaO:AC-PF (2:1), the main absorption bands were detected at 3564 cm^{-1} (O–H stretching from $Ca(OH)_2$ and the –OH group in AC-PF), 1387 cm^{-1} (C–O stretching), and 877 cm^{-1} and 713 cm^{-1} (bending vibration of CO_3^{2-}). This combination of bands indicates the formation of carbonate compounds ($CaCO_3$) due to the interaction between CaO and the oxygen groups of activated carbon. The presence of –OH groups from KOH activation also strengthens the basic properties on the surface, which can increase the chemical interaction between CaO and AC-PF[30].

At a CaO:AC-PF ratio of 1:1, the absorption bands at 3588 cm^{-1}, 1392 cm^{-1}, 867 cm^{-1}, and 711 cm^{-1} show a similar pattern, indicating the presence of hydroxyl (O–H) and carbonate (CO_3^{2-}) groups. The difference in peak intensity compared to the 2:1 ratio indicates variations in the level of interaction between CaO and the –OH groups resulting from KOH activation on AC-PF, which affects the formation of carbonate-hydroxide complexes on the material surface[31].

5. 3. BET Catalyst Result

Fig. 4 shows the adsorption–desorption isotherm curves for nitrogen for the AC, CaO:AC (1:1), and CaO:AC (2:1) samples are shown in Fig. 4. All three samples exhibit type IV isotherms with clear hysteresis loops at relatively high pressures (P/Po > 0.9). Based on the IUPAC classification, this characteristic indicates that the material has a mesoporous structure formed through capillary condensation within the pore channels. The difference between the adsorption and desorption pathways indicates that the pore shape is not perfectly cylindrical, but rather tends to be irregular or slit-like, which is commonly found in modified activated carbon materials[32].

The pure activated carbon (AC) sample showed a relatively low nitrogen adsorption volume with a specific surface area of 24.51 m^2/g and an average pore diameter of 0.74 nm, indicating a predominance of microporous structures. In the CaO:AC (1:1) composite, the surface area did not change significantly compared to pure AC, indicating that the addition of a moderate amount of CaO did not cover the carbon pores much, but only adhered to the external surface of the carbon matrix [33].



a *b*

Fig. 4. BET Result: *a* – AC Surface Analysis Adsorption Desorption Isotherm; *b* – BJH Adsorption Pore Size Distribution

Conversely, in the CaO:AC (2:1) mixture, there was a sharp increase in adsorption volume at relatively high pressure (P/Po > 0.9) to around 35 cm^3/g STP, while the BET surface area decreased dramatically to 5.06 m^2/g, and the pore diameter increased to 22.87 nm.

These changes in isotherm shape and pore size increase indicate that CaO impregnation not only modifies the surface chemistry but also significantly alters the pore structure of activated carbon. This transformation is positive in the context of catalytic applications in biomass gasification processes, as the mesoporous structure can enhance gas diffusion and accessibility to active sites during the tar reforming and water-gas shift reactions. Thus, even though the specific surface area decreases, the increase in mesoporousness and pore connectivity can actually improve catalyst performance in hydrogen gas production[34].

Fig. 4, *b* shows the BJH pore size distribution curves that provide further insight into the textural evolution of the palm-fiber-based activated carbon after CaO impregnation. The pristine AC exhibits a relatively low dV/dD value and a broad contribution only at large pore diameters (>60 nm), indicating that its pore system is dominated by macropores with a limited amount of mesopores. Such a texture is less favourable for gas-solid reactions because the accessible surface area in the mesopore range (2–50 nm) is relatively small.

After CaO loading, the shape and intensity of the BJH curves change markedly. For CaO:AC = 1:1, the distribution shifts toward smaller pore diameters with a pronounced contribution in the mesopore region of approximately 15–60 nm. This behaviour shows that CaO impregnation partially reconstructs the carbon matrix, enlarging existing micropores and opening blocked pores to generate additional mesoporosity. The effect becomes even more evident at CaO:AC = 2:1, where the curve displays the highest dV/dD values and a distinct maximum centred at about 30–40 nm. The strong peak in this range confirms that a higher CaO loading promotes the development of well-defined mesopores while reducing the relative fraction of very large macropores.

Overall, the BJH analysis demonstrates that CaO acts not only as a reactive sorbent but also as a textural promoter for the palm-fiber AC. The increase in mesopore volume and the shift of the dominant pore size toward 20–40 nm are expected to facilitate the diffusion of gasifying agents and tar molecules, as well as to improve the accessibility of CaO active sites for CO_2 capture and reforming reactions. These features are therefore beneficial for enhancing the catalytic performance of the CaO/AC composite in biomass gasification toward H_2-rich syngas production.

5. 4. Effect of ER on Syngas Product

The composition of syngas from updraft gasification is greatly influenced by the Equivalence Ratio (ER), which is the ratio of the mass flow rate of air compared to the mass flow rate of corncob in the experiment compared to the stoichiometry of air required for complete combustion of corncob. In this study, the ER used was 0.2–0.35 with the following formula

All formulas must be typed in the MathType formula editor version 7 or earlier. If you don't have this version of MathType, then type the formulas in the built-in formula editor

$$ER = \frac{(\dot{m}_a/\dot{m}_{cc})_{exp}}{(\dot{m}_a/\dot{m}_{cc})_{stc}}$$

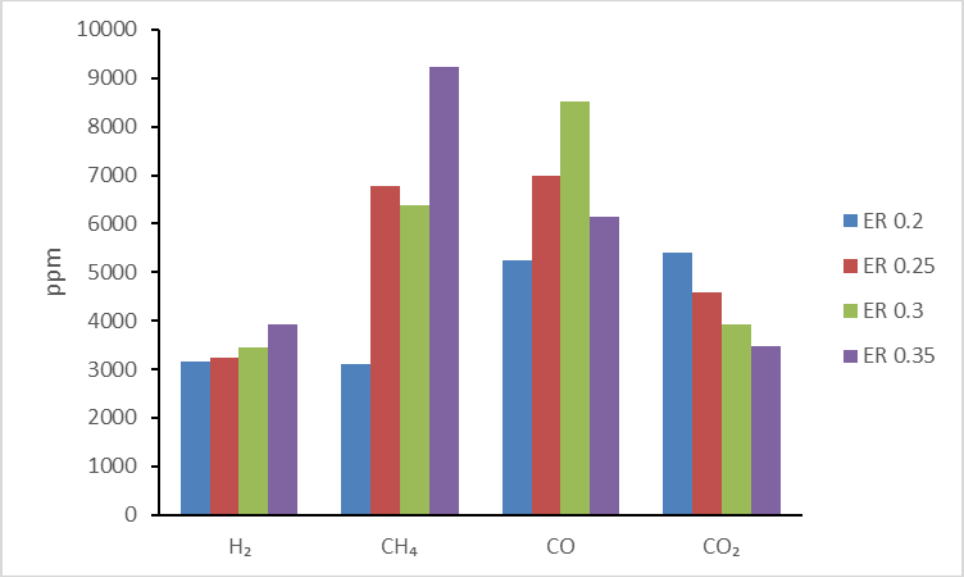


Fig. 5. Syngas Composition with Different ER

The graph above shows that the higher the ER, the higher the hydrogen composition produced. At ER 0.2, the ppm is 3150 ppm, at ER 0.25 it is 3241 ppm, at ER 0.3 it is 3457 ppm, and at ER 0.35 it is 3914 ppm. A higher oxidant supply promotes the formation of more stable autothermal conditions and higher reaction temperatures due to partial oxidation. This increase in temperature accelerates hydrogen-forming reactions, particularly the gasification of active carbon catalyst interactions with steam ($C + H_2O \rightarrow CO + H_2$), the reforming of volatile compounds/light hydrocarbons ($CxHy + H_2O \rightarrow CO + H_2$), and the cracking of tar/volatile into lighter gas species. At low ER, some volatiles tend to be incompletely converted and still have the potential to escape as condensable components, while increasing ER increases heat availability, making the conversion of volatiles into gas fractions (including H_2) more effective.

The higher the ER, the higher the CH4 composition produced. At ER 0.2, 3093 ppm was obtained, at ER 0.25 6767 ppm, ER 0.3 6377 ppm, and ER 0.35 9221 ppm. This trend indicates that the supply of oxidants not only increases autothermal conditions and the rate of devolatilization, but also shifts the reaction pathway towards the formation of light hydrocarbons through hydrogenation and/or methanation reactions in the reactor zone where the temperature still supports CH_4 formation. In particular, increased H_2 at higher ERs can promote the methanation reaction of CO ($CO + 3H_2 \rightleftharpoons CH_4 + H_2O$), so that CH_4 increases along with a tendency for CO to decrease at the highest ER. In addition, more intensive fragmentation of volatiles and tar at high ERs has the potential to produce light gas precursors which are then hydrogenated to CH_4.

CO formation increased up to an ER of 0.3 and decreased at an ER of 0.35. At an ER of 0.2, 5238 ppm was obtained, at an ER of 0.25, 6999 ppm, at an ER of 0.3, 8532 ppm, and decreased at an ER of 0.35 to 6145 ppm. At low ER (0.20–0.25), limited oxygen supply resulted in relatively low heat release, so that the reaction zone

temperature and char reactivity were not sufficient to intensify CO formation reactions, especially the Boudouard reaction ($C + CO_2 \rightleftharpoons 2CO$) and char gasification with steam ($C + H_2O \rightleftharpoons CO + H_2$). When the ER is increased towards 0.30, the increase in autothermal heat strengthens these reduction reactions, causing CO formation to increase and reach its peak. However, at higher ERs (0.35), the CO fraction tends to decrease because some CO can be converted to CH_4.

CO_2 formation continues to decrease as ER increases. At ER 0.2, 5412 ppm is obtained; at ER 0.25, 4592 ppm; at ER 0.3, 3916 ppm; and at ER 0.35, 3479 ppm. The increase in oxidant supply at this ER does not promote complete combustion, but rather strengthens the CO_2 reduction mechanism. At higher ERs, the heat generated from partial oxidation increases the temperature of the reduction zone, thereby accelerating the Boudouard reaction ($C + CO_2 \rightleftharpoons 2CO$), in which CO_2 is reduced by char to CO. This mechanism is consistent with the increase in CO until it reaches a maximum at an ER of 0.30, while also explaining the decrease in CO_2 under the same conditions. Interestingly, at an ER of 0.35, CO_2 remains at its lowest level even though CO decreases, indicating that the CO formed is not completely accumulated at the outlet but has the potential to undergo further conversion along the gas flow path.

5. 5. Effect of Catalyst Loading on Syngas Product

The catalyst load or amount of catalyst in this study was 4%, 6%, 8%, and 10% of the total biomass weight. The figure 6. shows that the composition of H_2 and CH_4 increases as the catalyst load decreases. The H_2 gas composition at catalyst loads of 4%, 6%, 8%, and 10% is 3742 ppm, 3471 ppm, 3372 ppm, and 3176 ppm, respectively. As the catalyst load increases, the reaction pathways that consume H_2 tend to strengthen, particularly the reverse water–gas shift ($CO_2 + H_2 \rightarrow CO + H_2O$) and H_2 interactions on the catalyst surface during the conversion of gasification compounds. As a result, even though reforming occurs, the measured net H_2 decreases because more H_2 is used for CO formation and surface reactions. The CH_4 gas composition at catalyst loads of 4%, 6%, 8%, and 10% was 7031 ppm, 6476 ppm, 6206 ppm, and 5746 ppm, respectively. An increase in catalyst load increases the number of active sites and gas-catalyst contact, so that methane/light hydrocarbon cracking and reforming occur more intensely. CH_4 then acts as a reactant that is converted into more reactive syngas components, causing the CH_4 concentration to decrease at higher catalyst loads.

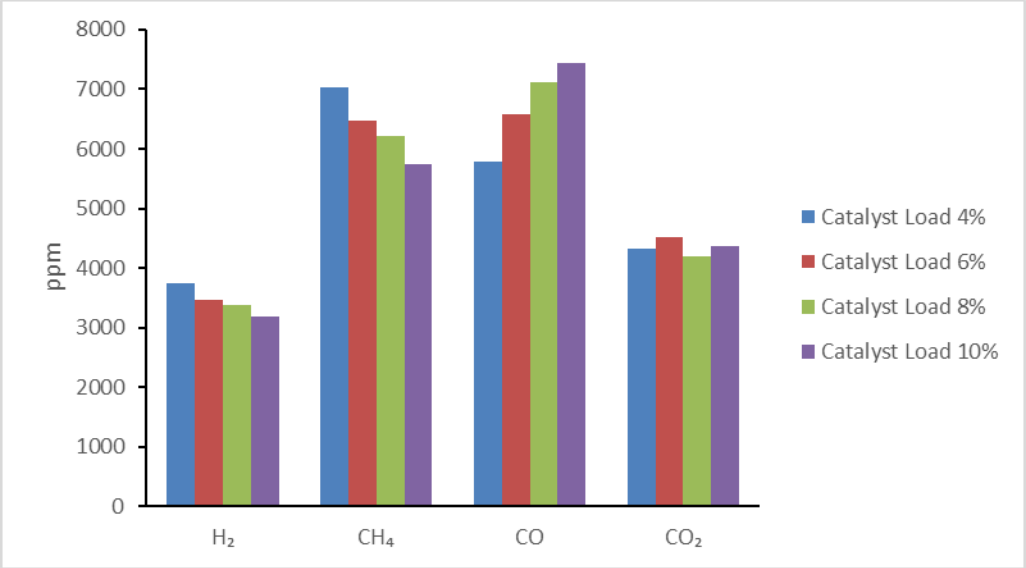


Fig. 6. Syngas Composition with Catalyst Load Variation

The CO gas composition increases with increasing catalyst load, namely for catalyst loads of 4%, 6%, 8% and 10% at 5782 ppm, 6576 ppm, 7111 ppm and 7445 ppm, respectively. The increase in catalyst loading strengthens the CO-forming reactions, particularly dry reforming ($CH_4 + CO_2 \rightarrow 2CO + 2H_2$), char–$CO_2$ reaction ($C + CO_2 \rightarrow 2CO$), and reverse water-gas shift. This combination shifts the product selectivity towards CO, so that the CO fraction increases consistently as the catalyst is increased. The CO_2 gas composition tends to stagnate with increasing catalyst loading, at catalyst loads of 4%, 6%, 8%, and 10% at 4322 ppm, 4510 ppm, 4198 ppm, and 4369 ppm, respectively. CO_2 shows minor changes because it is in a searching for a chemical equilibrium between the partial oxidation and the dry reforming. When the catalyst load increases, the rate of CO_2 consumption may rise, but this is often offset by CO_2 formation in the reaction zone, so that the CO_2 value appears stable or only fluctuates.

5. 6. Effect of Catalyst Ratio on Syngas Product

At a catalyst load of 4%, the CaO/AC ratio changes the gasification reaction through differences in the dominance of tar cracking/reforming and CO_2 capture by CaO, so that the gas composition is highly dependent on the number of active sites and the effectiveness of gas-catalyst contact. At 0:1 (AC), CH_4 and CO are relatively high because AC promotes volatile/tar cracking, but CO_2 remains high because there is no absorption. At 1:0 (CaO), CH_4 decreases but CO_2 is highest, indicating that CO_2 capture is not yet effective due to limited surface area/carbonate layer formation. The 1:1 ratio produces the highest CO with moderate CO_2, indicating CaO–AC synergy that increases the conversion of volatiles into reactive gases. Meanwhile, the 2:1 (CaO-rich) ratio provides the highest H_2 and lowest CO_2 due to the sorption-enhanced effect of CaO, but

CH_4 remains high due to the smaller contribution of AC, so methane reforming/cracking is not yet optimal.

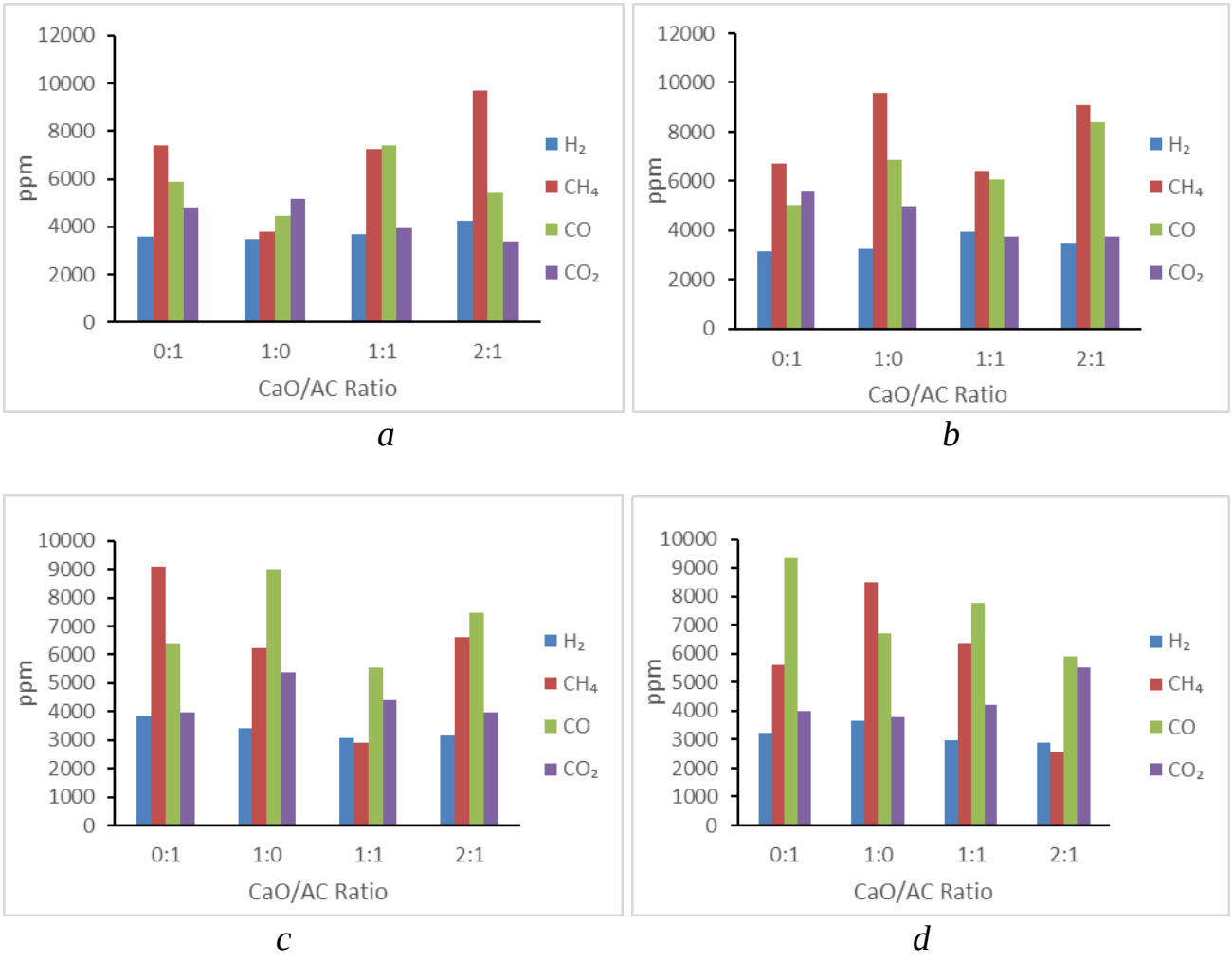


Fig. 7. Effect CaO/AC ratio with various catalyst load: *a* – 4%, *b* – 6%, *c* – 8%, *d* – 10%

At a catalyst load of 4%, the CaO/AC ratio changes the gasification reaction through differences in the dominance of tar cracking/reforming and CO_2 capture by CaO, so that the gas composition is highly dependent on the number of active sites and the effectiveness of gas-catalyst contact. At 0:1 (AC), CH_4 and CO are relatively high because AC promotes volatile/tar cracking, but CO_2 remains high because there is no absorption. At 1:0 (CaO), CH_4 decreases but CO_2 is highest, indicating that CO_2 capture is not yet effective due to limited surface area/carbonate layer formation. The 1:1 ratio produces the highest CO with moderate CO_2, indicating CaO–AC synergy that increases the conversion of volatiles into reactive gases. Meanwhile, the 2:1 (CaO-rich) ratio provides the highest H_2 and lowest CO_2 due to the sorption-enhanced effect of CaO, but

CH_4 remains high due to the smaller contribution of AC, so methane reforming/cracking is not yet optimal.

At a catalyst load of 6%, the CaO/AC ratio mainly shifts the selectivity of secondary reactions (tar cracking/reforming and CO_2 capture), where AC enhances the conversion of volatiles/light hydrocarbons, while CaO reduces CO_2 through carbonation ($CaO + CO_2 \rightarrow CaCO_3$) and changes the reaction equilibrium. At 0:1, CH_4 and CO_2 remain high because there is no CO_2 capture and methane reforming is not yet optimal, so volatiles still escape as CH_4. At 1:0, CO_2 tends to decrease, but CH_4 becomes the highest due to the absence of AC's role in cracking/reforming. The most favorable conditions occur at 1:1, with the highest H_2 and lowest CO_2, indicating CaO–AC synergy that promotes sorption-enhanced reforming and increases the conversion of hydrocarbons into syngas components. At 2:1, CO is highest and CO_2 remains low, but CH_4 rises again and H_2 is not maximized because excess CaO has the potential to rapidly carbonate/cause contact limitations, thereby reducing the contribution of AC in cracking/reforming.

At a catalyst load of 8%, the CaO/AC ratio significantly shifts the selectivity of the syngas reaction. At 0:1 (AC), CH_4 is still high because some light hydrocarbons have not been fully converted even though the tar cracking process is already active. At 1:0 (CaO), CO increases the most, but CO_2 also tends to be high, indicating that CaO in this condition is more dominant in promoting the CO formation pathway, while the CO_2 capture function is not yet optimal due to contact limitations or carbonation saturation. The 1:1 ratio produces the lowest CH_4, indicating the most effective CaO–AC synergy for cracking/reforming light hydrocarbons so that more methane is converted into reactive gas. At 2:1, CO increases again but CH_4 also rises, indicating that a smaller AC fraction reduces the intensity of methane reforming/cracking, while the decrease in CO_2 remains dependent on the effectiveness of CaO sorption.

At a catalyst load of 10%, the increase in total catalyst makes secondary reactions (tar cracking/reforming, solid-gas heterogeneous reactions, and equilibrium shifts) very dominant, so that the CaO/AC ratio mainly determines the direction of product selectivity. At 0:1 (AC), CO formation tends to be strongest because the porous carbon surface accelerates the cracking/reforming of volatiles and the conversion of tar into reactive gases. At ratios involving CaO (1:0, 1:1, 2:1), CaO can retain CO_2 through carbonation, but at high loads the effect is often non-linear because CaO rapidly carbonates/diffusion limitations and pore blocking occur, so that under CaO-rich conditions (2:1) CH_4 can decrease, but CO_2 may increase and H_2 is not maximized due to reaction competition. Overall, at a 10% load, a trade-off is observed: AC-dominant increases CO, while CaO-dominant suppresses light hydrocarbons but has the potential to trigger non-ideal conditions (saturation/mass transport) that reduce the benefits of H_2 and CO_2.

5.7 LHV Syngas

To calculate the LHV of syngas, it must first be converted from ppm to % volume of gas. The formula is $\%vol_i = \frac{ppmv_i}{10^4}$. To calculate the LHV, use the formula

$$LHV_{mix}\left(\frac{MJ}{Nm^3}\right) = \frac{10{,}8(\%H_2) + 12.63(\%CO) + 35.8(\%CH_4)}{100}$$

LHV H_2 = 10.8 MJ/Nm^3

LHV CO = 12.63 MJ/Nm^3

LHV CH_4 = 35.8 MJ/Nm^3

There must be a reference to the Fig. 8 in the text before the Figure

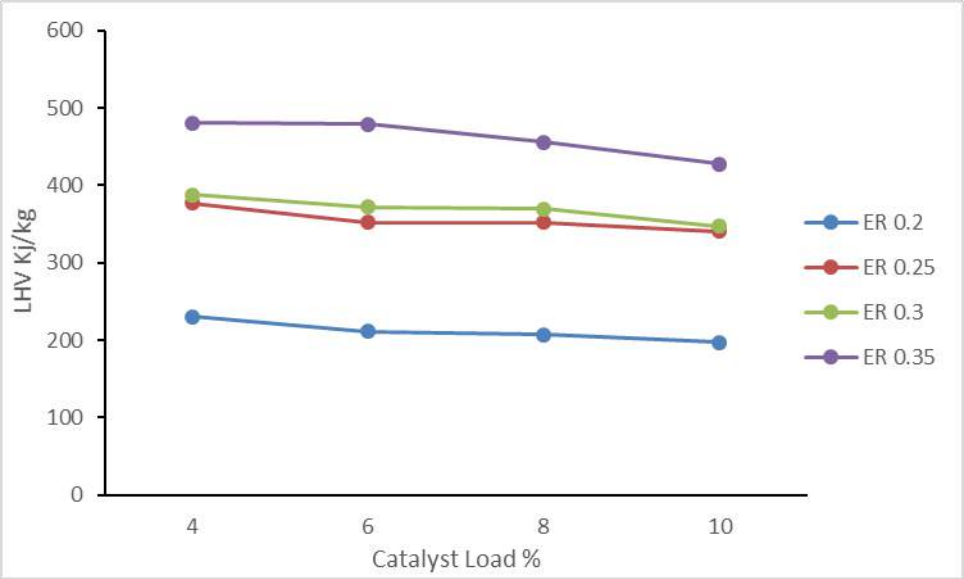


Fig. 8. LHV syngas with various ER

Fig. 8 shows that the LHV value increases with the ER, where a higher ER produces more intense autothermal conditions, causing the reactor temperature to rise. This increase in temperature accelerates the decomposition of volatiles and tar cracking, and promotes more complete gasification and reforming reactions, thereby increasing the fraction of permanent gases that contribute to the calorific value (mainly CO and CH_4, as well as some H_2). In addition, the increase in temperature is also associated with more effective hydrogen formation, because H_2 formation reactions (e.g., through steam-water and reforming reactions) are generally more optimal at high temperatures, with the temperature range often reported to be most conducive to H_2 formation being 800–1000°C.

However, all ER values show that LHV tends to decrease when the catalyst load is increased from 4% to 10%. This decrease indicates that excessive catalyst addition

under these operating conditions does not always improve gas energy quality, because the catalyst can shift the reaction selectivity towards the conversion of high calorific components especially CH_4 into CO and H_2 through reforming, while at the same time the fraction of diluent gases such as CO_2 (and steam) may increase due to reaction. Since CH_4 has a very large calorific value contribution in the syngas mixture, the decrease in its fraction is often more dominant than the increase in CO/H_2, so that the total LHV tends to decrease.

There must be a reference to the Fig. 9 in the text before the Figure

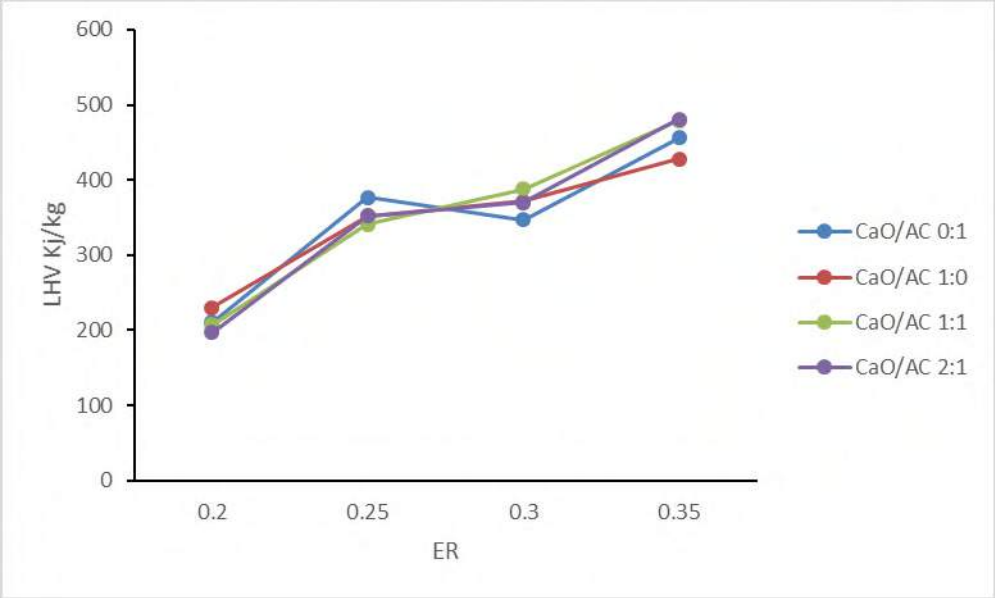


Fig. 9. LHV Syngas with Various CaO/AC Ratio

Fig. 9 shows that the LHV of syngas increases consistently with the increase in ER 0.2 to 0.35 for all CaO/AC ratios, indicating that a higher ER strengthens autothermal conditions so that the reaction temperature increases and the conversion of volatiles into syngas becomes more complete. At low ER (0.2), the difference in LHV between ratios is still small because secondary reactions such as cracking, reforming and heterogeneous reactions are not yet dominant; the system is still relatively influenced by incompletely converted volatiles. When the ER is increased to 0.25–0.30, the effect of the catalyst ratio becomes apparent: compositions involving AC tend to produce higher LHV because they accelerate tar cracking and increase the fraction of calorific gas, while the contribution of CaO can shift the reaction equilibrium through a decrease in CO_2. At the highest ER (0.35), the LHV reaches its maximum at all ratios, with CaO/AC 2:1 and 0:1 showing peak values, indicating that at high temperatures, the reactive gas formation pathway (via cracking/reforming on the carbon surface and/or CaO-rich-promoted heterogeneous reactions) becomes dominant. Overall, ER acts as the main controlling factor for LHV increase through the temperature effect, while the CaO/AC ratio

modulates LHV through the balance between cracking/reforming (AC) and CO_2 control (CaO), especially at medium-high ER.

6. Discussion **The title of the section should be specific and correspond to the essence of the article**

The section is structured like this:

Answer the question, what explains the results obtained? When answering this question, it is necessary to refer to those objects in the article, which display the discussed result. Such objects are formulas, figures, tables.

What are the peculiarities of the proposed method and the obtained results in comparison with the existing ones (it is necessary to make a comparison with the known data, indicating the references to the relevant works of colleagues)

What limitations are inherent in the given research (in general it can be: the applicability limits of the proposed solutions / results obtained, the applicability conditions of the proposed solutions / results obtained, reproducibility of the results / methods of obtaining results, stability of solutions to the change of influencing factors, the range of input data within which the results are adequate and can be reproduced, leading to the stated effects, etc.)

What disadvantages of this study can be noted and how they can be eliminated in the future. Warning. Disadvantages and limitations are not the same thing

What might be the development of this study and what difficulties (mathematical, methodological, experimental, or any other) might be encountered along the way?

The characteristics of AC-PF-based catalysts (activated carbon from palm fiber) show a rough, porous surface that supports tar/volatile adsorption and increases the chances of heterogeneous reactions (cracking/reforming) on the catalyst surface. This porous structure is crucial in updraft gasification because pyrolysis gases and volatiles move through the bed, so the presence of porous media has the potential to strengthen secondary reactions before the gas exits to the condenser. After the addition of CaO, CaO particle dispersion was observed on the carbon surface; however, at high CaO ratios (e.g., 2:1), the structure became denser, indicating that some of the micropores were closed. Nevertheless, BET data reveal an important phenomenon: the surface area decreases, but the pore diameter increases to the mesopore scale, which can improve the accessibility of tar/volatiles to active sites and improve mass transport in the reforming reaction. From a surface chemistry perspective, FTIR indicates the presence of –OH groups and Ca carbonate, confirming that CaO acts not only as a base catalyst but also as a CO_2 sorbent, enabling a sorption-enhanced mechanism that modulates the gasification reaction equilibrium [35].

On the process side, ER emerges as the dominant variable governing autothermal conditions, primarily through increases in effective temperature and secondary reaction intensity. An increase in ER from low to high levels consistently increases H_2, which can be explained by the acceleration of H_2 formation reactions such as char gasification

with steam ($C + H_2O \rightarrow CO + H_2$) [36], light hydrocarbon reforming, and more intense tar cracking at higher temperatures. At the same time, CH_4 also increases sharply at high ER, indicating that in updraft autothermal systems, increased temperature and changes in gas composition can facilitate the formation of light gases. Meanwhile, CO tends to peak at medium ER and then decreases at higher ER, consistent with competition between CO formation against CO consumption through subsequent reactions such as methanation [37]. The decrease in CO_2 at high ER indicates the role of high temperatures in enhancing the CO_2 reduction reaction by char (Boudouard) and/or the role of CaO sorption when available.

The effect of catalyst loading shows that adding catalyst does not always increase H_2. An increase in catalyst loading from low to high levels tends to decrease H_2 and CH_4 but increase CO. Mechanistically, this condition can occur when the catalyst strengthens pathways that increase CO and/or promotes RWGS ($CO_2 + H_2 \rightarrow CO + H_2O$)[38], which consumes H_2 so that net H_2 decreases. Additionally, at high catalyst loading, the possibility of diffusion/agglomeration penalties increases, so that selectivity may shift and some active sites become less effective. Thus, the target of H_2-rich syngas in this reactor is more dependent on ER adjustment and the selection of moderate/lower catalyst loading, rather than simply increasing the loading.

The CaO/AC-PF ratio exhibits synergistic but non-linear behaviour. AC-PF primarily acts as a porous medium that enhances cracking/reforming of volatiles, while CaO provides both basic sites and CO_2 sorbents to shift the equilibrium. At high CaO ratios, the sorption and base effects may increase, but the risk of micro-pore closure and diffusion pathway changes also increases. This explains why certain compositions are optimal at certain catalyst loads: the best performance arises from a balance between pore accessibility the role of AC-PF and sorption/base strength the role of CaO.

From an energy quality perspective, the LHV value of syngas is highly sensitive to changes in CH_4. Therefore, high ER conditions that increase CH_4 tend to increase LHV. However, the interpretation of LHV needs to be read in conjunction with the process objective, because an increase in LHV is not always synonymous with an increase in syngas quality for all applications.

However, there are several limitations. First, the gas composition is obtained from ppm-based MQ sensors, so absolute accuracy can be affected by cross-sensitivity, humidity, sensor drift, and gas sampling temperature; this can affect %vol and LHV estimates, especially when CO and CH_4 changes occur simultaneously. Second, catalyst characterization (SEM-FTIR-BET) already supports the role of surface texture and chemistry, but has not yet quantified active phase changes during operation. carbonation levels, and activity decline due to fouling/pore closure

Based on these limitations, several directions for future work are recommended. Perform gas composition calibration/validation using GC-TCD/GC-FID or micro-GC to convert sensor readings into more accurate %vol and include LHV uncertainty analysis. Evaluate catalyst stability and regeneration, particularly for easily carbonated CaO, through carbonation-calcination cycle tests and post-reaction characterization

(XRD/TGA/SEM-EDX) to assess phase changes and activity loss. Develop experimental designs towards ANOVA interactions or RSM so that interaction effects and predictive models can be obtained and validated through replication confirmation tests. Add process performance metrics such as gas yield (Nm^3/kg), cold gas efficiency, pressure drop, and air consumption so that "syngas quality improvement" can be demonstrated on the basis of mass-energy balance and operability, not just composition.

7. Conclusion

1. AC-PF with rich -OH group acts as a porous catalytic medium that facilitates volatile cracking and supports the reduction of condensable by-products, while CaO contributes to absorb CO_2. The BJH analysis confirms that CaO plays a dual role as a reactive sorbent and a textural promoter in palm-fiber activated carbon by enlarging mesopores (20–40 nm), thereby enhancing gas diffusion and improving access to CaO active sites, which ultimately strengthens catalytic performance.

2. Increasing ER to 0.35 enhances the combustible gas fraction H_2 and CH_4 and suppresses CO_2, whereas CO typically peaks at intermediate ER due to competing CO formation and consumption reactions along the updraft reaction zones. Increasing catalyst loading shifts syngas composition: CO increases, while H_2 and CH_4 decrease, indicating changes in dominant secondary reactions and possible diffusion or agglomeration limitations at higher loadings. Increasing ER lead to increase LHV syngas, but it can decrease at high catalyst loading. An increase in the CaO/AC ratio to 2:1 resulted in a higher syngas LHV, with a maximum value of 481 kJ/kg.

Conflict of interest

The authors declare that they have no conflict of interest in relation to this research, whether financial, personal, authorship or otherwise, that could affect the research and its results presented in this paper.

Financing

The authors sincerely thank the Ministry of Education, Culture, Research and Technology, Republic of Indonesia for fully supporting this research through the DRTPM Research Grant under Fundamental Research, Universitas Widyagama Malang, Indonesia 2025 (Grant Number:128/C3/DT.05.00/PL/2025;023/LL7/DT.05.00/PL/2025;010/ Kontrak/PT/PTS.030.7/PN/V/2025).

Data availability

Manuscript has no associated data.

Use of artificial intelligence

The authors declare that generative artificial intelligence tools were used exclusively for language editing, grammar checking, and technical formatting of the

manuscript under full human control. Artificial intelligence was not used to generate, process, or interpret scientific data, form conclusions, or other ele-ments of the scientific results in the paper. Tool used: ChatGPT (OpenAI GPT-5.2, version 2026). The authors bear full responsibility for the content, reli-ability, and scientific correctness of the submitted material.

Example:

It is necessary to declare the use of AI according to the scheme:

– model and number of AI,

– where exactly it was used (in which section of the article),

– what exactly was done using AI tools (specific description),

– how the authors checked the results provided by AI tools,

– how the result provided by the AI tool influenced the conclusions of the study.

Warning:

1. In the process of finalizing the manuscript based on the comments of editors and reviewers, the use of AI tools **is possible only if the permissible scope and tasks are observed** https://journals.uran.ua/eejet/artificial-intelligence

2. Detection of undeclared use of AI and/or use of AI outside the permissible tasks delegated to AI or the scope https://journals.uran.ua/eejet/artificial-intelligence

at the review stage or after it as part of quality assurance and ethical standards control will lead to the manuscript being withdrawn from consideration / removed from the editorial portfolio, and sanctions provided for by the License Agreement.

Acknowledgements

We as the Research Team would like to thank Ministry of Education, Culture, Research and Technology, Republic of Indonesia (Kemendiktisaintek Indonesia) for financing research activities.

Authors' contributions

Indicate the author's contribution according to CRediT (Author Role Taxonomy) in the format:

Author1 first name last name: contribution1, contribution2, contribution3; **Author2 first name last name**: contribution1, contribution2, contribution3

In this section, you should only indicate the name of the contribution, which must be selected from the list of contributions on the CRediT (Author Role Taxonomy)

We ask authors of the article in the literature to highlight (in purple color) references to articles in Scopus journals (Q1, Q2). If there is no reference, it should be

added by all means.

References

Please check, self-citation should not exceed 30 %.

If possible, please provide active hyperlinks to the entire list of literature.

1. ASEAN Statistical Brief, "Role of Agriculture , Forestry , and Fishing Industry in ASEAN Economy," vol. VII, no. June 2023, p. 511191, 2024.
2. V. K. Yadav *et al.*, "Emerging trends in the valorization of agricultural waste and their utilization in agricultural, pharmaceuticals, and environmental cleanup," *Waste and Biomass Valorization*, pp. 1–55, 2025.
3. W. M. Lewandowski, M. Ryms, and W. Kosakowski, "Thermal biomass conversion: A review," *Processes*, vol. 8, no. 5, p. 516, 2020.
4. D. Ariyanti *et al.*, "Valorization of corn cob waste for furfural production: A circular economy approach," *Biomass and Bioenergy*, vol. 194, p. 107665, 2025.
5. A. Raizada, A. Shukla, S. Yadav, P. Katiyar, and R. Kumar, "Enhancement of H2 production via catalytic steam gasification of food waste as feedstock and its ash as a support and promoter for Ni catalyst," *Int. J. Hydrogen Energy*, vol. 60, pp. 272–281, 2024.
6. Y. Dai *et al.*, "Co-gasification characteristics of Ca-rich sludge and Fe-rich sludge under CO2 atmosphere, and potential utilization of gasification residues as renewable catalyst in biomass pyrolysis," *Renew. Energy*, vol. 224, p. 120118, 2024.
7. H. Sun *et al.*, "Three-stage behaviors of K2CO3 catalyst during CO2 catalytic gasification of coal," *Fuel*, vol. 367, p. 131149, 2024.
8. J. Zhang, Z. Chu, R. Cao, X. Wu, and K. Han, "A review of resource recovery from waste plastics via pyrolysis and gasification," *Fuel*, vol. 404, p. 136319, 2026.
9. Y. Tangke Tosuli, Cahyadi, H. Dafiqurrohman, R. Hermawan, and A. Surjosatyo, "Gasification of sago dreg waste in a top-lit updraft fixed bed gasifier: Syngas composition and its effect with additional Al2O3 as catalyst," *Energy Convers. Manag. X*, vol. 24, no. October, p. 100775, 2024, doi: 10.1016/j.ecmx.2024.100775.
10. P. Dinh *et al.*, "Enrichment of hydrogen in product gas from a pilot-scale rice husk updraft gasification system," *Carbon Resour. Convers.*, vol. 5, no. 3, pp. 231–239, 2025, doi: 10.1016/j.crcon.2022.07.003.
11. S. Yousef and J. Eimontas, "International Journal of Hydrogen Energy Oxygen updraft gasification-catalytic reforming of cigarettes butts for hydrogen-rich syngas production," vol. 171, no. May, 2025, doi: 10.1016/j.ijhydene.2025.150650.
12. D. Contreras, E. Blanco, and D. Travieso, "Experimental assessment of the energy potential of pellets produced from beekeeping wastes by updraft gasification," vol. 343, no. January, 2025, doi: 10.1016/j.enconman.2025.120206.
13. N. Yesilova, O. Tezer, A. Ongen, and A. Ayol, "International Journal of Hydrogen Energy Enhancing biomass gasification : A comparative study of catalyst

applications in updraft and modifiable-downdraft fixed bed reactors," *Int. J. Hydrogen Energy*, vol. 76, no. April, pp. 290–303, 2024, doi: 10.1016/j.ijhydene.2024.05.075.

14. R. Skvor and A. Jan, "Experimental investigation of sorted municipal solid wastes producer gas composition in an updraft fixed bed gasifier," vol. 289, no. August 2022, 2024, doi: 10.1016/j.energy.2023.130063.

15. R. Junga, M. Tańczuk, S. Sobek, M. Chabiński, and Ł. Ziółkowski, "Effect of the addition of laying hens manure to the straw on gasification efficiency in updraft gasifier under air atmosphere," *Appl. Therm. Eng.*, vol. 226, no. February, p. 120269, 2023, doi: 10.1016/j.applthermaleng.2023.120269.

16. A. Ongen and A. Ayol, "ScienceDirect Gasification performance of olive pomace in updraft and downdraft fixed bed reactors," vol. I, 2023, doi: 10.1016/j.ijhydene.2023.02.088.

17. K. Ertas, "Gasification of MDF residue in an updraft fixed bed gasifier to produce heat and power via an ORC turbine," vol. 169, no. February, pp. 43–51, 2023, doi: 10.1016/j.wasman.2023.06.025.

18. S. Gorthy, S. Verma, N. Sinha, S. Shetty, H. Nguyen, and M. Neurock, "Theoretical Insights into the Effects of KOH Concentration and the Role of OH–in the Electrocatalytic Reduction of CO2 on Au," *ACS Catal.*, vol. 13, no. 19, pp. 12924–12940, 2023.

19] X. Wang, W. Zeng, C. Xin, X. Kong, X. Hu, and Q. Guo, "The development of activated carbon from corncob for CO2 capture," *RSC Adv.*, vol. 12, no. 51, pp. 33069–33078, 2022, doi: 10.1039/d2ra05979g.

20. D. Ali, H. Fakra, D. Armel, and S. Andriatoavina, "A simple and low-cost integrative sensor system for methane and hydrogen measurement," vol. 1, no. August, 2020, doi: 10.1016/j.sintl.2020.100032.

21. S. V. Co-digestion and H. Ram, "Assessment of a Low-Cost Hydrogen Sensor for Detection and Monitoring of Biohydrogen Production during Sugarcane," pp. 479–490, 2024.

22. H. Du *et al.*, "Lignocellulosic Films: Preparation, Properties, and Applications," *Chem. Rev.*, 2025.

23. S. De, A. M. Balu, J. C. Van Der Waal, and R. Luque, "Biomass-derived porous carbon materials: synthesis and catalytic applications," *ChemCatChem*, vol. 7, no. 11, pp. 1608–1629, 2015.

24. C. Li *et al.*, "Importance of oxidation reactions in creating pores in physical activation of biomasses," *Chem. Eng. J.*, vol. 474, p. 145748, 2023.

25. B. Zhou *et al.*, "Insights into effects of grain boundary engineering in composite metal oxide catalysts for improving catalytic performance," *J. Colloid Interface Sci.*, vol. 653, pp. 1177–1187, 2024.

26. Y. Zhu *et al.*, "Preparation of hierarchically porous carbon ash composite material from fine slag of coal gasification and ash slag of biomass combustion for CO2 capture," *Sep. Purif. Technol.*, vol. 330, p. 125452, 2024.

27. Y. Y. García-Guel, E. M. Múzquiz-Ramos, J. C. Ríos-Hurtado, A. Moreno-

Santos, S. E. Flores-Villaseñor, and G. B. Escalante-Ibarra, “Surface modification of activated carbon cloth with calcium silicate and hydroxyapatite: bioactive composite material,” *Heliyon*, vol. 8, no. 11, 2022.

28. M. Ilić *et al.*, “Surface functional groups and degree of carbonization of selected chars from different processes and feedstock,” *PLoS One*, vol. 17, no. 11, p. e0277365, 2022.

29. R. Ali, Z. Aslam, R. A. Shawabkeh, A. Asghar, and I. A. Hussein, “BET, FTIR, and RAMAN characterizations of activated carbon from waste oil fly ash,” *Turkish J. Chem.*, vol. 44, no. 2, pp. 279–295, 2020.

30. K. J. Stanienda-Pilecki, “The importance of Fourier-Transform Infrared Spectroscopy in the identification of carbonate phases differentiated in magnesium content,” 2019.

31. F. Dai, Q. Zhuang, G. Huang, H. Deng, and X. Zhang, “Infrared spectrum characteristics and quantification of OH groups in coal,” *ACS omega*, vol. 8, no. 19, pp. 17064–17076, 2023.

32. E. M. de Salazar Martínez, M. F. Alexandre-Franco, A. J. Nieto-Sanchez, and E. M. Cuerda-Correa, “Exploring the role of surface and porosity in CO2 capture by CaO-based adsorbents through response surface methodology (RSM) and artificial neural networks (ANN),” *J. CO2 Util.*, vol. 83, p. 102773, 2024.

33. J. A. Tavizón-Pozos, H. Cervantes-Cuevas, G. G. Garcia-Camacho, G. Chavez-Esquivel, and D. R. Acosta-Najarro, “Biodiesel Production Using K–Sr/CaO and CaO Catalysts Derived from Eggshells by Canola Oil Transesterification,” *ACS omega*, vol. 10, no. 7, pp. 6827–6838, 2025.

34. W. Koo-Amornpattana, P. Phadungbut, N. Kunthakudee, W. Jonglertjunya, S. Ratchahat, and M. Hunsom, “Innovative metal oxides (CaO, SrO, MgO) impregnated waste-derived activated carbon for biohydrogen purification,” *Sci. Rep.*, vol. 13, no. 1, p. 4705, 2023.

35. C. Quan, M. Wang, N. Gao, T. Yang, and R. Li, “In situ adsorption of CO2 to enhance biomass gasification for hydrogen production using Ca/Ni based composites,” *J. Energy Inst.*, vol. 108, p. 101229, 2023, doi: https://doi.org/10.1016/j.joei.2023.101229.

36. F. Micheli, E. Mattucci, C. Courson, and K. Gallucci, “Bi-Functional Catalyst/Sorbent for a H2-Rich Gas from Biomass Gasification,” 2021. doi: 10.3390/pr9071249.

37. M. Zhu, Q. Wang, and S. Wang, “Recent Advances and Future Perspectives in Catalyst Development for Efficient and Sustainable Biomass Gasification: A Comprehensive Review,” 2025. doi: 10.3390/su17167370.

38. N. Cerone, F. Zimbardi, L. Contuzzi, J. Baleta, and D. Cerinski, “Experimental investigation of syngas composition variation along updraft fixed bed gasifier,” *Energy Convers. Manag.*, vol. 221, no. July, p. 113116, 2020, doi: 10.1016/j.enconman.2020.113116.

Please fill in this table

Author's order	First Name	Middle name	Second Name
1			
2			
3			
4			
5			

We ask the authors indicate the Corresponding author in the information about the authors, after the full name (Corresponding author is the author who is in correspondence with the editors and whose email address will be indicated as feedback for readers if they want to contact the author/group of authors)

English

Purbo Suwandono
Master
Department of Mechanical Engineering
Widya Gama University
Borobudur str., 35, Mojolangu, Lowokwaru District, Malang City, East Java, 65142, Indonesia
The address of the university (in such sequence: street, house, city, country, index)
E-mail: purbo@widyagama.ac.id
ORCID: https://orcid.org/0000-0003-4085-1291
Contact phone: +6282132697144
Number of publications in national journals indexed (approximate; for Ukraine citizens only): -
Number of publications in international journals indexed (approximate): 14
H-index by Scopus (if available): 4
ResearchGate: https://www.researchgate.net/profile/Purbo-Suwandono
Scopus ID: 57204187970
Researcher ID: https://researchid.co/rid80879

Widya Wijayanti
PhD
Department of Mechanical Engineering
Brawijaya University
Veteran str., 10–11, Ketawanggede, Lowokwaru District, Malang City, East Java 65145, Indonesia
The address of the university (in such sequence: street, house, city, country, index)
E-mail: widya_dinata@ub.ac.id

ORCID: https://orcid.org/0000-0003-4215-5943
Contact phone: +6285334992164
Number of publications in national journals indexed (approximate; for Ukraine citizens only): -
Number of publications in international journals indexed (approximate): 78
H-index by Scopus (if available): 12
ResearchGate: https://www.researchgate.net/profile/Widya-Wijayanti
Scopus ID: 36006672800
Researcher ID: -

Nova Risdiyanto Ismail
Doctor
Department of Mechanical Engineering
Widya Gama University
Borobudur Str., 35, Mojolangu, Lowokwaru District, Malang City, East Java 65142, Indonesia
The address of the university (in such sequence: street, house, city, country, index)
E-mail: nova@widyagama.ac.id
ORCID: https://orcid.org/0000-0001-8439-6919
Contact phone:
Number of publications in national journals indexed (approximate; for Ukraine citizens only): -
Number of publications in international journals indexed (approximate): 7
H-index by Scopus (if available): 3
ResearchGate: https://www.researchgate.net/profile/Nova-Ismail-2
Scopus ID: 57204527065
Researcher ID: https://researchid.co/rid80876

Dzulfikar Johan Akbar
Master Student
Department of Mechanical Engineering
Brawijaya University
Veteran Str., 10–11, Ketawanggede, Lowokwaru District, Malang City, East Java 65145, Indonesia
The address of the university (in such sequence: street, house, city, country, index)
E-mail: johanakbar@student.ub.ac.id
ORCID: https://orcid.org/0009-0002-4652-8516
Contact phone: +6282241116998
Number of publications in national journals indexed (approximate; for Ukraine citizens only): -
Number of publications in international journals indexed (approximate): -

H-index by Scopus (if available): -
ResearchGate: https://www.researchgate.net/profile/Dzulfikar-Johan-Akbar
Scopus ID: -
Researcher ID: -

Muhammad Reza
Bachelor Student
Department of Mechanical Engineering
Widya Gama University
Borobudur Str., 35, Mojolangu, Lowokwaru District, Malang City, East Java 65142, Indonesia
The address of the university (in such sequence: street, house, city, country, index)
E-mail: muhapanjangreza@gmail.com
ORCID: https://orcid.org/0009-0009-9258-0586
Contact phone: +6282139682566
Number of publications in national journals indexed (approximate; for Ukraine citizens only): -
Number of publications in international journals indexed (approximate): -
H-index by Scopus (if available): -
ResearchGate: -
Scopus ID: -
Researcher ID: -

Please attach to the manuscript information about potential reviewers for the topic (at least 2 reviewers). The editor reserves the exclusive right to decide whether or not to use the services of the proposed reviewers. In either case, the editorial staff practices a double-blind review policy.
Example (Fields marked with an asterisk (*) are required.)
Name of reviewer *
Professor*
Tel:
E-mail: *
Work address:

REVISI REVIEW EDITOR

Received date: 20.02.2026
Accepted date:

UDC

ПОКРАЩЕННЯ ЯКОСТІ СИНТЕЗ-ГАЗУ ПРИ ВИСХІДНІЙ ГАЗИФІКАЦІЇ КУКУРУДЗЯНИХ КАЧАНІВ З ВИКОРИСТАННЯМ КАТАЛІЗАТОРА НА ОСНОВІ CAO/АКТИВОВАНОГО ВУГІЛЛЯ НА ПАЛЬМОВОМУ ВОЛОКН

Purbo Suwandono, Widya Wijayanti, Nova Risdiyanto Ismail, Dzulfikar Johan Akbar, Muhammad Reza

SYNGAS QUALITY IMPROVEMENT IN CORNCOB UPDRAFT GASIFICATION USING CAO/ACTIVATED CARBON PALM FIBER CATALYST

Purbo Suwandono, Widya Wijayanti, Nova Risdiyanto Ismail, Dzulfikar Johan Akbar, Muhammad Reza

Це дослідження зосереджується на поліпшенні якості синтез-газу, отриманого в результаті газифікації кукурудзяних качанів за допомогою висхідного потоку, з використанням подвійної каталітичної системи на основі CaO та активованого вугілля, отриманого з пальмового волокна (AC-PF). Основними досліджуваними робочими змінними були коефіцієнт еквівалентності (ER), навантаження каталізатора та співвідношення CaO/AC-PF (0:1, 1:0, 1:1 та 2:1). Характеристика каталізатора показує, що AC-PF забезпечує пористу структуру, яка покращує контакт газу з твердою речовиною та сприяє вторинним реакціям, тоді як включення CaO утворює композит із модифікованою структурою пор та поверхневими речовинами, пов'язаними з функцією сорбції CO_2. Експериментальні результати показують, що збільшення ER загалом підвищує частки H_2 та CH_4, одночасно зменшуючи CO_2, тоді як CO демонструє оптимальний результат при середньому ER, а потім зменшується при найвищому ER. Навпаки, більш високе навантаження каталізатора, як правило, зменшує H_2 і CH_4, але збільшує CO, що свідчить про зміну селективності вторинної реакції при більш інтенсивному каталітичному контакті. З енергетичної точки зору, LHV The abbreviations must be decrypted *синтез-газу збільшується з ER, але може знижуватися при більш високих навантаженнях каталізатора через зменшення внеску CH_4.*

Ключові слова: Газифікація висхідним потоком; Кукурудзяні качани; Синтетичний газ; Каталізатор CaO; Активоване вугілля

The sum of summary + keywords= should be 1800-1900 characters with spaces.

The summary should contain the following information:

- object of research

- problem that was solved

- results obtained

- brief interpretation of the results (what explains them)

- features and distinctive features of the results obtained, thanks to which they allowed to solve the problem under study

- the scope and conditions of practical use of the results obtained

This study focuses on improving syngas quality from corncob updraft gasification using a dual catalyst system based on CaO and palm-fiber-derived activated carbon (AC-PF). The main operating variables investigated were the equivalence ratio (ER), catalyst loading, and the CaO/AC-PF ratio (0:1, 1:0, 1:1, and 2:1). Catalyst characterization indicates that AC-PF provides a porous structure that enhances gas–solid contact and promotes secondary reactions, whereas CaO incorporation forms a composite with modified pore texture and surface species associated with CO_2 sorption functionality. Experimental results show that increasing ER generally raises the H_2 and CH_4 fractions while reducing CO_2, whereas CO exhibits an optimum at intermediate ER before decreasing at the highest ER. In contrast, higher catalyst loading tends to decrease H_2 and CH_4 but increase CO, suggesting a shift in secondary-reaction selectivity under more intensive catalytic contact. From an energy perspective, the syngas LHV increases with ER but may decline at higher catalyst loadings due to a reduced CH_4 contribution

Keywords: updraft gasification, corncob, syngas, CaO catalyst, activated carbon
10 words

Keywords are used to index jobs on electronic systems and the Internet. The better the keywords are chosen, the more people will be able to find the paper by typing in the same keywords as in the paper. This will increase the readability of the paper, and therefore the likelihood that the paper will be cited.

The main purpose of keywords is to allow you to quickly find an article on the desired topic.

Replace hyphens (-) with dashes (–) by text (except word combinations)

Анотація:

У цьому дослідженні вивчається можливість поліпшення якості синтез-газу, отриманого в результаті газифікації кукурудзяних качанів за допомогою системи з подвійним каталізатором на основі CaO та активованого вугілля з пальмового волокна (AC–PF). Основними проблемами є відносно низька теплотворна здатність синтез-газу з кукурудзяних качанів та висока вартість каталізаторів, що використовуються на даний момент. У цьому дослідженні в якості каталізаторів

використовувалися недорогий CaO та перероблені відходи пальмового волокна, перетворені на активоване вугілля. До досліджуваних робочих змінних належали коефіцієнт еквівалентності (0,2, 0,25, 0,3 та 0,35), навантаження каталізатора (4 %, 6 %, 8 % та 10 %) та масове співвідношення CaO/AC-PF (0:1, 1:0, 1:1 та 2:1).
Характеристика каталізатора показує, що AC-PF має пористу структуру, яка збільшує контакт газу з твердим тілом і сприяє вторинним реакціям, тоді як додавання CaO утворює композит із модифікованою структурою пор і поверхневими видами, пов'язаними з сорбцією CO_2. Експериментальні результати показують, що збільшення ER підвищує частку H_2 (ER 0,2: 3150 ppm, ER 0,35: 3914 ppm) і частку CH_4. Водночас частка CO_2 зменшилася. Тим часом CO показав оптимальне значення при ER: 0,3 ppm, перш ніж зменшитися при ER 0,35. І навпаки, збільшення навантаження каталізатора призводило до зменшення H_2 (4%: 3742 ppm, 10%: 3176 ppm) і CH_4, але збільшувало CO. З енергетичної точки зору, нижча теплота згоряння синтез-газу збільшується із збільшенням ER, але може зменшуватися при більш високих навантаженнях каталізатора через зменшення внеску CH_4.
Сильна сторона цього дослідження полягає у функціональній синергії між пористим AC-PF та поліпшенням якості сорбції CO_2 на основі CaO, завдяки чому можна досягти поліпшення якості синтез-газу за допомогою поєднання каталітичних та сорбційних ефектів в одній системі. Результати цього дослідження можуть бути застосовані до невеликих установок газифікації біомаси, зокрема до реакторів з висхідним потоком для відходів кукурудзяних качанів.
Ключові слова: газифікація, висхідний потік, кукурудзяні качани, синтетичний газ, CaO, активоване вугілля, пальмове волокно, низька теплотворна здатність, коефіцієнт еквівалентності, навантаження

Abstract:
This study investigates improving the quality of syngas from updraft corn cob gasification using a dual catalyst system based on CaO and activated carbon from palm fiber (AC–PF). The main problems encountered are the relatively low heating value of corn cob syngas and the high cost of the catalysts currently in use. In this study, inexpensive CaO and processed palm fiber waste into activated carbon were used as catalysts. The operating variables studied included the equivalence ratio (0.2, 0.25, 0.3, and 0.35), catalyst loading (4%, 6%, 8%, and 10%), and the CaO/AC-PF mass ratio (0:1, 1:0, 1:1, and 2:1).
Characterization of the catalyst shows that AC-PF has a porous structure that increases gas–solid contact and promotes secondary reactions, while the addition of CaO forms a composite with a modified pore texture and surface species associated with CO_2 sorption. Experimental results show that an increase in ER raises the H_2 fraction (ER 0.2: 3150 ppm, ER 0.35: 3914 ppm) and CH_4 fraction. Meanwhile, the CO_2 fraction decreased. Meanwhile, CO showed an optimum value at ER: 0.3 ppm before decreasing at ER 0.35. Conversely, an increase in catalyst loading tended to decrease H_2 (4%: 3742

ppm, 10%: 3176 ppm) and CH_4 but increases CO. From an energy perspective, the Lower Heating Value of syngas increases with increasing ER, but may decrease at higher catalyst loadings due to the reduced contribution of CH_4.

The strength of this research lies in the functional synergy between porous AC-PF and CaO-based CO_2 sorption quality improvement, so that syngas quality improvement can be achieved through a combination of catalytic and sorption effects in a single system. The results of this study have the potential to be applied to small scale biomass gasification units, particularly updraft reactors for corn cob waste.

Keywords: gasification, updraft, corncob, syngas, CaO, activated carbon, palm fiber, low heating value, equivalence ratio, load

1. Introduction

Indonesia is one of the largest corn producers in Southeast Asia, with national production reaching more than 18 million tons of dry kernels per year. Of this amount, about 15–20% is cobs after the kernel removal process, resulting in a very large amount of corn cob waste, estimated at 2.5–3.5 million tons annually [1]. Until now, most corn cobs have only been used to a limited extent, for example as traditional fuel, small amounts of animal feed, or even burned directly on post-harvest land, which has the potential to cause air pollution. Most of the rest are simply piled up or left to rot on the land, posing a risk of becoming a source of plant disease [2].

Corn cobs have quite promising chemical and energy characteristics. Their composition is dominated by cellulose, hemicellulose, and lignin, with a calorific value of around 15–17 MJ/kg, making them very suitable as raw materials in various biomass-based energy conversion technologies [3]. Their hard and fibrous nature also makes them suitable for processing into biochar, activated charcoal, or direct use in pyrolysis and gasification processes. This significant potential indicates that corn cobs are not merely waste but a renewable resource that can be optimized to support energy security and reduce dependence on fossil fuels.

Biomass gasification is a promising thermochemical technology for converting renewable resources into syngas consisting of H_2, CO, CH_4, and CO_2. Of the various types of biomass, corn cobs are a potential candidate due to their abundant availability in Indonesia and lignocellulose content that supports the energy conversion process [4]. However, the biomass gasification process still faces several obstacles, particularly the low hydrogen fraction in syngas and the formation of significant amounts of tar. Tar can cause reactor clogging, reduced thermal efficiency, and increased purification costs.

To overcome these problems, the use of catalysts is an important strategy. A number of studies have proven that metal catalysts such as Ni [5], Ca [6], and K [7] can increase hydrogen yield while suppressing tar formation. On the other hand, activated carbon is also widely used as a catalyst support because it has a high surface area, porous structure, and good chemical stability. The use of agricultural waste, particularly palm fiber, as raw material for activated carbon is not only economically valuable but also supports the concept of a circular economy in plantation waste management. In

addition, calcium oxide (CaO) is known to have a dual role, namely as a catalyst in the tar decomposition reaction and as a CO_2 absorber that promotes sorption-enhanced gasification to increase the hydrogen fraction in syngas [8].

Although various studies have examined the role of metal catalysts and activated carbon separately, research focusing on the combination of biomass bases catalyst such as palm fiber-based activated carbon with CaO in corn cob gasification is still limited. The uniqueness of this study lies in the integration of two catalyst, which is expected to provide a synergistic effect: activated carbon with high porosity increases catalyst dispersion and activity, while CaO simultaneously breaks down tar and absorbs CO_2. This approach has the potential to significantly increase hydrogen production and reduce carbon emissions.

However, there are several research gaps that remain unanswered. First, the optimal composition and ratio of activated carbon and CaO in corn cob gasification have not been extensively studied. Second, the synergistic mechanism using two catalyst in increasing syngas quality not yet fully understood. In addition, a systematic and statistically robust approach is required to disentangle the coupled effects of key operating and catalyst variables.

Based on this background and research gaps, this study aims to investigate the performance of a composite catalyst based on activated carbon from palm fiber combined with CaO in the corn cob gasification process. The main focus is on increasing hydrogen production, reducing tar, and evaluating the potential synergistic effects between materials. This research is expected to contribute to the development of low-cost, locally sourced, and sustainable catalyst systems that are relevant to supporting the clean energy transition and practical applications of biomass-to-hydrogen in the future.

2. Literature review and problem statement

How this section should be built: The paper [.] presents the results of research ..., Shown, that..., But there were unresolved issues related to ..., The reason for this may be (objective difficulties associated with ..., fundamental impossibility ..., cost part in terms of ..., which makes relevant research impractical, etc.). A way to overcome these difficulties can be ..., This approach was used in [.], however ..., All this suggests that it is advisable to conduct a study on ...

Names are not mentioned in scientific articles, references to works are enough

A study by ~~Tosuli~~ [9] explored Sago-based foods are staple in eastern Indonesia. Al_2O_3 (5–10 wt%) added to sago-dregs pellets in a TULD gasifier enhances syngas: H_2 is highest at 5% (31.65%), while CO (4.33%) and CH_4 (26.45%) peak at 10%. The H_2/CO ratio remains favorable (1.65–1.51) with low tar, indicating potential for internal combustion engine fuel.

A research by ~~Tuan~~ [10] explored an updraft gasifier processed 3 kg of dried rice husk using air, steam-air, and air with dolomite at varied conditions. Among the tested

agents, catalytic air gasification (air + dolomite) gave the best results, producing the highest H_2 (15.4 mol%) and LHV (5.1 MJ/Nm³), compared with steam-air (7.08 mol%, 3.6 MJ/Nm³) and air only (3.6 mol%). The optimum setting was an airflow of 3 m³/h with 15% dolomite.

A research by ~~Yousef~~ [11] explored Cigarette butts are hazardous urban waste rich in cellulose acetate and volatile matter, making them a potential renewable feedstock for hydrogen production. This study valorized as-received cigarette butts via continuous updraft gasification (700–900 °C; ER 0.15–0.25), followed by steam catalytic reforming over KATALCO™ 57-4GQ at 900 °C. Gasification alone produced high syngas yields (82.3–89.7%) but limited H_2 (<20.84 vol% at 900 °C, ER 0.15). The reforming step increased H_2 to 30.27 vol% and reduced tar from 18.15 to 13.38 g/m³, improving fuel quality (HHV from 11,038 to 11,528 kJ/kg).

A research by ~~Bilbao~~ [12] explored slumgum suitability as a gasification fuel. Slumgum and slumgum-pine sawdust pellets were produced (ISO 17225 tests) and gasified in a modified updraft reactor while measuring gas composition and LHV. Pure slumgum pellets showed very high durability (99.98%) and HHV (27.66 MJ/kg), likely due to high fat content, but high sulfur (2.17%) and nitrogen (3.52%) prevented ISO compliance. In gasification, adding sawdust increased LHV, reaching 7.62 MJ/Nm³ at a 50:50 blend, although ER stayed very low (0.0125–0.0204) because higher airflow raised fuel consumption.

A research by ~~Yesilova~~ [13] examined catalyst effects on biomass-mixture gasification using lab-scale updraft and modifiable-downdraft fixed-bed reactors. Red mud (RM) and an Al–Ni alloy were tested at high temperature, where H_2 levels of 51–65 vol% were obtained at 900 °C in both systems. The Al–Ni catalyst showed the strongest enhancement, achieving 65 vol% H_2 in the updraft reactor at 900 °C with 0.05 L/min dry air, and widening the H_2/CO range from 2–4 (no catalyst) to 1.6–7. RM generally increased H_2 in the updraft reactor by about 1–7 vol% at 900 °C, but in the modifiable-downdraft reactor it reduced H_2 by roughly 2–6%.

A research by ~~Jancauskas~~ [14] examined three MSW fractions (FDS, SRF, and plastic packaging mixture/PPM) from mechanical–biological treatment plants were gasified in an allothermal fixed-bed updraft reactor at 800 °C using air at ER ≈ 0.15 and 0.21. All feeds showed similar volatile-release peaks (~330 and ~500 °C). Lowering ER increased the heating value of combustible gases; PPM produced the highest H_2 (11.39%). SRF generated the most tar (47.44 g/m³), dominated by aromatic compounds.

A research by ~~Junga~~ [15] examined co-gasifying laying hens manure (LHM) with common litter such as wheat straw remains limited, particularly across a wide range of air–fuel equivalence ratios (AFER). This laboratory study used a fixed-bed updraft reactor to gasify straw-LHM blends (25–75% LHM) under low (0.12–0.28) and high (0.30–0.45) AFER to assess how LHM affects producer-gas quality and process efficiency. At higher AFER, the producer-gas LHV stayed around 3.3–3.4 MJ/m³ (depending on blend), with cold gas efficiency 60% and carbon conversion efficiency of 82–94%.

A study by ~~Tezer~~ [16] evaluated the gasification of olive pomace in fixed-bed updraft and downdraft systems. Dried olive pomace obtained from an olive-oil soap plant in Izmir (Türkiye) was characterized and gasified at 700–900 °C using dry air at 0.05–0.4 L/min, with additional tests using pure oxygen (0.01 L/min). With dry air, the syngas reached 48 vol% H_2 in the updraft and 45 vol% in the downdraft, with a heating value of about 12.4 MJ/Nm³. Under oxygen, H_2 increased to ~53 vol% in the updraft but was ~39 vol% in the downdraft.

A study by ~~Isik~~ [17] gasified MDF wood-waste in a 2100 kg/h updraft fixed-bed system (tested at 1500–2100 kg/h) using oak chips as a reference. Syngas yield was 2.5 Nm³/kg with LHV 6.0–7.0 MJ/Nm³, and the gas composition at full-load MDF was similar to oak. Hot syngas (430 °C) containing tar/soot was burned directly in a retrofitted thermal-oil heater (7 MWh) to supply an ORC turbine generating 955 kW electricity, converting 88 wt% of MDF residue into syngas.

Based on the above literature, it is evident that syngas quality in fixed-bed updraft gasification is primarily governed by catalytic strategy such as Al_2O_3, dolomite, Al/Ni, red mud, oxidant selection, and equivalence ratio, while secondary upgrading can further suppress tar and enrich H_2. However, most published studies still emphasize single catalyst systems or isolated additives, and comparatively few have investigated dual catalyst synergy in updraft configurations using a systematic, design-of-experiments optimization framework.

In this context, the present study on Syngas Quality Improvement in Corncob Updraft Gasification Using a CaO/Activated Carbon Palm-Fiber Catalyst addresses a clear research gap. The CaO-activated carbon combination is expected to deliver a dual-synergistic function: CaO acts as an in-situ CO_2 sorbent that can shift gasification equilibria toward higher H_2 formation, whereas palm-fiber-derived activated carbon provides high-surface-area catalytic sites to promote tar cracking and reforming of volatiles, thereby reducing condensable by-products while enhancing the combustible gas fraction. Consequently, this work is positioned to contribute both mechanistic and practical advances by demonstrating a scalable dual-catalyst route to produce cleaner, H_2-richer, and higher-LHV syngas from corncob waste in an updraft reactor.

Please add a summary of the section on literary data analysis and problem statement. All this allows us to conclude that it is expedient to conduct research devoted to...

The purpose of the study (section 3) should follow from the unresolved problem formulated at the end of section 2.

2. Literature review and problem statement

Previous studies have reported improvements in syngas quality in fixed-bed updraft gasification through the selection of gasification agents and catalytic strategies. The paper by [9] explored Sago-based foods are staple in eastern Indonesia. Single Al_2O_3

catalyst (5–10 wt%) was added to sago-dregs pellets in a TULD gasifier enhances syngas: H_2 is highest at 5% (31.65%), while CO (4.33%) and CH_4 (26.45%) peak at 10%. The H_2/CO ratio remains favorable (1.65–1.51) with low tar, indicating potential for internal combustion engine fuel.

The paper by [10] explored an updraft gasifier processed 3 kg of dried rice husk using air, steam-air, and air with dolomite at varied conditions. Among the tested agents, single catalytic air gasification (air + dolomite) gave the best results, producing the highest H_2 (15.4 mol%) and LHV (5.1 MJ/Nm³), compared with steam-air (7.08 mol%, 3.6 MJ/Nm³) and air only (3.6 mol%). The optimum setting was an airflow of 3 m³/h with 15% dolomite.

The paper by [11] explored Cigarette butts are hazardous urban waste rich in cellulose acetate and volatile matter, making them a potential renewable feedstock for hydrogen production. This study valorized as-received cigarette butts via continuous updraft gasification (700–900 °C; ER 0.15–0.25), followed by steam catalytic reforming over KATALCO™ 57-4GQ at 900 °C. Gasification alone produced high syngas yields (82.3–89.7%) but limited H_2 (<20.84 vol% at 900 °C, ER 0.15). The reforming step increased H_2 to 30.27 vol% and reduced tar from 18.15 to 13.38 g/m³, improving fuel quality (HHV from 11,038 to 11,528 kJ/kg).

The paper by [12] explored slumgum suitability as a gasification fuel. Slumgum and slumgum-pine sawdust pellets were produced (ISO 17225 tests) and gasified in a modified updraft reactor while measuring gas composition and LHV. Pure slumgum pellets showed very high durability (99.98%) and HHV (27.66 MJ/kg), likely due to high fat content, but high sulfur (2.17%) and nitrogen (3.52%) prevented ISO compliance. In gasification, adding sawdust increased LHV, reaching 7.62 MJ/Nm³ at a 50:50 blend, although ER stayed very low (0.0125–0.0204) because higher airflow raised fuel consumption.

The paper by [13] examined catalyst effects on biomass-mixture gasification using lab-scale updraft and modifiable-downdraft fixed-bed reactors. Red mud (RM) and an Al–Ni alloy were tested at high temperature, where H_2 levels of 51–65 vol% were obtained at 900 °C in both systems. The Al–Ni catalyst showed the strongest enhancement, achieving 65 vol% H_2 in the updraft reactor at 900 °C with 0.05 L/min dry air, and widening the H_2/CO range from 2–4 (no catalyst) to 1.6–7. RM generally increased H_2 in the updraft reactor by about 1–7 vol% at 900 °C, but in the modifiable-downdraft reactor it reduced H_2 by roughly 2–6%.

The paper by [14] examined three MSW fractions (FDS, SRF, and plastic packaging mixture/PPM) from mechanical–biological treatment plants were gasified in an allothermal fixed-bed updraft reactor at 800 °C using air at ER ≈ 0.15 and 0.21. All feeds showed similar volatile-release peaks (~330 and ~500 °C). Lowering ER increased the heating value of combustible gases; PPM produced the highest H_2 (11.39%). SRF generated the most tar (47.44 g/m³), dominated by aromatic compounds.

The paper by [15] examined co-gasifying laying hens manure (LHM) with common litter such as wheat straw remains limited, particularly across a wide range of air–fuel

equivalence ratios (AFER). This laboratory study used a fixed-bed updraft reactor to gasify straw-LHM blends (25–75% LHM) under low (0.12–0.28) and high (0.30–0.45) AFER to assess how LHM affects producer-gas quality and process efficiency. At higher AFER, the producer-gas LHV stayed around 3.3–3.4 MJ/m³ (depending on blend), with cold gas efficiency 60% and carbon conversion efficiency of 82–94%.

The paper by [16] evaluated the gasification of olive pomace in fixed-bed updraft and downdraft systems. Dried olive pomace obtained from an olive-oil soap plant in Izmir (Türkiye) was characterized and gasified at 700–900 °C using dry air at 0.05–0.4 L/min, with additional tests using pure oxygen (0.01 L/min). With dry air, the syngas reached 48 vol% H_2 in the updraft and 45 vol% in the downdraft, with a heating value of about 12.4 MJ/Nm³. Under oxygen, H_2 increased to ~53 vol% in the updraft but was ~39 vol% in the downdraft.

The paper by [17] gasified MDF wood-waste in a 2100 kg/h updraft fixed-bed system (tested at 1500–2100 kg/h) using oak chips as a reference. Syngas yield was 2.5 Nm³/kg with LHV 6.0–7.0 MJ/Nm³, and the gas composition at full-load MDF was similar to oak. Hot syngas (430 °C) containing tar/soot was burned directly in a retrofitted thermal-oil heater (7 MWh) to supply an ORC turbine generating 955 kW electricity, converting 88 wt% of MDF residue into syngas.

However, there are still unresolved issues regarding how to achieve simultaneous improvements in syngas quality increasing H_2/CH_4 and LHV while reducing CO_2/tar with an approach that remains simple, scalable, and economical for updraft reactors. One reason for this is that most studies still emphasize single catalysts or separate additives, while dual-catalyst synergy in updraft configurations has been relatively rarely studied systematically. Efforts to overcome these limitations can be made through the development of a dual-catalyst system that combines the function of CO_2 absorption to drive the equilibrium shift towards H_2 formation, and a high-surface catalytic function to enhance secondary reactions such as cracking of volatiles and suppressing condensed products.

This approach has the potential to be realized by combining CaO as a CO_2 sorbent and palm fiber-based activated carbon (AC–PF) as a porous material with a high surface area to increase contact and volatility reactivity. however, quantitative evidence regarding the level of synergy, the optimum CaO/ AC–PF ratio combination, and the effect of ER and catalyst loading on H_2, CO, CH_4, CO_2, and LHV in updraft corn cob gasification has not yet been comprehensively mapped.

All this allows us to conclude that it is expedient to conduct research devoted to improving syngas quality in updraft corn cob gasification through a CaO/ AC–PF dual catalyst system with systematic evaluation of the equivalence ratio, catalyst loading, and CaO/ AC–PF ratio, to obtain cleaner syngas that is rich in H_2 and has a higher calorific value.

3. The aim and objectives of the study

The purpose statement should include two components: scientific (The purpose of the study is...) and practical (This will allow...). The scientific part should correspond to the title of the article, the practical part should indicate what the scientific results obtained will give to practice (i.e., the achievement of the scientific component of the research goal)

The aim of the study is to enhance syngas quality from corncob updraft gasification by developing and optimizing a dual-synergy CaO/palm-fiber-derived activated carbon (CaO/AC-PF) catalytic system.

Objectives of the study:

It is strictly prohibited to use an automatic list. All lists are marked in manual mode!

- to synthesize and characterize the CaO and palm-fiber activated carbon catalysts using FTIR, SEM, and BET The abbreviations must be decrypted

- to investigate the effects of operating parameters, particularly equivalence ratio (ER), catalyst loading, and CaO/AC ratio, on syngas composition H_2, CO, CH_4, CO_2 and LHV.

3. The aim and objectives of the study

The purpose of the study is to enhance syngas quality from corncob updraft gasification by developing a dual-synergy catalytic system based on calcium oxide (CaO) and palm-fiber-derived activated carbon (AC–PF). This will allow the production of cleaner and more energy-dense producer gas, providing practical guidance for selecting operating conditions and catalyst configurations suitable for updraft gasifiers processing agricultural residues.

To achieve these aims, the following objectives are accomplished:

- to synthesize and characterize the CaO and palm-fiber activated carbon catalysts using Fourier Transform Infrared Spectroscopy (FTIR), scanning electron microscopy (SEM) and Brunauer–Emmett–Teller surface area analysis (BET)

- to investigate the effects of operating parameters, particularly equivalence ratio (ER), catalyst loading, and CaO/AC ratio, on syngas composition H_2, CO, CH_4, CO_2 and LHV.

4. Materials and methods

Section 4 should begin with the following:

The object of study (this is the practical physical object or process on which the results of the study will be used and, as a result, something will increase or decrease),

The research hypothesis is what underlies the achievement of the research goal, i.e., what was tested and had to be accepted or refuted.

Assumptions made before the start of the research.

Simplifications made in the course of the research.

4. Materials and methods

The object of the study is the updraft fixed-bed gasification process of corncob biomass using a dual catalyst system based on calcium oxide (CaO) and palm-fiber-derived activated carbon (AC–PF). The practical physical process under investigation is the catalytic upgrading of producer gas within the updraft reactor, where changes in operating parameters and catalyst configuration are expected to influence syngas composition and heating value. The results of this study are intended to be applied to improve the quality of syngas, specifically by increasing the combustible gas fraction (H_2 and CH_4) and the lower heating value (LHV), while reducing CO_2 content.

The research hypothesis is that a dual-synergy CaO/AC–PF catalytic system can improve syngas quality more effectively than single-catalyst configurations in updraft corncob gasification. It is hypothesized that CaO functions as a CO_2 sorbent, shifting reaction equilibria toward enhanced hydrogen formation, while activated carbon derived from palm fiber provides high-surface-area catalytic sites that promote secondary reactions such as tar cracking and volatile reforming. The combined catalytic–sorption mechanism is expected to increase H_2 and CH_4 fractions and improve LHV under optimized equivalence ratio (ER), catalyst loading, and CaO/AC–PF ratio conditions.

It was assumed that the corncob feedstock has relatively homogeneous composition and stable proximate/ultimate characteristics during the experiments. The gasification process was assumed to operate under steady-state conditions after stabilization. It was also assumed that the CaO maintains sufficient CO_2 sorption capacity within the experimental time frame and that the activated carbon structure remains stable under the applied temperature range.

During the course of the research, several methodological simplifications were adopted in order to maintain experimental feasibility and focus on the main objective of syngas quality evaluation. Detailed kinetic modeling of individual gasification reactions was not performed; instead, the process performance was assessed based on experimentally measured syngas composition and syngas low heating value. Furthermore, although CaO carbonation–decarbonation reactions may occur during operation, microstructural evolution, sintering behavior, and long-term cyclic stability of the catalyst were not investigated in this study. The catalytic performance was evaluated within the experimental duration without conducting extended durability or regeneration-cycle analysis.

4. 1. Catalyst Preparation

Approximately 6 grams of ground palm fiber was mixed with 60 mL of distilled water and stirred for 10 minutes. The mixture was then placed in an autoclave and heated to 200°C at a rate of 5°C per minute for 6 hours in an electric oven. After that, the reactor is allowed to cool naturally to room temperature. The resulting solid hydrocarbon product (hydrochar) is then separated using Whatman No. 42 filter paper. The filtered product is then dried at 105°C for 24 hours and stored in a glass vial. The next stage is the activation process. The hydrochar is immersed in a 3 M KOH solution

with a weight ratio of 1:3 (Hydrochar:KOH) for 16 hours, then dried at 85°C for 6 hours. Spectroscopic evidence indicates that KOH preferentially reacts with oxygenated sites and can increase the relative abundance of C–OH functionalities, while higher KOH ratio and activation temperature significantly enhance porosity and BET surface area [18, 19]. To obtain the CaO/AC mixture, CaO powder and activated carbon (AC) were mixed in specific proportions using a grinder until a homogeneous mixture was obtained. Next, CaO, AC, and CaO/AC were activated using a tube furnace at a temperature of 700°C for 1 hour with a continuous flow of nitrogen during the activation process. The resulting product was then washed using distilled water until it reached a neutral pH. This stage produced activated carbon that was ready for use in research.

4. 2. Experimental Setup

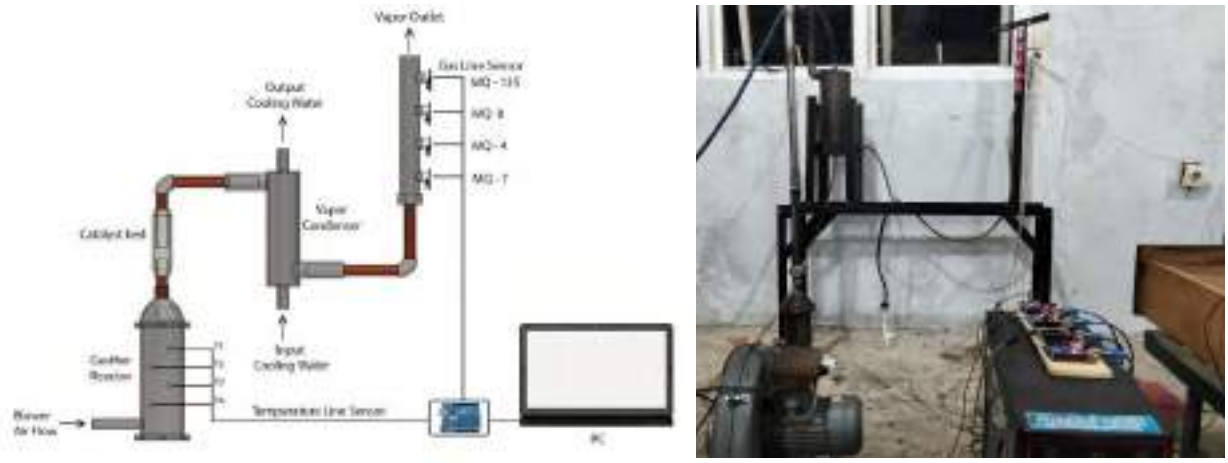
Corncob biomass was obtained from farmers in the South Malang region of East Java. Before use, the biomass was cleaned of impurities and dried in an oven for 6 hours at 100°C to remove moisture (water vapor) content. The ultimate and proximate test results are as follows.

There must be a reference to the table in the text before the table

The proximate and ultimate analyses of the corncob feedstock were conducted to determine its physicochemical characteristics prior to gasification. The results are presented in Table 1. The data indicate that corncob has high volatile matter content and relatively low ash content, which are favorable characteristics for gasification processes.

Table 1
Ultimate And Proximate Test Corn Cob

Parameter	Units	Corn cobs
Moisture	%	10
Volatile matter	%	71.38
Fixed carbon	%	12.11
Ash	%	6.51
C	%	43.6
H	%	6.3
O	%	46.8
N	%	0.22
HHV	MJ/kg	17.61



a *b*

Fig. 1. Updraft gasifier: *a* – schematic experiment; *b* – experimental setup

This study used an updraft gasification reactor designed with a total height of 20 cm. The lower part of the reactor consisted of an ash container with a height of 5 cm, while the active reactor had a height of 15 cm and a diameter of 3 inches. The reactor was equipped with a 1-inch diameter air inlet pipe connected to a blower. The blower was modified with a potentiometer so that the air speed could be adjusted as needed. To monitor the thermal conditions inside the reactor, four 3 cm long type K thermocouples were installed at several different points so that the temperature profile in the gasification zone could be observed in more detail. Each test was conducted with a fixed biomass mass, a mixture of corn cobs weighing 80 grams. The reactor was made of iron and equipped with a gas seal to prevent leaks during the gasification process.

The gas produced by the reactor was fed into a condenser, which cooled the hot gas so that the water vapor components could be separated. The condenser was made of a copper spiral pipe with a diameter of ½ inch and a height of 30 cm. Cooling water was circulated from the bottom of the condenser and exited through the top to ensure efficient heat transfer. This cooling system was driven by a 60-watt water pump, ensuring stable water flow and optimal condensation. The catalyst was positioned downstream after the reactor, where it was supported on steel wool and wrapped with an 80-μm wire mesh to secure the catalyst and prevent particle carryover with the gas flow

To analyse the gas composition, four types of MQ gas sensors were used. The MQ-8 sensor was used to detect H_2, MQ-4 for CH_4, MQ-135 for CO_2 and MQ-7 for CO. Each gas sensor was calibrated according to the manufacturer's datasheet, specifically by determining the Ro value, which is the sensor resistance in clean air conditions. This Ro value is used as a reference in calculating the measured gas concentration during the process [20, 21].

All data from the gas sensors and thermocouples were acquired using an Arduino Uno microcontroller. Each gas sensor is connected to a separate Arduino Uno to facilitate the calibration process and reduce the possibility of interference between

sensors. Arduino is also used to record temperature data from four thermocouples installed in the reactor, so that gas composition and temperature distribution data can be obtained simultaneously.

The ER range of 0.2, 0.25, 0.3 and 0.35. The catalyst load was between 4%, 6%, 8% and 10% from the mass of input feedstock. The CaO/AC-PF ratio was varied between 0:1, 1:0, 1:1, and 2:1. Design of experiment can be seen in Table 2.

Table 2
Design of Experiment using

Run	Equivalence Ratio (E.R)	Catalyst Load %	CaO/AC
1	0.2	4	1:0
2	0.2	6	0:1
3	0.2	8	1:1
4	0.2	10	2:1
5	0.25	4	0:1
6	0.25	6	1:0
7	0.25	8	2:1
8	0.25	10	1:1
9	0.3	4	1:1
10	0.3	6	2:1
11	0.3	8	1:0
12	0.3	10	0:1
13	0.35	4	2:1
14	0.35	6	1:1
15	0.35	8	0:1
16	0.35	10	1:0

IT IS NOT CORRECT TO END THE SECTION WITH THE TABLE. WE NEED SOME KIND OF INTERPRETATION

A total of 16 experimental runs were conducted systematically to enable evaluation of the main effects of each variable and the tendency of interactions between variables on the fractions of H_2, CO, CH_4, CO_2, and lower heating value (LHV). This approach enabled identification of the most effective combination of operating parameters in improving syngas quality quantitatively and measurably.

5. Results (which one, what one?)

The title of the section should be specific and correspond to the essence of the article

Structure the "Research Results" section according to the objectives (Section 3).

5. 1

5. 2

Each subsection should correspond to a specific task, showing exactly where each task begins and where each task ends.

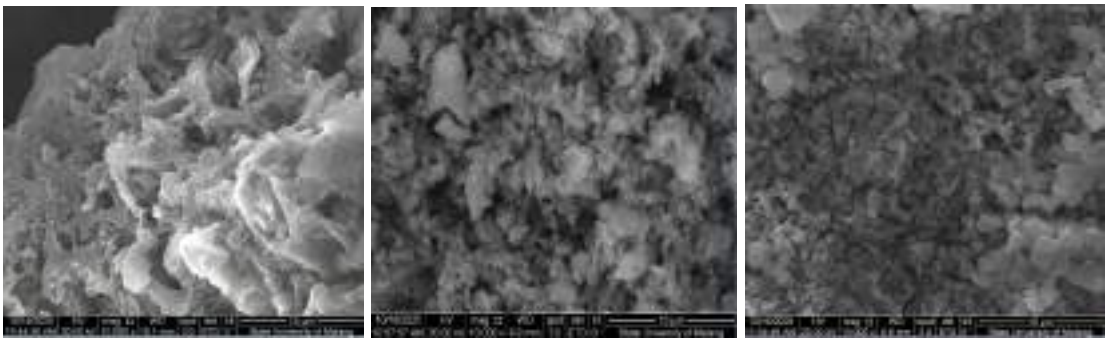
5. Results of syngas quality enhancement from corncob using calcium oxide (CaO) and palm-fiber-derived activated carbon (AC–PF).

5. 1. Characterization of Calcium Oxide (CaO) and Palm-Fiber-Derived Activated Carbon (AC–PF) Catalysts

5. 1 SEM Catalyst Result abbreviations in section names are not allowed

5. 1. 1. Scanning Electron Microscopy Catalyst Result

Fig. 2, *a* shows the image obtained from a Scanning Electron Microscope (SEM) with a magnification of 10,000× shows the surface morphology of palm fiber-based activated carbon (AC-PF). The surface structure appears porous and irregular, with a combination of void areas and layered surfaces. This characteristic indicates that the activation process that using KOH has successfully formed micropores and mesopores, which play an important role in increasing the specific surface area of activated carbon.



a *b* *c*

Fig. 2. SEM Catalyst Result: *a* – SEM AC-PF; *b* – SEM CaO:AC;1:1; *c* – SEM CaO:AC;2:1

Fig. 2. Scanning Electron Microscopy Catalyst Result: *a* – Scanning Electron Microscopy AC-PF; *b* – Scanning Electron Microscopy CaO:AC;1:1; *c* – Scanning Electron Microscopy CaO:AC-PF;2:1

abbreviations in the names of figures are not allowed

The rough and textured surface indicates that most of the material has undergone lignocellulose cell wall exfoliation, resulting in numerous interparticle gaps [22]. This porous structure greatly supports gas adsorption and diffusion capabilities when used as a catalyst in gasification or thermochemical reactions.

The presence of 1–5 μm voids indicates that most pores are in the mesopore category, supporting the adsorption of gas molecules such as H_2, CO, and tar during the gasification reaction [23].

The morphology of AC-PF shows the characteristics of porous activated carbon with a heterogeneous pore distribution, where the pores allow increased contact between gas reactants and active sites on the material surface, thereby increasing catalytic efficiency and the ability to absorb tar or CO_2 in biomass-based energy applications [24].

Fig. 2, *b* shows the surface morphology of the CaO:AC-PF catalyst with a ratio of 1:1. Visually, it can be seen that the surface of this material consists of fine particles ranging in size from microns to submicrons that stick together to form a layered and slightly agglomerated structure.

The presence of fine, light-colored grains indicates an even distribution of CaO particles impregnated on the surface of activated carbon (AC-PF). This CaO distribution fills some of the pores of the carbon, resulting in a denser surface compared to pure AC-PF. However, there are still small gaps and voids between the grains, indicating that the microporous and mesoporous structures are still formed and can support catalytic activity [25].

This morphology illustrates the success of the CaO impregnation process on activated carbon from palm fiber, where the interaction between CaO and the carbon pore walls produces a composite material that is more thermally and chemically stable. This structure is highly conducive to catalyst applications in biomass gasification processes, as CaO particles can function as CO_2 absorbers while accelerating the tar reforming reaction [26].

Fig. 2, c shows the surface morphology of the CaO:AC-PF (2:1) catalyst. The image shows that the surface of the material is dominated by agglomerations of fine, round, and irregular particles ranging in size from microns to submicrons. Compared to the CaO:AC-PF (1:1) sample, this structure appears denser and tighter, indicating that an increase in the CaO ratio causes partial closure of the activated carbon surface pores by CaO particles.

The distribution of CaO particles appears more uniform and covers the carbon surface, indicating the successful impregnation of a larger amount of CaO. The light

color in some areas indicates the presence of a calcium oxide phase that is strongly attached to the activated carbon matrix [27]. This structure indicates a strong interaction between CaO and AC-PF, forming a thermally stable composite.

Although some pores are covered, there are still microscopic gaps between the CaO grains that allow gas diffusion to occur, so that the catalyst retains its good adsorption capacity. The combination of the active area of CaO and the porous carbon structure makes this material very promising for biomass gasification or tar reforming applications, as CaO can act as a CO_2 absorber and increase the conversion of carbon to hydrogen gas.

5. 2. FTIR catalyst result abbreviations in section names are not allowed

5. 1. 2. Fourier Transform Infrared Spectroscopy catalyst result

The FTIR analysis results shown in the Fig. 3 reveal clear spectral differences between the AC-PF, CaO, and their mixtures (CaO:AC-PF) with ratios of 2:1 and 1:1. In the AC-PF spectrum, the absorption band at 2926 cm^{-1} is associated with the stretching vibration of the C–H group from –CH2 or –CH3 (methylene/methyl stretching), which indicates the presence of hydrocarbon chain residues from the lignocellulose structure. The peak at 1577 cm^{-1} indicates the presence of aromatic C=C or C=O stretching, while the band at 1056 cm^{-1} represents C–O stretching from alcohol or ether groups. In addition, the –OH group that appears in the 3500–3600 cm^{-1} region is identified as the result of AC-PF activation using a KOH solution, which causes the formation of hydroxyl groups on the activated carbon surface. This –OH group plays an important role in increasing the surface activity and adsorption capacity of AC-PF as a catalyst support medium [28, 29].

In pure CaO, the intense band at 3639 cm^{-1} is associated with the stretching of the O–H group from $Ca(OH)_2$, which is formed due to the partial hydration of CaO when exposed to humid air. Meanwhile, the absorption bands at 1426 cm^{-1} and 876 cm^{-1} are associated with C–O stretching and CO_3^{2-} bending, respectively, indicating the formation of $CaCO_3$ due to CO_2 adsorption from the air. This shows that CaO is highly reactive to moisture and carbon dioxide in the environment.

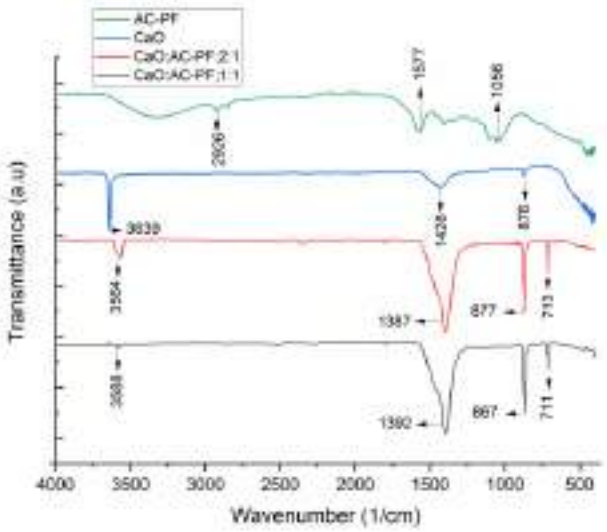


Fig. 3. FTIR Catalyst Result

Fig. 3. Fourier Transform Infrared Spectroscopy Catalyst Result

For the CaO:AC-PF (2:1), the main absorption bands were detected at 3564 cm^{-1} (O–H stretching from $Ca(OH)_2$ and the –OH group in AC-PF), 1387 cm^{-1} (C–O stretching), and 877 cm^{-1} and 713 cm^{-1} (bending vibration of CO_3^{2-}). This combination of bands indicates the formation of carbonate compounds ($CaCO_3$) due to the interaction between CaO and the oxygen groups of activated carbon. The presence of –OH groups from KOH activation also strengthens the basic properties on the surface, which can increase the chemical interaction between CaO and AC-PF[1].

At a CaO:AC-PF ratio of 1:1, the absorption bands at 3588 cm^{-1}, 1392 cm^{-1}, 867 cm^{-1}, and 711 cm^{-1} show a similar pattern, indicating the presence of hydroxyl (O–H) and carbonate (CO_3^{2-}) groups. The difference in peak intensity compared to the 2:1 ratio indicates variations in the level of interaction between CaO and the –OH groups resulting from KOH activation on AC-PF, which affects the formation of carbonate-hydroxide complexes on the material surface[2].

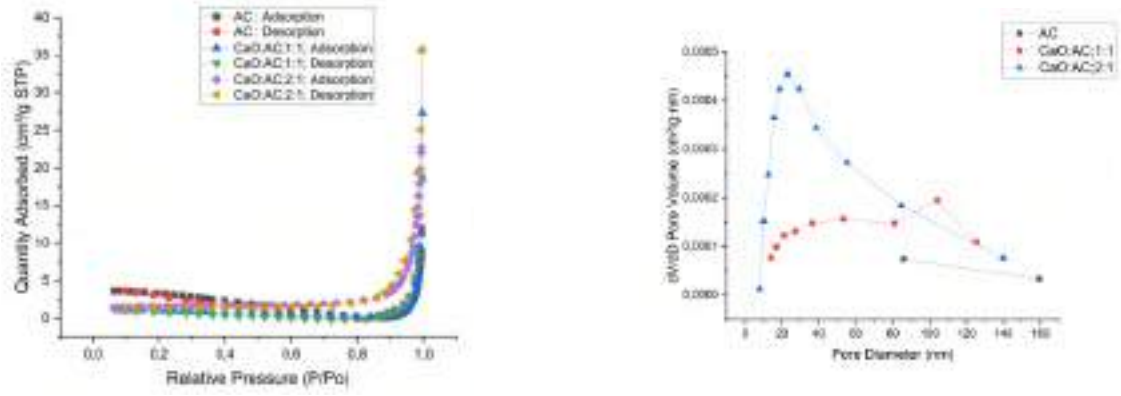
5. 3. BET Catalyst Result

5. 1. 3. Brunauer–Emmett–Teller Catalyst Result

Fig. 4 shows the adsorption–desorption isotherm curves for nitrogen for the AC, CaO:AC (1:1), and CaO:AC (2:1) samples are shown in Fig. 4. All three samples exhibit type IV isotherms with clear hysteresis loops at relatively high pressures (P/Po > 0.9). Based on the IUPAC classification, this characteristic indicates that the material has a mesoporous structure formed through capillary condensation within the pore channels. The difference between the adsorption and desorption pathways indicates that the pore

shape is not perfectly cylindrical, but rather tends to be irregular or slit-like, which is commonly found in modified activated carbon materials[3].

The pure activated carbon (AC) sample showed a relatively low nitrogen adsorption volume with a specific surface area of 24.51 m^2/g and an average pore diameter of 0.74 nm, indicating a predominance of microporous structures. In the CaO:AC (1:1) composite, the surface area did not change significantly compared to pure AC, indicating that the addition of a moderate amount of CaO did not cover the carbon pores much, but only adhered to the external surface of the carbon matrix [4].



a *b*

Fig. 4. BET Result: *a* – AC Surface Analysis Adsorption Desorption Isotherm; *b* – BJH Adsorption Pore Size Distribution

Fig. 4. Brunauer–Emmett–Teller Result: *a* – Surface Analysis Adsorption Desorption Isotherm; *b* – Barrett–Joyner–Halenda Adsorption Pore Size Distribution

Conversely, in the CaO:AC (2:1) mixture, there was a sharp increase in adsorption volume at relatively high pressure (P/Po > 0.9) to around 35 cm^3/g STP, while the BET surface area decreased dramatically to 5.06 m^2/g, and the pore diameter increased to 22.87 nm.

These changes in isotherm shape and pore size increase indicate that CaO impregnation not only modifies the surface chemistry but also significantly alters the pore structure of activated carbon. This transformation is positive in the context of catalytic applications in biomass gasification processes, as the mesoporous structure can enhance gas diffusion and accessibility to active sites during the tar reforming and water-gas shift reactions. Thus, even though the specific surface area decreases, the increase in mesoporousness and pore connectivity can actually improve catalyst performance in hydrogen gas production[5].

Fig. 4, *b* shows the BJH pore size distribution curves that provide further insight into the textural evolution of the palm-fiber-based activated carbon after CaO impregnation. The pristine AC exhibits a relatively low dV/dD value and a broad

contribution only at large pore diameters (>60 nm), indicating that its pore system is dominated by macropores with a limited amount of mesopores. Such a texture is less favourable for gas-solid reactions because the accessible surface area in the mesopore range (2–50 nm) is relatively small.

After CaO loading, the shape and intensity of the BJH curves change markedly. For CaO:AC-PF = 1:1, the distribution shifts toward smaller pore diameters with a pronounced contribution in the mesopore region of approximately 15–60 nm. This behaviour shows that CaO impregnation partially reconstructs the carbon matrix, enlarging existing micropores and opening blocked pores to generate additional mesoporosity. The effect becomes even more evident at CaO:AC-PF = 2:1, where the curve displays the highest dV/dD values and a distinct maximum centred at about 30–40 nm. The strong peak in this range confirms that a higher CaO loading promotes the development of well-defined mesopores while reducing the relative fraction of very large macropores.

Overall, the BJH analysis demonstrates that CaO acts not only as a reactive sorbent but also as a textural promoter for the palm-fiber AC. The increase in mesopore volume and the shift of the dominant pore size toward 20–40 nm are expected to facilitate the diffusion of gasifying agents and tar molecules, as well as to improve the accessibility of CaO active sites for CO_2 capture and reforming reactions. These features are therefore beneficial for enhancing the catalytic performance of the CaO/AC composite in biomass gasification toward H_2-rich syngas production.

5. 2. Effect of Operating Parameters on Syngas Composition and Low Heating Value

5. 2. 1. Effect of Equivalence Ratio on Syngas Product

The composition of syngas from updraft gasification is greatly influenced by the Equivalence Ratio (ER), which is the ratio of the mass flow rate of air compared to the mass flow rate of corncob in the experiment compared to the stoichiometry of air required for complete combustion of corncob. In this study, the ER used was 0.2–0.35 with the following formula

All formulas must be typed in the MathType formula editor version 7 or earlier. If you don't have this version of MathType, then type the formulas in the built-in formula editor

$$ER = \frac{(\dot{m}_a/\dot{m}_{cc})_{exp}}{(\dot{m}_a/\dot{m}_{cc})_{stc}}$$

$$ER = \frac{(m_a / m_{cc})_{\exp}}{(m_a / m_{cc})_{stc}}$$

where $\dot{m}_a$ is the air mass flow rate (kg/s), $\dot{m}_{cc}$ is the corncob mass flow rate (kg/s), exp denotes the experimental air–fuel ratio, and stc denotes the stoichiometric air–fuel ratio

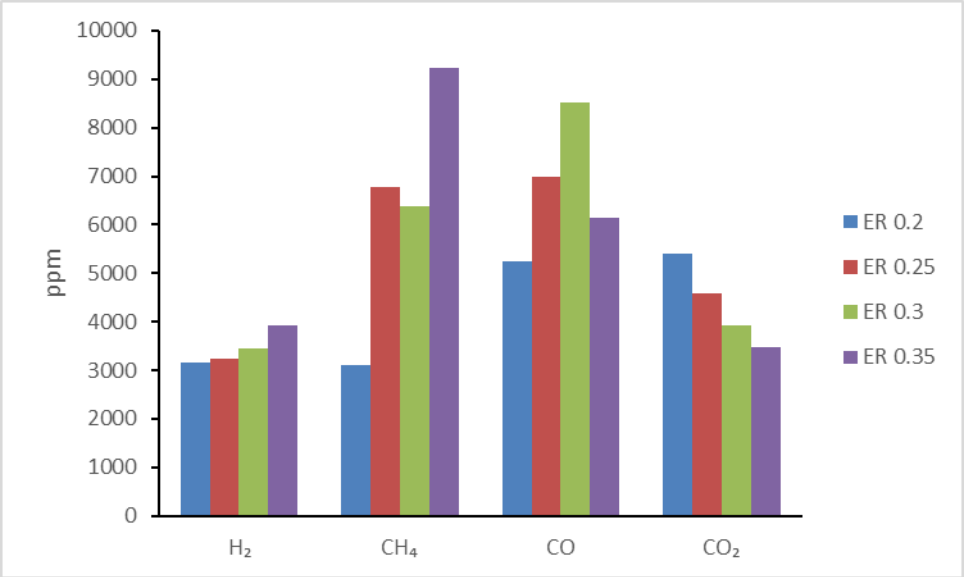


Fig. 5. Syngas Composition with Different ER
Fig. 5. Syngas Composition with Different Equivalence Ratio

The graph above shows that the higher the ER, the higher the hydrogen composition produced. At ER 0.2, the ppm is 3150 ppm, at ER 0.25 it is 3241 ppm, at ER 0.3 it is 3457 ppm, and at ER 0.35 it is 3914 ppm. A higher oxidant supply promotes the formation of more stable autothermal conditions and higher reaction temperatures due to partial oxidation. This increase in temperature accelerates hydrogen-forming reactions, particularly the gasification of active carbon catalyst interactions with steam ($C + H_2O \rightarrow CO + H_2$), the reforming of volatile compounds/light hydrocarbons ($CxHy + H_2O \rightarrow CO + H_2$), and the cracking of tar/volatile into lighter gas species. At low ER, some volatiles tend to be incompletely converted and still have the potential to escape as condensable components, while increasing ER increases heat availability, making the conversion of volatiles into gas fractions (including H_2) more effective.

The higher the ER, the higher the CH4 composition produced. At ER 0.2, 3093 ppm was obtained, at ER 0.25 6767 ppm, ER 0.3 6377 ppm, and ER 0.35 9221 ppm. This trend indicates that the supply of oxidants not only increases autothermal conditions and the rate of devolatilization, but also shifts the reaction pathway towards the formation of light hydrocarbons through hydrogenation and/or methanation reactions in the reactor zone where the temperature still supports CH_4 formation. In particular, increased H_2 at higher ERs can promote the methanation reaction of CO ($CO + 3H_2 \rightleftharpoons CH_4 + H_2O$), so that CH_4 increases along with a tendency for CO to decrease at the

highest ER. In addition, more intensive fragmentation of volatiles and tar at high ERs has the potential to produce light gas precursors which are then hydrogenated to CH_4.

CO formation increased up to an ER of 0.3 and decreased at an ER of 0.35. At an ER of 0.2, 5238 ppm was obtained, at an ER of 0.25, 6999 ppm, at an ER of 0.3, 8532 ppm, and decreased at an ER of 0.35 to 6145 ppm. At low ER (0.20–0.25), limited oxygen supply resulted in relatively low heat release, so that the reaction zone temperature and char reactivity were not sufficient to intensify CO formation reactions, especially the Boudouard reaction ($C + CO_2 \rightleftharpoons 2CO$) and char gasification with steam ($C + H_2O \rightleftharpoons CO + H_2$). When the ER is increased towards 0.30, the increase in autothermal heat strengthens these reduction reactions, causing CO formation to increase and reach its peak. However, at higher ERs (0.35), the CO fraction tends to decrease because some CO can be converted to CH_4.

CO_2 formation continues to decrease as ER increases. At ER 0.2, 5412 ppm is obtained; at ER 0.25, 4592 ppm; at ER 0.3, 3916 ppm; and at ER 0.35, 3479 ppm. The increase in oxidant supply at this ER does not promote complete combustion, but rather strengthens the CO_2 reduction mechanism. At higher ERs, the heat generated from partial oxidation increases the temperature of the reduction zone, thereby accelerating the Boudouard reaction ($C + CO_2 \rightleftharpoons 2CO$), in which CO_2 is reduced by char to CO. This mechanism is consistent with the increase in CO until it reaches a maximum at an ER of 0.30, while also explaining the decrease in CO_2 under the same conditions. Interestingly, at an ER of 0.35, CO_2 remains at its lowest level even though CO decreases, indicating that the CO formed is not completely accumulated at the outlet but has the potential to undergo further conversion along the gas flow path.

5. 5. Effect of Catalyst Loading on Syngas Product

5. 2. 2. Effect of Catalyst Loading on Syngas Product

The catalyst load or amount of catalyst in this study was 4%, 6%, 8%, and 10% of the total biomass weight. The figure 6. shows that the composition of H_2 and CH_4 increases as the catalyst load decreases. The H_2 gas composition at catalyst loads of 4%, 6%, 8%, and 10% is 3742 ppm, 3471 ppm, 3372 ppm, and 3176 ppm, respectively. As the catalyst load increases, the reaction pathways that consume H_2 tend to strengthen, particularly the reverse water–gas shift ($CO_2 + H_2 \rightarrow CO + H_2O$) and H_2 interactions on the catalyst surface during the conversion of gasification compounds. As a result, even though reforming occurs, the measured net H_2 decreases because more H_2 is used for CO formation and surface reactions. The CH_4 gas composition at catalyst loads of 4%, 6%, 8%, and 10% was 7031 ppm, 6476 ppm, 6206 ppm, and 5746 ppm, respectively. An increase in catalyst load increases the number of active sites and gas-catalyst contact, so that methane/light hydrocarbon cracking and reforming occur more intensely. CH_4 then acts as a reactant that is converted into more reactive syngas components, causing the CH_4 concentration to decrease at higher catalyst loads.

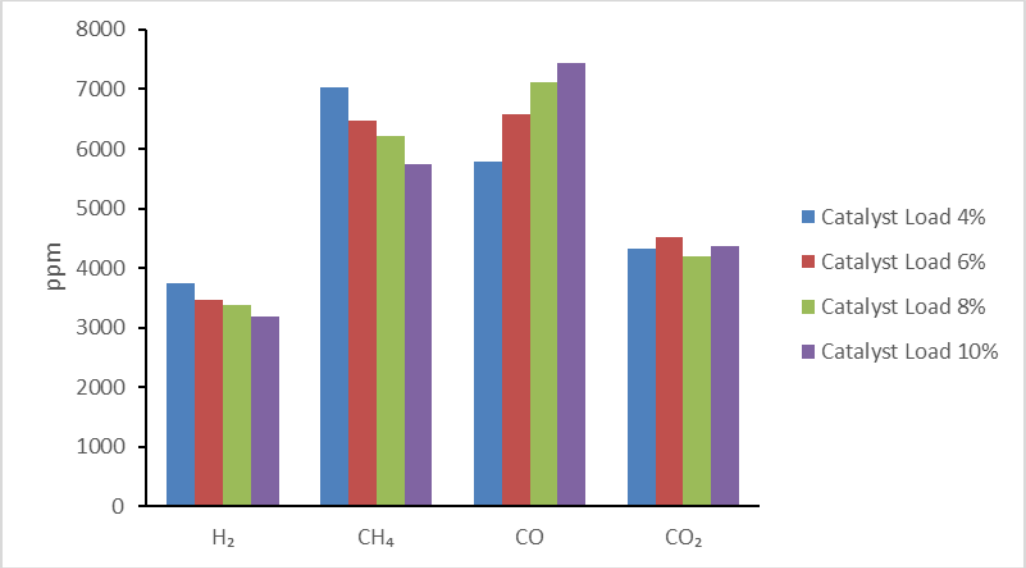


Fig. 6. Syngas Composition with Catalyst Load Variation

The CO gas composition increases with increasing catalyst load, namely for catalyst loads of 4%, 6%, 8% and 10% at 5782 ppm, 6576 ppm, 7111 ppm and 7445 ppm, respectively. The increase in catalyst loading strengthens the CO-forming reactions, particularly dry reforming ($CH_4 + CO_2 \rightarrow 2CO + 2H_2$), char–$CO_2$ reaction ($C + CO_2 \rightarrow 2CO$), and reverse water-gas shift. This combination shifts the product selectivity towards CO, so that the CO fraction increases consistently as the catalyst is increased. The CO_2 gas composition tends to stagnate with increasing catalyst loading, at catalyst loads of 4%, 6%, 8%, and 10% at 4322 ppm, 4510 ppm, 4198 ppm, and 4369 ppm, respectively. CO_2 shows minor changes because it is in a searching for a chemical equilibrium between the partial oxidation and the dry reforming. When the catalyst load increases, the rate of CO_2 consumption may rise, but this is often offset by CO_2 formation in the reaction zone, so that the CO_2 value appears stable or only fluctuates.

5. 6. Effect of Catalyst Ratio on Syngas Product

5. 2. 3. Effect of Catalyst Ratio on Syngas Product

At a catalyst load of 4%, the CaO/AC ratio changes the gasification reaction through differences in the dominance of tar cracking/reforming and CO_2 capture by CaO, so that the gas composition is highly dependent on the number of active sites and the effectiveness of gas-catalyst contact. At 0:1 (AC), CH_4 and CO are relatively high because AC promotes volatile/tar cracking, but CO_2 remains high because there is no absorption. At 1:0 (CaO), CH_4 decreases but CO_2 is highest, indicating that CO_2 capture is not yet effective due to limited surface area/carbonate layer formation. The 1:1 ratio produces the highest CO with moderate CO_2, indicating CaO–AC synergy that increases the conversion of volatiles into reactive gases. Meanwhile, the 2:1 (CaO-rich) ratio provides the highest H_2 and lowest CO_2 due to the sorption-enhanced effect of CaO, but

CH_4 remains high due to the smaller contribution of AC, so methane reforming/cracking is not yet optimal.

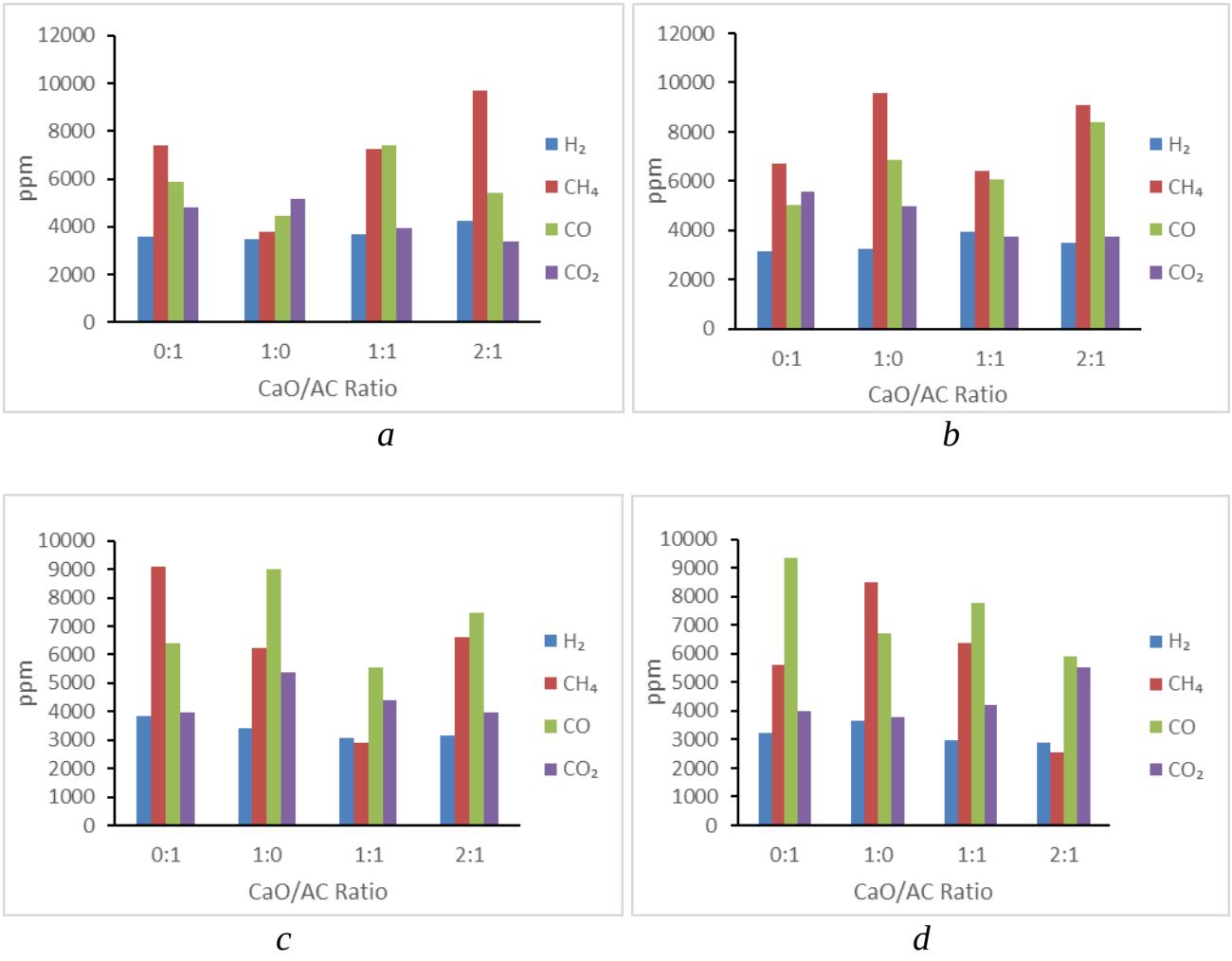


Fig. 7. Effect CaO/AC ratio with various catalyst load: *a* – 4%, *b* – 6%, *c* – 8%, *d* – 10%

At a catalyst load of 4%, the CaO/AC ratio changes the gasification reaction through differences in the dominance of tar cracking/reforming and CO_2 capture by CaO, so that the gas composition is highly dependent on the number of active sites and the effectiveness of gas-catalyst contact. At 0:1 (AC), CH_4 and CO are relatively high because AC promotes volatile/tar cracking, but CO_2 remains high because there is no absorption. At 1:0 (CaO), CH_4 decreases but CO_2 is highest, indicating that CO_2 capture is not yet effective due to limited surface area/carbonate layer formation. The 1:1 ratio produces the highest CO with moderate CO_2, indicating CaO–AC synergy that increases the conversion of volatiles into reactive gases. Meanwhile, the 2:1 (CaO-rich) ratio provides the highest H_2 and lowest CO_2 due to the sorption-enhanced effect of CaO, but

CH_4 remains high due to the smaller contribution of AC, so methane reforming/cracking is not yet optimal.

At a catalyst load of 6%, the CaO/AC ratio mainly shifts the selectivity of secondary reactions (tar cracking/reforming and CO_2 capture), where AC enhances the conversion of volatiles/light hydrocarbons, while CaO reduces CO_2 through carbonation ($CaO + CO_2 \rightarrow CaCO_3$) and changes the reaction equilibrium. At 0:1, CH_4 and CO_2 remain high because there is no CO_2 capture and methane reforming is not yet optimal, so volatiles still escape as CH_4. At 1:0, CO_2 tends to decrease, but CH_4 becomes the highest due to the absence of AC's role in cracking/reforming. The most favorable conditions occur at 1:1, with the highest H_2 and lowest CO_2, indicating CaO–AC synergy that promotes sorption-enhanced reforming and increases the conversion of hydrocarbons into syngas components. At 2:1, CO is highest and CO_2 remains low, but CH_4 rises again and H_2 is not maximized because excess CaO has the potential to rapidly carbonate/cause contact limitations, thereby reducing the contribution of AC in cracking/reforming.

At a catalyst load of 8%, the CaO/AC ratio significantly shifts the selectivity of the syngas reaction. At 0:1 (AC), CH_4 is still high because some light hydrocarbons have not been fully converted even though the tar cracking process is already active. At 1:0 (CaO), CO increases the most, but CO_2 also tends to be high, indicating that CaO in this condition is more dominant in promoting the CO formation pathway, while the CO_2 capture function is not yet optimal due to contact limitations or carbonation saturation. The 1:1 ratio produces the lowest CH_4, indicating the most effective CaO–AC synergy for cracking/reforming light hydrocarbons so that more methane is converted into reactive gas. At 2:1, CO increases again but CH_4 also rises, indicating that a smaller AC fraction reduces the intensity of methane reforming/cracking, while the decrease in CO_2 remains dependent on the effectiveness of CaO sorption.

At a catalyst load of 10%, the increase in total catalyst makes secondary reactions, reforming, solid-gas heterogeneous reactions, and equilibrium shifts very dominant, so that the CaO/AC ratio mainly determines the direction of product selectivity. At 0:1 (AC), CO formation tends to be strongest because the porous carbon surface accelerates the cracking/reforming of volatiles and the conversion of tar into reactive gases. At ratios involving CaO (1:0, 1:1, 2:1), CaO can retain CO_2 through carbonation, but at high loads the effect is often non-linear because CaO rapidly carbonates/diffusion limitations and pore blocking occur, so that under CaO-rich conditions (2:1) CH_4 can decrease, but CO_2 may increase and H_2 is not maximized due to reaction competition. Overall, at a 10% load, a trade-off is observed: AC-dominant increases CO, while CaO-dominant suppresses light hydrocarbons but has the potential to trigger non-ideal conditions (saturation/mass transport) that reduce the benefits of H_2 and CO_2.

5.7 LHV Syngas

5. 2. 4. Syngas Low Heating Value

To calculate the LHV of syngas, it must first be converted from ppm to % volume of gas. The formula is $\%vol_i = \frac{ppmv_i}{10^4}$. To calculate the LHV, use the formula

$$LHV_{mix}\left(\frac{MJ}{Nm^3}\right) = \frac{10{,}8(\%H_2) + 12.63(\%CO) + 35.8(\%CH_4)}{100}$$

LHV H_2 = 10.8 MJ/Nm^3

LHV CO = 12.63 MJ/Nm^3

LHV CH_4 = 35.8 MJ/Nm^3

As shown in Fig. 8, the syngas low heating value (LHV) varies with the equivalence ratio (ER) and catalyst load.

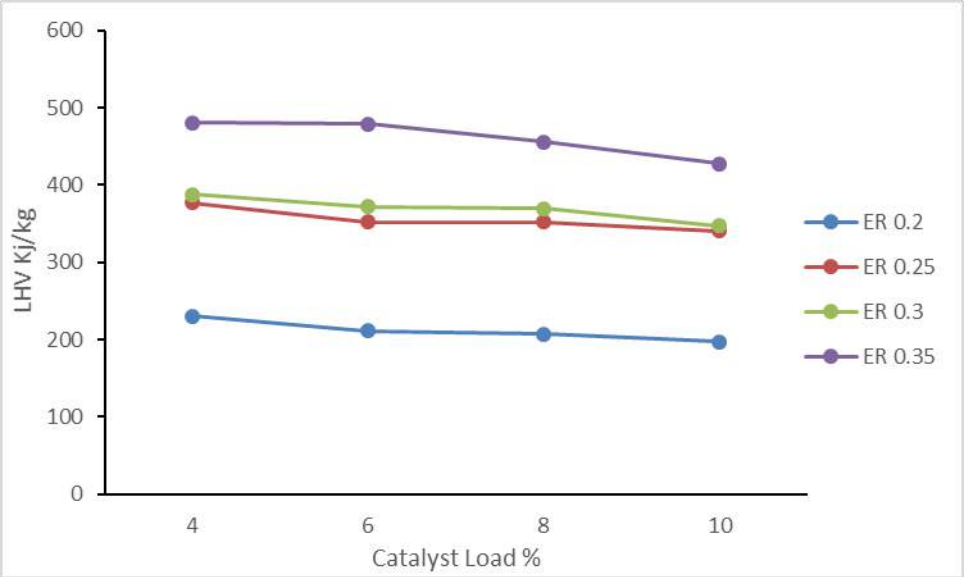


Fig. 8. LHV syngas with various ER

Fig. 8. Syngas Low Heating Value with various Equivalence Ratio

Fig. 8 shows that the LHV value increases with the ER. At the same catalyst load of 4%, the LHV will increase in line with the increase in ER. ER 0.2 has an LHV of 230 kJ/kg and ER 0.35 has an LHV of 481 kJ/kg. Higher ER produces more intense autothermal conditions, causing the reactor temperature to rise. This increase in temperature accelerates the decomposition of volatiles and tar cracking, and promotes more complete gasification and reforming reactions, thereby increasing the fraction of permanent gases that contribute to the calorific value, mainly CO and CH_4, as well as some H_2. In addition, the increase in temperature is also associated with more effective

hydrogen formation, because H_2 formation reactions (e.g., through steam-water and reforming reactions) are generally more optimal at high temperatures, with the temperature range often reported to be most conducive to H_2 formation being 800–1000°C.

At ER 0.2, the highest LHV was obtained at a catalyst load of 4% at 230 kJ/kg and continued to decrease with increasing catalyst load to 197 kJ/kg at 10%. At ER 0.25, the highest LHV was also obtained at a catalyst load of 4% at 377 kJ/kg and also decreased to 341 kJ/kg at a catalyst load of 10%. At ER 0.3, the highest LHV was obtained at a catalyst load of 4% at 388 kJ/kg and also decreased at a catalyst load of 10% to 347 kJ/kg. At ER 0.35, the highest LHV was obtained at 481 kJ/kg and decreased at a catalyst load of 10% to 428 kJ/kg.

However, all ER values show that LHV tends to decrease when the catalyst load is increased from 4% to 10%. This decrease indicates that excessive catalyst addition under these operating conditions does not always improve gas energy quality, because the catalyst can shift the reaction selectivity towards the conversion of high calorific components especially CH_4 into CO and H_2 through reforming, while at the same time the fraction of diluent gases such as CO_2 (and steam) may increase due to reaction. Since CH_4 has a very large calorific value contribution in the syngas mixture, the decrease in its fraction is often more dominant than the increase in CO/H_2, so that the total LHV tends to decrease.

There must be a reference to the Fig. 9 in the text before the Figure

In energy system analysis, particularly in combustion, gasification, and fuel gas utilisation processes such as syngas, the LHV value is often used because it better represents the heat energy that can actually be utilised by the system. The LHV value of a fuel gas is usually influenced by the composition of combustible gases such as carbon monoxide (CO), hydrogen (H_2), and methane (CH_4). The higher the content of these gases, the greater the LHV value produced. The LHV of syngas from this study with variations in ER and CaO/AC-PF ratio can be seen in Figure 9.

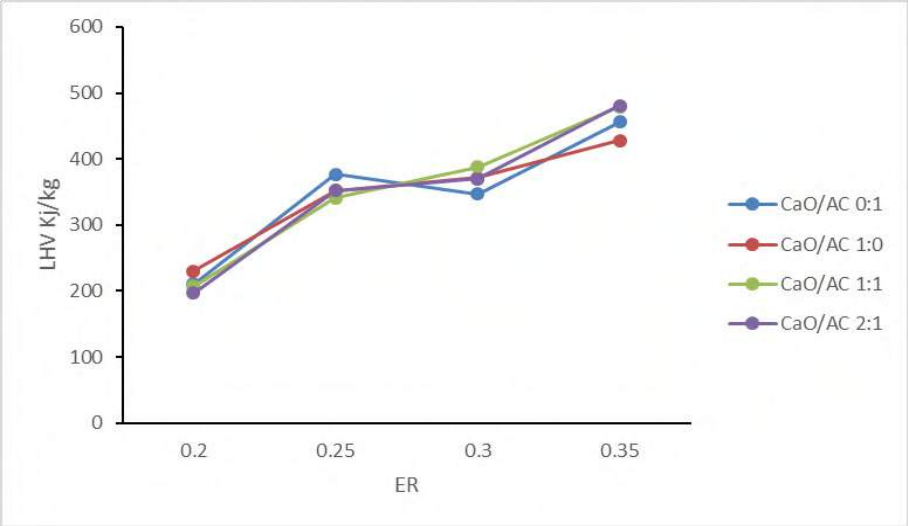


Fig. 9. LHV Syngas with Various CaO/AC Ratio
Fig. 9. Syngas Low Heating Value with Various CaO/AC Ratio

Fig. 9 shows that the LHV of syngas increases consistently with the increase in ER 0.2 to 0.35 for all CaO/AC ratios, indicating that a higher ER strengthens autothermal conditions so that the reaction temperature increases and the conversion of volatiles into syngas becomes more complete. At low ER (0.2), the difference in LHV between ratios is still small because secondary reactions such as cracking, reforming and heterogeneous reactions are not yet dominant; the system is still relatively influenced by incompletely converted volatiles. When the ER is increased to 0.25–0.30, the effect of the catalyst ratio becomes apparent: compositions involving AC tend to produce higher LHV because they accelerate tar cracking and increase the fraction of calorific gas, while the contribution of CaO can shift the reaction equilibrium through a decrease in CO_2. At the highest ER (0.35), the LHV reaches its maximum at all ratios, with CaO/AC 2:1 and 0:1 showing peak values, indicating that at high temperatures, the reactive gas formation pathway (via cracking/reforming on the carbon surface and/or CaO-rich-promoted heterogeneous reactions) becomes dominant. Overall, ER acts as the main controlling factor for LHV increase through the temperature effect, while the CaO/AC ratio modulates LHV through the balance between cracking/reforming (AC) and CO_2 control (CaO), especially at medium-high ER.

6. Discussion **The title of the section should be specific and correspond to the essence of the article**

The section is structured like this:

Answer the question, what explains the results obtained? When answering this question, it is necessary to refer to those objects in the article, which display the discussed result. Such objects are formulas, figures, tables.

What are the peculiarities of the proposed method and the obtained results in comparison with the existing ones (it is necessary to make a comparison with the known data, indicating the references to the relevant works of colleagues)

What limitations are inherent in the given research (in general it can be: the applicability limits of the proposed solutions / results obtained, the applicability conditions of the proposed solutions / results obtained, reproducibility of the results / methods of obtaining results, stability of solutions to the change of influencing factors, the range of input data within which the results are adequate and can be reproduced, leading to the stated effects, etc.)

What disadvantages of this study can be noted and how they can be eliminated in the future. Warning. Disadvantages and limitations are not the same thing

What might be the development of this study and what difficulties (mathematical, methodological, experimental, or any other) might be encountered along the way?

The characteristics of AC-PF-based catalysts (activated carbon from palm fiber) show a rough, porous surface that supports tar/volatile adsorption and increases the chances of heterogeneous reactions (cracking/reforming) on the catalyst surface. This porous structure is crucial in updraft gasification because pyrolysis gases and volatiles move through the bed, so the presence of porous media has the potential to strengthen secondary reactions before the gas exits to the condenser. After the addition of CaO, CaO particle dispersion was observed on the carbon surface; however, at high CaO ratios (e.g., 2:1), the structure became denser, indicating that some of the micropores were closed. Nevertheless, BET data reveal an important phenomenon: the surface area decreases, but the pore diameter increases to the mesopore scale, which can improve the accessibility of tar/volatiles to active sites and improve mass transport in the reforming reaction. From a surface chemistry perspective, FTIR indicates the presence of –OH groups and Ca carbonate, confirming that CaO acts not only as a base catalyst but also as a CO_2 sorbent, enabling a sorption-enhanced mechanism that modulates the gasification reaction equilibrium [35].

On the process side, ER emerges as the dominant variable governing autothermal conditions, primarily through increases in effective temperature and secondary reaction intensity. An increase in ER from low to high levels consistently increases H_2, which can be explained by the acceleration of H_2 formation reactions such as char gasification with steam ($C + H_2O \rightarrow CO + H_2$) [36], light hydrocarbon reforming, and more intense tar cracking at higher temperatures. At the same time, CH_4 also increases sharply at high ER, indicating that in updraft autothermal systems, increased temperature and changes in gas composition can facilitate the formation of light gases. Meanwhile, CO tends to peak at medium ER and then decreases at higher ER, consistent with competition between CO formation against CO consumption through subsequent reactions such as methanation [37]. The decrease in CO_2 at high ER indicates the role of high temperatures in enhancing the CO_2 reduction reaction by char (Boudouard) and/or the role of CaO sorption when available.

The effect of catalyst loading shows that adding catalyst does not always increase H_2. An increase in catalyst loading from low to high levels tends to decrease H_2 and CH_4 but increase CO. Mechanistically, this condition can occur when the catalyst strengthens pathways that increase CO and/or promotes RWGS ($CO_2 + H_2 \rightarrow CO + H_2O$)[38], which consumes H_2 so that net H_2 decreases. Additionally, at high catalyst loading, the possibility of diffusion/agglomeration penalties increases, so that selectivity may shift and some active sites become less effective. Thus, the target of H_2-rich syngas in this reactor is more dependent on ER adjustment and the selection of moderate/lower catalyst loading, rather than simply increasing the loading.

The CaO/AC-PF ratio exhibits synergistic but non-linear behaviour. AC-PF primarily acts as a porous medium that enhances cracking/reforming of volatiles, while CaO provides both basic sites and CO_2 sorbents to shift the equilibrium. At high CaO ratios, the sorption and base effects may increase, but the risk of micro-pore closure and diffusion pathway changes also increases. This explains why certain compositions are

optimal at certain catalyst loads: the best performance arises from a balance between pore accessibility the role of AC-PF and sorption/base strength the role of CaO.

From an energy quality perspective, the LHV value of syngas is highly sensitive to changes in CH_4. Therefore, high ER conditions that increase CH_4 tend to increase LHV. However, the interpretation of LHV needs to be read in conjunction with the process objective, because an increase in LHV is not always synonymous with an increase in syngas quality for all applications.

However, there are several limitations. First, the gas composition is obtained from ppm-based MQ sensors, so absolute accuracy can be affected by cross-sensitivity, humidity, sensor drift, and gas sampling temperature; this can affect %vol and LHV estimates, especially when CO and CH_4 changes occur simultaneously. Second, catalyst characterization (SEM-FTIR-BET) already supports the role of surface texture and chemistry, but has not yet quantified active phase changes during operation. carbonation levels, and activity decline due to fouling/pore closure

Based on these limitations, several directions for future work are recommended. Perform gas composition calibration/validation using GC-TCD/GC-FID or micro-GC to convert sensor readings into more accurate %vol and include LHV uncertainty analysis. Evaluate catalyst stability and regeneration, particularly for easily carbonated CaO, through carbonation-calcination cycle tests and post-reaction characterization (XRD/TGA/SEM-EDX) to assess phase changes and activity loss. Develop experimental designs towards ANOVA interactions or RSM so that interaction effects and predictive models can be obtained and validated through replication confirmation tests. Add process performance metrics such as gas yield (Nm^3/kg), cold gas efficiency, pressure drop, and air consumption so that "syngas quality improvement" can be demonstrated on the basis of mass-energy balance and operability, not just composition.

6. Discussion on the Catalytic Effect of AC-PF/CaO and Operating Conditions on Syngas Composition and LHV

The interaction of the CaO-AC-PF catalyst to improve syngas quality can be seen from the characterisation of the catalyst, the composition of the syngas and the LHV produced. From the Scanning Electron Microscopy results in Fig. 2, it can be seen that the CaO:AC-PF;2:1 catalyst (Fig. 2. c) appears denser than the other catalysts. With the addition of CaO, CaO particle dispersion can be seen on the white carbon surface, indicating that some micro pores are closed by CaO. With the addition of CaO, a lot of CO2 is absorbed and becomes $CaCO_3$. This porous structure is very important in top-flow gasification because pyrolysis gas and volatiles move through the layer, so the presence of a porous medium has the potential to strengthen secondary reactions and act as carbon capture before the gas exits to the condenser.

From a surface chemistry perspective, Fourier Transform Infrared Spectroscopy (FTIR) shows the presence of –OH and calcium carbonate groups, as shown in Fig. 3. This is due to the results of KOH impregnation carried out during the manufacture of AC-PF. The presence of -OH groups functions as polar active sites capable of adsorbing

polar molecules such as H_2O, CO_2, and volatile compounds. Surfaces with -OH groups tend to be hydrophilic and reactive, thereby enhancing interactions with tar compounds or heavy hydrocarbons. These tar compounds can then undergo thermal cracking or catalytic reforming into light gases such as H_2, CO, and CH_4. In addition to -OH, there are also O-H and C-O groups. The O-H group has characteristics that are almost the same as the -OH group, while the C-O group plays a role in enhancing the redox properties and chemical interactions between the carbon surface and gas molecules. In the gasification process, the C-O group can be part of the partial oxidation mechanism and carbon gasification reaction, which produces CO[35].

The BET data in Fig. 4 shows that the surface area decreased to 5.06 m^2/g, but the pore diameter increased to a mesopore scale of 22.87 nm, which can improve the accessibility of volatiles to active sites and improve mass transport in the reforming reaction. In Fig. 4.b, the BJH curve at CaO:AC-PF = 2:1 shows the highest dV/dD values of 30–40 nm, indicating a catalyst in the mesopore size range. The presence of these mesopores will further increase the active sites for CO_2 adsorption.

From a process perspective, in Fig. 5, ER appears as the dominant variable that regulates autothermal conditions, primarily through an increase in effective temperature and secondary reaction intensity. An increase in ER from low to high levels consistently increases H_2, which can be explained by the acceleration of H_2 formation reactions such as charcoal gasification with steam ($C + H_2O \rightarrow CO + H_2$) [36], light hydrocarbon reforming, and more intense tar cracking at high temperatures. At the same time, CH_4 also increases sharply at high ER, indicating that in an autothermal upflow system, increased temperature and changes in gas composition can facilitate the formation of light gases. Meanwhile, CO tends to peak at moderate ER and then decreases at high ER, consistent with competition between CO formation and CO consumption through subsequent reactions such as methanation [37]. The decrease in CO_2 at high ER indicates the role of high temperatures in enhancing the reduction of CO_2 by charcoal (Boudouard reaction) and/or the role of CaO adsorption if available.

The effect of catalyst loading in Fig. 6 shows that adding catalyst does not always increase H_2. Increasing the catalyst loading from low to high tends to reduce H_2 and CH_4 but increase CO. Mechanistically, this condition can occur when the catalyst strengthens pathways that increase CO and/or promotes RWGS ($CO_2 + H_2 \rightarrow CO + H_2O$)[38], which consumes H_2 so that net H_2 is reduced. Furthermore, at high catalyst loadings, the possibility of diffusion/aggregation penalties increases, so that selectivity may shift and some active sites become less effective. Therefore, the target of H_2-rich synthesis gas in this reactor is more dependent on ER adjustment and the selection of moderate/low catalyst loadings, rather than simply increasing the loading.

The CaO/AC-PF ratio in Fig. 7 shows synergistic but non-linear behaviour. AC-PF plays a major role as a porous medium that enhances the cracking/reforming process of volatile compounds, while CaO provides a basic site and CO_2 absorber to shift the equilibrium. At high CaO ratios, sorption and base effects may increase, but the risk of micro-pore closure and diffusion pathway changes also increases. This explains why

certain compositions are optimal at certain catalyst loads: the best performance arises from a balance between pore accessibility (the role of AC-PF) and sorption/base strength (the role of CaO).

From an energy quality perspective, in Figures 8 and 9, the LHV value of synthetic gas is highly sensitive to changes in CH_4. Therefore, high ER conditions that increase CH_4 tend to increase LHV. H_2, CH_4 and CO are the main factors for obtaining high LHV. CO_2 has no calorific value so it must be captured. In this study, CaO was used so that CO_2 could be suppressed, meaning that the total LHV could be increased. The highest LHV in this study was 481 kJ/kg, while in another study, the highest was 550 kJ/kg using pinewood with dolomite, activated carbon, silica gel, and limestone catalysts [39]. The higher the ER, the more oxygen enters the system, thereby increasing the reforming reaction [40].

There are several limitations to this study. First, the gas composition was obtained from an MQ sensor based on ppm, so absolute accuracy may be affected by cross-sensitivity, humidity, sensor drift, and gas sampling temperature; this may affect the estimation of %vol and LHV, especially when changes in CO and CH_4 occur simultaneously. Second, catalyst characterisation (SEM-FTIR-BET) supports the role of surface texture and chemistry, but has not quantified changes in the active phase during operation, the degree of carbonation, and the decrease in activity due to pore closure accumulation.

The disadvantage of this research is that the CaO catalyst reacts very easily with CO_2. After the calcination process, CaO must be stored in an airtight container to prevent it from clumping into $CaCO_3$. The catalyst has a specific usage period because it is covered with tar or ash.

Based on these limitations, several future directions are recommended. Calibrate the gas composition using GC-TCD/GC-FID to convert the sensor readings into more accurate %vol and include LHV uncertainty analysis. Evaluate catalyst stability and regeneration, especially for CaO which is easily carbonated, through carbonation-calcination cycle tests and post-reaction characterisation (XRD/TGA/SEM-EDX) to assess phase changes and activity loss. Develop experimental designs towards ANOVA or RSM interactions so that interaction effects and predictive models can be obtained and verified through replication confirmation tests. Add process performance metrics such as gas yield (Nm^3/kg), cold gas efficiency, pressure drop, and air consumption so that ‘syngas quality improvement’ can be demonstrated based on mass-energy balance and operability, not just composition.

7. Conclusion

1. AC-PF with rich -OH group acts as a porous catalytic medium that facilitates volatile cracking and supports the reduction of condensable by-products, while CaO contributes to absorb CO_2. The BJH analysis confirms that CaO plays a dual role as a reactive sorbent and a textural promoter in palm-fiber activated carbon by enlarging mesopores (20–40 nm), thereby enhancing gas diffusion and improving access to CaO active sites, which ultimately strengthens catalytic performance.

2. Increasing ER to 0.35 enhances the combustible gas fraction H_2 and CH_4 and suppresses CO_2, whereas CO typically peaks at intermediate ER due to competing CO formation and consumption reactions along the updraft reaction zones. Increasing catalyst loading shifts syngas composition: CO increases, while H_2 and CH_4 decrease, indicating changes in dominant secondary reactions and possible diffusion or agglomeration limitations at higher loadings. Increasing ER lead to increase LHV syngas, but it can decrease at high catalyst loading. An increase in the CaO/AC ratio to 2:1 resulted in a higher syngas LHV, with a maximum value of 481 kJ/kg.

Conflict of interest

The authors declare that they have no conflict of interest in relation to this research, whether financial, personal, authorship or otherwise, that could affect the research and its results presented in this paper.

Financing

The authors sincerely thank the Ministry of Education, Culture, Research and Technology, Republic of Indonesia for fully supporting this research through the DRTPM Research Grant under Fundamental Research, Universitas Widyagama Malang, Indonesia 2025 (Grant Number:128/C3/DT.05.00/PL/2025;023/LL7/DT.05.00/PL/2025;010/ Kontrak/PT/PTS.030.7/PN/V/2025).

Data availability

Manuscript has no associated data.

Use of artificial intelligence

The authors declare that generative artificial intelligence tools were used exclusively for language editing, grammar checking, and technical formatting of the manuscript under full human control. Artificial intelligence was not used to generate, process, or interpret scientific data, form conclusions, or other ele-ments of the scientific results in the paper. Tool used: ChatGPT (OpenAI GPT-5.2, version 2026). The authors bear full responsibility for the content, reliability, and scientific correctness of the submitted material.

Example:

It is necessary to declare the use of AI according to the scheme:
– model and number of AI,
– where exactly it was used (in which section of the article),
– what exactly was done using AI tools (specific description),
– how the authors checked the results provided by AI tools,
– how the result provided by the AI tool influenced the conclusions of the study.

Warning:

1. In the process of finalizing the manuscript based on the comments of editors and reviewers, the use of AI tools **is possible only if the permissible scope and tasks are observed** https://journals.uran.ua/eejet/artificial-intelligence

2. Detection of undeclared use of AI and/or use of AI outside the permissible tasks delegated to AI or the scope https://journals.uran.ua/eejet/artificial-intelligence at the review stage or after it as part of quality assurance and ethical standards control will lead to the manuscript being withdrawn from consideration / removed from the editorial portfolio, and sanctions provided for by the License Agreement.

The authors used the AI-based language model ChatGPT (GPT-5.3) only to assist in improving the clarity of English language and grammar in several sections of the manuscript, particularly in the Introduction and Literature Review sections.
The AI tool was used solely for language editing and paraphrasing purposes. All scientific content, experimental design, data analysis, and interpretation of the results were conducted entirely by the authors.
The authors carefully reviewed and verified all AI-assisted text to ensure accuracy and consistency with the experimental results. The use of AI tools did not influence the scientific conclusions of this study.

Acknowledgements

We as the Research Team would like to thank Ministry of Education, Culture, Research and Technology, Republic of Indonesia (Kemendiktisaintek Indonesia) for financing research activities.

Authors' contributions

Indicate the author's contribution according to CRediT (Author Role Taxonomy) in the format:

Author1 first name last name: contribution1, contribution2, contribution3; **Author2 first name last name**: contribution1, contribution2, contribution3

In this section, you should only indicate the name of the contribution, which must be selected from the list of contributions on the CRediT (Author Role Taxonomy)

Purbo Suwandono: Conceptualization, Writing–original draft, Investigation, Supervision, Formal analysis, Writing–review & editing
Widya Wijayanti: Validation, Investigation, Data Curation, Formal analysis, Writing–original draft
Nova Risdiyanto Ismail: Writing – review & editing, Formal analysis
Dzulfikar Johan Akbar: Visualization, Writing – original draft, Data curation.
Muhammad Reza: Project administration, Resources, Data curation.

We ask authors of the article in the literature to highlight (in purple color) references to articles in Scopus journals (Q1, Q2). If there is no reference, it should be added by all means.

References

Please check, self-citation should not exceed 30 %.
If possible, please provide active hyperlinks to the entire list of literature.

1. ASEAN Statistical Brief, "Role of Agriculture , Forestry , and Fishing Industry in ASEAN Economy," vol. VII, no. June 2023, p. 511191, 2024.
2. V. K. Yadav *et al.*, "Emerging trends in the valorization of agricultural waste and their utilization in agricultural, pharmaceuticals, and environmental cleanup," *Waste and Biomass Valorization*, pp. 1–55, 2025.
3. W. M. Lewandowski, M. Ryms, and W. Kosakowski, "Thermal biomass conversion: A review," *Processes*, vol. 8, no. 5, p. 516, 2020.
4. D. Ariyanti *et al.*, "Valorization of corn cob waste for furfural production: A circular economy approach," *Biomass and Bioenergy*, vol. 194, p. 107665, 2025.
5. A. Raizada, A. Shukla, S. Yadav, P. Katiyar, and R. Kumar, "Enhancement of H2 production via catalytic steam gasification of food waste as feedstock and its ash as a support and promoter for Ni catalyst," *Int. J. Hydrogen Energy*, vol. 60, pp. 272–281, 2024.
6. Y. Dai *et al.*, "Co-gasification characteristics of Ca-rich sludge and Fe-rich sludge under CO2 atmosphere, and potential utilization of gasification residues as renewable catalyst in biomass pyrolysis," *Renew. Energy*, vol. 224, p. 120118, 2024.
7. H. Sun *et al.*, "Three-stage behaviors of K2CO3 catalyst during CO2 catalytic gasification of coal," *Fuel*, vol. 367, p. 131149, 2024.
8. J. Zhang, Z. Chu, R. Cao, X. Wu, and K. Han, "A review of resource recovery from waste plastics via pyrolysis and gasification," *Fuel*, vol. 404, p. 136319, 2026.
9. Y. Tangke Tosuli, Cahyadi, H. Dafiqurrohman, R. Hermawan, and A.

Surjosatyo, “Gasification of sago dreg waste in a top-lit updraft fixed bed gasifier: Syngas composition and its effect with additional Al2O3 as catalyst,” *Energy Convers. Manag. X*, vol. 24, no. October, p. 100775, 2024, doi: 10.1016/j.ecmx.2024.100775.

10. P. Dinh *et al.*, “Enrichment of hydrogen in product gas from a pilot-scale rice husk updraft gasification system,” *Carbon Resour. Convers.*, vol. 5, no. 3, pp. 231–239, 2025, doi: 10.1016/j.crcon.2022.07.003.

11. S. Yousef and J. Eimontas, “International Journal of Hydrogen Energy Oxygen updraft gasification-catalytic reforming of cigarettes butts for hydrogen-rich syngas production,” vol. 171, no. May, 2025, doi: 10.1016/j.ijhydene.2025.150650.

12. D. Contreras, E. Blanco, and D. Travieso, “Experimental assessment of the energy potential of pellets produced from beekeeping wastes by updraft gasification,” vol. 343, no. January, 2025, doi: 10.1016/j.enconman.2025.120206.

13. N. Yesilova, O. Tezer, A. Ongen, and A. Ayol, “International Journal of Hydrogen Energy Enhancing biomass gasification : A comparative study of catalyst applications in updraft and modifiable-downdraft fixed bed reactors,” *Int. J. Hydrogen Energy*, vol. 76, no. April, pp. 290–303, 2024, doi: 10.1016/j.ijhydene.2024.05.075.

14. R. Skvor and A. Jan, “Experimental investigation of sorted municipal solid wastes producer gas composition in an updraft fixed bed gasifier,” vol. 289, no. August 2022, 2024, doi: 10.1016/j.energy.2023.130063.

15. R. Junga, M. Tańczuk, S. Sobek, M. Chabiński, and Ł. Ziółkowski, “Effect of the addition of laying hens manure to the straw on gasification efficiency in updraft gasifier under air atmosphere,” *Appl. Therm. Eng.*, vol. 226, no. February, p. 120269, 2023, doi: 10.1016/j.applthermaleng.2023.120269.

16. A. Ongen and A. Ayol, “ScienceDirect Gasification performance of olive pomace in updraft and downdraft fixed bed reactors,” vol. I, 2023, doi: 10.1016/j.ijhydene.2023.02.088.

17. K. Ertas, “Gasification of MDF residue in an updraft fixed bed gasifier to produce heat and power via an ORC turbine,” vol. 169, no. February, pp. 43–51, 2023, doi: 10.1016/j.wasman.2023.06.025.

18. S. Gorthy, S. Verma, N. Sinha, S. Shetty, H. Nguyen, and M. Neurock, “Theoretical Insights into the Effects of KOH Concentration and the Role of OH–in the Electrocatalytic Reduction of CO2 on Au,” *ACS Catal.*, vol. 13, no. 19, pp. 12924–12940, 2023.

19] X. Wang, W. Zeng, C. Xin, X. Kong, X. Hu, and Q. Guo, “The development of activated carbon from corncob for CO2 capture,” *RSC Adv.*, vol. 12, no. 51, pp. 33069–33078, 2022, doi: 10.1039/d2ra05979g.

20. D. Ali, H. Fakra, D. Armel, and S. Andriatoavina, “A simple and low-cost integrative sensor system for methane and hydrogen measurement,” vol. 1, no. August, 2020, doi: 10.1016/j.sintl.2020.100032.

21. S. V. Co-digestion and H. Ram, “Assessment of a Low-Cost Hydrogen Sensor for Detection and Monitoring of Biohydrogen Production during Sugarcane,” pp. 479–490, 2024.

22. H. Du *et al.*, “Lignocellulosic Films: Preparation, Properties, and Applications,” *Chem. Rev.*, 2025.
23. S. De, A. M. Balu, J. C. Van Der Waal, and R. Luque, “Biomass-derived porous carbon materials: synthesis and catalytic applications,” *ChemCatChem*, vol. 7, no. 11, pp. 1608–1629, 2015.
24. C. Li *et al.*, “Importance of oxidation reactions in creating pores in physical activation of biomasses,” *Chem. Eng. J.*, vol. 474, p. 145748, 2023.
25. B. Zhou *et al.*, “Insights into effects of grain boundary engineering in composite metal oxide catalysts for improving catalytic performance,” *J. Colloid Interface Sci.*, vol. 653, pp. 1177–1187, 2024.
26. Y. Zhu *et al.*, “Preparation of hierarchically porous carbon ash composite material from fine slag of coal gasification and ash slag of biomass combustion for CO2 capture,” *Sep. Purif. Technol.*, vol. 330, p. 125452, 2024.
27. Y. Y. García-Guel, E. M. Múzquiz-Ramos, J. C. Ríos-Hurtado, A. Moreno-Santos, S. E. Flores-Villaseñor, and G. B. Escalante-Ibarra, “Surface modification of activated carbon cloth with calcium silicate and hydroxyapatite: bioactive composite material,” *Heliyon*, vol. 8, no. 11, 2022.
28. M. Ilić *et al.*, “Surface functional groups and degree of carbonization of selected chars from different processes and feedstock,” *PLoS One*, vol. 17, no. 11, p. e0277365, 2022.
29. R. Ali, Z. Aslam, R. A. Shawabkeh, A. Asghar, and I. A. Hussein, “BET, FTIR, and RAMAN characterizations of activated carbon from waste oil fly ash,” *Turkish J. Chem.*, vol. 44, no. 2, pp. 279–295, 2020.
30. K. J. Stanienda-Pilecki, “The importance of Fourier-Transform Infrared Spectroscopy in the identification of carbonate phases differentiated in magnesium content,” 2019.
31. F. Dai, Q. Zhuang, G. Huang, H. Deng, and X. Zhang, “Infrared spectrum characteristics and quantification of OH groups in coal,” *ACS omega*, vol. 8, no. 19, pp. 17064–17076, 2023.
32. E. M. de Salazar Martínez, M. F. Alexandre-Franco, A. J. Nieto-Sanchez, and E. M. Cuerda-Correa, “Exploring the role of surface and porosity in CO2 capture by CaO-based adsorbents through response surface methodology (RSM) and artificial neural networks (ANN),” *J. CO2 Util.*, vol. 83, p. 102773, 2024.
33. J. A. Tavizón-Pozos, H. Cervantes-Cuevas, G. G. Garcia-Camacho, G. Chavez-Esquivel, and D. R. Acosta-Najarro, “Biodiesel Production Using K–Sr/CaO and CaO Catalysts Derived from Eggshells by Canola Oil Transesterification,” *ACS omega*, vol. 10, no. 7, pp. 6827–6838, 2025.
34. W. Koo-Amornpattana, P. Phadungbut, N. Kunthakudee, W. Jonglertjunya, S. Ratchahat, and M. Hunsom, “Innovative metal oxides (CaO, SrO, MgO) impregnated waste-derived activated carbon for biohydrogen purification,” *Sci. Rep.*, vol. 13, no. 1, p. 4705, 2023.
35. C. Quan, M. Wang, N. Gao, T. Yang, and R. Li, “In situ adsorption of CO2

to enhance biomass gasification for hydrogen production using Ca/Ni based composites," *J. Energy Inst.*, vol. 108, p. 101229, 2023, doi: https://doi.org/10.1016/j.joei.2023.101229.

36. F. Micheli, E. Mattucci, C. Courson, and K. Gallucci, "Bi-Functional Catalyst/Sorbent for a H2-Rich Gas from Biomass Gasification," 2021. doi: 10.3390/pr9071249.

37. M. Zhu, Q. Wang, and S. Wang, "Recent Advances and Future Perspectives in Catalyst Development for Efficient and Sustainable Biomass Gasification: A Comprehensive Review," 2025. doi: 10.3390/su17167370.

38. N. Cerone, F. Zimbardi, L. Contuzzi, J. Baleta, and D. Cerinski, "Experimental investigation of syngas composition variation along updraft fixed bed gasifier," *Energy Convers. Manag.*, vol. 221, no. July, p. 113116, 2020, doi: 10.1016/j.enconman.2020.113116.

39. R. Mohanty, P. Mahanta, A. Mahapatro, and R. Prakash, "Catalytic gasification of pinewood biomass in a fluidized bed reactor with dolomite , limestone , and activated carbon : An experimental study," *Energy*, vol. 325, no. April, p. 136131, 2025, doi: 10.1016/j.energy.2025.136131.

40. C. Liu, Y. Huang, M. Niu, and H. Pei, "ScienceDirect Influences of equivalence ratio , oxygen concentration and fluidization velocity on the characteristics of oxygen-enriched gasification products from biomass in a pilot-scale fluidized bed," *Int. J. Hydrogen Energy*, vol. 43, no. 31, pp. 14214–14225, 2018, doi: 10.1016/j.ijhydene.2018.05.154.

Please fill in this table

Author's order	First Name	Middle name	Second Name
1	*Purbo*		*Suwandono*
2	*Widya*		*Wijayanti*
3	*Nova*	*Risdiyanto*	*Ismail*
4	*Dzulfikar*	*Johan*	*Akbar*
5	*Muhammad*		*Reza*

We ask the authors indicate the Corresponding author in the information about the authors, after the full name (Corresponding author is the author who is in correspondence with the editors and whose email address will be indicated as feedback for readers if they want to contact the author/group of authors)

English
Purbo Suwandono Master

Department of Mechanical Engineering
Widya Gama University
Borobudur str., 35, Mojolangu, Lowokwaru District, Malang City, East Java, 65142, Indonesia
The address of the university (in such sequence: street, house, city, country, index)
Borobudur str., 35, Malang, Indonesia, 65142
E-mail: purbo@widyagama.ac.id
ORCID: https://orcid.org/0000-0003-4085-1291
Contact phone: +6282132697144
Number of publications in national journals indexed (approximate; for Ukraine citizens only): -
Number of publications in international journals indexed (approximate): 14
H-index by Scopus (if available): 4
ResearchGate: https://www.researchgate.net/profile/Purbo-Suwandono
Scopus ID: 57204187970
Researcher ID: https://researchid.co/rid80879

Widya Wijayanti
PhD
Department of Mechanical Engineering
Brawijaya University
Veteran str., 10–11, Ketawanggede, Lowokwaru District, Malang City, East Java 65145, Indonesia
The address of the university (in such sequence: street, house, city, country, index)
Veteran str., 10–11, Malang, Indonesia, 65145
E-mail: widya_dinata@ub.ac.id
ORCID: https://orcid.org/0000-0003-4215-5943
Contact phone: +6285334992164
Number of publications in national journals indexed (approximate; for Ukraine citizens only): -
Number of publications in international journals indexed (approximate): 78
H-index by Scopus (if available): 12
ResearchGate: https://www.researchgate.net/profile/Widya-Wijayanti
Scopus ID: 36006672800
Researcher ID: -

Nova Risdiyanto Ismail
Doctor
Department of Mechanical Engineering
Widya Gama University
Borobudur Str., 35, Mojolangu, Lowokwaru District, Malang City, East Java 65142,

Indonesia
The address of the university (in such sequence: street, house, city, country, index)
Borobudur str., 35, Malang, Indonesia, 65142
E-mail: nova@widyagama.ac.id
ORCID: https://orcid.org/0000-0001-8439-6919
Contact phone:
Number of publications in national journals indexed (approximate; for Ukraine citizens only): -
Number of publications in international journals indexed (approximate): 7
H-index by Scopus (if available): 3
ResearchGate: https://www.researchgate.net/profile/Nova-Ismail-2
Scopus ID: 57204527065
Researcher ID: https://researchid.co/rid80876

Dzulfikar Johan Akbar
Master Student
Department of Mechanical Engineering
Brawijaya University
Veteran Str., 10–11, Ketawanggede, Lowokwaru District, Malang City, East Java 65145, Indonesia
The address of the university (in such sequence: street, house, city, country, index)
Veteran str., 10–11, Malang, Indonesia, 65145
E-mail: johanakbar@student.ub.ac.id
ORCID: https://orcid.org/0009-0002-4652-8516
Contact phone: +6282241116998
Number of publications in national journals indexed (approximate; for Ukraine citizens only): -
Number of publications in international journals indexed (approximate): -
H-index by Scopus (if available): -
ResearchGate: https://www.researchgate.net/profile/Dzulfikar-Johan-Akbar
Scopus ID: -
Researcher ID: -

Muhammad Reza
Bachelor Student
Department of Mechanical Engineering
Widya Gama University
Borobudur Str., 35, Mojolangu, Lowokwaru District, Malang City, East Java 65142, Indonesia
The address of the university (in such sequence: street, house, city, country, index)
Borobudur str., 35, Malang, Indonesia, 65142

E-mail: muhapanjangreza@gmail.com
ORCID: https://orcid.org/0009-0009-9258-0586
Contact phone: +6282139682566
Number of publications in national journals indexed (approximate; for Ukraine citizens only): -
Number of publications in international journals indexed (approximate): -
H-index by Scopus (if available): -
ResearchGate: -
Scopus ID: -
Researcher ID: -

Please attach to the manuscript information about potential reviewers for the topic (at least 2 reviewers). The editor reserves the exclusive right to decide whether or not to use the services of the proposed reviewers. In either case, the editorial staff practices a double-blind review policy.
Example (Fields marked with an asterisk (*) are required.)
Name of reviewer *
Professor*
Tel:
E-mail: *
Work address:

Name of reviewer: Prof. Dr. Muji Setiyo, ST., MT.
Professor: Mechanical Engineering
Tel: +6281211020288
E-mail: muji@unimma.ac.id.
Work address: Universitas Muhammadiyah Magelang

Name of reviewer: Prof. Dr. Eng. Nurkholis Hamidi, ST., MT.
Professor: Mechanical Engineering
Tel: +62 81259293165
E-mail: hamidy@ub.ac.id
Work address: Brawijaya University

TAHAP 3

REVIEW EDITOR TAHAP 3

8 Maret 2026

Purbo Suwandono <purbo@widyagama.ac.id>

from "Eastern-European Journal of Enterprise Technologies" - Suwandono P. (stage 3, No. 2(140).2026 (April))

4 messages

Oksana Nikitina <0661966nauka@gmail.com> Sun, Mar 8, 2026 at 3:48 AM
To: Purbo Suwandono <purbo@widyagama.ac.id>

Good afternoon, dear authors.

The article was accepted for consideration of the possibility of publication in (No. 2(140).2026).

At the 3rd stage of editing, please take into account the comments of the editor (article in the application, color notes are highlighted).

We ask you to right strictly in the option which is in the attachment (see attachment).

We ask you not to delete the comments so that we can see all your edits. All corrections by the author, please highlight in green.

Please provide an edited version of the article **by 10.03.2026.**

If you have any questions, please call or write; we will be happy to answer them.

With best regards, Manager Yu. Prylutska
TECHNOLOGY CENTER GROUP LTD
Viber/ WhatsApp/ Telegram: +380 (50) 3033801
Editorial staff of the "Eastern-European Journal of Enterprise Technologies"
Website: https://jet.com.ua/en/, http://journals.uran.ua/eejet/



Відвідати сайт Відвідати сайт

Attention! The author (team of authors) submitting the manuscript to the editorial office of the journal **«Eastern-European Journal of Enterprise Technologies»** agrees with all requirements for registration, submission of the manuscript of the article and payment and be responsible in case of violation of these requirements.

Our company may rely on your freely given consent at the time you provided your personal data to us replying on this email then the lawfulness of such processing is based on that consent under EU GDPR 2016/679. You have the right to withdraw consent at any time.

Subscribe

Suwandono 22-an-(2).doc
1098K

Oksana Nikitina <0661966nauka@gmail.com> Tue, Mar 10, 2026 at 6:54 PM
To: Purbo Suwandono <purbo@widyagama.ac.id>

Good afternoon, dear authors,
This is a friendly reminder that we expect the corrected version of your article **by March 11, 2026.**
Please feel free to reach out if you need any assistance.
We are always happy to help!
Best regards, Oksana

сб, 7 мар. 2026 г. в 22:48, Oksana Nikitina <0661966nauka@gmail.com>:

[Quoted text hidden]

--

[Quoted text hidden]

Purbo Suwandono <purbo@widyagama.ac.id> Wed, Mar 11, 2026 at 12:18 AM
To: Oksana Nikitina <0661966nauka@gmail.com>

Good afternoon, dear Editor,

Thank you for your kind reminder.

I would like to inform you that I am currently finalizing the corrected version of the article. I sincerely apologize for the delay.

Thank you very much for your patience and support. Please let me know if any additional information is needed.

Best regards,
Purbo Suwandono

[Quoted text hidden]

Suwandono 22-an-(2)_Revision.doc
1164K

Oksana Nikitina <0661966nauka@gmail.com> Wed, Mar 11, 2026 at 2:24 PM
To: Purbo Suwandono <purbo@widyagama.ac.id>

Good day!
The article has been sent to the editor for checking.
If you have any questions, please call or write. We will be happy to answer them.
We wish you a great day and a good mood!
Regards, Oksana

вт, 10 мар. 2026 г. в 19:19, Purbo Suwandono <purbo@widyagama.ac.id>:
[Quoted text hidden]
[Quoted text hidden]

Received date: 20.02.2026
Accepted date:

UDC

ПОКРАЩЕННЯ ЯКОСТІ СИНТЕЗ-ГАЗУ ПРИ ВИСХІДНІЙ ГАЗИФІКАЦІЇ КУКУРУДЗЯНИХ КАЧАНІВ З ВИКОРИСТАННЯМ КАТАЛІЗАТОРА НА ОСНОВІ CAO/АКТИВОВАНОГО ВУГІЛЛЯ НА ПАЛЬМОВОМУ ВОЛОКН

Purbo Suwandono, Widya Wijayanti, Nova Risdiyanto Ismail, Dzulfikar Johan Akbar, Muhammad Reza

SYNGAS QUALITY IMPROVEMENT IN CORNCOB UPDRAFT GASIFICATION USING CAO/ACTIVATED CARBON PALM FIBER CATALYST

Purbo Suwandono, Widya Wijayanti, Nova Risdiyanto Ismail, Dzulfikar Johan Akbar, Muhammad Reza

The sum of summary + keywords= should be 1800-1900 characters with spaces.

The summary should contain the following information:
- object of research
- problem that was solved
- results obtained
- brief interpretation of the results (what explains them)
- features and distinctive features of the results obtained, thanks to which they allowed to solve the problem under study
- the scope and conditions of practical use of the results obtained

Replace hyphens (-) with dashes (–) by text (except word combinations)

У цьому дослідженні вивчається можливість поліпшення якості синтез-газу, отриманого в результаті газифікації кукурудзяних качанів за допомогою системи з подвійним каталізатором на основі CaO та активованого вугілля з пальмового волокна (AC–PF). Основними проблемами є відносно низька теплотворна здатність синтез-газу з кукурудзяних качанів та висока вартість каталізаторів, що використовуються на даний момент. У цьому дослідженні в якості каталізаторів використовувалися недорогий CaO та перероблені відходи пальмового волокна, перетворені на активоване вугілля. До досліджуваних робочих змінних належали коефіцієнт еквівалентності (0,2, 0,25, 0,3 та 0,35), навантаження каталізатора (4%, 6%, 8% та 10%) та масове співвідношення CaO/AC-PF (0:1, 1:0, 1:1 та 2:1).

Характеристика каталізатора показує, що AC-PF має пористу структуру, яка збільшує контакт газу з твердим тілом і сприяє вторинним реакціям, тоді як додавання CaO утворює композит із модифікованою структурою пор і поверхневими видами, пов'язаними з сорбцією CO_2. Експериментальні результати показують, що збільшення ER підвищує частку H_2 (ER 0,2: 3150 ppm, ER 0,35: 3914 ppm) і частку CH_4. Водночас частка CO_2 зменшилася. Тим часом CO показав оптимальне значення при ER: 0,3 ppm, перш ніж зменшитися при ER 0,35. І навпаки, збільшення навантаження каталізатора призводило до зменшення H_2 (4%: 3742 ppm, 10%: 3176 ppm) і CH_4, але збільшувало CO. З енергетичної точки зору, нижча теплота згоряння синтез-газу збільшується із збільшенням ER, але може зменшуватися при більш високих навантаженнях каталізатора через зменшення внеску CH_4.

Сильна сторона цього дослідження полягає у функціональній синергії між пористим AC-PF та поліпшенням якості сорбції CO_2 на основі CaO, завдяки чому можна досягти поліпшення якості синтез-газу за допомогою поєднання каталітичних та сорбційних ефектів в одній системі. Результати цього дослідження можуть бути застосовані до невеликих установок газифікації біомаси, зокрема до реакторів з висхідним потоком для відходів кукурудзяних качанів.

Ключові слова: газифікація, висхідний потік, кукурудзяні качани, синтетичний газ, CaO, активоване вугілля, пальмове волокно, низька теплотворна здатність, коефіцієнт еквівалентності, навантаження You have 18 words, there should be 10

This study investigates improving the quality of syngas from updraft corn cob gasification using a dual catalyst system based on CaO and activated carbon from palm fiber (AC–PF). The main problems encountered are the relatively low heating value of corn cob syngas and the high cost of the catalysts currently in use. In this study, inexpensive CaO and processed palm fiber waste into activated carbon were used as catalysts. The operating variables studied included the equivalence ratio (0.2, 0.25, 0.3, and 0.35), catalyst loading (4%, 6%, 8%, and 10%), and the CaO/AC-PF mass ratio (0:1, 1:0, 1:1, and 2:1).

Characterization of the catalyst shows that AC-PF has a porous structure that increases gas-solid contact and promotes secondary reactions, while the addition of CaO forms a composite with a modified pore texture and surface species associated with CO_2 sorption. Experimental results show that an increase in ER raises the H_2 fraction (ER 0.2: 3150 ppm, ER 0.35: 3914 ppm) and CH_4 fraction. Meanwhile, the CO_2 fraction decreased. Meanwhile, CO showed an optimum value at ER: 0.3 ppm before decreasing at ER 0.35. Conversely, an increase in catalyst loading tended to decrease H_2 (4%: 3742 ppm, 10%: 3176 ppm) and CH_4 but increases CO. From an energy perspective, the Lower Heating Value of syngas increases with increasing ER, but may decrease at higher catalyst loadings due to the reduced contribution of CH_4.

The strength of this research lies in the functional synergy between porous AC-PF and CaO-based CO_2 sorption quality improvement, so that syngas quality improvement can be achieved through a combination of catalytic and sorption effects in a single system. The results of this study have the potential to be applied to small scale biomass gasification units, particularly updraft reactors for corn cob waste

Keywords: gasification, updraft, corncob, syngas, CaO, activated carbon, palm fiber, low heating value, equivalence ratio, load You have 15 words, there should be 10

1. Introduction

Indonesia is one of the largest corn producers in Southeast Asia, with national production reaching more than 18 million tons of dry kernels per year. Of this amount, about 15–20% is cobs after the kernel removal process, resulting in a very large amount of corn cob waste, estimated at 2.5–3.5 million tons annually [1]. Until now, most corn cobs have only been used to a limited extent, for example as traditional fuel, small amounts of animal feed, or even burned directly on post-harvest land, which has the potential to cause air pollution. Most of the rest are simply piled up or left to rot on the land, posing a risk of becoming a source of plant disease [2].

Corn cobs have quite promising chemical and energy characteristics. Their composition is dominated by cellulose, hemicellulose, and lignin, with a calorific value of around 15–17 MJ/kg, making them very suitable as raw materials in various biomass-based energy conversion technologies [3]. Their hard and fibrous nature also makes them suitable for processing into biochar, activated charcoal, or direct use in pyrolysis and gasification processes. This significant potential indicates that corn cobs are not merely waste but a renewable resource that can be optimized to support energy security and reduce dependence on fossil fuels.

Biomass gasification is a promising thermochemical technology for converting renewable resources into syngas consisting of H_2, CO, CH_4, and CO_2. Of the various types of biomass, corn cobs are a potential candidate due to their abundant availability in Indonesia and lignocellulose content that supports the energy conversion process [4]. However, the biomass gasification process still faces several obstacles, particularly the low hydrogen fraction in syngas and the formation of significant amounts of tar. Tar can cause reactor clogging, reduced thermal efficiency, and increased purification costs.

To overcome these problems, the use of catalysts is an important strategy. A number of studies have proven that metal catalysts such as Ni [5], Ca [6], and K [7] can increase hydrogen yield while suppressing tar formation. On the other hand, activated carbon is also widely used as a catalyst support because it has a high surface area, porous structure, and good chemical stability. The use of agricultural waste, particularly palm fiber, as raw material for activated carbon is not only economically valuable but also supports the concept of a circular economy in plantation waste management. In addition, calcium oxide (CaO) is known to have a dual role, namely as a catalyst in the tar decomposition reaction and as a CO_2 absorber that promotes sorption-enhanced gasification to increase the hydrogen fraction in syngas [8].

Although various studies have examined the role of metal catalysts and activated carbon separately, research focusing on the combination of biomass bases catalyst such as palm fiber-based activated carbon with CaO in corn cob gasification is still limited. The uniqueness of this study lies in the integration of two catalyst, which is expected to provide a synergistic effect: activated carbon with high porosity increases catalyst dispersion and activity, while CaO simultaneously breaks down tar and absorbs CO_2. This approach has the potential to significantly increase hydrogen production and reduce carbon emissions.

However, there are several research gaps that remain unanswered. First, the optimal composition and ratio of activated carbon and CaO in corn cob gasification have not been extensively studied. Second, the synergistic mechanism using two catalyst in increasing syngas quality not yet fully understood. In addition, a systematic and statistically robust approach is required to disentangle the coupled effects of key operating and catalyst variables.

Based on this background and research gaps, this study aims to investigate the performance of a composite catalyst based on activated carbon from palm fiber combined with CaO in the corn cob gasification process. The main focus is on increasing hydrogen production, reducing tar, and evaluating the potential synergistic effects between materials. This research is expected to contribute to the development of low-cost, locally sourced, and sustainable catalyst systems that are relevant to supporting the clean energy transition and practical applications of biomass-to-hydrogen in the future.

2. Literature review and problem statement

How this section should be built: The paper [.] presents the results of research ..., Shown, that..., But there were unresolved issues related to ..., The reason for this may be (objective difficulties associated with ..., fundamental impossibility ..., cost part in terms of ..., which makes relevant research impractical, etc.). A way to overcome these difficulties can be ..., This approach was used in [.], however ..., All this suggests that it is advisable to conduct a study on ...

Previous studies have reported improvements in syngas quality in fixed-bed updraft gasification through the selection of gasification agents and catalytic strategies. The paper by [9] explored Sago-based foods are staple in eastern Indonesia. Single Al_2O_3 catalyst (5–10 wt%) was added to sago-dregs pellets in a TULD gasifier enhances syngas: H_2 is highest at 5% (31.65%), while CO (4.33%) and CH_4 (26.45%) peak at 10%. The H_2/CO ratio remains favorable (1.65–1.51) with low tar, indicating potential for internal combustion engine fuel.

The paper by [10] explored an updraft gasifier processed 3 kg of dried rice husk using air, steam-air, and air with dolomite at varied conditions. Among the tested agents, single catalytic air gasification (air + dolomite) gave the best results, producing the highest H_2 (15.4 mol%) and LHV (5.1 MJ/Nm^3), compared with steam-air (7.08 mol%,

3.6 MJ/Nm³) and air only (3.6 mol%). The optimum setting was an airflow of 3 m³/h with 15% dolomite.

The paper by [11] explored Cigarette butts are hazardous urban waste rich in cellulose acetate and volatile matter, making them a potential renewable feedstock for hydrogen production. This study valorized as-received cigarette butts via continuous updraft gasification (700–900°C; ER 0.15–0.25), followed by steam catalytic reforming over KATALCO™ 57-4GQ at 900°C. Gasification alone produced high syngas yields (82.3–89.7%) but limited H_2 (<20.84 vol% at 900°C, ER 0.15). The reforming step increased H_2 to 30.27 vol% and reduced tar from 18.15 to 13.38 g/m³, improving fuel quality (HHV from 11,038 to 11,528 kJ/kg).

The paper by [12] explored slumgum suitability as a gasification fuel. Slumgum and slumgum-pine sawdust pellets were produced (ISO 17225 tests) and gasified in a modified updraft reactor while measuring gas composition and LHV. Pure slumgum pellets showed very high durability (99.98%) and HHV (27.66 MJ/kg), likely due to high fat content, but high sulfur (2.17%) and nitrogen (3.52%) prevented ISO compliance. In gasification, adding sawdust increased LHV, reaching 7.62 MJ/Nm³ at a 50:50 blend, although ER stayed very low (0.0125–0.0204) because higher airflow raised fuel consumption.

The paper by [13] examined catalyst effects on biomass-mixture gasification using lab-scale updraft and modifiable-downdraft fixed-bed reactors. Red mud (RM) and an Al–Ni alloy were tested at high temperature, where H_2 levels of 51–65 vol% were obtained at 900°C in both systems. The Al–Ni catalyst showed the strongest enhancement, achieving 65 vol% H_2 in the updraft reactor at 900°C with 0.05 L/min dry air, and widening the H_2/CO range from 2–4 (no catalyst) to 1.6–7. RM generally increased H_2 in the updraft reactor by about 1–7 vol% at 900°C, but in the modifiable-downdraft reactor it reduced H_2 by roughly 2–6%.

The paper by [14] examined three MSW fractions (FDS, SRF, and plastic packaging mixture/PPM) from mechanical-biological treatment plants were gasified in an allothermal fixed-bed updraft reactor at 800°C using air at ER ≈ 0.15 and 0.21. All feeds showed similar volatile-release peaks (~330 and ~500°C). Lowering ER increased the heating value of combustible gases; PPM produced the highest H_2 (11.39%). SRF generated the most tar (47.44 g/m³), dominated by aromatic compounds.

The paper by [15] examined co-gasifying laying hens manure (LHM) with common litter such as wheat straw remains limited, particularly across a wide range of air–fuel equivalence ratios (AFER). This laboratory study used a fixed-bed updraft reactor to gasify straw-LHM blends (25–75% LHM) under low (0.12–0.28) and high (0.30–0.45) AFER to assess how LHM affects producer-gas quality and process efficiency. At higher AFER, the producer-gas LHV stayed around 3.3–3.4 MJ/m³ (depending on blend), with cold gas efficiency 60% and carbon conversion efficiency of 82–94%.

The paper by [16] evaluated the gasification of olive pomace in fixed-bed updraft and downdraft systems. Dried olive pomace obtained from an olive-oil soap plant in Izmir (Türkiye) was characterized and gasified at 700–900 °C using dry air at 0.05–0.4

L/min, with additional tests using pure oxygen (0.01 L / min). With dry air, the syngas reached 48 vol% H_2 in the updraft and 45 vol% in the downdraft, with a heating value of about 12.4 MJ / Nm^3. Under oxygen, H_2 increased to ~53 vol% in the updraft but was ~39 vol% in the downdraft.

The paper by [17] gasified MDF wood-waste in a 2100 kg/h updraft fixed-bed system (tested at 1500–2100 kg/h) using oak chips as a reference. Syngas yield was 2.5 Nm^3/kg with LHV 6.0–7.0 MJ/Nm^3, and the gas composition at full-load MDF was similar to oak. Hot syngas (430°C) containing tar/soot was burned directly in a retrofitted thermal-oil heater (7 MWh) to supply an ORC turbine generating 955 kW electricity, converting 88 wt% of MDF residue into syngas.

However, there are still unresolved issues regarding how to achieve simultaneous improvements in syngas quality increasing H_2/CH_4 and LHV while reducing CO_2/tar with an approach that remains simple, scalable, and economical for updraft reactors. One reason for this is that most studies still emphasize single catalysts or separate additives, while dual-catalyst synergy in updraft configurations has been relatively rarely studied systematically. Efforts to overcome these limitations can be made through the development of a dual-catalyst system that combines the function of CO_2 absorption to drive the equilibrium shift towards H_2 formation, and a high-surface catalytic function to enhance secondary reactions such as cracking of volatiles and suppressing condensed products.

This approach has the potential to be realized by combining CaO as a CO_2 sorbent and palm fiber-based activated carbon (AC–PF) as a porous material with a high surface area to increase contact and volatility reactivity. however, quantitative evidence regarding the level of synergy, the optimum CaO / AC–PF ratio combination, and the effect of ER and catalyst loading on H_2, CO, CH_4, CO_2, and LHV in updraft corn cob gasification has not yet been comprehensively mapped.

All this allows us to conclude that it is expedient to conduct research devoted to improving syngas quality in updraft corn cob gasification through a CaO / AC–PF dual catalyst system with systematic evaluation of the equivalence ratio, catalyst loading, and CaO / AC–PF ratio, to obtain cleaner syngas that is rich in H_2 and has a higher calorific value.

3. The aim and objectives of the study

The purpose of the study is to enhance syngas quality from corncob updraft gasification by developing a dual-synergy catalytic system based on calcium oxide (CaO) and palm-fiber-derived activated carbon (AC–PF). This will allow the production of cleaner and more energy-dense producer gas, providing practical guidance for selecting operating conditions and catalyst configurations suitable for updraft gasifiers processing agricultural residues.

To achieve these aims, the following objectives are accomplished:

– to synthesize and characterize the CaO and palm-fiber activated carbon catalysts using Fourier Transform Infrared Spectroscopy (FTIR), scanning electron microscopy (SEM) and Brunauer–Emmett–Teller surface area analysis (BET);

– to investigate the effects of operating parameters, particularly equivalence ratio (ER), catalyst loading, and CaO/AC ratio, on syngas composition H_2, CO, CH_4, CO_2 and LHV.

4. Materials and methods

The object of the study is the updraft fixed-bed gasification process of corncob biomass using a dual catalyst system based on calcium oxide (CaO) and palm-fiber-derived activated carbon (AC-PF). The practical physical process under investigation is the catalytic upgrading of producer gas within the updraft reactor, where changes in operating parameters and catalyst configuration are expected to influence syngas composition and heating value. The results of this study are intended to be applied to improve the quality of syngas, specifically by increasing the combustible gas fraction (H_2 and CH_4) and the lower heating value (LHV), while reducing CO_2 content.

The research hypothesis is that a dual-synergy CaO/AC-PF catalytic system can improve syngas quality more effectively than single-catalyst configurations in updraft corncob gasification. It is hypothesized that CaO functions as a CO_2 sorbent, shifting reaction equilibria toward enhanced hydrogen formation, while activated carbon derived from palm fiber provides high-surface-area catalytic sites that promote secondary reactions such as tar cracking and volatile reforming. The combined catalytic-sorption mechanism is expected to increase H_2 and CH_4 fractions and improve LHV under optimized equivalence ratio (ER), catalyst loading, and CaO/AC-PF ratio conditions.

It was assumed that the corncob feedstock has relatively homogeneous composition and stable proximate/ultimate characteristics during the experiments. The gasification process was assumed to operate under steady-state conditions after stabilization. It was also assumed that the CaO maintains sufficient CO_2 sorption capacity within the experimental time frame and that the activated carbon structure remains stable under the applied temperature range.

During the course of the research, several methodological simplifications were adopted in order to maintain experimental feasibility and focus on the main objective of syngas quality evaluation. Detailed kinetic modeling of individual gasification reactions was not performed; instead, the process performance was assessed based on experimentally measured syngas composition and syngas low heating value. Furthermore, although CaO carbonation-decarbonation reactions may occur during operation, microstructural evolution, sintering behavior, and long-term cyclic stability of the catalyst were not investigated in this study. The catalytic performance was evaluated within the experimental duration without conducting extended durability or regeneration-cycle analysis.

4. 1. Catalyst Preparation

Approximately 6 grams of ground palm fiber was mixed with 60 mL of distilled water and stirred for 10 minutes. The mixture was then placed in an autoclave and heated to 200°C at a rate of 5°C per minute for 6 hours in an electric oven. After that, the reactor is allowed to cool naturally to room temperature. The resulting solid hydrocarbon product (hydrochar) is then separated using Whatman No. 42 filter paper. The filtered product is then dried at 105°C for 24 hours and stored in a glass vial. The next stage is the activation process. The hydrochar is immersed in a 3 M KOH solution with a weight ratio of 1:3 (Hydrochar:KOH) for 16 hours, then dried at 85°C for 6 hours. Spectroscopic evidence indicates that KOH preferentially reacts with oxygenated sites and can increase the relative abundance of C–OH functionalities, while higher KOH ratio and activation temperature significantly enhance porosity and BET surface area [18, 19]. To obtain the CaO/AC mixture, CaO powder and activated carbon (AC) were mixed in specific proportions using a grinder until a homogeneous mixture was obtained. Next, CaO, AC, and CaO/AC were activated using a tube furnace at a temperature of 700°C for 1 hour with a continuous flow of nitrogen during the activation process. The resulting product was then washed using distilled water until it reached a neutral pH. This stage produced activated carbon that was ready for use in research.

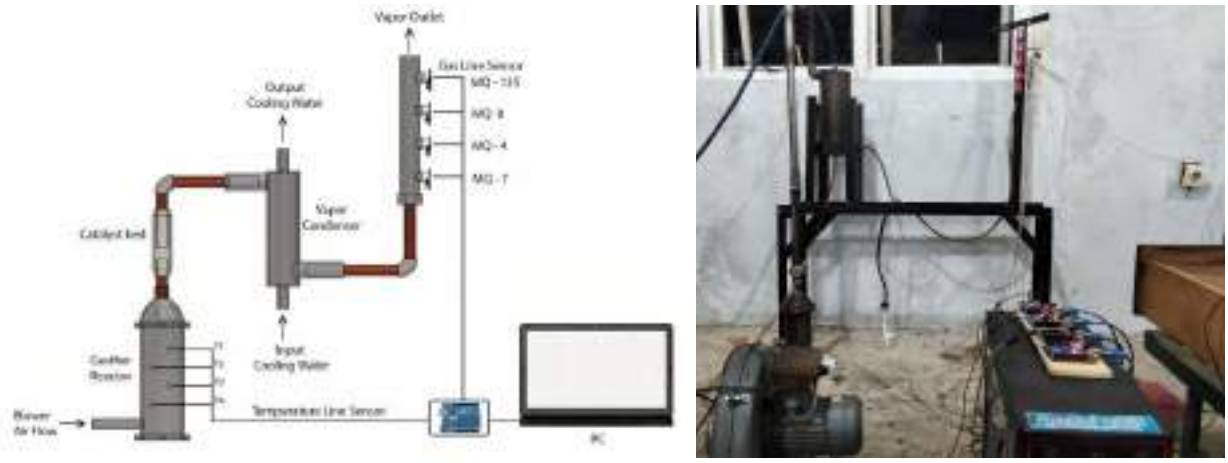
4. 2. Experimental Setup

Corncob biomass was obtained from farmers in the South Malang region of East Java. Before use, the biomass was cleaned of impurities and dried in an oven for 6 hours at 100°C to remove moisture (water vapor) content. The ultimate and proximate test results are as follows.

The proximate and ultimate analyses of the corncob feedstock were conducted to determine its physicochemical characteristics prior to gasification. The results are presented in Table 1. The data indicate that corncob has high volatile matter content and relatively low ash content, which are favorable characteristics for gasification processes.

Table 1
Ultimate and Proximate Test Corn Cob

Parameter	Units	Corn cobs
Moisture	%	10
Volatile matter	%	71.38
Fixed carbon	%	12.11
Ash	%	6.51
C	%	43.6
H	%	6.3
O	%	46.8
N	%	0.22
HHV	MJ/kg	17.61



a *b*

Fig. 1. Updraft gasifier: *a* – schematic experiment; *b* – experimental setup

This study used an updraft gasification reactor designed with a total height of 20 cm. The lower part of the reactor consisted of an ash container with a height of 5 cm, while the active reactor had a height of 15 cm and a diameter of 3 inches. The reactor was equipped with a 1-inch diameter air inlet pipe connected to a blower. The blower was modified with a potentiometer so that the air speed could be adjusted as needed. To monitor the thermal conditions inside the reactor, four 3 cm long type K thermocouples were installed at several different points so that the temperature profile in the gasification zone could be observed in more detail. Each test was conducted with a fixed biomass mass, a mixture of corn cobs weighing 80 grams. The reactor was made of iron and equipped with a gas seal to prevent leaks during the gasification process.

The gas produced by the reactor was fed into a condenser, which cooled the hot gas so that the water vapor components could be separated. The condenser was made of a copper spiral pipe with a diameter of ½ inch and a height of 30 cm. Cooling water was circulated from the bottom of the condenser and exited through the top to ensure efficient heat transfer. This cooling system was driven by a 60-watt water pump, ensuring stable water flow and optimal condensation. The catalyst was positioned downstream after the reactor, where it was supported on steel wool and wrapped with an 80-µm wire mesh to secure the catalyst and prevent particle carryover with the gas flow

To analyse the gas composition, four types of MQ gas sensors were used. The MQ-8 sensor was used to detect H_2, MQ-4 for CH_4, MQ-135 for CO_2 and MQ-7 for CO. Each gas sensor was calibrated according to the manufacturer's datasheet, specifically by determining the Ro value, which is the sensor resistance in clean air conditions. This Ro value is used as a reference in calculating the measured gas concentration during the process [20, 21].

All data from the gas sensors and thermocouples were acquired using an Arduino Uno microcontroller. Each gas sensor is connected to a separate Arduino Uno to facilitate the calibration process and reduce the possibility of interference between

sensors. Arduino is also used to record temperature data from four thermocouples installed in the reactor, so that gas composition and temperature distribution data can be obtained simultaneously.

The ER range of 0.2, 0.25, 0.3 and 0.35. The catalyst load was between 4%, 6%, 8% and 10% from the mass of input feedstock. The CaO/AC-PF ratio was varied between 0:1, 1:0, 1:1, and 2:1. Design of experiment can be seen in Table 2.

Table 2
Design of Experiment using

Run	Equivalence Ratio (E.R)	Catalyst Load %	CaO/AC
1	0.2	4	1:0
2	0.2	6	0:1
3	0.2	8	1:1
4	0.2	10	2:1
5	0.25	4	0:1
6	0.25	6	1:0
7	0.25	8	2:1
8	0.25	10	1:1
9	0.3	4	1:1
10	0.3	6	2:1
11	0.3	8	1:0
12	0.3	10	0:1
13	0.35	4	2:1
14	0.35	6	1:1
15	0.35	8	0:1
16	0.35	10	1:0

A total of 16 experimental runs were conducted systematically to enable evaluation of the main effects of each variable and the tendency of interactions between variables on the fractions of H_2, CO, CH_4, CO_2, and lower heating value (LHV). This approach enabled identification of the most effective combination of operating parameters in improving syngas quality quantitatively and measurably.

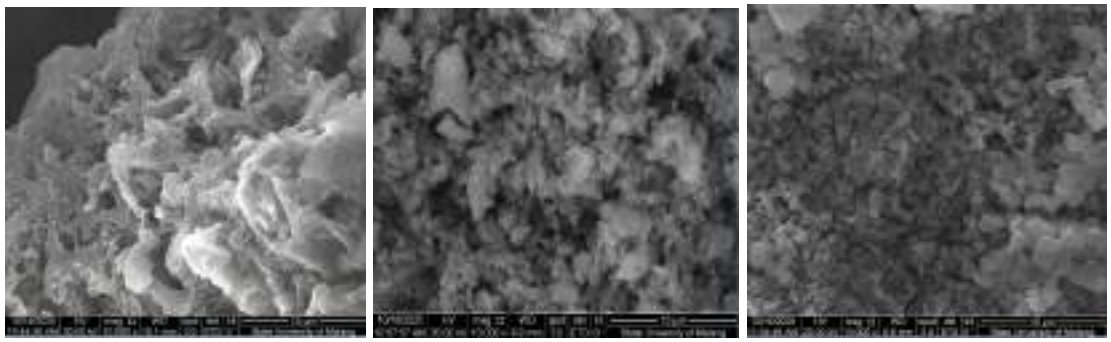
5. Results of syngas quality enhancement from corncob using calcium oxide (CaO) and palm-fiber-derived activated carbon (AC–PF).

5. 1. Characterization of Calcium Oxide (CaO) and Palm-Fiber-Derived Activated Carbon (AC–PF) Catalysts

5. 1. 1. Scanning Electron Microscopy Catalyst Result

Fig. 2, *a* shows the image obtained from a Scanning Electron Microscope (SEM) with a magnification of 10,000× shows the surface morphology of palm fiber-based activated carbon (AC-PF). The surface structure appears porous and irregular, with a

combination of void areas and layered surfaces. This characteristic indicates that the activation process that using KOH has successfully formed micropores and mesopores, which play an important role in increasing the specific surface area of activated carbon.



a *b* *c*

Fig. 2. Scanning Electron Microscopy Catalyst Result: *a* – Scanning Electron Microscopy AC-PF; *b* – Scanning Electron Microscopy CaO:AC;1:1; *c* – Scanning Electron Microscopy CaO:AC-PF;2:1

The rough and textured surface indicates that most of the material has undergone lignocellulose cell wall exfoliation, resulting in numerous interparticle gaps [22]. This porous structure greatly supports gas adsorption and diffusion capabilities when used as a catalyst in gasification or thermochemical reactions.

The presence of 1–5 μm voids indicates that most pores are in the mesopore category, supporting the adsorption of gas molecules such as H_2, CO, and tar during the gasification reaction [23].

The morphology of AC-PF shows the characteristics of porous activated carbon with a heterogeneous pore distribution, where the pores allow increased contact between gas reactants and active sites on the material surface, thereby increasing catalytic efficiency and the ability to absorb tar or CO_2 in biomass-based energy applications [24].

Fig. 2, *b* shows the surface morphology of the CaO:AC-PF catalyst with a ratio of 1:1. Visually, it can be seen that the surface of this material consists of fine particles ranging in size from microns to submicrons that stick together to form a layered and slightly agglomerated structure.

The presence of fine, light-colored grains indicates an even distribution of CaO particles impregnated on the surface of activated carbon (AC-PF). This CaO distribution fills some of the pores of the carbon, resulting in a denser surface compared to pure AC-PF. However, there are still small gaps and voids between the grains, indicating that the microporous and mesoporous structures are still formed and can support catalytic activity [25].

This morphology illustrates the success of the CaO impregnation process on activated carbon from palm fiber, where the interaction between CaO and the carbon pore walls produces a composite material that is more thermally and chemically stable. This structure is highly conducive to catalyst applications in biomass gasification processes, as CaO particles can function as CO_2 absorbers while accelerating the tar reforming reaction [26].

Fig. 2, *c* shows the surface morphology of the CaO:AC-PF (2:1) catalyst. The image shows that the surface of the material is dominated by agglomerations of fine, round, and irregular particles ranging in size from microns to submicrons. Compared to the CaO:AC-PF (1:1) sample, this structure appears denser and tighter, indicating that an increase in the CaO ratio causes partial closure of the activated carbon surface pores by CaO particles.

The distribution of CaO particles appears more uniform and covers the carbon surface, indicating the successful impregnation of a larger amount of CaO. The light color in some areas indicates the presence of a calcium oxide phase that is strongly attached to the activated carbon matrix [27]. This structure indicates a strong interaction between CaO and AC-PF, forming a thermally stable composite.

Although some pores are covered, there are still microscopic gaps between the CaO grains that allow gas diffusion to occur, so that the catalyst retains its good adsorption capacity. The combination of the active area of CaO and the porous carbon structure makes this material very promising for biomass gasification or tar reforming applications, as CaO can act as a CO_2 absorber and increase the conversion of carbon to hydrogen gas.

5. 1. 2. Fourier Transform Infrared Spectroscopy catalyst result

The FTIR analysis results shown in the Fig. 3 reveal clear spectral differences between the AC-PF, CaO, and their mixtures (CaO:AC-PF) with ratios of 2:1 and 1:1. In the AC-PF spectrum, the absorption band at 2926 cm^{-1} is associated with the stretching vibration of the C–H group from $–CH_2$ or $–CH_3$ (methylene/methyl stretching), which indicates the presence of hydrocarbon chain residues from the lignocellulose structure. The peak at 1577 cm^{-1} indicates the presence of aromatic C=C or C=O stretching, while the band at 1056 cm^{-1} represents C–O stretching from alcohol or ether groups. In addition, the –OH group that appears in the 3500–3600 cm^{-1} region is identified as the result of AC-PF activation using a KOH solution, which causes the formation of hydroxyl groups on the activated carbon surface. This –OH group plays an important role in increasing the surface activity and adsorption capacity of AC-PF as a catalyst support medium [28, 29].

In pure CaO, the intense band at 3639 cm^{-1} is associated with the stretching of the O–H group from $Ca(OH)_2$, which is formed due to the partial hydration of CaO when exposed to humid air. Meanwhile, the absorption bands at 1426 cm^{-1} and 876 cm^{-1} are associated with C–O stretching and CO_3^{2-} Please reduce the number of sources to 30 references. bending, respectively, indicating the formation of $CaCO_3$ due to CO_2

adsorption from the air. This shows that CaO is highly reactive to moisture and carbon dioxide in the environment.

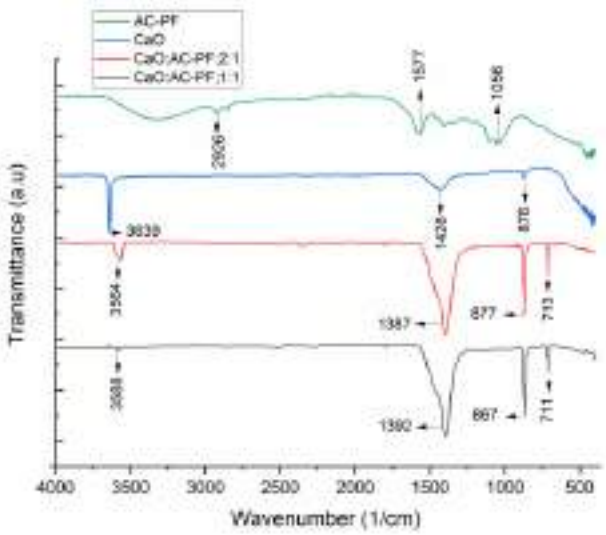


Fig. 3. Fourier Transform Infrared Spectroscopy Catalyst Result

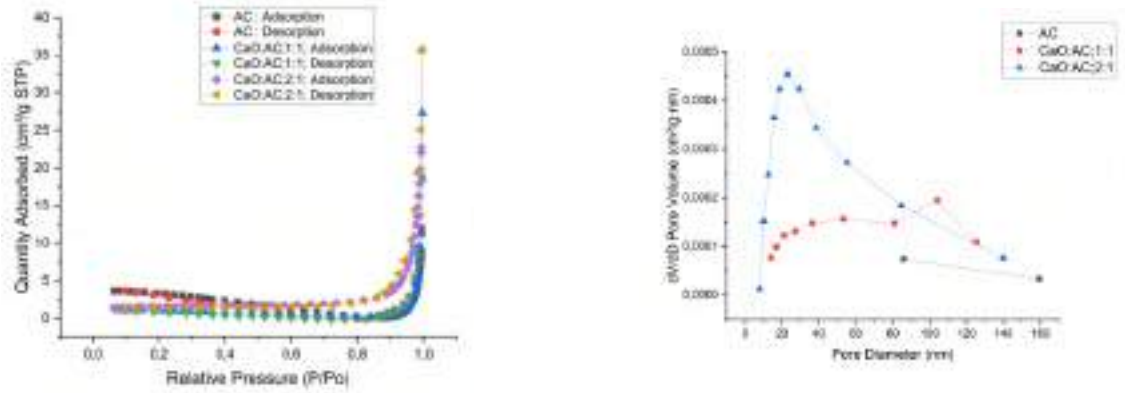
For the CaO:AC-PF (2:1), the main absorption bands were detected at 3564 cm^{-1} (O–H stretching from $Ca(OH)_2$ and the –OH group in AC-PF), 1387 cm^{-1} (C–O stretching), and 877 cm^{-1} and 713 cm^{-1} (bending vibration of CO_3^{2-}). This combination of bands indicates the formation of carbonate compounds ($CaCO_3$) due to the interaction between CaO and the oxygen groups of activated carbon. The presence of –OH groups from KOH activation also strengthens the basic properties on the surface, which can increase the chemical interaction between CaO and AC-PF [1].

At a CaO:AC-PF ratio of 1:1, the absorption bands at 3588 cm^{-1}, 1392 cm^{-1}, 867 cm^{-1}, and 711 cm^{-1} show a similar pattern, indicating the presence of hydroxyl (O–H) and carbonate (CO_3^{2-}) groups. The difference in peak intensity compared to the 2:1 ratio indicates variations in the level of interaction between CaO and the –OH groups resulting from KOH activation on AC-PF, which affects the formation of carbonate-hydroxide complexes on the material surface [2].

5. 1. 3. Brunauer-Emmett-Teller Catalyst Result

Fig. 4 shows the adsorption-desorption isotherm curves for nitrogen for the AC, CaO:AC (1:1), and CaO:AC (2:1) samples are shown in Fig. 4. All three samples exhibit type IV isotherms with clear hysteresis loops at relatively high pressures ($P/Po > 0.9$). Based on the IUPAC classification, this characteristic indicates that the material has a mesoporous structure formed through capillary condensation within the pore channels. The difference between the adsorption and desorption pathways indicates that the pore shape is not perfectly cylindrical, but rather tends to be irregular or slit-like, which is commonly found in modified activated carbon materials [3].

The pure activated carbon (AC) sample showed a relatively low nitrogen adsorption volume with a specific surface area of 24.51 m²/g and an average pore diameter of 0.74 nm, indicating a predominance of microporous structures. In the CaO:AC (1:1) composite, the surface area did not change significantly compared to pure AC, indicating that the addition of a moderate amount of CaO did not cover the carbon pores much, but only adhered to the external surface of the carbon matrix [4].



a *b*

Fig. 4. Brunauer-Emmett-Teller Result: *a* – Surface Analysis Adsorption Desorption Isotherm; *b* – Barrett-Joyner-Halenda Adsorption Pore Size Distribution

Conversely, in the CaO:AC (2:1) mixture, there was a sharp increase in adsorption volume at relatively high pressure (P/Po > 0.9) to around 35 cm³/g STP, while the BET surface area decreased dramatically to 5.06 m²/g, and the pore diameter increased to 22.87 nm.

These changes in isotherm shape and pore size increase indicate that CaO impregnation not only modifies the surface chemistry but also significantly alters the pore structure of activated carbon. This transformation is positive in the context of catalytic applications in biomass gasification processes, as the mesoporous structure can enhance gas diffusion and accessibility to active sites during the tar reforming and water-gas shift reactions. Thus, even though the specific surface area decreases, the increase in mesoporousness and pore connectivity can actually improve catalyst performance in hydrogen gas production [5].

Fig. 4, *b* shows the BJH pore size distribution curves that provide further insight into the textural evolution of the palm-fiber-based activated carbon after CaO impregnation. The pristine AC exhibits a relatively low dV/dD value and a broad contribution only at large pore diameters (>60 nm), indicating that its pore system is dominated by macropores with a limited amount of mesopores. Such a texture is less favourable for gas-solid reactions because the accessible surface area in the mesopore range (2–50 nm) is relatively small.

After CaO loading, the shape and intensity of the BJH curves change markedly. For CaO:AC-PF = 1:1, the distribution shifts toward smaller pore diameters with a pronounced contribution in the mesopore region of approximately 15–60 nm. This behaviour shows that CaO impregnation partially reconstructs the carbon matrix, enlarging existing micropores and opening blocked pores to generate additional mesoporosity. The effect becomes even more evident at CaO:AC-PF = 2:1, where the curve displays the highest dV/dD values and a distinct maximum centred at about 30–40 nm. The strong peak in this range confirms that a higher CaO loading promotes the development of well-defined mesopores while reducing the relative fraction of very large macropores.

Overall, the BJH analysis demonstrates that CaO acts not only as a reactive sorbent but also as a textural promoter for the palm-fiber AC. The increase in mesopore volume and the shift of the dominant pore size toward 20–40 nm are expected to facilitate the diffusion of gasifying agents and tar molecules, as well as to improve the accessibility of CaO active sites for CO_2 capture and reforming reactions. These features are therefore beneficial for enhancing the catalytic performance of the CaO/AC composite in biomass gasification toward H_2-rich syngas production.

5. 2. Effect of Operating Parameters on Syngas Composition and Low Heating Value

5. 2. 1. Effect of Equivalence Ratio on Syngas Product

The composition of syngas from updraft gasification is greatly influenced by the Equivalence Ratio (ER), which is the ratio of the mass flow rate of air compared to the mass flow rate of corncob in the experiment compared to the stoichiometry of air required for complete combustion of corncob. In this study, the ER used was 0.2–0.35 with the following formula

$$ER = \frac{(\dot{m}_a / \dot{m}_{cc})_{\exp}}{(\dot{m}_a / m_{cc})_{stc}},$$

where $\dot{m}_a$ is the air mass flow rate (kg/s), $\dot{m}_{cc}$ is the corncob mass flow rate (kg/s), exp denotes the experimental air-fuel ratio, and stc denotes the stoichiometric air-fuel ratio.

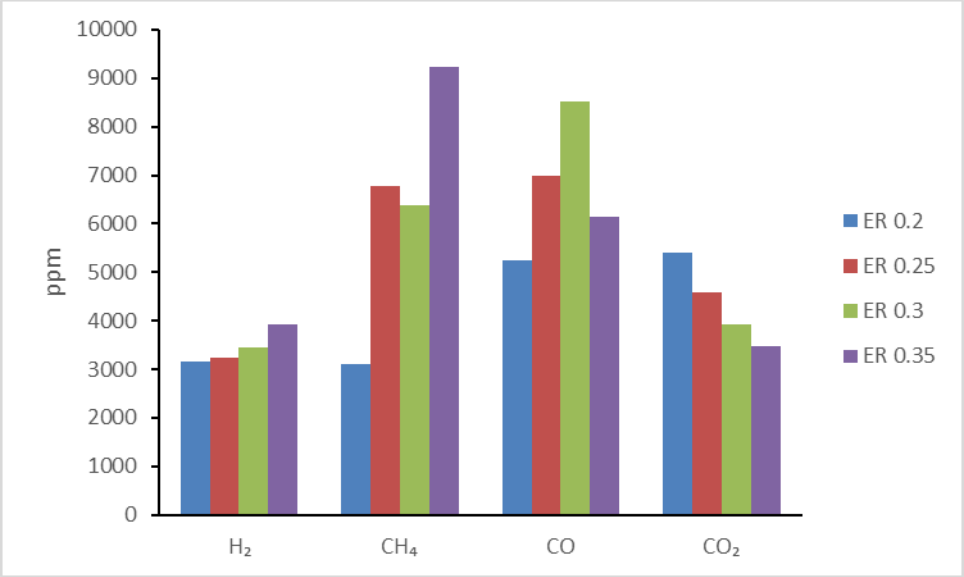


Fig. 5. Syngas composition with different equivalence ratio

The graph above shows that the higher the ER, the higher the hydrogen composition produced. At ER 0.2, the ppm is 3150 ppm, at ER 0.25 it is 3241 ppm, at ER 0.3 it is 3457 ppm, and at ER 0.35 it is 3914 ppm. A higher oxidant supply promotes the formation of more stable autothermal conditions and higher reaction temperatures due to partial oxidation. This increase in temperature accelerates hydrogen-forming reactions, particularly the gasification of active carbon catalyst interactions with steam ($C + H_2O \rightarrow CO + H_2$), the reforming of volatile compounds/light hydrocarbons ($CxHy + H_2O \rightarrow CO + H_2$), and the cracking of tar/volatile into lighter gas species. At low ER, some volatiles tend to be incompletely converted and still have the potential to escape as condensable components, while increasing ER increases heat availability, making the conversion of volatiles into gas fractions (including H_2) more effective.

The higher the ER, the higher the CH4 composition produced. At ER 0.2, 3093 ppm was obtained, at ER 0.25 6767 ppm, ER 0.3 6377 ppm, and ER 0.35 9221 ppm. This trend indicates that the supply of oxidants not only increases autothermal conditions and the rate of devolatilization, but also shifts the reaction pathway towards the formation of light hydrocarbons through hydrogenation and/or methanation reactions in the reactor zone where the temperature still supports CH_4 formation. In particular, increased H_2 at higher ERs can promote the methanation reaction of CO ($CO + 3H_2 \rightleftharpoons CH_4 + H_2O$), so that CH_4 increases along with a tendency for CO to decrease at the highest ER. In addition, more intensive fragmentation of volatiles and tar at high ERs has the potential to produce light gas precursors which are then hydrogenated to CH_4.

CO formation increased up to an ER of 0.3 and decreased at an ER of 0.35. At an ER of 0.2, 5238 ppm was obtained, at an ER of 0.25, 6999 ppm, at an ER of 0.3, 8532 ppm, and decreased at an ER of 0.35 to 6145 ppm. At low ER (0.20–0.25), limited oxygen supply resulted in relatively low heat release, so that the reaction zone

temperature and char reactivity were not sufficient to intensify CO formation reactions, especially the Boudouard reaction ($C + CO_2 \rightleftharpoons 2CO$) and char gasification with steam ($C + H_2O \rightleftharpoons CO + H_2$). When the ER is increased towards 0.30, the increase in autothermal heat strengthens these reduction reactions, causing CO formation to increase and reach its peak. However, at higher ERs (0.35), the CO fraction tends to decrease because some CO can be converted to CH_4.

CO_2 formation continues to decrease as ER increases. At ER 0.2, 5412 ppm is obtained; at ER 0.25, 4592 ppm; at ER 0.3, 3916 ppm; and at ER 0.35, 3479 ppm. The increase in oxidant supply at this ER does not promote complete combustion, but rather strengthens the CO_2 reduction mechanism. At higher ERs, the heat generated from partial oxidation increases the temperature of the reduction zone, thereby accelerating the Boudouard reaction ($C + CO_2 \rightleftharpoons 2CO$), in which CO_2 is reduced by char to CO. This mechanism is consistent with the increase in CO until it reaches a maximum at an ER of 0.30, while also explaining the decrease in CO_2 under the same conditions. Interestingly, at an ER of 0.35, CO_2 remains at its lowest level even though CO decreases, indicating that the CO formed is not completely accumulated at the outlet but has the potential to undergo further conversion along the gas flow path.

5. 2. 2. Effect of Catalyst Loading on Syngas Product

The catalyst load or amount of catalyst in this study was 4%, 6%, 8%, and 10% of the total biomass weight. The figure 6. shows that the composition of H_2 and CH_4 increases as the catalyst load decreases. The H_2 gas composition at catalyst loads of 4%, 6%, 8%, and 10% is 3742 ppm, 3471 ppm, 3372 ppm, and 3176 ppm, respectively. As the catalyst load increases, the reaction pathways that consume H_2 tend to strengthen, particularly the reverse water–gas shift ($CO_2 + H_2 \rightarrow CO + H_2O$) and H_2 interactions on the catalyst surface during the conversion of gasification compounds. As a result, even though reforming occurs, the measured net H_2 decreases because more H_2 is used for CO formation and surface reactions. The CH_4 gas composition at catalyst loads of 4%, 6%, 8%, and 10% was 7031 ppm, 6476 ppm, 6206 ppm, and 5746 ppm, respectively. An increase in catalyst load increases the number of active sites and gas-catalyst contact, so that methane/light hydrocarbon cracking and reforming occur more intensely. CH_4 then acts as a reactant that is converted into more reactive syngas components, causing the CH_4 concentration to decrease at higher catalyst loads.

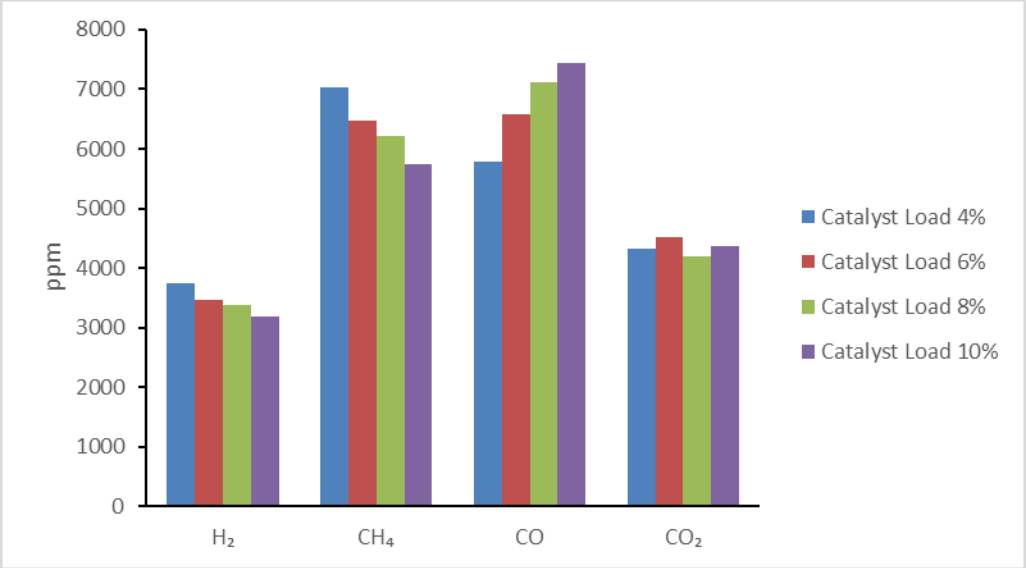


Fig. 6. Syngas Composition with Catalyst Load Variation

The CO gas composition increases with increasing catalyst load, namely for catalyst loads of 4%, 6%, 8% and 10% at 5782 ppm, 6576 ppm, 7111 ppm and 7445 ppm, respectively. The increase in catalyst loading strengthens the CO-forming reactions, particularly dry reforming ($CH_4 + CO_2 \rightarrow 2CO + 2H_2$), char–$CO_2$ reaction ($C + CO_2 \rightarrow 2CO$), and reverse water-gas shift. This combination shifts the product selectivity towards CO, so that the CO fraction increases consistently as the catalyst is increased. The CO_2 gas composition tends to stagnate with increasing catalyst loading, at catalyst loads of 4%, 6%, 8%, and 10% at 4322 ppm, 4510 ppm, 4198 ppm, and 4369 ppm, respectively. CO_2 shows minor changes because it is in a searching for a chemical equilibrium between the partial oxidation and the dry reforming. When the catalyst load increases, the rate of CO_2 consumption may rise, but this is often offset by CO_2 formation in the reaction zone, so that the CO_2 value appears stable or only fluctuates.

5. 2. 3. Effect of Catalyst Ratio on Syngas Product

At a catalyst load of 4%, the CaO/AC ratio changes the gasification reaction through differences in the dominance of tar cracking/reforming and CO_2 capture by CaO, so that the gas composition is highly dependent on the number of active sites and the effectiveness of gas-catalyst contact. At 0:1 (AC), CH_4 and CO are relatively high because AC promotes volatile/tar cracking, but CO_2 remains high because there is no absorption. At 1:0 (CaO), CH_4 decreases but CO_2 is highest, indicating that CO_2 capture is not yet effective due to limited surface area/carbonate layer formation. The 1:1 ratio produces the highest CO with moderate CO_2, indicating CaO–AC synergy that increases the conversion of volatiles into reactive gases. Meanwhile, the 2:1 (CaO-rich) ratio provides the highest H_2 and lowest CO_2 due to the sorption-enhanced effect of CaO, but

CH_4 remains high due to the smaller contribution of AC, so methane reforming/cracking is not yet optimal.

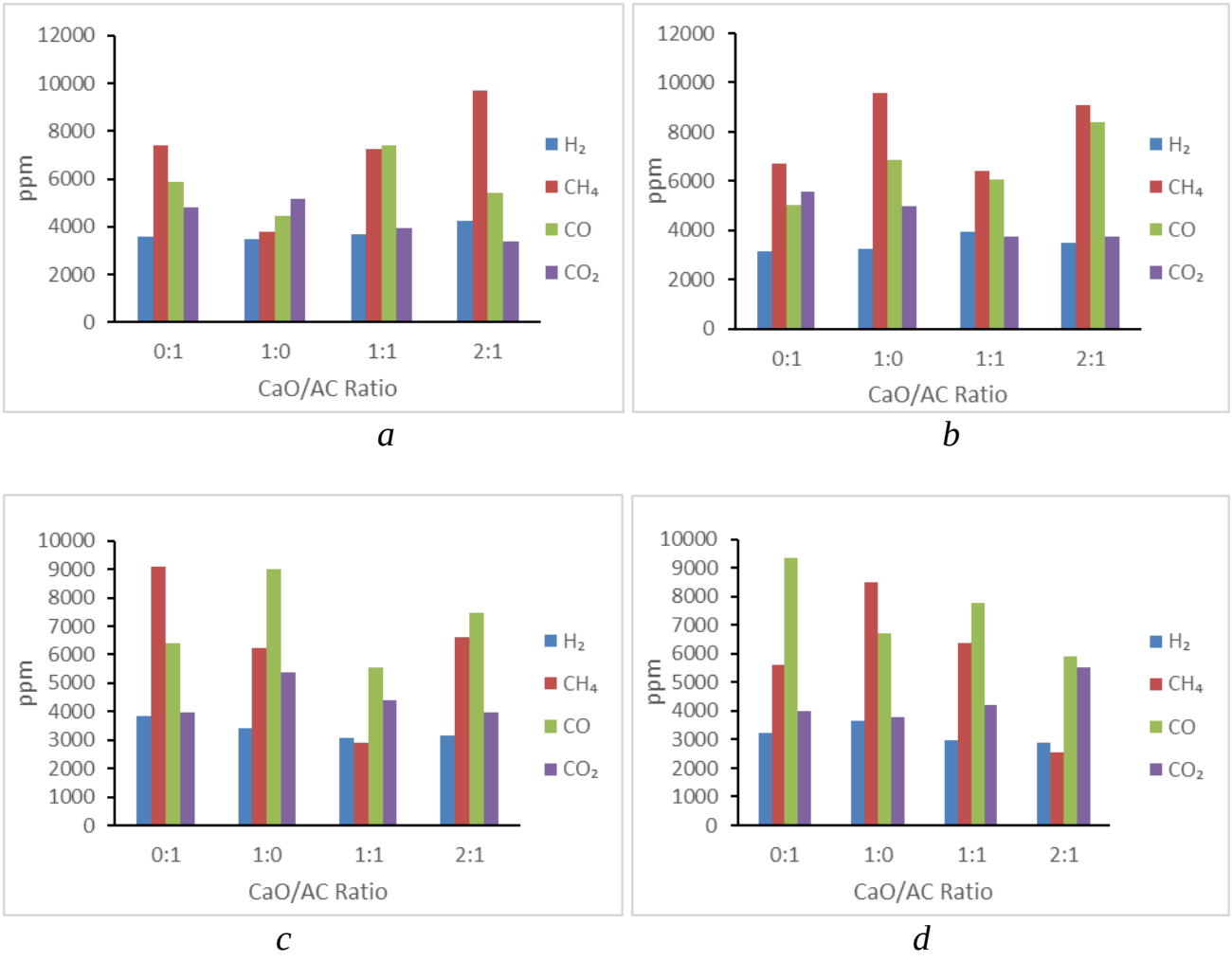


Fig. 7. Effect CaO/AC ratio with various catalyst load: *a* – 4%, *b* – 6%, *c* – 8%, *d* – 10%

At a catalyst load of 4%, the CaO/AC ratio changes the gasification reaction through differences in the dominance of tar cracking/reforming and CO_2 capture by CaO, so that the gas composition is highly dependent on the number of active sites and the effectiveness of gas-catalyst contact. At 0:1 (AC), CH_4 and CO are relatively high because AC promotes volatile/tar cracking, but CO_2 remains high because there is no absorption. At 1:0 (CaO), CH_4 decreases but CO_2 is highest, indicating that CO_2 capture is not yet effective due to limited surface area/carbonate layer formation. The 1:1 ratio produces the highest CO with moderate CO_2, indicating CaO–AC synergy that increases the conversion of volatiles into reactive gases. Meanwhile, the 2:1 (CaO-rich) ratio provides the highest H_2 and lowest CO_2 due to the sorption-enhanced effect of CaO, but

CH_4 remains high due to the smaller contribution of AC, so methane reforming/cracking is not yet optimal.

At a catalyst load of 6%, the CaO/AC ratio mainly shifts the selectivity of secondary reactions (tar cracking/reforming and CO_2 capture), where AC enhances the conversion of volatiles/light hydrocarbons, while CaO reduces CO_2 through carbonation ($CaO + CO_2 \rightarrow CaCO_3$) and changes the reaction equilibrium. At 0:1, CH_4 and CO_2 remain high because there is no CO_2 capture and methane reforming is not yet optimal, so volatiles still escape as CH_4. At 1:0, CO_2 tends to decrease, but CH_4 becomes the highest due to the absence of AC's role in cracking/reforming. The most favorable conditions occur at 1:1, with the highest H_2 and lowest CO_2, indicating CaO–AC synergy that promotes sorption-enhanced reforming and increases the conversion of hydrocarbons into syngas components. At 2:1, CO is highest and CO_2 remains low, but CH_4 rises again and H_2 is not maximized because excess CaO has the potential to rapidly carbonate/cause contact limitations, thereby reducing the contribution of AC in cracking/reforming.

At a catalyst load of 8%, the CaO/AC ratio significantly shifts the selectivity of the syngas reaction. At 0:1 (AC), CH_4 is still high because some light hydrocarbons have not been fully converted even though the tar cracking process is already active. At 1:0 (CaO), CO increases the most, but CO_2 also tends to be high, indicating that CaO in this condition is more dominant in promoting the CO formation pathway, while the CO_2 capture function is not yet optimal due to contact limitations or carbonation saturation. The 1:1 ratio produces the lowest CH_4, indicating the most effective CaO–AC synergy for cracking/reforming light hydrocarbons so that more methane is converted into reactive gas. At 2:1, CO increases again but CH_4 also rises, indicating that a smaller AC fraction reduces the intensity of methane reforming/cracking, while the decrease in CO_2 remains dependent on the effectiveness of CaO sorption.

At a catalyst load of 10%, the increase in total catalyst makes secondary reactions, reforming, solid-gas heterogeneous reactions, and equilibrium shifts very dominant, so that the CaO/AC ratio mainly determines the direction of product selectivity. At 0:1 (AC), CO formation tends to be strongest because the porous carbon surface accelerates the cracking/reforming of volatiles and the conversion of tar into reactive gases. At ratios involving CaO (1:0, 1:1, 2:1), CaO can retain CO_2 through carbonation, but at high loads the effect is often non-linear because CaO rapidly carbonates/diffusion limitations and pore blocking occur, so that under CaO-rich conditions (2:1) CH_4 can decrease, but CO_2 may increase and H_2 is not maximized due to reaction competition. Overall, at a 10% load, a trade-off is observed: AC-dominant increases CO, while CaO-dominant suppresses light hydrocarbons but has the potential to trigger non-ideal conditions (saturation/mass transport) that reduce the benefits of H_2 and CO_2.

5. 2. 4. Syngas Low Heating Value

To calculate the LHV of syngas, it must first be converted from ppm to % volume of gas. The formula is $\%vol_i = \frac{ppmv_i}{10^4}$. To calculate the LHV, use the formula

The values highlighted in turquoise need to be re-typed in the MathType formula editor so that the indices are one below the other

All formulas must be typed in the MathType formula editor version 7 or earlier. If you don't have this version of MathType, then type the formulas in the built-in formula editor

$$LHV_{mix}\left(\frac{MJ}{Nm^3}\right) = \frac{10{,}8(\%H_2) + 12.63(\%CO) + 35.8(\%CH_4)}{100}$$

LHV H_2 = 10.8 MJ/Nm^3

LHV CO = 12.63 MJ/Nm^3

LHV CH_4 = 35.8 MJ/Nm^3

As shown in Fig. 8, the syngas low heating value (LHV) varies with the equivalence ratio (ER) and catalyst load.

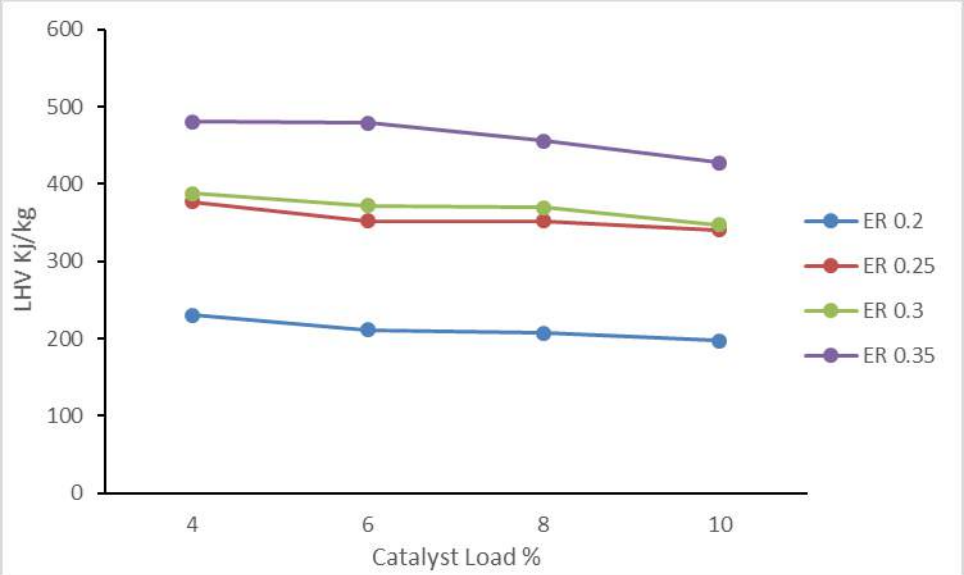


Fig. 8. Syngas Low Heating Value with various Equivalence Ratio

Fig. 8 shows that the LHV value increases with the ER. At the same catalyst load of 4%, the LHV will increase in line with the increase in ER. ER 0.2 has an LHV of 230 kJ/kg and ER 0.35 has an LHV of 481 kJ/kg. Higher ER produces more intense autothermal conditions, causing the reactor temperature to rise. This increase in temperature accelerates the decomposition of volatiles and tar cracking, and promotes

more complete gasification and reforming reactions, thereby increasing the fraction of permanent gases that contribute to the calorific value, mainly CO and CH_4, as well as some H_2. In addition, the increase in temperature is also associated with more effective hydrogen formation, because H_2 formation reactions (e.g., through steam-water and reforming reactions) are generally more optimal at high temperatures, with the temperature range often reported to be most conducive to H_2 formation being 800–1000°C.

At ER 0.2, the highest LHV was obtained at a catalyst load of 4% at 230 kJ/kg and continued to decrease with increasing catalyst load to 197 kJ/kg at 10%. At ER 0.25, the highest LHV was also obtained at a catalyst load of 4% at 377 kJ/kg and also decreased to 341 kJ/kg at a catalyst load of 10%. At ER 0.3, the highest LHV was obtained at a catalyst load of 4% at 388 kJ/kg and also decreased at a catalyst load of 10% to 347 kJ/kg. At ER 0.35, the highest LHV was obtained at 481 kJ/kg and decreased at a catalyst load of 10% to 428 kJ/kg.

However, all ER values show that LHV tends to decrease when the catalyst load is increased from 4% to 10%. This decrease indicates that excessive catalyst addition under these operating conditions does not always improve gas energy quality, because the catalyst can shift the reaction selectivity towards the conversion of high calorific components especially CH_4 into CO and H_2 through reforming, while at the same time the fraction of diluent gases such as CO_2 (and steam) may increase due to reaction. Since CH_4 has a very large calorific value contribution in the syngas mixture, the decrease in its fraction is often more dominant than the increase in CO/H_2, so that the total LHV tends to decrease.

In energy system analysis, particularly in combustion, gasification, and fuel gas utilisation processes such as syngas, the LHV value is often used because it better represents the heat energy that can actually be utilised by the system. The LHV value of a fuel gas is usually influenced by the composition of combustible gases such as carbon monoxide (CO), hydrogen (H_2), and methane (CH_4). The higher the content of these gases, the greater the LHV value produced. The LHV of syngas from this study with variations in ER and CaO/AC-PF ratio can be seen in Fig. 9.

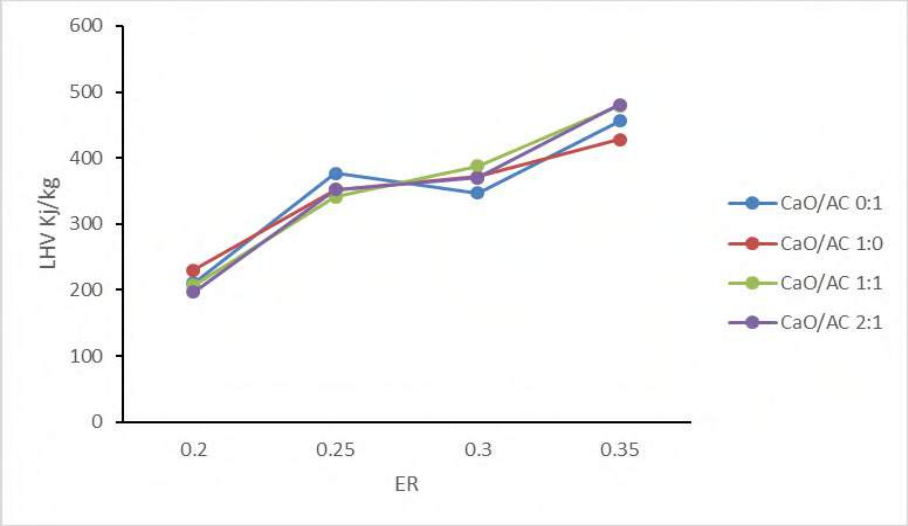


Fig. 9. Syngas Low Heating Value with Various CaO/AC Ratio

Fig. 9 shows that the LHV of syngas increases consistently with the increase in ER 0.2 to 0.35 for all CaO/AC ratios, indicating that a higher ER strengthens autothermal conditions so that the reaction temperature increases and the conversion of volatiles into syngas becomes more complete. At low ER (0.2), the difference in LHV between ratios is still small because secondary reactions such as cracking, reforming and heterogeneous reactions are not yet dominant; the system is still relatively influenced by incompletely converted volatiles. When the ER is increased to 0.25–0.30, the effect of the catalyst ratio becomes apparent: compositions involving AC tend to produce higher LHV because they accelerate tar cracking and increase the fraction of calorific gas, while the contribution of CaO can shift the reaction equilibrium through a decrease in CO_2. At the highest ER (0.35), the LHV reaches its maximum at all ratios, with CaO/AC 2:1 and 0:1 showing peak values, indicating that at high temperatures, the reactive gas formation pathway (via cracking/reforming on the carbon surface and/or CaO-rich-promoted heterogeneous reactions) becomes dominant. Overall, ER acts as the main controlling factor for LHV increase through the temperature effect, while the CaO/AC ratio modulates LHV through the balance between cracking/reforming (AC) and CO_2 control (CaO), especially at medium-high ER.

6. Discussion on the Catalytic Effect of AC-PF/CaO and Operating Conditions on Syngas Composition and LHV

The interaction of the CaO-AC-PF catalyst to improve syngas quality can be seen from the characterisation of the catalyst, the composition of the syngas and the LHV produced. From the Scanning Electron Microscopy results in Fig. 2, it can be seen that the CaO:AC-PF;2:1 catalyst (Fig. 2, *c*) appears denser than the other catalysts. With the addition of CaO, CaO particle dispersion can be seen on the white carbon surface, indicating that some micro pores are closed by CaO. With the addition of CaO, a lot of

CO_2 is absorbed and becomes $CaCO_3$. This porous structure is very important in top-flow gasification because pyrolysis gas and volatiles move through the layer, so the presence of a porous medium has the potential to strengthen secondary reactions and act as carbon capture before the gas exits to the condenser.

From a surface chemistry perspective, Fourier Transform Infrared Spectroscopy (FTIR) shows the presence of –OH and calcium carbonate groups, as shown in Fig. 3. This is due to the results of KOH impregnation carried out during the manufacture of AC-PF. The presence of -OH groups functions as polar active sites capable of adsorbing polar molecules such as H_2O, CO_2, and volatile compounds. Surfaces with -OH groups tend to be hydrophilic and reactive, thereby enhancing interactions with tar compounds or heavy hydrocarbons. These tar compounds can then undergo thermal cracking or catalytic reforming into light gases such as H_2, CO, and CH_4. In addition to -OH, there are also O-H and C-O groups. The O-H group has characteristics that are almost the same as the -OH group, while the C-O group plays a role in enhancing the redox properties and chemical interactions between the carbon surface and gas molecules. In the gasification process, the C-O group can be part of the partial oxidation mechanism and carbon gasification reaction, which produces CO [35].

The BET data in Fig. 4 shows that the surface area decreased to 5.06 m^2/g, but the pore diameter increased to a mesopore scale of 22.87 nm, which can improve the accessibility of volatiles to active sites and improve mass transport in the reforming reaction. In Fig. 4, *b*, the BJH curve at CaO:AC-PF = 2:1 shows the highest dV/dD values of 30–40 nm, indicating a catalyst in the mesopore size range. The presence of these mesopores will further increase the active sites for CO_2 adsorption.

From a process perspective, in Fig. 5, ER appears as the dominant variable that regulates autothermal conditions, primarily through an increase in effective temperature and secondary reaction intensity. An increase in ER from low to high levels consistently increases H_2, which can be explained by the acceleration of H_2 formation reactions such as charcoal gasification with steam ($C + H_2O \rightarrow CO + H_2$) [36], light hydrocarbon reforming, and more intense tar cracking at high temperatures. At the same time, CH_4 also increases sharply at high ER, indicating that in an autothermal upflow system, increased temperature and changes in gas composition can facilitate the formation of light gases. Meanwhile, CO tends to peak at moderate ER and then decreases at high ER, consistent with competition between CO formation and CO consumption through subsequent reactions such as methanation [37]. The decrease in CO_2 at high ER indicates the role of high temperatures in enhancing the reduction of CO_2 by charcoal (Boudouard reaction) and/or the role of CaO adsorption if available.

The effect of catalyst loading in Fig. 6 shows that adding catalyst does not always increase H_2. Increasing the catalyst loading from low to high tends to reduce H_2 and CH_4 but increase CO. Mechanistically, this condition can occur when the catalyst strengthens pathways that increase CO and/or promotes RWGS ($CO_2 + H_2 \rightarrow CO + H_2O$) [38], which consumes H_2 so that net H_2 is reduced. Furthermore, at high catalyst loadings, the possibility of diffusion/aggregation penalties increases, so that selectivity may shift and

some active sites become less effective. Therefore, the target of H_2-rich synthesis gas in this reactor is more dependent on ER adjustment and the selection of moderate/low catalyst loadings, rather than simply increasing the loading.

The CaO/AC-PF ratio in Fig. 7 shows synergistic but non-linear behaviour. AC-PF plays a major role as a porous medium that enhances the cracking/reforming process of volatile compounds, while CaO provides a basic site and CO_2 absorber to shift the equilibrium. At high CaO ratios, sorption and base effects may increase, but the risk of micro-pore closure and diffusion pathway changes also increases. This explains why certain compositions are optimal at certain catalyst loads: the best performance arises from a balance between pore accessibility (the role of AC-PF) and sorption/base strength (the role of CaO).

From an energy quality perspective, in Fig. 8, 9, the LHV value of synthetic gas is highly sensitive to changes in CH_4. Therefore, high ER conditions that increase CH_4 tend to increase LHV. H_2, CH_4 and CO are the main factors for obtaining high LHV. CO_2 has no calorific value so it must be captured. In this study, CaO was used so that CO_2 could be suppressed, meaning that the total LHV could be increased. The highest LHV in this study was 481 kJ/kg, while in another study, the highest was 550 kJ/kg using pinewood with dolomite, activated carbon, silica gel, and limestone catalysts [39]. The higher the ER, the more oxygen enters the system, thereby increasing the reforming reaction [40].

There are several limitations to this study. First, the gas composition was obtained from an MQ sensor based on ppm, so absolute accuracy may be affected by cross-sensitivity, humidity, sensor drift, and gas sampling temperature; this may affect the estimation of %vol and LHV, especially when changes in CO and CH_4 occur simultaneously. Second, catalyst characterisation (SEM-FTIR-BET) supports the role of surface texture and chemistry, but has not quantified changes in the active phase during operation, the degree of carbonation, and the decrease in activity due to pore closure accumulation.

The disadvantage of this research is that the CaO catalyst reacts very easily with CO_2. After the calcination process, CaO must be stored in an airtight container to prevent it from clumping into $CaCO_3$. The catalyst has a specific usage period because it is covered with tar or ash.

Based on these limitations, several future directions are recommended. Calibrate the gas composition using GC-TCD/GC-FID to convert the sensor readings into more accurate %vol and include LHV uncertainty analysis. Evaluate catalyst stability and regeneration, especially for CaO which is easily carbonated, through carbonation-calcination cycle tests and post-reaction characterisation (XRD/TGA/SEM-EDX) to assess phase changes and activity loss. Develop experimental designs towards ANOVA or RSM interactions so that interaction effects and predictive models can be obtained and verified through replication confirmation tests. Add process performance metrics such as gas yield (Nm^3/kg), cold gas efficiency, pressure drop, and air consumption so

that ‘syngas quality improvement’ can be demonstrated based on mass-energy balance and operability, not just composition.

7. Conclusion

1. AC-PF with rich -OH group acts as a porous catalytic medium that facilitates volatile cracking and supports the reduction of condensable by-products, while CaO contributes to absorb CO_2. The BJH analysis confirms that CaO plays a dual role as a reactive sorbent and a textural promoter in palm-fiber activated carbon by enlarging mesopores (20–40 nm), thereby enhancing gas diffusion and improving access to CaO active sites, which ultimately strengthens catalytic performance.

2. Increasing ER to 0.35 enhances the combustible gas fraction H_2 and CH_4 and suppresses CO_2, whereas CO typically peaks at intermediate ER due to competing CO formation and consumption reactions along the updraft reaction zones. Increasing catalyst loading shifts syngas composition: CO increases, while H_2 and CH_4 decrease, indicating changes in dominant secondary reactions and possible diffusion or agglomeration limitations at higher loadings. Increasing ER lead to increase LHV syngas, but it can decrease at high catalyst loading. An increase in the CaO/AC ratio to 2:1 resulted in a higher syngas LHV, with a maximum value of 481 kJ/kg.

Conflict of interest

The authors declare that they have no conflict of interest in relation to this research, whether financial, personal, authorship or otherwise, that could affect the research and its results presented in this paper.

Financing

The authors sincerely thank the Ministry of Education, Culture, Research and Technology, Republic of Indonesia for fully supporting this research through the DRTPM Research Grant under Fundamental Research, Universitas Widyagama Malang, Indonesia 2025 (Grant Number:128/C3/DT.05.00/PL/2025;023/LL7/DT.05.00/PL/2025;010/ Kontrak/PT/PTS.030.7/PN/V/2025).

Data availability

Manuscript has no associated data.

Use of artificial intelligence

The authors used the AI-based language model ChatGPT (GPT-5.3) only to assist in improving the clarity of English language and grammar in several sections of the manuscript, particularly in the Introduction and Literature Review sections.

The AI tool was used solely for language editing and paraphrasing purposes. All scientific content, experimental design, data analysis, and interpretation of the results were conducted entirely by the authors.

The authors carefully reviewed and verified all AI-assisted text to ensure accuracy and consistency with the experimental results. The use of AI tools did not influence the scientific conclusions of this study.

Acknowledgements

We as the Research Team would like to thank Ministry of Education, Culture, Research and Technology, Republic of Indonesia (Kemendiktisaintek Indonesia) for financing research activities.

Authors' contributions

Purbo Suwandono: Conceptualization, Writing-original draft, Investigation, Supervision, Formal analysis, Writing – review & editing; **Widya Wijayanti**: Validation, Investigation, Data Curation, Formal analysis, Writing – original draft; **Nova Risdiyanto Ismail**: Writing – review & editing, Formal analysis; **Dzulfikar Johan Akbar:** Visualization, Writing – original draft, Data curation; **Muhammad Reza**: Project administration, Resources, Data curation.

Please reduce the number of sources to 30 references.

References

If possible, please provide active hyperlinks to the entire list of literature.

1. ASEAN Statistical Brief, "Role of Agriculture , Forestry , and Fishing Industry in ASEAN Economy," vol. VII, no. June 2023, p. 511191, 2024.
2. V. K. Yadav *et al.*, "Emerging trends in the valorization of agricultural waste and their utilization in agricultural, pharmaceuticals, and environmental cleanup," *Waste and Biomass Valorization*, pp. 1–55, 2025.
3. W. M. Lewandowski, M. Ryms, and W. Kosakowski, "Thermal biomass conversion: A review," *Processes*, vol. 8, no. 5, p. 516, 2020.
4. D. Ariyanti *et al.*, "Valorization of corn cob waste for furfural production: A circular economy approach," *Biomass and Bioenergy*, vol. 194, p. 107665, 2025.
5. A. Raizada, A. Shukla, S. Yadav, P. Katiyar, and R. Kumar, "Enhancement of H2 production via catalytic steam gasification of food waste as feedstock and its ash as a support and promoter for Ni catalyst," *Int. J. Hydrogen Energy*, vol. 60, pp. 272–281, 2024.
6. Y. Dai *et al.*, "Co-gasification characteristics of Ca-rich sludge and Fe-rich sludge under CO2 atmosphere, and potential utilization of gasification residues as renewable catalyst in biomass pyrolysis," *Renew. Energy*, vol. 224, p. 120118, 2024.
7. H. Sun *et al.*, "Three-stage behaviors of K2CO3 catalyst during CO2 catalytic gasification of coal," *Fuel*, vol. 367, p. 131149, 2024.
8. J. Zhang, Z. Chu, R. Cao, X. Wu, and K. Han, "A review of resource recovery from waste plastics via pyrolysis and gasification," *Fuel*, vol. 404, p. 136319,

2026.
9. Y. Tangke Tosuli, Cahyadi, H. Dafiqurrohman, R. Hermawan, and A. Surjosatyo, “Gasification of sago dreg waste in a top-lit updraft fixed bed gasifier: Syngas composition and its effect with additional Al2O3 as catalyst,” *Energy Convers. Manag. X*, vol. 24, no. October, p. 100775, 2024, doi: 10.1016/j.ecmx.2024.100775.
10. P. Dinh *et al.*, “Enrichment of hydrogen in product gas from a pilot-scale rice husk updraft gasification system,” *Carbon Resour. Convers.*, vol. 5, no. 3, pp. 231–239, 2025, doi: 10.1016/j.crcon.2022.07.003.
11. S. Yousef and J. Eimontas, “International Journal of Hydrogen Energy Oxygen updraft gasification-catalytic reforming of cigarettes butts for hydrogen-rich syngas production,” vol. 171, no. May, 2025, doi: 10.1016/j.ijhydene.2025.150650.
12. D. Contreras, E. Blanco, and D. Travieso, “Experimental assessment of the energy potential of pellets produced from beekeeping wastes by updraft gasification,” vol. 343, no. January, 2025, doi: 10.1016/j.enconman.2025.120206.
13. N. Yesilova, O. Tezer, A. Ongen, and A. Ayol, “International Journal of Hydrogen Energy Enhancing biomass gasification : A comparative study of catalyst applications in updraft and modifiable-downdraft fixed bed reactors,” *Int. J. Hydrogen Energy*, vol. 76, no. April, pp. 290–303, 2024, doi: 10.1016/j.ijhydene.2024.05.075.
14. R. Skvor and A. Jan, “Experimental investigation of sorted municipal solid wastes producer gas composition in an updraft fixed bed gasifier,” vol. 289, no. August 2022, 2024, doi: 10.1016/j.energy.2023.130063.
15. R. Junga, M. Tańczuk, S. Sobek, M. Chabiński, and Ł. Ziółkowski, “Effect of the addition of laying hens manure to the straw on gasification efficiency in updraft gasifier under air atmosphere,” *Appl. Therm. Eng.*, vol. 226, no. February, p. 120269, 2023, doi: 10.1016/j.applthermaleng.2023.120269.
16. A. Ongen and A. Ayol, “ScienceDirect Gasification performance of olive pomace in updraft and downdraft fixed bed reactors,” vol. I, 2023, doi: 10.1016/j.ijhydene.2023.02.088.
17. K. Ertas, “Gasification of MDF residue in an updraft fixed bed gasifier to produce heat and power via an ORC turbine,” vol. 169, no. February, pp. 43–51, 2023, doi: 10.1016/j.wasman.2023.06.025.
18. S. Gorthy, S. Verma, N. Sinha, S. Shetty, H. Nguyen, and M. Neurock, “Theoretical Insights into the Effects of KOH Concentration and the Role of OH–in the Electrocatalytic Reduction of CO2 on Au,” *ACS Catal.*, vol. 13, no. 19, pp. 12924–12940, 2023.
19] X. Wang, W. Zeng, C. Xin, X. Kong, X. Hu, and Q. Guo, “The development of activated carbon from corncob for CO2 capture,” *RSC Adv.*, vol. 12, no. 51, pp. 33069–33078, 2022, doi: 10.1039/d2ra05979g.
20. D. Ali, H. Fakra, D. Armel, and S. Andriatoavina, “A simple and low-cost integrative sensor system for methane and hydrogen measurement,” vol. 1, no. August, 2020, doi: 10.1016/j.sintl.2020.100032.
21. S. V. Co-digestion and H. Ram, “Assessment of a Low-Cost Hydrogen

Sensor for Detection and Monitoring of Biohydrogen Production during Sugarcane," pp. 479–490, 2024.

22. H. Du *et al.*, "Lignocellulosic Films: Preparation, Properties, and Applications," *Chem. Rev.*, 2025.

23. S. De, A. M. Balu, J. C. Van Der Waal, and R. Luque, "Biomass-derived porous carbon materials: synthesis and catalytic applications," *ChemCatChem*, vol. 7, no. 11, pp. 1608–1629, 2015.

24. C. Li *et al.*, "Importance of oxidation reactions in creating pores in physical activation of biomasses," *Chem. Eng. J.*, vol. 474, p. 145748, 2023.

25. B. Zhou *et al.*, "Insights into effects of grain boundary engineering in composite metal oxide catalysts for improving catalytic performance," *J. Colloid Interface Sci.*, vol. 653, pp. 1177–1187, 2024.

26. Y. Zhu *et al.*, "Preparation of hierarchically porous carbon ash composite material from fine slag of coal gasification and ash slag of biomass combustion for CO2 capture," *Sep. Purif. Technol.*, vol. 330, p. 125452, 2024.

27. Y. Y. García-Guel, E. M. Múzquiz-Ramos, J. C. Ríos-Hurtado, A. Moreno-Santos, S. E. Flores-Villaseñor, and G. B. Escalante-Ibarra, "Surface modification of activated carbon cloth with calcium silicate and hydroxyapatite: bioactive composite material," *Heliyon*, vol. 8, no. 11, 2022.

28. M. Ilić *et al.*, "Surface functional groups and degree of carbonization of selected chars from different processes and feedstock," *PLoS One*, vol. 17, no. 11, p. e0277365, 2022.

29. R. Ali, Z. Aslam, R. A. Shawabkeh, A. Asghar, and I. A. Hussein, "BET, FTIR, and RAMAN characterizations of activated carbon from waste oil fly ash," *Turkish J. Chem.*, vol. 44, no. 2, pp. 279–295, 2020.

30. K. J. Stanienda-Pilecki, "The importance of Fourier-Transform Infrared Spectroscopy in the identification of carbonate phases differentiated in magnesium content," 2019.

31. F. Dai, Q. Zhuang, G. Huang, H. Deng, and X. Zhang, "Infrared spectrum characteristics and quantification of OH groups in coal," *ACS omega*, vol. 8, no. 19, pp. 17064–17076, 2023.

32. E. M. de Salazar Martínez, M. F. Alexandre-Franco, A. J. Nieto-Sanchez, and E. M. Cuerda-Correa, "Exploring the role of surface and porosity in CO2 capture by CaO-based adsorbents through response surface methodology (RSM) and artificial neural networks (ANN)," *J. CO2 Util.*, vol. 83, p. 102773, 2024.

33. J. A. Tavizón-Pozos, H. Cervantes-Cuevas, G. G. Garcia-Camacho, G. Chavez-Esquivel, and D. R. Acosta-Najarro, "Biodiesel Production Using K–Sr/CaO and CaO Catalysts Derived from Eggshells by Canola Oil Transesterification," *ACS omega*, vol. 10, no. 7, pp. 6827–6838, 2025.

34. W. Koo-Amornpattana, P. Phadungbut, N. Kunthakudee, W. Jonglertjunya, S. Ratchahat, and M. Hunsom, "Innovative metal oxides (CaO, SrO, MgO) impregnated waste-derived activated carbon for biohydrogen purification," *Sci. Rep.*, vol. 13, no. 1, p.

4705, 2023.
35. C. Quan, M. Wang, N. Gao, T. Yang, and R. Li, “In situ adsorption of CO2 to enhance biomass gasification for hydrogen production using Ca/Ni based composites,” *J. Energy Inst.*, vol. 108, p. 101229, 2023, doi: https://doi.org/10.1016/j.joei.2023.101229.
36. F. Micheli, E. Mattucci, C. Courson, and K. Gallucci, “Bi-Functional Catalyst/Sorbent for a H2-Rich Gas from Biomass Gasification,” 2021. doi: 10.3390/pr9071249.
37. M. Zhu, Q. Wang, and S. Wang, “Recent Advances and Future Perspectives in Catalyst Development for Efficient and Sustainable Biomass Gasification: A Comprehensive Review,” 2025. doi: 10.3390/su17167370.
38. N. Cerone, F. Zimbardi, L. Contuzzi, J. Baleta, and D. Cerinski, “Experimental investigation of syngas composition variation along updraft fixed bed gasifier,” *Energy Convers. Manag.*, vol. 221, no. July, p. 113116, 2020, doi: 10.1016/j.enconman.2020.113116.
39. R. Mohanty, P. Mahanta, A. Mahapatro, and R. Prakash, “Catalytic gasification of pinewood biomass in a fluidized bed reactor with dolomite , limestone , and activated carbon : An experimental study,” *Energy*, vol. 325, no. April, p. 136131, 2025, doi: 10.1016/j.energy.2025.136131.
40. C. Liu, Y. Huang, M. Niu, and H. Pei, “ScienceDirect Influences of equivalence ratio , oxygen concentration and fluidization velocity on the characteristics of oxygen-enriched gasification products from biomass in a pilot-scale fluidized bed,” *Int. J. Hydrogen Energy*, vol. 43, no. 31, pp. 14214–14225, 2018, doi: 10.1016/j.ijhydene.2018.05.154.

Author’s order	First Name	Middle name	Second Name
1	*Purbo*		*Suwandono*
2	*Widya*		*Wijayanti*
3	*Nova*	*Risdiyanto*	*Ismail*
4	*Dzulfikar*	*Johan*	*Akbar*
5	*Muhammad*		*Reza*

We ask the authors indicate the Corresponding author in the information about the authors, after the full name (Corresponding author is the author who is in correspondence with the editors and whose email address will be indicated as feedback for readers if they want to contact the author/group of authors)

English
Purbo Suwandono Master

Department of Mechanical Engineering
Widya Gama University
Borobudur str., 35, Malang, Indonesia, 65142
E-mail: purbo@widyagama.ac.id
ORCID: https://orcid.org/0000-0003-4085-1291
Contact phone: +6282132697144
Number of publications in national journals indexed (approximate; for Ukraine citizens only): -
Number of publications in international journals indexed (approximate): 14
H-index by Scopus (if available): 4
ResearchGate: https://www.researchgate.net/profile/Purbo-Suwandono
Scopus ID: 57204187970
Researcher ID: https://researchid.co/rid80879

Widya Wijayanti
PhD
Department of Mechanical Engineering
Brawijaya University
Veteran str., 10–11, Malang, Indonesia, 65145
E-mail: widya_dinata@ub.ac.id
ORCID: https://orcid.org/0000-0003-4215-5943
Contact phone: +6285334992164
Number of publications in national journals indexed (approximate; for Ukraine citizens only): -
Number of publications in international journals indexed (approximate): 78
H-index by Scopus (if available): 12
ResearchGate: https://www.researchgate.net/profile/Widya-Wijayanti
Scopus ID: 36006672800
Researcher ID: -

Nova Risdiyanto Ismail
Doctor Which sciences?
Department of Mechanical Engineering
Widya Gama University
Borobudur str., 35, Malang, Indonesia, 65142
E-mail: nova@widyagama.ac.id
ORCID: https://orcid.org/0000-0001-8439-6919
Contact phone:
Number of publications in national journals indexed (approximate; for Ukraine citizens only): -
Number of publications in international journals indexed (approximate): 7

H-index by Scopus (if available): 3
ResearchGate: https://www.researchgate.net/profile/Nova-Ismail-2
Scopus ID: 57204527065
Researcher ID: https://researchid.co/rid80876

Dzulfikar Johan Akbar
Master Student
Department of Mechanical Engineering
Brawijaya University
Veteran str., 10–11, Malang, Indonesia, 65145
E-mail: johanakbar@student.ub.ac.id
ORCID: https://orcid.org/0009-0002-4652-8516
Contact phone: +6282241116998
Number of publications in national journals indexed (approximate; for Ukraine citizens only): -
Number of publications in international journals indexed (approximate): -
H-index by Scopus (if available): -
ResearchGate: https://www.researchgate.net/profile/Dzulfikar-Johan-Akbar
Scopus ID: -
Researcher ID: -

Muhammad Reza
Bachelor Student
Department of Mechanical Engineering
Widya Gama University
Borobudur str., 35, Malang, Indonesia, 65142
E-mail: muhapanjangreza@gmail.com
ORCID: https://orcid.org/0009-0009-9258-0586
Contact phone: +6282139682566
Number of publications in national journals indexed (approximate; for Ukraine citizens only): -
Number of publications in international journals indexed (approximate): -
H-index by Scopus (if available): -
ResearchGate: -
Scopus ID: -
Researcher ID: -

Name of reviewer: Prof. Dr. Muji Setiyo, ST., MT.
Professor: Mechanical Engineering
Tel: +6281211020288
E-mail: muji@unimma.ac.id.

Work address: Universitas Muhammadiyah Magelang

Name of reviewer: Prof. Dr. Eng. Nurkholis Hamidi, ST., MT.
Professor: Mechanical Engineering
Tel: +62 81259293165
E-mail: hamidy@ub.ac.id
Work address: Brawijaya University

REVISI REVIEW EDITOR

Received date: 20.02.2026
Accepted date:

UDC

ПОКРАЩЕННЯ ЯКОСТІ СИНТЕЗ-ГАЗУ ПРИ ВИСХІДНІЙ ГАЗИФІКАЦІЇ КУКУРУДЗЯНИХ КАЧАНІВ З ВИКОРИСТАННЯМ КАТАЛІЗАТОРА НА ОСНОВІ CAO/АКТИВОВАНОГО ВУГІЛЛЯ НА ПАЛЬМОВОМУ ВОЛОКН

Purbo Suwandono, Widya Wijayanti, Nova Risdiyanto Ismail, Dzulfikar Johan Akbar, Muhammad Reza

SYNGAS QUALITY IMPROVEMENT IN CORNCOB UPDRAFT GASIFICATION USING CAO/ACTIVATED CARBON PALM FIBER CATALYST

Purbo Suwandono, Widya Wijayanti, Nova Risdiyanto Ismail, Dzulfikar Johan Akbar, Muhammad Reza

The sum of summary + keywords= should be 1800-1900 characters with spaces.

The summary should contain the following information:
- object of research
- problem that was solved
- results obtained
- brief interpretation of the results (what explains them)
- features and distinctive features of the results obtained, thanks to which they allowed to solve the problem under study
- the scope and conditions of practical use of the results obtained

Replace hyphens (-) with dashes (–) by text (except word combinations)

У цьому дослідженні вивчається можливість поліпшення якості синтез-газу, отриманого в результаті газифікації кукурудзяних качанів за допомогою системи з подвійним каталізатором на основі CaO та активованого вугілля з пальмового волокна (AC–PF). Основними проблемами є відносно низька теплотворна здатність синтез-газу з кукурудзяних качанів та висока вартість каталізаторів, що використовуються на даний момент. У цьому дослідженні в якості каталізаторів використовувалися недорогий CaO та перероблені відходи пальмового волокна, перетворені на активоване вугілля. До досліджуваних робочих змінних належали коефіцієнт еквівалентності (0,2, 0,25, 0,3 та 0,35), навантаження каталізатора (4%, 6%, 8% та 10%) та масове співвідношення CaO/AC-PF (0:1, 1:0, 1:1 та 2:1).

Характеристика каталізатора показує, що AC-PF має пористу структуру, яка збільшує контакт газу з твердим тілом і сприяє вторинним реакціям, тоді як додавання CaO утворює композит із модифікованою структурою пор і поверхневими видами, пов'язаними з сорбцією CO_2. Експериментальні результати показують, що збільшення ER підвищує частку H_2 (ER 0,2: 3150 ppm, ER 0,35: 3914 ppm) і частку CH_4. Водночас частка CO_2 зменшилася. Тим часом CO показав оптимальне значення при ER: 0,3 ppm, перш ніж зменшитися при ER 0,35. І навпаки, збільшення навантаження каталізатора призводило до зменшення H_2 (4%: 3742 ppm, 10%: 3176 ppm) і CH_4, але збільшувало CO. З енергетичної точки зору, нижча теплота згоряння синтез-газу збільшується із збільшенням ER, але може зменшуватися при більш високих навантаженнях каталізатора через зменшення внеску CH_4.

Сильна сторона цього дослідження полягає у функціональній синергії між пористим AC-PF та поліпшенням якості сорбції CO_2 на основі CaO, завдяки чому можна досягти поліпшення якості синтез-газу за допомогою поєднання каталітичних та сорбційних ефектів в одній системі. Результати цього дослідження можуть бути застосовані до невеликих установок газифікації біомаси, зокрема до реакторів з висхідним потоком для відходів кукурудзяних качанів.

Ключові слова: газифікація, висхідний потік, кукурудзяні качани, синтетичний газ, CaO, активоване вугілля, пальмове волокно, низька теплотворна здатність, коефіцієнт еквівалентності, навантаження You have 18 words, there should be 10

This study investigates improving the quality of syngas from updraft corn cob gasification using a dual catalyst system based on CaO and activated carbon from palm fiber (AC–PF). The main problems encountered are the relatively low heating value of corn cob syngas and the high cost of the catalysts currently in use. In this study, inexpensive CaO and processed palm fiber waste into activated carbon were used as catalysts. The operating variables studied included the equivalence ratio (0.2, 0.25, 0.3, and 0.35), catalyst loading (4%, 6%, 8%, and 10%), and the CaO/AC-PF mass ratio (0:1, 1:0, 1:1, and 2:1).

Characterization of the catalyst shows that AC-PF has a porous structure that increases gas-solid contact and promotes secondary reactions, while the addition of CaO forms a composite with a modified pore texture and surface species associated with CO_2 sorption. Experimental results show that an increase in ER raises the H_2 fraction (ER 0.2: 3150 ppm, ER 0.35: 3914 ppm) and CH_4 fraction. Meanwhile, the CO_2 fraction decreased. Meanwhile, CO showed an optimum value at ER: 0.3 ppm before decreasing at ER 0.35. Conversely, an increase in catalyst loading tended to decrease H_2 (4%: 3742 ppm, 10%: 3176 ppm) and CH_4 but increases CO. From an energy perspective, the Lower Heating Value of syngas increases with increasing ER, but may decrease at higher catalyst loadings due to the reduced contribution of CH_4.

The strength of this research lies in the functional synergy between porous AC-PF and CaO-based CO_2 sorption quality improvement, so that syngas quality improvement can be achieved through a combination of catalytic and sorption effects in a single system. The results of this study have the potential to be applied to small scale biomass gasification units, particularly updraft reactors for corn cob waste

Keywords: gasification, updraft, corncob, syngas, CaO, activated carbon, palm fiber, low heating value, equivalence ratio, load You have 15 words, there should be 10

Анотація:
Метою даного дослідження є поліпшення якості синтез-газу, отриманого в результаті газифікації кукурудзяних качанів за допомогою системи з подвійним каталізатором, що складається з CaO та активованого вугілля, отриманого з пальмового волокна (AC–PF). Проблема, вирішена в даному дослідженні, полягає у відносно низькій теплотворній здатності синтез-газу з кукурудзяних качанів та високій вартості традиційних каталізаторів, що використовуються для його поліпшення. Дослідження проводилося з використанням різних значень еквівалентного співвідношення (0,2; 0,25; 0,3; 0,35), навантаження каталізатора (4%; 6%; 8%; 10%) та масового співвідношення CaO/AC–PF (0:1; 1:0; 1:1; 2:1) у поєднанні з характеристикою подвійної каталітичної системи. Отримані результати показують, що збільшення ER збільшує частки H_2 і CH_4 та нижчу теплоту згоряння синтез-газу, одночасно зменшуючи CO_2, причому CO досягає оптимального значення при ER = 0,3. У той час як більш високе навантаження каталізатора має тенденцію до зменшення H_2 і CH_4, але збільшує CO, потенційно знижуючи теплоту згоряння при високих навантаженнях Характеристика каталізатора показує, що AC-PF має пористу структуру, яка збільшує контакт газу з твердим тілом і сприяє вторинним реакціям, тоді як додавання CaO утворює композит із модифікованою структурою пор і поверхневими видами, пов'язаними з сорбцією CO_2. З енергетичної точки зору, нижня теплота згоряння синтез-газу збільшується із зростанням ER, але зменшується при більш високих навантаженнях каталізатора через зменшення внеску CH_4. Ключовою особливістю отриманих результатів є продемонстрована функціональна синергія між пористим AC–PF і сорбцією CO_2 на основі CaO, що дозволяє одночасно здійснювати каталітичне поліпшення якості та уловлювання CO_2 в єдиній, недорогій системі з подвійним каталізатором. Ці висновки можуть стати практичною основою для проектування та експлуатації невеликих установок газифікації біомаси, зокрема реакторів з висхідним потоком для відходів кукурудзяних качанів, в межах досліджених діапазонів ER та навантаження каталізатора.

Ключові слова: газифікація, висхідний потік, кукурудзяні качани, синтез-газ, CaO, активоване вугілля

Abstract:
The object of this study is the improvement of syngas quality from updraft corn cob gasification using a dual catalyst system consisting of CaO and activated carbon derived from palm fiber (AC–PF). The problem solved in this study is the relatively low heating value of corn cob syngas and the high cost of conventional catalysts used for its upgrading. The study was conducted using variations of equivalence ratio (0.2, 0.25, 0.3, 0.35), catalyst loading (4%, 6%, 8%, 10%), and CaO/AC–PF mass ratio (0:1, 1:0, 1:1, 2:1), combined with characterization of the dual catalyst system. The results obtained show that increasing ER increases the H_2 and CH_4 fractions and the syngas lower heating value while decreasing CO_2, with CO reaching an optimum at ER = 0.3. Whereas higher catalyst loading tends to decrease H_2 and CH_4 but increase CO, potentially reducing the heating value at high loadings Characterization of the catalyst shows that AC-PF has a porous structure that increases gas-solid contact and promotes secondary reactions, while the addition of CaO forms a composite with a modified pore texture and surface species associated with CO_2 sorption. From an energy perspective, the Lower Heating Value of syngas increases with increasing ER, but decrease at higher catalyst loadings due to the reduced contribution of CH_4. A key feature of obtained results is the demonstrated functional synergy between porous AC–PF and CaO-based CO_2 sorption, which enables simultaneous catalytic upgrading and CO_2 capture in a single, low-cost dual catalyst system. These findings could be a practical basis for designing and operating small-scale biomass gasification units, particularly updraft reactors for corn cob waste, within the studied ER and catalyst loading ranges.
Keywords: gasification, updraft, corncob, syngas, CaO, activated carbon

1. Introduction

Indonesia is one of the largest corn producers in Southeast Asia, with national production reaching more than 18 million tons of dry kernels per year. Of this amount, about 15–20% is cobs after the kernel removal process, resulting in a very large amount of corn cob waste, estimated at 2.5–3.5 million tons annually. Until now, most corn cobs have only been used to a limited extent, for example as traditional fuel, small amounts of animal feed, or even burned directly on post-harvest land, which has the potential to cause air pollution. Most of the rest are simply piled up or left to rot on the land, posing a risk of becoming a source of plant disease [1].

Corn cobs have quite promising chemical and energy characteristics. Their composition is dominated by cellulose, hemicellulose, and lignin, with a calorific value of around 15–17 MJ/kg, making them very suitable as raw materials in various biomass-based energy conversion technologies [2]. Their hard and fibrous nature also makes them suitable for processing into biochar, activated charcoal, or direct use in pyrolysis and gasification processes. This significant potential indicates that corn cobs are not merely waste but a renewable resource that can be optimized to support energy security and reduce dependence on fossil fuels.

Biomass gasification is a promising thermochemical technology for converting renewable resources into syngas consisting of H_2, CO, CH_4, and CO_2. Of the various types of biomass, corn cobs are a potential candidate due to their abundant availability in Indonesia and lignocellulose content that supports the energy conversion process [3]. However, the biomass gasification process still faces several obstacles, particularly the low hydrogen fraction in syngas and the formation of significant amounts of tar. Tar can cause reactor clogging, reduced thermal efficiency, and increased purification costs.

To overcome these problems, the use of catalysts is an important strategy. A number of studies have proven that metal catalysts such as Ni, Ca, and K can increase hydrogen yield while suppressing tar formation. On the other hand, activated carbon is also widely used as a catalyst support because it has a high surface area, porous structure, and good chemical stability. The use of agricultural waste, particularly palm fiber, as raw material for activated carbon is not only economically valuable but also supports the concept of a circular economy in plantation waste management. In addition, calcium oxide (CaO) is known to have a dual role, namely as a catalyst in the tar decomposition reaction and as a CO_2 absorber that promotes sorption-enhanced gasification to increase the hydrogen fraction in syngas [4].

Although various studies have examined the role of metal catalysts and activated carbon separately, research focusing on the combination of biomass bases catalyst such as palm fiber-based activated carbon with CaO in corn cob gasification is still limited. The uniqueness of this study lies in the integration of two catalyst, which is expected to provide a synergistic effect: activated carbon with high porosity increases catalyst dispersion and activity, while CaO simultaneously breaks down tar and absorbs CO_2. This approach has the potential to significantly increase hydrogen production and reduce carbon emissions.

However, there are several research gaps that remain unanswered. First, the optimal composition and ratio of activated carbon and CaO in corn cob gasification have not been extensively studied. Second, the synergistic mechanism using two catalyst in increasing syngas quality not yet fully understood. In addition, a systematic and statistically robust approach is required to disentangle the coupled effects of key operating and catalyst variables.

Based on this background and research gaps, this study aims to investigate the performance of a composite catalyst based on activated carbon from palm fiber combined with CaO in the corn cob gasification process. The main focus is on increasing hydrogen production, reducing tar, and evaluating the potential synergistic effects between materials. This research is expected to contribute to the development of low-cost, locally sourced, and sustainable catalyst systems that are relevant to supporting the clean energy transition and practical applications of biomass-to-hydrogen in the future.

2. Literature review and problem statement

How this section should be built: The paper [.] presents the results of research ..., Shown, that..., But there were unresolved issues related to ..., The reason for this may be (objective difficulties associated with ..., fundamental impossibility ..., cost part in terms of ..., which makes relevant research impractical, etc.). A way to overcome these difficulties can be ..., This approach was used in [.], however ..., All this suggests that it is advisable to conduct a study on ...

Previous studies have reported improvements in syngas quality in fixed-bed updraft gasification through the selection of gasification agents and catalytic strategies. The paper by [9] explored Sago-based foods are staple in eastern Indonesia. Single Al_2O_3 catalyst (5–10 wt%) was added to sago-dregs pellets in a TULD gasifier enhances syngas: H_2 is highest at 5% (31.65%), while CO (4.33%) and CH_4 (26.45%) peak at 10%. The H_2/CO ratio remains favorable (1.65–1.51) with low tar, indicating potential for internal combustion engine fuel.

The paper by [10] explored an updraft gasifier processed 3 kg of dried rice husk using air, steam-air, and air with dolomite at varied conditions. Among the tested agents, single catalytic air gasification (air + dolomite) gave the best results, producing the highest H_2 (15.4 mol%) and LHV (5.1 MJ/Nm³), compared with steam-air (7.08 mol%, 3.6 MJ/Nm³) and air only (3.6 mol%). The optimum setting was an airflow of 3 m³/h with 15% dolomite.

The paper by [11] explored Cigarette butts are hazardous urban waste rich in cellulose acetate and volatile matter, making them a potential renewable feedstock for hydrogen production. This study valorized as-received cigarette butts via continuous updraft gasification (700–900°C; ER 0.15–0.25), followed by steam catalytic reforming over KATALCO™ 57-4GQ at 900°C. Gasification alone produced high syngas yields (82.3–89.7%) but limited H_2 (<20.84 vol% at 900°C, ER 0.15). The reforming step increased H_2 to 30.27 vol% and reduced tar from 18.15 to 13.38 g/m³, improving fuel quality (HHV from 11,038 to 11,528 kJ/kg).

The paper by [12] explored slumgum suitability as a gasification fuel. Slumgum and slumgum-pine sawdust pellets were produced (ISO 17225 tests) and gasified in a modified updraft reactor while measuring gas composition and LHV. Pure slumgum pellets showed very high durability (99.98%) and HHV (27.66 MJ/kg), likely due to high fat content, but high sulfur (2.17%) and nitrogen (3.52%) prevented ISO compliance. In gasification, adding sawdust increased LHV, reaching 7.62 MJ/Nm³ at a 50:50 blend, although ER stayed very low (0.0125–0.0204) because higher airflow raised fuel consumption.

The paper by [13] examined catalyst effects on biomass-mixture gasification using lab-scale updraft and modifiable-downdraft fixed-bed reactors. Red mud (RM) and an Al–Ni alloy were tested at high temperature, where H_2 levels of 51–65 vol% were obtained at 900°C in both systems. The Al–Ni catalyst showed the strongest enhancement, achieving 65 vol% H_2 in the updraft reactor at 900°C with 0.05 L/min dry

air, and widening the H_2/CO range from 2–4 (no catalyst) to 1.6–7. RM generally increased H_2 in the updraft reactor by about 1–7 vol% at 900°C, but in the modifiable-downdraft reactor it reduced H_2 by roughly 2–6%.

The paper by [14] examined three MSW fractions (FDS, SRF, and plastic packaging mixture/PPM) from mechanical-biological treatment plants were gasified in an allothermal fixed-bed updraft reactor at 800°C using air at ER ≈ 0.15 and 0.21. All feeds showed similar volatile-release peaks (~330 and ~500°C). Lowering ER increased the heating value of combustible gases; PPM produced the highest H_2 (11.39%). SRF generated the most tar (47.44 g/m³), dominated by aromatic compounds.

The paper by [15] examined co-gasifying laying hens manure (LHM) with common litter such as wheat straw remains limited, particularly across a wide range of air–fuel equivalence ratios (AFER). This laboratory study used a fixed-bed updraft reactor to gasify straw-LHM blends (25–75% LHM) under low (0.12–0.28) and high (0.30–0.45) AFER to assess how LHM affects producer-gas quality and process efficiency. At higher AFER, the producer-gas LHV stayed around 3.3–3.4 MJ/m³ (depending on blend), with cold gas efficiency 60% and carbon conversion efficiency of 82–94%.

The paper by [16] evaluated the gasification of olive pomace in fixed-bed updraft and downdraft systems. Dried olive pomace obtained from an olive-oil soap plant in Izmir (Türkiye) was characterized and gasified at 700–900 °C using dry air at 0.05–0.4 L/min, with additional tests using pure oxygen (0.01 L / min). With dry air, the syngas reached 48 vol% H_2 in the updraft and 45 vol% in the downdraft, with a heating value of about 12.4 MJ / Nm³. Under oxygen, H_2 increased to ~53 vol% in the updraft but was ~39 vol% in the downdraft.

The paper by [17] gasified MDF wood-waste in a 2100 kg/h updraft fixed-bed system (tested at 1500–2100 kg/h) using oak chips as a reference. Syngas yield was 2.5 Nm³/kg with LHV 6.0–7.0 MJ/Nm³, and the gas composition at full-load MDF was similar to oak. Hot syngas (430°C) containing tar/soot was burned directly in a retrofitted thermal-oil heater (7 MWh) to supply an ORC turbine generating 955 kW electricity, converting 88 wt% of MDF residue into syngas.

However, there are still unresolved issues regarding how to achieve simultaneous improvements in syngas quality increasing H_2/CH_4 and LHV while reducing CO_2/tar with an approach that remains simple, scalable, and economical for updraft reactors. One reason for this is that most studies still emphasize single catalysts or separate additives, while dual-catalyst synergy in updraft configurations has been relatively rarely studied systematically. Efforts to overcome these limitations can be made through the development of a dual-catalyst system that combines the function of CO_2 absorption to drive the equilibrium shift towards H_2 formation, and a high-surface catalytic function to enhance secondary reactions such as cracking of volatiles and suppressing condensed products.

This approach has the potential to be realized by combining CaO as a CO_2 sorbent and palm fiber-based activated carbon (AC–PF) as a porous material with a high surface area to increase contact and volatility reactivity. however, quantitative evidence

regarding the level of synergy, the optimum CaO / AC–PF ratio combination, and the effect of ER and catalyst loading on H_2, CO, CH_4, CO_2, and LHV in updraft corn cob gasification has not yet been comprehensively mapped.

All this allows us to conclude that it is expedient to conduct research devoted to improving syngas quality in updraft corn cob gasification through a CaO / AC–PF dual catalyst system with systematic evaluation of the equivalence ratio, catalyst loading, and CaO / AC–PF ratio, to obtain cleaner syngas that is rich in H_2 and has a higher calorific value.

2. Literature review and problem statement

The paper [5] presents the result on the gasification of sago dreg waste pellets in a top-lit updraft fixed-bed gasifier. The results show that the addition of Al_2O_3 improved syngas quality, especially by increasing H_2 content up to 31.65% at 5% Al_2O_3 and enhancing CO and CH_4 production, while also increasing the H_2/CO ratio to 1.65 and 1.51 for 5% and 10% Al_2O_3, respectively, improving LHV, and reducing tar content by about 25–27.5% compared with pellets without catalyst. However, this study is limited because it was conducted only on one biomass type, within a laboratory-scale TULD fixed-bed gasifier, and only considered two catalyst loadings.

The paper [6] presents the result on hydrogen enrichment in product gas from a pilot-scale rice husk updraft gasification. The results show that dolomite-assisted air gasification gave the best performance, increasing the H_2 content up to 15.4 mol%, with an LHV of 5.1 MJ/Nm³, while steam/air gasification improved H_2 to 9.6 mol% and air alone produced only about 7.08 mol% H_2, the optimum operating condition was reported at an airflow rate of 3 m³/h and a dolomite mixing ratio of 15 wt%. However, this study is limited because it focused only on rice husk feedstock, used a pilot-scale updraft gasifier with a batch capacity of 3 kg, and evaluated only a limited range of operating conditions and catalyst type.

The paper [7] presents the result on oxygen updraft gasification coupled with catalytic steam reforming of cigarette butts for hydrogen-rich syngas production. The results show that the integrated process was effective in converting cigarette butts into syngas, with gasification producing 82.3–89.7 wt.% syngas, 6.3–8.6 wt.% soot, and 1.4–1.9 wt.% tar, while the catalytic reforming stage significantly improved the gas quality by increasing the H_2 content up to 30.27 vol.%, increasing the HHV up to 11,528 kJ/kg, and reducing tar concentration from about 18.15 g/m³ to 13.38 g/m³ under the optimum condition. However, this study is limited because it investigated only cigarette butt waste as feedstock, used a specific oxygen updraft gasifier–catalytic reformer configuration, and fixed most catalytic reforming parameters.

The paper [8] presents the result on the experimental assessment of pellets produced from beekeeping waste and slumgum–pine sawdust mixtures through updraft gasification. The results show that pure slumgum pellets exhibited very high mechanical durability (99.98%) and high HHV (27.66 MJ/kg), while during gasification the 50% slumgum–50% sawdust pellets produced the highest producer gas LHV of 7.62 MJ/Nm³,

indicating that the addition of sawdust improved gas quality and energy recovery potential. However, this study is limited because the equivalence ratio remained very low (0.0125–0.0204) compared with typical gasification conditions, the experiments were conducted only in a modified laboratory-scale updraft gasifier.

The paper [9] presents the result on a comparative investigation of catalyst applications in updraft and modifiable-downdraft fixed-bed biomass gasifiers, using a biomass mixture of green waste, sewage sludge, and olive pomace together with red mud (RM) and Al–Ni alloy catalysts to improve syngas quality and hydrogen production. The results show that catalyst type and reactor configuration strongly influenced gasification performance, with the Al–Ni catalyst giving the best hydrogen enrichment, reaching up to 65 vol.% H_2 in the updraft gasifier at 900 °C, while RM increased H_2 to about 50 vol.%, the updraft gasifier produced better hydrogen-rich syngas than the modifiable-downdraft reactor. However, this study is limited because it, used a specific mixed biomass composition and mainly focused on high temperature operation around 900 °C with limited gasifying-agent flow conditions.

The paper [10] presents the result on the experimental investigation of producer gas composition from sorted municipal solid wastes in an updraft fixed-bed gasifier. The results show that reducing the equivalence ratio from 0.21 to 0.15 increased the heating value of the combustible gases. The study indicated that the allothermal updraft fixed-bed gasifier is suitable for producing gas that can be utilized in gas engines. However, this study is limited because it used a laboratory-scale 10 kW allothermal updraft gasifier at a fixed temperature of 800 °C, and evaluated only two ER conditions.

The paper [11] presents the result on the effect of adding laying hens manure (LHM) to wheat straw on gasification efficiency in an air-blown updraft fixed-bed gasifier. The results show that increasing ER improved the gasification performance, with the producer gas LHV reaching 3.3–3.4 MJ/m^3, cold gas efficiency around 60%, and carbon conversion efficiency in the range of 82–94% . However, this study is limited because it was focused on one specific co-feed system and produced a relatively low-calorific gas.

The paper [12] presents the result on the gasification performance of olive pomace in updraft and downdraft fixed-bed reactors using dry air and pure oxygen. The results show that updraft reactor achieving up to 48 vol.% H_2 with dry air and 53 vol.% H_2 with pure oxygen, while the downdraft reactor reached up to 45 vol.% H_2 with dry air and 39 vol.% H_2 with pure oxygen. However, this study is limited because only a limited range of gasifying agents, temperatures, and flow rates.

The paper [13] presents the result on the gasification of MDF residue in an industrial-scale updraft fixed-bed gasifier. The results show that MDF residue can be effectively converted into useful energy, with a syngas production rate of about 2.5 Nm^3/kg, syngas LHV of around 6.0–7.0 MJ/Nm^3, about 88 wt.% of MDF residue converted into syngas, and a system capable of delivering 7 MWth of thermal energy and about 955 kW net electrical power through the ORC turbine. However, this study is limited because it focused on one specific industrial waste stream (MDF residue) in one

updraft gasifier configuration, mainly evaluated performance under a limited number of feed rates, and relied on direct combustion of raw hot syngas containing tar.

The paper presents the results of research on biomass gasification in updraft fixed-bed reactors aimed at improving syngas quality and thermal conversion efficiency. Shown that syngas composition and heating value are strongly influenced by feedstock properties, gasification conditions, and catalyst application. But there were unresolved issues related to the lack of effective and low-cost catalyst systems capable of simultaneously enhancing hydrogen formation and improving overall syngas quality during corncob gasification. The reason is the complexity of catalytic reactions in the gasification zone, including reforming, cracking, and CO_2 capture mechanisms, as well as the economic limitations of commercially available catalysts. A way to overcome these difficulties can be the development of composite catalysts based on CaO and activated carbon palm fiber, where CaO may promote CO_2 absorption and shift reactions, while activated carbon palm fiber may provide a porous surface and active sites for secondary cracking reactions. This approach was used in previous studies, however, the combined use of CaO and activated carbon palm fiber in corncob updraft gasification has not been sufficiently investigated. All this suggests that it is advisable to conduct a study on syngas quality improvement in corncob updraft gasification using CaO/activated carbon palm fiber catalyst.

3. The aim and objectives of the study

The purpose of the study is to enhance syngas quality from corncob updraft gasification by developing a dual-synergy catalytic system based on calcium oxide (CaO) and palm-fiber-derived activated carbon (AC–PF). This will allow the production of cleaner and more energy-dense producer gas, providing practical guidance for selecting operating conditions and catalyst configurations suitable for updraft gasifiers processing agricultural residues.

To achieve these aims, the following objectives are accomplished:

– to synthesize and characterize the CaO and palm-fiber activated carbon catalysts using Fourier Transform Infrared Spectroscopy (FTIR), scanning electron microscopy (SEM) and Brunauer–Emmett–Teller surface area analysis (BET);

– to investigate the effects of operating parameters, particularly equivalence ratio (ER), catalyst loading, and CaO/AC ratio, on syngas composition H_2, CO, CH_4, CO_2 and LHV.

4. Materials and methods

The object of the study is the updraft fixed-bed gasification process of corncob biomass using a dual catalyst system based on calcium oxide (CaO) and palm-fiber-derived activated carbon (AC-PF). The practical physical process under investigation is the catalytic upgrading of producer gas within the updraft reactor, where changes in operating parameters and catalyst configuration are expected to influence syngas

composition and heating value. The results of this study are intended to be applied to improve the quality of syngas, specifically by increasing the combustible gas fraction (H_2 and CH_4) and the lower heating value (LHV), while reducing CO_2 content.

The research hypothesis is that a dual-synergy CaO/AC-PF catalytic system can improve syngas quality more effectively than single-catalyst configurations in updraft corncob gasification. It is hypothesized that CaO functions as a CO_2 sorbent, shifting reaction equilibria toward enhanced hydrogen formation, while activated carbon derived from palm fiber provides high-surface-area catalytic sites that promote secondary reactions such as tar cracking and volatile reforming. The combined catalytic-sorption mechanism is expected to increase H_2 and CH_4 fractions and improve LHV under optimized equivalence ratio (ER), catalyst loading, and CaO/AC-PF ratio conditions.

It was assumed that the corncob feedstock has relatively homogeneous composition and stable proximate/ultimate characteristics during the experiments. The gasification process was assumed to operate under steady-state conditions after stabilization. It was also assumed that the CaO maintains sufficient CO_2 sorption capacity within the experimental time frame and that the activated carbon structure remains stable under the applied temperature range.

During the course of the research, several methodological simplifications were adopted in order to maintain experimental feasibility and focus on the main objective of syngas quality evaluation. Detailed kinetic modeling of individual gasification reactions was not performed; instead, the process performance was assessed based on experimentally measured syngas composition and syngas low heating value. Furthermore, although CaO carbonation-decarbonation reactions may occur during operation, microstructural evolution, sintering behavior, and long-term cyclic stability of the catalyst were not investigated in this study. The catalytic performance was evaluated within the experimental duration without conducting extended durability or regeneration-cycle analysis.

4. 1. Catalyst Preparation

Approximately 6 grams of ground palm fiber was mixed with 60 mL of distilled water and stirred for 10 minutes. The mixture was then placed in an autoclave and heated to 200°C at a rate of 5°C per minute for 6 hours in an electric oven. After that, the reactor is allowed to cool naturally to room temperature. The resulting solid hydrocarbon product (hydrochar) is then separated using Whatman No. 42 filter paper. The filtered product is then dried at 105°C for 24 hours and stored in a glass vial. The next stage is the activation process. The hydrochar is immersed in a 3 M KOH solution with a weight ratio of 1:3 (Hydrochar:KOH) for 16 hours, then dried at 85°C for 6 hours. Spectroscopic evidence indicates that KOH preferentially reacts with oxygenated sites and can increase the relative abundance of C–OH functionalities, while higher KOH ratio and activation temperature significantly enhance porosity and BET surface area [14, 15]. To obtain the CaO/AC mixture, CaO powder and activated carbon (AC) were mixed in specific proportions using a grinder until a homogeneous mixture was

obtained. Next, CaO, AC, and CaO/AC were activated using a tube furnace at a temperature of 700°C for 1 hour with a continuous flow of nitrogen during the activation process. The resulting product was then washed using distilled water until it reached a neutral pH. This stage produced activated carbon that was ready for use in research.

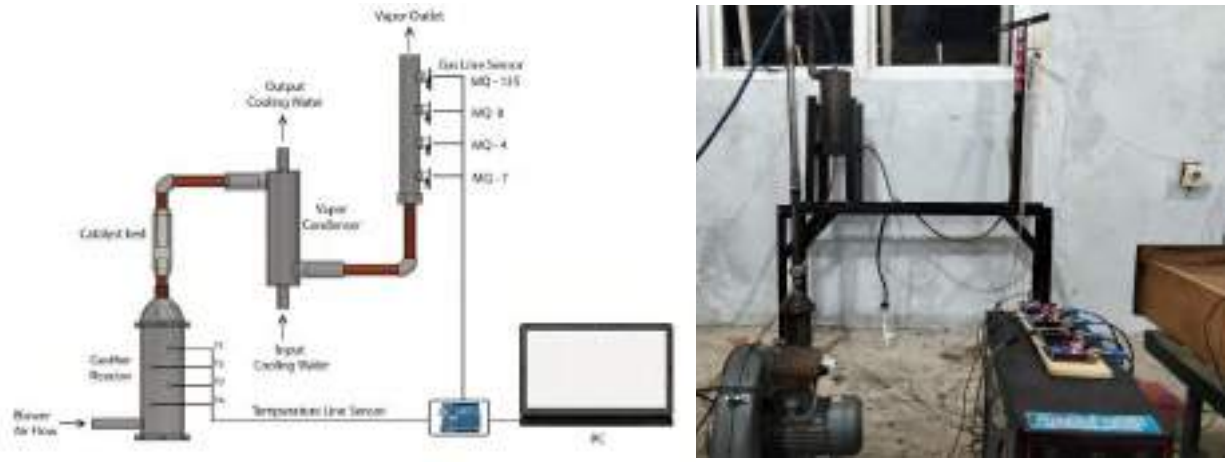
4. 2. Experimental Setup

Corncob biomass was obtained from farmers in the South Malang region of East Java. Before use, the biomass was cleaned of impurities and dried in an oven for 6 hours at 100°C to remove moisture (water vapor) content. The ultimate and proximate test results are as follows.

The proximate and ultimate analyses of the corncob feedstock were conducted to determine its physicochemical characteristics prior to gasification. The results are presented in Table 1. The data indicate that corncob has high volatile matter content and relatively low ash content, which are favorable characteristics for gasification processes.

Table 1
Ultimate and Proximate Test Corn Cob

Parameter	Units	Corn cobs
Moisture	%	10
Volatile matter	%	71.38
Fixed carbon	%	12.11
Ash	%	6.51
C	%	43.6
H	%	6.3
O	%	46.8
N	%	0.22
HHV	MJ/kg	17.61



a *b*

Fig. 1. Updraft gasifier: *a* – schematic experiment; *b* – experimental setup

This study used an updraft gasification reactor designed with a total height of 20 cm. The lower part of the reactor consisted of an ash container with a height of 5 cm, while the active reactor had a height of 15 cm and a diameter of 3 inches. The reactor was equipped with a 1-inch diameter air inlet pipe connected to a blower. The blower was modified with a potentiometer so that the air speed could be adjusted as needed. To monitor the thermal conditions inside the reactor, four 3 cm long type K thermocouples were installed at several different points so that the temperature profile in the gasification zone could be observed in more detail. Each test was conducted with a fixed biomass mass, a mixture of corn cobs weighing 80 grams. The reactor was made of iron and equipped with a gas seal to prevent leaks during the gasification process.

The gas produced by the reactor was fed into a condenser, which cooled the hot gas so that the water vapor components could be separated. The condenser was made of a copper spiral pipe with a diameter of ½ inch and a height of 30 cm. Cooling water was circulated from the bottom of the condenser and exited through the top to ensure efficient heat transfer. This cooling system was driven by a 60-watt water pump, ensuring stable water flow and optimal condensation. The catalyst was positioned downstream after the reactor, where it was supported on steel wool and wrapped with an 80-µm wire mesh to secure the catalyst and prevent particle carryover with the gas flow

To analyse the gas composition, four types of MQ gas sensors were used. The MQ-8 sensor was used to detect H_2, MQ-4 for CH_4, MQ-135 for CO_2 and MQ-7 for CO. Each gas sensor was calibrated according to the manufacturer's datasheet, specifically by determining the Ro value, which is the sensor resistance in clean air conditions. This Ro value is used as a reference in calculating the measured gas concentration during the process.

All data from the gas sensors and thermocouples were acquired using an Arduino Uno microcontroller. Each gas sensor is connected to a separate Arduino Uno to facilitate the calibration process and reduce the possibility of interference between sensors. Arduino is also used to record temperature data from four thermocouples installed in the reactor, so that gas composition and temperature distribution data can be obtained simultaneously.

The ER range of 0.2, 0.25, 0.3 and 0.35. The catalyst load was between 4%, 6%, 8% and 10% from the mass of input feedstock. The CaO/AC-PF ratio was varied between 0:1, 1:0, 1:1, and 2:1. Design of experiment can be seen in Table 2.

Table 2
Design of Experiment using

Run	Equivalence Ratio (E.R)	Catalyst Load %	CaO/AC
1	0.2	4	1:0
2	0.2	6	0:1
3	0.2	8	1:1

4	0.2	10	2:1
5	0.25	4	0:1
6	0.25	6	1:0
7	0.25	8	2:1
8	0.25	10	1:1
9	0.3	4	1:1
10	0.3	6	2:1
11	0.3	8	1:0
12	0.3	10	0:1
13	0.35	4	2:1
14	0.35	6	1:1
15	0.35	8	0:1
16	0.35	10	1:0

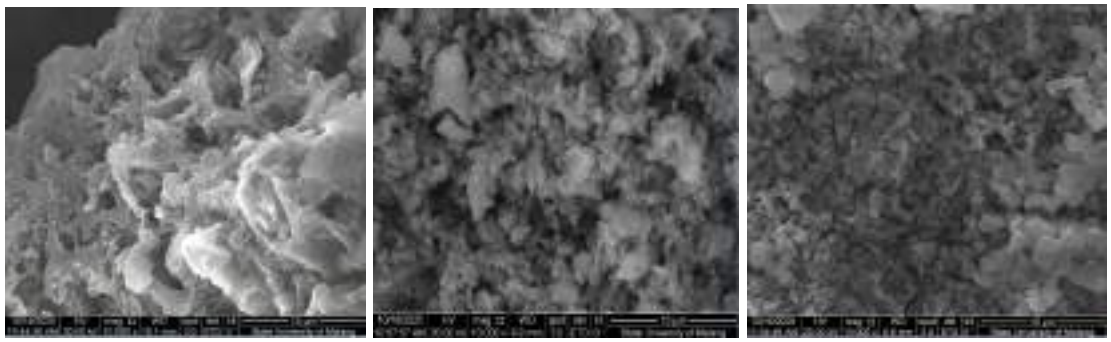
A total of 16 experimental runs were conducted systematically to enable evaluation of the main effects of each variable and the tendency of interactions between variables on the fractions of H_2, CO, CH_4, CO_2, and lower heating value (LHV). This approach enabled identification of the most effective combination of operating parameters in improving syngas quality quantitatively and measurably.

5. Results of syngas quality enhancement from corncob using calcium oxide (CaO) and palm-fiber-derived activated carbon (AC–PF).

5. 1. Characterization of Calcium Oxide (CaO) and Palm-Fiber-Derived Activated Carbon (AC–PF) Catalysts

5. 1. 1. Scanning Electron Microscopy Catalyst Result

Fig. 2, *a* shows the image obtained from a Scanning Electron Microscope (SEM) with a magnification of 10,000× shows the surface morphology of palm fiber-based activated carbon (AC-PF). The surface structure appears porous and irregular, with a combination of void areas and layered surfaces. This characteristic indicates that the activation process that using KOH has successfully formed micropores and mesopores, which play an important role in increasing the specific surface area of activated carbon.



a *b* *c*

Fig. 2. Scanning Electron Microscopy Catalyst Result: *a* – Scanning Electron Microscopy AC-PF; *b* – Scanning Electron Microscopy CaO:AC;1:1; *c* – Scanning Electron Microscopy CaO:AC-PF;2:1

The rough and textured surface indicates that most of the material has undergone lignocellulose cell wall exfoliation, resulting in numerous interparticle gaps. This porous structure greatly supports gas adsorption and diffusion capabilities when used as a catalyst in gasification or thermochemical reactions.

The presence of 1–5 μm voids indicates that most pores are in the mesopore category, supporting the adsorption of gas molecules such as H_2, CO, and tar during the gasification reaction.

The morphology of AC-PF shows the characteristics of porous activated carbon with a heterogeneous pore distribution, where the pores allow increased contact between gas reactants and active sites on the material surface, thereby increasing catalytic efficiency and the ability to absorb tar or CO_2 in biomass-based energy applications.

Fig. 2, *b* shows the surface morphology of the CaO:AC-PF catalyst with a ratio of 1:1. Visually, it can be seen that the surface of this material consists of fine particles ranging in size from microns to submicrons that stick together to form a layered and slightly agglomerated structure.

The presence of fine, light-colored grains indicates an even distribution of CaO particles impregnated on the surface of activated carbon (AC-PF). This CaO distribution fills some of the pores of the carbon, resulting in a denser surface compared to pure AC-PF. However, there are still small gaps and voids between the grains, indicating that the microporous and mesoporous structures are still formed and can support catalytic activity [16].

This morphology illustrates the success of the CaO impregnation process on activated carbon from palm fiber, where the interaction between CaO and the carbon pore walls produces a composite material that is more thermally and chemically stable. This structure is highly conducive to catalyst applications in biomass gasification processes, as CaO particles can function as CO_2 absorbers while accelerating the tar reforming reaction [17].

Fig. 2, *c* shows the surface morphology of the CaO:AC-PF (2:1) catalyst. The image shows that the surface of the material is dominated by agglomerations of fine, round, and irregular particles ranging in size from microns to submicrons. Compared to the CaO:AC-PF (1:1) sample, this structure appears denser and tighter, indicating that an increase in the CaO ratio causes partial closure of the activated carbon surface pores by CaO particles.

The distribution of CaO particles appears more uniform and covers the carbon surface, indicating the successful impregnation of a larger amount of CaO. The light color in some areas indicates the presence of a calcium oxide phase that is strongly

attached to the activated carbon matrix. This structure indicates a strong interaction between CaO and AC-PF, forming a thermally stable composite.

Although some pores are covered, there are still microscopic gaps between the CaO grains that allow gas diffusion to occur, so that the catalyst retains its good adsorption capacity. The combination of the active area of CaO and the porous carbon structure makes this material very promising for biomass gasification or tar reforming applications, as CaO can act as a CO_2 absorber and increase the conversion of carbon to hydrogen gas.

5. 1. 2. Fourier Transform Infrared Spectroscopy catalyst result

The FTIR analysis results shown in the Fig. 3 reveal clear spectral differences between the AC-PF, CaO, and their mixtures (CaO:AC-PF) with ratios of 2:1 and 1:1. In the AC-PF spectrum, the absorption band at 2926 cm^{-1} is associated with the stretching vibration of the C–H group from $–CH_2$ or $–CH_3$ (methylene/methyl stretching), which indicates the presence of hydrocarbon chain residues from the lignocellulose structure. The peak at 1577 cm^{-1} indicates the presence of aromatic C=C or C=O stretching, while the band at 1056 cm^{-1} represents C–O stretching from alcohol or ether groups. In addition, the –OH group that appears in the 3500–3600 cm^{-1} region is identified as the result of AC-PF activation using a KOH solution, which causes the formation of hydroxyl groups on the activated carbon surface. This –OH group plays an important role in increasing the surface activity and adsorption capacity of AC-PF as a catalyst support medium [18, 19].

In pure CaO, the intense band at 3639 cm^{-1} is associated with the stretching of the O–H group from $Ca(OH)_2$, which is formed due to the partial hydration of CaO when exposed to humid air. Meanwhile, the absorption bands at 1426 cm^{-1} and 876 cm^{-1} are associated with C–O stretching and CO_3^{2-} Please reduce the number of sources to 30 references. bending, respectively, indicating the formation of $CaCO_3$ due to CO_2 adsorption from the air. This shows that CaO is highly reactive to moisture and carbon dioxide in the environment.

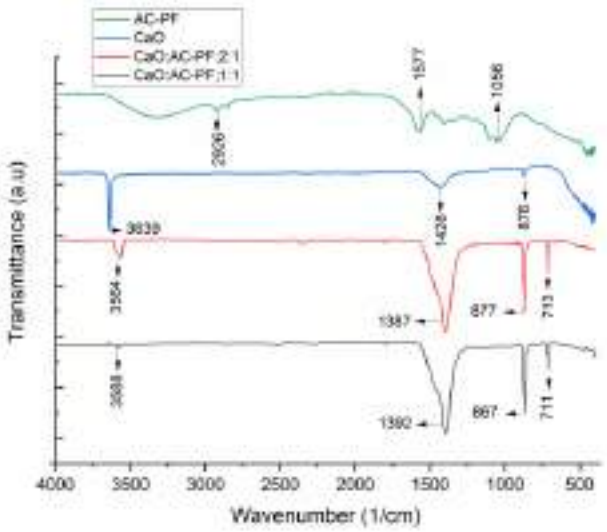


Fig. 3. Fourier Transform Infrared Spectroscopy Catalyst Result

For the CaO:AC-PF (2:1), the main absorption bands were detected at 3564 cm^{-1} (O–H stretching from $Ca(OH)_2$ and the –OH group in AC-PF), 1387 cm^{-1} (C–O stretching), and 877 cm^{-1} and 713 cm^{-1} (bending vibration of CO_3^{2-}). This combination of bands indicates the formation of carbonate compounds ($CaCO_3$) due to the interaction between CaO and the oxygen groups of activated carbon. The presence of –OH groups from KOH activation also strengthens the basic properties on the surface, which can increase the chemical interaction between CaO and AC-PF [20].

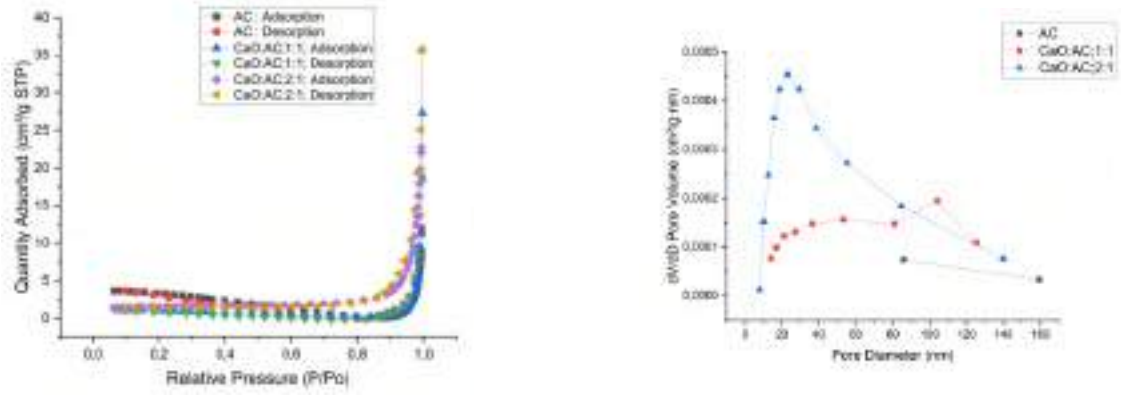
At a CaO:AC-PF ratio of 1:1, the absorption bands at 3588 cm^{-1}, 1392 cm^{-1}, 867 cm^{-1}, and 711 cm^{-1} show a similar pattern, indicating the presence of hydroxyl (O–H) and carbonate (CO_3^{2-}) groups. The difference in peak intensity compared to the 2:1 ratio indicates variations in the level of interaction between CaO and the –OH groups resulting from KOH activation on AC-PF, which affects the formation of carbonate-hydroxide complexes on the material surface [21].

5. 1. 3. Brunauer-Emmett-Teller Catalyst Result

Fig. 4 shows the adsorption-desorption isotherm curves for nitrogen for the AC, CaO:AC (1:1), and CaO:AC (2:1) samples are shown in Fig. 4. All three samples exhibit type IV isotherms with clear hysteresis loops at relatively high pressures (P/Po > 0.9). Based on the IUPAC classification, this characteristic indicates that the material has a mesoporous structure formed through capillary condensation within the pore channels. The difference between the adsorption and desorption pathways indicates that the pore shape is not perfectly cylindrical, but rather tends to be irregular or slit-like, which is commonly found in modified activated carbon materials [22].

The pure activated carbon (AC) sample showed a relatively low nitrogen adsorption volume with a specific surface area of 24.51 m^2/g and an average pore diameter of 0.74 nm, indicating a predominance of microporous structures. In the

CaO:AC (1:1) composite, the surface area did not change significantly compared to pure AC, indicating that the addition of a moderate amount of CaO did not cover the carbon pores much, but only adhered to the external surface of the carbon matrix [23].



a *b*

Fig. 4. Brunauer-Emmett-Teller Result: *a* – Surface Analysis Adsorption Desorption Isotherm; *b* – Barrett-Joyner-Halenda Adsorption Pore Size Distribution

Conversely, in the CaO:AC (2:1) mixture, there was a sharp increase in adsorption volume at relatively high pressure (P/Po > 0.9) to around 35 cm^3/g STP, while the BET surface area decreased dramatically to 5.06 m^2/g, and the pore diameter increased to 22.87 nm.

These changes in isotherm shape and pore size increase indicate that CaO impregnation not only modifies the surface chemistry but also significantly alters the pore structure of activated carbon. This transformation is positive in the context of catalytic applications in biomass gasification processes, as the mesoporous structure can enhance gas diffusion and accessibility to active sites during the tar reforming and water-gas shift reactions. Thus, even though the specific surface area decreases, the increase in mesoporousness and pore connectivity can actually improve catalyst performance in hydrogen gas production [24].

Fig. 4, *b* shows the BJH pore size distribution curves that provide further insight into the textural evolution of the palm-fiber-based activated carbon after CaO impregnation. The pristine AC exhibits a relatively low dV/dD value and a broad contribution only at large pore diameters (>60 nm), indicating that its pore system is dominated by macropores with a limited amount of mesopores. Such a texture is less favourable for gas-solid reactions because the accessible surface area in the mesopore range (2–50 nm) is relatively small.

After CaO loading, the shape and intensity of the BJH curves change markedly. For CaO:AC-PF = 1:1, the distribution shifts toward smaller pore diameters with a pronounced contribution in the mesopore region of approximately 15–60 nm. This behaviour shows that CaO impregnation partially reconstructs the carbon matrix,

enlarging existing micropores and opening blocked pores to generate additional mesoporosity. The effect becomes even more evident at CaO:AC-PF = 2:1, where the curve displays the highest dV/dD values and a distinct maximum centred at about 30–40 nm. The strong peak in this range confirms that a higher CaO loading promotes the development of well-defined mesopores while reducing the relative fraction of very large macropores.

Overall, the BJH analysis demonstrates that CaO acts not only as a reactive sorbent but also as a textural promoter for the palm-fiber AC. The increase in mesopore volume and the shift of the dominant pore size toward 20–40 nm are expected to facilitate the diffusion of gasifying agents and tar molecules, as well as to improve the accessibility of CaO active sites for CO_2 capture and reforming reactions. These features are therefore beneficial for enhancing the catalytic performance of the CaO/AC composite in biomass gasification toward H_2-rich syngas production.

5. 2. Effect of Operating Parameters on Syngas Composition and Low Heating Value

5. 2. 1. Effect of Equivalence Ratio on Syngas Product

The composition of syngas from updraft gasification is greatly influenced by the Equivalence Ratio (ER), which is the ratio of the mass flow rate of air compared to the mass flow rate of corncob in the experiment compared to the stoichiometry of air required for complete combustion of corncob. In this study, the ER used was 0.2–0.35 with the following formula

$$ER = \frac{(\dot{m}_a / \dot{m}_{cc})_{\exp}}{(\dot{m}_a / m_{cc})_{stc}},$$

where $\dot{m}_a$ is the air mass flow rate (kg/s), $\dot{m}_{cc}$ is the corncob mass flow rate (kg/s), exp denotes the experimental air-fuel ratio, and stc denotes the stoichiometric air-fuel ratio.

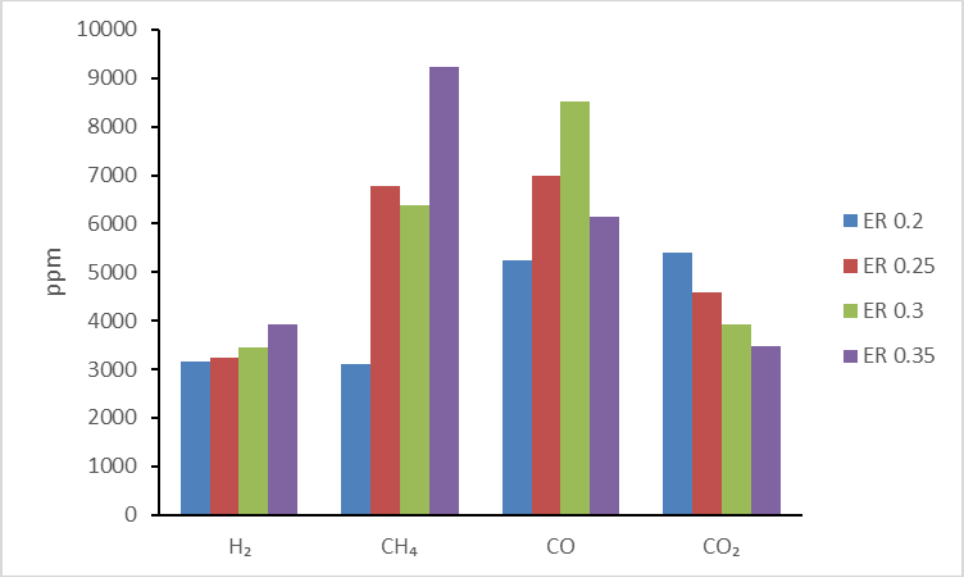


Fig. 5. Syngas composition with different equivalence ratio

The graph above shows that the higher the ER, the higher the hydrogen composition produced. At ER 0.2, the ppm is 3150 ppm, at ER 0.25 it is 3241 ppm, at ER 0.3 it is 3457 ppm, and at ER 0.35 it is 3914 ppm. A higher oxidant supply promotes the formation of more stable autothermal conditions and higher reaction temperatures due to partial oxidation. This increase in temperature accelerates hydrogen-forming reactions, particularly the gasification of active carbon catalyst interactions with steam ($C + H_2O \rightarrow CO + H_2$), the reforming of volatile compounds/light hydrocarbons ($CxHy + H_2O \rightarrow CO + H_2$), and the cracking of tar/volatile into lighter gas species. At low ER, some volatiles tend to be incompletely converted and still have the potential to escape as condensable components, while increasing ER increases heat availability, making the conversion of volatiles into gas fractions (including H_2) more effective.

The higher the ER, the higher the CH4 composition produced. At ER 0.2, 3093 ppm was obtained, at ER 0.25 6767 ppm, ER 0.3 6377 ppm, and ER 0.35 9221 ppm. This trend indicates that the supply of oxidants not only increases autothermal conditions and the rate of devolatilization, but also shifts the reaction pathway towards the formation of light hydrocarbons through hydrogenation and/or methanation reactions in the reactor zone where the temperature still supports CH_4 formation. In particular, increased H_2 at higher ERs can promote the methanation reaction of CO ($CO + 3H_2 \rightleftharpoons CH_4 + H_2O$), so that CH_4 increases along with a tendency for CO to decrease at the highest ER. In addition, more intensive fragmentation of volatiles and tar at high ERs has the potential to produce light gas precursors which are then hydrogenated to CH_4.

CO formation increased up to an ER of 0.3 and decreased at an ER of 0.35. At an ER of 0.2, 5238 ppm was obtained, at an ER of 0.25, 6999 ppm, at an ER of 0.3, 8532 ppm, and decreased at an ER of 0.35 to 6145 ppm. At low ER (0.20–0.25), limited oxygen supply resulted in relatively low heat release, so that the reaction zone

temperature and char reactivity were not sufficient to intensify CO formation reactions, especially the Boudouard reaction ($C + CO_2 \rightleftharpoons 2CO$) and char gasification with steam ($C + H_2O \rightleftharpoons CO + H_2$). When the ER is increased towards 0.30, the increase in autothermal heat strengthens these reduction reactions, causing CO formation to increase and reach its peak. However, at higher ERs (0.35), the CO fraction tends to decrease because some CO can be converted to CH_4.

CO_2 formation continues to decrease as ER increases. At ER 0.2, 5412 ppm is obtained; at ER 0.25, 4592 ppm; at ER 0.3, 3916 ppm; and at ER 0.35, 3479 ppm. The increase in oxidant supply at this ER does not promote complete combustion, but rather strengthens the CO_2 reduction mechanism. At higher ERs, the heat generated from partial oxidation increases the temperature of the reduction zone, thereby accelerating the Boudouard reaction ($C + CO_2 \rightleftharpoons 2CO$), in which CO_2 is reduced by char to CO. This mechanism is consistent with the increase in CO until it reaches a maximum at an ER of 0.30, while also explaining the decrease in CO_2 under the same conditions. Interestingly, at an ER of 0.35, CO_2 remains at its lowest level even though CO decreases, indicating that the CO formed is not completely accumulated at the outlet but has the potential to undergo further conversion along the gas flow path.

5. 2. 2. Effect of Catalyst Loading on Syngas Product

The catalyst load or amount of catalyst in this study was 4%, 6%, 8%, and 10% of the total biomass weight. The figure 6. shows that the composition of H_2 and CH_4 increases as the catalyst load decreases. The H_2 gas composition at catalyst loads of 4%, 6%, 8%, and 10% is 3742 ppm, 3471 ppm, 3372 ppm, and 3176 ppm, respectively. As the catalyst load increases, the reaction pathways that consume H_2 tend to strengthen, particularly the reverse water–gas shift ($CO_2 + H_2 \rightarrow CO + H_2O$) and H_2 interactions on the catalyst surface during the conversion of gasification compounds. As a result, even though reforming occurs, the measured net H_2 decreases because more H_2 is used for CO formation and surface reactions. The CH_4 gas composition at catalyst loads of 4%, 6%, 8%, and 10% was 7031 ppm, 6476 ppm, 6206 ppm, and 5746 ppm, respectively. An increase in catalyst load increases the number of active sites and gas-catalyst contact, so that methane/light hydrocarbon cracking and reforming occur more intensely. CH_4 then acts as a reactant that is converted into more reactive syngas components, causing the CH_4 concentration to decrease at higher catalyst loads.

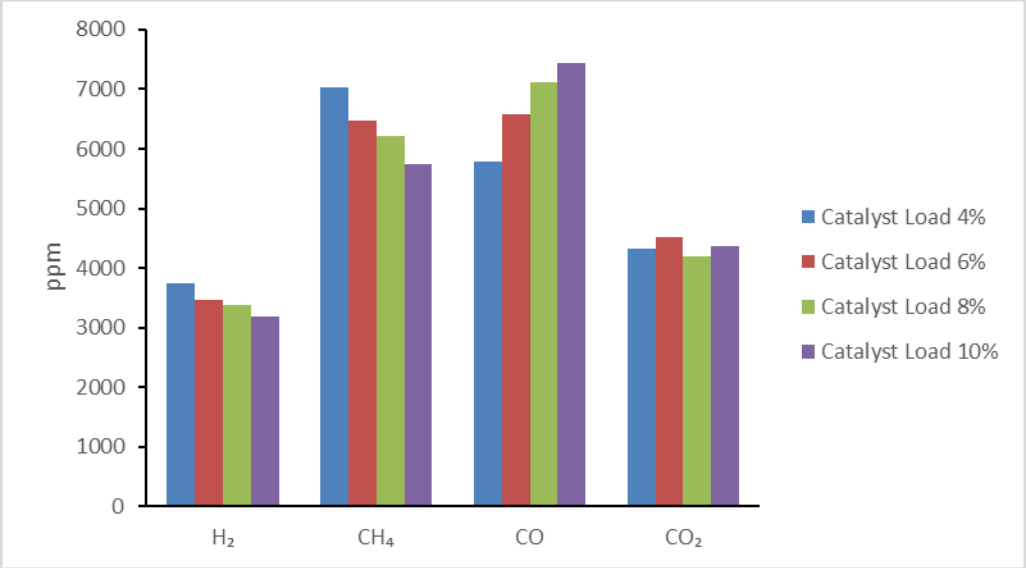


Fig. 6. Syngas Composition with Catalyst Load Variation

The CO gas composition increases with increasing catalyst load, namely for catalyst loads of 4%, 6%, 8% and 10% at 5782 ppm, 6576 ppm, 7111 ppm and 7445 ppm, respectively. The increase in catalyst loading strengthens the CO-forming reactions, particularly dry reforming ($CH_4 + CO_2 \rightarrow 2CO + 2H_2$), char–$CO_2$ reaction ($C + CO_2 \rightarrow 2CO$), and reverse water-gas shift. This combination shifts the product selectivity towards CO, so that the CO fraction increases consistently as the catalyst is increased. The CO_2 gas composition tends to stagnate with increasing catalyst loading, at catalyst loads of 4%, 6%, 8%, and 10% at 4322 ppm, 4510 ppm, 4198 ppm, and 4369 ppm, respectively. CO_2 shows minor changes because it is in a searching for a chemical equilibrium between the partial oxidation and the dry reforming. When the catalyst load increases, the rate of CO_2 consumption may rise, but this is often offset by CO_2 formation in the reaction zone, so that the CO_2 value appears stable or only fluctuates.

5. 2. 3. Effect of Catalyst Ratio on Syngas Product

At a catalyst load of 4%, the CaO/AC ratio changes the gasification reaction through differences in the dominance of tar cracking/reforming and CO_2 capture by CaO, so that the gas composition is highly dependent on the number of active sites and the effectiveness of gas-catalyst contact. At 0:1 (AC), CH_4 and CO are relatively high because AC promotes volatile/tar cracking, but CO_2 remains high because there is no absorption. At 1:0 (CaO), CH_4 decreases but CO_2 is highest, indicating that CO_2 capture is not yet effective due to limited surface area/carbonate layer formation. The 1:1 ratio produces the highest CO with moderate CO_2, indicating CaO–AC synergy that increases the conversion of volatiles into reactive gases. Meanwhile, the 2:1 (CaO-rich) ratio provides the highest H_2 and lowest CO_2 due to the sorption-enhanced effect of CaO, but

CH_4 remains high due to the smaller contribution of AC, so methane reforming/cracking is not yet optimal.

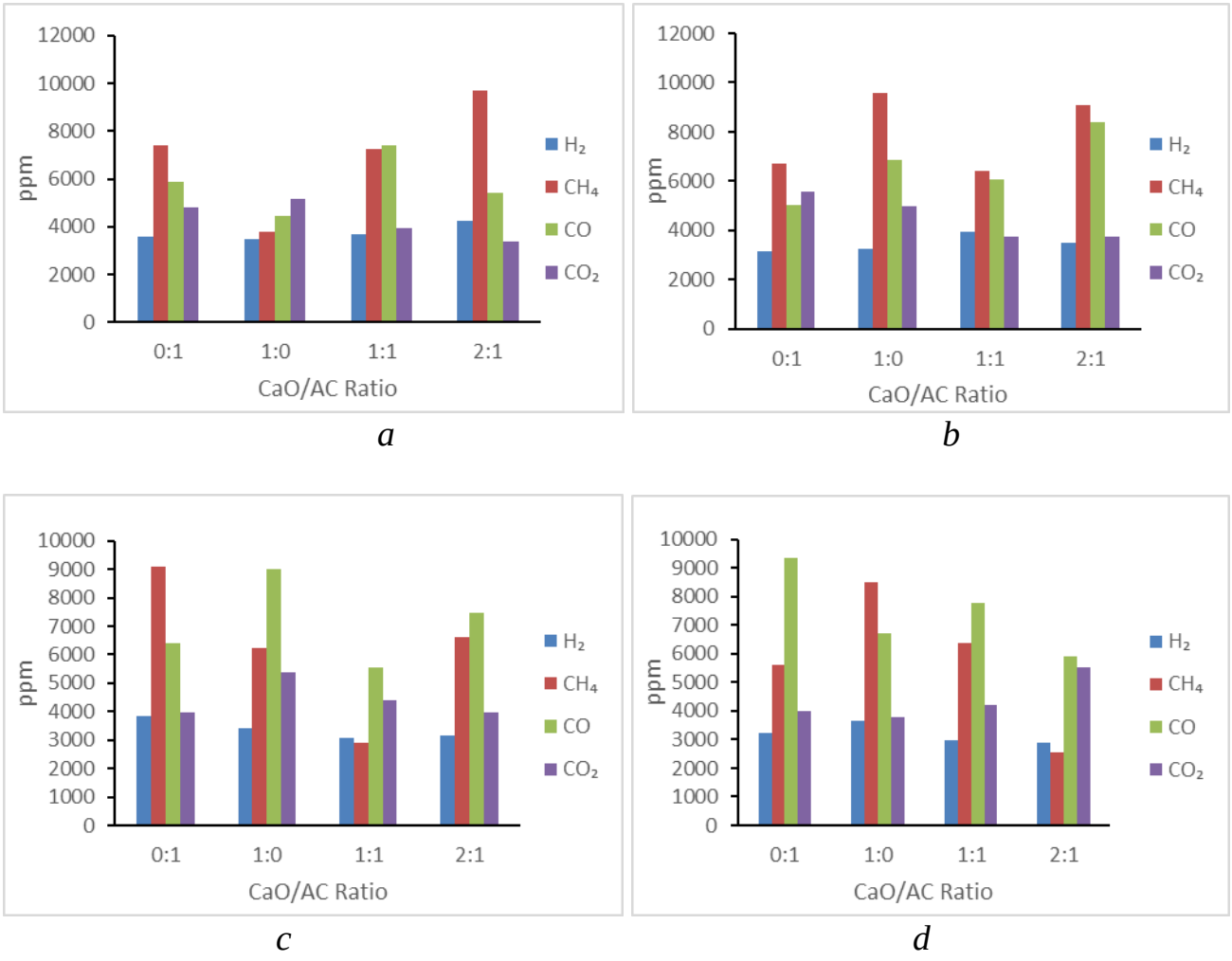


Fig. 7. Effect CaO/AC ratio with various catalyst load: *a* – 4%, *b* – 6%, *c* – 8%, *d* – 10%

At a catalyst load of 4%, the CaO/AC ratio changes the gasification reaction through differences in the dominance of tar cracking/reforming and CO_2 capture by CaO, so that the gas composition is highly dependent on the number of active sites and the effectiveness of gas-catalyst contact. At 0:1 (AC), CH_4 and CO are relatively high because AC promotes volatile/tar cracking, but CO_2 remains high because there is no absorption. At 1:0 (CaO), CH_4 decreases but CO_2 is highest, indicating that CO_2 capture is not yet effective due to limited surface area/carbonate layer formation. The 1:1 ratio produces the highest CO with moderate CO_2, indicating CaO–AC synergy that increases the conversion of volatiles into reactive gases. Meanwhile, the 2:1 (CaO-rich) ratio provides the highest H_2 and lowest CO_2 due to the sorption-enhanced effect of CaO, but

CH_4 remains high due to the smaller contribution of AC, so methane reforming/cracking is not yet optimal.

At a catalyst load of 6%, the CaO/AC ratio mainly shifts the selectivity of secondary reactions (tar cracking/reforming and CO_2 capture), where AC enhances the conversion of volatiles/light hydrocarbons, while CaO reduces CO_2 through carbonation ($CaO + CO_2 \rightarrow CaCO_3$) and changes the reaction equilibrium. At 0:1, CH_4 and CO_2 remain high because there is no CO_2 capture and methane reforming is not yet optimal, so volatiles still escape as CH_4. At 1:0, CO_2 tends to decrease, but CH_4 becomes the highest due to the absence of AC's role in cracking/reforming. The most favorable conditions occur at 1:1, with the highest H_2 and lowest CO_2, indicating CaO–AC synergy that promotes sorption-enhanced reforming and increases the conversion of hydrocarbons into syngas components. At 2:1, CO is highest and CO_2 remains low, but CH_4 rises again and H_2 is not maximized because excess CaO has the potential to rapidly carbonate/cause contact limitations, thereby reducing the contribution of AC in cracking/reforming.

At a catalyst load of 8%, the CaO/AC ratio significantly shifts the selectivity of the syngas reaction. At 0:1 (AC), CH_4 is still high because some light hydrocarbons have not been fully converted even though the tar cracking process is already active. At 1:0 (CaO), CO increases the most, but CO_2 also tends to be high, indicating that CaO in this condition is more dominant in promoting the CO formation pathway, while the CO_2 capture function is not yet optimal due to contact limitations or carbonation saturation. The 1:1 ratio produces the lowest CH_4, indicating the most effective CaO–AC synergy for cracking/reforming light hydrocarbons so that more methane is converted into reactive gas. At 2:1, CO increases again but CH_4 also rises, indicating that a smaller AC fraction reduces the intensity of methane reforming/cracking, while the decrease in CO_2 remains dependent on the effectiveness of CaO sorption.

At a catalyst load of 10%, the increase in total catalyst makes secondary reactions, reforming, solid-gas heterogeneous reactions, and equilibrium shifts very dominant, so that the CaO/AC ratio mainly determines the direction of product selectivity. At 0:1 (AC), CO formation tends to be strongest because the porous carbon surface accelerates the cracking/reforming of volatiles and the conversion of tar into reactive gases. At ratios involving CaO (1:0, 1:1, 2:1), CaO can retain CO_2 through carbonation, but at high loads the effect is often non-linear because CaO rapidly carbonates/diffusion limitations and pore blocking occur, so that under CaO-rich conditions (2:1) CH_4 can decrease, but CO_2 may increase and H_2 is not maximized due to reaction competition. Overall, at a 10% load, a trade-off is observed: AC-dominant increases CO, while CaO-dominant suppresses light hydrocarbons but has the potential to trigger non-ideal conditions (saturation/mass transport) that reduce the benefits of H_2 and CO_2.

5. 2. 4. Syngas Low Heating Value

To calculate the LHV of syngas, it must first be converted from ppm to % volume of gas. The formula is $\%vol_i = \frac{ppmv_i}{10^4}$ $\%vol_i = \frac{ppmv_i}{10^4}$. To calculate the LHV, use the formula

The values highlighted in turquoise need to be re-typed in the MathType formula editor so that the indices are one below the other

All formulas must be typed in the MathType formula editor version 7 or earlier. If you don't have this version of MathType, then type the formulas in the built-in formula editor

$$LHV_{mix}\left(\frac{MJ}{Nm^3}\right) = \frac{10{,}8(\%H_2) + 12.63(\%CO) + 35.8(\%CH_4)}{100}$$

$$LHV_{mix}\left(\frac{MJ}{Nm^3}\right) = \frac{10.8(\%H_2) + 12.63(\%CO) + 35.8(\%CH_4)}{100}$$

LHV H_2 = 10.8 MJ/Nm^3

LHV CO = 12.63 MJ/Nm^3

LHV CH_4 = 35.8 MJ/Nm^3

As shown in Fig. 8, the syngas low heating value (LHV) varies with the equivalence ratio (ER) and catalyst load.

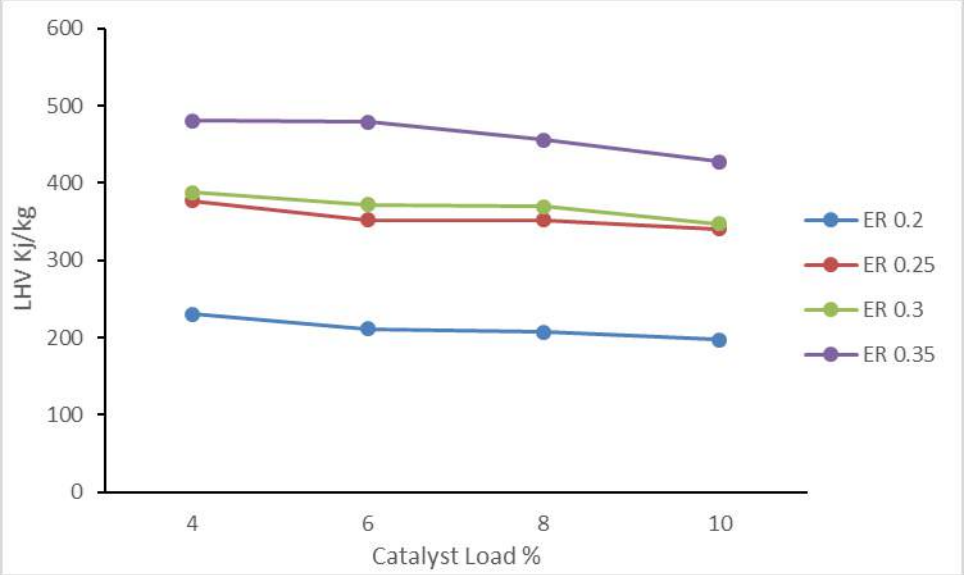


Fig. 8. Syngas Low Heating Value with various Equivalence Ratio

Fig. 8 shows that the LHV value increases with the ER. At the same catalyst load of 4%, the LHV will increase in line with the increase in ER. ER 0.2 has an LHV of 230 kJ/kg and ER 0.35 has an LHV of 481 kJ/kg. Higher ER produces more intense autothermal conditions, causing the reactor temperature to rise. This increase in temperature accelerates the decomposition of volatiles and tar cracking, and promotes more complete gasification and reforming reactions, thereby increasing the fraction of permanent gases that contribute to the calorific value, mainly CO and CH_4, as well as some H_2. In addition, the increase in temperature is also associated with more effective hydrogen formation, because H_2 formation reactions (e.g., through steam-water and reforming reactions) are generally more optimal at high temperatures, with the temperature range often reported to be most conducive to H_2 formation being 800–1000°C.

At ER 0.2, the highest LHV was obtained at a catalyst load of 4% at 230 kJ/kg and continued to decrease with increasing catalyst load to 197 kJ/kg at 10%. At ER 0.25, the highest LHV was also obtained at a catalyst load of 4% at 377 kJ/kg and also decreased to 341 kJ/kg at a catalyst load of 10%. At ER 0.3, the highest LHV was obtained at a catalyst load of 4% at 388 kJ/kg and also decreased at a catalyst load of 10% to 347 kJ/kg. At ER 0.35, the highest LHV was obtained at 481 kJ/kg and decreased at a catalyst load of 10% to 428 kJ/kg.

However, all ER values show that LHV tends to decrease when the catalyst load is increased from 4% to 10%. This decrease indicates that excessive catalyst addition under these operating conditions does not always improve gas energy quality, because the catalyst can shift the reaction selectivity towards the conversion of high calorific components especially CH_4 into CO and H_2 through reforming, while at the same time the fraction of diluent gases such as CO_2 (and steam) may increase due to reaction. Since CH_4 has a very large calorific value contribution in the syngas mixture, the decrease in its fraction is often more dominant than the increase in CO/H_2, so that the total LHV tends to decrease.

In energy system analysis, particularly in combustion, gasification, and fuel gas utilisation processes such as syngas, the LHV value is often used because it better represents the heat energy that can actually be utilised by the system. The LHV value of a fuel gas is usually influenced by the composition of combustible gases such as carbon monoxide (CO), hydrogen (H_2), and methane (CH_4). The higher the content of these gases, the greater the LHV value produced. The LHV of syngas from this study with variations in ER and CaO/AC-PF ratio can be seen in Fig. 9.

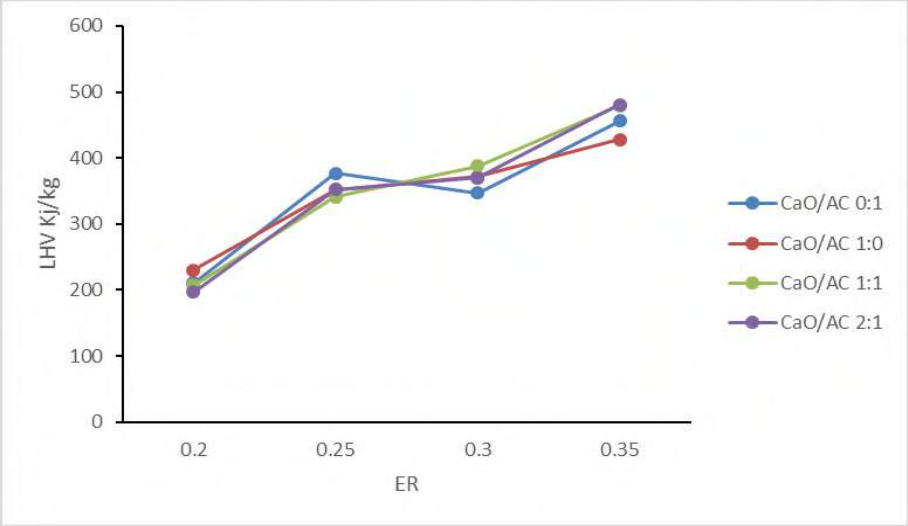


Fig. 9. Syngas Low Heating Value with Various CaO/AC Ratio

Fig. 9 shows that the LHV of syngas increases consistently with the increase in ER 0.2 to 0.35 for all CaO/AC ratios, indicating that a higher ER strengthens autothermal conditions so that the reaction temperature increases and the conversion of volatiles into syngas becomes more complete. At low ER (0.2), the difference in LHV between ratios is still small because secondary reactions such as cracking, reforming and heterogeneous reactions are not yet dominant; the system is still relatively influenced by incompletely converted volatiles. When the ER is increased to 0.25–0.30, the effect of the catalyst ratio becomes apparent: compositions involving AC tend to produce higher LHV because they accelerate tar cracking and increase the fraction of calorific gas, while the contribution of CaO can shift the reaction equilibrium through a decrease in CO_2. At the highest ER (0.35), the LHV reaches its maximum at all ratios, with CaO/AC 2:1 and 0:1 showing peak values, indicating that at high temperatures, the reactive gas formation pathway (via cracking/reforming on the carbon surface and/or CaO-rich-promoted heterogeneous reactions) becomes dominant. Overall, ER acts as the main controlling factor for LHV increase through the temperature effect, while the CaO/AC ratio modulates LHV through the balance between cracking/reforming (AC) and CO_2 control (CaO), especially at medium-high ER.

6. Discussion on the Catalytic Effect of AC-PF/CaO and Operating Conditions on Syngas Composition and LHV

The interaction of the CaO-AC-PF catalyst to improve syngas quality can be seen from the characterisation of the catalyst, the composition of the syngas and the LHV produced. From the Scanning Electron Microscopy results in Fig. 2, it can be seen that the CaO:AC-PF;2:1 catalyst (Fig. 2, *c*) appears denser than the other catalysts. With the addition of CaO, CaO particle dispersion can be seen on the white carbon surface, indicating that some micro pores are closed by CaO. With the addition of CaO, a lot of

CO_2 is absorbed and becomes $CaCO_3$. This porous structure is very important in top-flow gasification because pyrolysis gas and volatiles move through the layer, so the presence of a porous medium has the potential to strengthen secondary reactions and act as carbon capture before the gas exits to the condenser.

From a surface chemistry perspective, Fourier Transform Infrared Spectroscopy (FTIR) shows the presence of –OH and calcium carbonate groups, as shown in Fig. 3. This is due to the results of KOH impregnation carried out during the manufacture of AC-PF. The presence of -OH groups functions as polar active sites capable of adsorbing polar molecules such as H_2O, CO_2, and volatile compounds. Surfaces with -OH groups tend to be hydrophilic and reactive, thereby enhancing interactions with tar compounds or heavy hydrocarbons. These tar compounds can then undergo thermal cracking or catalytic reforming into light gases such as H_2, CO, and CH_4. In addition to -OH, there are also O-H and C-O groups. The O-H group has characteristics that are almost the same as the -OH group, while the C-O group plays a role in enhancing the redox properties and chemical interactions between the carbon surface and gas molecules. In the gasification process, the C-O group can be part of the partial oxidation mechanism and carbon gasification reaction, which produces CO [25].

The BET data in Fig. 4 shows that the surface area decreased to 5.06 m^2/g, but the pore diameter increased to a mesopore scale of 22.87 nm, which can improve the accessibility of volatiles to active sites and improve mass transport in the reforming reaction. In Fig. 4, *b*, the BJH curve at CaO:AC-PF = 2:1 shows the highest dV/dD values of 30–40 nm, indicating a catalyst in the mesopore size range. The presence of these mesopores will further increase the active sites for CO_2 adsorption.

From a process perspective, in Fig. 5, ER appears as the dominant variable that regulates autothermal conditions, primarily through an increase in effective temperature and secondary reaction intensity. An increase in ER from low to high levels consistently increases H_2, which can be explained by the acceleration of H_2 formation reactions such as charcoal gasification with steam ($C + H_2O \rightarrow CO + H_2$) [26], light hydrocarbon reforming, and more intense tar cracking at high temperatures. At the same time, CH_4 also increases sharply at high ER, indicating that in an autothermal upflow system, increased temperature and changes in gas composition can facilitate the formation of light gases. Meanwhile, CO tends to peak at moderate ER and then decreases at high ER, consistent with competition between CO formation and CO consumption through subsequent reactions such as methanation [27]. The decrease in CO_2 at high ER indicates the role of high temperatures in enhancing the reduction of CO_2 by charcoal (Boudouard reaction) and/or the role of CaO adsorption if available.

The effect of catalyst loading in Fig. 6 shows that adding catalyst does not always increase H_2. Increasing the catalyst loading from low to high tends to reduce H_2 and CH_4 but increase CO. Mechanistically, this condition can occur when the catalyst strengthens pathways that increase CO and/or promotes RWGS ($CO_2 + H_2 \rightarrow CO + H_2O$) [28], which consumes H_2 so that net H_2 is reduced. Furthermore, at high catalyst loadings, the possibility of diffusion/aggregation penalties increases, so that selectivity may shift and

some active sites become less effective. Therefore, the target of H_2-rich synthesis gas in this reactor is more dependent on ER adjustment and the selection of moderate/low catalyst loadings, rather than simply increasing the loading.

The CaO/AC-PF ratio in Fig. 7 shows synergistic but non-linear behaviour. AC-PF plays a major role as a porous medium that enhances the cracking/reforming process of volatile compounds, while CaO provides a basic site and CO_2 absorber to shift the equilibrium. At high CaO ratios, sorption and base effects may increase, but the risk of micro-pore closure and diffusion pathway changes also increases. This explains why certain compositions are optimal at certain catalyst loads: the best performance arises from a balance between pore accessibility (the role of AC-PF) and sorption/base strength (the role of CaO).

From an energy quality perspective, in Fig. 8, 9, the LHV value of synthetic gas is highly sensitive to changes in CH_4. Therefore, high ER conditions that increase CH_4 tend to increase LHV. H_2, CH_4 and CO are the main factors for obtaining high LHV. CO_2 has no calorific value so it must be captured. In this study, CaO was used so that CO_2 could be suppressed, meaning that the total LHV could be increased. The highest LHV in this study was 481 kJ/kg, while in another study, the highest was 550 kJ/kg using pinewood with dolomite, activated carbon, silica gel, and limestone catalysts [29]. The higher the ER, the more oxygen enters the system, thereby increasing the reforming reaction [30].

There are several limitations to this study. First, the gas composition was obtained from an MQ sensor based on ppm, so absolute accuracy may be affected by cross-sensitivity, humidity, sensor drift, and gas sampling temperature; this may affect the estimation of %vol and LHV, especially when changes in CO and CH_4 occur simultaneously. Second, catalyst characterisation (SEM-FTIR-BET) supports the role of surface texture and chemistry, but has not quantified changes in the active phase during operation, the degree of carbonation, and the decrease in activity due to pore closure accumulation.

The disadvantage of this research is that the CaO catalyst reacts very easily with CO_2. After the calcination process, CaO must be stored in an airtight container to prevent it from clumping into $CaCO_3$. The catalyst has a specific usage period because it is covered with tar or ash.

Based on these limitations, several future directions are recommended. Calibrate the gas composition using GC-TCD/GC-FID to convert the sensor readings into more accurate %vol and include LHV uncertainty analysis. Evaluate catalyst stability and regeneration, especially for CaO which is easily carbonated, through carbonation-calcination cycle tests and post-reaction characterisation (XRD/TGA/SEM-EDX) to assess phase changes and activity loss. Develop experimental designs towards ANOVA or RSM interactions so that interaction effects and predictive models can be obtained and verified through replication confirmation tests. Add process performance metrics such as gas yield (Nm^3/kg), cold gas efficiency, pressure drop, and air consumption so

that ‘syngas quality improvement’ can be demonstrated based on mass-energy balance and operability, not just composition.

7. Conclusion

1. AC-PF with rich -OH group acts as a porous catalytic medium that facilitates volatile cracking and supports the reduction of condensable by-products, while CaO contributes to absorb CO_2. The BJH analysis confirms that CaO plays a dual role as a reactive sorbent and a textural promoter in palm-fiber activated carbon by enlarging mesopores (20–40 nm), thereby enhancing gas diffusion and improving access to CaO active sites, which ultimately strengthens catalytic performance.

2. Increasing ER to 0.35 enhances the combustible gas fraction H_2 and CH_4 and suppresses CO_2, whereas CO typically peaks at intermediate ER due to competing CO formation and consumption reactions along the updraft reaction zones. Increasing catalyst loading shifts syngas composition: CO increases, while H_2 and CH_4 decrease, indicating changes in dominant secondary reactions and possible diffusion or agglomeration limitations at higher loadings. Increasing ER lead to increase LHV syngas, but it can decrease at high catalyst loading. An increase in the CaO/AC ratio to 2:1 resulted in a higher syngas LHV, with a maximum value of 481 kJ/kg.

Conflict of interest

The authors declare that they have no conflict of interest in relation to this research, whether financial, personal, authorship or otherwise, that could affect the research and its results presented in this paper.

Financing

The authors sincerely thank the Ministry of Education, Culture, Research and Technology, Republic of Indonesia for fully supporting this research through the DRTPM Research Grant under Fundamental Research, Universitas Widyagama Malang, Indonesia 2025 (Grant Number:128/C3/DT.05.00/PL/2025;023/LL7/DT.05.00/PL/2025;010/ Kontrak/PT/PTS.030.7/PN/V/2025).

Data availability

Manuscript has no associated data.

Use of artificial intelligence

The authors used the AI-based language model ChatGPT (GPT-5.3) only to assist in improving the clarity of English language and grammar in several sections of the manuscript, particularly in the Introduction and Literature Review sections.

The AI tool was used solely for language editing and paraphrasing purposes. All scientific content, experimental design, data analysis, and interpretation of the results were conducted entirely by the authors.

The authors carefully reviewed and verified all AI-assisted text to ensure accuracy and consistency with the experimental results. The use of AI tools did not influence the scientific conclusions of this study.

Acknowledgements

We as the Research Team would like to thank Ministry of Education, Culture, Research and Technology, Republic of Indonesia (Kemendiktisaintek Indonesia) for financing research activities.

Authors' contributions

Purbo Suwandono: Conceptualization, Writing-original draft, Investigation, Supervision, Formal analysis, Writing – review & editing; **Widya Wijayanti**: Validation, Investigation, Data Curation, Formal analysis, Writing – original draft; **Nova Risdiyanto Ismail**: Writing – review & editing, Formal analysis; **Dzulfikar Johan Akbar:** Visualization, Writing – original draft, Data curation; **Muhammad Reza**: Project administration, Resources, Data curation.

Please reduce the number of sources to 30 references.

References

If possible, please provide active hyperlinks to the entire list of literature.

1. V. K. Yadav *et al.*, "Emerging trends in the valorization of agricultural waste and their utilization in agricultural, pharmaceuticals, and environmental cleanup," *Waste and Biomass Valorization*, pp. 1–55, 2025. DOI:10.1007/s12649-025-03002-y
2. W. M. Lewandowski, M. Ryms, and W. Kosakowski, "Thermal biomass conversion: A review," *Processes*, vol. 8, no. 5, p. 516, 2020. https://doi.org/10.3390/pr8050516
3. D. Ariyanti *et al.*, "Valorization of corn cob waste for furfural production: A circular economy approach," *Biomass and Bioenergy*, vol. 194, p. 107665, 2025. DOI:10.1016/j.biombioe.2025.107665
4. J. Zhang, Z. Chu, R. Cao, X. Wu, and K. Han, "A review of resource recovery from waste plastics via pyrolysis and gasification," *Fuel*, vol. 404, p. 136319, 2026. https://doi.org/10.1016/j.fuel.2025.136319
5. Y. Tangke Tosuli, Cahyadi, H. Dafiqurrohman, R. Hermawan, and A. Surjosatyo, "Gasification of sago dreg waste in a top-lit updraft fixed bed gasifier: Syngas composition and its effect with additional Al2O3 as catalyst," *Energy Convers. Manag. X*, vol. 24, no. October, p. 100775, 2024, doi: 10.1016/j.ecmx.2024.100775. https://doi.org/10.1016/j.ecmx.2024.100775
6. P. Dinh *et al.*, "Enrichment of hydrogen in product gas from a pilot-scale rice husk updraft gasification system," *Carbon Resour. Convers.*, vol. 5, no. 3, pp. 231–239, 2025, doi: 10.1016/j.crcon.2022.07.003.

7. S. Yousef and J. Eimontas, “International Journal of Hydrogen Energy Oxygen updraft gasification-catalytic reforming of cigarettes butts for hydrogen-rich syngas production,” vol. 171, no. May, 2025, https://doi.org/10.1016/j.ijhydene.2025.150650

8. D. Contreras, E. Blanco, and D. Travieso, “Experimental assessment of the energy potential of pellets produced from beekeeping wastes by updraft gasification,” vol. 343, no. January, 2025, https://doi.org/10.1016/j.enconman.2025.120206

9. N. Yesilova, O. Tezer, A. Ongen, and A. Ayol, “International Journal of Hydrogen Energy Enhancing biomass gasification : A comparative study of catalyst applications in updraft and modifiable-downdraft fixed bed reactors,” *Int. J. Hydrogen Energy*, vol. 76, no. April, pp. 290–303, 2024, https://doi.org/10.1016/j.ijhydene.2024.05.075

10. R. Skvor and A. Jan, “Experimental investigation of sorted municipal solid wastes producer gas composition in an updraft fixed bed gasifier,” vol. 289, no. August 2022, 2024, https://doi.org/10.1016/j.energy.2023.130063

11. R. Junga, M. Tańczuk, S. Sobek, M. Chabiński, and Ł. Ziółkowski, “Effect of the addition of laying hens manure to the straw on gasification efficiency in updraft gasifier under air atmosphere,” *Appl. Therm. Eng.*, vol. 226, no. February, p. 120269, 2023, https://doi.org/10.1016/j.applthermaleng.2023.120269.

12. A. Ongen and A. Ayol, “ScienceDirect Gasification performance of olive pomace in updraft and downdraft fixed bed reactors,” vol. I, 2023, https://doi.org/10.1016/j.ijhydene.2023.02.088

13. K. Ertas, “Gasification of MDF residue in an updraft fixed bed gasifier to produce heat and power via an ORC turbine,” vol. 169, no. February, pp. 43–51, 2023, https://doi.org/10.1016/j.wasman.2023.06.025

14. S. Gorthy, S. Verma, N. Sinha, S. Shetty, H. Nguyen, and M. Neurock, “Theoretical Insights into the Effects of KOH Concentration and the Role of OH–in the Electrocatalytic Reduction of CO2 on Au,” *ACS Catal.*, vol. 13, no. 19, pp. 12924–12940, 2023. DOI:10.1021/acscatal.2c06115

15. X. Wang, W. Zeng, C. Xin, X. Kong, X. Hu, and Q. Guo, “The development of activated carbon from corncob for CO2 capture,” *RSC Adv.*, vol. 12, no. 51, pp. 33069–33078, 2022, https://doi.org/10.1039/D2RA05979G

16. B. Zhou *et al.*, “Insights into effects of grain boundary engineering in composite metal oxide catalysts for improving catalytic performance,” *J. Colloid Interface Sci.*, vol. 653, pp. 1177–1187, 2024. https://doi.org/10.1016/j.jcis.2023.09.148

17. Y. Zhu *et al.*, “Preparation of hierarchically porous carbon ash composite material from fine slag of coal gasification and ash slag of biomass combustion for CO2 capture,” *Sep. Purif. Technol.*, vol. 330, p. 125452, 2024. https://doi.org/10.1016/j.seppur.2023.125452

18. M. Ilić *et al.*, “Surface functional groups and degree of carbonization of *selected* chars from different processes and feedstock,” *PLoS One*, vol. 17, no. 11, p. e0277365, 2022. https://doi.org/10.1371/journal.pone.0277365

19. R. Ali, Z. Aslam, R. A. Shawabkeh, A. Asghar, and I. A. Hussein, “BET, FTIR, and RAMAN characterizations of activated carbon from waste oil fly ash,” *Turkish J. Chem.*, vol. 44, no. 2, pp. 279–295, 2020. doi: 10.3906/kim-1909-20

20. K. J. Stanienda-Pilecki, “The importance of Fourier-Transform Infrared Spectroscopy in the identification of carbonate phases differentiated in magnesium content,” 2019.

21. F. Dai, Q. Zhuang, G. Huang, H. Deng, and X. Zhang, “Infrared spectrum characteristics and quantification of OH groups in coal,” *ACS omega*, vol. 8, no. 19, pp. 17064–17076, 2023. https://doi.org/10.1021/acsomega.3c01336

22. E. M. de Salazar Martínez, M. F. Alexandre-Franco, A. J. Nieto-Sanchez, and E. M. Cuerda-Correa, “Exploring the role of surface and porosity in CO2 capture by CaO-based adsorbents through response surface methodology (RSM) and artificial neural networks (ANN),” *J. CO2 Util.*, vol. 83, p. 102773, 2024. https://doi.org/10.1016/j.jcou.2024.102773

23. J. A. Tavizón-Pozos, H. Cervantes-Cuevas, G. G. Garcia-Camacho, G. Chavez-Esquivel, and D. R. Acosta-Najarro, “Biodiesel Production Using K–Sr/CaO and CaO Catalysts Derived from Eggshells by Canola Oil Transesterification,” *ACS omega*, vol. 10, no. 7, pp. 6827–6838, 2025. https://doi.org/10.1021/acsomega.4c09118

24. W. Koo-Amornpattana, P. Phadungbut, N. Kunthakudee, W. Jonglertjunya, S. Ratchahat, and M. Hunsom, “Innovative metal oxides (CaO, SrO, MgO) impregnated waste-derived activated carbon for biohydrogen purification,” *Sci. Rep.*, vol. 13, no. 1, p. 4705, 2023. DOI:10.1038/s41598-023-31723-4

25. C. Quan, M. Wang, N. Gao, T. Yang, and R. Li, “In situ adsorption of CO2 to enhance biomass gasification for hydrogen production using Ca/Ni based composites,” *J. Energy Inst.*, vol. 108, p. 101229, 2023, doi: https://doi.org/10.1016/j.joei.2023.101229. https://doi.org/10.1016/j.joei.2023.101229

26. F. Micheli, E. Mattucci, C. Courson, and K. Gallucci, “Bi-Functional Catalyst/Sorbent for a H2-Rich Gas from Biomass Gasification,” 2021. doi: 10.3390/pr9071249. DOI:10.3390/PR9071249

27. M. Zhu, Q. Wang, and S. Wang, “Recent Advances and Future Perspectives in Catalyst Development for Efficient and Sustainable Biomass Gasification: A Comprehensive Review,” 2025, https://doi.org/10.3390/su17167370

28. N. Cerone, F. Zimbardi, L. Contuzzi, J. Baleta, and D. Cerinski, “Experimental investigation of syngas composition variation along updraft fixed bed gasifier,” *Energy Convers. Manag.*, vol. 221, no. July, p. 113116, 2020, https://doi.org/10.1016/j.enconman.2020.113116

29. R. Mohanty, P. Mahanta, A. Mahapatro, and R. Prakash, “Catalytic gasification of pinewood biomass in a fluidized bed reactor with dolomite , limestone , and activated carbon : An experimental study,” *Energy*, vol. 325, no. April, p. 136131, 2025, doi: 10.1016/j.energy.2025.136131. https://doi.org/10.1016/j.energy.2025.136131

30. C. Liu, Y. Huang, M. Niu, and H. Pei, “ScienceDirect Influences of

equivalence ratio , oxygen concentration and fluidization velocity on the characteristics of oxygen-enriched gasification products from biomass in a pilot-scale fluidized bed," *Int. J. Hydrogen Energy*, vol. 43, no. 31, pp. 14214–14225, 2018, https://doi.org/10.1016/j.ijhydene.2018.05.154

Author's order	First Name	Middle name	Second Name
1	*Purbo*		*Suwandono*
2	*Widya*		*Wijayanti*
3	*Nova*	*Risdiyanto*	*Ismail*
4	*Dzulfikar*	*Johan*	*Akbar*
5	*Muhammad*		*Reza*

We ask the authors indicate the Corresponding author in the information about the authors, after the full name (Corresponding author is the author who is in correspondence with the editors and whose email address will be indicated as feedback for readers if they want to contact the author/group of authors)

English

Purbo Suwandono (Corresponding author)
Master
Department of Mechanical Engineering
Widya Gama University
Borobudur str., 35, Malang, Indonesia, 65142
E-mail: purbo@widyagama.ac.id
ORCID: https://orcid.org/0000-0003-4085-1291
Contact phone: +6282132697144
Number of publications in national journals indexed (approximate; for Ukraine citizens only): -
Number of publications in international journals indexed (approximate): 14
H-index by Scopus (if available): 4
ResearchGate: https://www.researchgate.net/profile/Purbo-Suwandono
Scopus ID: 57204187970
Researcher ID: https://researchid.co/rid80879

Widya Wijayanti
PhD
Department of Mechanical Engineering
Brawijaya University
Veteran str., 10–11, Malang, Indonesia, 65145
E-mail: widya_dinata@ub.ac.id

ORCID: https://orcid.org/0000-0003-4215-5943
Contact phone: +6285334992164
Number of publications in national journals indexed (approximate; for Ukraine citizens only): -
Number of publications in international journals indexed (approximate): 78
H-index by Scopus (if available): 12
ResearchGate: https://www.researchgate.net/profile/Widya-Wijayanti
Scopus ID: 36006672800
Researcher ID: -

Nova Risdiyanto Ismail
Doctor Which sciences? PhD
Department of Mechanical Engineering
Widya Gama University
Borobudur str., 35, Malang, Indonesia, 65142
E-mail: nova@widyagama.ac.id
ORCID: https://orcid.org/0000-0001-8439-6919
Contact phone:
Number of publications in national journals indexed (approximate; for Ukraine citizens only): -
Number of publications in international journals indexed (approximate): 7
H-index by Scopus (if available): 3
ResearchGate: https://www.researchgate.net/profile/Nova-Ismail-2
Scopus ID: 57204527065
Researcher ID: https://researchid.co/rid80876

Dzulfikar Johan Akbar
Master Student
Department of Mechanical Engineering
Brawijaya University
Veteran str., 10–11, Malang, Indonesia, 65145
E-mail: johanakbar@student.ub.ac.id
ORCID: https://orcid.org/0009-0002-4652-8516
Contact phone: +6282241116998
Number of publications in national journals indexed (approximate; for Ukraine citizens only): -
Number of publications in international journals indexed (approximate): -
H-index by Scopus (if available): -
ResearchGate: https://www.researchgate.net/profile/Dzulfikar-Johan-Akbar
Scopus ID: -
Researcher ID: -

Muhammad Reza
Bachelor Student
Department of Mechanical Engineering
Widya Gama University
Borobudur str., 35, Malang, Indonesia, 65142
E-mail: muhapanjangreza@gmail.com
ORCID: https://orcid.org/0009-0009-9258-0586
Contact phone: +6282139682566
Number of publications in national journals indexed (approximate; for Ukraine citizens only): -
Number of publications in international journals indexed (approximate): -
H-index by Scopus (if available): -
ResearchGate: -
Scopus ID: -
Researcher ID: -

Name of reviewer: Prof. Dr. Muji Setiyo, ST., MT.
Professor: Mechanical Engineering
Tel: +6281211020288
E-mail: muji@unimma.ac.id.
Work address: Universitas Muhammadiyah Magelang

Name of reviewer: Prof. Dr. Eng. Nurkholis Hamidi, ST., MT.
Professor: Mechanical Engineering
Tel: +62 81259293165
E-mail: hamidy@ub.ac.id
Work address: Brawijaya University

TAHAP 4

REVIEW EDITOR TAHAP 4

27 Maret 2026

Purbo Suwandono <purbo@widyagama.ac.id>

from "Eastern-European Journal of Enterprise Technologies"_4th stage_No.2(140).2026

4 messages

Oksana Nikitina <0661966nauka@gmail.com> Mon, Mar 23, 2026 at 4:56 PM
To: purbo@widyagama.ac.id, "Widya Wijayanti, ST.,MT" <widya_dinata@ub.ac.id>, nova@widyagama.ac.id, johanakbar@student.ub.ac.id, muhapanjangreza@gmail.com

Good afternoon, dear authors.

The article was accepted for consideration of the possibility of publication in (No. 2(140).2026).

At the 4th stage of editing, please consider the comments of the reviews (article in the application, color notes are highlighted).

We ask you to right strictly in the option which is in the attachment (see attachment).

We ask you not to delete the comments so that we can see all your edits. Please highlight all the author's corrections in green.

Please provide an edited version of the article **by 26.03.2026.**

If you have any questions, please call or write; we will be happy to answer them.

With best regards, Manager Yu. Prylutska
TECHNOLOGY CENTER GROUP LTD
Viber/ WhatsApp/ Telegram: +380 (50) 3033801
Editorial staff of the "Eastern-European Journal of Enterprise Technologies"
Website: https://jet.com.ua/en/, http://journals.uran.ua/eejet/

Відвідати сайт



Відвідати сайт

Attention! The author (team of authors) submitting the manuscript to the editorial office of the journal **«Eastern-European Journal of Enterprise Technologies»** agrees with all requirements for registration, submission of the manuscript of the article and payment and be responsible in case of violation of these requirements.

Our company may rely on your freely given consent at the time you provided your personal data to us replying on this email then the lawfulness of such processing is based on that consent under EU GDPR 2016/679. You have the right to withdraw consent at any time.

Subscribe

Suwandono 27-+p.doc
1148K

Purbo Suwandono <purbo@widyagama.ac.id> Fri, Mar 27, 2026 at 12:23 AM
To: Oksana Nikitina <0661966nauka@gmail.com>

Good afternoon,

Thank you for your email.

We have completed the revision of the manuscript according to the reviewers' comments and the editorial instructions. All author corrections have been highlighted in green, and the comments were not deleted.

Please find the revised manuscript attached. If there are any remaining mistakes or further corrections needed, we will be ready to revise it accordingly.

Best regards,
Purbo Suwandono

[Quoted text hidden]

Suwandono 22-ап-(3) - Revision.doc
1153K

Oksana Nikitina <0661966nauka@gmail.com> Fri, Mar 27, 2026 at 4:42 AM
To: Purbo Suwandono <purbo@widyagama.ac.id>

Dear authors,
Thank you for your message.
Please note that the file you have sent is not the correct version required by the editorial office.
Kindly ask you to carefully check the attachment we previously provided and submit the corrected manuscript based strictly on that version.
We look forward to receiving the correct file.
Best regards, Oksana

чт, 26 мар. 2026 г. в 19:23, Purbo Suwandono <purbo@widyagama.ac.id>:
[Quoted text hidden]

--
[Quoted text hidden]

Suwandono 27-+p.doc
1148K

Purbo Suwandono <purbo@widyagama.ac.id> Fri, Mar 27, 2026 at 9:33 AM
To: Oksana Nikitina <0661966nauka@gmail.com>

Dear Editor,

Thank you for your message.

I sincerely apologize, as I mistakenly sent the wrong file.

Thank you for your patience and understanding.

Best regards,
Purbo Suwandono

Suwandono 27-+p - Revision.doc
1172K

Received date: 20.02.2026
Accepted date:

UDC

ПОКРАЩЕННЯ ЯКОСТІ СИНТЕЗ-ГАЗУ ПРИ ВИСХІДНІЙ ГАЗИФІКАЦІЇ КУКУРУДЗЯНИХ КАЧАНІВ З ВИКОРИСТАННЯМ КАТАЛІЗАТОРА НА ОСНОВІ CAO/АКТИВОВАНОГО ВУГІЛЛЯ НА ПАЛЬМОВОМУ ВОЛОКН

Purbo Suwandono, Widya Wijayanti, Nova Risdiyanto Ismail, Dzulfikar Johan Akbar, Muhammad Reza

SYNGAS QUALITY IMPROVEMENT IN CORNCOB UPDRAFT GASIFICATION USING CAO/ACTIVATED CARBON PALM FIBER CATALYST

Purbo Suwandono, Widya Wijayanti, Nova Risdiyanto Ismail, Dzulfikar Johan Akbar, Muhammad Reza

Об’єктом даного дослідження є поліпшення якості синтез-газу, отриманого в результаті газифікації кукурудзяних качанів за допомогою системи з подвійним каталізатором, що складається з CaO та активованого вугілля, отриманого з пальмового волокна (AC–PF). Проблема, вирішена в даному дослідженні, полягає у відносно низькій теплотворній здатності синтез-газу з кукурудзяних качанів та високій вартості традиційних каталізаторів, що використовуються для його поліпшення. Дослідження проводилося з використанням різних значень еквівалентного співвідношення (0,2; 0,25; 0,3; 0,35), навантаження каталізатора (4%; 6%; 8%; 10%) та масового співвідношення CaO/AC–PF (0:1; 1:0; 1:1; 2:1) у поєднанні з характеристикою подвійної каталітичної системи. Отримані результати показують, що збільшення ER збільшує частки H_2 і CH_4 та нижчу теплоту згоряння синтез-газу, одночасно зменшуючи CO_2, причому CO досягає оптимального значення при ER = 0,3. У той час як більш високе навантаження каталізатора має тенденцію до зменшення H_2 і CH_4, але збільшує CO, потенційно знижуючи теплоту згоряння при високих навантаженнях Характеристика каталізатора показує, що AC-PF має пористу структуру, яка збільшує контакт газу з твердим тілом і сприяє вторинним реакціям, тоді як додавання CaO утворює композит із модифікованою структурою пор і поверхневими видами, пов'язаними з сорбцією CO_2. З енергетичної точки зору, нижня теплота згоряння синтез-газу збільшується із зростанням ER, але зменшується при більш високих навантаженнях каталізатора через зменшення внеску CH_4. Ключовою особливістю отриманих результатів є продемонстрована функціональна синергія між пористим AC–PF і сорбцією CO_2 на основі CaO, що дозволяє одночасно

здійснювати каталітичне поліпшення якості та уловлювання CO_2 в єдиній, недорогій системі з подвійним каталізатором. Ці висновки можуть стати практичною основою для проектування та експлуатації невеликих установок газифікації біомаси, зокрема реакторів з висхідним потоком для відходів кукурудзяних качанів, в межах досліджених діапазонів ER та навантаження каталізатора.

Ключові слова: газифікація, висхідний потік, кукурудзяні качани, синтез-газ, CaO, активоване вугілля.

The object of this study is the improvement of syngas quality from updraft corn cob gasification using a dual catalyst system consisting of CaO and activated carbon derived from palm fiber (AC–PF). The problem solved in this study is the relatively low heating value of corn cob syngas and the high cost of conventional catalysts used for its upgrading. The study was conducted using variations of equivalence ratio (0.2, 0.25, 0.3, 0.35), catalyst loading (4%, 6%, 8%, 10%), and CaO/AC–PF mass ratio (0:1, 1:0, 1:1, 2:1), combined with characterization of the dual catalyst system. The results obtained show that increasing ER increases the H_2 and CH_4 fractions and the syngas lower heating value while decreasing CO_2, with CO reaching an optimum at ER = 0.3. Whereas higher catalyst loading tends to decrease H_2 and CH_4 but increase CO, potentially reducing the heating value at high loadings Characterization of the catalyst shows that AC-PF has a porous structure that increases gas-solid contact and promotes secondary reactions, while the addition of CaO forms a composite with a modified pore texture and surface species associated with CO_2 sorption. From an energy perspective, the Lower Heating Value of syngas increases with increasing ER, but decrease at higher catalyst loadings due to the reduced contribution of CH_4. A key feature of obtained results is the demonstrated functional synergy between porous AC–PF and CaO-based CO_2 sorption, which enables simultaneous catalytic upgrading and CO_2 capture in a single, low-cost dual catalyst system. These findings could be a practical basis for designing and operating small-scale biomass gasification units, particularly updraft reactors for corn cob waste, within the studied ER and catalyst loading ranges

Keywords: gasification, updraft, corncob, syngas, CaO, activated carbon

1. Introduction

Indonesia is one of the largest corn producers in Southeast Asia, with national production reaching more than 18 million tons of dry kernels per year. Of this amount, about 15–20% is cobs after the kernel removal process, resulting in a very large amount of corn cob waste, estimated at 2.5–3.5 million tons annually. Until now, most corn cobs have only been used to a limited extent, for example as traditional fuel, small amounts of animal feed, or even burned directly on post-harvest land, which has the potential to cause air pollution. Most of the rest are simply piled up or left to rot on the land, posing a risk of becoming a source of plant disease [1].

Corn cobs have quite promising chemical and energy characteristics. Their composition is dominated by cellulose, hemicellulose, and lignin, with a calorific value of around 15–17 MJ/kg, making them very suitable as raw materials in various biomass-based energy conversion technologies [2]. Their hard and fibrous nature also makes them suitable for processing into biochar, activated charcoal, or direct use in pyrolysis and gasification processes. This significant potential indicates that corn cobs are not merely waste but a renewable resource that can be optimized to support energy security and reduce dependence on fossil fuels.

Biomass gasification is a promising thermochemical technology for converting renewable resources into syngas consisting of H_2, CO, CH_4, and CO_2. Of the various types of biomass, corn cobs are a potential candidate due to their abundant availability in Indonesia and lignocellulose content that supports the energy conversion process [3]. However, the biomass gasification process still faces several obstacles, particularly the low hydrogen fraction in syngas and the formation of significant amounts of tar. Tar can cause reactor clogging, reduced thermal efficiency, and increased purification costs.

To overcome these problems, the use of catalysts is an important strategy. A number of studies have proven that metal catalysts such as Ni, Ca, and K can increase hydrogen yield while suppressing tar formation. On the other hand, activated carbon is also widely used as a catalyst support because it has a high surface area, porous structure, and good chemical stability. The use of agricultural waste, particularly palm fiber, as raw material for activated carbon is not only economically valuable but also supports the concept of a circular economy in plantation waste management. In addition, calcium oxide (CaO) is known to have a dual role, namely as a catalyst in the tar decomposition reaction and as a CO_2 absorber that promotes sorption-enhanced gasification to increase the hydrogen fraction in syngas [4].

Although various studies have examined the role of metal catalysts and activated carbon separately, research focusing on the combination of biomass bases catalyst such as palm fiber-based activated carbon with CaO in corn cob gasification is still limited. The uniqueness of this study lies in the integration of two catalyst, which is expected to provide a synergistic effect: activated carbon with high porosity increases catalyst dispersion and activity, while CaO simultaneously breaks down tar and absorbs CO_2. This approach has the potential to significantly increase hydrogen production and reduce carbon emissions.

However, there are several research gaps that remain unanswered. First, the optimal composition and ratio of activated carbon and CaO in corn cob gasification have not been extensively studied. Second, the synergistic mechanism using two catalyst in increasing syngas quality not yet fully understood. In addition, a systematic and statistically robust approach is required to disentangle the coupled effects of key operating and catalyst variables.

Based on this background and research gaps, this study aims to investigate the performance of a composite catalyst based on activated carbon from palm fiber combined with CaO in the corn cob gasification process. The main focus is on

increasing hydrogen production, reducing tar, and evaluating the potential synergistic effects between materials. This research is expected to contribute to the development of low-cost, locally sourced, and sustainable catalyst systems that are relevant to supporting the clean energy transition and practical applications of biomass-to-hydrogen in the future.

2. Literature review and problem statement

The paper [5] presents the result on the gasification of sago dreg waste pellets in a top-lit updraft fixed-bed gasifier. The results show that the addition of Al_2O_3 improved syngas quality, especially by increasing H_2 content up to 31.65% at 5% Al_2O_3 and enhancing CO and CH_4 production, while also increasing the H_2/CO ratio to 1.65 and 1.51 for 5% and 10% Al_2O_3, respectively, improving LHV, and reducing tar content by about 25–27.5% compared with pellets without catalyst. However, this study is limited because it was conducted only on one biomass type, within a laboratory-scale TULD fixed-bed gasifier, and only considered two catalyst loadings.

The paper [6] presents the result on hydrogen enrichment in product gas from a pilot-scale rice husk updraft gasification. The results show that dolomite-assisted air gasification gave the best performance, increasing the H_2 content up to 15.4 mol%, with an LHV of 5.1 MJ/Nm³, while steam/air gasification improved H_2 to 9.6 mol% and air alone produced only about 7.08 mol% H_2, the optimum operating condition was reported at an airflow rate of 3 m³/h and a dolomite mixing ratio of 15 wt%. However, this study is limited because it focused only on rice husk feedstock, used a pilot-scale updraft gasifier with a batch capacity of 3 kg, and evaluated only a limited range of operating conditions and catalyst type.

The paper [7] presents the result on oxygen updraft gasification coupled with catalytic steam reforming of cigarette butts for hydrogen-rich syngas production. The results show that the integrated process was effective in converting cigarette butts into syngas, with gasification producing 82.3–89.7 wt.% syngas, 6.3–8.6 wt.% soot, and 1.4–1.9 wt.% tar, while the catalytic reforming stage significantly improved the gas quality by increasing the H_2 content up to 30.27 vol.%, increasing the HHV up to 11,528 kJ/kg, and reducing tar concentration from about 18.15 g/m³ to 13.38 g/m³ under the optimum condition. However, this study is limited because it investigated only cigarette butt waste as feedstock, used a specific oxygen updraft gasifier–catalytic reformer configuration, and fixed most catalytic reforming parameters.

The paper [8] presents the result on the experimental assessment of pellets produced from beekeeping waste and slumgum–pine sawdust mixtures through updraft gasification. The results show that pure slumgum pellets exhibited very high mechanical durability (99.98%) and high HHV (27.66 MJ/kg), while during gasification the 50% slumgum–50% sawdust pellets produced the highest producer gas LHV of 7.62 MJ/Nm³, indicating that the addition of sawdust improved gas quality and energy recovery potential. However, this study is limited because the equivalence ratio remained very

low (0.0125–0.0204) compared with typical gasification conditions, the experiments were conducted only in a modified laboratory-scale updraft gasifier.

The paper [9] presents the result on a comparative investigation of catalyst applications in updraft and modifiable-downdraft fixed-bed biomass gasifiers, using a biomass mixture of green waste, sewage sludge, and olive pomace together with red mud (RM) and Al–Ni alloy catalysts to improve syngas quality and hydrogen production. The results show that catalyst type and reactor configuration strongly influenced gasification performance, with the Al–Ni catalyst giving the best hydrogen enrichment, reaching up to 65 vol.% H_2 in the updraft gasifier at 900 °C, while RM increased H_2 to about 50 vol.%, the updraft gasifier produced better hydrogen-rich syngas than the modifiable-downdraft reactor. However, this study is limited because it, used a specific mixed biomass composition and mainly focused on high temperature operation around 900 °C with limited gasifying-agent flow conditions.

The paper [10] presents the result on the experimental investigation of producer gas composition from sorted municipal solid wastes in an updraft fixed-bed gasifier. The results show that reducing the equivalence ratio from 0.21 to 0.15 increased the heating value of the combustible gases. The study indicated that the allothermal updraft fixed-bed gasifier is suitable for producing gas that can be utilized in gas engines. However, this study is limited because it used a laboratory-scale 10 kW allothermal updraft gasifier at a fixed temperature of 800 °C, and evaluated only two ER conditions.

The paper [11] presents the result on the effect of adding laying hens manure (LHM) to wheat straw on gasification efficiency in an air-blown updraft fixed-bed gasifier. The results show that increasing ER improved the gasification performance, with the producer gas LHV reaching 3.3–3.4 MJ/m^3, cold gas efficiency around 60%, and carbon conversion efficiency in the range of 82–94% . However, this study is limited because it was focused on one specific co-feed system and produced a relatively low-calorific gas.

The paper [12] presents the result on the gasification performance of olive pomace in updraft and downdraft fixed-bed reactors using dry air and pure oxygen. The results show that updraft reactor achieving up to 48 vol.% H_2 with dry air and 53 vol.% H_2 with pure oxygen, while the downdraft reactor reached up to 45 vol.% H_2 with dry air and 39 vol.% H_2 with pure oxygen. However, this study is limited because only a limited range of gasifying agents, temperatures, and flow rates.

The paper [13] presents the result on the gasification of MDF residue in an industrial-scale updraft fixed-bed gasifier. The results show that MDF residue can be effectively converted into useful energy, with a syngas production rate of about 2.5 Nm^3/kg, syngas LHV of around 6.0–7.0 MJ/Nm^3, about 88 wt.% of MDF residue converted into syngas, and a system capable of delivering 7 MWth of thermal energy and about 955 kW net electrical power through the ORC turbine. However, this study is limited because it focused on one specific industrial waste stream (MDF residue) in one updraft gasifier configuration, mainly evaluated performance under a limited number of feed rates, and relied on direct combustion of raw hot syngas containing tar.

The paper presents the results of research on biomass gasification in updraft fixed-bed reactors aimed at improving syngas quality and thermal conversion efficiency. Shown that syngas composition and heating value are strongly influenced by feedstock properties, gasification conditions, and catalyst application. But there were unresolved issues related to the lack of effective and low-cost catalyst systems capable of simultaneously enhancing hydrogen formation and improving overall syngas quality during corncob gasification. The reason is the complexity of catalytic reactions in the gasification zone, including reforming, cracking, and CO_2 capture mechanisms, as well as the economic limitations of commercially available catalysts. A way to overcome these difficulties can be the development of composite catalysts based on CaO and activated carbon palm fiber, where CaO may promote CO_2 absorption and shift reactions, while activated carbon palm fiber may provide a porous surface and active sites for secondary cracking reactions. This approach was used in previous studies, however, the combined use of CaO and activated carbon palm fiber in corncob updraft gasification has not been sufficiently investigated. All this suggests that it is advisable to conduct a study on syngas quality improvement in corncob updraft gasification using CaO/activated carbon palm fiber catalyst.

3. The aim and objectives of the study

The purpose of the study is to enhance syngas quality from corncob updraft gasification by developing a dual-synergy catalytic system based on calcium oxide (CaO) and palm-fiber-derived activated carbon (AC-PF). This will allow the production of cleaner and more energy-dense producer gas, providing practical guidance for selecting operating conditions and catalyst configurations suitable for updraft gasifiers processing agricultural residues.

To achieve these aims, the following objectives are accomplished:

– to synthesize and characterize the CaO and palm-fiber activated carbon catalysts using Fourier Transform Infrared Spectroscopy (FTIR), scanning electron microscopy (SEM) and Brunauer-Emmett-Teller surface area analysis (BET);

– to investigate the effects of operating parameters, particularly equivalence ratio (ER), catalyst loading, and CaO/AC ratio, on syngas composition H_2, CO, CH_4, CO_2 and LHV.

4. Materials and methods

The object of the study is the updraft fixed-bed gasification process of corncob biomass using a dual catalyst system based on calcium oxide (CaO) and palm-fiber-derived activated carbon (AC-PF). The practical physical process under investigation is the catalytic upgrading of producer gas within the updraft reactor, where changes in operating parameters and catalyst configuration are expected to influence syngas composition and heating value. The results of this study are intended to be applied to improve the quality of syngas, specifically by increasing the combustible gas fraction (H_2 and CH_4) and the lower heating value (LHV), while reducing CO_2 content.

The research hypothesis is that a dual-synergy CaO/AC-PF catalytic system can improve syngas quality more effectively than single-catalyst configurations in updraft corncob gasification. It is hypothesized that CaO functions as a CO_2 sorbent, shifting reaction equilibria toward enhanced hydrogen formation, while activated carbon derived from palm fiber provides high-surface-area catalytic sites that promote secondary reactions such as tar cracking and volatile reforming. The combined catalytic-sorption mechanism is expected to increase H_2 and CH_4 fractions and improve LHV under optimized equivalence ratio (ER), catalyst loading, and CaO/AC-PF ratio conditions.

It was assumed that the corncob feedstock has relatively homogeneous composition and stable proximate/ultimate characteristics during the experiments. The gasification process was assumed to operate under steady-state conditions after stabilization. It was also assumed that the CaO maintains sufficient CO_2 sorption capacity within the experimental time frame and that the activated carbon structure remains stable under the applied temperature range.

During the course of the research, several methodological simplifications were adopted in order to maintain experimental feasibility and focus on the main objective of syngas quality evaluation. Detailed kinetic modeling of individual gasification reactions was not performed; instead, the process performance was assessed based on experimentally measured syngas composition and syngas low heating value. Furthermore, although CaO carbonation-decarbonation reactions may occur during operation, microstructural evolution, sintering behavior, and long-term cyclic stability of the catalyst were not investigated in this study. The catalytic performance was evaluated within the experimental duration without conducting extended durability or regeneration-cycle analysis.

4. 1. Catalyst Preparation

Approximately 6 grams of ground palm fiber was mixed with 60 mL of distilled water and stirred for 10 minutes. The mixture was then placed in an autoclave and heated to 200°C at a rate of 5°C per minute for 6 hours in an electric oven. After that, the reactor is allowed to cool naturally to room temperature. The resulting solid hydrocarbon product (hydrochar) is then separated using Whatman No. 42 filter paper. The filtered product is then dried at 105°C for 24 hours and stored in a glass vial. The next stage is the activation process. The hydrochar is immersed in a 3 M KOH solution with a weight ratio of 1:3 (Hydrochar:KOH) for 16 hours, then dried at 85°C for 6 hours. Spectroscopic evidence indicates that KOH preferentially reacts with oxygenated sites and can increase the relative abundance of C–OH functionalities, while higher KOH ratio and activation temperature significantly enhance porosity and BET surface area [14, 15]. To obtain the CaO/AC mixture, CaO powder and activated carbon (AC) were mixed in specific proportions using a grinder until a homogeneous mixture was obtained. Next, CaO, AC, and CaO/AC were activated using a tube furnace at a temperature of 700°C for 1 hour with a continuous flow of nitrogen during the activation

process. The resulting product was then washed using distilled water until it reached a neutral pH. This stage produced activated carbon that was ready for use in research.

4. 2. Experimental Setup

Corncob biomass was obtained from farmers in the South Malang region of East Java. Before use, the biomass was cleaned of impurities and dried in an oven for 6 hours at 100°C to remove moisture (water vapor) content. The ultimate and proximate test results are as follows.

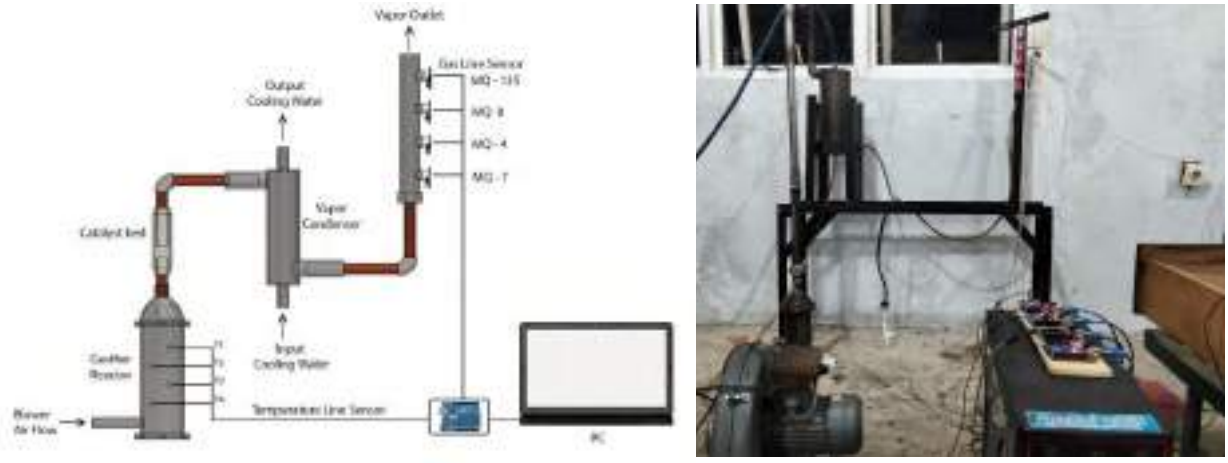
The proximate and ultimate analyses of the corncob feedstock were conducted to determine its physicochemical characteristics prior to gasification. The results are presented in Table 1. The data indicate that corncob has high volatile matter content and relatively low ash content, which are favorable characteristics for gasification processes.

There must be a reference to the Fig. 1 in the text before the Figure

Table 1

Ultimate and Proximate Test Corn Cob

Parameter	Units	Corn cobs
Moisture	%	10
Volatile matter	%	71.38
Fixed carbon	%	12.11
Ash	%	6.51
C	%	43.6
H	%	6.3
O	%	46.8
N	%	0.22
HHV	MJ/kg	17.61



a *b*

Fig. 1. Updraft gasifier: *a* – schematic experiment; *b* – experimental setup

This study used an updraft gasification reactor designed with a total height of 20 cm. The lower part of the reactor consisted of an ash container with a height of 5 cm, while the active reactor had a height of 15 cm and a diameter of 3 inches. The reactor was equipped with a 1-inch diameter air inlet pipe connected to a blower. The blower was modified with a potentiometer so that the air speed could be adjusted as needed. To monitor the thermal conditions inside the reactor, four 3 cm long type K thermocouples were installed at several different points so that the temperature profile in the gasification zone could be observed in more detail. Each test was conducted with a fixed biomass mass, a mixture of corn cobs weighing 80 grams. The reactor was made of iron and equipped with a gas seal to prevent leaks during the gasification process.

The gas produced by the reactor was fed into a condenser, which cooled the hot gas so that the water vapor components could be separated. The condenser was made of a copper spiral pipe with a diameter of ½ inch and a height of 30 cm. Cooling water was circulated from the bottom of the condenser and exited through the top to ensure efficient heat transfer. This cooling system was driven by a 60-watt water pump, ensuring stable water flow and optimal condensation. The catalyst was positioned downstream after the reactor, where it was supported on steel wool and wrapped with an 80-µm wire mesh to secure the catalyst and prevent particle carryover with the gas flow

To analyse the gas composition, four types of MQ gas sensors were used. The MQ-8 sensor was used to detect H_2, MQ-4 for CH_4, MQ-135 for CO_2 and MQ-7 for CO. Each gas sensor was calibrated according to the manufacturer's datasheet, specifically by determining the Ro value, which is the sensor resistance in clean air conditions. This Ro value is used as a reference in calculating the measured gas concentration during the process.

All data from the gas sensors and thermocouples were acquired using an Arduino Uno microcontroller. Each gas sensor is connected to a separate Arduino Uno to facilitate the calibration process and reduce the possibility of interference between sensors. Arduino is also used to record temperature data from four thermocouples installed in the reactor, so that gas composition and temperature distribution data can be obtained simultaneously.

The ER range of 0.2, 0.25, 0.3 and 0.35. The catalyst load was between 4%, 6%, 8% and 10% from the mass of input feedstock. The CaO/AC-PF ratio was varied between 0:1, 1:0, 1:1, and 2:1. Design of experiment can be seen in Table 2.

Table 2
Design of Experiment using

Run	Equivalence Ratio (E.R)	Catalyst Load %	CaO/AC
1	0.2	4	1:0
2	0.2	6	0:1
3	0.2	8	1:1
4	0.2	10	2:1

5	0.25	4	0:1
6	0.25	6	1:0
7	0.25	8	2:1
8	0.25	10	1:1
9	0.3	4	1:1
10	0.3	6	2:1
11	0.3	8	1:0
12	0.3	10	0:1
13	0.35	4	2:1
14	0.35	6	1:1
15	0.35	8	0:1
16	0.35	10	1:0

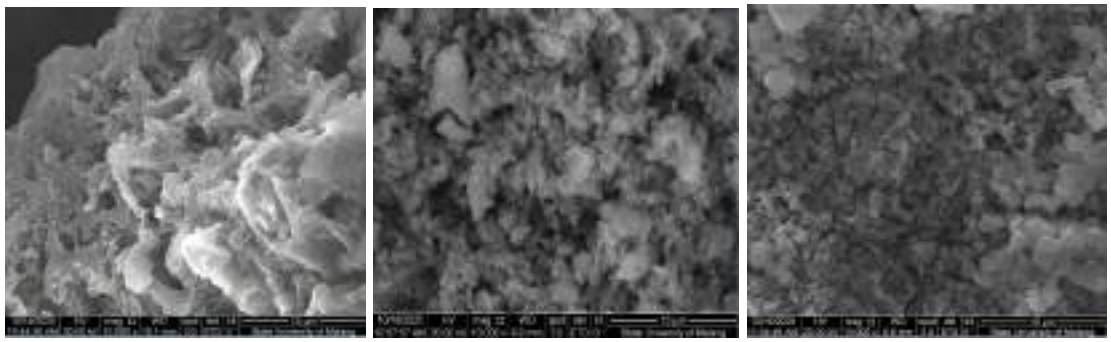
A total of 16 experimental runs were conducted systematically to enable evaluation of the main effects of each variable and the tendency of interactions between variables on the fractions of H_2, CO, CH_4, CO_2, and lower heating value (LHV). This approach enabled identification of the most effective combination of operating parameters in improving syngas quality quantitatively and measurably.

5. Results of syngas quality enhancement from corncob using calcium oxide (CaO) and palm-fiber-derived activated carbon (AC–PF).

5. 1. Characterization of Calcium Oxide (CaO) and Palm-Fiber-Derived Activated Carbon (AC–PF) Catalysts

5. 1. 1. Scanning Electron Microscopy Catalyst Result

Fig. 2, *a* shows the image obtained from a Scanning Electron Microscope (SEM) with a magnification of 10,000× shows the surface morphology of palm fiber-based activated carbon (AC-PF). The surface structure appears porous and irregular, with a combination of void areas and layered surfaces. This characteristic indicates that the activation process that using KOH has successfully formed micropores and mesopores, which play an important role in increasing the specific surface area of activated carbon.



a *b* *c*

Fig. 2. Scanning Electron Microscopy Catalyst Result: *a* – Scanning Electron Microscopy AC-PF; *b* – Scanning Electron Microscopy CaO:AC;1:1; *c* – Scanning Electron Microscopy CaO:AC-PF;2:1

The rough and textured surface indicates that most of the material has undergone lignocellulose cell wall exfoliation, resulting in numerous interparticle gaps. This porous structure greatly supports gas adsorption and diffusion capabilities when used as a catalyst in gasification or thermochemical reactions.

The presence of 1–5 μm voids indicates that most pores are in the mesopore category, supporting the adsorption of gas molecules such as H_2, CO, and tar during the gasification reaction.

The morphology of AC-PF shows the characteristics of porous activated carbon with a heterogeneous pore distribution, where the pores allow increased contact between gas reactants and active sites on the material surface, thereby increasing catalytic efficiency and the ability to absorb tar or CO_2 in biomass-based energy applications.

Fig. 2, *b* shows the surface morphology of the CaO:AC-PF catalyst with a ratio of 1:1. Visually, it can be seen that the surface of this material consists of fine particles ranging in size from microns to submicrons that stick together to form a layered and slightly agglomerated structure.

The presence of fine, light-colored grains indicates an even distribution of CaO particles impregnated on the surface of activated carbon (AC-PF). This CaO distribution fills some of the pores of the carbon, resulting in a denser surface compared to pure AC-PF. However, there are still small gaps and voids between the grains, indicating that the microporous and mesoporous structures are still formed and can support catalytic activity [16].

This morphology illustrates the success of the CaO impregnation process on activated carbon from palm fiber, where the interaction between CaO and the carbon pore walls produces a composite material that is more thermally and chemically stable. This structure is highly conducive to catalyst applications in biomass gasification processes, as CaO particles can function as CO_2 absorbers while accelerating the tar reforming reaction [17].

Fig. 2, *c* shows the surface morphology of the CaO:AC-PF (2:1) catalyst. The image shows that the surface of the material is dominated by agglomerations of fine, round, and irregular particles ranging in size from microns to submicrons. Compared to the CaO:AC-PF (1:1) sample, this structure appears denser and tighter, indicating that an increase in the CaO ratio causes partial closure of the activated carbon surface pores by CaO particles.

The distribution of CaO particles appears more uniform and covers the carbon surface, indicating the successful impregnation of a larger amount of CaO. The light color in some areas indicates the presence of a calcium oxide phase that is strongly

attached to the activated carbon matrix. This structure indicates a strong interaction between CaO and AC-PF, forming a thermally stable composite.

Although some pores are covered, there are still microscopic gaps between the CaO grains that allow gas diffusion to occur, so that the catalyst retains its good adsorption capacity. The combination of the active area of CaO and the porous carbon structure makes this material very promising for biomass gasification or tar reforming applications, as CaO can act as a CO_2 absorber and increase the conversion of carbon to hydrogen gas.

5. 1. 2. Fourier Transform Infrared Spectroscopy catalyst result

The FTIR analysis results shown in the Fig. 3 reveal clear spectral differences between the AC-PF, CaO, and their mixtures (CaO:AC-PF) with ratios of 2:1 and 1:1. In the AC-PF spectrum, the absorption band at 2926 cm^{-1} is associated with the stretching vibration of the C–H group from $–CH_2$ or $–CH_3$ (methylene/methyl stretching), which indicates the presence of hydrocarbon chain residues from the lignocellulose structure. The peak at 1577 cm^{-1} indicates the presence of aromatic C=C or C=O stretching, while the band at 1056 cm^{-1} represents C–O stretching from alcohol or ether groups. In addition, the –OH group that appears in the 3500–3600 cm^{-1} region is identified as the result of AC-PF activation using a KOH solution, which causes the formation of hydroxyl groups on the activated carbon surface. This –OH group plays an important role in increasing the surface activity and adsorption capacity of AC-PF as a catalyst support medium [18, 19].

In pure CaO, the intense band at 3639 cm^{-1} is associated with the stretching of the O–H group from $Ca(OH)_2$, which is formed due to the partial hydration of CaO when exposed to humid air. Meanwhile, the absorption bands at 1426 cm^{-1} and 876 cm^{-1} are associated with C–O stretching and CO_3^{2-} bending, respectively, indicating the formation of $CaCO_3$ due to CO_2 adsorption from the air. This shows that CaO is highly reactive to moisture and carbon dioxide in the environment.

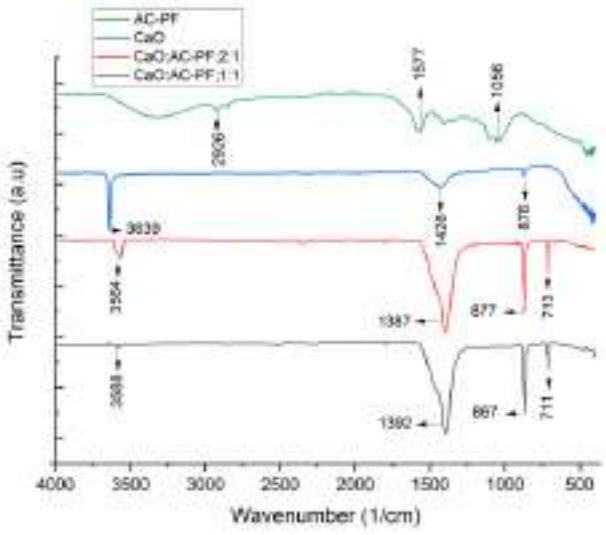


Fig. 3. Fourier Transform Infrared Spectroscopy Catalyst Result

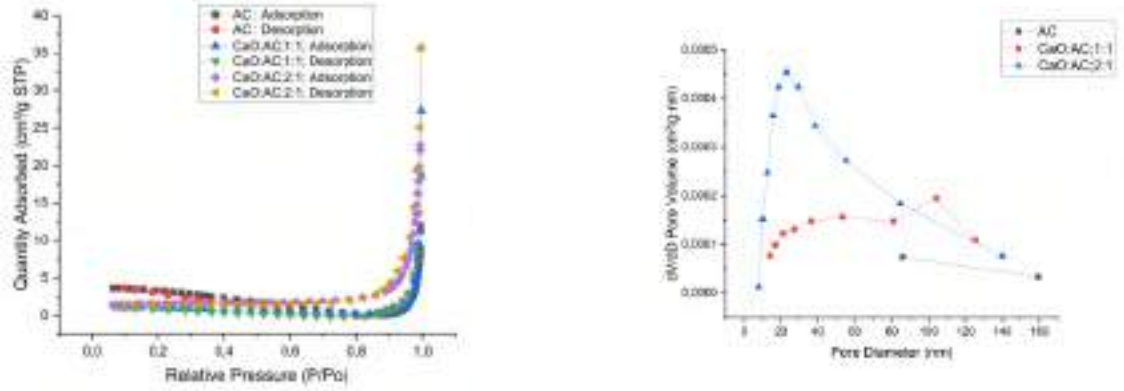
For the CaO:AC-PF (2:1), the main absorption bands were detected at 3564 cm^{-1} (O–H stretching from $Ca(OH)_2$ and the –OH group in AC-PF), 1387 cm^{-1} (C–O stretching), and 877 cm^{-1} and 713 cm^{-1} (bending vibration of CO_3^{2-}). This combination of bands indicates the formation of carbonate compounds ($CaCO_3$) due to the interaction between CaO and the oxygen groups of activated carbon. The presence of –OH groups from KOH activation also strengthens the basic properties on the surface, which can increase the chemical interaction between CaO and AC-PF [20].

At a CaO:AC-PF ratio of 1:1, the absorption bands at 3588 cm^{-1}, 1392 cm^{-1}, 867 cm^{-1}, and 711 cm^{-1} show a similar pattern, indicating the presence of hydroxyl (O–H) and carbonate (CO_3^{2-}) groups. The difference in peak intensity compared to the 2:1 ratio indicates variations in the level of interaction between CaO and the –OH groups resulting from KOH activation on AC-PF, which affects the formation of carbonate-hydroxide complexes on the material surface [21].

5. 1. 3. Brunauer-Emmett-Teller Catalyst Result

Fig. 4 shows the adsorption-desorption isotherm curves for nitrogen for the AC, CaO:AC (1:1), and CaO:AC (2:1) samples are shown in Fig. 4. All three samples exhibit type IV isotherms with clear hysteresis loops at relatively high pressures ($P/Po > 0.9$). Based on the IUPAC classification, this characteristic indicates that the material has a mesoporous structure formed through capillary condensation within the pore channels. The difference between the adsorption and desorption pathways indicates that the pore shape is not perfectly cylindrical, but rather tends to be irregular or slit-like, which is commonly found in modified activated carbon materials [22].

The pure activated carbon (AC) sample showed a relatively low nitrogen adsorption volume with a specific surface area of 24.51 m^2/g and an average pore diameter of 0.74 nm, indicating a predominance of microporous structures. In the CaO:AC (1:1) composite, the surface area did not change significantly compared to pure AC, indicating that the addition of a moderate amount of CaO did not cover the carbon pores much, but only adhered to the external surface of the carbon matrix [23].



a *b*

Fig. 4. Brunauer-Emmett-Teller Result: *a* – Surface Analysis Adsorption Desorption Isotherm; *b* – Barrett-Joyner-Halenda Adsorption Pore Size Distribution

Conversely, in the CaO:AC (2:1) mixture, there was a sharp increase in adsorption volume at relatively high pressure (P/Po > 0.9) to around 35 cm³/g STP, while the BET surface area decreased dramatically to 5.06 m²/g, and the pore diameter increased to 22.87 nm.

These changes in isotherm shape and pore size increase indicate that CaO impregnation not only modifies the surface chemistry but also significantly alters the pore structure of activated carbon. This transformation is positive in the context of catalytic applications in biomass gasification processes, as the mesoporous structure can enhance gas diffusion and accessibility to active sites during the tar reforming and water-gas shift reactions. Thus, even though the specific surface area decreases, the increase in mesoporousness and pore connectivity can actually improve catalyst performance in hydrogen gas production [24].

Fig. 4, *b* shows the BJH pore size distribution curves that provide further insight into the textural evolution of the palm-fiber-based activated carbon after CaO impregnation. The pristine AC exhibits a relatively low dV/dD value and a broad contribution only at large pore diameters (>60 nm), indicating that its pore system is dominated by macropores with a limited amount of mesopores. Such a texture is less favourable for gas-solid reactions because the accessible surface area in the mesopore range (2–50 nm) is relatively small.

After CaO loading, the shape and intensity of the BJH curves change markedly. For CaO:AC-PF = 1:1, the distribution shifts toward smaller pore diameters with a pronounced contribution in the mesopore region of approximately 15–60 nm. This behaviour shows that CaO impregnation partially reconstructs the carbon matrix, enlarging existing micropores and opening blocked pores to generate additional mesoporosity. The effect becomes even more evident at CaO:AC-PF = 2:1, where the curve displays the highest dV/dD values and a distinct maximum centred at about 30–40 nm. The strong peak in this range confirms that a higher CaO loading promotes the

development of well-defined mesopores while reducing the relative fraction of very large macropores.

Overall, the BJH analysis demonstrates that CaO acts not only as a reactive sorbent but also as a textural promoter for the palm-fiber AC. The increase in mesopore volume and the shift of the dominant pore size toward 20–40 nm are expected to facilitate the diffusion of gasifying agents and tar molecules, as well as to improve the accessibility of CaO active sites for CO_2 capture and reforming reactions. These features are therefore beneficial for enhancing the catalytic performance of the CaO/AC composite in biomass gasification toward H_2-rich syngas production.

5. 2. Effect of operating parameters on syngas composition and low heating value

5. 2. 1. Effect of Equivalence Ratio on Syngas Product

The composition of syngas from updraft gasification is greatly influenced by the Equivalence Ratio (ER), which is the ratio of the mass flow rate of air compared to the mass flow rate of corncob in the experiment compared to the stoichiometry of air required for complete combustion of corncob. In this study, the ER used was 0.2–0.35 with the following formula

$$ER = \frac{(\dot{m}_a / \dot{m}_{cc})_{\exp}}{(\dot{m}_a / m_{cc})_{stc}},$$

where $\dot{m}_a$ is the air mass flow rate (kg/s), $\dot{m}_{cc}$ is the corncob mass flow rate (kg/s), exp denotes the experimental air-fuel ratio, and stc denotes the stoichiometric air-fuel ratio.

There must be a reference to the Fig. 5 in the text before the Figure

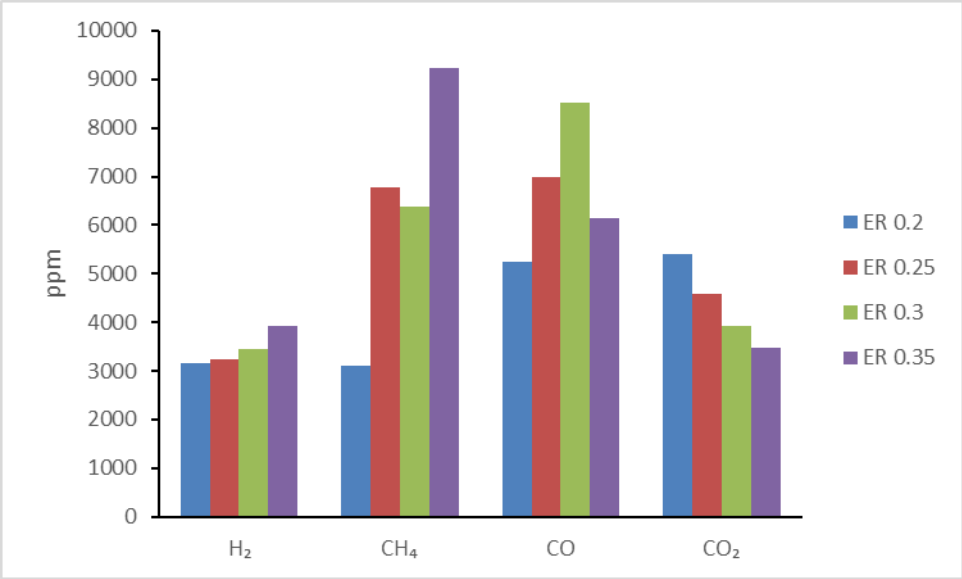


Fig. 5. Syngas composition with different equivalence ratio

The graph above shows that the higher the ER, the higher the hydrogen composition produced. At ER 0.2, the ppm is 3150 ppm, at ER 0.25 it is 3241 ppm, at ER 0.3 it is 3457 ppm, and at ER 0.35 it is 3914 ppm. A higher oxidant supply promotes the formation of more stable autothermal conditions and higher reaction temperatures due to partial oxidation. This increase in temperature accelerates hydrogen-forming reactions, particularly the gasification of active carbon catalyst interactions with steam ($C + H_2O \rightarrow CO + H_2$), the reforming of volatile compounds/light hydrocarbons ($C_xH_y + H_2O \rightarrow CO + H_2$), and the cracking of tar/volatile into lighter gas species. At low ER, some volatiles tend to be incompletely converted and still have the potential to escape as condensable components, while increasing ER increases heat availability, making the conversion of volatiles into gas fractions (including H_2) more effective.

The higher the ER, the higher the CH_4 composition produced. At ER 0.2, 3093 ppm was obtained, at ER 0.25 6767 ppm, ER 0.3 6377 ppm, and ER 0.35 9221 ppm. This trend indicates that the supply of oxidants not only increases autothermal conditions and the rate of devolatilization, but also shifts the reaction pathway towards the formation of light hydrocarbons through hydrogenation and/or methanation reactions in the reactor zone where the temperature still supports CH_4 formation. In particular, increased H_2 at higher ERs can promote the methanation reaction of CO ($CO + 3H_2 \rightleftharpoons CH_4 + H_2O$), so that CH_4 increases along with a tendency for CO to decrease at the highest ER. In addition, more intensive fragmentation of volatiles and tar at high ERs has the potential to produce light gas precursors which are then hydrogenated to CH_4.

CO formation increased up to an ER of 0.3 and decreased at an ER of 0.35. At an ER of 0.2, 5238 ppm was obtained, at an ER of 0.25, 6999 ppm, at an ER of 0.3, 8532 ppm, and decreased at an ER of 0.35 to 6145 ppm. At low ER (0.20–0.25), limited oxygen supply resulted in relatively low heat release, so that the reaction zone temperature and char reactivity were not sufficient to intensify CO formation reactions, especially the Boudouard reaction ($C + CO_2 \rightleftharpoons 2CO$) and char gasification with steam ($C + H_2O \rightleftharpoons CO + H_2$). When the ER is increased towards 0.30, the increase in autothermal heat strengthens these reduction reactions, causing CO formation to increase and reach its peak. However, at higher ERs (0.35), the CO fraction tends to decrease because some CO can be converted to CH_4.

CO_2 formation continues to decrease as ER increases. At ER 0.2, 5412 ppm is obtained; at ER 0.25, 4592 ppm; at ER 0.3, 3916 ppm; and at ER 0.35, 3479 ppm. The increase in oxidant supply at this ER does not promote complete combustion, but rather strengthens the CO_2 reduction mechanism. At higher ERs, the heat generated from partial oxidation increases the temperature of the reduction zone, thereby accelerating the Boudouard reaction ($C + CO_2 \rightleftharpoons 2CO$), in which CO_2 is reduced by char to CO. This mechanism is consistent with the increase in CO until it reaches a maximum at an ER of 0.30, while also explaining the decrease in CO_2 under the same conditions. Interestingly, at an ER of 0.35, CO_2 remains at its lowest level even though CO decreases, indicating

that the CO formed is not completely accumulated at the outlet but has the potential to undergo further conversion along the gas flow path.

5. 2. 2. Effect of Catalyst Loading on Syngas Product

The catalyst load or amount of catalyst in this study was 4%, 6%, 8%, and 10% of the total biomass weight. The Fig. 6. shows that the composition of H_2 and CH_4 increases as the catalyst load decreases. The H_2 gas composition at catalyst loads of 4%, 6%, 8%, and 10% is 3742 ppm, 3471 ppm, 3372 ppm, and 3176 ppm, respectively. As the catalyst load increases, the reaction pathways that consume H_2 tend to strengthen, particularly the reverse water–gas shift ($CO_2 + H_2 \rightarrow CO + H_2O$) and H_2 interactions on the catalyst surface during the conversion of gasification compounds. As a result, even though reforming occurs, the measured net H_2 decreases because more H_2 is used for CO formation and surface reactions. The CH_4 gas composition at catalyst loads of 4%, 6%, 8%, and 10% was 7031 ppm, 6476 ppm, 6206 ppm, and 5746 ppm, respectively. An increase in catalyst load increases the number of active sites and gas-catalyst contact, so that methane/light hydrocarbon cracking and reforming occur more intensely. CH_4 then acts as a reactant that is converted into more reactive syngas components, causing the CH_4 concentration to decrease at higher catalyst loads.

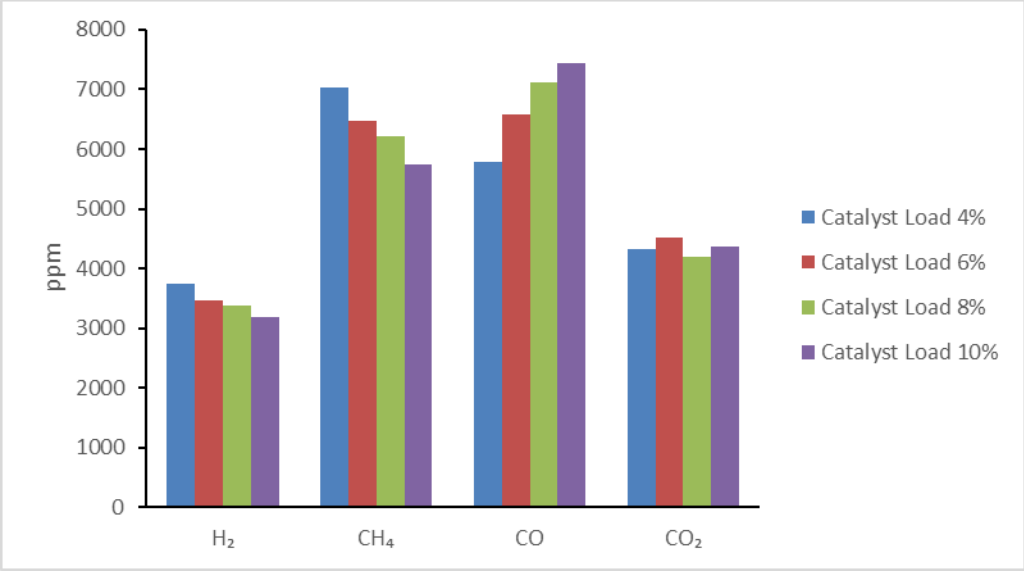


Fig. 6. Syngas Composition with Catalyst Load Variation

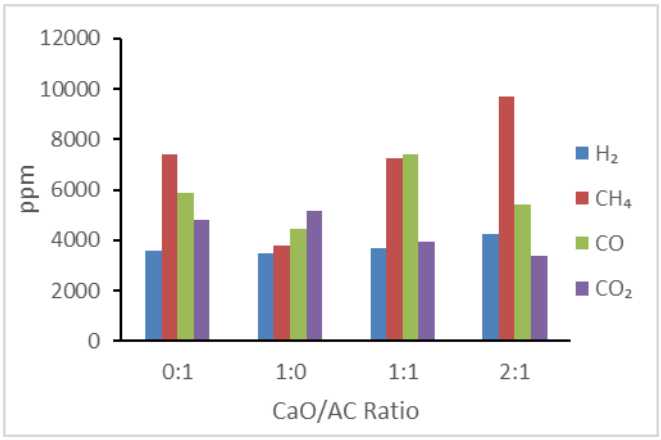
The CO gas composition increases with increasing catalyst load, namely for catalyst loads of 4%, 6%, 8% and 10% at 5782 ppm, 6576 ppm, 7111 ppm and 7445 ppm, respectively. The increase in catalyst loading strengthens the CO-forming reactions, particularly dry reforming ($CH_4 + CO_2 \rightarrow 2CO + 2H_2$), char–$CO_2$ reaction ($C + CO_2 \rightarrow 2CO$), and reverse water-gas shift. This combination shifts the product selectivity towards CO, so that the CO fraction increases consistently as the catalyst is

increased. The CO_2 gas composition tends to stagnate with increasing catalyst loading, at catalyst loads of 4%, 6%, 8%, and 10% at 4322 ppm, 4510 ppm, 4198 ppm, and 4369 ppm, respectively. CO_2 shows minor changes because it is in a searching for a chemical equilibrium between the partial oxidation and the dry reforming. When the catalyst load increases, the rate of CO_2 consumption may rise, but this is often offset by CO_2 formation in the reaction zone, so that the CO_2 value appears stable or only fluctuates.

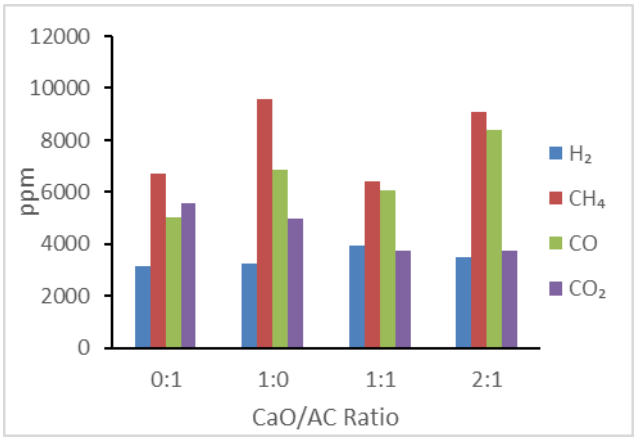
5. 2. 3. Effect of Catalyst Ratio on Syngas Product

At a catalyst load of 4%, the CaO/AC ratio changes the gasification reaction through differences in the dominance of tar cracking/reforming and CO_2 capture by CaO, so that the gas composition is highly dependent on the number of active sites and the effectiveness of gas-catalyst contact. At 0:1 (AC), CH_4 and CO are relatively high because AC promotes volatile/tar cracking, but CO_2 remains high because there is no absorption. At 1:0 (CaO), CH_4 decreases but CO_2 is highest, indicating that CO_2 capture is not yet effective due to limited surface area/carbonate layer formation. The 1:1 ratio produces the highest CO with moderate CO_2, indicating CaO–AC synergy that increases the conversion of volatiles into reactive gases. Meanwhile, the 2:1 (CaO-rich) ratio provides the highest H_2 and lowest CO_2 due to the sorption-enhanced effect of CaO, but CH_4 remains high due to the smaller contribution of AC, so methane reforming/cracking is not yet optimal.

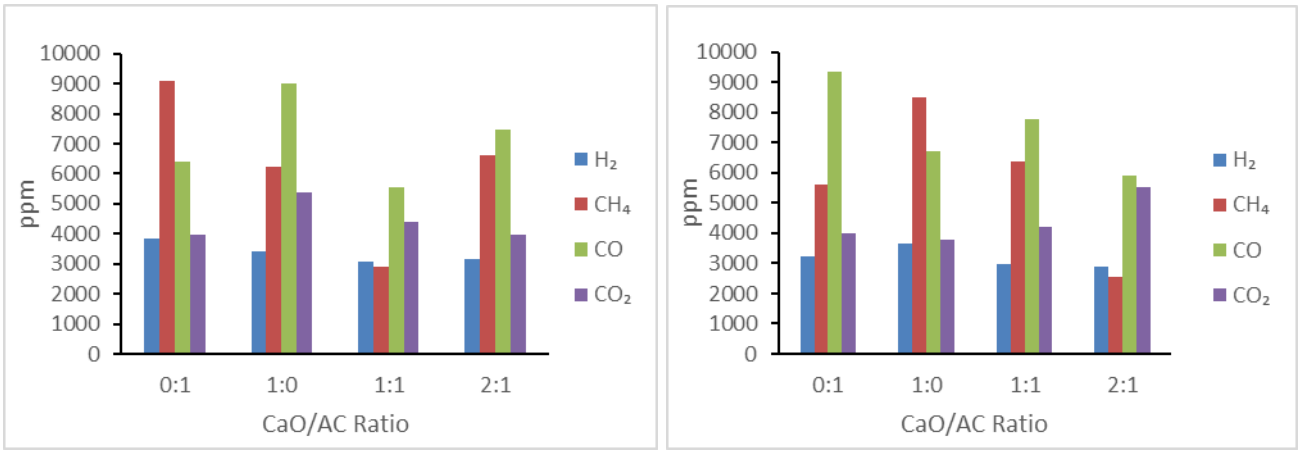
There must be a reference to the Fig. 7 in the text before the Figure



a



b



c *d*

Fig. 7. Effect CaO/AC ratio with various catalyst load: *a* – 4%; *b* – 6%; *c* – 8%; *d* – 10%

At a catalyst load of 4%, the CaO/AC ratio changes the gasification reaction through differences in the dominance of tar cracking/reforming and CO_2 capture by CaO, so that the gas composition is highly dependent on the number of active sites and the effectiveness of gas-catalyst contact. At 0:1 (AC), CH_4 and CO are relatively high because AC promotes volatile/tar cracking, but CO_2 remains high because there is no absorption. At 1:0 (CaO), CH_4 decreases but CO_2 is highest, indicating that CO_2 capture is not yet effective due to limited surface area/carbonate layer formation. The 1:1 ratio produces the highest CO with moderate CO_2, indicating CaO–AC synergy that increases the conversion of volatiles into reactive gases. Meanwhile, the 2:1 (CaO-rich) ratio provides the highest H_2 and lowest CO_2 due to the sorption-enhanced effect of CaO, but CH_4 remains high due to the smaller contribution of AC, so methane reforming/cracking is not yet optimal.

At a catalyst load of 6%, the CaO/AC ratio mainly shifts the selectivity of secondary reactions (tar cracking/reforming and CO_2 capture), where AC enhances the conversion of volatiles/light hydrocarbons, while CaO reduces CO_2 through carbonation ($CaO + CO_2 \rightarrow CaCO_3$) and changes the reaction equilibrium. At 0:1, CH_4 and CO_2 remain high because there is no CO_2 capture and methane reforming is not yet optimal, so volatiles still escape as CH_4. At 1:0, CO_2 tends to decrease, but CH_4 becomes the highest due to the absence of AC's role in cracking/reforming. The most favorable conditions occur at 1:1, with the highest H_2 and lowest CO_2, indicating CaO–AC synergy that promotes sorption-enhanced reforming and increases the conversion of hydrocarbons into syngas components. At 2:1, CO is highest and CO_2 remains low, but CH_4 rises again and H_2 is not maximized because excess CaO has the potential to rapidly carbonate/cause contact limitations, thereby reducing the contribution of AC in cracking/reforming.

At a catalyst load of 8%, the CaO/AC ratio significantly shifts the selectivity of the syngas reaction. At 0:1 (AC), CH_4 is still high because some light hydrocarbons have not been fully converted even though the tar cracking process is already active. At 1:0 (CaO), CO increases the most, but CO_2 also tends to be high, indicating that CaO in this condition is more dominant in promoting the CO formation pathway, while the CO_2 capture function is not yet optimal due to contact limitations or carbonation saturation. The 1:1 ratio produces the lowest CH_4, indicating the most effective CaO–AC synergy for cracking/reforming light hydrocarbons so that more methane is converted into reactive gas. At 2:1, CO increases again but CH_4 also rises, indicating that a smaller AC fraction reduces the intensity of methane reforming/cracking, while the decrease in CO_2 remains dependent on the effectiveness of CaO sorption.

At a catalyst load of 10%, the increase in total catalyst makes secondary reactions, reforming, solid-gas heterogeneous reactions, and equilibrium shifts very dominant, so that the CaO/AC ratio mainly determines the direction of product selectivity. At 0:1 (AC), CO formation tends to be strongest because the porous carbon surface accelerates the cracking/reforming of volatiles and the conversion of tar into reactive gases. At ratios involving CaO (1:0, 1:1, 2:1), CaO can retain CO_2 through carbonation, but at high loads the effect is often non-linear because CaO rapidly carbonates/diffusion limitations and pore blocking occur, so that under CaO-rich conditions (2:1) CH_4 can decrease, but CO_2 may increase and H_2 is not maximized due to reaction competition. Overall, at a 10% load, a trade-off is observed: AC-dominant increases CO, while CaO-dominant suppresses light hydrocarbons but has the potential to trigger non-ideal conditions (saturation/mass transport) that reduce the benefits of H_2 and CO_2.

5. 2. 4. Syngas Low Heating Value

To calculate the LHV of syngas, it must first be converted from ppm to % volume of gas. The formula is $\%vol_i = \frac{ppmv_i}{10^4}$ to calculate the LHV, use the formula

$$LHV_{mix}\left(\frac{MJ}{Nm^3}\right) = \frac{10.8(\%H_2) + 12.63(\%CO) + 35.8(\%CH_4)}{100},$$

LHV H_2 = 10.8 MJ/Nm^3,

LHV CO = 12.63 MJ/Nm^3,

LHV CH_4 = 35.8 MJ/Nm^3.

As shown in Fig. 8, the syngas low heating value (LHV) varies with the equivalence ratio (ER) and catalyst load.

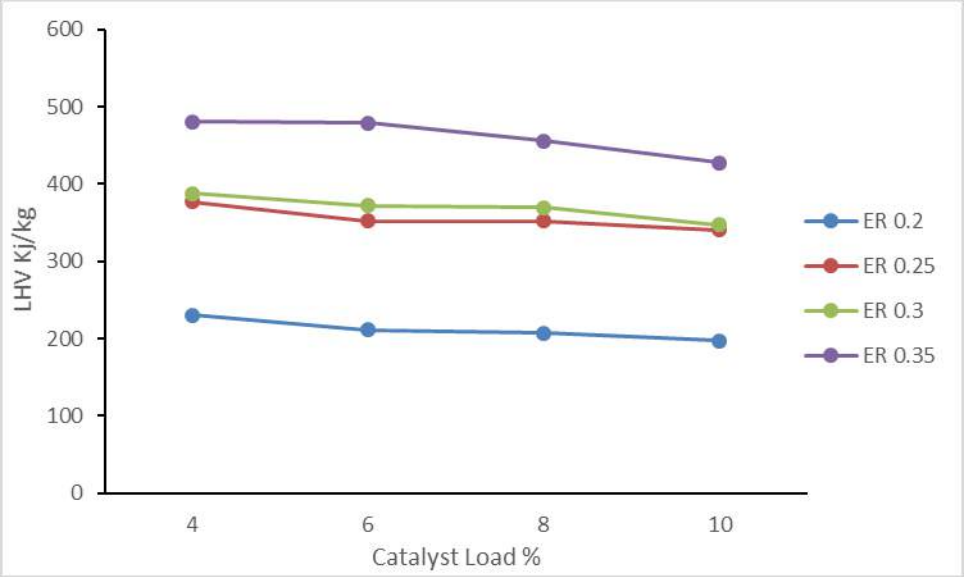


Fig. 8. Syngas low heating value with various equivalence ratio

Fig. 8 shows that the LHV value increases with the ER. At the same catalyst load of 4%, the LHV will increase in line with the increase in ER. ER 0.2 has an LHV of 230 kJ/kg and ER 0.35 has an LHV of 481 kJ/kg. Higher ER produces more intense autothermal conditions, causing the reactor temperature to rise. This increase in temperature accelerates the decomposition of volatiles and tar cracking, and promotes more complete gasification and reforming reactions, thereby increasing the fraction of permanent gases that contribute to the calorific value, mainly CO and CH_4, as well as some H_2. In addition, the increase in temperature is also associated with more effective hydrogen formation, because H_2 formation reactions (e.g., through steam-water and reforming reactions) are generally more optimal at high temperatures, with the temperature range often reported to be most conducive to H_2 formation being 800–1000°C.

At ER 0.2, the highest LHV was obtained at a catalyst load of 4% at 230 kJ/kg and continued to decrease with increasing catalyst load to 197 kJ/kg at 10%. At ER 0.25, the highest LHV was also obtained at a catalyst load of 4% at 377 kJ/kg and also decreased to 341 kJ/kg at a catalyst load of 10%. At ER 0.3, the highest LHV was obtained at a catalyst load of 4% at 388 kJ/kg and also decreased at a catalyst load of 10% to 347 kJ/kg. At ER 0.35, the highest LHV was obtained at 481 kJ/kg and decreased at a catalyst load of 10% to 428 kJ/kg.

However, all ER values show that LHV tends to decrease when the catalyst load is increased from 4% to 10%. This decrease indicates that excessive catalyst addition under these operating conditions does not always improve gas energy quality, because the catalyst can shift the reaction selectivity towards the conversion of high calorific components especially CH_4 into CO and H_2 through reforming, while at the same time the fraction of diluent gases such as CO_2 (and steam) may increase due to reaction. Since

CH_4 has a very large calorific value contribution in the syngas mixture, the decrease in its fraction is often more dominant than the increase in CO/H_2, so that the total LHV tends to decrease.

In energy system analysis, particularly in combustion, gasification, and fuel gas utilisation processes such as syngas, the LHV value is often used because it better represents the heat energy that can actually be utilised by the system. The LHV value of a fuel gas is usually influenced by the composition of combustible gases such as carbon monoxide (CO), hydrogen (H_2), and methane (CH_4). The higher the content of these gases, the greater the LHV value produced. The LHV of syngas from this study with variations in ER and CaO/AC-PF ratio can be seen in Fig. 9.

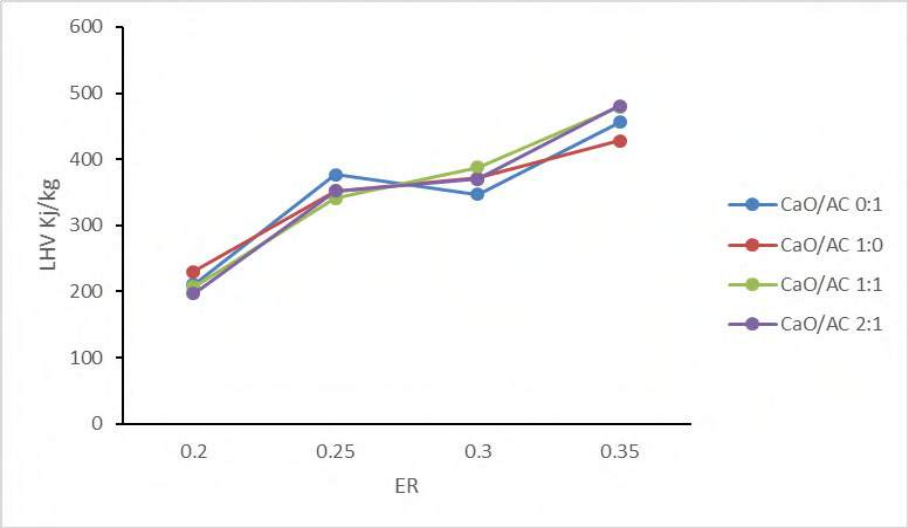


Fig. 9. Syngas Low Heating Value with Various CaO/AC Ratio

Fig. 9 shows that the LHV of syngas increases consistently with the increase in ER 0.2 to 0.35 for all CaO/AC ratios, indicating that a higher ER strengthens autothermal conditions so that the reaction temperature increases and the conversion of volatiles into syngas becomes more complete. At low ER (0.2), the difference in LHV between ratios is still small because secondary reactions such as cracking, reforming and heterogeneous reactions are not yet dominant; the system is still relatively influenced by incompletely converted volatiles. When the ER is increased to 0.25–0.30, the effect of the catalyst ratio becomes apparent: compositions involving AC tend to produce higher LHV because they accelerate tar cracking and increase the fraction of calorific gas, while the contribution of CaO can shift the reaction equilibrium through a decrease in CO_2. At the highest ER (0.35), the LHV reaches its maximum at all ratios, with CaO/AC 2:1 and 0:1 showing peak values, indicating that at high temperatures, the reactive gas formation pathway (via cracking/reforming on the carbon surface and/or CaO-rich-promoted heterogeneous reactions) becomes dominant. Overall, ER acts as the main controlling factor for LHV increase through the temperature effect, while the CaO/AC ratio

modulates LHV through the balance between cracking/reforming (AC) and CO_2 control (CaO), especially at medium-high ER.

6. Discussion on the Catalytic Effect of AC-PF/CaO and Operating Conditions on Syngas Composition and LHV

The interaction of the CaO-AC-PF catalyst to improve syngas quality can be seen from the characterisation of the catalyst, the composition of the syngas and the LHV produced. From the Scanning Electron Microscopy results in Fig. 2, it can be seen that the CaO:AC-PF;2:1 catalyst (Fig. 2, *c*) appears denser than the other catalysts. With the addition of CaO, CaO particle dispersion can be seen on the white carbon surface, indicating that some micro pores are closed by CaO. With the addition of CaO, a lot of CO_2 is absorbed and becomes $CaCO_3$. This porous structure is very important in top-flow gasification because pyrolysis gas and volatiles move through the layer, so the presence of a porous medium has the potential to strengthen secondary reactions and act as carbon capture before the gas exits to the condenser.

From a surface chemistry perspective, Fourier Transform Infrared Spectroscopy (FTIR) shows the presence of –OH and calcium carbonate groups, as shown in Fig. 3. This is due to the results of KOH impregnation carried out during the manufacture of AC-PF. The presence of -OH groups functions as polar active sites capable of adsorbing polar molecules such as H_2O, CO_2, and volatile compounds. Surfaces with -OH groups tend to be hydrophilic and reactive, thereby enhancing interactions with tar compounds or heavy hydrocarbons. These tar compounds can then undergo thermal cracking or catalytic reforming into light gases such as H_2, CO, and CH_4. In addition to -OH, there are also O-H and C-O groups. The O-H group has characteristics that are almost the same as the -OH group, while the C-O group plays a role in enhancing the redox properties and chemical interactions between the carbon surface and gas molecules. In the gasification process, the C-O group can be part of the partial oxidation mechanism and carbon gasification reaction, which produces CO [25].

The BET data in Fig. 4 shows that the surface area decreased to 5.06 m^2/g, but the pore diameter increased to a mesopore scale of 22.87 nm, which can improve the accessibility of volatiles to active sites and improve mass transport in the reforming reaction. In Fig. 4, *b*, the BJH curve at CaO:AC-PF = 2:1 shows the highest dV/dD values of 30–40 nm, indicating a catalyst in the mesopore size range. The presence of these mesopores will further increase the active sites for CO_2 adsorption.

From a process perspective, in Fig. 5, ER appears as the dominant variable that regulates autothermal conditions, primarily through an increase in effective temperature and secondary reaction intensity. An increase in ER from low to high levels consistently increases H_2, which can be explained by the acceleration of H_2 formation reactions such as charcoal gasification with steam ($C + H_2O \rightarrow CO + H_2$) [26], light hydrocarbon reforming, and more intense tar cracking at high temperatures. At the same time, CH_4 also increases sharply at high ER, indicating that in an autothermal upflow system, increased temperature and changes in gas composition can facilitate the formation of

light gases. Meanwhile, CO tends to peak at moderate ER and then decreases at high ER, consistent with competition between CO formation and CO consumption through subsequent reactions such as methanation [27]. The decrease in CO_2 at high ER indicates the role of high temperatures in enhancing the reduction of CO_2 by charcoal (Boudouard reaction) and/or the role of CaO adsorption if available.

The effect of catalyst loading in Fig. 6 shows that adding catalyst does not always increase H_2. Increasing the catalyst loading from low to high tends to reduce H_2 and CH_4 but increase CO. Mechanistically, this condition can occur when the catalyst strengthens pathways that increase CO and/or promotes RWGS ($CO_2 + H_2 \rightarrow CO + H_2O$) [28], which consumes H_2 so that net H_2 is reduced. Furthermore, at high catalyst loadings, the possibility of diffusion/aggregation penalties increases, so that selectivity may shift and some active sites become less effective. Therefore, the target of H_2-rich synthesis gas in this reactor is more dependent on ER adjustment and the selection of moderate/low catalyst loadings, rather than simply increasing the loading.

The CaO/AC-PF ratio in Fig. 7 shows synergistic but non-linear behaviour. AC-PF plays a major role as a porous medium that enhances the cracking/reforming process of volatile compounds, while CaO provides a basic site and CO_2 absorber to shift the equilibrium. At high CaO ratios, sorption and base effects may increase, but the risk of micro-pore closure and diffusion pathway changes also increases. This explains why certain compositions are optimal at certain catalyst loads: the best performance arises from a balance between pore accessibility (the role of AC-PF) and sorption/base strength (the role of CaO).

From an energy quality perspective, in Fig. 8, 9, the LHV value of synthetic gas is highly sensitive to changes in CH_4. Therefore, high ER conditions that increase CH_4 tend to increase LHV. H_2, CH_4 and CO are the main factors for obtaining high LHV. CO_2 has no calorific value so it must be captured. In this study, CaO was used so that CO_2 could be suppressed, meaning that the total LHV could be increased. The highest LHV in this study was 481 kJ/kg, while in another study, the highest was 550 kJ/kg using pinewood with dolomite, activated carbon, silica gel, and limestone catalysts [29]. The higher the ER, the more oxygen enters the system, thereby increasing the reforming reaction [30].

There are several limitations to this study. First, the gas composition was obtained from an MQ sensor based on ppm, so absolute accuracy may be affected by cross-sensitivity, humidity, sensor drift, and gas sampling temperature; this may affect the estimation of %vol and LHV, especially when changes in CO and CH_4 occur simultaneously. Second, catalyst characterisation (SEM-FTIR-BET) supports the role of surface texture and chemistry, but has not quantified changes in the active phase during operation, the degree of carbonation, and the decrease in activity due to pore closure accumulation.

The disadvantage of this research is that the CaO catalyst reacts very easily with CO_2. After the calcination process, CaO must be stored in an airtight container to

prevent it from clumping into $CaCO_3$. The catalyst has a specific usage period because it is covered with tar or ash.

Based on these limitations, several future directions are recommended. Calibrate the gas composition using GC-TCD/GC-FID to convert the sensor readings into more accurate %vol and include LHV uncertainty analysis. Evaluate catalyst stability and regeneration, especially for CaO which is easily carbonated, through carbonation-calcination cycle tests and post-reaction characterisation (XRD/TGA/SEM-EDX) to assess phase changes and activity loss. Develop experimental designs towards ANOVA or RSM interactions so that interaction effects and predictive models can be obtained and verified through replication confirmation tests. Add process performance metrics such as gas yield (Nm^3/kg), cold gas efficiency, pressure drop, and air consumption so that 'syngas quality improvement' can be demonstrated based on mass-energy balance and operability, not just composition.

7. Conclusion

1. AC-PF with rich -OH group acts as a porous catalytic medium that facilitates volatile cracking and supports the reduction of condensable by-products, while CaO contributes to absorb CO_2. The BJH analysis confirms that CaO plays a dual role as a reactive sorbent and a textural promoter in palm-fiber activated carbon by enlarging mesopores (20–40 nm), thereby enhancing gas diffusion and improving access to CaO active sites, which ultimately strengthens catalytic performance.

2. Increasing ER to 0.35 enhances the combustible gas fraction H_2 and CH_4 and suppresses CO_2, whereas CO typically peaks at intermediate ER due to competing CO formation and consumption reactions along the updraft reaction zones. Increasing catalyst loading shifts syngas composition: CO increases, while H_2 and CH_4 decrease, indicating changes in dominant secondary reactions and possible diffusion or agglomeration limitations at higher loadings. Increasing ER lead to increase LHV syngas, but it can decrease at high catalyst loading. An increase in the CaO/AC ratio to 2:1 resulted in a higher syngas LHV, with a maximum value of 481 kJ/kg.

Conflict of interest

The authors declare that they have no conflict of interest in relation to this research, whether financial, personal, authorship or otherwise, that could affect the research and its results presented in this paper.

Financing

The authors sincerely thank the Ministry of Education, Culture, Research and Technology, Republic of Indonesia for fully supporting this research through the DRTPM Research Grant under Fundamental Research, Universitas Widyagama Malang, Indonesia 2025 (Grant Number:128/C3/DT.05.00/PL/2025;023/LL7/DT.05.00/PL/2025;010/ Kontrak/PT/PTS.030.7/PN/V/2025).

Data availability

Manuscript has no associated data.

Use of artificial intelligence

The authors used the AI-based language model ChatGPT (GPT-5.3) only to assist in improving the clarity of English language and grammar in several sections of the manuscript, particularly in the Introduction and Literature Review sections.

The AI tool was used solely for language editing and paraphrasing purposes. All scientific content, experimental design, data analysis, and interpretation of the results were conducted entirely by the authors.

The authors carefully reviewed and verified all AI-assisted text to ensure accuracy and consistency with the experimental results. The use of AI tools did not influence the scientific conclusions of this study.

Acknowledgements

We as the Research Team would like to thank Ministry of Education, Culture, Research and Technology, Republic of Indonesia (Kemendiktisaintek Indonesia) for financing research activities.

Authors' contributions

Purbo Suwandono: Conceptualization, Writing-original draft, Investigation, Supervision, Formal analysis, Writing – review & editing; **Widya Wijayanti**: Validation, Investigation, Data Curation, Formal analysis, Writing – original draft; **Nova Risdiyanto Ismail**: Writing – review & editing, Formal analysis; **Dzulfikar Johan Akbar:** Visualization, Writing – original draft, Data curation; **Muhammad Reza**: Project administration, Resources, Data curation.

References

1. V. K. Yadav *et al.*, “Emerging trends in the valorization of agricultural waste and their utilization in agricultural, pharmaceuticals, and environmental cleanup,” *Waste and Biomass Valorization*, pp. 1–55, 2025. DOI:10.1007/s12649-025-03002-y
2. W. M. Lewandowski, M. Ryms, and W. Kosakowski, “Thermal biomass conversion: A review,” *Processes*, vol. 8, no. 5, p. 516, 2020. https://doi.org/10.3390/pr8050516
3. D. Ariyanti *et al.*, “Valorization of corn cob waste for furfural production: A circular economy approach,” *Biomass and Bioenergy*, vol. 194, p. 107665, 2025. DOI:10.1016/j.biombioe.2025.107665
4. J. Zhang, Z. Chu, R. Cao, X. Wu, and K. Han, “A review of resource recovery from waste plastics via pyrolysis and gasification,” *Fuel*, vol. 404, p. 136319, 2026. https://doi.org/10.1016/j.fuel.2025.136319
5. Y. Tangke Tosuli, Cahyadi, H. Dafiqurrohman, R. Hermawan, and A.

Surjosatyo, “Gasification of sago dreg waste in a top-lit updraft fixed bed gasifier: Syngas composition and its effect with additional Al2O3 as catalyst,” *Energy Convers. Manag. X*, vol. 24, no. October, p. 100775, 2024, doi: 10.1016/j.ecmx.2024.100775. https://doi.org/10.1016/j.ecmx.2024.100775

6. P. Dinh *et al.*, “Enrichment of hydrogen in product gas from a pilot-scale rice husk updraft gasification system,” *Carbon Resour. Convers.*, vol. 5, no. 3, pp. 231–239, 2025, doi: 10.1016/j.crcon.2022.07.003.

7. S. Yousef and J. Eimontas, “International Journal of Hydrogen Energy Oxygen updraft gasification-catalytic reforming of cigarettes butts for hydrogen-rich syngas production,” vol. 171, no. May, 2025, https://doi.org/10.1016/j.ijhydene.2025.150650

8. D. Contreras, E. Blanco, and D. Travieso, “Experimental assessment of the energy potential of pellets produced from beekeeping wastes by updraft gasification,” vol. 343, no. January, 2025, https://doi.org/10.1016/j.enconman.2025.120206

9. N. Yesilova, O. Tezer, A. Ongen, and A. Ayol, “International Journal of Hydrogen Energy Enhancing biomass gasification : A comparative study of catalyst applications in updraft and modifiable-downdraft fixed bed reactors,” *Int. J. Hydrogen Energy*, vol. 76, no. April, pp. 290–303, 2024, https://doi.org/10.1016/j.ijhydene.2024.05.075

10. R. Skvor and A. Jan, “Experimental investigation of sorted municipal solid wastes producer gas composition in an updraft fixed bed gasifier,” vol. 289, no. August 2022, 2024, https://doi.org/10.1016/j.energy.2023.130063

11. R. Junga, M. Tańczuk, S. Sobek, M. Chabiński, and Ł. Ziółkowski, “Effect of the addition of laying hens manure to the straw on gasification efficiency in updraft gasifier under air atmosphere,” *Appl. Therm. Eng.*, vol. 226, no. February, p. 120269, 2023, https://doi.org/10.1016/j.applthermaleng.2023.120269.

12. A. Ongen and A. Ayol, “ScienceDirect Gasification performance of olive pomace in updraft and downdraft fixed bed reactors,” vol. I, 2023, https://doi.org/10.1016/j.ijhydene.2023.02.088

13. K. Ertas, “Gasification of MDF residue in an updraft fixed bed gasifier to produce heat and power via an ORC turbine,” vol. 169, no. February, pp. 43–51, 2023, https://doi.org/10.1016/j.wasman.2023.06.025

14. S. Gorthy, S. Verma, N. Sinha, S. Shetty, H. Nguyen, and M. Neurock, “Theoretical Insights into the Effects of KOH Concentration and the Role of OH–in the Electrocatalytic Reduction of CO2 on Au,” *ACS Catal.*, vol. 13, no. 19, pp. 12924–12940, 2023. DOI:10.1021/acscatal.2c06115

15. X. Wang, W. Zeng, C. Xin, X. Kong, X. Hu, and Q. Guo, “The development of activated carbon from corncob for CO2 capture,” *RSC Adv.*, vol. 12, no. 51, pp. 33069–33078, 2022, https://doi.org/10.1039/D2RA05979G

16. B. Zhou *et al.*, “Insights into effects of grain boundary engineering in composite metal oxide catalysts for improving catalytic performance,” *J. Colloid Interface Sci.*, vol. 653, pp. 1177–1187, 2024. https://doi.org/10.1016/j.jcis.2023.09.148

17. Y. Zhu *et al.*, “Preparation of hierarchically porous carbon ash composite material from fine slag of coal gasification and ash slag of biomass combustion for CO2 capture,” *Sep. Purif. Technol.*, vol. 330, p. 125452, 2024. https://doi.org/10.1016/j.seppur.2023.125452
18. M. Ilić *et al.*, “Surface functional groups and degree of carbonization of *selected* chars from different processes and feedstock,” *PLoS One*, vol. 17, no. 11, p. e0277365, 2022. https://doi.org/10.1371/journal.pone.0277365
19. R. Ali, Z. Aslam, R. A. Shawabkeh, A. Asghar, and I. A. Hussein, “BET, FTIR, and RAMAN characterizations of activated carbon from waste oil fly ash,” *Turkish J. Chem.*, vol. 44, no. 2, pp. 279–295, 2020. doi: 10.3906/kim-1909-20
20. K. J. Stanienda-Pilecki, “The importance of Fourier-Transform Infrared Spectroscopy in the identification of carbonate phases differentiated in magnesium content,” 2019.
21. F. Dai, Q. Zhuang, G. Huang, H. Deng, and X. Zhang, “Infrared spectrum characteristics and quantification of OH groups in coal,” *ACS omega*, vol. 8, no. 19, pp. 17064–17076, 2023. https://doi.org/10.1021/acsomega.3c01336
22. E. M. de Salazar Martínez, M. F. Alexandre-Franco, A. J. Nieto-Sanchez, and E. M. Cuerda-Correa, “Exploring the role of surface and porosity in CO2 capture by CaO-based adsorbents through response surface methodology (RSM) and artificial neural networks (ANN),” *J. CO2 Util.*, vol. 83, p. 102773, 2024. https://doi.org/10.1016/j.jcou.2024.102773
23. J. A. Tavizón-Pozos, H. Cervantes-Cuevas, G. G. Garcia-Camacho, G. Chavez-Esquivel, and D. R. Acosta-Najarro, “Biodiesel Production Using K–Sr/CaO and CaO Catalysts Derived from Eggshells by Canola Oil Transesterification,” *ACS omega*, vol. 10, no. 7, pp. 6827–6838, 2025. https://doi.org/10.1021/acsomega.4c09118
24. W. Koo-Amornpattana, P. Phadungbut, N. Kunthakudee, W. Jonglertjunya, S. Ratchahat, and M. Hunsom, “Innovative metal oxides (CaO, SrO, MgO) impregnated waste-derived activated carbon for biohydrogen purification,” *Sci. Rep.*, vol. 13, no. 1, p. 4705, 2023. DOI:10.1038/s41598-023-31723-4
25. C. Quan, M. Wang, N. Gao, T. Yang, and R. Li, “In situ adsorption of CO2 to enhance biomass gasification for hydrogen production using Ca/Ni based composites,” *J. Energy Inst.*, vol. 108, p. 101229, 2023, doi: https://doi.org/10.1016/j.joei.2023.101229. https://doi.org/10.1016/j.joei.2023.101229
26. F. Micheli, E. Mattucci, C. Courson, and K. Gallucci, “Bi-Functional Catalyst/Sorbent for a H2-Rich Gas from Biomass Gasification,” 2021. doi: 10.3390/pr9071249. DOI:10.3390/PR9071249
27. M. Zhu, Q. Wang, and S. Wang, “Recent Advances and Future Perspectives in Catalyst Development for Efficient and Sustainable Biomass Gasification: A Comprehensive Review,” 2025, https://doi.org/10.3390/su17167370
28. N. Cerone, F. Zimbardi, L. Contuzzi, J. Baleta, and D. Cerinski, “Experimental investigation of syngas composition variation along updraft fixed bed gasifier,” *Energy Convers. Manag.*, vol. 221, no. July, p. 113116, 2020,

https://doi.org/10.1016/j.enconman.2020.113116
29. R. Mohanty, P. Mahanta, A. Mahapatro, and R. Prakash, “Catalytic gasification of pinewood biomass in a fluidized bed reactor with dolomite , limestone , and activated carbon : An experimental study,” *Energy*, vol. 325, no. April, p. 136131, 2025, doi: 10.1016/j.energy.2025.136131. https://doi.org/10.1016/j.energy.2025.136131
30. C. Liu, Y. Huang, M. Niu, and H. Pei, “ScienceDirect Influences of equivalence ratio , oxygen concentration and fluidization velocity on the characteristics of oxygen-enriched gasification products from biomass in a pilot-scale fluidized bed,” *Int. J. Hydrogen Energy*, vol. 43, no. 31, pp. 14214–14225, 2018, https://doi.org/10.1016/j.ijhydene.2018.05.154

References

1. V. K. Yadav *et al.*, “Emerging trends in the valorization of agricultural waste and their utilization in agricultural, pharmaceuticals, and environmental cleanup,” *Waste and Biomass Valorization*, pp. 1–55, 2025. DOI:10.1007/s12649-025-03002-y
2. W. M. Lewandowski, M. Ryms, and W. Kosakowski, “Thermal biomass conversion: A review,” *Processes*, vol. 8, no. 5, p. 516, 2020. https://doi.org/10.3390/pr8050516
3. D. Ariyanti *et al.*, “Valorization of corn cob waste for furfural production: A circular economy approach,” *Biomass and Bioenergy*, vol. 194, p. 107665, 2025. DOI:10.1016/j.biombioe.2025.107665
4. J. Zhang, Z. Chu, R. Cao, X. Wu, and K. Han, “A review of resource recovery from waste plastics via pyrolysis and gasification,” *Fuel*, vol. 404, p. 136319, 2026. https://doi.org/10.1016/j.fuel.2025.136319
5. Y. Tangke Tosuli, Cahyadi, H. Dafiqurrohman, R. Hermawan, and A. Surjosatyo, “Gasification of sago dreg waste in a top-lit updraft fixed bed gasifier: Syngas composition and its effect with additional Al2O3 as catalyst,” *Energy Convers. Manag. X*, vol. 24, no. October, p. 100775, 2024, doi: 10.1016/j.ecmx.2024.100775. https://doi.org/10.1016/j.ecmx.2024.100775
6. P. Dinh *et al.*, “Enrichment of hydrogen in product gas from a pilot-scale rice husk updraft gasification system,” *Carbon Resour. Convers.*, vol. 5, no. 3, pp. 231–239, 2025, doi: 10.1016/j.crcon.2022.07.003.
7. S. Yousef and J. Eimontas, “International Journal of Hydrogen Energy Oxygen updraft gasification-catalytic reforming of cigarettes butts for hydrogen-rich syngas production,” vol. 171, no. May, 2025, https://doi.org/10.1016/j.ijhydene.2025.150650
8. D. Contreras, E. Blanco, and D. Travieso, “Experimental assessment of the energy potential of pellets produced from beekeeping wastes by updraft gasification,” vol. 343, no. January, 2025, https://doi.org/10.1016/j.enconman.2025.120206
9. N. Yesilova, O. Tezer, A. Ongen, and A. Ayol, “International Journal of Hydrogen Energy Enhancing biomass gasification : A comparative study of catalyst applications in updraft and modifiable-downdraft fixed bed reactors,” *Int. J. Hydrogen*

Energy, vol. 76, no. April, pp. 290–303, 2024, https://doi.org/10.1016/j.ijhydene.2024.05.075

10. R. Skvor and A. Jan, "Experimental investigation of sorted municipal solid wastes producer gas composition in an updraft fixed bed gasifier," vol. 289, no. August 2022, 2024, https://doi.org/10.1016/j.energy.2023.130063

11. R. Junga, M. Tańczuk, S. Sobek, M. Chabiński, and Ł. Ziółkowski, "Effect of the addition of laying hens manure to the straw on gasification efficiency in updraft gasifier under air atmosphere," *Appl. Therm. Eng.*, vol. 226, no. February, p. 120269, 2023, https://doi.org/10.1016/j.applthermaleng.2023.120269.

12. A. Ongen and A. Ayol, "ScienceDirect Gasification performance of olive pomace in updraft and downdraft fixed bed reactors," vol. I, 2023, https://doi.org/10.1016/j.ijhydene.2023.02.088

13. K. Ertas, "Gasification of MDF residue in an updraft fixed bed gasifier to produce heat and power via an ORC turbine," vol. 169, no. February, pp. 43–51, 2023, https://doi.org/10.1016/j.wasman.2023.06.025

14. S. Gorthy, S. Verma, N. Sinha, S. Shetty, H. Nguyen, and M. Neurock, "Theoretical Insights into the Effects of KOH Concentration and the Role of OH–in the Electrocatalytic Reduction of CO2 on Au," *ACS Catal.*, vol. 13, no. 19, pp. 12924–12940, 2023. DOI:10.1021/acscatal.2c06115

15. X. Wang, W. Zeng, C. Xin, X. Kong, X. Hu, and Q. Guo, "The development of activated carbon from corncob for CO2 capture," *RSC Adv.*, vol. 12, no. 51, pp. 33069–33078, 2022, https://doi.org/10.1039/D2RA05979G

16. B. Zhou *et al.*, "Insights into effects of grain boundary engineering in composite metal oxide catalysts for improving catalytic performance," *J. Colloid Interface Sci.*, vol. 653, pp. 1177–1187, 2024. https://doi.org/10.1016/j.jcis.2023.09.148

17. Y. Zhu *et al.*, "Preparation of hierarchically porous carbon ash composite material from fine slag of coal gasification and ash slag of biomass combustion for CO2 capture," *Sep. Purif. Technol.*, vol. 330, p. 125452, 2024. https://doi.org/10.1016/j.seppur.2023.125452

18. M. Ilić *et al.*, "Surface functional groups and degree of carbonization of *selected* chars from different processes and feedstock," *PLoS One*, vol. 17, no. 11, p. e0277365, 2022. https://doi.org/10.1371/journal.pone.0277365

19. R. Ali, Z. Aslam, R. A. Shawabkeh, A. Asghar, and I. A. Hussein, "BET, FTIR, and RAMAN characterizations of activated carbon from waste oil fly ash," *Turkish J. Chem.*, vol. 44, no. 2, pp. 279–295, 2020. doi: 10.3906/kim-1909-20

20. K. J. Stanienda-Pilecki, "The importance of Fourier-Transform Infrared Spectroscopy in the identification of carbonate phases differentiated in magnesium content," 2019.

21. F. Dai, Q. Zhuang, G. Huang, H. Deng, and X. Zhang, "Infrared spectrum characteristics and quantification of OH groups in coal," *ACS omega*, vol. 8, no. 19, pp. 17064–17076, 2023. https://doi.org/10.1021/acsomega.3c01336

22. E. M. de Salazar Martínez, M. F. Alexandre-Franco, A. J. Nieto-Sanchez,

and E. M. Cuerda-Correa, “Exploring the role of surface and porosity in CO2 capture by CaO-based adsorbents through response surface methodology (RSM) and artificial neural networks (ANN),” *J. CO2 Util.*, vol. 83, p. 102773, 2024. https://doi.org/10.1016/j.jcou.2024.102773

23. J. A. Tavizón-Pozos, H. Cervantes-Cuevas, G. G. Garcia-Camacho, G. Chavez-Esquivel, and D. R. Acosta-Najarro, “Biodiesel Production Using K–Sr/CaO and CaO Catalysts Derived from Eggshells by Canola Oil Transesterification,” *ACS omega*, vol. 10, no. 7, pp. 6827–6838, 2025. https://doi.org/10.1021/acsomega.4c09118

24. W. Koo-Amornpattana, P. Phadungbut, N. Kunthakudee, W. Jonglertjunya, S. Ratchahat, and M. Hunsom, “Innovative metal oxides (CaO, SrO, MgO) impregnated waste-derived activated carbon for biohydrogen purification,” *Sci. Rep.*, vol. 13, no. 1, p. 4705, 2023. DOI:10.1038/s41598-023-31723-4

25. C. Quan, M. Wang, N. Gao, T. Yang, and R. Li, “In situ adsorption of CO2 to enhance biomass gasification for hydrogen production using Ca/Ni based composites,” *J. Energy Inst.*, vol. 108, p. 101229, 2023, doi: https://doi.org/10.1016/j.joei.2023.101229. https://doi.org/10.1016/j.joei.2023.101229

26. F. Micheli, E. Mattucci, C. Courson, and K. Gallucci, “Bi-Functional Catalyst/Sorbent for a H2-Rich Gas from Biomass Gasification,” 2021. doi: 10.3390/pr9071249. DOI:10.3390/PR9071249

27. M. Zhu, Q. Wang, and S. Wang, “Recent Advances and Future Perspectives in Catalyst Development for Efficient and Sustainable Biomass Gasification: A Comprehensive Review,” 2025, https://doi.org/10.3390/su17167370

28. N. Cerone, F. Zimbardi, L. Contuzzi, J. Baleta, and D. Cerinski, “Experimental investigation of syngas composition variation along updraft fixed bed gasifier,” *Energy Convers. Manag.*, vol. 221, no. July, p. 113116, 2020, https://doi.org/10.1016/j.enconman.2020.113116

29. R. Mohanty, P. Mahanta, A. Mahapatro, and R. Prakash, “Catalytic gasification of pinewood biomass in a fluidized bed reactor with dolomite , limestone , and activated carbon : An experimental study,” *Energy*, vol. 325, no. April, p. 136131, 2025, doi: 10.1016/j.energy.2025.136131. https://doi.org/10.1016/j.energy.2025.136131

30. C. Liu, Y. Huang, M. Niu, and H. Pei, “ScienceDirect Influences of equivalence ratio , oxygen concentration and fluidization velocity on the characteristics of oxygen-enriched gasification products from biomass in a pilot-scale fluidized bed,” *Int. J. Hydrogen Energy*, vol. 43, no. 31, pp. 14214–14225, 2018, https://doi.org/10.1016/j.ijhydene.2018.05.154

Author’s order	First Name	Middle name	Second Name
1	*Purbo*		*Suwandono*
2	*Widya*		*Wijayanti*
3	*Nova*	*Risdiyanto*	*Ismail*
4	*Dzulfikar*	*Johan*	*Akbar*

5	*Muhammad*		*Reza*

English

Purbo Suwandono
Corresponding author
Master
Department of Mechanical Engineering
Widya Gama University
Borobudur str., 35, Malang, Indonesia, 65142
E-mail: purbo@widyagama.ac.id
ORCID: https://orcid.org/0000-0003-4085-1291
Contact phone: +6282132697144
Number of publications in national journals indexed (approximate; for Ukraine citizens only): -
Number of publications in international journals indexed (approximate): 14
H-index by Scopus (if available): 4
ResearchGate: https://www.researchgate.net/profile/Purbo-Suwandono
Scopus ID: 57204187970
Researcher ID: https://researchid.co/rid80879

Widya Wijayanti
PhD
Department of Mechanical Engineering
Brawijaya University
Veteran str., 10–11, Malang, Indonesia, 65145
E-mail: widya_dinata@ub.ac.id
ORCID: https://orcid.org/0000-0003-4215-5943
Contact phone: +6285334992164
Number of publications in national journals indexed (approximate; for Ukraine citizens only): -
Number of publications in international journals indexed (approximate): 78
H-index by Scopus (if available): 12
ResearchGate: https://www.researchgate.net/profile/Widya-Wijayanti
Scopus ID: 36006672800
Researcher ID: -

Nova Risdiyanto Ismail
PhD
Department of Mechanical Engineering
Widya Gama University
Borobudur str., 35, Malang, Indonesia, 65142

E-mail: nova@widyagama.ac.id
ORCID: https://orcid.org/0000-0001-8439-6919
Contact phone:
Number of publications in national journals indexed (approximate; for Ukraine citizens only): -
Number of publications in international journals indexed (approximate): 7
H-index by Scopus (if available): 3
ResearchGate: https://www.researchgate.net/profile/Nova-Ismail-2
Scopus ID: 57204527065
Researcher ID: https://researchid.co/rid80876

Dzulfikar Johan Akbar
Master Student
Department of Mechanical Engineering
Brawijaya University
Veteran str., 10–11, Malang, Indonesia, 65145
E-mail: johanakbar@student.ub.ac.id
ORCID: https://orcid.org/0009-0002-4652-8516
Contact phone: +6282241116998
Number of publications in national journals indexed (approximate; for Ukraine citizens only): -
Number of publications in international journals indexed (approximate): -
H-index by Scopus (if available): -
ResearchGate: https://www.researchgate.net/profile/Dzulfikar-Johan-Akbar
Scopus ID: -
Researcher ID: -

Muhammad Reza
Bachelor Student
Department of Mechanical Engineering
Widya Gama University
Borobudur str., 35, Malang, Indonesia, 65142
E-mail: muhapanjangreza@gmail.com
ORCID: https://orcid.org/0009-0009-9258-0586
Contact phone: +6282139682566
Number of publications in national journals indexed (approximate; for Ukraine citizens only): -
Number of publications in international journals indexed (approximate): -
H-index by Scopus (if available): -
ResearchGate: -
Scopus ID: -

Researcher ID: -

Name of reviewer: Prof. Dr. Muji Setiyo, ST., MT.
Professor: Mechanical Engineering
Tel: +6281211020288
E-mail: muji@unimma.ac.id.
Work address: Universitas Muhammadiyah Magelang

Name of reviewer: Prof. Dr. Eng. Nurkholis Hamidi, ST., MT.
Professor: Mechanical Engineering
Tel: +62 81259293165
E-mail: hamidy@ub.ac.id
Work address: Brawijaya University

REVISI REVIEW EDITOR

Received date: 20.02.2026
Accepted date:

UDC

ПОКРАЩЕННЯ ЯКОСТІ СИНТЕЗ-ГАЗУ ПРИ ВИСХІДНІЙ ГАЗИФІКАЦІЇ КУКУРУДЗЯНИХ КАЧАНІВ З ВИКОРИСТАННЯМ КАТАЛІЗАТОРА НА ОСНОВІ CAO/АКТИВОВАНОГО ВУГІЛЛЯ НА ПАЛЬМОВОМУ ВОЛОКН

Purbo Suwandono, Widya Wijayanti, Nova Risdiyanto Ismail, Dzulfikar Johan Akbar, Muhammad Reza

SYNGAS QUALITY IMPROVEMENT IN CORNCOB UPDRAFT GASIFICATION USING CAO/ACTIVATED CARBON PALM FIBER CATALYST

Purbo Suwandono, Widya Wijayanti, Nova Risdiyanto Ismail, Dzulfikar Johan Akbar, Muhammad Reza

Об’єктом даного дослідження є поліпшення якості синтез-газу, отриманого в результаті газифікації кукурудзяних качанів за допомогою системи з подвійним каталізатором, що складається з CaO та активованого вугілля, отриманого з пальмового волокна (AC–PF). Проблема, вирішена в даному дослідженні, полягає у відносно низькій теплотворній здатності синтез-газу з кукурудзяних качанів та високій вартості традиційних каталізаторів, що використовуються для його поліпшення. Дослідження проводилося з використанням різних значень еквівалентного співвідношення (0,2; 0,25; 0,3; 0,35), навантаження каталізатора (4%; 6%; 8%; 10%) та масового співвідношення CaO/AC–PF (0:1; 1:0; 1:1; 2:1) у поєднанні з характеристикою подвійної каталітичної системи. Отримані результати показують, що збільшення ER збільшує частки H_2 і CH_4 та нижчу теплоту згоряння синтез-газу, одночасно зменшуючи CO_2, причому CO досягає оптимального значення при ER = 0,3. У той час як більш високе навантаження каталізатора має тенденцію до зменшення H_2 і CH_4, але збільшує CO, потенційно знижуючи теплоту згоряння при високих навантаженнях Характеристика каталізатора показує, що AC-PF має пористу структуру, яка збільшує контакт газу з твердим тілом і сприяє вторинним реакціям, тоді як додавання CaO утворює композит із модифікованою структурою пор і поверхневими видами, пов'язаними з сорбцією CO_2. З енергетичної точки зору, нижня теплота згоряння синтез-газу збільшується із зростанням ER, але зменшується при більш високих навантаженнях каталізатора через зменшення внеску CH_4. Ключовою особливістю отриманих результатів є продемонстрована функціональна синергія між пористим AC–PF і сорбцією CO_2 на основі CaO, що дозволяє одночасно

здійснювати каталітичне поліпшення якості та уловлювання CO_2 в єдиній, недорогій системі з подвійним каталізатором. Ці висновки можуть стати практичною основою для проектування та експлуатації невеликих установок газифікації біомаси, зокрема реакторів з висхідним потоком для відходів кукурудзяних качанів, в межах досліджених діапазонів ER та навантаження каталізатора.

Ключові слова: газифікація, висхідний потік, кукурудзяні качани, синтез-газ, CaO, активоване вугілля.

The object of this study is the improvement of syngas quality from updraft corn cob gasification using a dual catalyst system consisting of CaO and activated carbon derived from palm fiber (AC–PF). The problem solved in this study is the relatively low heating value of corn cob syngas and the high cost of conventional catalysts used for its upgrading. The study was conducted using variations of equivalence ratio (0.2, 0.25, 0.3, 0.35), catalyst loading (4%, 6%, 8%, 10%), and CaO/AC–PF mass ratio (0:1, 1:0, 1:1, 2:1), combined with characterization of the dual catalyst system. The results obtained show that increasing ER increases the H_2 and CH_4 fractions and the syngas lower heating value while decreasing CO_2, with CO reaching an optimum at ER = 0.3. Whereas higher catalyst loading tends to decrease H_2 and CH_4 but increase CO, potentially reducing the heating value at high loadings Characterization of the catalyst shows that AC-PF has a porous structure that increases gas-solid contact and promotes secondary reactions, while the addition of CaO forms a composite with a modified pore texture and surface species associated with CO_2 sorption. From an energy perspective, the Lower Heating Value of syngas increases with increasing ER, but decrease at higher catalyst loadings due to the reduced contribution of CH_4. A key feature of obtained results is the demonstrated functional synergy between porous AC–PF and CaO-based CO_2 sorption, which enables simultaneous catalytic upgrading and CO_2 capture in a single, low-cost dual catalyst system. These findings could be a practical basis for designing and operating small-scale biomass gasification units, particularly updraft reactors for corn cob waste, within the studied ER and catalyst loading ranges

Keywords: gasification, updraft, corncob, syngas, CaO, activated carbon

1. Introduction

Indonesia is one of the largest corn producers in Southeast Asia, with national production reaching more than 18 million tons of dry kernels per year. Of this amount, about 15–20% is cobs after the kernel removal process, resulting in a very large amount of corn cob waste, estimated at 2.5–3.5 million tons annually. Until now, most corn cobs have only been used to a limited extent, for example as traditional fuel, small amounts of animal feed, or even burned directly on post-harvest land, which has the potential to cause air pollution. Most of the rest are simply piled up or left to rot on the land, posing a risk of becoming a source of plant disease [1].

Corn cobs have quite promising chemical and energy characteristics. Their composition is dominated by cellulose, hemicellulose, and lignin, with a calorific value of around 15–17 MJ/kg, making them very suitable as raw materials in various biomass-based energy conversion technologies [2]. Their hard and fibrous nature also makes them suitable for processing into biochar, activated charcoal, or direct use in pyrolysis and gasification processes. This significant potential indicates that corn cobs are not merely waste but a renewable resource that can be optimized to support energy security and reduce dependence on fossil fuels.

Biomass gasification is a promising thermochemical technology for converting renewable resources into syngas consisting of H_2, CO, CH_4, and CO_2. Of the various types of biomass, corn cobs are a potential candidate due to their abundant availability in Indonesia and lignocellulose content that supports the energy conversion process [3]. However, the biomass gasification process still faces several obstacles, particularly the low hydrogen fraction in syngas and the formation of significant amounts of tar. Tar can cause reactor clogging, reduced thermal efficiency, and increased purification costs.

To overcome these problems, the use of catalysts is an important strategy. A number of studies have proven that metal catalysts such as Ni, Ca, and K can increase hydrogen yield while suppressing tar formation. On the other hand, activated carbon is also widely used as a catalyst support because it has a high surface area, porous structure, and good chemical stability. The use of agricultural waste, particularly palm fiber, as raw material for activated carbon is not only economically valuable but also supports the concept of a circular economy in plantation waste management. In addition, calcium oxide (CaO) is known to have a dual role, namely as a catalyst in the tar decomposition reaction and as a CO_2 absorber that promotes sorption-enhanced gasification to increase the hydrogen fraction in syngas [4].

Although various studies have examined the role of metal catalysts and activated carbon separately, research focusing on the combination of biomass bases catalyst such as palm fiber-based activated carbon with CaO in corn cob gasification is still limited. The uniqueness of this study lies in the integration of two catalyst, which is expected to provide a synergistic effect: activated carbon with high porosity increases catalyst dispersion and activity, while CaO simultaneously breaks down tar and absorbs CO_2. This approach has the potential to significantly increase hydrogen production and reduce carbon emissions.

However, there are several research gaps that remain unanswered. First, the optimal composition and ratio of activated carbon and CaO in corn cob gasification have not been extensively studied. Second, the synergistic mechanism using two catalyst in increasing syngas quality not yet fully understood. In addition, a systematic and statistically robust approach is required to disentangle the coupled effects of key operating and catalyst variables.

Based on this background and research gaps, this study aims to investigate the performance of a composite catalyst based on activated carbon from palm fiber combined with CaO in the corn cob gasification process. The main focus is on

increasing hydrogen production, reducing tar, and evaluating the potential synergistic effects between materials. This research is expected to contribute to the development of low-cost, locally sourced, and sustainable catalyst systems that are relevant to supporting the clean energy transition and practical applications of biomass-to-hydrogen in the future.

2. Literature review and problem statement

The paper [5] presents the result on the gasification of sago dreg waste pellets in a top-lit updraft fixed-bed gasifier. The results show that the addition of Al_2O_3 improved syngas quality, especially by increasing H_2 content up to 31.65% at 5% Al_2O_3 and enhancing CO and CH_4 production, while also increasing the H_2/CO ratio to 1.65 and 1.51 for 5% and 10% Al_2O_3, respectively, improving LHV, and reducing tar content by about 25–27.5% compared with pellets without catalyst. However, this study is limited because it was conducted only on one biomass type, within a laboratory-scale TULD fixed-bed gasifier, and only considered two catalyst loadings.

The paper [6] presents the result on hydrogen enrichment in product gas from a pilot-scale rice husk updraft gasification. The results show that dolomite-assisted air gasification gave the best performance, increasing the H_2 content up to 15.4 mol%, with an LHV of 5.1 MJ/Nm³, while steam/air gasification improved H_2 to 9.6 mol% and air alone produced only about 7.08 mol% H_2, the optimum operating condition was reported at an airflow rate of 3 m³/h and a dolomite mixing ratio of 15 wt%. However, this study is limited because it focused only on rice husk feedstock, used a pilot-scale updraft gasifier with a batch capacity of 3 kg, and evaluated only a limited range of operating conditions and catalyst type.

The paper [7] presents the result on oxygen updraft gasification coupled with catalytic steam reforming of cigarette butts for hydrogen-rich syngas production. The results show that the integrated process was effective in converting cigarette butts into syngas, with gasification producing 82.3–89.7 wt.% syngas, 6.3–8.6 wt.% soot, and 1.4–1.9 wt.% tar, while the catalytic reforming stage significantly improved the gas quality by increasing the H_2 content up to 30.27 vol.%, increasing the HHV up to 11,528 kJ/kg, and reducing tar concentration from about 18.15 g/m³ to 13.38 g/m³ under the optimum condition. However, this study is limited because it investigated only cigarette butt waste as feedstock, used a specific oxygen updraft gasifier–catalytic reformer configuration, and fixed most catalytic reforming parameters.

The paper [8] presents the result on the experimental assessment of pellets produced from beekeeping waste and slumgum–pine sawdust mixtures through updraft gasification. The results show that pure slumgum pellets exhibited very high mechanical durability (99.98%) and high HHV (27.66 MJ/kg), while during gasification the 50% slumgum–50% sawdust pellets produced the highest producer gas LHV of 7.62 MJ/Nm³, indicating that the addition of sawdust improved gas quality and energy recovery potential. However, this study is limited because the equivalence ratio remained very

low (0.0125–0.0204) compared with typical gasification conditions, the experiments were conducted only in a modified laboratory-scale updraft gasifier.

The paper [9] presents the result on a comparative investigation of catalyst applications in updraft and modifiable-downdraft fixed-bed biomass gasifiers, using a biomass mixture of green waste, sewage sludge, and olive pomace together with red mud (RM) and Al–Ni alloy catalysts to improve syngas quality and hydrogen production. The results show that catalyst type and reactor configuration strongly influenced gasification performance, with the Al–Ni catalyst giving the best hydrogen enrichment, reaching up to 65 vol.% H_2 in the updraft gasifier at 900 °C, while RM increased H_2 to about 50 vol.%, the updraft gasifier produced better hydrogen-rich syngas than the modifiable-downdraft reactor. However, this study is limited because it, used a specific mixed biomass composition and mainly focused on high temperature operation around 900 °C with limited gasifying-agent flow conditions.

The paper [10] presents the result on the experimental investigation of producer gas composition from sorted municipal solid wastes in an updraft fixed-bed gasifier. The results show that reducing the equivalence ratio from 0.21 to 0.15 increased the heating value of the combustible gases. The study indicated that the allothermal updraft fixed-bed gasifier is suitable for producing gas that can be utilized in gas engines. However, this study is limited because it used a laboratory-scale 10 kW allothermal updraft gasifier at a fixed temperature of 800 °C, and evaluated only two ER conditions.

The paper [11] presents the result on the effect of adding laying hens manure (LHM) to wheat straw on gasification efficiency in an air-blown updraft fixed-bed gasifier. The results show that increasing ER improved the gasification performance, with the producer gas LHV reaching 3.3–3.4 MJ/m^3, cold gas efficiency around 60%, and carbon conversion efficiency in the range of 82–94% . However, this study is limited because it was focused on one specific co-feed system and produced a relatively low-calorific gas.

The paper [12] presents the result on the gasification performance of olive pomace in updraft and downdraft fixed-bed reactors using dry air and pure oxygen. The results show that updraft reactor achieving up to 48 vol.% H_2 with dry air and 53 vol.% H_2 with pure oxygen, while the downdraft reactor reached up to 45 vol.% H_2 with dry air and 39 vol.% H_2 with pure oxygen. However, this study is limited because only a limited range of gasifying agents, temperatures, and flow rates.

The paper [13] presents the result on the gasification of MDF residue in an industrial-scale updraft fixed-bed gasifier. The results show that MDF residue can be effectively converted into useful energy, with a syngas production rate of about 2.5 Nm^3/kg, syngas LHV of around 6.0–7.0 MJ/Nm^3, about 88 wt.% of MDF residue converted into syngas, and a system capable of delivering 7 MWth of thermal energy and about 955 kW net electrical power through the ORC turbine. However, this study is limited because it focused on one specific industrial waste stream (MDF residue) in one updraft gasifier configuration, mainly evaluated performance under a limited number of feed rates, and relied on direct combustion of raw hot syngas containing tar.

The paper presents the results of research on biomass gasification in updraft fixed-bed reactors aimed at improving syngas quality and thermal conversion efficiency. Shown that syngas composition and heating value are strongly influenced by feedstock properties, gasification conditions, and catalyst application. But there were unresolved issues related to the lack of effective and low-cost catalyst systems capable of simultaneously enhancing hydrogen formation and improving overall syngas quality during corncob gasification. The reason is the complexity of catalytic reactions in the gasification zone, including reforming, cracking, and CO_2 capture mechanisms, as well as the economic limitations of commercially available catalysts. A way to overcome these difficulties can be the development of composite catalysts based on CaO and activated carbon palm fiber, where CaO may promote CO_2 absorption and shift reactions, while activated carbon palm fiber may provide a porous surface and active sites for secondary cracking reactions. This approach was used in previous studies, however, the combined use of CaO and activated carbon palm fiber in corncob updraft gasification has not been sufficiently investigated. All this suggests that it is advisable to conduct a study on syngas quality improvement in corncob updraft gasification using CaO/activated carbon palm fiber catalyst.

3. The aim and objectives of the study

The purpose of the study is to enhance syngas quality from corncob updraft gasification by developing a dual-synergy catalytic system based on calcium oxide (CaO) and palm-fiber-derived activated carbon (AC-PF). This will allow the production of cleaner and more energy-dense producer gas, providing practical guidance for selecting operating conditions and catalyst configurations suitable for updraft gasifiers processing agricultural residues.

To achieve these aims, the following objectives are accomplished:

– to synthesize and characterize the CaO and palm-fiber activated carbon catalysts using Fourier Transform Infrared Spectroscopy (FTIR), scanning electron microscopy (SEM) and Brunauer-Emmett-Teller surface area analysis (BET);

– to investigate the effects of operating parameters, particularly equivalence ratio (ER), catalyst loading, and CaO/AC ratio, on syngas composition H_2, CO, CH_4, CO_2 and LHV.

4. Materials and methods

The object of the study is the updraft fixed-bed gasification process of corncob biomass using a dual catalyst system based on calcium oxide (CaO) and palm-fiber-derived activated carbon (AC-PF). The practical physical process under investigation is the catalytic upgrading of producer gas within the updraft reactor, where changes in operating parameters and catalyst configuration are expected to influence syngas composition and heating value. The results of this study are intended to be applied to improve the quality of syngas, specifically by increasing the combustible gas fraction (H_2 and CH_4) and the lower heating value (LHV), while reducing CO_2 content.

The research hypothesis is that a dual-synergy CaO/AC-PF catalytic system can improve syngas quality more effectively than single-catalyst configurations in updraft corncob gasification. It is hypothesized that CaO functions as a CO_2 sorbent, shifting reaction equilibria toward enhanced hydrogen formation, while activated carbon derived from palm fiber provides high-surface-area catalytic sites that promote secondary reactions such as tar cracking and volatile reforming. The combined catalytic-sorption mechanism is expected to increase H_2 and CH_4 fractions and improve LHV under optimized equivalence ratio (ER), catalyst loading, and CaO/AC-PF ratio conditions.

It was assumed that the corncob feedstock has relatively homogeneous composition and stable proximate/ultimate characteristics during the experiments. The gasification process was assumed to operate under steady-state conditions after stabilization. It was also assumed that the CaO maintains sufficient CO_2 sorption capacity within the experimental time frame and that the activated carbon structure remains stable under the applied temperature range.

During the course of the research, several methodological simplifications were adopted in order to maintain experimental feasibility and focus on the main objective of syngas quality evaluation. Detailed kinetic modeling of individual gasification reactions was not performed; instead, the process performance was assessed based on experimentally measured syngas composition and syngas low heating value. Furthermore, although CaO carbonation-decarbonation reactions may occur during operation, microstructural evolution, sintering behavior, and long-term cyclic stability of the catalyst were not investigated in this study. The catalytic performance was evaluated within the experimental duration without conducting extended durability or regeneration-cycle analysis.

4. 1. Catalyst Preparation

Approximately 6 grams of ground palm fiber was mixed with 60 mL of distilled water and stirred for 10 minutes. The mixture was then placed in an autoclave and heated to 200°C at a rate of 5°C per minute for 6 hours in an electric oven. After that, the reactor is allowed to cool naturally to room temperature. The resulting solid hydrocarbon product (hydrochar) is then separated using Whatman No. 42 filter paper. The filtered product is then dried at 105°C for 24 hours and stored in a glass vial. The next stage is the activation process. The hydrochar is immersed in a 3 M KOH solution with a weight ratio of 1:3 (Hydrochar:KOH) for 16 hours, then dried at 85°C for 6 hours. Spectroscopic evidence indicates that KOH preferentially reacts with oxygenated sites and can increase the relative abundance of C–OH functionalities, while higher KOH ratio and activation temperature significantly enhance porosity and BET surface area [14, 15]. To obtain the CaO/AC mixture, CaO powder and activated carbon (AC) were mixed in specific proportions using a grinder until a homogeneous mixture was obtained. Next, CaO, AC, and CaO/AC were activated using a tube furnace at a temperature of 700°C for 1 hour with a continuous flow of nitrogen during the activation

process. The resulting product was then washed using distilled water until it reached a neutral pH. This stage produced activated carbon that was ready for use in research.

4. 2. Experimental Setup

Corncob biomass was obtained from farmers in the South Malang region of East Java. Before use, the biomass was cleaned of impurities and dried in an oven for 6 hours at 100°C to remove moisture (water vapor) content. The ultimate and proximate test results are as follows.

The proximate and ultimate analyses of the corncob feedstock were conducted to determine its physicochemical characteristics prior to gasification. The results are presented in Table 1. The data indicate that corncob has high volatile matter content and relatively low ash content, which are favorable characteristics for gasification processes.

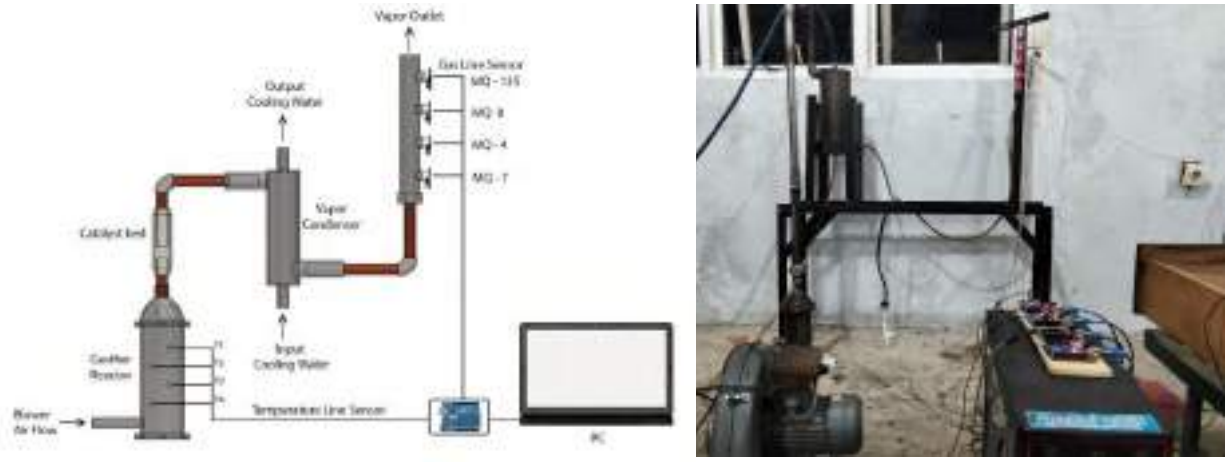
There must be a reference to the Fig. 1 in the text before the Figure

Table 1

Ultimate and Proximate Test Corn Cob

Parameter	Units	Corn cobs
Moisture	%	10
Volatile matter	%	71.38
Fixed carbon	%	12.11
Ash	%	6.51
C	%	43.6
H	%	6.3
O	%	46.8
N	%	0.22
HHV	MJ/kg	17.61

The experimental apparatus employed in this study consisted of an updraft gasifier integrated with a catalyst bed, a vapor condensation unit, gas sensors, and temperature measurement points to enable comprehensive monitoring of the gasification process. Fig. 1 shows the updraft gasifier system used in this study, including the schematic experiment (a) and the experimental setup (b).



a *b*

Fig. 1. Updraft gasifier: *a* – schematic experiment; *b* – experimental setup

This study used an updraft gasification reactor designed with a total height of 20 cm. The lower part of the reactor consisted of an ash container with a height of 5 cm, while the active reactor had a height of 15 cm and a diameter of 3 inches. The reactor was equipped with a 1-inch diameter air inlet pipe connected to a blower. The blower was modified with a potentiometer so that the air speed could be adjusted as needed. To monitor the thermal conditions inside the reactor, four 3 cm long type K thermocouples were installed at several different points so that the temperature profile in the gasification zone could be observed in more detail. Each test was conducted with a fixed biomass mass, a mixture of corn cobs weighing 80 grams. The reactor was made of iron and equipped with a gas seal to prevent leaks during the gasification process.

The gas produced by the reactor was fed into a condenser, which cooled the hot gas so that the water vapor components could be separated. The condenser was made of a copper spiral pipe with a diameter of ½ inch and a height of 30 cm. Cooling water was circulated from the bottom of the condenser and exited through the top to ensure efficient heat transfer. This cooling system was driven by a 60-watt water pump, ensuring stable water flow and optimal condensation. The catalyst was positioned downstream after the reactor, where it was supported on steel wool and wrapped with an 80-µm wire mesh to secure the catalyst and prevent particle carryover with the gas flow

To analyse the gas composition, four types of MQ gas sensors were used. The MQ-8 sensor was used to detect H_2, MQ-4 for CH_4, MQ-135 for CO_2 and MQ-7 for CO. Each gas sensor was calibrated according to the manufacturer's datasheet, specifically by determining the Ro value, which is the sensor resistance in clean air conditions. This Ro value is used as a reference in calculating the measured gas concentration during the process.

All data from the gas sensors and thermocouples were acquired using an Arduino Uno microcontroller. Each gas sensor is connected to a separate Arduino Uno to facilitate the calibration process and reduce the possibility of interference between

sensors. Arduino is also used to record temperature data from four thermocouples installed in the reactor, so that gas composition and temperature distribution data can be obtained simultaneously.

The ER range of 0.2, 0.25, 0.3 and 0.35. The catalyst load was between 4%, 6%, 8% and 10% from the mass of input feedstock. The CaO/AC-PF ratio was varied between 0:1, 1:0, 1:1, and 2:1. Design of experiment can be seen in Table 2.

Table 2
Design of Experiment using

Run	Equivalence Ratio (E.R)	Catalyst Load %	CaO/AC
1	0.2	4	1:0
2	0.2	6	0:1
3	0.2	8	1:1
4	0.2	10	2:1
5	0.25	4	0:1
6	0.25	6	1:0
7	0.25	8	2:1
8	0.25	10	1:1
9	0.3	4	1:1
10	0.3	6	2:1
11	0.3	8	1:0
12	0.3	10	0:1
13	0.35	4	2:1
14	0.35	6	1:1
15	0.35	8	0:1
16	0.35	10	1:0

A total of 16 experimental runs were conducted systematically to enable evaluation of the main effects of each variable and the tendency of interactions between variables on the fractions of H_2, CO, CH_4, CO_2, and lower heating value (LHV). This approach enabled identification of the most effective combination of operating parameters in improving syngas quality quantitatively and measurably.

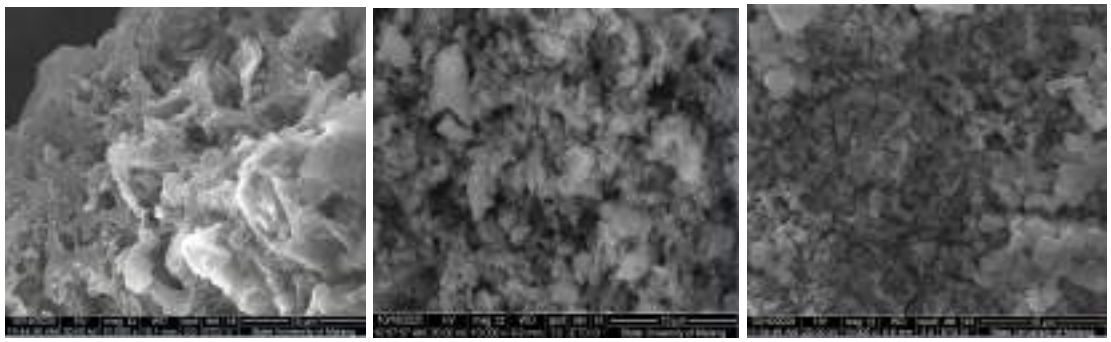
5. Results of syngas quality enhancement from corncob using calcium oxide (CaO) and palm-fiber-derived activated carbon (AC–PF).

5. 1. Characterization of Calcium Oxide (CaO) and Palm-Fiber-Derived Activated Carbon (AC–PF) Catalysts

5. 1. 1. Scanning Electron Microscopy Catalyst Result

Fig. 2, *a* shows the image obtained from a Scanning Electron Microscope (SEM) with a magnification of 10,000× shows the surface morphology of palm fiber-based activated carbon (AC-PF). The surface structure appears porous and irregular, with a

combination of void areas and layered surfaces. This characteristic indicates that the activation process that using KOH has successfully formed micropores and mesopores, which play an important role in increasing the specific surface area of activated carbon.



a *b* *c*

Fig. 2. Scanning Electron Microscopy Catalyst Result: *a* – Scanning Electron Microscopy AC-PF; *b* – Scanning Electron Microscopy CaO:AC;1:1; *c* – Scanning Electron Microscopy CaO:AC-PF;2:1

The rough and textured surface indicates that most of the material has undergone lignocellulose cell wall exfoliation, resulting in numerous interparticle gaps. This porous structure greatly supports gas adsorption and diffusion capabilities when used as a catalyst in gasification or thermochemical reactions.

The presence of 1–5 µm voids indicates that most pores are in the mesopore category, supporting the adsorption of gas molecules such as H_2, CO, and tar during the gasification reaction.

The morphology of AC-PF shows the characteristics of porous activated carbon with a heterogeneous pore distribution, where the pores allow increased contact between gas reactants and active sites on the material surface, thereby increasing catalytic efficiency and the ability to absorb tar or CO_2 in biomass-based energy applications.

Fig. 2, *b* shows the surface morphology of the CaO:AC-PF catalyst with a ratio of 1:1. Visually, it can be seen that the surface of this material consists of fine particles ranging in size from microns to submicrons that stick together to form a layered and slightly agglomerated structure.

The presence of fine, light-colored grains indicates an even distribution of CaO particles impregnated on the surface of activated carbon (AC-PF). This CaO distribution fills some of the pores of the carbon, resulting in a denser surface compared to pure AC-PF. However, there are still small gaps and voids between the grains, indicating that the microporous and mesoporous structures are still formed and can support catalytic activity [16].

This morphology illustrates the success of the CaO impregnation process on activated carbon from palm fiber, where the interaction between CaO and the carbon

pore walls produces a composite material that is more thermally and chemically stable. This structure is highly conducive to catalyst applications in biomass gasification processes, as CaO particles can function as CO_2 absorbers while accelerating the tar reforming reaction [17].

Fig. 2, *c* shows the surface morphology of the CaO:AC-PF (2:1) catalyst. The image shows that the surface of the material is dominated by agglomerations of fine, round, and irregular particles ranging in size from microns to submicrons. Compared to the CaO:AC-PF (1:1) sample, this structure appears denser and tighter, indicating that an increase in the CaO ratio causes partial closure of the activated carbon surface pores by CaO particles.

The distribution of CaO particles appears more uniform and covers the carbon surface, indicating the successful impregnation of a larger amount of CaO. The light color in some areas indicates the presence of a calcium oxide phase that is strongly attached to the activated carbon matrix. This structure indicates a strong interaction between CaO and AC-PF, forming a thermally stable composite.

Although some pores are covered, there are still microscopic gaps between the CaO grains that allow gas diffusion to occur, so that the catalyst retains its good adsorption capacity. The combination of the active area of CaO and the porous carbon structure makes this material very promising for biomass gasification or tar reforming applications, as CaO can act as a CO_2 absorber and increase the conversion of carbon to hydrogen gas.

5. 1. 2. Fourier Transform Infrared Spectroscopy catalyst result

The FTIR analysis results shown in the Fig. 3 reveal clear spectral differences between the AC-PF, CaO, and their mixtures (CaO:AC-PF) with ratios of 2:1 and 1:1. In the AC-PF spectrum, the absorption band at 2926 cm^{-1} is associated with the stretching vibration of the C–H group from $–CH_2$ or $–CH_3$ (methylene/methyl stretching), which indicates the presence of hydrocarbon chain residues from the lignocellulose structure. The peak at 1577 cm^{-1} indicates the presence of aromatic C=C or C=O stretching, while the band at 1056 cm^{-1} represents C–O stretching from alcohol or ether groups. In addition, the –OH group that appears in the 3500–3600 cm^{-1} region is identified as the result of AC-PF activation using a KOH solution, which causes the formation of hydroxyl groups on the activated carbon surface. This –OH group plays an important role in increasing the surface activity and adsorption capacity of AC-PF as a catalyst support medium [18, 19].

In pure CaO, the intense band at 3639 cm^{-1} is associated with the stretching of the O–H group from $Ca(OH)_2$, which is formed due to the partial hydration of CaO when exposed to humid air. Meanwhile, the absorption bands at 1426 cm^{-1} and 876 cm^{-1} are associated with C–O stretching and CO_3^{2-} bending, respectively, indicating the formation of $CaCO_3$ due to CO_2 adsorption from the air. This shows that CaO is highly reactive to moisture and carbon dioxide in the environment.

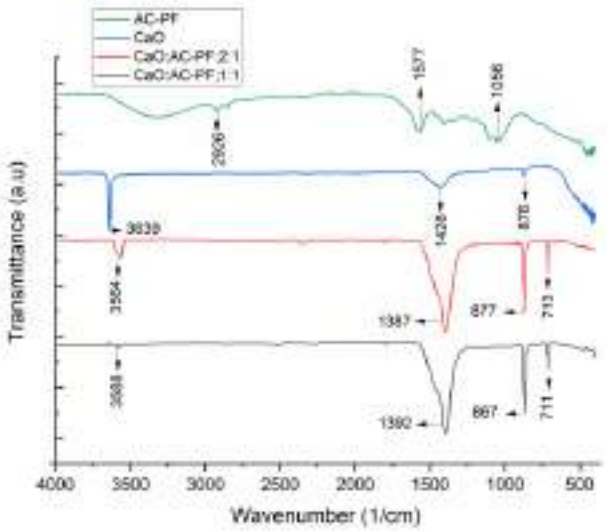


Fig. 3. Fourier Transform Infrared Spectroscopy Catalyst Result

For the CaO:AC-PF (2:1), the main absorption bands were detected at 3564 cm^{-1} (O–H stretching from $Ca(OH)_2$ and the –OH group in AC-PF), 1387 cm^{-1} (C–O stretching), and 877 cm^{-1} and 713 cm^{-1} (bending vibration of CO_3^{2-}). This combination of bands indicates the formation of carbonate compounds ($CaCO_3$) due to the interaction between CaO and the oxygen groups of activated carbon. The presence of –OH groups from KOH activation also strengthens the basic properties on the surface, which can increase the chemical interaction between CaO and AC-PF [20].

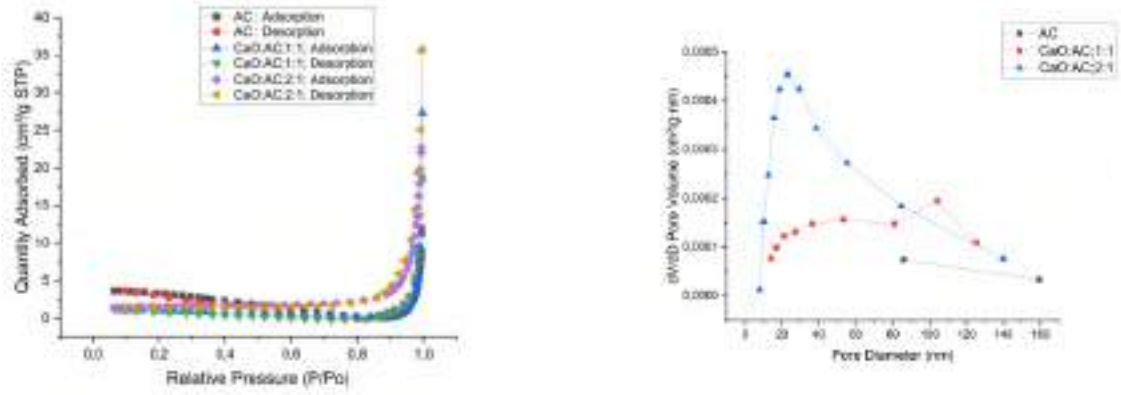
At a CaO:AC-PF ratio of 1:1, the absorption bands at 3588 cm^{-1}, 1392 cm^{-1}, 867 cm^{-1}, and 711 cm^{-1} show a similar pattern, indicating the presence of hydroxyl (O–H) and carbonate (CO_3^{2-}) groups. The difference in peak intensity compared to the 2:1 ratio indicates variations in the level of interaction between CaO and the –OH groups resulting from KOH activation on AC-PF, which affects the formation of carbonate-hydroxide complexes on the material surface [21].

5. 1. 3. Brunauer-Emmett-Teller Catalyst Result

Fig. 4 shows the adsorption-desorption isotherm curves for nitrogen for the AC, CaO:AC (1:1), and CaO:AC (2:1) samples are shown in Fig. 4. All three samples exhibit type IV isotherms with clear hysteresis loops at relatively high pressures (P/Po > 0.9). Based on the IUPAC classification, this characteristic indicates that the material has a mesoporous structure formed through capillary condensation within the pore channels. The difference between the adsorption and desorption pathways indicates that the pore shape is not perfectly cylindrical, but rather tends to be irregular or slit-like, which is commonly found in modified activated carbon materials [22].

The pure activated carbon (AC) sample showed a relatively low nitrogen adsorption volume with a specific surface area of 24.51 m^2/g and an average pore diameter of 0.74 nm, indicating a predominance of microporous structures. In the

CaO:AC (1:1) composite, the surface area did not change significantly compared to pure AC, indicating that the addition of a moderate amount of CaO did not cover the carbon pores much, but only adhered to the external surface of the carbon matrix [23].



a *b*

Fig. 4. Brunauer-Emmett-Teller Result: *a* – Surface Analysis Adsorption Desorption Isotherm; *b* – Barrett-Joyner-Halenda Adsorption Pore Size Distribution

Conversely, in the CaO:AC (2:1) mixture, there was a sharp increase in adsorption volume at relatively high pressure (P/Po > 0.9) to around 35 cm^3/g STP, while the BET surface area decreased dramatically to 5.06 m^2/g, and the pore diameter increased to 22.87 nm.

These changes in isotherm shape and pore size increase indicate that CaO impregnation not only modifies the surface chemistry but also significantly alters the pore structure of activated carbon. This transformation is positive in the context of catalytic applications in biomass gasification processes, as the mesoporous structure can enhance gas diffusion and accessibility to active sites during the tar reforming and water-gas shift reactions. Thus, even though the specific surface area decreases, the increase in mesoporousness and pore connectivity can actually improve catalyst performance in hydrogen gas production [24].

Fig. 4, *b* shows the BJH pore size distribution curves that provide further insight into the textural evolution of the palm-fiber-based activated carbon after CaO impregnation. The pristine AC exhibits a relatively low dV/dD value and a broad contribution only at large pore diameters (>60 nm), indicating that its pore system is dominated by macropores with a limited amount of mesopores. Such a texture is less favourable for gas-solid reactions because the accessible surface area in the mesopore range (2–50 nm) is relatively small.

After CaO loading, the shape and intensity of the BJH curves change markedly. For CaO:AC-PF = 1:1, the distribution shifts toward smaller pore diameters with a pronounced contribution in the mesopore region of approximately 15–60 nm. This behaviour shows that CaO impregnation partially reconstructs the carbon matrix,

enlarging existing micropores and opening blocked pores to generate additional mesoporosity. The effect becomes even more evident at CaO:AC-PF = 2:1, where the curve displays the highest dV/dD values and a distinct maximum centred at about 30–40 nm. The strong peak in this range confirms that a higher CaO loading promotes the development of well-defined mesopores while reducing the relative fraction of very large macropores.

Overall, the BJH analysis demonstrates that CaO acts not only as a reactive sorbent but also as a textural promoter for the palm-fiber AC. The increase in mesopore volume and the shift of the dominant pore size toward 20–40 nm are expected to facilitate the diffusion of gasifying agents and tar molecules, as well as to improve the accessibility of CaO active sites for CO_2 capture and reforming reactions. These features are therefore beneficial for enhancing the catalytic performance of the CaO/AC composite in biomass gasification toward H_2-rich syngas production.

5. 2. Effect of operating parameters on syngas composition and low heating value

5. 2. 1. Effect of Equivalence Ratio on Syngas Product

The composition of syngas from updraft gasification is greatly influenced by the Equivalence Ratio (ER), which is the ratio of the mass flow rate of air compared to the mass flow rate of corncob in the experiment compared to the stoichiometry of air required for complete combustion of corncob. In this study, the ER used was 0.2–0.35 with the following formula

$$ER = \frac{(\dot{m}_a / \dot{m}_{cc})_{\exp}}{(\dot{m}_a / m_{cc})_{stc}},$$

where $\dot{m}_a$ is the air mass flow rate (kg/s), $\dot{m}_{cc}$ is the corncob mass flow rate (kg/s), exp denotes the experimental air-fuel ratio, and stc denotes the stoichiometric air-fuel ratio.

There must be a reference to the Fig. 5 in the text before the Figure

The composition of syngas produced from corncob gasification was evaluated at different equivalence ratios to determine the variation in the main combustible and non-combustible gas components. Changes in the equivalence ratio significantly affected the concentrations of H_2, CH_4, CO, and CO_2, indicating that the air supply plays an important role in the gasification performance and gas quality. Fig. 5 shows the syngas composition obtained at different equivalence ratios.

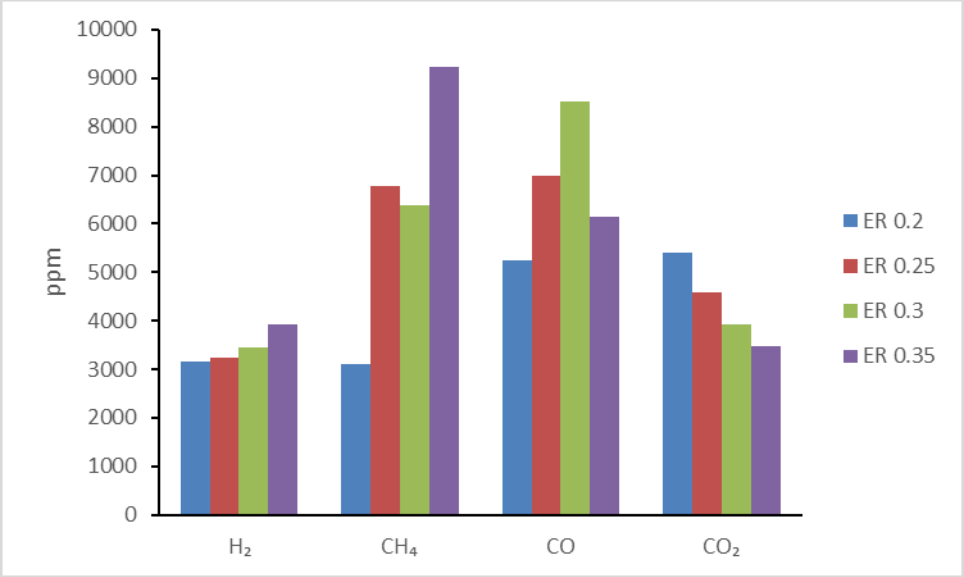


Fig. 5. Syngas composition with different equivalence ratio

The graph above shows that the higher the ER, the higher the hydrogen composition produced. At ER 0.2, the ppm is 3150 ppm, at ER 0.25 it is 3241 ppm, at ER 0.3 it is 3457 ppm, and at ER 0.35 it is 3914 ppm. A higher oxidant supply promotes the formation of more stable autothermal conditions and higher reaction temperatures due to partial oxidation. This increase in temperature accelerates hydrogen-forming reactions, particularly the gasification of active carbon catalyst interactions with steam ($C + H_2O \rightarrow CO + H_2$), the reforming of volatile compounds/light hydrocarbons ($CxHy + H_2O \rightarrow CO + H_2$), and the cracking of tar/volatile into lighter gas species. At low ER, some volatiles tend to be incompletely converted and still have the potential to escape as condensable components, while increasing ER increases heat availability, making the conversion of volatiles into gas fractions (including H_2) more effective.

The higher the ER, the higher the CH_4 composition produced. At ER 0.2, 3093 ppm was obtained, at ER 0.25 6767 ppm, ER 0.3 6377 ppm, and ER 0.35 9221 ppm. This trend indicates that the supply of oxidants not only increases autothermal conditions and the rate of devolatilization, but also shifts the reaction pathway towards the formation of light hydrocarbons through hydrogenation and/or methanation reactions in the reactor zone where the temperature still supports CH_4 formation. In particular, increased H_2 at higher ERs can promote the methanation reaction of CO ($CO + 3H_2 \rightleftharpoons CH_4 + H_2O$), so that CH_4 increases along with a tendency for CO to decrease at the highest ER. In addition, more intensive fragmentation of volatiles and tar at high ERs has the potential to produce light gas precursors which are then hydrogenated to CH_4.

CO formation increased up to an ER of 0.3 and decreased at an ER of 0.35. At an ER of 0.2, 5238 ppm was obtained, at an ER of 0.25, 6999 ppm, at an ER of 0.3, 8532 ppm, and decreased at an ER of 0.35 to 6145 ppm. At low ER (0.20–0.25), limited oxygen supply resulted in relatively low heat release, so that the reaction zone

temperature and char reactivity were not sufficient to intensify CO formation reactions, especially the Boudouard reaction ($C + CO_2 \rightleftharpoons 2CO$) and char gasification with steam ($C + H_2O \rightleftharpoons CO + H_2$). When the ER is increased towards 0.30, the increase in autothermal heat strengthens these reduction reactions, causing CO formation to increase and reach its peak. However, at higher ERs (0.35), the CO fraction tends to decrease because some CO can be converted to CH_4.

CO_2 formation continues to decrease as ER increases. At ER 0.2, 5412 ppm is obtained; at ER 0.25, 4592 ppm; at ER 0.3, 3916 ppm; and at ER 0.35, 3479 ppm. The increase in oxidant supply at this ER does not promote complete combustion, but rather strengthens the CO_2 reduction mechanism. At higher ERs, the heat generated from partial oxidation increases the temperature of the reduction zone, thereby accelerating the Boudouard reaction ($C + CO_2 \rightleftharpoons 2CO$), in which CO_2 is reduced by char to CO. This mechanism is consistent with the increase in CO until it reaches a maximum at an ER of 0.30, while also explaining the decrease in CO_2 under the same conditions. Interestingly, at an ER of 0.35, CO_2 remains at its lowest level even though CO decreases, indicating that the CO formed is not completely accumulated at the outlet but has the potential to undergo further conversion along the gas flow path.

5. 2. 2. Effect of Catalyst Loading on Syngas Product

The catalyst load or amount of catalyst in this study was 4%, 6%, 8%, and 10% of the total biomass weight. The Fig. 6. shows that the composition of H_2 and CH_4 increases as the catalyst load decreases. The H_2 gas composition at catalyst loads of 4%, 6%, 8%, and 10% is 3742 ppm, 3471 ppm, 3372 ppm, and 3176 ppm, respectively. As the catalyst load increases, the reaction pathways that consume H_2 tend to strengthen, particularly the reverse water–gas shift ($CO_2 + H_2 \rightarrow CO + H_2O$) and H_2 interactions on the catalyst surface during the conversion of gasification compounds. As a result, even though reforming occurs, the measured net H_2 decreases because more H_2 is used for CO formation and surface reactions. The CH_4 gas composition at catalyst loads of 4%, 6%, 8%, and 10% was 7031 ppm, 6476 ppm, 6206 ppm, and 5746 ppm, respectively. An increase in catalyst load increases the number of active sites and gas-catalyst contact, so that methane/light hydrocarbon cracking and reforming occur more intensely. CH_4 then acts as a reactant that is converted into more reactive syngas components, causing the CH_4 concentration to decrease at higher catalyst loads.

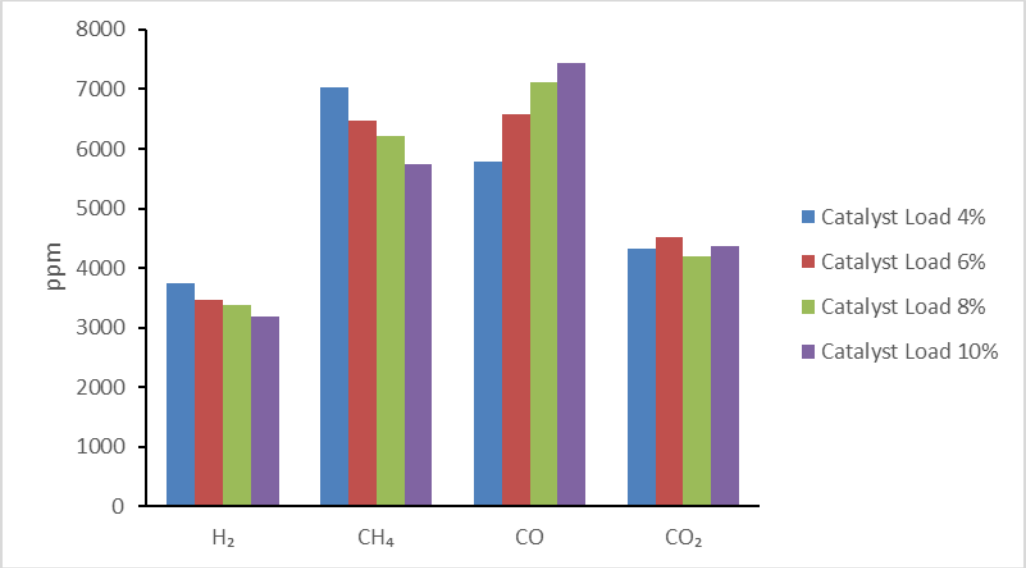


Fig. 6. Syngas Composition with Catalyst Load Variation

The CO gas composition increases with increasing catalyst load, namely for catalyst loads of 4%, 6%, 8% and 10% at 5782 ppm, 6576 ppm, 7111 ppm and 7445 ppm, respectively. The increase in catalyst loading strengthens the CO-forming reactions, particularly dry reforming ($CH_4 + CO_2 \rightarrow 2CO + 2H_2$), char–$CO_2$ reaction ($C + CO_2 \rightarrow 2CO$), and reverse water-gas shift. This combination shifts the product selectivity towards CO, so that the CO fraction increases consistently as the catalyst is increased. The CO_2 gas composition tends to stagnate with increasing catalyst loading, at catalyst loads of 4%, 6%, 8%, and 10% at 4322 ppm, 4510 ppm, 4198 ppm, and 4369 ppm, respectively. CO_2 shows minor changes because it is in a searching for a chemical equilibrium between the partial oxidation and the dry reforming. When the catalyst load increases, the rate of CO_2 consumption may rise, but this is often offset by CO_2 formation in the reaction zone, so that the CO_2 value appears stable or only fluctuates.

5. 2. 3. Effect of Catalyst Ratio on Syngas Product

At a catalyst load of 4%, the CaO/AC ratio changes the gasification reaction through differences in the dominance of tar cracking/reforming and CO_2 capture by CaO, so that the gas composition is highly dependent on the number of active sites and the effectiveness of gas-catalyst contact. At 0:1 (AC), CH_4 and CO are relatively high because AC promotes volatile/tar cracking, but CO_2 remains high because there is no absorption. At 1:0 (CaO), CH_4 decreases but CO_2 is highest, indicating that CO_2 capture is not yet effective due to limited surface area/carbonate layer formation. The 1:1 ratio produces the highest CO with moderate CO_2, indicating CaO–AC synergy that increases the conversion of volatiles into reactive gases. Meanwhile, the 2:1 (CaO-rich) ratio provides the highest H_2 and lowest CO_2 due to the sorption-enhanced effect of CaO, but

CH_4 remains high due to the smaller contribution of AC, so methane reforming/cracking is not yet optimal.

There must be a reference to the Fig. 7 in the text before the Figure

To further examine the catalytic performance, the effect of CaO/AC ratio on syngas composition was investigated under various catalyst loading conditions. This analysis was conducted to determine how the proportion of CaO and activated carbon, combined with different catalyst loads, affected the distribution of H_2, CH_4, CO, and CO_2 during corncob gasification. Fig. 7 illustrates the effect of CaO/AC ratio at catalyst loads of 4% (a), 6% (b), 8% (c), and 10% (d).

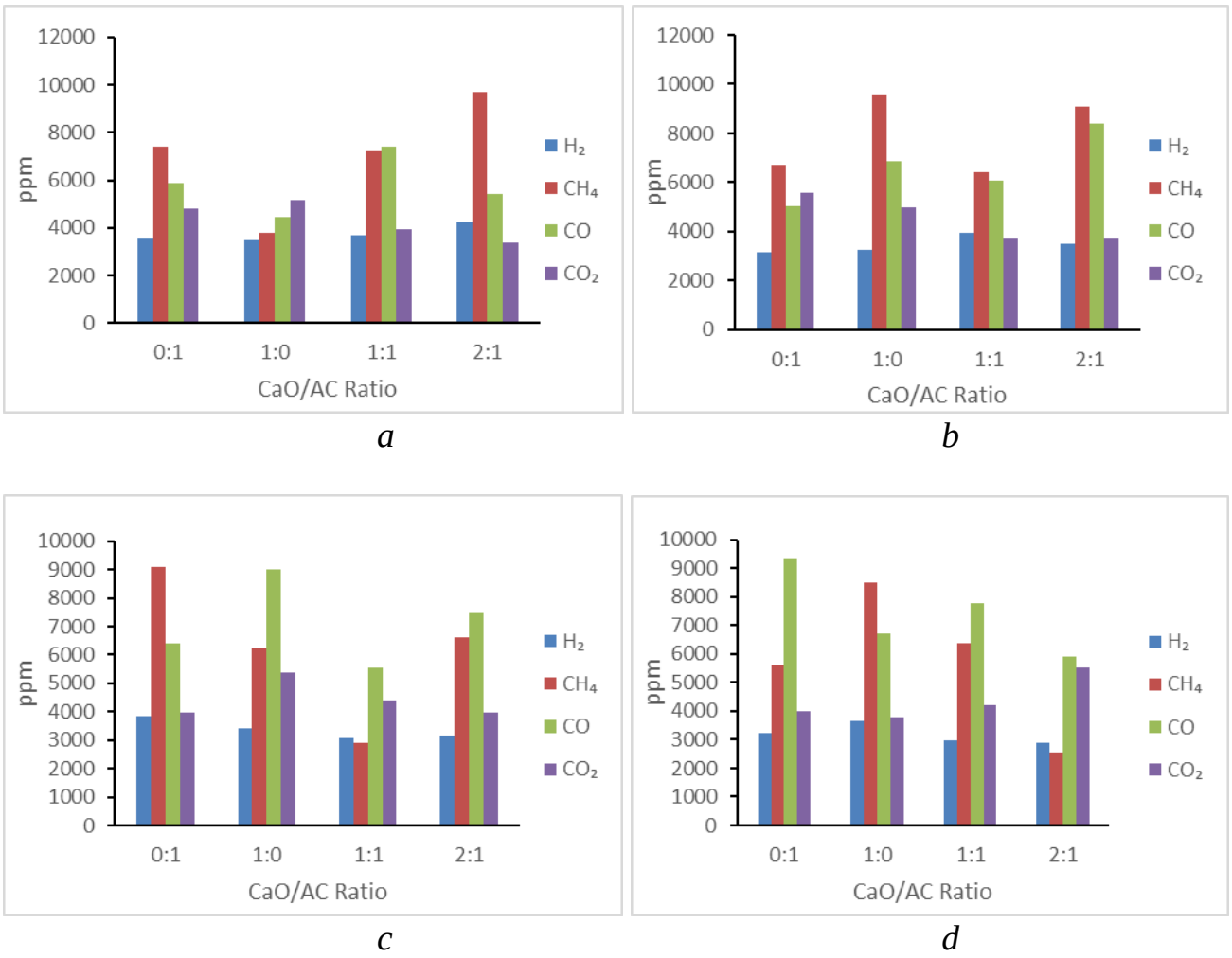


Fig. 7. Effect CaO/AC ratio with various catalyst load: *a* – 4%; *b* – 6%; *c* – 8%; *d* – 10%

At a catalyst load of 4%, the CaO/AC ratio changes the gasification reaction through differences in the dominance of tar cracking/reforming and CO_2 capture by CaO, so that the gas composition is highly dependent on the number of active sites and

the effectiveness of gas-catalyst contact. At 0:1 (AC), CH_4 and CO are relatively high because AC promotes volatile/tar cracking, but CO_2 remains high because there is no absorption. At 1:0 (CaO), CH_4 decreases but CO_2 is highest, indicating that CO_2 capture is not yet effective due to limited surface area/carbonate layer formation. The 1:1 ratio produces the highest CO with moderate CO_2, indicating CaO–AC synergy that increases the conversion of volatiles into reactive gases. Meanwhile, the 2:1 (CaO-rich) ratio provides the highest H_2 and lowest CO_2 due to the sorption-enhanced effect of CaO, but CH_4 remains high due to the smaller contribution of AC, so methane reforming/cracking is not yet optimal.

At a catalyst load of 6%, the CaO/AC ratio mainly shifts the selectivity of secondary reactions (tar cracking/reforming and CO_2 capture), where AC enhances the conversion of volatiles/light hydrocarbons, while CaO reduces CO_2 through carbonation ($CaO + CO_2 \rightarrow CaCO_3$) and changes the reaction equilibrium. At 0:1, CH_4 and CO_2 remain high because there is no CO_2 capture and methane reforming is not yet optimal, so volatiles still escape as CH_4. At 1:0, CO_2 tends to decrease, but CH_4 becomes the highest due to the absence of AC's role in cracking/reforming. The most favorable conditions occur at 1:1, with the highest H_2 and lowest CO_2, indicating CaO–AC synergy that promotes sorption-enhanced reforming and increases the conversion of hydrocarbons into syngas components. At 2:1, CO is highest and CO_2 remains low, but CH_4 rises again and H_2 is not maximized because excess CaO has the potential to rapidly carbonate/cause contact limitations, thereby reducing the contribution of AC in cracking/reforming.

At a catalyst load of 8%, the CaO/AC ratio significantly shifts the selectivity of the syngas reaction. At 0:1 (AC), CH_4 is still high because some light hydrocarbons have not been fully converted even though the tar cracking process is already active. At 1:0 (CaO), CO increases the most, but CO_2 also tends to be high, indicating that CaO in this condition is more dominant in promoting the CO formation pathway, while the CO_2 capture function is not yet optimal due to contact limitations or carbonation saturation. The 1:1 ratio produces the lowest CH_4, indicating the most effective CaO–AC synergy for cracking/reforming light hydrocarbons so that more methane is converted into reactive gas. At 2:1, CO increases again but CH_4 also rises, indicating that a smaller AC fraction reduces the intensity of methane reforming/cracking, while the decrease in CO_2 remains dependent on the effectiveness of CaO sorption.

At a catalyst load of 10%, the increase in total catalyst makes secondary reactions, reforming, solid-gas heterogeneous reactions, and equilibrium shifts very dominant, so that the CaO/AC ratio mainly determines the direction of product selectivity. At 0:1 (AC), CO formation tends to be strongest because the porous carbon surface accelerates the cracking/reforming of volatiles and the conversion of tar into reactive gases. At ratios involving CaO (1:0, 1:1, 2:1), CaO can retain CO_2 through carbonation, but at high loads the effect is often non-linear because CaO rapidly carbonates/diffusion limitations and pore blocking occur, so that under CaO-rich conditions (2:1) CH_4 can decrease, but CO_2 may increase and H_2 is not maximized due to reaction competition.

Overall, at a 10% load, a trade-off is observed: AC-dominant increases CO, while CaO-dominant suppresses light hydrocarbons but has the potential to trigger non-ideal conditions (saturation/mass transport) that reduce the benefits of H_2 and CO_2.

5. 2. 4. Syngas Low Heating Value

To calculate the LHV of syngas, it must first be converted from ppm to % volume of gas. The formula is $\%vol_i = \frac{ppmv_i}{10^4}$ to calculate the LHV, use the formula

$$LHV_{mix}\left(\frac{MJ}{Nm^3}\right) = \frac{10.8(\%H_2) + 12.63(\%CO) + 35.8(\%CH_4)}{100},$$

LHV H_2 = 10.8 MJ/Nm^3,

LHV CO = 12.63 MJ/Nm^3,

LHV CH_4 = 35.8 MJ/Nm^3.

As shown in Fig. 8, the syngas low heating value (LHV) varies with the equivalence ratio (ER) and catalyst load.

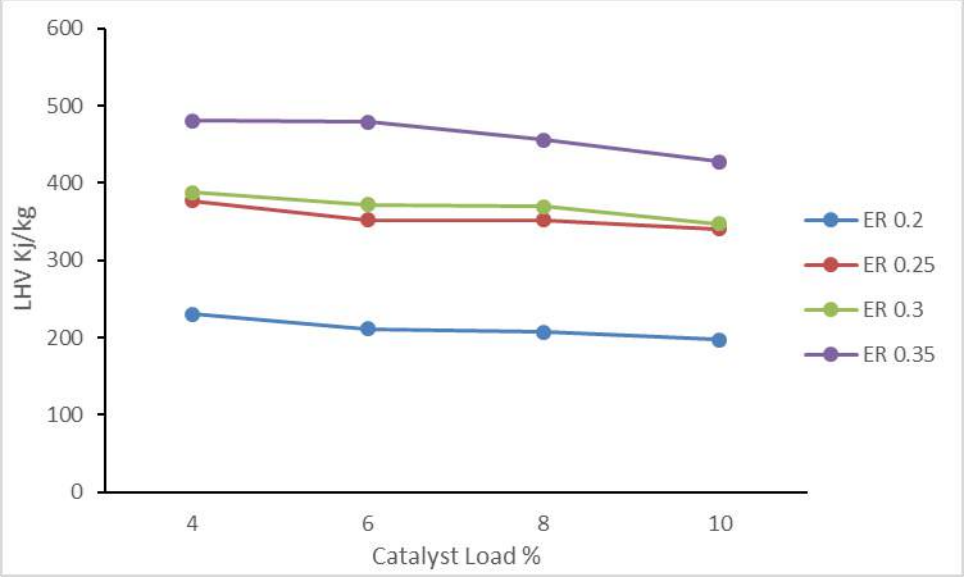


Fig. 8. Syngas low heating value with various equivalence ratio

Fig. 8 shows that the LHV value increases with the ER. At the same catalyst load of 4%, the LHV will increase in line with the increase in ER. ER 0.2 has an LHV of 230 kJ/kg and ER 0.35 has an LHV of 481 kJ/kg. Higher ER produces more intense autothermal conditions, causing the reactor temperature to rise. This increase in

temperature accelerates the decomposition of volatiles and tar cracking, and promotes more complete gasification and reforming reactions, thereby increasing the fraction of permanent gases that contribute to the calorific value, mainly CO and CH_4, as well as some H_2. In addition, the increase in temperature is also associated with more effective hydrogen formation, because H_2 formation reactions (e.g., through steam-water and reforming reactions) are generally more optimal at high temperatures, with the temperature range often reported to be most conducive to H_2 formation being 800–1000°C.

At ER 0.2, the highest LHV was obtained at a catalyst load of 4% at 230 kJ/kg and continued to decrease with increasing catalyst load to 197 kJ/kg at 10%. At ER 0.25, the highest LHV was also obtained at a catalyst load of 4% at 377 kJ/kg and also decreased to 341 kJ/kg at a catalyst load of 10%. At ER 0.3, the highest LHV was obtained at a catalyst load of 4% at 388 kJ/kg and also decreased at a catalyst load of 10% to 347 kJ/kg. At ER 0.35, the highest LHV was obtained at 481 kJ/kg and decreased at a catalyst load of 10% to 428 kJ/kg.

However, all ER values show that LHV tends to decrease when the catalyst load is increased from 4% to 10%. This decrease indicates that excessive catalyst addition under these operating conditions does not always improve gas energy quality, because the catalyst can shift the reaction selectivity towards the conversion of high calorific components especially CH_4 into CO and H_2 through reforming, while at the same time the fraction of diluent gases such as CO_2 (and steam) may increase due to reaction. Since CH_4 has a very large calorific value contribution in the syngas mixture, the decrease in its fraction is often more dominant than the increase in CO/H_2, so that the total LHV tends to decrease.

In energy system analysis, particularly in combustion, gasification, and fuel gas utilisation processes such as syngas, the LHV value is often used because it better represents the heat energy that can actually be utilised by the system. The LHV value of a fuel gas is usually influenced by the composition of combustible gases such as carbon monoxide (CO), hydrogen (H_2), and methane (CH_4). The higher the content of these gases, the greater the LHV value produced. The LHV of syngas from this study with variations in ER and CaO/AC-PF ratio can be seen in Fig. 9.

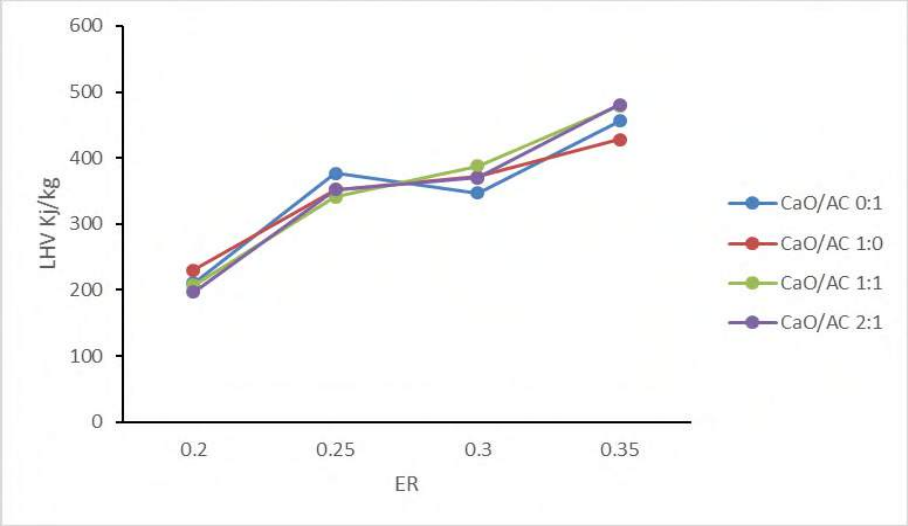


Fig. 9. Syngas Low Heating Value with Various CaO/AC Ratio

Fig. 9 shows that the LHV of syngas increases consistently with the increase in ER 0.2 to 0.35 for all CaO/AC ratios, indicating that a higher ER strengthens autothermal conditions so that the reaction temperature increases and the conversion of volatiles into syngas becomes more complete. At low ER (0.2), the difference in LHV between ratios is still small because secondary reactions such as cracking, reforming and heterogeneous reactions are not yet dominant; the system is still relatively influenced by incompletely converted volatiles. When the ER is increased to 0.25–0.30, the effect of the catalyst ratio becomes apparent: compositions involving AC tend to produce higher LHV because they accelerate tar cracking and increase the fraction of calorific gas, while the contribution of CaO can shift the reaction equilibrium through a decrease in CO_2. At the highest ER (0.35), the LHV reaches its maximum at all ratios, with CaO/AC 2:1 and 0:1 showing peak values, indicating that at high temperatures, the reactive gas formation pathway (via cracking/reforming on the carbon surface and/or CaO-rich-promoted heterogeneous reactions) becomes dominant. Overall, ER acts as the main controlling factor for LHV increase through the temperature effect, while the CaO/AC ratio modulates LHV through the balance between cracking/reforming (AC) and CO_2 control (CaO), especially at medium-high ER.

6. Discussion on the Catalytic Effect of AC-PF/CaO and Operating Conditions on Syngas Composition and LHV

The interaction of the CaO-AC-PF catalyst to improve syngas quality can be seen from the characterisation of the catalyst, the composition of the syngas and the LHV produced. From the Scanning Electron Microscopy results in Fig. 2, it can be seen that the CaO:AC-PF;2:1 catalyst (Fig. 2, *c*) appears denser than the other catalysts. With the addition of CaO, CaO particle dispersion can be seen on the white carbon surface, indicating that some micro pores are closed by CaO. With the addition of CaO, a lot of

CO_2 is absorbed and becomes $CaCO_3$. This porous structure is very important in top-flow gasification because pyrolysis gas and volatiles move through the layer, so the presence of a porous medium has the potential to strengthen secondary reactions and act as carbon capture before the gas exits to the condenser.

From a surface chemistry perspective, Fourier Transform Infrared Spectroscopy (FTIR) shows the presence of –OH and calcium carbonate groups, as shown in Fig. 3. This is due to the results of KOH impregnation carried out during the manufacture of AC-PF. The presence of -OH groups functions as polar active sites capable of adsorbing polar molecules such as H_2O, CO_2, and volatile compounds. Surfaces with -OH groups tend to be hydrophilic and reactive, thereby enhancing interactions with tar compounds or heavy hydrocarbons. These tar compounds can then undergo thermal cracking or catalytic reforming into light gases such as H_2, CO, and CH_4. In addition to -OH, there are also O-H and C-O groups. The O-H group has characteristics that are almost the same as the -OH group, while the C-O group plays a role in enhancing the redox properties and chemical interactions between the carbon surface and gas molecules. In the gasification process, the C-O group can be part of the partial oxidation mechanism and carbon gasification reaction, which produces CO [25].

The BET data in Fig. 4 shows that the surface area decreased to 5.06 m^2/g, but the pore diameter increased to a mesopore scale of 22.87 nm, which can improve the accessibility of volatiles to active sites and improve mass transport in the reforming reaction. In Fig. 4, *b*, the BJH curve at CaO:AC-PF = 2:1 shows the highest dV/dD values of 30–40 nm, indicating a catalyst in the mesopore size range. The presence of these mesopores will further increase the active sites for CO_2 adsorption.

From a process perspective, in Fig. 5, ER appears as the dominant variable that regulates autothermal conditions, primarily through an increase in effective temperature and secondary reaction intensity. An increase in ER from low to high levels consistently increases H_2, which can be explained by the acceleration of H_2 formation reactions such as charcoal gasification with steam ($C + H_2O \rightarrow CO + H_2$) [26], light hydrocarbon reforming, and more intense tar cracking at high temperatures. At the same time, CH_4 also increases sharply at high ER, indicating that in an autothermal upflow system, increased temperature and changes in gas composition can facilitate the formation of light gases. Meanwhile, CO tends to peak at moderate ER and then decreases at high ER, consistent with competition between CO formation and CO consumption through subsequent reactions such as methanation [27]. The decrease in CO_2 at high ER indicates the role of high temperatures in enhancing the reduction of CO_2 by charcoal (Boudouard reaction) and/or the role of CaO adsorption if available.

The effect of catalyst loading in Fig. 6 shows that adding catalyst does not always increase H_2. Increasing the catalyst loading from low to high tends to reduce H_2 and CH_4 but increase CO. Mechanistically, this condition can occur when the catalyst strengthens pathways that increase CO and/or promotes RWGS ($CO_2 + H_2 \rightarrow CO + H_2O$) [28], which consumes H_2 so that net H_2 is reduced. Furthermore, at high catalyst loadings, the possibility of diffusion/aggregation penalties increases, so that selectivity may shift and

some active sites become less effective. Therefore, the target of H_2-rich synthesis gas in this reactor is more dependent on ER adjustment and the selection of moderate/low catalyst loadings, rather than simply increasing the loading.

The CaO/AC-PF ratio in Fig. 7 shows synergistic but non-linear behaviour. AC-PF plays a major role as a porous medium that enhances the cracking/reforming process of volatile compounds, while CaO provides a basic site and CO_2 absorber to shift the equilibrium. At high CaO ratios, sorption and base effects may increase, but the risk of micro-pore closure and diffusion pathway changes also increases. This explains why certain compositions are optimal at certain catalyst loads: the best performance arises from a balance between pore accessibility (the role of AC-PF) and sorption/base strength (the role of CaO).

From an energy quality perspective, in Fig. 8, 9, the LHV value of synthetic gas is highly sensitive to changes in CH_4. Therefore, high ER conditions that increase CH_4 tend to increase LHV. H_2, CH_4 and CO are the main factors for obtaining high LHV. CO_2 has no calorific value so it must be captured. In this study, CaO was used so that CO_2 could be suppressed, meaning that the total LHV could be increased. The highest LHV in this study was 481 kJ/kg, while in another study, the highest was 550 kJ/kg using pinewood with dolomite, activated carbon, silica gel, and limestone catalysts [29]. The higher the ER, the more oxygen enters the system, thereby increasing the reforming reaction [30].

There are several limitations to this study. First, the gas composition was obtained from an MQ sensor based on ppm, so absolute accuracy may be affected by cross-sensitivity, humidity, sensor drift, and gas sampling temperature; this may affect the estimation of %vol and LHV, especially when changes in CO and CH_4 occur simultaneously. Second, catalyst characterisation (SEM-FTIR-BET) supports the role of surface texture and chemistry, but has not quantified changes in the active phase during operation, the degree of carbonation, and the decrease in activity due to pore closure accumulation.

The disadvantage of this research is that the CaO catalyst reacts very easily with CO_2. After the calcination process, CaO must be stored in an airtight container to prevent it from clumping into $CaCO_3$. The catalyst has a specific usage period because it is covered with tar or ash.

Based on these limitations, several future directions are recommended. Calibrate the gas composition using GC-TCD/GC-FID to convert the sensor readings into more accurate %vol and include LHV uncertainty analysis. Evaluate catalyst stability and regeneration, especially for CaO which is easily carbonated, through carbonation-calcination cycle tests and post-reaction characterisation (XRD/TGA/SEM-EDX) to assess phase changes and activity loss. Develop experimental designs towards ANOVA or RSM interactions so that interaction effects and predictive models can be obtained and verified through replication confirmation tests. Add process performance metrics such as gas yield (Nm^3/kg), cold gas efficiency, pressure drop, and air consumption so

that ‘syngas quality improvement’ can be demonstrated based on mass-energy balance and operability, not just composition.

7. Conclusion

1. AC-PF with rich -OH group acts as a porous catalytic medium that facilitates volatile cracking and supports the reduction of condensable by-products, while CaO contributes to absorb CO_2. The BJH analysis confirms that CaO plays a dual role as a reactive sorbent and a textural promoter in palm-fiber activated carbon by enlarging mesopores (20–40 nm), thereby enhancing gas diffusion and improving access to CaO active sites, which ultimately strengthens catalytic performance.

2. Increasing ER to 0.35 enhances the combustible gas fraction H_2 and CH_4 and suppresses CO_2, whereas CO typically peaks at intermediate ER due to competing CO formation and consumption reactions along the updraft reaction zones. Increasing catalyst loading shifts syngas composition: CO increases, while H_2 and CH_4 decrease, indicating changes in dominant secondary reactions and possible diffusion or agglomeration limitations at higher loadings. Increasing ER lead to increase LHV syngas, but it can decrease at high catalyst loading. An increase in the CaO/AC ratio to 2:1 resulted in a higher syngas LHV, with a maximum value of 481 kJ/kg.

Conflict of interest

The authors declare that they have no conflict of interest in relation to this research, whether financial, personal, authorship or otherwise, that could affect the research and its results presented in this paper.

Financing

The authors sincerely thank the Ministry of Education, Culture, Research and Technology, Republic of Indonesia for fully supporting this research through the DRTPM Research Grant under Fundamental Research, Universitas Widyagama Malang, Indonesia 2025 (Grant Number:128/C3/DT.05.00/PL/2025;023/LL7/DT.05.00/PL/2025;010/ Kontrak/PT/PTS.030.7/PN/V/2025).

Data availability

Manuscript has no associated data.

Use of artificial intelligence

The authors used the AI-based language model ChatGPT (GPT-5.3) only to assist in improving the clarity of English language and grammar in several sections of the manuscript, particularly in the Introduction and Literature Review sections.

The AI tool was used solely for language editing and paraphrasing purposes. All scientific content, experimental design, data analysis, and interpretation of the results were conducted entirely by the authors.

The authors carefully reviewed and verified all AI-assisted text to ensure accuracy and consistency with the experimental results. The use of AI tools did not influence the scientific conclusions of this study.

Acknowledgements

We as the Research Team would like to thank Ministry of Education, Culture, Research and Technology, Republic of Indonesia (Kemendiktisaintek Indonesia) for financing research activities.

Authors' contributions

Purbo Suwandono: Conceptualization, Writing-original draft, Investigation, Supervision, Formal analysis, Writing – review & editing; **Widya Wijayanti**: Validation, Investigation, Data Curation, Formal analysis, Writing – original draft; **Nova Risdiyanto Ismail**: Writing – review & editing, Formal analysis; **Dzulfikar Johan Akbar:** Visualization, Writing – original draft, Data curation; **Muhammad Reza**: Project administration, Resources, Data curation.

References

1. V. K. Yadav *et al.*, "Emerging trends in the valorization of agricultural waste and their utilization in agricultural, pharmaceuticals, and environmental cleanup," *Waste and Biomass Valorization*, pp. 1–55, 2025. DOI:10.1007/s12649-025-03002-y
2. W. M. Lewandowski, M. Ryms, and W. Kosakowski, "Thermal biomass conversion: A review," *Processes*, vol. 8, no. 5, p. 516, 2020. https://doi.org/10.3390/pr8050516
3. D. Ariyanti *et al.*, "Valorization of corn cob waste for furfural production: A circular economy approach," *Biomass and Bioenergy*, vol. 194, p. 107665, 2025. DOI:10.1016/j.biombioe.2025.107665
4. J. Zhang, Z. Chu, R. Cao, X. Wu, and K. Han, "A review of resource recovery from waste plastics via pyrolysis and gasification," *Fuel*, vol. 404, p. 136319, 2026. https://doi.org/10.1016/j.fuel.2025.136319
5. Y. Tangke Tosuli, Cahyadi, H. Dafiqurrohman, R. Hermawan, and A. Surjosatyo, "Gasification of sago dreg waste in a top-lit updraft fixed bed gasifier: Syngas composition and its effect with additional Al2O3 as catalyst," *Energy Convers. Manag. X*, vol. 24, no. October, p. 100775, 2024, doi: 10.1016/j.ecmx.2024.100775. https://doi.org/10.1016/j.ecmx.2024.100775
6. P. Dinh *et al.*, "Enrichment of hydrogen in product gas from a pilot-scale rice husk updraft gasification system," *Carbon Resour. Convers.*, vol. 5, no. 3, pp. 231–239, 2025, doi: 10.1016/j.crcon.2022.07.003.
7. S. Yousef and J. Eimontas, "International Journal of Hydrogen Energy Oxygen updraft gasification-catalytic reforming of cigarettes butts for hydrogen-rich syngas production," vol. 171, no. May, 2025, https://doi.org/10.1016/j.ijhydene.2025.150650

8. D. Contreras, E. Blanco, and D. Travieso, “Experimental assessment of the energy potential of pellets produced from beekeeping wastes by updraft gasification,” vol. 343, no. January, 2025, https://doi.org/10.1016/j.enconman.2025.120206
9. N. Yesilova, O. Tezer, A. Ongen, and A. Ayol, “International Journal of Hydrogen Energy Enhancing biomass gasification : A comparative study of catalyst applications in updraft and modifiable-downdraft fixed bed reactors,” *Int. J. Hydrogen Energy*, vol. 76, no. April, pp. 290–303, 2024, https://doi.org/10.1016/j.ijhydene.2024.05.075
10. R. Skvor and A. Jan, “Experimental investigation of sorted municipal solid wastes producer gas composition in an updraft fixed bed gasifier,” vol. 289, no. August 2022, 2024, https://doi.org/10.1016/j.energy.2023.130063
11. R. Junga, M. Tańczuk, S. Sobek, M. Chabiński, and Ł. Ziółkowski, “Effect of the addition of laying hens manure to the straw on gasification efficiency in updraft gasifier under air atmosphere,” *Appl. Therm. Eng.*, vol. 226, no. February, p. 120269, 2023, https://doi.org/10.1016/j.applthermaleng.2023.120269.
12. A. Ongen and A. Ayol, “ScienceDirect Gasification performance of olive pomace in updraft and downdraft fixed bed reactors,” vol. I, 2023, https://doi.org/10.1016/j.ijhydene.2023.02.088
13. K. Ertas, “Gasification of MDF residue in an updraft fixed bed gasifier to produce heat and power via an ORC turbine,” vol. 169, no. February, pp. 43–51, 2023, https://doi.org/10.1016/j.wasman.2023.06.025
14. S. Gorthy, S. Verma, N. Sinha, S. Shetty, H. Nguyen, and M. Neurock, “Theoretical Insights into the Effects of KOH Concentration and the Role of OH–in the Electrocatalytic Reduction of CO2 on Au,” *ACS Catal.*, vol. 13, no. 19, pp. 12924–12940, 2023. DOI:10.1021/acscatal.2c06115
15. X. Wang, W. Zeng, C. Xin, X. Kong, X. Hu, and Q. Guo, “The development of activated carbon from corncob for CO2 capture,” *RSC Adv.*, vol. 12, no. 51, pp. 33069–33078, 2022, https://doi.org/10.1039/D2RA05979G
16. B. Zhou *et al.*, “Insights into effects of grain boundary engineering in composite metal oxide catalysts for improving catalytic performance,” *J. Colloid Interface Sci.*, vol. 653, pp. 1177–1187, 2024. https://doi.org/10.1016/j.jcis.2023.09.148
17. Y. Zhu *et al.*, “Preparation of hierarchically porous carbon ash composite material from fine slag of coal gasification and ash slag of biomass combustion for CO2 capture,” *Sep. Purif. Technol.*, vol. 330, p. 125452, 2024. https://doi.org/10.1016/j.seppur.2023.125452
18. M. Ilić *et al.*, “Surface functional groups and degree of carbonization of *selected* chars from different processes and feedstock,” *PLoS One*, vol. 17, no. 11, p. e0277365, 2022. https://doi.org/10.1371/journal.pone.0277365
19. R. Ali, Z. Aslam, R. A. Shawabkeh, A. Asghar, and I. A. Hussein, “BET, FTIR, and RAMAN characterizations of activated carbon from waste oil fly ash,” *Turkish J. Chem.*, vol. 44, no. 2, pp. 279–295, 2020. doi: 10.3906/kim-1909-20
20. K. J. Stanienda-Pilecki, “The importance of Fourier-Transform Infrared

Spectroscopy in the identification of carbonate phases differentiated in magnesium content," 2019.

21. F. Dai, Q. Zhuang, G. Huang, H. Deng, and X. Zhang, "Infrared spectrum characteristics and quantification of OH groups in coal," *ACS omega*, vol. 8, no. 19, pp. 17064–17076, 2023. https://doi.org/10.1021/acsomega.3c01336

22. E. M. de Salazar Martínez, M. F. Alexandre-Franco, A. J. Nieto-Sanchez, and E. M. Cuerda-Correa, "Exploring the role of surface and porosity in CO2 capture by CaO-based adsorbents through response surface methodology (RSM) and artificial neural networks (ANN)," *J. CO2 Util.*, vol. 83, p. 102773, 2024. https://doi.org/10.1016/j.jcou.2024.102773

23. J. A. Tavizón-Pozos, H. Cervantes-Cuevas, G. G. Garcia-Camacho, G. Chavez-Esquivel, and D. R. Acosta-Najarro, "Biodiesel Production Using K–Sr/CaO and CaO Catalysts Derived from Eggshells by Canola Oil Transesterification," *ACS omega*, vol. 10, no. 7, pp. 6827–6838, 2025. https://doi.org/10.1021/acsomega.4c09118

24. W. Koo-Amornpattana, P. Phadungbut, N. Kunthakudee, W. Jonglertjunya, S. Ratchahat, and M. Hunsom, "Innovative metal oxides (CaO, SrO, MgO) impregnated waste-derived activated carbon for biohydrogen purification," *Sci. Rep.*, vol. 13, no. 1, p. 4705, 2023. DOI:10.1038/s41598-023-31723-4

25. C. Quan, M. Wang, N. Gao, T. Yang, and R. Li, "In situ adsorption of CO2 to enhance biomass gasification for hydrogen production using Ca/Ni based composites," *J. Energy Inst.*, vol. 108, p. 101229, 2023, doi: https://doi.org/10.1016/j.joei.2023.101229. https://doi.org/10.1016/j.joei.2023.101229

26. F. Micheli, E. Mattucci, C. Courson, and K. Gallucci, "Bi-Functional Catalyst/Sorbent for a H2-Rich Gas from Biomass Gasification," 2021. doi: 10.3390/pr9071249. DOI:10.3390/PR9071249

27. M. Zhu, Q. Wang, and S. Wang, "Recent Advances and Future Perspectives in Catalyst Development for Efficient and Sustainable Biomass Gasification: A Comprehensive Review," 2025, https://doi.org/10.3390/su17167370

28. N. Cerone, F. Zimbardi, L. Contuzzi, J. Baleta, and D. Cerinski, "Experimental investigation of syngas composition variation along updraft fixed bed gasifier," *Energy Convers. Manag.*, vol. 221, no. July, p. 113116, 2020, https://doi.org/10.1016/j.enconman.2020.113116

29. R. Mohanty, P. Mahanta, A. Mahapatro, and R. Prakash, "Catalytic gasification of pinewood biomass in a fluidized bed reactor with dolomite , limestone , and activated carbon : An experimental study," *Energy*, vol. 325, no. April, p. 136131, 2025, doi: 10.1016/j.energy.2025.136131. https://doi.org/10.1016/j.energy.2025.136131

30. C. Liu, Y. Huang, M. Niu, and H. Pei, "ScienceDirect Influences of equivalence ratio , oxygen concentration and fluidization velocity on the characteristics of oxygen-enriched gasification products from biomass in a pilot-scale fluidized bed," *Int. J. Hydrogen Energy*, vol. 43, no. 31, pp. 14214–14225, 2018, https://doi.org/10.1016/j.ijhydene.2018.05.154

References

1. V. K. Yadav *et al.*, “Emerging trends in the valorization of agricultural waste and their utilization in agricultural, pharmaceuticals, and environmental cleanup,” *Waste and Biomass Valorization*, pp. 1–55, 2025. DOI:10.1007/s12649-025-03002-y
2. W. M. Lewandowski, M. Ryms, and W. Kosakowski, “Thermal biomass conversion: A review,” *Processes*, vol. 8, no. 5, p. 516, 2020. https://doi.org/10.3390/pr8050516
3. D. Ariyanti *et al.*, “Valorization of corn cob waste for furfural production: A circular economy approach,” *Biomass and Bioenergy*, vol. 194, p. 107665, 2025. DOI:10.1016/j.biombioe.2025.107665
4. J. Zhang, Z. Chu, R. Cao, X. Wu, and K. Han, “A review of resource recovery from waste plastics via pyrolysis and gasification,” *Fuel*, vol. 404, p. 136319, 2026. https://doi.org/10.1016/j.fuel.2025.136319
5. Y. Tangke Tosuli, Cahyadi, H. Dafiqurrohman, R. Hermawan, and A. Surjosatyo, “Gasification of sago dreg waste in a top-lit updraft fixed bed gasifier: Syngas composition and its effect with additional Al2O3 as catalyst,” *Energy Convers. Manag. X*, vol. 24, no. October, p. 100775, 2024, doi: 10.1016/j.ecmx.2024.100775. https://doi.org/10.1016/j.ecmx.2024.100775
6. P. Dinh *et al.*, “Enrichment of hydrogen in product gas from a pilot-scale rice husk updraft gasification system,” *Carbon Resour. Convers.*, vol. 5, no. 3, pp. 231–239, 2025, doi: 10.1016/j.crcon.2022.07.003.
7. S. Yousef and J. Eimontas, “International Journal of Hydrogen Energy Oxygen updraft gasification-catalytic reforming of cigarettes butts for hydrogen-rich syngas production,” vol. 171, no. May, 2025, https://doi.org/10.1016/j.ijhydene.2025.150650
8. D. Contreras, E. Blanco, and D. Travieso, “Experimental assessment of the energy potential of pellets produced from beekeeping wastes by updraft gasification,” vol. 343, no. January, 2025, https://doi.org/10.1016/j.enconman.2025.120206
9. N. Yesilova, O. Tezer, A. Ongen, and A. Ayol, “International Journal of Hydrogen Energy Enhancing biomass gasification : A comparative study of catalyst applications in updraft and modifiable-downdraft fixed bed reactors,” *Int. J. Hydrogen Energy*, vol. 76, no. April, pp. 290–303, 2024, https://doi.org/10.1016/j.ijhydene.2024.05.075
10. R. Skvor and A. Jan, “Experimental investigation of sorted municipal solid wastes producer gas composition in an updraft fixed bed gasifier,” vol. 289, no. August 2022, 2024, https://doi.org/10.1016/j.energy.2023.130063
11. R. Junga, M. Tańczuk, S. Sobek, M. Chabiński, and Ł. Ziółkowski, “Effect of the addition of laying hens manure to the straw on gasification efficiency in updraft gasifier under air atmosphere,” *Appl. Therm. Eng.*, vol. 226, no. February, p. 120269, 2023, https://doi.org/10.1016/j.applthermaleng.2023.120269.
12. A. Ongen and A. Ayol, “ScienceDirect Gasification performance of olive pomace in updraft and downdraft fixed bed reactors,” vol. I, 2023,

https://doi.org/10.1016/j.ijhydene.2023.02.088
13. K. Ertas, “Gasification of MDF residue in an updraft fixed bed gasifier to produce heat and power via an ORC turbine,” vol. 169, no. February, pp. 43–51, 2023, https://doi.org/10.1016/j.wasman.2023.06.025
14. S. Gorthy, S. Verma, N. Sinha, S. Shetty, H. Nguyen, and M. Neurock, “Theoretical Insights into the Effects of KOH Concentration and the Role of OH–in the Electrocatalytic Reduction of CO2 on Au,” *ACS Catal.*, vol. 13, no. 19, pp. 12924–12940, 2023. DOI:10.1021/acscatal.2c06115
15. X. Wang, W. Zeng, C. Xin, X. Kong, X. Hu, and Q. Guo, “The development of activated carbon from corncob for CO2 capture,” *RSC Adv.*, vol. 12, no. 51, pp. 33069–33078, 2022, https://doi.org/10.1039/D2RA05979G
16. B. Zhou *et al.*, “Insights into effects of grain boundary engineering in composite metal oxide catalysts for improving catalytic performance,” *J. Colloid Interface Sci.*, vol. 653, pp. 1177–1187, 2024. https://doi.org/10.1016/j.jcis.2023.09.148
17. Y. Zhu *et al.*, “Preparation of hierarchically porous carbon ash composite material from fine slag of coal gasification and ash slag of biomass combustion for CO2 capture,” *Sep. Purif. Technol.*, vol. 330, p. 125452, 2024. https://doi.org/10.1016/j.seppur.2023.125452
18. M. Ilić *et al.*, “Surface functional groups and degree of carbonization of *selected* chars from different processes and feedstock,” *PLoS One*, vol. 17, no. 11, p. e0277365, 2022. https://doi.org/10.1371/journal.pone.0277365
19. R. Ali, Z. Aslam, R. A. Shawabkeh, A. Asghar, and I. A. Hussein, “BET, FTIR, and RAMAN characterizations of activated carbon from waste oil fly ash,” *Turkish J. Chem.*, vol. 44, no. 2, pp. 279–295, 2020. doi: 10.3906/kim-1909-20
20. K. J. Stanienda-Pilecki, “The importance of Fourier-Transform Infrared Spectroscopy in the identification of carbonate phases differentiated in magnesium content,” 2019.
21. F. Dai, Q. Zhuang, G. Huang, H. Deng, and X. Zhang, “Infrared spectrum characteristics and quantification of OH groups in coal,” *ACS omega*, vol. 8, no. 19, pp. 17064–17076, 2023. https://doi.org/10.1021/acsomega.3c01336
22. E. M. de Salazar Martínez, M. F. Alexandre-Franco, A. J. Nieto-Sanchez, and E. M. Cuerda-Correa, “Exploring the role of surface and porosity in CO2 capture by CaO-based adsorbents through response surface methodology (RSM) and artificial neural networks (ANN),” *J. CO2 Util.*, vol. 83, p. 102773, 2024. https://doi.org/10.1016/j.jcou.2024.102773
23. J. A. Tavizón-Pozos, H. Cervantes-Cuevas, G. G. Garcia-Camacho, G. Chavez-Esquivel, and D. R. Acosta-Najarro, “Biodiesel Production Using K–Sr/CaO and CaO Catalysts Derived from Eggshells by Canola Oil Transesterification,” *ACS omega*, vol. 10, no. 7, pp. 6827–6838, 2025. https://doi.org/10.1021/acsomega.4c09118
24. W. Koo-Amornpattana, P. Phadungbut, N. Kunthakudee, W. Jonglertjunya, S. Ratchahat, and M. Hunsom, “Innovative metal oxides (CaO, SrO, MgO) impregnated waste-derived activated carbon for biohydrogen purification,” *Sci. Rep.*, vol. 13, no. 1, p.

4705, 2023. DOI:10.1038/s41598-023-31723-4
25. C. Quan, M. Wang, N. Gao, T. Yang, and R. Li, “In situ adsorption of CO2 to enhance biomass gasification for hydrogen production using Ca/Ni based composites,” *J. Energy Inst.*, vol. 108, p. 101229, 2023, doi: https://doi.org/10.1016/j.joei.2023.101229. https://doi.org/10.1016/j.joei.2023.101229
26. F. Micheli, E. Mattucci, C. Courson, and K. Gallucci, “Bi-Functional Catalyst/Sorbent for a H2-Rich Gas from Biomass Gasification,” 2021. doi: 10.3390/pr9071249. DOI:10.3390/PR9071249
27. M. Zhu, Q. Wang, and S. Wang, “Recent Advances and Future Perspectives in Catalyst Development for Efficient and Sustainable Biomass Gasification: A Comprehensive Review,” 2025, https://doi.org/10.3390/su17167370
28. N. Cerone, F. Zimbardi, L. Contuzzi, J. Baleta, and D. Cerinski, “Experimental investigation of syngas composition variation along updraft fixed bed gasifier,” *Energy Convers. Manag.*, vol. 221, no. July, p. 113116, 2020, https://doi.org/10.1016/j.enconman.2020.113116
29. R. Mohanty, P. Mahanta, A. Mahapatro, and R. Prakash, “Catalytic gasification of pinewood biomass in a fluidized bed reactor with dolomite , limestone , and activated carbon : An experimental study,” *Energy*, vol. 325, no. April, p. 136131, 2025, doi: 10.1016/j.energy.2025.136131. https://doi.org/10.1016/j.energy.2025.136131
30. C. Liu, Y. Huang, M. Niu, and H. Pei, “ScienceDirect Influences of equivalence ratio , oxygen concentration and fluidization velocity on the characteristics of oxygen-enriched gasification products from biomass in a pilot-scale fluidized bed,” *Int. J. Hydrogen Energy*, vol. 43, no. 31, pp. 14214–14225, 2018, https://doi.org/10.1016/j.ijhydene.2018.05.154

Author’s order	First Name	Middle name	Second Name
1	*Purbo*		*Suwandono*
2	*Widya*		*Wijayanti*
3	*Nova*	*Risdiyanto*	*Ismail*
4	*Dzulfikar*	*Johan*	*Akbar*
5	*Muhammad*		*Reza*

English

Purbo Suwandono
Corresponding author
Master
Department of Mechanical Engineering
Widya Gama University
Borobudur str., 35, Malang, Indonesia, 65142
E-mail: purbo@widyagama.ac.id

ORCID: https://orcid.org/0000-0003-4085-1291
Contact phone: +6282132697144
Number of publications in national journals indexed (approximate; for Ukraine citizens only): -
Number of publications in international journals indexed (approximate): 14
H-index by Scopus (if available): 4
ResearchGate: https://www.researchgate.net/profile/Purbo-Suwandono
Scopus ID: 57204187970
Researcher ID: https://researchid.co/rid80879

Widya Wijayanti
PhD
Department of Mechanical Engineering
Brawijaya University
Veteran str., 10–11, Malang, Indonesia, 65145
E-mail: widya_dinata@ub.ac.id
ORCID: https://orcid.org/0000-0003-4215-5943
Contact phone: +6285334992164
Number of publications in national journals indexed (approximate; for Ukraine citizens only): -
Number of publications in international journals indexed (approximate): 78
H-index by Scopus (if available): 12
ResearchGate: https://www.researchgate.net/profile/Widya-Wijayanti
Scopus ID: 36006672800
Researcher ID: -

Nova Risdiyanto Ismail
PhD
Department of Mechanical Engineering
Widya Gama University
Borobudur str., 35, Malang, Indonesia, 65142
E-mail: nova@widyagama.ac.id
ORCID: https://orcid.org/0000-0001-8439-6919
Contact phone:
Number of publications in national journals indexed (approximate; for Ukraine citizens only): -
Number of publications in international journals indexed (approximate): 7
H-index by Scopus (if available): 3
ResearchGate: https://www.researchgate.net/profile/Nova-Ismail-2
Scopus ID: 57204527065
Researcher ID: https://researchid.co/rid80876

Dzulfikar Johan Akbar
Master Student
Department of Mechanical Engineering
Brawijaya University
Veteran str., 10–11, Malang, Indonesia, 65145
E-mail: johanakbar@student.ub.ac.id
ORCID: https://orcid.org/0009-0002-4652-8516
Contact phone: +6282241116998
Number of publications in national journals indexed (approximate; for Ukraine citizens only): -
Number of publications in international journals indexed (approximate): -
H-index by Scopus (if available): -
ResearchGate: https://www.researchgate.net/profile/Dzulfikar-Johan-Akbar
Scopus ID: -
Researcher ID: -

Muhammad Reza
Bachelor Student
Department of Mechanical Engineering
Widya Gama University
Borobudur str., 35, Malang, Indonesia, 65142
E-mail: muhapanjangreza@gmail.com
ORCID: https://orcid.org/0009-0009-9258-0586
Contact phone: +6282139682566
Number of publications in national journals indexed (approximate; for Ukraine citizens only): -
Number of publications in international journals indexed (approximate): -
H-index by Scopus (if available): -
ResearchGate: -
Scopus ID: -
Researcher ID: -

Name of reviewer: Prof. Dr. Muji Setiyo, ST., MT.
Professor: Mechanical Engineering
Tel: +6281211020288
E-mail: muji@unimma.ac.id.
Work address: Universitas Muhammadiyah Magelang

Name of reviewer: Prof. Dr. Eng. Nurkholis Hamidi, ST., MT.
Professor: Mechanical Engineering
Tel: +62 81259293165

E-mail: hamidy@ub.ac.id
Work address: Brawijaya University

TAHAP 5

REVIEW REVIEWER TAHAP 5

30 Maret 2026

Purbo Suwandono <purbo@widyagama.ac.id>

from "Eastern-European Journal of Enterprise Technologies"_5th stage_No.2(140).2026

3 messages

Oksana Nikitina <0661966nauka@gmail.com> Mon, Mar 30, 2026 at 6:29 PM
To: purbo@widyagama.ac.id, "Widya Wijayanti, ST.,MT" <widya_dinata@ub.ac.id>, nova@widyagama.ac.id, johanakbar@student.ub.ac.id, muhapanjangreza@gmail.com

Good afternoon, dear authors.

The article was accepted for consideration of the possibility of publication in (No. 2(140).2026).

At the 5th stage of editing, please consider the comments of the reviews (article in the application, color notes are highlighted).

We ask you to right strictly in the option which is in the attachment (see attachment).

We ask you not to delete the comments so that we can see all your edits. Please highlight all the author's corrections in green.

Please provide an edited version of the article **by 02.04.2026.**

If you have any questions, please call or write; we will be happy to answer them.

With best regards, Manager Yu. Prylutska
TECHNOLOGY CENTER GROUP LTD
Viber/ WhatsApp/ Telegram: +380 (50) 3033801
Editorial staff of the "Eastern-European Journal of Enterprise Technologies"
Website: https://jet.com.ua/en/, http://journals.uran.ua/eejet/



Відвідати сайт



Відвідати сайт

Attention! The author (team of authors) submitting the manuscript to the editorial office of the journal **«Eastern-European Journal of Enterprise Technologies»** agrees with all requirements for registration, submission of the manuscript of the article and payment and be responsible in case of violation of these requirements.

Our company may rely on your freely given consent at the time you provided your personal data to us replying on this email then the lawfulness of such processing is based on that consent under EU GDPR 2016/679. You have the right to withdraw consent at any time.

Subscribe

Suwandono 27+-7.doc
1169K

Purbo Suwandono <purbo@widyagama.ac.id> Wed, Apr 1, 2026 at 10:12 PM
To: Oksana Nikitina <0661966nauka@gmail.com>

Good afternoon,

Thank you for your email.

We have completed the revision of the manuscript according to the reviewers' comments and the editorial instructions.

Please find the revised manuscript attached. If there are any remaining mistakes or further corrections needed, we will be ready to revise it accordingly.

Best regards,
Purbo Suwandono

[Quoted text hidden]

Suwandono 27+-7 - Revision.doc
1197K

Oksana Nikitina <0661966nauka@gmail.com> Thu, Apr 2, 2026 at 1:39 AM
To: Purbo Suwandono <purbo@widyagama.ac.id>

Good afternoon!
Your article has been sent for review. Please wait.
We wish you a great day and a good mood!
If you have any questions, please call or write. We will be happy to answer them.
Regards, Oksana

ср, 1 апр. 2026 г. в 18:12, Purbo Suwandono <purbo@widyagama.ac.id>:
[Quoted text hidden]

--
[Quoted text hidden]

Received date: 20.02.2026
Accepted date:

From Reviewer

1. Section 1: The authors justified the relevance of the research topic appropriately. Currently, most scientists are conducting research related to "green technologies". "Green technologies" are the production of biogas from agricultural waste. Then the biogas is converted into synthesis gas as a raw material for further syntheses or a product of energy direction. The authors considered another process of converting plant raw materials, which is gasification. The authors should first provide information about the situation in the world and the country about the environmental situation. Provide information about the prospects of "green technologies".

2. The authors considered the topic and direction of research in 10 articles. The articles are related to the transformation of various plant raw materials. Catalytic transformations using different types of catalysts and in different types of reactors are considered. Most of the information material is used from Scopus format articles. The authors formulated the questions not very clearly, which ones have already been investigated and which ones the authors want to investigate further.

Question to the editors: the list of information materials is highlighted in color. How should I understand this? Is this the final list or will it be further adjusted?
If the list of references is adjusted, then this section of the review makes no sense.

3. The purpose of the study is set by the authors according to the topic. But the authors should formulate the research tasks more clearly. This is the creation of a catalyst, then the analysis of its surface by appropriate methods and the study of the parameters of the gasification process with the production of synthesis gas.

4. The authors of the article have defined the object of the research. The authors have also formulated a hypothesis regarding the research. The authors have made some assumptions regarding the course of the process. The article also provides a system of simplifications regarding the conduct of the research. But the authors should more clearly state why the authors use such research methods.

5. In the article, the authors should provide a comparison of the results with existing data when analyzing them. This will allow the research to be perceived as promising.

6. Regarding the analysis and discussion of the research results provided by spectrometric analysis, it is appropriate. The authors should substantiate the results of

the experimental research in more detail. The justification should be built in comparison with existing literature data.

7. The authors of the article conduct research that has scientific and practical activities. The products of the reaction are declared synthesis gas, which is both the target product and an intermediate for obtaining other products of the chemical industry. Synthesis gas is also a good source of energy for use in energy technologies. The authors should provide more details on the practicality of the research in the article.

8. The article does not clearly state the purpose and objectives. Therefore, the conclusions look formulaic. The authors should formulate the conclusions in such a way that it is clear that the research is successful on already known data.

9. The article contains all the necessary sections. It has a promising research direction and is related to the processing of plant raw materials. The manuscript is written clearly, but some points need to be made clearer.

Generally:

The article is related to a promising area of biotechnology. The authors investigated the process of processing plant raw materials by gasification. The authors created a catalyst production plant and the course of the gasification process. The authors conducted a number of studies on the influence of process parameters on the course of the reaction. In the article, the authors presented the results of the research and their analysis. But the authors should correct some points. The goal and objectives of the article should be stated more clearly. In particular, the authors should formulate the tasks more clearly. In the article, the authors considered such points as the creation of a catalyst, surface analysis by spectrometric methods, and the study of various parameters of the reaction course to obtain synthesis gas. When analyzing the research results, the authors should not only describe the values. They should also note their positive impact in comparison with known values. When justifying the goal, the authors should also more clearly provide the scientific and practicality of the selected study. Such updates should also be noted in the conclusions for a clearer understanding.
In the article, the authors should: more clearly formulate the goal and objectives; When analyzing research results, one should provide their justifications regarding their prospects; add a little information regarding the scientificity and practicality of the results; the conclusions of the article should also be formed according to the tasks and provide results in comparison with their prospects.
These comments to the article do not reduce its relevance. These corrections to the article will give it a clearer perception and understanding of prospects.

The article requires revision

UDC 662.7:662.767:66.097

ПОКРАЩЕННЯ ЯКОСТІ СИНТЕЗ-ГАЗУ ПРИ ВИСХІДНІЙ ГАЗИФІКАЦІЇ КУКУРУДЗЯНИХ КАЧАНІВ З ВИКОРИСТАННЯМ КАТАЛІЗАТОРА НА ОСНОВІ CAO/АКТИВОВАНОГО ВУГІЛЛЯ НА ПАЛЬМОВОМУ ВОЛОКН

Purbo Suwandono, Widya Wijayanti, Nova Risdiyanto Ismail, Dzulfikar Johan Akbar, Muhammad Reza

SYNGAS QUALITY IMPROVEMENT IN CORNCOB UPDRAFT GASIFICATION USING CAO/ACTIVATED CARBON PALM FIBER CATALYST

Purbo Suwandono, Widya Wijayanti, Nova Risdiyanto Ismail, Dzulfikar Johan Akbar, Muhammad Reza

Об’єктом даного дослідження є поліпшення якості синтез-газу, отриманого в результаті газифікації кукурудзяних качанів за допомогою системи з подвійним каталізатором, що складається з CaO та активованого вугілля, отриманого з пальмового волокна (AC–PF). Проблема, вирішена в даному дослідженні, полягає у відносно низькій теплотворній здатності синтез-газу з кукурудзяних качанів та високій вартості традиційних каталізаторів, що використовуються для його поліпшення. Дослідження проводилося з використанням різних значень еквівалентного співвідношення (0,2; 0,25; 0,3; 0,35), навантаження каталізатора (4%; 6%; 8%; 10%) та масового співвідношення CaO/AC–PF (0:1; 1:0; 1:1; 2:1) у поєднанні з характеристикою подвійної каталітичної системи. Отримані результати показують, що збільшення ER збільшує частки H_2 і CH_4 та нижчу теплоту згоряння синтез-газу, одночасно зменшуючи CO_2, причому CO досягає оптимального значення при ER = 0,3. У той час як більш високе навантаження каталізатора має тенденцію до зменшення H_2 і CH_4, але збільшує CO, потенційно знижуючи теплоту згоряння при високих навантаженнях Характеристика каталізатора показує, що AC-PF має пористу структуру, яка збільшує контакт газу з твердим тілом і сприяє вторинним реакціям, тоді як додавання CaO утворює композит із модифікованою структурою пор і поверхневими видами, пов'язаними з сорбцією CO_2. З енергетичної точки зору, нижня теплота згоряння синтез-газу збільшується із зростанням ER, але зменшується при більш високих навантаженнях каталізатора через зменшення внеску CH_4. Ключовою особливістю отриманих результатів є продемонстрована функціональна синергія між пористим AC–PF і сорбцією CO_2 на основі CaO, що дозволяє одночасно здійснювати каталітичне поліпшення якості та уловлювання CO_2 в єдиній,

недорогій системі з подвійним каталізатором. Ці висновки можуть стати практичною основою для проектування та експлуатації невеликих установок газифікації біомаси, зокрема реакторів з висхідним потоком для відходів кукурудзяних качанів, в межах досліджених діапазонів ER та навантаження каталізатора.

Ключові слова: газифікація, висхідний потік, кукурудзяні качани, синтез-газ, CaO, активоване вугілля.

The object of this study is the improvement of syngas quality from updraft corn cob gasification using a dual catalyst system consisting of CaO and activated carbon derived from palm fiber (AC–PF). The problem solved in this study is the relatively low heating value of corn cob syngas and the high cost of conventional catalysts used for its upgrading. The study was conducted using variations of equivalence ratio (0.2, 0.25, 0.3, 0.35), catalyst loading (4%, 6%, 8%, 10%), and CaO/AC–PF mass ratio (0:1, 1:0, 1:1, 2:1), combined with characterization of the dual catalyst system. The results obtained show that increasing ER increases the H_2 and CH_4 fractions and the syngas lower heating value while decreasing CO_2, with CO reaching an optimum at ER = 0.3. Whereas higher catalyst loading tends to decrease H_2 and CH_4 but increase CO, potentially reducing the heating value at high loadings Characterization of the catalyst shows that AC-PF has a porous structure that increases gas-solid contact and promotes secondary reactions, while the addition of CaO forms a composite with a modified pore texture and surface species associated with CO_2 sorption. From an energy perspective, the Lower Heating Value of syngas increases with increasing ER, but decrease at higher catalyst loadings due to the reduced contribution of CH_4. A key feature of obtained results is the demonstrated functional synergy between porous AC–PF and CaO-based CO_2 sorption, which enables simultaneous catalytic upgrading and CO_2 capture in a single, low-cost dual catalyst system. These findings could be a practical basis for designing and operating small-scale biomass gasification units, particularly updraft reactors for corn cob waste, within the studied ER and catalyst loading ranges

Keywords: gasification, updraft, corncob, syngas, CaO, activated carbon

1. Introduction

Indonesia is one of the largest corn producers in Southeast Asia, with national production reaching more than 18 million tons of dry kernels per year. Of this amount, about 15–20% is cobs after the kernel removal process, resulting in a very large amount of corn cob waste, estimated at 2.5–3.5 million tons annually. Until now, most corn cobs have only been used to a limited extent, for example as traditional fuel, small amounts of animal feed, or even burned directly on post-harvest land, which has the potential to cause air pollution. Most of the rest are simply piled up or left to rot on the land, posing a risk of becoming a source of plant disease [1].

Corn cobs have quite promising chemical and energy characteristics. Their composition is dominated by cellulose, hemicellulose, and lignin, with a calorific value

of around 15–17 MJ/kg, making them very suitable as raw materials in various biomass-based energy conversion technologies [2]. Their hard and fibrous nature also makes them suitable for processing into biochar, activated charcoal, or direct use in pyrolysis and gasification processes. This significant potential indicates that corn cobs are not merely waste but a renewable resource that can be optimized to support energy security and reduce dependence on fossil fuels.

Biomass gasification is a promising thermochemical technology for converting renewable resources into syngas consisting of H_2, CO, CH_4, and CO_2. Of the various types of biomass, corn cobs are a potential candidate due to their abundant availability in Indonesia and lignocellulose content that supports the energy conversion process [3]. However, the biomass gasification process still faces several obstacles, particularly the low hydrogen fraction in syngas and the formation of significant amounts of tar. Tar can cause reactor clogging, reduced thermal efficiency, and increased purification costs.

To overcome these problems, the use of catalysts is an important strategy. A number of studies have proven that metal catalysts such as Ni, Ca, and K can increase hydrogen yield while suppressing tar formation. On the other hand, activated carbon is also widely used as a catalyst support because it has a high surface area, porous structure, and good chemical stability. The use of agricultural waste, particularly palm fiber, as raw material for activated carbon is not only economically valuable but also supports the concept of a circular economy in plantation waste management. In addition, calcium oxide (CaO) is known to have a dual role, namely as a catalyst in the tar decomposition reaction and as a CO_2 absorber that promotes sorption-enhanced gasification to increase the hydrogen fraction in syngas [4].

Although various studies have examined the role of metal catalysts and activated carbon separately, research focusing on the combination of biomass bases catalyst such as palm fiber-based activated carbon with CaO in corn cob gasification is still limited. The uniqueness of this study lies in the integration of two catalyst, which is expected to provide a synergistic effect: activated carbon with high porosity increases catalyst dispersion and activity, while CaO simultaneously breaks down tar and absorbs CO_2. This approach has the potential to significantly increase hydrogen production and reduce carbon emissions.

However, there are several research gaps that remain unanswered. First, the optimal composition and ratio of activated carbon and CaO in corn cob gasification have not been extensively studied. Second, the synergistic mechanism using two catalyst in increasing syngas quality not yet fully understood. In addition, a systematic and statistically robust approach is required to disentangle the coupled effects of key operating and catalyst variables.

Based on this background and research gaps, this study aims to investigate the performance of a composite catalyst based on activated carbon from palm fiber combined with CaO in the corn cob gasification process. The main focus is on increasing hydrogen production, reducing tar, and evaluating the potential synergistic effects between materials. This research is expected to contribute to the development of

low-cost, locally sourced, and sustainable catalyst systems that are relevant to supporting the clean energy transition and practical applications of biomass-to-hydrogen in the future.

2. Literature review and problem statement

The paper [5] presents the result on the gasification of sago dreg waste pellets in a top-lit updraft fixed-bed gasifier. The results show that the addition of Al_2O_3 improved syngas quality, especially by increasing H_2 content up to 31.65% at 5% Al_2O_3 and enhancing CO and CH_4 production, while also increasing the H_2/CO ratio to 1.65 and 1.51 for 5% and 10% Al_2O_3, respectively, improving LHV, and reducing tar content by about 25–27.5% compared with pellets without catalyst. However, this study is limited because it was conducted only on one biomass type, within a laboratory-scale TULD fixed-bed gasifier, and only considered two catalyst loadings.

The paper [6] presents the result on hydrogen enrichment in product gas from a pilot-scale rice husk updraft gasification. The results show that dolomite-assisted air gasification gave the best performance, increasing the H_2 content up to 15.4 mol%, with an LHV of 5.1 MJ/Nm³, while steam/air gasification improved H_2 to 9.6 mol% and air alone produced only about 7.08 mol% H_2, the optimum operating condition was reported at an airflow rate of 3 m³/h and a dolomite mixing ratio of 15 wt%. However, this study is limited because it focused only on rice husk feedstock, used a pilot-scale updraft gasifier with a batch capacity of 3 kg, and evaluated only a limited range of operating conditions and catalyst type.

The paper [7] presents the result on oxygen updraft gasification coupled with catalytic steam reforming of cigarette butts for hydrogen-rich syngas production. The results show that the integrated process was effective in converting cigarette butts into syngas, with gasification producing 82.3–89.7 wt.% syngas, 6.3–8.6 wt.% soot, and 1.4–1.9 wt.% tar, while the catalytic reforming stage significantly improved the gas quality by increasing the H_2 content up to 30.27 vol.%, increasing the HHV up to 11,528 kJ/kg, and reducing tar concentration from about 18.15 g/m³ to 13.38 g/m³ under the optimum condition. However, this study is limited because it investigated only cigarette butt waste as feedstock, used a specific oxygen updraft gasifier–catalytic reformer configuration, and fixed most catalytic reforming parameters.

The paper [8] presents the result on the experimental assessment of pellets produced from beekeeping waste and slumgum–pine sawdust mixtures through updraft gasification. The results show that pure slumgum pellets exhibited very high mechanical durability (99.98%) and high HHV (27.66 MJ/kg), while during gasification the 50% slumgum–50% sawdust pellets produced the highest producer gas LHV of 7.62 MJ/Nm³, indicating that the addition of sawdust improved gas quality and energy recovery potential. However, this study is limited because the equivalence ratio remained very low (0.0125–0.0204) compared with typical gasification conditions, the experiments were conducted only in a modified laboratory-scale updraft gasifier.

The paper [9] presents the result on a comparative investigation of catalyst applications in updraft and modifiable-downdraft fixed-bed biomass gasifiers, using a biomass mixture of green waste, sewage sludge, and olive pomace together with red mud (RM) and Al–Ni alloy catalysts to improve syngas quality and hydrogen production. The results show that catalyst type and reactor configuration strongly influenced gasification performance, with the Al–Ni catalyst giving the best hydrogen enrichment, reaching up to 65 vol.% H_2 in the updraft gasifier at 900 °C, while RM increased H_2 to about 50 vol.%, the updraft gasifier produced better hydrogen-rich syngas than the modifiable-downdraft reactor. However, this study is limited because it, used a specific mixed biomass composition and mainly focused on high temperature operation around 900 °C with limited gasifying-agent flow conditions.

The paper [10] presents the result on the experimental investigation of producer gas composition from sorted municipal solid wastes in an updraft fixed-bed gasifier. The results show that reducing the equivalence ratio from 0.21 to 0.15 increased the heating value of the combustible gases. The study indicated that the allothermal updraft fixed-bed gasifier is suitable for producing gas that can be utilized in gas engines. However, this study is limited because it used a laboratory-scale 10 kW allothermal updraft gasifier at a fixed temperature of 800 °C, and evaluated only two ER conditions.

The paper [11] presents the result on the effect of adding laying hens manure (LHM) to wheat straw on gasification efficiency in an air-blown updraft fixed-bed gasifier. The results show that increasing ER improved the gasification performance, with the producer gas LHV reaching 3.3–3.4 MJ/m³, cold gas efficiency around 60%, and carbon conversion efficiency in the range of 82–94% . However, this study is limited because it was focused on one specific co-feed system and produced a relatively low-calorific gas.

The paper [12] presents the result on the gasification performance of olive pomace in updraft and downdraft fixed-bed reactors using dry air and pure oxygen. The results show that updraft reactor achieving up to 48 vol.% H_2 with dry air and 53 vol.% H_2 with pure oxygen, while the downdraft reactor reached up to 45 vol.% H_2 with dry air and 39 vol.% H_2 with pure oxygen. However, this study is limited because only a limited range of gasifying agents, temperatures, and flow rates.

The paper [13] presents the result on the gasification of MDF residue in an industrial-scale updraft fixed-bed gasifier. The results show that MDF residue can be effectively converted into useful energy, with a syngas production rate of about 2.5 Nm³/kg, syngas LHV of around 6.0–7.0 MJ/Nm³, about 88 wt.% of MDF residue converted into syngas, and a system capable of delivering 7 MWth of thermal energy and about 955 kW net electrical power through the ORC turbine. However, this study is limited because it focused on one specific industrial waste stream (MDF residue) in one updraft gasifier configuration, mainly evaluated performance under a limited number of feed rates, and relied on direct combustion of raw hot syngas containing tar.

The paper presents the results of research on biomass gasification in updraft fixed-bed reactors aimed at improving syngas quality and thermal conversion efficiency.

Shown that syngas composition and heating value are strongly influenced by feedstock properties, gasification conditions, and catalyst application. But there were unresolved issues related to the lack of effective and low-cost catalyst systems capable of simultaneously enhancing hydrogen formation and improving overall syngas quality during corncob gasification. The reason is the complexity of catalytic reactions in the gasification zone, including reforming, cracking, and CO_2 capture mechanisms, as well as the economic limitations of commercially available catalysts. A way to overcome these difficulties can be the development of composite catalysts based on CaO and activated carbon palm fiber, where CaO may promote CO_2 absorption and shift reactions, while activated carbon palm fiber may provide a porous surface and active sites for secondary cracking reactions. This approach was used in previous studies, however, the combined use of CaO and activated carbon palm fiber in corncob updraft gasification has not been sufficiently investigated. All this suggests that it is advisable to conduct a study on syngas quality improvement in corncob updraft gasification using CaO/activated carbon palm fiber catalyst.

3. The aim and objectives of the study

The purpose of the study is to enhance syngas quality from corncob updraft gasification by developing a dual-synergy catalytic system based on calcium oxide (CaO) and palm-fiber-derived activated carbon (AC-PF). This will allow the production of cleaner and more energy-dense producer gas, providing practical guidance for selecting operating conditions and catalyst configurations suitable for updraft gasifiers processing agricultural residues.

To achieve these aims, the following objectives are accomplished:

– to synthesize and characterize the CaO and palm-fiber activated carbon catalysts using Fourier Transform Infrared Spectroscopy (FTIR), scanning electron microscopy (SEM) and Brunauer-Emmett-Teller surface area analysis (BET);

– to investigate the effects of operating parameters, particularly equivalence ratio (ER), catalyst loading, and CaO/AC ratio, on syngas composition H_2, CO, CH_4, CO_2 and LHV.

4. Materials and methods

The object of the study is the updraft fixed-bed gasification process of corncob biomass using a dual catalyst system based on calcium oxide (CaO) and palm-fiber-derived activated carbon (AC-PF). The practical physical process under investigation is the catalytic upgrading of producer gas within the updraft reactor, where changes in operating parameters and catalyst configuration are expected to influence syngas composition and heating value. The results of this study are intended to be applied to improve the quality of syngas, specifically by increasing the combustible gas fraction (H_2 and CH_4) and the lower heating value (LHV), while reducing CO_2 content.

The research hypothesis is that a dual-synergy CaO/AC-PF catalytic system can improve syngas quality more effectively than single-catalyst configurations in updraft

corncob gasification. It is hypothesized that CaO functions as a CO_2 sorbent, shifting reaction equilibria toward enhanced hydrogen formation, while activated carbon derived from palm fiber provides high-surface-area catalytic sites that promote secondary reactions such as tar cracking and volatile reforming. The combined catalytic-sorption mechanism is expected to increase H_2 and CH_4 fractions and improve LHV under optimized equivalence ratio (ER), catalyst loading, and CaO/AC-PF ratio conditions.

It was assumed that the corncob feedstock has relatively homogeneous composition and stable proximate/ultimate characteristics during the experiments. The gasification process was assumed to operate under steady-state conditions after stabilization. It was also assumed that the CaO maintains sufficient CO_2 sorption capacity within the experimental time frame and that the activated carbon structure remains stable under the applied temperature range.

During the course of the research, several methodological simplifications were adopted in order to maintain experimental feasibility and focus on the main objective of syngas quality evaluation. Detailed kinetic modeling of individual gasification reactions was not performed; instead, the process performance was assessed based on experimentally measured syngas composition and syngas low heating value. Furthermore, although CaO carbonation-decarbonation reactions may occur during operation, microstructural evolution, sintering behavior, and long-term cyclic stability of the catalyst were not investigated in this study. The catalytic performance was evaluated within the experimental duration without conducting extended durability or regeneration-cycle analysis.

4. 1. Catalyst Preparation

Approximately 6 grams of ground palm fiber was mixed with 60 mL of distilled water and stirred for 10 minutes. The mixture was then placed in an autoclave and heated to 200°C at a rate of 5°C per minute for 6 hours in an electric oven. After that, the reactor is allowed to cool naturally to room temperature. The resulting solid hydrocarbon product (hydrochar) is then separated using Whatman No. 42 filter paper. The filtered product is then dried at 105°C for 24 hours and stored in a glass vial. The next stage is the activation process. The hydrochar is immersed in a 3 M KOH solution with a weight ratio of 1:3 (Hydrochar:KOH) for 16 hours, then dried at 85°C for 6 hours. Spectroscopic evidence indicates that KOH preferentially reacts with oxygenated sites and can increase the relative abundance of C–OH functionalities, while higher KOH ratio and activation temperature significantly enhance porosity and BET surface area [14, 15]. To obtain the CaO/AC mixture, CaO powder and activated carbon (AC) were mixed in specific proportions using a grinder until a homogeneous mixture was obtained. Next, CaO, AC, and CaO/AC were activated using a tube furnace at a temperature of 700°C for 1 hour with a continuous flow of nitrogen during the activation process. The resulting product was then washed using distilled water until it reached a neutral pH. This stage produced activated carbon that was ready for use in research.

4. 2. Experimental Setup

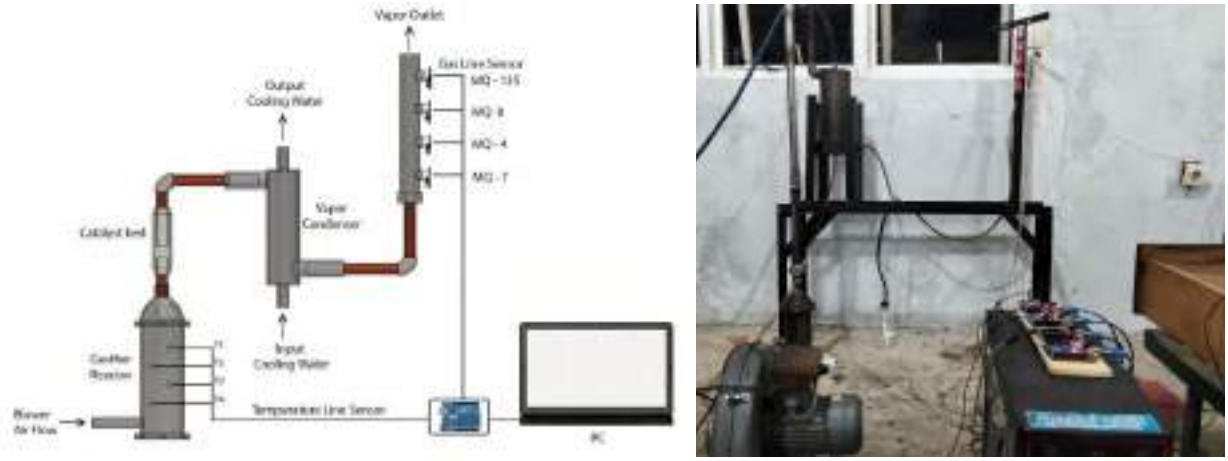
Corncob biomass was obtained from farmers in the South Malang region of East Java. Before use, the biomass was cleaned of impurities and dried in an oven for 6 hours at 100°C to remove moisture (water vapor) content. The ultimate and proximate test results are as follows.

The proximate and ultimate analyses of the corncob feedstock were conducted to determine its physicochemical characteristics prior to gasification. The results are presented in Table 1. The data indicate that corncob has high volatile matter content and relatively low ash content, which are favorable characteristics for gasification processes.

Table 1
Ultimate and Proximate Test Corn Cob

Parameter	Units	Corn cobs
Moisture	%	10
Volatile matter	%	71.38
Fixed carbon	%	12.11
Ash	%	6.51
C	%	43.6
H	%	6.3
O	%	46.8
N	%	0.22
HHV	MJ/kg	17.61

The experimental apparatus employed in this study consisted of an updraft gasifier integrated with a catalyst bed, a vapor condensation unit, gas sensors, and temperature measurement points to enable comprehensive monitoring of the gasification process. Fig. 1 shows the updraft gasifier system used in this study, including the schematic experiment (a) and the experimental setup (b).



a *b*

Fig. 1. Updraft gasifier: *a* – schematic experiment; *b* – experimental setup

This study used an updraft gasification reactor designed with a total height of 20 cm. The lower part of the reactor consisted of an ash container with a height of 5 cm, while the active reactor had a height of 15 cm and a diameter of 3 inches. The reactor was equipped with a 1-inch diameter air inlet pipe connected to a blower. The blower was modified with a potentiometer so that the air speed could be adjusted as needed. To monitor the thermal conditions inside the reactor, four 3 cm long type K thermocouples were installed at several different points so that the temperature profile in the gasification zone could be observed in more detail. Each test was conducted with a fixed biomass mass, a mixture of corn cobs weighing 80 grams. The reactor was made of iron and equipped with a gas seal to prevent leaks during the gasification process.

The gas produced by the reactor was fed into a condenser, which cooled the hot gas so that the water vapor components could be separated. The condenser was made of a copper spiral pipe with a diameter of ½ inch and a height of 30 cm. Cooling water was circulated from the bottom of the condenser and exited through the top to ensure efficient heat transfer. This cooling system was driven by a 60-watt water pump, ensuring stable water flow and optimal condensation. The catalyst was positioned downstream after the reactor, where it was supported on steel wool and wrapped with an 80-µm wire mesh to secure the catalyst and prevent particle carryover with the gas flow

To analyse the gas composition, four types of MQ gas sensors were used. The MQ-8 sensor was used to detect H_2, MQ-4 for CH_4, MQ-135 for CO_2 and MQ-7 for CO. Each gas sensor was calibrated according to the manufacturer's datasheet, specifically by determining the Ro value, which is the sensor resistance in clean air conditions. This Ro value is used as a reference in calculating the measured gas concentration during the process.

All data from the gas sensors and thermocouples were acquired using an Arduino Uno microcontroller. Each gas sensor is connected to a separate Arduino Uno to facilitate the calibration process and reduce the possibility of interference between sensors. Arduino is also used to record temperature data from four thermocouples installed in the reactor, so that gas composition and temperature distribution data can be obtained simultaneously.

The ER range of 0.2, 0.25, 0.3 and 0.35. The catalyst load was between 4%, 6%, 8% and 10% from the mass of input feedstock. The CaO/AC-PF ratio was varied between 0:1, 1:0, 1:1, and 2:1. Design of experiment can be seen in Table 2.

Table 2
Design of Experiment using

Run	Equivalence Ratio (E.R)	Catalyst Load %	CaO/AC
1	0.2	4	1:0
2	0.2	6	0:1

3	0.2	8	1:1
4	0.2	10	2:1
5	0.25	4	0:1
6	0.25	6	1:0
7	0.25	8	2:1
8	0.25	10	1:1
9	0.3	4	1:1
10	0.3	6	2:1
11	0.3	8	1:0
12	0.3	10	0:1
13	0.35	4	2:1
14	0.35	6	1:1
15	0.35	8	0:1
16	0.35	10	1:0

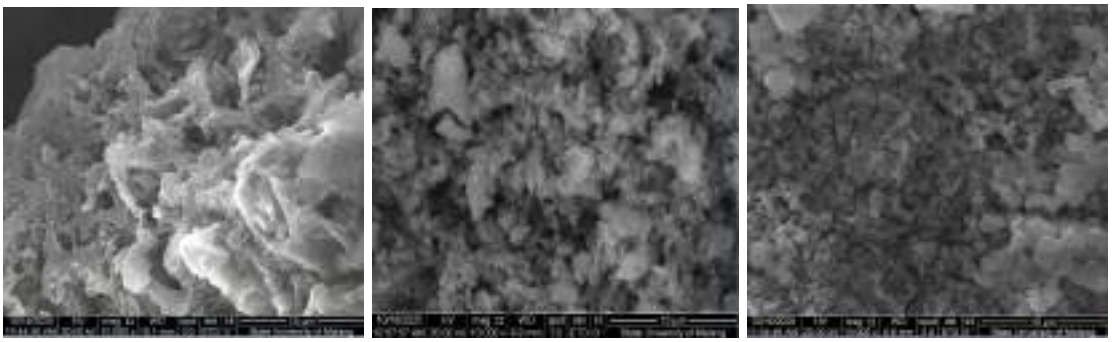
A total of 16 experimental runs were conducted systematically to enable evaluation of the main effects of each variable and the tendency of interactions between variables on the fractions of H_2, CO, CH_4, CO_2, and lower heating value (LHV). This approach enabled identification of the most effective combination of operating parameters in improving syngas quality quantitatively and measurably.

5. Results of syngas quality enhancement from corncob using calcium oxide (CaO) and palm-fiber-derived activated carbon (AC–PF).

5. 1. Characterization of Calcium Oxide (CaO) and Palm-Fiber-Derived Activated Carbon (AC–PF) Catalysts

5. 1. 1. Scanning Electron Microscopy Catalyst Result

Fig. 2, *a* shows the image obtained from a Scanning Electron Microscope (SEM) with a magnification of 10,000× shows the surface morphology of palm fiber-based activated carbon (AC-PF). The surface structure appears porous and irregular, with a combination of void areas and layered surfaces. This characteristic indicates that the activation process that using KOH has successfully formed micropores and mesopores, which play an important role in increasing the specific surface area of activated carbon.



a *b* *c*

Fig. 2. Scanning Electron Microscopy Catalyst Result: *a* – Scanning Electron Microscopy AC-PF; *b* – Scanning Electron Microscopy CaO:AC;1:1; *c* – Scanning Electron Microscopy CaO:AC-PF;2:1

The rough and textured surface indicates that most of the material has undergone lignocellulose cell wall exfoliation, resulting in numerous interparticle gaps. This porous structure greatly supports gas adsorption and diffusion capabilities when used as a catalyst in gasification or thermochemical reactions.

The presence of 1–5 μm voids indicates that most pores are in the mesopore category, supporting the adsorption of gas molecules such as H_2, CO, and tar during the gasification reaction.

The morphology of AC-PF shows the characteristics of porous activated carbon with a heterogeneous pore distribution, where the pores allow increased contact between gas reactants and active sites on the material surface, thereby increasing catalytic efficiency and the ability to absorb tar or CO_2 in biomass-based energy applications.

Fig. 2, *b* shows the surface morphology of the CaO:AC-PF catalyst with a ratio of 1:1. Visually, it can be seen that the surface of this material consists of fine particles ranging in size from microns to submicrons that stick together to form a layered and slightly agglomerated structure.

The presence of fine, light-colored grains indicates an even distribution of CaO particles impregnated on the surface of activated carbon (AC-PF). This CaO distribution fills some of the pores of the carbon, resulting in a denser surface compared to pure AC-PF. However, there are still small gaps and voids between the grains, indicating that the microporous and mesoporous structures are still formed and can support catalytic activity [16].

This morphology illustrates the success of the CaO impregnation process on activated carbon from palm fiber, where the interaction between CaO and the carbon pore walls produces a composite material that is more thermally and chemically stable. This structure is highly conducive to catalyst applications in biomass gasification processes, as CaO particles can function as CO_2 absorbers while accelerating the tar reforming reaction [17].

Fig. 2, *c* shows the surface morphology of the CaO:AC-PF (2:1) catalyst. The image shows that the surface of the material is dominated by agglomerations of fine, round, and irregular particles ranging in size from microns to submicrons. Compared to the CaO:AC-PF (1:1) sample, this structure appears denser and tighter, indicating that an increase in the CaO ratio causes partial closure of the activated carbon surface pores by CaO particles.

The distribution of CaO particles appears more uniform and covers the carbon surface, indicating the successful impregnation of a larger amount of CaO. The light

color in some areas indicates the presence of a calcium oxide phase that is strongly attached to the activated carbon matrix. This structure indicates a strong interaction between CaO and AC-PF, forming a thermally stable composite.

Although some pores are covered, there are still microscopic gaps between the CaO grains that allow gas diffusion to occur, so that the catalyst retains its good adsorption capacity. The combination of the active area of CaO and the porous carbon structure makes this material very promising for biomass gasification or tar reforming applications, as CaO can act as a CO_2 absorber and increase the conversion of carbon to hydrogen gas.

5. 1. 2. Fourier Transform Infrared Spectroscopy catalyst result

The FTIR analysis results shown in the Fig. 3 reveal clear spectral differences between the AC-PF, CaO, and their mixtures (CaO:AC-PF) with ratios of 2:1 and 1:1. In the AC-PF spectrum, the absorption band at 2926 cm^{-1} is associated with the stretching vibration of the C–H group from $–CH_2$ or $–CH_3$ (methylene/methyl stretching), which indicates the presence of hydrocarbon chain residues from the lignocellulose structure. The peak at 1577 cm^{-1} indicates the presence of aromatic C=C or C=O stretching, while the band at 1056 cm^{-1} represents C–O stretching from alcohol or ether groups. In addition, the –OH group that appears in the 3500–3600 cm^{-1} region is identified as the result of AC-PF activation using a KOH solution, which causes the formation of hydroxyl groups on the activated carbon surface. This –OH group plays an important role in increasing the surface activity and adsorption capacity of AC-PF as a catalyst support medium [18, 19].

In pure CaO, the intense band at 3639 cm^{-1} is associated with the stretching of the O–H group from $Ca(OH)_2$, which is formed due to the partial hydration of CaO when exposed to humid air. Meanwhile, the absorption bands at 1426 cm^{-1} and 876 cm^{-1} are associated with C–O stretching and CO_3^{2-} bending, respectively, indicating the formation of $CaCO_3$ due to CO_2 adsorption from the air. This shows that CaO is highly reactive to moisture and carbon dioxide in the environment.

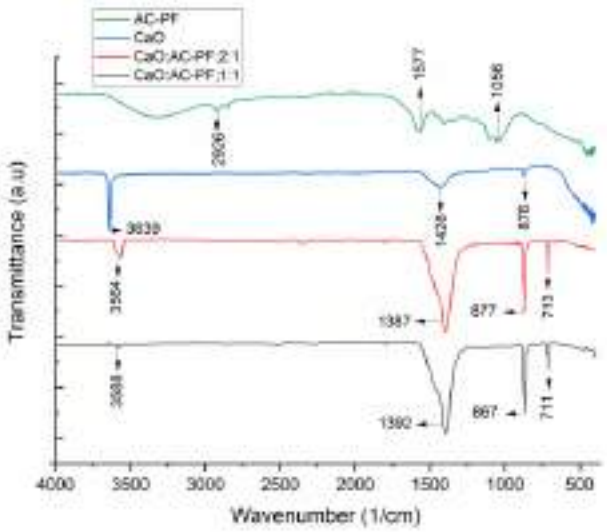


Fig. 3. Fourier Transform Infrared Spectroscopy Catalyst Result

For the CaO:AC-PF (2:1), the main absorption bands were detected at 3564 cm^{-1} (O–H stretching from $Ca(OH)_2$ and the –OH group in AC-PF), 1387 cm^{-1} (C–O stretching), and 877 cm^{-1} and 713 cm^{-1} (bending vibration of CO_3^{2-}). This combination of bands indicates the formation of carbonate compounds ($CaCO_3$) due to the interaction between CaO and the oxygen groups of activated carbon. The presence of –OH groups from KOH activation also strengthens the basic properties on the surface, which can increase the chemical interaction between CaO and AC-PF [20].

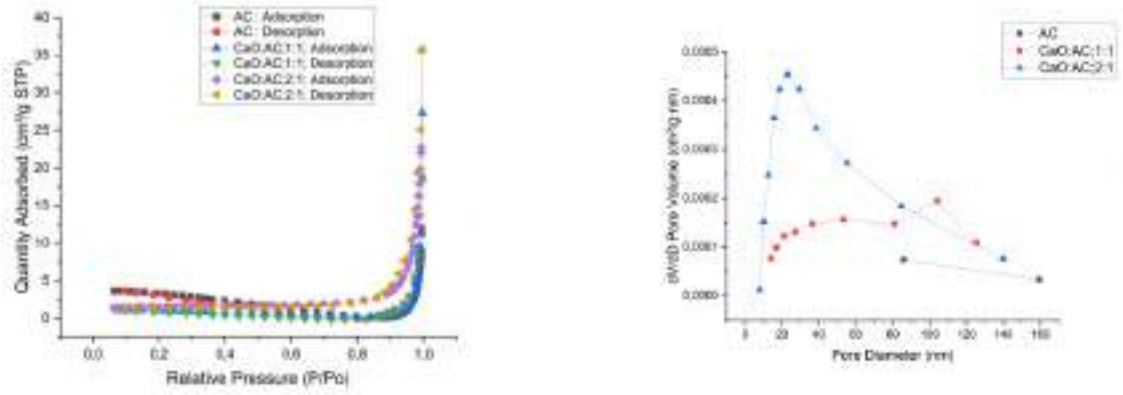
At a CaO:AC-PF ratio of 1:1, the absorption bands at 3588 cm^{-1}, 1392 cm^{-1}, 867 cm^{-1}, and 711 cm^{-1} show a similar pattern, indicating the presence of hydroxyl (O–H) and carbonate (CO_3^{2-}) groups. The difference in peak intensity compared to the 2:1 ratio indicates variations in the level of interaction between CaO and the –OH groups resulting from KOH activation on AC-PF, which affects the formation of carbonate-hydroxide complexes on the material surface [21].

5. 1. 3. Brunauer-Emmett-Teller Catalyst Result

Fig. 4 shows the adsorption-desorption isotherm curves for nitrogen for the AC, CaO:AC (1:1), and CaO:AC (2:1) samples are shown in Fig. 4. All three samples exhibit type IV isotherms with clear hysteresis loops at relatively high pressures (P/Po > 0.9). Based on the IUPAC classification, this characteristic indicates that the material has a mesoporous structure formed through capillary condensation within the pore channels. The difference between the adsorption and desorption pathways indicates that the pore shape is not perfectly cylindrical, but rather tends to be irregular or slit-like, which is commonly found in modified activated carbon materials [22].

The pure activated carbon (AC) sample showed a relatively low nitrogen adsorption volume with a specific surface area of 24.51 m^2/g and an average pore diameter of 0.74 nm, indicating a predominance of microporous structures. In the

CaO:AC (1:1) composite, the surface area did not change significantly compared to pure AC, indicating that the addition of a moderate amount of CaO did not cover the carbon pores much, but only adhered to the external surface of the carbon matrix [23].



a *b*

Fig. 4. Brunauer-Emmett-Teller Result: *a* – Surface Analysis Adsorption Desorption Isotherm; *b* – Barrett-Joyner-Halenda Adsorption Pore Size Distribution

Conversely, in the CaO:AC (2:1) mixture, there was a sharp increase in adsorption volume at relatively high pressure (P/Po > 0.9) to around 35 cm^3/g STP, while the BET surface area decreased dramatically to 5.06 m^2/g, and the pore diameter increased to 22.87 nm.

These changes in isotherm shape and pore size increase indicate that CaO impregnation not only modifies the surface chemistry but also significantly alters the pore structure of activated carbon. This transformation is positive in the context of catalytic applications in biomass gasification processes, as the mesoporous structure can enhance gas diffusion and accessibility to active sites during the tar reforming and water-gas shift reactions. Thus, even though the specific surface area decreases, the increase in mesoporousness and pore connectivity can actually improve catalyst performance in hydrogen gas production [24].

Fig. 4, *b* shows the BJH pore size distribution curves that provide further insight into the textural evolution of the palm-fiber-based activated carbon after CaO impregnation. The pristine AC exhibits a relatively low dV/dD value and a broad contribution only at large pore diameters (>60 nm), indicating that its pore system is dominated by macropores with a limited amount of mesopores. Such a texture is less favourable for gas-solid reactions because the accessible surface area in the mesopore range (2–50 nm) is relatively small.

After CaO loading, the shape and intensity of the BJH curves change markedly. For CaO:AC-PF = 1:1, the distribution shifts toward smaller pore diameters with a pronounced contribution in the mesopore region of approximately 15–60 nm. This behaviour shows that CaO impregnation partially reconstructs the carbon matrix,

enlarging existing micropores and opening blocked pores to generate additional mesoporosity. The effect becomes even more evident at CaO:AC-PF = 2:1, where the curve displays the highest dV/dD values and a distinct maximum centred at about 30–40 nm. The strong peak in this range confirms that a higher CaO loading promotes the development of well-defined mesopores while reducing the relative fraction of very large macropores.

Overall, the BJH analysis demonstrates that CaO acts not only as a reactive sorbent but also as a textural promoter for the palm-fiber AC. The increase in mesopore volume and the shift of the dominant pore size toward 20–40 nm are expected to facilitate the diffusion of gasifying agents and tar molecules, as well as to improve the accessibility of CaO active sites for CO_2 capture and reforming reactions. These features are therefore beneficial for enhancing the catalytic performance of the CaO/AC composite in biomass gasification toward H_2-rich syngas production.

5. 2. Effect of operating parameters on syngas composition and low heating value

5. 2. 1. Effect of Equivalence Ratio on Syngas Product

The composition of syngas from updraft gasification is greatly influenced by the Equivalence Ratio (ER), which is the ratio of the mass flow rate of air compared to the mass flow rate of corncob in the experiment compared to the stoichiometry of air required for complete combustion of corncob. In this study, the ER used was 0.2–0.35 with the following formula

$$ER = \frac{(\dot{m}_a / \dot{m}_{cc})_{\exp}}{(\dot{m}_a / m_{cc})_{stc}},$$

where $\dot{m}_a$ is the air mass flow rate (kg/s), $\dot{m}_{cc}$ is the corncob mass flow rate (kg/s), exp denotes the experimental air-fuel ratio, and stc denotes the stoichiometric air-fuel ratio.

The composition of syngas produced from corncob gasification was evaluated at different equivalence ratios to determine the variation in the main combustible and non-combustible gas components. Changes in the equivalence ratio significantly affected the concentrations of H_2, CH_4, CO, and CO_2, indicating that the air supply plays an important role in the gasification performance and gas quality. Fig. 5 shows the syngas composition obtained at different equivalence ratios.

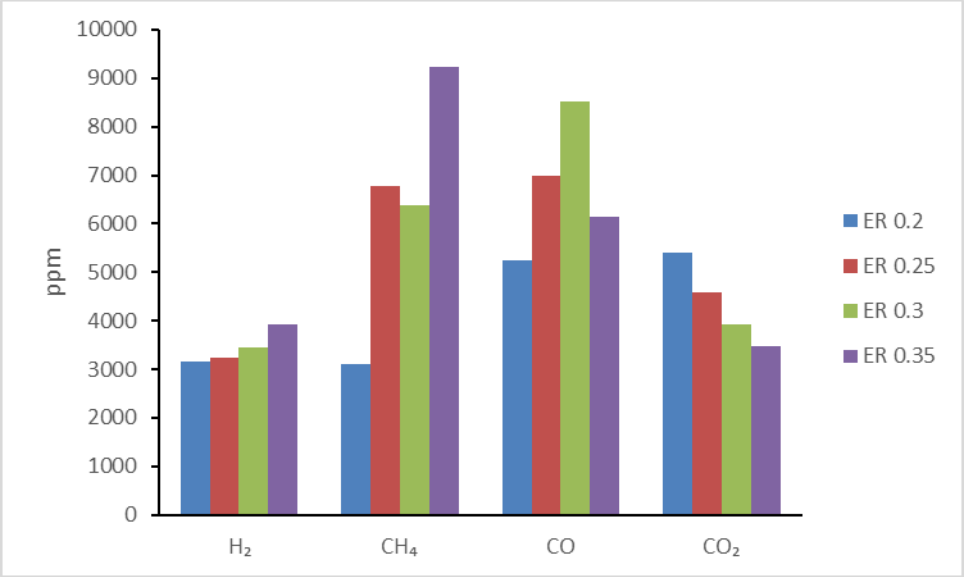


Fig. 5. Syngas composition with different equivalence ratio

The graph above shows that the higher the ER, the higher the hydrogen composition produced. At ER 0.2, the ppm is 3150 ppm, at ER 0.25 it is 3241 ppm, at ER 0.3 it is 3457 ppm, and at ER 0.35 it is 3914 ppm. A higher oxidant supply promotes the formation of more stable autothermal conditions and higher reaction temperatures due to partial oxidation. This increase in temperature accelerates hydrogen-forming reactions, particularly the gasification of active carbon catalyst interactions with steam ($C + H_2O \rightarrow CO + H_2$), the reforming of volatile compounds/light hydrocarbons ($C_xH_y + H_2O \rightarrow CO + H_2$), and the cracking of tar/volatile into lighter gas species. At low ER, some volatiles tend to be incompletely converted and still have the potential to escape as condensable components, while increasing ER increases heat availability, making the conversion of volatiles into gas fractions (including H_2) more effective.

The higher the ER, the higher the CH_4 composition produced. At ER 0.2, 3093 ppm was obtained, at ER 0.25 6767 ppm, ER 0.3 6377 ppm, and ER 0.35 9221 ppm. This trend indicates that the supply of oxidants not only increases autothermal conditions and the rate of devolatilization, but also shifts the reaction pathway towards the formation of light hydrocarbons through hydrogenation and/or methanation reactions in the reactor zone where the temperature still supports CH_4 formation. In particular, increased H_2 at higher ERs can promote the methanation reaction of CO ($CO + 3H_2 \rightleftharpoons CH_4 + H_2O$), so that CH_4 increases along with a tendency for CO to decrease at the highest ER. In addition, more intensive fragmentation of volatiles and tar at high ERs has the potential to produce light gas precursors which are then hydrogenated to CH_4.

CO formation increased up to an ER of 0.3 and decreased at an ER of 0.35. At an ER of 0.2, 5238 ppm was obtained, at an ER of 0.25, 6999 ppm, at an ER of 0.3, 8532 ppm, and decreased at an ER of 0.35 to 6145 ppm. At low ER (0.20–0.25), limited oxygen supply resulted in relatively low heat release, so that the reaction zone

temperature and char reactivity were not sufficient to intensify CO formation reactions, especially the Boudouard reaction ($C + CO_2 \rightleftharpoons 2CO$) and char gasification with steam ($C + H_2O \rightleftharpoons CO + H_2$). When the ER is increased towards 0.30, the increase in autothermal heat strengthens these reduction reactions, causing CO formation to increase and reach its peak. However, at higher ERs (0.35), the CO fraction tends to decrease because some CO can be converted to CH_4.

CO_2 formation continues to decrease as ER increases. At ER 0.2, 5412 ppm is obtained; at ER 0.25, 4592 ppm; at ER 0.3, 3916 ppm; and at ER 0.35, 3479 ppm. The increase in oxidant supply at this ER does not promote complete combustion, but rather strengthens the CO_2 reduction mechanism. At higher ERs, the heat generated from partial oxidation increases the temperature of the reduction zone, thereby accelerating the Boudouard reaction ($C + CO_2 \rightleftharpoons 2CO$), in which CO_2 is reduced by char to CO. This mechanism is consistent with the increase in CO until it reaches a maximum at an ER of 0.30, while also explaining the decrease in CO_2 under the same conditions. Interestingly, at an ER of 0.35, CO_2 remains at its lowest level even though CO decreases, indicating that the CO formed is not completely accumulated at the outlet but has the potential to undergo further conversion along the gas flow path.

5. 2. 2. Effect of Catalyst Loading on Syngas Product

The catalyst load or amount of catalyst in this study was 4%, 6%, 8%, and 10% of the total biomass weight. The Fig. 6. shows that the composition of H_2 and CH_4 increases as the catalyst load decreases. The H_2 gas composition at catalyst loads of 4%, 6%, 8%, and 10% is 3742 ppm, 3471 ppm, 3372 ppm, and 3176 ppm, respectively. As the catalyst load increases, the reaction pathways that consume H_2 tend to strengthen, particularly the reverse water–gas shift ($CO_2 + H_2 \rightarrow CO + H_2O$) and H_2 interactions on the catalyst surface during the conversion of gasification compounds. As a result, even though reforming occurs, the measured net H_2 decreases because more H_2 is used for CO formation and surface reactions. The CH_4 gas composition at catalyst loads of 4%, 6%, 8%, and 10% was 7031 ppm, 6476 ppm, 6206 ppm, and 5746 ppm, respectively. An increase in catalyst load increases the number of active sites and gas-catalyst contact, so that methane/light hydrocarbon cracking and reforming occur more intensely. CH_4 then acts as a reactant that is converted into more reactive syngas components, causing the CH_4 concentration to decrease at higher catalyst loads.

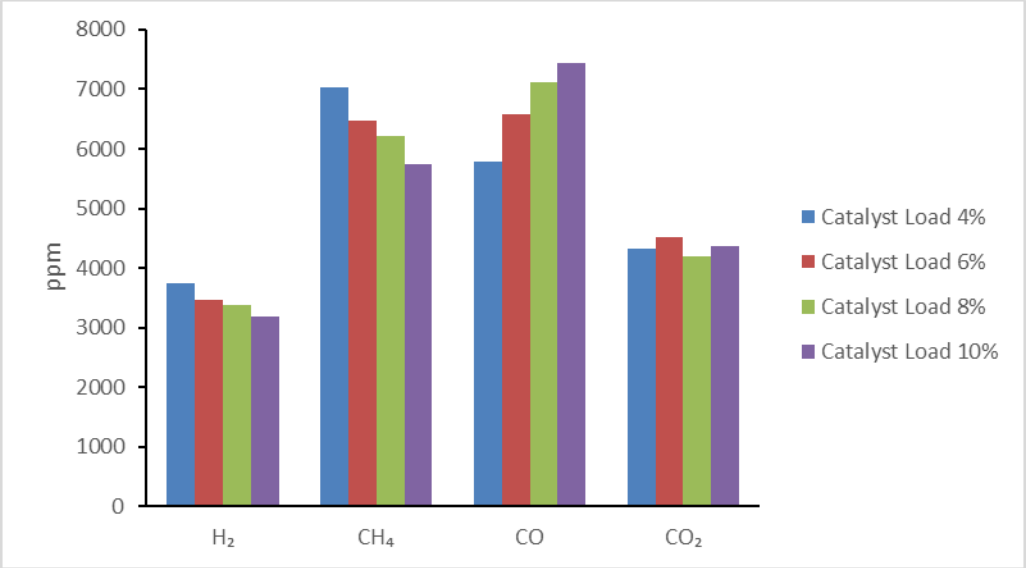


Fig. 6. Syngas Composition with Catalyst Load Variation

The CO gas composition increases with increasing catalyst load, namely for catalyst loads of 4%, 6%, 8% and 10% at 5782 ppm, 6576 ppm, 7111 ppm and 7445 ppm, respectively. The increase in catalyst loading strengthens the CO-forming reactions, particularly dry reforming ($CH_4 + CO_2 \rightarrow 2CO + 2H_2$), char–$CO_2$ reaction ($C + CO_2 \rightarrow 2CO$), and reverse water-gas shift. This combination shifts the product selectivity towards CO, so that the CO fraction increases consistently as the catalyst is increased. The CO_2 gas composition tends to stagnate with increasing catalyst loading, at catalyst loads of 4%, 6%, 8%, and 10% at 4322 ppm, 4510 ppm, 4198 ppm, and 4369 ppm, respectively. CO_2 shows minor changes because it is in a searching for a chemical equilibrium between the partial oxidation and the dry reforming. When the catalyst load increases, the rate of CO_2 consumption may rise, but this is often offset by CO_2 formation in the reaction zone, so that the CO_2 value appears stable or only fluctuates.

5. 2. 3. Effect of Catalyst Ratio on Syngas Product

At a catalyst load of 4%, the CaO/AC ratio changes the gasification reaction through differences in the dominance of tar cracking/reforming and CO_2 capture by CaO, so that the gas composition is highly dependent on the number of active sites and the effectiveness of gas-catalyst contact. At 0:1 (AC), CH_4 and CO are relatively high because AC promotes volatile/tar cracking, but CO_2 remains high because there is no absorption. At 1:0 (CaO), CH_4 decreases but CO_2 is highest, indicating that CO_2 capture is not yet effective due to limited surface area/carbonate layer formation. The 1:1 ratio produces the highest CO with moderate CO_2, indicating CaO–AC synergy that increases the conversion of volatiles into reactive gases. Meanwhile, the 2:1 (CaO-rich) ratio provides the highest H_2 and lowest CO_2 due to the sorption-enhanced effect of CaO, but

CH_4 remains high due to the smaller contribution of AC, so methane reforming/cracking is not yet optimal.

To further examine the catalytic performance, the effect of CaO/AC ratio on syngas composition was investigated under various catalyst loading conditions. This analysis was conducted to determine how the proportion of CaO and activated carbon, combined with different catalyst loads, affected the distribution of H_2, CH_4, CO, and CO_2 during corncob gasification. Fig. 7 illustrates the effect of CaO/AC ratio at catalyst loads of 4% (a), 6% (b), 8% (c), and 10% (d).

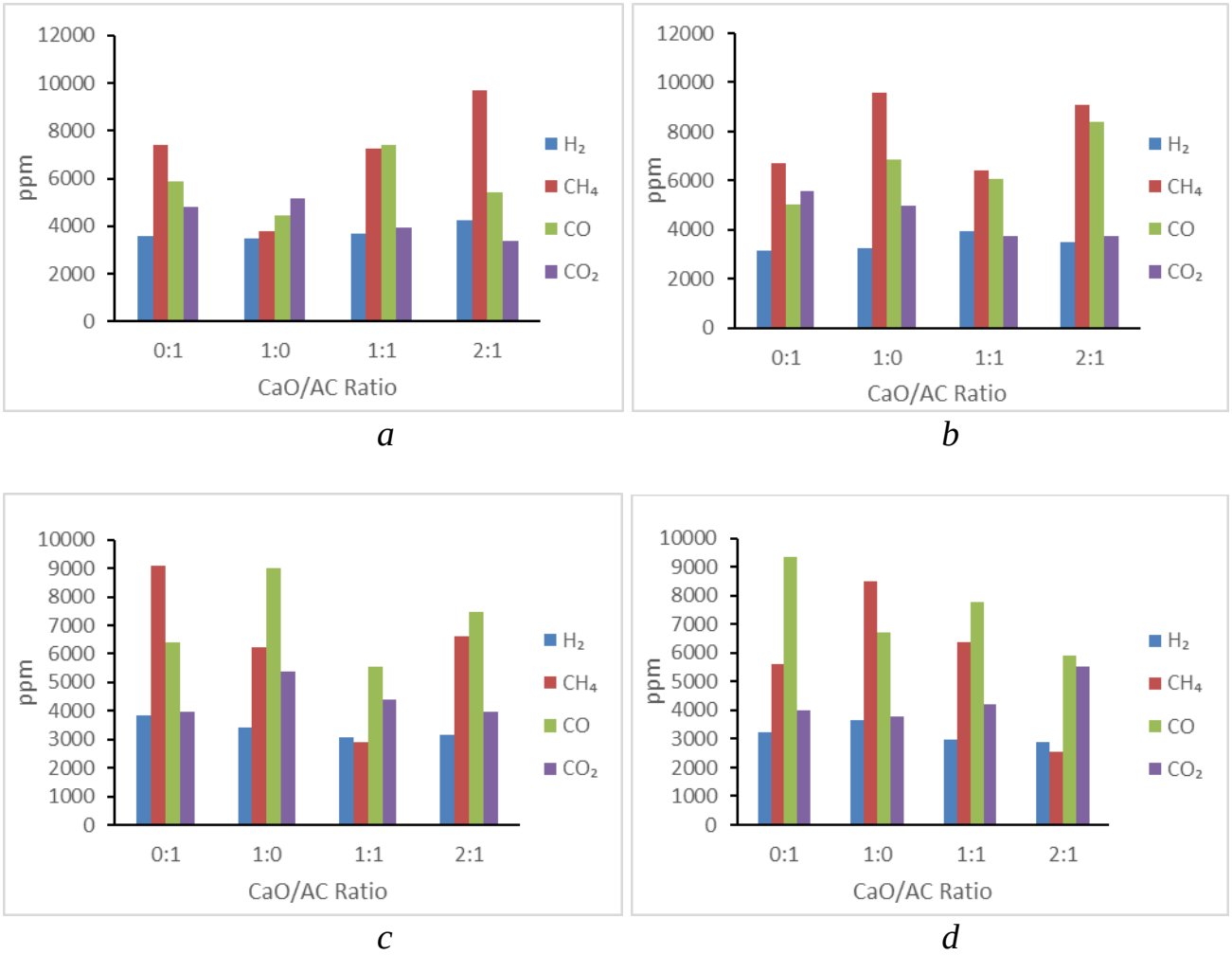


Fig. 7. Effect CaO/AC ratio with various catalyst load: *a* – 4%; *b* – 6%; *c* – 8%; *d* – 10%

At a catalyst load of 4%, the CaO/AC ratio changes the gasification reaction through differences in the dominance of tar cracking/reforming and CO_2 capture by CaO, so that the gas composition is highly dependent on the number of active sites and the effectiveness of gas-catalyst contact. At 0:1 (AC), CH_4 and CO are relatively high because AC promotes volatile/tar cracking, but CO_2 remains high because there is no

absorption. At 1:0 (CaO), CH_4 decreases but CO_2 is highest, indicating that CO_2 capture is not yet effective due to limited surface area/carbonate layer formation. The 1:1 ratio produces the highest CO with moderate CO_2, indicating CaO–AC synergy that increases the conversion of volatiles into reactive gases. Meanwhile, the 2:1 (CaO-rich) ratio provides the highest H_2 and lowest CO_2 due to the sorption-enhanced effect of CaO, but CH_4 remains high due to the smaller contribution of AC, so methane reforming/cracking is not yet optimal.

At a catalyst load of 6%, the CaO/AC ratio mainly shifts the selectivity of secondary reactions (tar cracking/reforming and CO_2 capture), where AC enhances the conversion of volatiles/light hydrocarbons, while CaO reduces CO_2 through carbonation ($CaO + CO_2 \rightarrow CaCO_3$) and changes the reaction equilibrium. At 0:1, CH_4 and CO_2 remain high because there is no CO_2 capture and methane reforming is not yet optimal, so volatiles still escape as CH_4. At 1:0, CO_2 tends to decrease, but CH_4 becomes the highest due to the absence of AC's role in cracking/reforming. The most favorable conditions occur at 1:1, with the highest H_2 and lowest CO_2, indicating CaO–AC synergy that promotes sorption-enhanced reforming and increases the conversion of hydrocarbons into syngas components. At 2:1, CO is highest and CO_2 remains low, but CH_4 rises again and H_2 is not maximized because excess CaO has the potential to rapidly carbonate/cause contact limitations, thereby reducing the contribution of AC in cracking/reforming.

At a catalyst load of 8%, the CaO/AC ratio significantly shifts the selectivity of the syngas reaction. At 0:1 (AC), CH_4 is still high because some light hydrocarbons have not been fully converted even though the tar cracking process is already active. At 1:0 (CaO), CO increases the most, but CO_2 also tends to be high, indicating that CaO in this condition is more dominant in promoting the CO formation pathway, while the CO_2 capture function is not yet optimal due to contact limitations or carbonation saturation. The 1:1 ratio produces the lowest CH_4, indicating the most effective CaO–AC synergy for cracking/reforming light hydrocarbons so that more methane is converted into reactive gas. At 2:1, CO increases again but CH_4 also rises, indicating that a smaller AC fraction reduces the intensity of methane reforming/cracking, while the decrease in CO_2 remains dependent on the effectiveness of CaO sorption.

At a catalyst load of 10%, the increase in total catalyst makes secondary reactions, reforming, solid-gas heterogeneous reactions, and equilibrium shifts very dominant, so that the CaO/AC ratio mainly determines the direction of product selectivity. At 0:1 (AC), CO formation tends to be strongest because the porous carbon surface accelerates the cracking/reforming of volatiles and the conversion of tar into reactive gases. At ratios involving CaO (1:0, 1:1, 2:1), CaO can retain CO_2 through carbonation, but at high loads the effect is often non-linear because CaO rapidly carbonates/diffusion limitations and pore blocking occur, so that under CaO-rich conditions (2:1) CH_4 can decrease, but CO_2 may increase and H_2 is not maximized due to reaction competition. Overall, at a 10% load, a trade-off is observed: AC-dominant increases CO, while CaO-

dominant suppresses light hydrocarbons but has the potential to trigger non-ideal conditions (saturation/mass transport) that reduce the benefits of H_2 and CO_2.

5. 2. 4. Syngas Low Heating Value

To calculate the LHV of syngas, it must first be converted from ppm to % volume of gas. The formula is $\%vol_i = \frac{ppmv_i}{10^4}$ to calculate the LHV, use the formula

$$LHV_{mix}\left(\frac{MJ}{Nm^3}\right) = \frac{10.8(\%H_2) + 12.63(\%CO) + 35.8(\%CH_4)}{100},$$

LHV H_2 = 10.8 MJ/Nm^3,

LHV CO = 12.63 MJ/Nm^3,

LHV CH_4 = 35.8 MJ/Nm^3.

As shown in Fig. 8, the syngas low heating value (LHV) varies with the equivalence ratio (ER) and catalyst load.

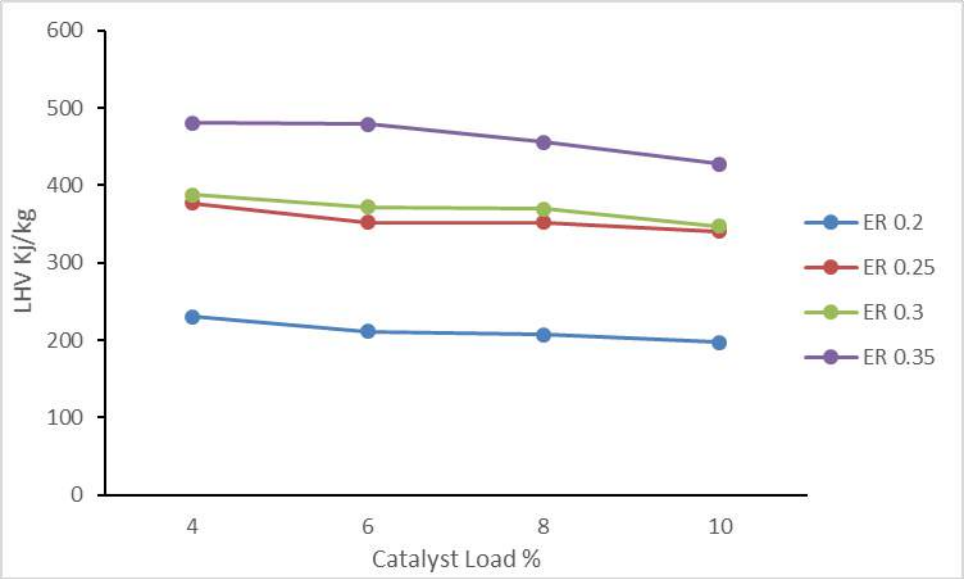


Fig. 8. Syngas low heating value with various equivalence ratio

Fig. 8 shows that the LHV value increases with the ER. At the same catalyst load of 4%, the LHV will increase in line with the increase in ER. ER 0.2 has an LHV of 230 kJ/kg and ER 0.35 has an LHV of 481 kJ/kg. Higher ER produces more intense autothermal conditions, causing the reactor temperature to rise. This increase in temperature accelerates the decomposition of volatiles and tar cracking, and promotes

more complete gasification and reforming reactions, thereby increasing the fraction of permanent gases that contribute to the calorific value, mainly CO and CH_4, as well as some H_2. In addition, the increase in temperature is also associated with more effective hydrogen formation, because H_2 formation reactions (e.g., through steam-water and reforming reactions) are generally more optimal at high temperatures, with the temperature range often reported to be most conducive to H_2 formation being 800–1000°C.

At ER 0.2, the highest LHV was obtained at a catalyst load of 4% at 230 kJ/kg and continued to decrease with increasing catalyst load to 197 kJ/kg at 10%. At ER 0.25, the highest LHV was also obtained at a catalyst load of 4% at 377 kJ/kg and also decreased to 341 kJ/kg at a catalyst load of 10%. At ER 0.3, the highest LHV was obtained at a catalyst load of 4% at 388 kJ/kg and also decreased at a catalyst load of 10% to 347 kJ/kg. At ER 0.35, the highest LHV was obtained at 481 kJ/kg and decreased at a catalyst load of 10% to 428 kJ/kg.

However, all ER values show that LHV tends to decrease when the catalyst load is increased from 4% to 10%. This decrease indicates that excessive catalyst addition under these operating conditions does not always improve gas energy quality, because the catalyst can shift the reaction selectivity towards the conversion of high calorific components especially CH_4 into CO and H_2 through reforming, while at the same time the fraction of diluent gases such as CO_2 (and steam) may increase due to reaction. Since CH_4 has a very large calorific value contribution in the syngas mixture, the decrease in its fraction is often more dominant than the increase in CO/H_2, so that the total LHV tends to decrease.

In energy system analysis, particularly in combustion, gasification, and fuel gas utilisation processes such as syngas, the LHV value is often used because it better represents the heat energy that can actually be utilised by the system. The LHV value of a fuel gas is usually influenced by the composition of combustible gases such as carbon monoxide (CO), hydrogen (H_2), and methane (CH_4). The higher the content of these gases, the greater the LHV value produced. The LHV of syngas from this study with variations in ER and CaO/AC-PF ratio can be seen in Fig. 9.

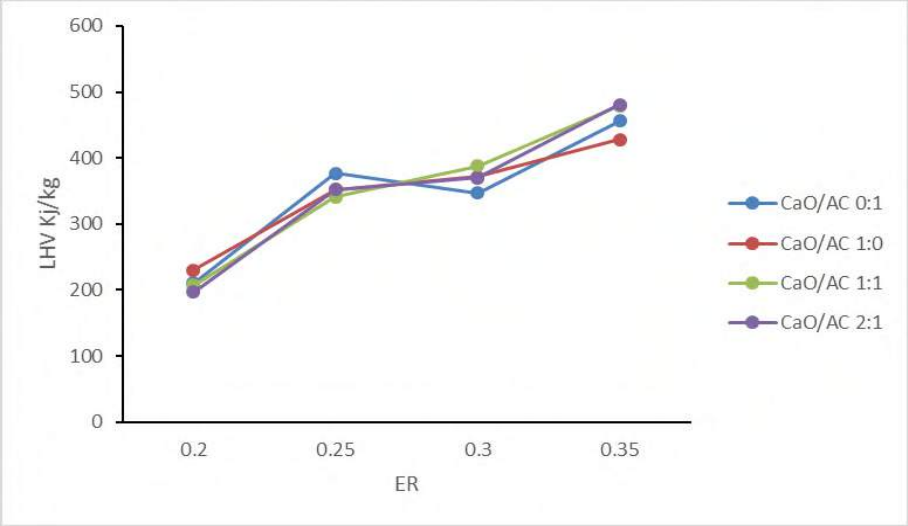


Fig. 9. Syngas Low Heating Value with Various CaO/AC Ratio

Fig. 9 shows that the LHV of syngas increases consistently with the increase in ER 0.2 to 0.35 for all CaO/AC ratios, indicating that a higher ER strengthens autothermal conditions so that the reaction temperature increases and the conversion of volatiles into syngas becomes more complete. At low ER (0.2), the difference in LHV between ratios is still small because secondary reactions such as cracking, reforming and heterogeneous reactions are not yet dominant; the system is still relatively influenced by incompletely converted volatiles. When the ER is increased to 0.25–0.30, the effect of the catalyst ratio becomes apparent: compositions involving AC tend to produce higher LHV because they accelerate tar cracking and increase the fraction of calorific gas, while the contribution of CaO can shift the reaction equilibrium through a decrease in CO_2. At the highest ER (0.35), the LHV reaches its maximum at all ratios, with CaO/AC 2:1 and 0:1 showing peak values, indicating that at high temperatures, the reactive gas formation pathway (via cracking/reforming on the carbon surface and/or CaO-rich-promoted heterogeneous reactions) becomes dominant. Overall, ER acts as the main controlling factor for LHV increase through the temperature effect, while the CaO/AC ratio modulates LHV through the balance between cracking/reforming (AC) and CO_2 control (CaO), especially at medium-high ER.

6. Discussion on the Catalytic Effect of AC-PF/CaO and Operating Conditions on Syngas Composition and LHV

The interaction of the CaO-AC-PF catalyst to improve syngas quality can be seen from the characterisation of the catalyst, the composition of the syngas and the LHV produced. From the Scanning Electron Microscopy results in Fig. 2, it can be seen that the CaO:AC-PF;2:1 catalyst (Fig. 2, *c*) appears denser than the other catalysts. With the addition of CaO, CaO particle dispersion can be seen on the white carbon surface, indicating that some micro pores are closed by CaO. With the addition of CaO, a lot of

CO_2 is absorbed and becomes $CaCO_3$. This porous structure is very important in top-flow gasification because pyrolysis gas and volatiles move through the layer, so the presence of a porous medium has the potential to strengthen secondary reactions and act as carbon capture before the gas exits to the condenser.

From a surface chemistry perspective, Fourier Transform Infrared Spectroscopy (FTIR) shows the presence of –OH and calcium carbonate groups, as shown in Fig. 3. This is due to the results of KOH impregnation carried out during the manufacture of AC-PF. The presence of -OH groups functions as polar active sites capable of adsorbing polar molecules such as H_2O, CO_2, and volatile compounds. Surfaces with -OH groups tend to be hydrophilic and reactive, thereby enhancing interactions with tar compounds or heavy hydrocarbons. These tar compounds can then undergo thermal cracking or catalytic reforming into light gases such as H_2, CO, and CH_4. In addition to -OH, there are also O-H and C-O groups. The O-H group has characteristics that are almost the same as the -OH group, while the C-O group plays a role in enhancing the redox properties and chemical interactions between the carbon surface and gas molecules. In the gasification process, the C-O group can be part of the partial oxidation mechanism and carbon gasification reaction, which produces CO [25].

The BET data in Fig. 4 shows that the surface area decreased to 5.06 m^2/g, but the pore diameter increased to a mesopore scale of 22.87 nm, which can improve the accessibility of volatiles to active sites and improve mass transport in the reforming reaction. In Fig. 4, *b*, the BJH curve at CaO:AC-PF = 2:1 shows the highest dV/dD values of 30–40 nm, indicating a catalyst in the mesopore size range. The presence of these mesopores will further increase the active sites for CO_2 adsorption.

From a process perspective, in Fig. 5, ER appears as the dominant variable that regulates autothermal conditions, primarily through an increase in effective temperature and secondary reaction intensity. An increase in ER from low to high levels consistently increases H_2, which can be explained by the acceleration of H_2 formation reactions such as charcoal gasification with steam ($C + H_2O \rightarrow CO + H_2$) [26], light hydrocarbon reforming, and more intense tar cracking at high temperatures. At the same time, CH_4 also increases sharply at high ER, indicating that in an autothermal upflow system, increased temperature and changes in gas composition can facilitate the formation of light gases. Meanwhile, CO tends to peak at moderate ER and then decreases at high ER, consistent with competition between CO formation and CO consumption through subsequent reactions such as methanation [27]. The decrease in CO_2 at high ER indicates the role of high temperatures in enhancing the reduction of CO_2 by charcoal (Boudouard reaction) and/or the role of CaO adsorption if available.

The effect of catalyst loading in Fig. 6 shows that adding catalyst does not always increase H_2. Increasing the catalyst loading from low to high tends to reduce H_2 and CH_4 but increase CO. Mechanistically, this condition can occur when the catalyst strengthens pathways that increase CO and/or promotes RWGS ($CO_2 + H_2 \rightarrow CO + H_2O$) [28], which consumes H_2 so that net H_2 is reduced. Furthermore, at high catalyst loadings, the possibility of diffusion/aggregation penalties increases, so that selectivity may shift and

some active sites become less effective. Therefore, the target of H_2-rich synthesis gas in this reactor is more dependent on ER adjustment and the selection of moderate/low catalyst loadings, rather than simply increasing the loading.

The CaO/AC-PF ratio in Fig. 7 shows synergistic but non-linear behaviour. AC-PF plays a major role as a porous medium that enhances the cracking/reforming process of volatile compounds, while CaO provides a basic site and CO_2 absorber to shift the equilibrium. At high CaO ratios, sorption and base effects may increase, but the risk of micro-pore closure and diffusion pathway changes also increases. This explains why certain compositions are optimal at certain catalyst loads: the best performance arises from a balance between pore accessibility (the role of AC-PF) and sorption/base strength (the role of CaO).

From an energy quality perspective, in Fig. 8, 9, the LHV value of synthetic gas is highly sensitive to changes in CH_4. Therefore, high ER conditions that increase CH_4 tend to increase LHV. H_2, CH_4 and CO are the main factors for obtaining high LHV. CO_2 has no calorific value so it must be captured. In this study, CaO was used so that CO_2 could be suppressed, meaning that the total LHV could be increased. The highest LHV in this study was 481 kJ/kg, while in another study, the highest was 550 kJ/kg using pinewood with dolomite, activated carbon, silica gel, and limestone catalysts [29]. The higher the ER, the more oxygen enters the system, thereby increasing the reforming reaction [30].

There are several limitations to this study. First, the gas composition was obtained from an MQ sensor based on ppm, so absolute accuracy may be affected by cross-sensitivity, humidity, sensor drift, and gas sampling temperature; this may affect the estimation of %vol and LHV, especially when changes in CO and CH_4 occur simultaneously. Second, catalyst characterisation (SEM-FTIR-BET) supports the role of surface texture and chemistry, but has not quantified changes in the active phase during operation, the degree of carbonation, and the decrease in activity due to pore closure accumulation.

The disadvantage of this research is that the CaO catalyst reacts very easily with CO_2. After the calcination process, CaO must be stored in an airtight container to prevent it from clumping into $CaCO_3$. The catalyst has a specific usage period because it is covered with tar or ash.

Based on these limitations, several future directions are recommended. Calibrate the gas composition using GC-TCD/GC-FID to convert the sensor readings into more accurate %vol and include LHV uncertainty analysis. Evaluate catalyst stability and regeneration, especially for CaO which is easily carbonated, through carbonation-calcination cycle tests and post-reaction characterisation (XRD/TGA/SEM-EDX) to assess phase changes and activity loss. Develop experimental designs towards ANOVA or RSM interactions so that interaction effects and predictive models can be obtained and verified through replication confirmation tests. Add process performance metrics such as gas yield (Nm^3/kg), cold gas efficiency, pressure drop, and air consumption so

that ‘syngas quality improvement’ can be demonstrated based on mass-energy balance and operability, not just composition.

7. Conclusion

1. AC-PF with rich -OH group acts as a porous catalytic medium that facilitates volatile cracking and supports the reduction of condensable by-products, while CaO contributes to absorb CO_2. The BJH analysis confirms that CaO plays a dual role as a reactive sorbent and a textural promoter in palm-fiber activated carbon by enlarging mesopores (20–40 nm), thereby enhancing gas diffusion and improving access to CaO active sites, which ultimately strengthens catalytic performance.

2. Increasing ER to 0.35 enhances the combustible gas fraction H_2 and CH_4 and suppresses CO_2, whereas CO typically peaks at intermediate ER due to competing CO formation and consumption reactions along the updraft reaction zones. Increasing catalyst loading shifts syngas composition: CO increases, while H_2 and CH_4 decrease, indicating changes in dominant secondary reactions and possible diffusion or agglomeration limitations at higher loadings. Increasing ER lead to increase LHV syngas, but it can decrease at high catalyst loading. An increase in the CaO/AC ratio to 2:1 resulted in a higher syngas LHV, with a maximum value of 481 kJ/kg.

Conflict of interest

The authors declare that they have no conflict of interest in relation to this research, whether financial, personal, authorship or otherwise, that could affect the research and its results presented in this paper.

Financing

The authors sincerely thank the Ministry of Education, Culture, Research and Technology, Republic of Indonesia for fully supporting this research through the DRTPM Research Grant under Fundamental Research, Universitas Widyagama Malang, Indonesia 2025 (Grant Number:128/C3/DT.05.00/PL/2025;023/LL7/DT.05.00/PL/2025;010/ Kontrak/PT/PTS.030.7/PN/V/2025).

Data availability

Manuscript has no associated data.

Use of artificial intelligence

The authors used the AI-based language model ChatGPT (GPT-5.3) only to assist in improving the clarity of English language and grammar in several sections of the manuscript, particularly in the Introduction and Literature Review sections.

The AI tool was used solely for language editing and paraphrasing purposes. All scientific content, experimental design, data analysis, and interpretation of the results were conducted entirely by the authors.

The authors carefully reviewed and verified all AI-assisted text to ensure accuracy and consistency with the experimental results. The use of AI tools did not influence the scientific conclusions of this study.

Acknowledgements

We as the Research Team would like to thank Ministry of Education, Culture, Research and Technology, Republic of Indonesia (Kemendiktisaintek Indonesia) for financing research activities.

Authors' contributions

Purbo Suwandono: Conceptualization, Writing-original draft, Investigation, Supervision, Formal analysis, Writing – review & editing; **Widya Wijayanti**: Validation, Investigation, Data Curation, Formal analysis, Writing – original draft; **Nova Risdiyanto Ismail**: Writing – review & editing, Formal analysis; **Dzulfikar Johan Akbar:** Visualization, Writing – original draft, Data curation; **Muhammad Reza**: Project administration, Resources, Data curation.

References

1. V. K. Yadav *et al.*, "Emerging trends in the valorization of agricultural waste and their utilization in agricultural, pharmaceuticals, and environmental cleanup," *Waste and Biomass Valorization*, pp. 1–55, 2025. DOI:10.1007/s12649-025-03002-y
2. W. M. Lewandowski, M. Ryms, and W. Kosakowski, "Thermal biomass conversion: A review," *Processes*, vol. 8, no. 5, p. 516, 2020. https://doi.org/10.3390/pr8050516
3. D. Ariyanti *et al.*, "Valorization of corn cob waste for furfural production: A circular economy approach," *Biomass and Bioenergy*, vol. 194, p. 107665, 2025. DOI:10.1016/j.biombioe.2025.107665
4. J. Zhang, Z. Chu, R. Cao, X. Wu, and K. Han, "A review of resource recovery from waste plastics via pyrolysis and gasification," *Fuel*, vol. 404, p. 136319, 2026. https://doi.org/10.1016/j.fuel.2025.136319
5. Y. Tangke Tosuli, Cahyadi, H. Dafiqurrohman, R. Hermawan, and A. Surjosatyo, "Gasification of sago dreg waste in a top-lit updraft fixed bed gasifier: Syngas composition and its effect with additional Al2O3 as catalyst," *Energy Convers. Manag. X*, vol. 24, no. October, p. 100775, 2024, doi: 10.1016/j.ecmx.2024.100775. https://doi.org/10.1016/j.ecmx.2024.100775
6. P. Dinh *et al.*, "Enrichment of hydrogen in product gas from a pilot-scale rice husk updraft gasification system," *Carbon Resour. Convers.*, vol. 5, no. 3, pp. 231–239, 2025, doi: 10.1016/j.crcon.2022.07.003.
7. S. Yousef and J. Eimontas, "International Journal of Hydrogen Energy Oxygen updraft gasification-catalytic reforming of cigarettes butts for hydrogen-rich syngas production," vol. 171, no. May, 2025, https://doi.org/10.1016/j.ijhydene.2025.150650

8. D. Contreras, E. Blanco, and D. Travieso, “Experimental assessment of the energy potential of pellets produced from beekeeping wastes by updraft gasification,” vol. 343, no. January, 2025, https://doi.org/10.1016/j.enconman.2025.120206
9. N. Yesilova, O. Tezer, A. Ongen, and A. Ayol, “International Journal of Hydrogen Energy Enhancing biomass gasification : A comparative study of catalyst applications in updraft and modifiable-downdraft fixed bed reactors,” *Int. J. Hydrogen Energy*, vol. 76, no. April, pp. 290–303, 2024, https://doi.org/10.1016/j.ijhydene.2024.05.075
10. R. Skvor and A. Jan, “Experimental investigation of sorted municipal solid wastes producer gas composition in an updraft fixed bed gasifier,” vol. 289, no. August 2022, 2024, https://doi.org/10.1016/j.energy.2023.130063
11. R. Junga, M. Tańczuk, S. Sobek, M. Chabiński, and Ł. Ziółkowski, “Effect of the addition of laying hens manure to the straw on gasification efficiency in updraft gasifier under air atmosphere,” *Appl. Therm. Eng.*, vol. 226, no. February, p. 120269, 2023, https://doi.org/10.1016/j.applthermaleng.2023.120269.
12. A. Ongen and A. Ayol, “ScienceDirect Gasification performance of olive pomace in updraft and downdraft fixed bed reactors,” vol. I, 2023, https://doi.org/10.1016/j.ijhydene.2023.02.088
13. K. Ertas, “Gasification of MDF residue in an updraft fixed bed gasifier to produce heat and power via an ORC turbine,” vol. 169, no. February, pp. 43–51, 2023, https://doi.org/10.1016/j.wasman.2023.06.025
14. S. Gorthy, S. Verma, N. Sinha, S. Shetty, H. Nguyen, and M. Neurock, “Theoretical Insights into the Effects of KOH Concentration and the Role of OH–in the Electrocatalytic Reduction of CO2 on Au,” *ACS Catal.*, vol. 13, no. 19, pp. 12924–12940, 2023. DOI:10.1021/acscatal.2c06115
15. X. Wang, W. Zeng, C. Xin, X. Kong, X. Hu, and Q. Guo, “The development of activated carbon from corncob for CO2 capture,” *RSC Adv.*, vol. 12, no. 51, pp. 33069–33078, 2022, https://doi.org/10.1039/D2RA05979G
16. B. Zhou *et al.*, “Insights into effects of grain boundary engineering in composite metal oxide catalysts for improving catalytic performance,” *J. Colloid Interface Sci.*, vol. 653, pp. 1177–1187, 2024. https://doi.org/10.1016/j.jcis.2023.09.148
17. Y. Zhu *et al.*, “Preparation of hierarchically porous carbon ash composite material from fine slag of coal gasification and ash slag of biomass combustion for CO2 capture,” *Sep. Purif. Technol.*, vol. 330, p. 125452, 2024. https://doi.org/10.1016/j.seppur.2023.125452
18. M. Ilić *et al.*, “Surface functional groups and degree of carbonization of *selected* chars from different processes and feedstock,” *PLoS One*, vol. 17, no. 11, p. e0277365, 2022. https://doi.org/10.1371/journal.pone.0277365
19. R. Ali, Z. Aslam, R. A. Shawabkeh, A. Asghar, and I. A. Hussein, “BET, FTIR, and RAMAN characterizations of activated carbon from waste oil fly ash,” *Turkish J. Chem.*, vol. 44, no. 2, pp. 279–295, 2020. doi: 10.3906/kim-1909-20
20. K. J. Stanienda-Pilecki, “The importance of Fourier-Transform Infrared

Spectroscopy in the identification of carbonate phases differentiated in magnesium content," 2019.

21. F. Dai, Q. Zhuang, G. Huang, H. Deng, and X. Zhang, "Infrared spectrum characteristics and quantification of OH groups in coal," *ACS omega*, vol. 8, no. 19, pp. 17064–17076, 2023. https://doi.org/10.1021/acsomega.3c01336

22. E. M. de Salazar Martínez, M. F. Alexandre-Franco, A. J. Nieto-Sanchez, and E. M. Cuerda-Correa, "Exploring the role of surface and porosity in CO2 capture by CaO-based adsorbents through response surface methodology (RSM) and artificial neural networks (ANN)," *J. CO2 Util.*, vol. 83, p. 102773, 2024. https://doi.org/10.1016/j.jcou.2024.102773

23. J. A. Tavizón-Pozos, H. Cervantes-Cuevas, G. G. Garcia-Camacho, G. Chavez-Esquivel, and D. R. Acosta-Najarro, "Biodiesel Production Using K–Sr/CaO and CaO Catalysts Derived from Eggshells by Canola Oil Transesterification," *ACS omega*, vol. 10, no. 7, pp. 6827–6838, 2025. https://doi.org/10.1021/acsomega.4c09118

24. W. Koo-Amornpattana, P. Phadungbut, N. Kunthakudee, W. Jonglertjunya, S. Ratchahat, and M. Hunsom, "Innovative metal oxides (CaO, SrO, MgO) impregnated waste-derived activated carbon for biohydrogen purification," *Sci. Rep.*, vol. 13, no. 1, p. 4705, 2023. DOI:10.1038/s41598-023-31723-4

25. C. Quan, M. Wang, N. Gao, T. Yang, and R. Li, "In situ adsorption of CO2 to enhance biomass gasification for hydrogen production using Ca/Ni based composites," *J. Energy Inst.*, vol. 108, p. 101229, 2023, doi: https://doi.org/10.1016/j.joei.2023.101229. https://doi.org/10.1016/j.joei.2023.101229

26. F. Micheli, E. Mattucci, C. Courson, and K. Gallucci, "Bi-Functional Catalyst/Sorbent for a H2-Rich Gas from Biomass Gasification," 2021. doi: 10.3390/pr9071249. DOI:10.3390/PR9071249

27. M. Zhu, Q. Wang, and S. Wang, "Recent Advances and Future Perspectives in Catalyst Development for Efficient and Sustainable Biomass Gasification: A Comprehensive Review," 2025, https://doi.org/10.3390/su17167370

28. N. Cerone, F. Zimbardi, L. Contuzzi, J. Baleta, and D. Cerinski, "Experimental investigation of syngas composition variation along updraft fixed bed gasifier," *Energy Convers. Manag.*, vol. 221, no. July, p. 113116, 2020, https://doi.org/10.1016/j.enconman.2020.113116

29. R. Mohanty, P. Mahanta, A. Mahapatro, and R. Prakash, "Catalytic gasification of pinewood biomass in a fluidized bed reactor with dolomite , limestone , and activated carbon : An experimental study," *Energy*, vol. 325, no. April, p. 136131, 2025, doi: 10.1016/j.energy.2025.136131. https://doi.org/10.1016/j.energy.2025.136131

30. C. Liu, Y. Huang, M. Niu, and H. Pei, "ScienceDirect Influences of equivalence ratio , oxygen concentration and fluidization velocity on the characteristics of oxygen-enriched gasification products from biomass in a pilot-scale fluidized bed," *Int. J. Hydrogen Energy*, vol. 43, no. 31, pp. 14214–14225, 2018, https://doi.org/10.1016/j.ijhydene.2018.05.154

References

1. V. K. Yadav *et al.*, “Emerging trends in the valorization of agricultural waste and their utilization in agricultural, pharmaceuticals, and environmental cleanup,” *Waste and Biomass Valorization*, pp. 1–55, 2025. DOI:10.1007/s12649-025-03002-y
2. W. M. Lewandowski, M. Ryms, and W. Kosakowski, “Thermal biomass conversion: A review,” *Processes*, vol. 8, no. 5, p. 516, 2020. https://doi.org/10.3390/pr8050516
3. D. Ariyanti *et al.*, “Valorization of corn cob waste for furfural production: A circular economy approach,” *Biomass and Bioenergy*, vol. 194, p. 107665, 2025. DOI:10.1016/j.biombioe.2025.107665
4. J. Zhang, Z. Chu, R. Cao, X. Wu, and K. Han, “A review of resource recovery from waste plastics via pyrolysis and gasification,” *Fuel*, vol. 404, p. 136319, 2026. https://doi.org/10.1016/j.fuel.2025.136319
5. Y. Tangke Tosuli, Cahyadi, H. Dafiqurrohman, R. Hermawan, and A. Surjosatyo, “Gasification of sago dreg waste in a top-lit updraft fixed bed gasifier: Syngas composition and its effect with additional Al2O3 as catalyst,” *Energy Convers. Manag. X*, vol. 24, no. October, p. 100775, 2024, doi: 10.1016/j.ecmx.2024.100775. https://doi.org/10.1016/j.ecmx.2024.100775
6. P. Dinh *et al.*, “Enrichment of hydrogen in product gas from a pilot-scale rice husk updraft gasification system,” *Carbon Resour. Convers.*, vol. 5, no. 3, pp. 231–239, 2025, doi: 10.1016/j.crcon.2022.07.003.
7. S. Yousef and J. Eimontas, “International Journal of Hydrogen Energy Oxygen updraft gasification-catalytic reforming of cigarettes butts for hydrogen-rich syngas production,” vol. 171, no. May, 2025, https://doi.org/10.1016/j.ijhydene.2025.150650
8. D. Contreras, E. Blanco, and D. Travieso, “Experimental assessment of the energy potential of pellets produced from beekeeping wastes by updraft gasification,” vol. 343, no. January, 2025, https://doi.org/10.1016/j.enconman.2025.120206
9. N. Yesilova, O. Tezer, A. Ongen, and A. Ayol, “International Journal of Hydrogen Energy Enhancing biomass gasification : A comparative study of catalyst applications in updraft and modifiable-downdraft fixed bed reactors,” *Int. J. Hydrogen Energy*, vol. 76, no. April, pp. 290–303, 2024, https://doi.org/10.1016/j.ijhydene.2024.05.075
10. R. Skvor and A. Jan, “Experimental investigation of sorted municipal solid wastes producer gas composition in an updraft fixed bed gasifier,” vol. 289, no. August 2022, 2024, https://doi.org/10.1016/j.energy.2023.130063
11. R. Junga, M. Tańczuk, S. Sobek, M. Chabiński, and Ł. Ziółkowski, “Effect of the addition of laying hens manure to the straw on gasification efficiency in updraft gasifier under air atmosphere,” *Appl. Therm. Eng.*, vol. 226, no. February, p. 120269, 2023, https://doi.org/10.1016/j.applthermaleng.2023.120269.
12. A. Ongen and A. Ayol, “ScienceDirect Gasification performance of olive pomace in updraft and downdraft fixed bed reactors,” vol. I, 2023,

https://doi.org/10.1016/j.ijhydene.2023.02.088
13. K. Ertas, “Gasification of MDF residue in an updraft fixed bed gasifier to produce heat and power via an ORC turbine,” vol. 169, no. February, pp. 43–51, 2023, https://doi.org/10.1016/j.wasman.2023.06.025
14. S. Gorthy, S. Verma, N. Sinha, S. Shetty, H. Nguyen, and M. Neurock, “Theoretical Insights into the Effects of KOH Concentration and the Role of OH–in the Electrocatalytic Reduction of CO2 on Au,” *ACS Catal.*, vol. 13, no. 19, pp. 12924–12940, 2023. DOI:10.1021/acscatal.2c06115
15. X. Wang, W. Zeng, C. Xin, X. Kong, X. Hu, and Q. Guo, “The development of activated carbon from corncob for CO2 capture,” *RSC Adv.*, vol. 12, no. 51, pp. 33069–33078, 2022, https://doi.org/10.1039/D2RA05979G
16. B. Zhou *et al.*, “Insights into effects of grain boundary engineering in composite metal oxide catalysts for improving catalytic performance,” *J. Colloid Interface Sci.*, vol. 653, pp. 1177–1187, 2024. https://doi.org/10.1016/j.jcis.2023.09.148
17. Y. Zhu *et al.*, “Preparation of hierarchically porous carbon ash composite material from fine slag of coal gasification and ash slag of biomass combustion for CO2 capture,” *Sep. Purif. Technol.*, vol. 330, p. 125452, 2024. https://doi.org/10.1016/j.seppur.2023.125452
18. M. Ilić *et al.*, “Surface functional groups and degree of carbonization of *selected* chars from different processes and feedstock,” *PLoS One*, vol. 17, no. 11, p. e0277365, 2022. https://doi.org/10.1371/journal.pone.0277365
19. R. Ali, Z. Aslam, R. A. Shawabkeh, A. Asghar, and I. A. Hussein, “BET, FTIR, and RAMAN characterizations of activated carbon from waste oil fly ash,” *Turkish J. Chem.*, vol. 44, no. 2, pp. 279–295, 2020. doi: 10.3906/kim-1909-20
20. K. J. Stanienda-Pilecki, “The importance of Fourier-Transform Infrared Spectroscopy in the identification of carbonate phases differentiated in magnesium content,” 2019.
21. F. Dai, Q. Zhuang, G. Huang, H. Deng, and X. Zhang, “Infrared spectrum characteristics and quantification of OH groups in coal,” *ACS omega*, vol. 8, no. 19, pp. 17064–17076, 2023. https://doi.org/10.1021/acsomega.3c01336
22. E. M. de Salazar Martínez, M. F. Alexandre-Franco, A. J. Nieto-Sanchez, and E. M. Cuerda-Correa, “Exploring the role of surface and porosity in CO2 capture by CaO-based adsorbents through response surface methodology (RSM) and artificial neural networks (ANN),” *J. CO2 Util.*, vol. 83, p. 102773, 2024. https://doi.org/10.1016/j.jcou.2024.102773
23. J. A. Tavizón-Pozos, H. Cervantes-Cuevas, G. G. Garcia-Camacho, G. Chavez-Esquivel, and D. R. Acosta-Najarro, “Biodiesel Production Using K–Sr/CaO and CaO Catalysts Derived from Eggshells by Canola Oil Transesterification,” *ACS omega*, vol. 10, no. 7, pp. 6827–6838, 2025. https://doi.org/10.1021/acsomega.4c09118
24. W. Koo-Amornpattana, P. Phadungbut, N. Kunthakudee, W. Jonglertjunya, S. Ratchahat, and M. Hunsom, “Innovative metal oxides (CaO, SrO, MgO) impregnated waste-derived activated carbon for biohydrogen purification,” *Sci. Rep.*, vol. 13, no. 1, p.

4705, 2023. DOI:10.1038/s41598-023-31723-4
25. C. Quan, M. Wang, N. Gao, T. Yang, and R. Li, “In situ adsorption of CO2 to enhance biomass gasification for hydrogen production using Ca/Ni based composites,” *J. Energy Inst.*, vol. 108, p. 101229, 2023, doi: https://doi.org/10.1016/j.joei.2023.101229. https://doi.org/10.1016/j.joei.2023.101229
26. F. Micheli, E. Mattucci, C. Courson, and K. Gallucci, “Bi-Functional Catalyst/Sorbent for a H2-Rich Gas from Biomass Gasification,” 2021. doi: 10.3390/pr9071249. DOI:10.3390/PR9071249
27. M. Zhu, Q. Wang, and S. Wang, “Recent Advances and Future Perspectives in Catalyst Development for Efficient and Sustainable Biomass Gasification: A Comprehensive Review,” 2025, https://doi.org/10.3390/su17167370
28. N. Cerone, F. Zimbardi, L. Contuzzi, J. Baleta, and D. Cerinski, “Experimental investigation of syngas composition variation along updraft fixed bed gasifier,” *Energy Convers. Manag.*, vol. 221, no. July, p. 113116, 2020, https://doi.org/10.1016/j.enconman.2020.113116
29. R. Mohanty, P. Mahanta, A. Mahapatro, and R. Prakash, “Catalytic gasification of pinewood biomass in a fluidized bed reactor with dolomite , limestone , and activated carbon : An experimental study,” *Energy*, vol. 325, no. April, p. 136131, 2025, doi: 10.1016/j.energy.2025.136131. https://doi.org/10.1016/j.energy.2025.136131
30. C. Liu, Y. Huang, M. Niu, and H. Pei, “ScienceDirect Influences of equivalence ratio , oxygen concentration and fluidization velocity on the characteristics of oxygen-enriched gasification products from biomass in a pilot-scale fluidized bed,” *Int. J. Hydrogen Energy*, vol. 43, no. 31, pp. 14214–14225, 2018, https://doi.org/10.1016/j.ijhydene.2018.05.154

Author’s order	First Name	Middle name	Second Name
1	*Purbo*		*Suwandono*
2	*Widya*		*Wijayanti*
3	*Nova*	*Risdiyanto*	*Ismail*
4	*Dzulfikar*	*Johan*	*Akbar*
5	*Muhammad*		*Reza*

English

Purbo Suwandono
Corresponding author
Master
Department of Mechanical Engineering
Widya Gama University
Borobudur str., 35, Malang, Indonesia, 65142
E-mail: purbo@widyagama.ac.id

ORCID: https://orcid.org/0000-0003-4085-1291
Contact phone: +6282132697144
Number of publications in national journals indexed (approximate; for Ukraine citizens only): -
Number of publications in international journals indexed (approximate): 14
H-index by Scopus (if available): 4
ResearchGate: https://www.researchgate.net/profile/Purbo-Suwandono
Scopus ID: 57204187970
Researcher ID: https://researchid.co/rid80879

Widya Wijayanti
PhD
Department of Mechanical Engineering
Brawijaya University
Veteran str., 10–11, Malang, Indonesia, 65145
E-mail: widya_dinata@ub.ac.id
ORCID: https://orcid.org/0000-0003-4215-5943
Contact phone: +6285334992164
Number of publications in national journals indexed (approximate; for Ukraine citizens only): -
Number of publications in international journals indexed (approximate): 78
H-index by Scopus (if available): 12
ResearchGate: https://www.researchgate.net/profile/Widya-Wijayanti
Scopus ID: 36006672800
Researcher ID: -

Nova Risdiyanto Ismail
PhD
Department of Mechanical Engineering
Widya Gama University
Borobudur str., 35, Malang, Indonesia, 65142
E-mail: nova@widyagama.ac.id
ORCID: https://orcid.org/0000-0001-8439-6919
Contact phone:
Number of publications in national journals indexed (approximate; for Ukraine citizens only): -
Number of publications in international journals indexed (approximate): 7
H-index by Scopus (if available): 3
ResearchGate: https://www.researchgate.net/profile/Nova-Ismail-2
Scopus ID: 57204527065
Researcher ID: https://researchid.co/rid80876

Dzulfikar Johan Akbar
Master Student
Department of Mechanical Engineering
Brawijaya University
Veteran str., 10–11, Malang, Indonesia, 65145
E-mail: johanakbar@student.ub.ac.id
ORCID: https://orcid.org/0009-0002-4652-8516
Contact phone: +6282241116998
Number of publications in national journals indexed (approximate; for Ukraine citizens only): -
Number of publications in international journals indexed (approximate): -
H-index by Scopus (if available): -
ResearchGate: https://www.researchgate.net/profile/Dzulfikar-Johan-Akbar
Scopus ID: -
Researcher ID: -

Muhammad Reza
Bachelor Student
Department of Mechanical Engineering
Widya Gama University
Borobudur str., 35, Malang, Indonesia, 65142
E-mail: muhapanjangreza@gmail.com
ORCID: https://orcid.org/0009-0009-9258-0586
Contact phone: +6282139682566
Number of publications in national journals indexed (approximate; for Ukraine citizens only): -
Number of publications in international journals indexed (approximate): -
H-index by Scopus (if available): -
ResearchGate: -
Scopus ID: -
Researcher ID: -

Name of reviewer: Prof. Dr. Muji Setiyo, ST., MT.
Professor: Mechanical Engineering
Tel: +6281211020288
E-mail: muji@unimma.ac.id.
Work address: Universitas Muhammadiyah Magelang

Name of reviewer: Prof. Dr. Eng. Nurkholis Hamidi, ST., MT.
Professor: Mechanical Engineering
Tel: +62 81259293165

E-mail: hamidy@ub.ac.id
Work address: Brawijaya University

Received date: 20.02.2026
Accepted date:

From Reviewer

1. Section 1: The authors justified the relevance of the research topic appropriately. Currently, most scientists are conducting research related to "green technologies". "Green technologies" are the production of biogas from agricultural waste. Then the biogas is converted into synthesis gas as a raw material for further syntheses or a product of energy direction. The authors considered another process of converting plant raw materials, which is gasification. The authors should first provide information about the situation in the world and the country about the environmental situation. Provide information about the prospects of "green technologies".

2. The authors considered the topic and direction of research in 10 articles. The articles are related to the transformation of various plant raw materials. Catalytic transformations using different types of catalysts and in different types of reactors are considered. Most of the information material is used from Scopus format articles. The authors formulated the questions not very clearly, which ones have already been investigated and which ones the authors want to investigate further.

Question to the editors: the list of information materials is highlighted in color. How should I understand this? Is this the final list or will it be further adjusted?
If the list of references is adjusted, then this section of the review makes no sense.

3. The purpose of the study is set by the authors according to the topic. But the authors should formulate the research tasks more clearly. This is the creation of a catalyst, then the analysis of its surface by appropriate methods and the study of the parameters of the gasification process with the production of synthesis gas.

4. The authors of the article have defined the object of the research. The authors have also formulated a hypothesis regarding the research. The authors have made some assumptions regarding the course of the process. The article also provides a system of simplifications regarding the conduct of the research. But the authors should more clearly state why the authors use such research methods.

5. In the article, the authors should provide a comparison of the results with existing data when analyzing them. This will allow the research to be perceived as promising.

6. Regarding the analysis and discussion of the research results provided by spectrometric analysis, it is appropriate. The authors should substantiate the results of

the experimental research in more detail. The justification should be built in comparison with existing literature data.

7. The authors of the article conduct research that has scientific and practical activities. The products of the reaction are declared synthesis gas, which is both the target product and an intermediate for obtaining other products of the chemical industry. Synthesis gas is also a good source of energy for use in energy technologies. The authors should provide more details on the practicality of the research in the article.

8. The article does not clearly state the purpose and objectives. Therefore, the conclusions look formulaic. The authors should formulate the conclusions in such a way that it is clear that the research is successful on already known data.

9. The article contains all the necessary sections. It has a promising research direction and is related to the processing of plant raw materials. The manuscript is written clearly, but some points need to be made clearer.

Generally:

The article is related to a promising area of biotechnology. The authors investigated the process of processing plant raw materials by gasification. The authors created a catalyst production plant and the course of the gasification process. The authors conducted a number of studies on the influence of process parameters on the course of the reaction. In the article, the authors presented the results of the research and their analysis. But the authors should correct some points. The goal and objectives of the article should be stated more clearly. In particular, the authors should formulate the tasks more clearly. In the article, the authors considered such points as the creation of a catalyst, surface analysis by spectrometric methods, and the study of various parameters of the reaction course to obtain synthesis gas. When analyzing the research results, the authors should not only describe the values. They should also note their positive impact in comparison with known values. When justifying the goal, the authors should also more clearly provide the scientific and practicality of the selected study. Such updates should also be noted in the conclusions for a clearer understanding.
In the article, the authors should: more clearly formulate the goal and objectives; When analyzing research results, one should provide their justifications regarding their prospects; add a little information regarding the scientificity and practicality of the results; the conclusions of the article should also be formed according to the tasks and provide results in comparison with their prospects.
These comments to the article do not reduce its relevance. These corrections to the article will give it a clearer perception and understanding of prospects.

The article requires revision

UDC 662.7:662.767:66.097

ПОКРАЩЕННЯ ЯКОСТІ СИНТЕЗ-ГАЗУ ПРИ ВИСХІДНІЙ ГАЗИФІКАЦІЇ КУКУРУДЗЯНИХ КАЧАНІВ З ВИКОРИСТАННЯМ КАТАЛІЗАТОРА НА ОСНОВІ CAO/АКТИВОВАНОГО ВУГІЛЛЯ НА ПАЛЬМОВОМУ ВОЛОКН

Purbo Suwandono, Widya Wijayanti, Nova Risdiyanto Ismail, Dzulfikar Johan Akbar, Muhammad Reza

SYNGAS QUALITY IMPROVEMENT IN CORNCOB UPDRAFT GASIFICATION USING CAO/ACTIVATED CARBON PALM FIBER CATALYST

Purbo Suwandono, Widya Wijayanti, Nova Risdiyanto Ismail, Dzulfikar Johan Akbar, Muhammad Reza

Об’єктом даного дослідження є поліпшення якості синтез-газу, отриманого в результаті газифікації кукурудзяних качанів за допомогою системи з подвійним каталізатором, що складається з CaO та активованого вугілля, отриманого з пальмового волокна (AC–PF). Проблема, вирішена в даному дослідженні, полягає у відносно низькій теплотворній здатності синтез-газу з кукурудзяних качанів та високій вартості традиційних каталізаторів, що використовуються для його поліпшення. Дослідження проводилося з використанням різних значень еквівалентного співвідношення (0,2; 0,25; 0,3; 0,35), навантаження каталізатора (4%; 6%; 8%; 10%) та масового співвідношення CaO/AC–PF (0:1; 1:0; 1:1; 2:1) у поєднанні з характеристикою подвійної каталітичної системи. Отримані результати показують, що збільшення ER збільшує частки H_2 і CH_4 та нижчу теплоту згоряння синтез-газу, одночасно зменшуючи CO_2, причому CO досягає оптимального значення при ER = 0,3. У той час як більш високе навантаження каталізатора має тенденцію до зменшення H_2 і CH_4, але збільшує CO, потенційно знижуючи теплоту згоряння при високих навантаженнях Характеристика каталізатора показує, що AC-PF має пористу структуру, яка збільшує контакт газу з твердим тілом і сприяє вторинним реакціям, тоді як додавання CaO утворює композит із модифікованою структурою пор і поверхневими видами, пов'язаними з сорбцією CO_2. З енергетичної точки зору, нижня теплота згоряння синтез-газу збільшується із зростанням ER, але зменшується при більш високих навантаженнях каталізатора через зменшення внеску CH_4. Ключовою особливістю отриманих результатів є продемонстрована функціональна синергія між пористим AC–PF і сорбцією CO_2 на основі CaO, що дозволяє одночасно здійснювати каталітичне поліпшення якості та уловлювання CO_2 в єдиній,

недорогій системі з подвійним каталізатором. Ці висновки можуть стати практичною основою для проектування та експлуатації невеликих установок газифікації біомаси, зокрема реакторів з висхідним потоком для відходів кукурудзяних качанів, в межах досліджених діапазонів ER та навантаження каталізатора.

Ключові слова: газифікація, висхідний потік, кукурудзяні качани, синтез-газ, CaO, активоване вугілля.

The object of this study is the improvement of syngas quality from updraft corn cob gasification using a dual catalyst system consisting of CaO and activated carbon derived from palm fiber (AC–PF). The problem solved in this study is the relatively low heating value of corn cob syngas and the high cost of conventional catalysts used for its upgrading. The study was conducted using variations of equivalence ratio (0.2, 0.25, 0.3, 0.35), catalyst loading (4%, 6%, 8%, 10%), and CaO/AC–PF mass ratio (0:1, 1:0, 1:1, 2:1), combined with characterization of the dual catalyst system. The results obtained show that increasing ER increases the H_2 and CH_4 fractions and the syngas lower heating value while decreasing CO_2, with CO reaching an optimum at ER = 0.3. Whereas higher catalyst loading tends to decrease H_2 and CH_4 but increase CO, potentially reducing the heating value at high loadings Characterization of the catalyst shows that AC-PF has a porous structure that increases gas-solid contact and promotes secondary reactions, while the addition of CaO forms a composite with a modified pore texture and surface species associated with CO_2 sorption. From an energy perspective, the Lower Heating Value of syngas increases with increasing ER, but decrease at higher catalyst loadings due to the reduced contribution of CH_4. A key feature of obtained results is the demonstrated functional synergy between porous AC–PF and CaO-based CO_2 sorption, which enables simultaneous catalytic upgrading and CO_2 capture in a single, low-cost dual catalyst system. These findings could be a practical basis for designing and operating small-scale biomass gasification units, particularly updraft reactors for corn cob waste, within the studied ER and catalyst loading ranges

Keywords: gasification, updraft, corncob, syngas, CaO, activated carbon

1. Introduction

In recent years, environmental challenges such as rising greenhouse gas emissions, fossil fuel depletion, and increasing agricultural waste have strengthened the global push toward green energy and sustainable technologies. These issues have become major concerns because they affect not only environmental quality but also long-term energy security and sustainable economic development. Green energy development is not only about reducing emissions but also about creating cleaner, more efficient ways to utilize available resources and minimize waste generation. Conversion of biomass residues into useful energy has attracted considerable attention as a practical and environmentally responsible solution. One promising approach is the thermochemical conversion of biomass through gasification, which can transform solid biomass into synthesis gas that

can be used directly as a fuel or further processed as a feedstock for chemical production and other energy applications.

Indonesia is one of the largest corn producers in Southeast Asia, with national production reaching more than 18 million tons of dry kernels per year. Of this amount, about 15–20% is cobs after the kernel removal process, resulting in a very large amount of corn cob waste, estimated at 2.5–3.5 million tons annually. Until now, most corn cobs have only been used to a limited extent, for example as traditional fuel, small amounts of animal feed, or even burned directly on post-harvest land, which has the potential to cause air pollution. Most of the rest are simply piled up or left to rot on the land, posing a risk of becoming a source of plant disease [1].

Corn cobs have quite promising chemical and energy characteristics. Their composition is dominated by cellulose, hemicellulose, and lignin, with a calorific value of around 15–17 MJ/kg, making them very suitable as raw materials in various biomass-based energy conversion technologies [2]. Their hard and fibrous nature also makes them suitable for processing into biochar, activated charcoal, or direct use in pyrolysis and gasification processes. This significant potential indicates that corn cobs are not merely waste but a renewable resource that can be optimized to support energy security and reduce dependence on fossil fuels.

Biomass gasification is a promising thermochemical technology for converting renewable resources into syngas consisting of H_2, CO, CH_4, and CO_2. Of the various types of biomass, corn cobs are a potential candidate due to their abundant availability in Indonesia and lignocellulose content that supports the energy conversion process [3]. However, the biomass gasification process still faces several obstacles, particularly the low hydrogen fraction in syngas and the formation of significant amounts of tar. Tar can cause reactor clogging, reduced thermal efficiency, and increased purification costs.

To overcome these problems, the use of catalysts is an important strategy. A number of studies have proven that metal catalysts such as Ni, Ca, and K can increase hydrogen yield while suppressing tar formation. On the other hand, activated carbon is also widely used as a catalyst support because it has a high surface area, porous structure, and good chemical stability. The use of agricultural waste, particularly palm fiber, as raw material for activated carbon is not only economically valuable but also supports the concept of a circular economy in plantation waste management. In addition, calcium oxide (CaO) is known to have a dual role, namely as a catalyst in the tar decomposition reaction and as a CO_2 absorber that promotes sorption-enhanced gasification to increase the hydrogen fraction in syngas [4].

Although various studies have examined the role of metal catalysts and activated carbon separately, research focusing on the combination of biomass bases catalyst such as palm fiber-based activated carbon with CaO in corn cob gasification is still limited. The uniqueness of this study lies in the integration of two catalyst, which is expected to provide a synergistic effect: activated carbon with high porosity increases catalyst dispersion and activity, while CaO simultaneously breaks down tar and absorbs CO_2.

This approach has the potential to significantly increase hydrogen production and reduce carbon emissions.

However, there are several research gaps that remain unanswered. First, the optimal composition and ratio of activated carbon and CaO in corn cob gasification have not been extensively studied. Second, the synergistic mechanism using two catalyst in increasing syngas quality not yet fully understood. In addition, a systematic and statistically robust approach is required to disentangle the coupled effects of key operating and catalyst variables.

Based on this background and research gaps, this study aims to investigate the performance of a composite catalyst based on activated carbon from palm fiber combined with CaO in the corn cob gasification process. The main focus is on increasing hydrogen production, reducing tar, and evaluating the potential synergistic effects between materials. This research is expected to contribute to the development of low-cost, locally sourced, and sustainable catalyst systems that are relevant to supporting the clean energy transition and practical applications of biomass-to-hydrogen in the future.

2. Literature review and problem statement

The paper [5] presents the result on the gasification of sago dreg waste pellets in a top-lit updraft fixed-bed gasifier. The results show that the addition of Al_2O_3 improved syngas quality, especially by increasing H_2 content up to 31.65% at 5% Al_2O_3 and enhancing CO and CH_4 production, while also increasing the H_2/CO ratio to 1.65 and 1.51 for 5% and 10% Al_2O_3, respectively, improving LHV, and reducing tar content by about 25–27.5% compared with pellets without catalyst. However, this study is limited because it was conducted only on one biomass type, within a laboratory-scale TULD fixed-bed gasifier, and only considered two catalyst loadings.

The paper [6] presents the result on hydrogen enrichment in product gas from a pilot-scale rice husk updraft gasification. The results show that dolomite-assisted air gasification gave the best performance, increasing the H_2 content up to 15.4 mol%, with an LHV of 5.1 MJ/Nm³, while steam/air gasification improved H_2 to 9.6 mol% and air alone produced only about 7.08 mol% H_2, the optimum operating condition was reported at an airflow rate of 3 m³/h and a dolomite mixing ratio of 15 wt%. However, this study is limited because it focused only on rice husk feedstock, used a pilot-scale updraft gasifier with a batch capacity of 3 kg, and evaluated only a limited range of operating conditions and catalyst type.

The paper [7] presents the result on oxygen updraft gasification coupled with catalytic steam reforming of cigarette butts for hydrogen-rich syngas production. The results show that the integrated process was effective in converting cigarette butts into syngas, with gasification producing 82.3–89.7 wt.% syngas, 6.3–8.6 wt.% soot, and 1.4–1.9 wt.% tar, while the catalytic reforming stage significantly improved the gas quality by increasing the H_2 content up to 30.27 vol.%, increasing the HHV up to 11,528 kJ/kg, and reducing tar concentration from about 18.15 g/m³ to 13.38 g/m³ under the optimum

condition. However, this study is limited because it investigated only cigarette butt waste as feedstock, used a specific oxygen updraft gasifier–catalytic reformer configuration, and fixed most catalytic reforming parameters.

The paper [8] presents the result on the experimental assessment of pellets produced from beekeeping waste and slumgum–pine sawdust mixtures through updraft gasification. The results show that pure slumgum pellets exhibited very high mechanical durability (99.98%) and high HHV (27.66 MJ/kg), while during gasification the 50% slumgum–50% sawdust pellets produced the highest producer gas LHV of 7.62 MJ/Nm³, indicating that the addition of sawdust improved gas quality and energy recovery potential. However, this study is limited because the equivalence ratio remained very low (0.0125–0.0204) compared with typical gasification conditions, the experiments were conducted only in a modified laboratory-scale updraft gasifier.

The paper [9] presents the result on a comparative investigation of catalyst applications in updraft and modifiable-downdraft fixed-bed biomass gasifiers, using a biomass mixture of green waste, sewage sludge, and olive pomace together with red mud (RM) and Al–Ni alloy catalysts to improve syngas quality and hydrogen production. The results show that catalyst type and reactor configuration strongly influenced gasification performance, with the Al–Ni catalyst giving the best hydrogen enrichment, reaching up to 65 vol.% H_2 in the updraft gasifier at 900 °C, while RM increased H_2 to about 50 vol.%, the updraft gasifier produced better hydrogen-rich syngas than the modifiable-downdraft reactor. However, this study is limited because it, used a specific mixed biomass composition and mainly focused on high temperature operation around 900 °C with limited gasifying-agent flow conditions.

The paper [10] presents the result on the experimental investigation of producer gas composition from sorted municipal solid wastes in an updraft fixed-bed gasifier. The results show that reducing the equivalence ratio from 0.21 to 0.15 increased the heating value of the combustible gases. The study indicated that the allothermal updraft fixed-bed gasifier is suitable for producing gas that can be utilized in gas engines. However, this study is limited because it used a laboratory-scale 10 kW allothermal updraft gasifier at a fixed temperature of 800 °C, and evaluated only two ER conditions.

The paper [11] presents the result on the effect of adding laying hens manure (LHM) to wheat straw on gasification efficiency in an air-blown updraft fixed-bed gasifier. The results show that increasing ER improved the gasification performance, with the producer gas LHV reaching 3.3–3.4 MJ/m³, cold gas efficiency around 60%, and carbon conversion efficiency in the range of 82–94% . However, this study is limited because it was focused on one specific co-feed system and produced a relatively low-calorific gas.

The paper [12] presents the result on the gasification performance of olive pomace in updraft and downdraft fixed-bed reactors using dry air and pure oxygen. The results show that updraft reactor achieving up to 48 vol.% H_2 with dry air and 53 vol.% H_2 with pure oxygen, while the downdraft reactor reached up to 45 vol.% H_2 with dry air and 39

vol.% H_2 with pure oxygen. However, this study is limited because only a limited range of gasifying agents, temperatures, and flow rates.

The paper [13] presents the result on the gasification of MDF residue in an industrial-scale updraft fixed-bed gasifier. The results show that MDF residue can be effectively converted into useful energy, with a syngas production rate of about 2.5 Nm^3/kg, syngas LHV of around 6.0–7.0 MJ/Nm^3, about 88 wt.% of MDF residue converted into syngas, and a system capable of delivering 7 MWth of thermal energy and about 955 kW net electrical power through the ORC turbine. However, this study is limited because it focused on one specific industrial waste stream (MDF residue) in one updraft gasifier configuration, mainly evaluated performance under a limited number of feed rates, and relied on direct combustion of raw hot syngas containing tar.

The paper presents the results of research on biomass gasification in updraft fixed-bed reactors aimed at improving syngas quality and thermal conversion efficiency. Shown that syngas composition and heating value are strongly influenced by feedstock properties, gasification conditions, and catalyst application. But there were unresolved issues related to the lack of effective and low-cost catalyst systems capable of simultaneously enhancing hydrogen formation and improving overall syngas quality during corncob gasification. The reason is the complexity of catalytic reactions in the gasification zone, including reforming, cracking, and CO_2 capture mechanisms, as well as the economic limitations of commercially available catalysts. A way to overcome these difficulties can be the development of composite catalysts based on CaO and activated carbon palm fiber, where CaO may promote CO_2 absorption and shift reactions, while activated carbon palm fiber may provide a porous surface and active sites for secondary cracking reactions. This approach was used in previous studies, however, the combined use of CaO and activated carbon palm fiber in corncob updraft gasification has not been sufficiently investigated. All this suggests that it is advisable to conduct a study on syngas quality improvement in corncob updraft gasification using CaO/activated carbon palm fiber catalyst.

Previous studies have shown that biomass gasification is a promising route for converting agricultural residues into synthesis gas, and that catalytic materials such as CaO and carbon-based adsorbents can improve gas quality through tar reduction, reforming reactions, and CO_2 capture. Several researchers have also investigated different biomass feedstocks, catalyst types, and reactor configurations to enhance syngas production. However, most of these studies mainly focused on the individual performance of catalysts or on gasification systems other than corncob updraft gasification. In addition, the combined effect of CaO and activated carbon palm fiber catalyst, especially in terms of catalyst ratio, catalyst loading, and equivalence ratio, has not been systematically discussed.

Therefore, further study is needed to clarify the synergistic role of CaO as a CO_2 sorbent and activated carbon palm fiber as a porous catalytic support in improving syngas composition and heating value. Based on this research gap, the present study specifically investigates the use of combined CaO/activated carbon palm fiber catalyst in

corncob updraft gasification and evaluates the influence of key operating parameters on synthesis gas quality. In this way, the study is intended to provide both a clearer scientific understanding of catalyst interaction and practical guidance for improving biomass gasification performance.

3. The aim and objectives of the study

The purpose of the study is to enhance syngas quality from corncob updraft gasification by developing a dual-synergy catalytic system based on calcium oxide (CaO) and palm-fiber-derived activated carbon (AC-PF). This will allow the production of cleaner and more energy-dense producer gas, providing practical guidance for selecting operating conditions and catalyst configurations suitable for updraft gasifiers processing agricultural residues.

To achieve these aims, the following objectives are accomplished:

– to synthesize and characterize the CaO and palm-fiber activated carbon catalysts using Fourier Transform Infrared Spectroscopy (FTIR), scanning electron microscopy (SEM) and Brunauer-Emmett-Teller surface area analysis (BET);

– to investigate the effects of operating parameters, particularly equivalence ratio (ER), catalyst loading, and CaO/AC ratio, on syngas composition H_2, CO, CH_4, CO_2 and LHV.

To achieve these aims, the following objectives are accomplished:

– to prepare and characterize CaO and AC-PF catalysts by analyzing their morphology, surface functional groups, and pore characteristics using SEM, FTIR, and BET methods;

– to evaluate the influence of equivalence ratio, catalyst loading, and CaO/AC ratio on syngas composition and lower heating value in corncob updraft gasification, and to identify the catalyst condition that provides improved gas quality.

4. Materials and methods

The object of the study is the updraft fixed-bed gasification process of corncob biomass using a dual catalyst system based on calcium oxide (CaO) and palm-fiber-derived activated carbon (AC-PF). The practical physical process under investigation is the catalytic upgrading of producer gas within the updraft reactor, where changes in operating parameters and catalyst configuration are expected to influence syngas composition and heating value. The results of this study are intended to be applied to improve the quality of syngas, specifically by increasing the combustible gas fraction (H_2 and CH_4) and the lower heating value (LHV), while reducing CO_2 content.

The selected methods were intended to explain both the catalyst characteristics and their effect on syngas quality. SEM, FTIR, and BET were used because they provide complementary information on catalyst morphology, surface functional groups, and pore structure, which are important for catalytic reforming, adsorption, and CO_2 capture during gasification. The investigated operating parameters, namely equivalence ratio,

catalyst loading, and CaO/AC ratio, were chosen because they are the main variables governing the reaction environment, catalyst effectiveness, and synergistic interaction between CaO and activated carbon in the updraft gasification process.

The research hypothesis is that a dual-synergy CaO/AC-PF catalytic system can improve syngas quality more effectively than single-catalyst configurations in updraft corncob gasification. It is hypothesized that CaO functions as a CO_2 sorbent, shifting reaction equilibria toward enhanced hydrogen formation, while activated carbon derived from palm fiber provides high-surface-area catalytic sites that promote secondary reactions such as tar cracking and volatile reforming. The combined catalytic-sorption mechanism is expected to increase H_2 and CH_4 fractions and improve LHV under optimized equivalence ratio (ER), catalyst loading, and CaO/AC-PF ratio conditions.

It was assumed that the corncob feedstock has relatively homogeneous composition and stable proximate/ultimate characteristics during the experiments. The gasification process was assumed to operate under steady-state conditions after stabilization. It was also assumed that the CaO maintains sufficient CO_2 sorption capacity within the experimental time frame and that the activated carbon structure remains stable under the applied temperature range.

During the course of the research, several methodological simplifications were adopted in order to maintain experimental feasibility and focus on the main objective of syngas quality evaluation. Detailed kinetic modeling of individual gasification reactions was not performed; instead, the process performance was assessed based on experimentally measured syngas composition and syngas low heating value. Furthermore, although CaO carbonation-decarbonation reactions may occur during operation, microstructural evolution, sintering behavior, and long-term cyclic stability of the catalyst were not investigated in this study. The catalytic performance was evaluated within the experimental duration without conducting extended durability or regeneration-cycle analysis.

4. 1. Catalyst Preparation

Approximately 6 grams of ground palm fiber was mixed with 60 mL of distilled water and stirred for 10 minutes. The mixture was then placed in an autoclave and heated to 200°C at a rate of 5°C per minute for 6 hours in an electric oven. After that, the reactor is allowed to cool naturally to room temperature. The resulting solid hydrocarbon product (hydrochar) is then separated using Whatman No. 42 filter paper. The filtered product is then dried at 105°C for 24 hours and stored in a glass vial. The next stage is the activation process. The hydrochar is immersed in a 3 M KOH solution with a weight ratio of 1:3 (Hydrochar:KOH) for 16 hours, then dried at 85°C for 6 hours. Spectroscopic evidence indicates that KOH preferentially reacts with oxygenated sites and can increase the relative abundance of C–OH functionalities, while higher KOH ratio and activation temperature significantly enhance porosity and BET surface area [14, 15]. To obtain the CaO/AC mixture, CaO powder and activated carbon (AC) were mixed in specific proportions using a grinder until a homogeneous mixture was

obtained. Next, CaO, AC, and CaO/AC were activated using a tube furnace at a temperature of 700°C for 1 hour with a continuous flow of nitrogen during the activation process. The resulting product was then washed using distilled water until it reached a neutral pH. This stage produced activated carbon that was ready for use in research.

4. 2. Experimental Setup

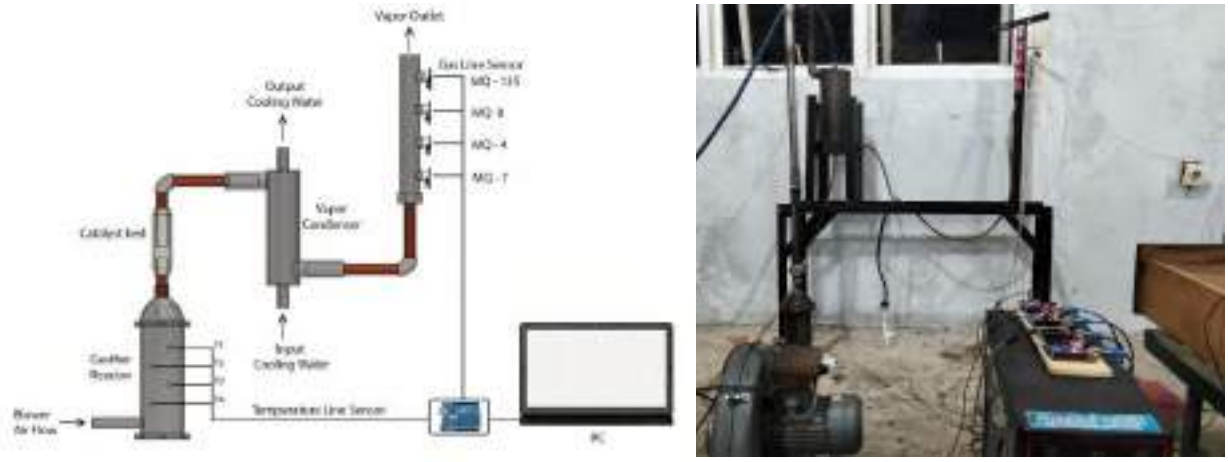
Corncob biomass was obtained from farmers in the South Malang region of East Java. Before use, the biomass was cleaned of impurities and dried in an oven for 6 hours at 100°C to remove moisture (water vapor) content. The ultimate and proximate test results are as follows.

The proximate and ultimate analyses of the corncob feedstock were conducted to determine its physicochemical characteristics prior to gasification. The results are presented in Table 1. The data indicate that corncob has high volatile matter content and relatively low ash content, which are favorable characteristics for gasification processes.

Table 1
Ultimate and Proximate Test Corn Cob

Parameter	Units	Corn cobs
Moisture	%	10
Volatile matter	%	71.38
Fixed carbon	%	12.11
Ash	%	6.51
C	%	43.6
H	%	6.3
O	%	46.8
N	%	0.22
HHV	MJ/kg	17.61

The experimental apparatus employed in this study consisted of an updraft gasifier integrated with a catalyst bed, a vapor condensation unit, gas sensors, and temperature measurement points to enable comprehensive monitoring of the gasification process. Fig. 1 shows the updraft gasifier system used in this study, including the schematic experiment (a) and the experimental setup (b).



a *b*

Fig. 1. Updraft gasifier: *a* – schematic experiment; *b* – experimental setup

This study used an updraft gasification reactor designed with a total height of 20 cm. The lower part of the reactor consisted of an ash container with a height of 5 cm, while the active reactor had a height of 15 cm and a diameter of 3 inches. The reactor was equipped with a 1-inch diameter air inlet pipe connected to a blower. The blower was modified with a potentiometer so that the air speed could be adjusted as needed. To monitor the thermal conditions inside the reactor, four 3 cm long type K thermocouples were installed at several different points so that the temperature profile in the gasification zone could be observed in more detail. Each test was conducted with a fixed biomass mass, a mixture of corn cobs weighing 80 grams. The reactor was made of iron and equipped with a gas seal to prevent leaks during the gasification process.

The gas produced by the reactor was fed into a condenser, which cooled the hot gas so that the water vapor components could be separated. The condenser was made of a copper spiral pipe with a diameter of ½ inch and a height of 30 cm. Cooling water was circulated from the bottom of the condenser and exited through the top to ensure efficient heat transfer. This cooling system was driven by a 60-watt water pump, ensuring stable water flow and optimal condensation. The catalyst was positioned downstream after the reactor, where it was supported on steel wool and wrapped with an 80-μm wire mesh to secure the catalyst and prevent particle carryover with the gas flow

To analyse the gas composition, four types of MQ gas sensors were used. The MQ-8 sensor was used to detect H_2, MQ-4 for CH_4, MQ-135 for CO_2 and MQ-7 for CO. Each gas sensor was calibrated according to the manufacturer's datasheet, specifically by determining the Ro value, which is the sensor resistance in clean air conditions. This Ro value is used as a reference in calculating the measured gas concentration during the process.

All data from the gas sensors and thermocouples were acquired using an Arduino Uno microcontroller. Each gas sensor is connected to a separate Arduino Uno to facilitate the calibration process and reduce the possibility of interference between

sensors. Arduino is also used to record temperature data from four thermocouples installed in the reactor, so that gas composition and temperature distribution data can be obtained simultaneously.

The ER range of 0.2, 0.25, 0.3 and 0.35. The catalyst load was between 4%, 6%, 8% and 10% from the mass of input feedstock. The CaO/AC-PF ratio was varied between 0:1, 1:0, 1:1, and 2:1. Design of experiment can be seen in Table 2.

Table 2
Design of Experiment using

Run	Equivalence Ratio (E.R)	Catalyst Load %	CaO/AC
1	0.2	4	1:0
2	0.2	6	0:1
3	0.2	8	1:1
4	0.2	10	2:1
5	0.25	4	0:1
6	0.25	6	1:0
7	0.25	8	2:1
8	0.25	10	1:1
9	0.3	4	1:1
10	0.3	6	2:1
11	0.3	8	1:0
12	0.3	10	0:1
13	0.35	4	2:1
14	0.35	6	1:1
15	0.35	8	0:1
16	0.35	10	1:0

A total of 16 experimental runs were conducted systematically to enable evaluation of the main effects of each variable and the tendency of interactions between variables on the fractions of H_2, CO, CH_4, CO_2, and lower heating value (LHV). This approach enabled identification of the most effective combination of operating parameters in improving syngas quality quantitatively and measurably.

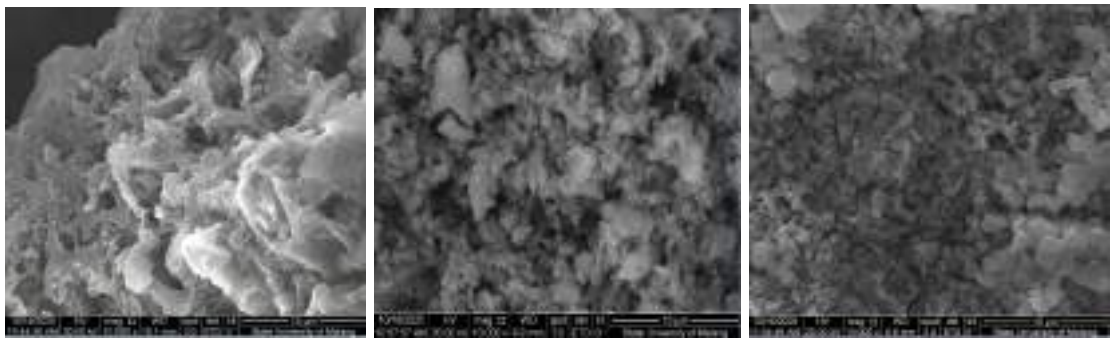
5. Results of syngas quality enhancement from corncob using calcium oxide (CaO) and palm-fiber-derived activated carbon (AC–PF).

5. 1. Characterization of Calcium Oxide (CaO) and Palm-Fiber-Derived Activated Carbon (AC–PF) Catalysts

5. 1. 1. Scanning Electron Microscopy Catalyst Result

Fig. 2, *a* shows the image obtained from a Scanning Electron Microscope (SEM) with a magnification of 10,000× shows the surface morphology of palm fiber-based activated carbon (AC-PF). The surface structure appears porous and irregular, with a

combination of void areas and layered surfaces. This characteristic indicates that the activation process that using KOH has successfully formed micropores and mesopores, which play an important role in increasing the specific surface area of activated carbon.



a *b* *c*

Fig. 2. Scanning Electron Microscopy Catalyst Result: *a* – Scanning Electron Microscopy AC-PF; *b* – Scanning Electron Microscopy CaO:AC;1:1; *c* – Scanning Electron Microscopy CaO:AC-PF;2:1

The rough and textured surface indicates that most of the material has undergone lignocellulose cell wall exfoliation, resulting in numerous interparticle gaps. This porous structure greatly supports gas adsorption and diffusion capabilities when used as a catalyst in gasification or thermochemical reactions.

The presence of 1–5 µm voids indicates that most pores are in the mesopore category, supporting the adsorption of gas molecules such as H_2, CO, and tar during the gasification reaction.

The morphology of AC-PF shows the characteristics of porous activated carbon with a heterogeneous pore distribution, where the pores allow increased contact between gas reactants and active sites on the material surface, thereby increasing catalytic efficiency and the ability to absorb tar or CO_2 in biomass-based energy applications.

Fig. 2, *b* shows the surface morphology of the CaO:AC-PF catalyst with a ratio of 1:1. Visually, it can be seen that the surface of this material consists of fine particles ranging in size from microns to submicrons that stick together to form a layered and slightly agglomerated structure.

The presence of fine, light-colored grains indicates an even distribution of CaO particles impregnated on the surface of activated carbon (AC-PF). This CaO distribution fills some of the pores of the carbon, resulting in a denser surface compared to pure AC-PF. However, there are still small gaps and voids between the grains, indicating that the microporous and mesoporous structures are still formed and can support catalytic activity [16].

This morphology illustrates the success of the CaO impregnation process on activated carbon from palm fiber, where the interaction between CaO and the carbon

pore walls produces a composite material that is more thermally and chemically stable. This structure is highly conducive to catalyst applications in biomass gasification processes, as CaO particles can function as CO_2 absorbers while accelerating the tar reforming reaction [17].

Fig. 2, *c* shows the surface morphology of the CaO:AC-PF (2:1) catalyst. The image shows that the surface of the material is dominated by agglomerations of fine, round, and irregular particles ranging in size from microns to submicrons. Compared to the CaO:AC-PF (1:1) sample, this structure appears denser and tighter, indicating that an increase in the CaO ratio causes partial closure of the activated carbon surface pores by CaO particles.

The distribution of CaO particles appears more uniform and covers the carbon surface, indicating the successful impregnation of a larger amount of CaO. The light color in some areas indicates the presence of a calcium oxide phase that is strongly attached to the activated carbon matrix. This structure indicates a strong interaction between CaO and AC-PF, forming a thermally stable composite.

Although some pores are covered, there are still microscopic gaps between the CaO grains that allow gas diffusion to occur, so that the catalyst retains its good adsorption capacity. The combination of the active area of CaO and the porous carbon structure makes this material very promising for biomass gasification or tar reforming applications, as CaO can act as a CO_2 absorber and increase the conversion of carbon to hydrogen gas.

5. 1. 2. Fourier Transform Infrared Spectroscopy catalyst result

The FTIR analysis results shown in the Fig. 3 reveal clear spectral differences between the AC-PF, CaO, and their mixtures (CaO:AC-PF) with ratios of 2:1 and 1:1. In the AC-PF spectrum, the absorption band at 2926 cm^{-1} is associated with the stretching vibration of the C–H group from $–CH_2$ or $–CH_3$ (methylene/methyl stretching), which indicates the presence of hydrocarbon chain residues from the lignocellulose structure. The peak at 1577 cm^{-1} indicates the presence of aromatic C=C or C=O stretching, while the band at 1056 cm^{-1} represents C–O stretching from alcohol or ether groups. In addition, the –OH group that appears in the 3500–3600 cm^{-1} region is identified as the result of AC-PF activation using a KOH solution, which causes the formation of hydroxyl groups on the activated carbon surface. This –OH group plays an important role in increasing the surface activity and adsorption capacity of AC-PF as a catalyst support medium [18, 19].

In pure CaO, the intense band at 3639 cm^{-1} is associated with the stretching of the O–H group from $Ca(OH)_2$, which is formed due to the partial hydration of CaO when exposed to humid air. Meanwhile, the absorption bands at 1426 cm^{-1} and 876 cm^{-1} are associated with C–O stretching and CO_3^{2-} bending, respectively, indicating the formation of $CaCO_3$ due to CO_2 adsorption from the air. This shows that CaO is highly reactive to moisture and carbon dioxide in the environment.

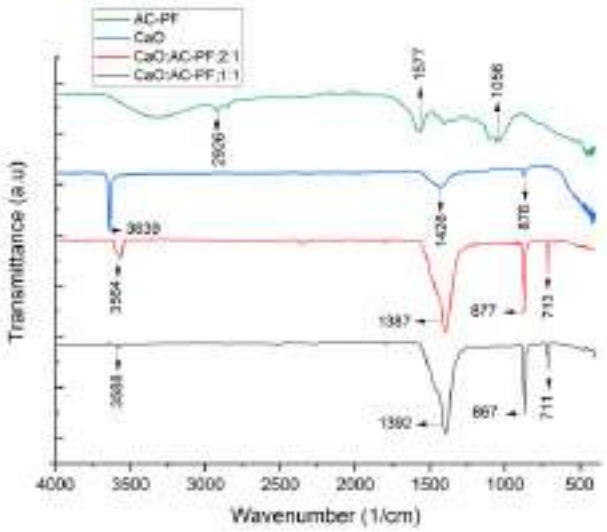


Fig. 3. Fourier Transform Infrared Spectroscopy Catalyst Result

For the CaO:AC-PF (2:1), the main absorption bands were detected at 3564 cm^{-1} (O–H stretching from $Ca(OH)_2$ and the –OH group in AC-PF), 1387 cm^{-1} (C–O stretching), and 877 cm^{-1} and 713 cm^{-1} (bending vibration of CO_3^{2-}). This combination of bands indicates the formation of carbonate compounds ($CaCO_3$) due to the interaction between CaO and the oxygen groups of activated carbon. The presence of –OH groups from KOH activation also strengthens the basic properties on the surface, which can increase the chemical interaction between CaO and AC-PF [20].

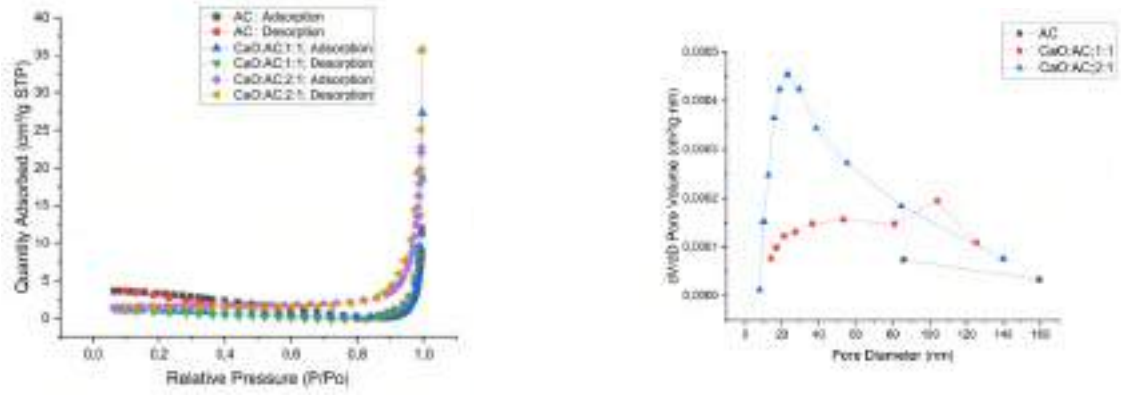
At a CaO:AC-PF ratio of 1:1, the absorption bands at 3588 cm^{-1}, 1392 cm^{-1}, 867 cm^{-1}, and 711 cm^{-1} show a similar pattern, indicating the presence of hydroxyl (O–H) and carbonate (CO_3^{2-}) groups. The difference in peak intensity compared to the 2:1 ratio indicates variations in the level of interaction between CaO and the –OH groups resulting from KOH activation on AC-PF, which affects the formation of carbonate-hydroxide complexes on the material surface [21].

5. 1. 3. Brunauer-Emmett-Teller Catalyst Result

Fig. 4 shows the adsorption-desorption isotherm curves for nitrogen for the AC, CaO:AC (1:1), and CaO:AC (2:1) samples are shown in Fig. 4. All three samples exhibit type IV isotherms with clear hysteresis loops at relatively high pressures (P/Po > 0.9). Based on the IUPAC classification, this characteristic indicates that the material has a mesoporous structure formed through capillary condensation within the pore channels. The difference between the adsorption and desorption pathways indicates that the pore shape is not perfectly cylindrical, but rather tends to be irregular or slit-like, which is commonly found in modified activated carbon materials [22].

The pure activated carbon (AC) sample showed a relatively low nitrogen adsorption volume with a specific surface area of 24.51 m^2/g and an average pore diameter of 0.74 nm, indicating a predominance of microporous structures. In the

CaO:AC (1:1) composite, the surface area did not change significantly compared to pure AC, indicating that the addition of a moderate amount of CaO did not cover the carbon pores much, but only adhered to the external surface of the carbon matrix [23].



a *b*

Fig. 4. Brunauer-Emmett-Teller Result: *a* – Surface Analysis Adsorption Desorption Isotherm; *b* – Barrett-Joyner-Halenda Adsorption Pore Size Distribution

Conversely, in the CaO:AC (2:1) mixture, there was a sharp increase in adsorption volume at relatively high pressure (P/Po > 0.9) to around 35 cm^3/g STP, while the BET surface area decreased dramatically to 5.06 m^2/g, and the pore diameter increased to 22.87 nm.

These changes in isotherm shape and pore size increase indicate that CaO impregnation not only modifies the surface chemistry but also significantly alters the pore structure of activated carbon. This transformation is positive in the context of catalytic applications in biomass gasification processes, as the mesoporous structure can enhance gas diffusion and accessibility to active sites during the tar reforming and water-gas shift reactions. Thus, even though the specific surface area decreases, the increase in mesoporousness and pore connectivity can actually improve catalyst performance in hydrogen gas production [24].

Fig. 4, *b* shows the BJH pore size distribution curves that provide further insight into the textural evolution of the palm-fiber-based activated carbon after CaO impregnation. The pristine AC exhibits a relatively low dV/dD value and a broad contribution only at large pore diameters (>60 nm), indicating that its pore system is dominated by macropores with a limited amount of mesopores. Such a texture is less favourable for gas-solid reactions because the accessible surface area in the mesopore range (2–50 nm) is relatively small.

After CaO loading, the shape and intensity of the BJH curves change markedly. For CaO:AC-PF = 1:1, the distribution shifts toward smaller pore diameters with a pronounced contribution in the mesopore region of approximately 15–60 nm. This behaviour shows that CaO impregnation partially reconstructs the carbon matrix,

enlarging existing micropores and opening blocked pores to generate additional mesoporosity. The effect becomes even more evident at CaO:AC-PF = 2:1, where the curve displays the highest dV/dD values and a distinct maximum centred at about 30–40 nm. The strong peak in this range confirms that a higher CaO loading promotes the development of well-defined mesopores while reducing the relative fraction of very large macropores.

Overall, the BJH analysis demonstrates that CaO acts not only as a reactive sorbent but also as a textural promoter for the palm-fiber AC. The increase in mesopore volume and the shift of the dominant pore size toward 20–40 nm are expected to facilitate the diffusion of gasifying agents and tar molecules, as well as to improve the accessibility of CaO active sites for CO_2 capture and reforming reactions. These features are therefore beneficial for enhancing the catalytic performance of the CaO/AC composite in biomass gasification toward H_2-rich syngas production.

5. 2. Effect of operating parameters on syngas composition and low heating value

5. 2. 1. Effect of Equivalence Ratio on Syngas Product

The composition of syngas from updraft gasification is greatly influenced by the Equivalence Ratio (ER), which is the ratio of the mass flow rate of air compared to the mass flow rate of corncob in the experiment compared to the stoichiometry of air required for complete combustion of corncob. In this study, the ER used was 0.2–0.35 with the following formula

$$ER = \frac{(\dot{m}_a / \dot{m}_{cc})_{\exp}}{(\dot{m}_a / m_{cc})_{stc}},$$

where $\dot{m}_a$ is the air mass flow rate (kg/s), $\dot{m}_{cc}$ is the corncob mass flow rate (kg/s), exp denotes the experimental air-fuel ratio, and stc denotes the stoichiometric air-fuel ratio.

The composition of syngas produced from corncob gasification was evaluated at different equivalence ratios to determine the variation in the main combustible and non-combustible gas components. Changes in the equivalence ratio significantly affected the concentrations of H_2, CH_4, CO, and CO_2, indicating that the air supply plays an important role in the gasification performance and gas quality. Fig. 5 shows the syngas composition obtained at different equivalence ratios.

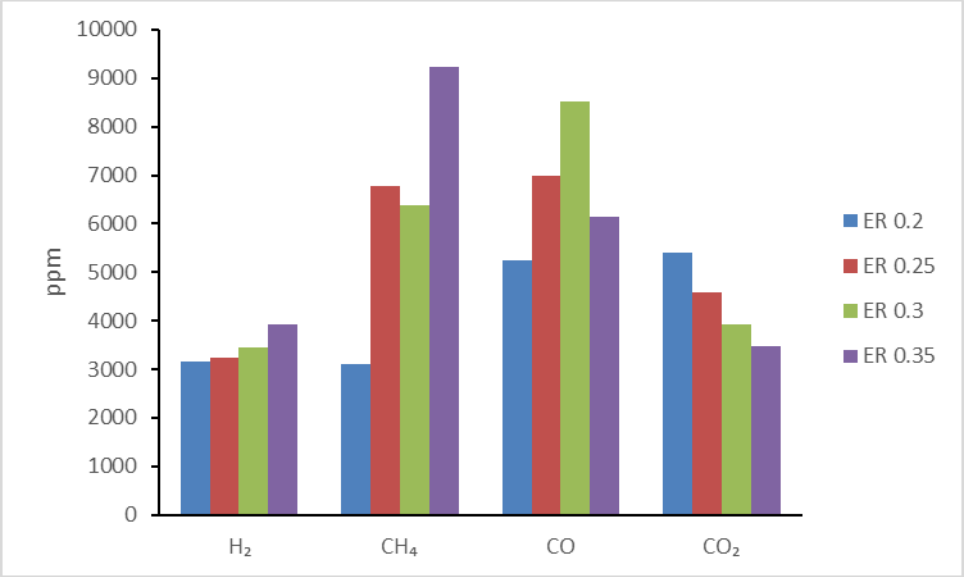


Fig. 5. Syngas composition with different equivalence ratio

The graph above shows that the higher the ER, the higher the hydrogen composition produced. At ER 0.2, the ppm is 3150 ppm, at ER 0.25 it is 3241 ppm, at ER 0.3 it is 3457 ppm, and at ER 0.35 it is 3914 ppm. A higher oxidant supply promotes the formation of more stable autothermal conditions and higher reaction temperatures due to partial oxidation. This increase in temperature accelerates hydrogen-forming reactions, particularly the gasification of active carbon catalyst interactions with steam ($C + H_2O \rightarrow CO + H_2$), the reforming of volatile compounds/light hydrocarbons ($C_xH_y + H_2O \rightarrow CO + H_2$), and the cracking of tar/volatile into lighter gas species. At low ER, some volatiles tend to be incompletely converted and still have the potential to escape as condensable components, while increasing ER increases heat availability, making the conversion of volatiles into gas fractions (including H_2) more effective.

The higher the ER, the higher the CH_4 composition produced. At ER 0.2, 3093 ppm was obtained, at ER 0.25 6767 ppm, ER 0.3 6377 ppm, and ER 0.35 9221 ppm. This trend indicates that the supply of oxidants not only increases autothermal conditions and the rate of devolatilization, but also shifts the reaction pathway towards the formation of light hydrocarbons through hydrogenation and/or methanation reactions in the reactor zone where the temperature still supports CH_4 formation. In particular, increased H_2 at higher ERs can promote the methanation reaction of CO ($CO + 3H_2 \rightleftharpoons CH_4 + H_2O$), so that CH_4 increases along with a tendency for CO to decrease at the highest ER. In addition, more intensive fragmentation of volatiles and tar at high ERs has the potential to produce light gas precursors which are then hydrogenated to CH_4.

CO formation increased up to an ER of 0.3 and decreased at an ER of 0.35. At an ER of 0.2, 5238 ppm was obtained, at an ER of 0.25, 6999 ppm, at an ER of 0.3, 8532 ppm, and decreased at an ER of 0.35 to 6145 ppm. At low ER (0.20–0.25), limited oxygen supply resulted in relatively low heat release, so that the reaction zone

temperature and char reactivity were not sufficient to intensify CO formation reactions, especially the Boudouard reaction ($C + CO_2 \rightleftharpoons 2CO$) and char gasification with steam ($C + H_2O \rightleftharpoons CO + H_2$). When the ER is increased towards 0.30, the increase in autothermal heat strengthens these reduction reactions, causing CO formation to increase and reach its peak. However, at higher ERs (0.35), the CO fraction tends to decrease because some CO can be converted to CH_4.

CO_2 formation continues to decrease as ER increases. At ER 0.2, 5412 ppm is obtained; at ER 0.25, 4592 ppm; at ER 0.3, 3916 ppm; and at ER 0.35, 3479 ppm. The increase in oxidant supply at this ER does not promote complete combustion, but rather strengthens the CO_2 reduction mechanism. At higher ERs, the heat generated from partial oxidation increases the temperature of the reduction zone, thereby accelerating the Boudouard reaction ($C + CO_2 \rightleftharpoons 2CO$), in which CO_2 is reduced by char to CO. This mechanism is consistent with the increase in CO until it reaches a maximum at an ER of 0.30, while also explaining the decrease in CO_2 under the same conditions. Interestingly, at an ER of 0.35, CO_2 remains at its lowest level even though CO decreases, indicating that the CO formed is not completely accumulated at the outlet but has the potential to undergo further conversion along the gas flow path.

5. 2. 2. Effect of Catalyst Loading on Syngas Product

The catalyst load or amount of catalyst in this study was 4%, 6%, 8%, and 10% of the total biomass weight. The Fig. 6. shows that the composition of H_2 and CH_4 increases as the catalyst load decreases. The H_2 gas composition at catalyst loads of 4%, 6%, 8%, and 10% is 3742 ppm, 3471 ppm, 3372 ppm, and 3176 ppm, respectively. As the catalyst load increases, the reaction pathways that consume H_2 tend to strengthen, particularly the reverse water–gas shift ($CO_2 + H_2 \rightarrow CO + H_2O$) and H_2 interactions on the catalyst surface during the conversion of gasification compounds. As a result, even though reforming occurs, the measured net H_2 decreases because more H_2 is used for CO formation and surface reactions. The CH_4 gas composition at catalyst loads of 4%, 6%, 8%, and 10% was 7031 ppm, 6476 ppm, 6206 ppm, and 5746 ppm, respectively. An increase in catalyst load increases the number of active sites and gas-catalyst contact, so that methane/light hydrocarbon cracking and reforming occur more intensely. CH_4 then acts as a reactant that is converted into more reactive syngas components, causing the CH_4 concentration to decrease at higher catalyst loads.

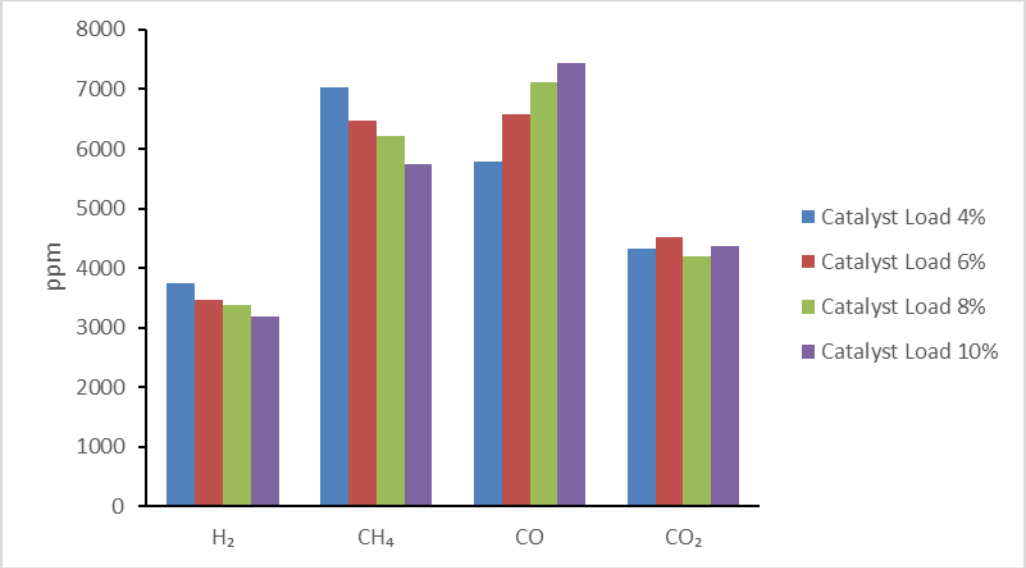


Fig. 6. Syngas Composition with Catalyst Load Variation

The CO gas composition increases with increasing catalyst load, namely for catalyst loads of 4%, 6%, 8% and 10% at 5782 ppm, 6576 ppm, 7111 ppm and 7445 ppm, respectively. The increase in catalyst loading strengthens the CO-forming reactions, particularly dry reforming ($CH_4 + CO_2 \rightarrow 2CO + 2H_2$), char–$CO_2$ reaction ($C + CO_2 \rightarrow 2CO$), and reverse water-gas shift. This combination shifts the product selectivity towards CO, so that the CO fraction increases consistently as the catalyst is increased. The CO_2 gas composition tends to stagnate with increasing catalyst loading, at catalyst loads of 4%, 6%, 8%, and 10% at 4322 ppm, 4510 ppm, 4198 ppm, and 4369 ppm, respectively. CO_2 shows minor changes because it is in a searching for a chemical equilibrium between the partial oxidation and the dry reforming. When the catalyst load increases, the rate of CO_2 consumption may rise, but this is often offset by CO_2 formation in the reaction zone, so that the CO_2 value appears stable or only fluctuates.

5. 2. 3. Effect of Catalyst Ratio on Syngas Product

At a catalyst load of 4%, the CaO/AC ratio changes the gasification reaction through differences in the dominance of tar cracking/reforming and CO_2 capture by CaO, so that the gas composition is highly dependent on the number of active sites and the effectiveness of gas-catalyst contact. At 0:1 (AC), CH_4 and CO are relatively high because AC promotes volatile/tar cracking, but CO_2 remains high because there is no absorption. At 1:0 (CaO), CH_4 decreases but CO_2 is highest, indicating that CO_2 capture is not yet effective due to limited surface area/carbonate layer formation. The 1:1 ratio produces the highest CO with moderate CO_2, indicating CaO–AC synergy that increases the conversion of volatiles into reactive gases. Meanwhile, the 2:1 (CaO-rich) ratio provides the highest H_2 and lowest CO_2 due to the sorption-enhanced effect of CaO, but

CH_4 remains high due to the smaller contribution of AC, so methane reforming/cracking is not yet optimal.

To further examine the catalytic performance, the effect of CaO/AC ratio on syngas composition was investigated under various catalyst loading conditions. This analysis was conducted to determine how the proportion of CaO and activated carbon, combined with different catalyst loads, affected the distribution of H_2, CH_4, CO, and CO_2 during corncob gasification. Fig. 7 illustrates the effect of CaO/AC ratio at catalyst loads of 4% (a), 6% (b), 8% (c), and 10% (d).

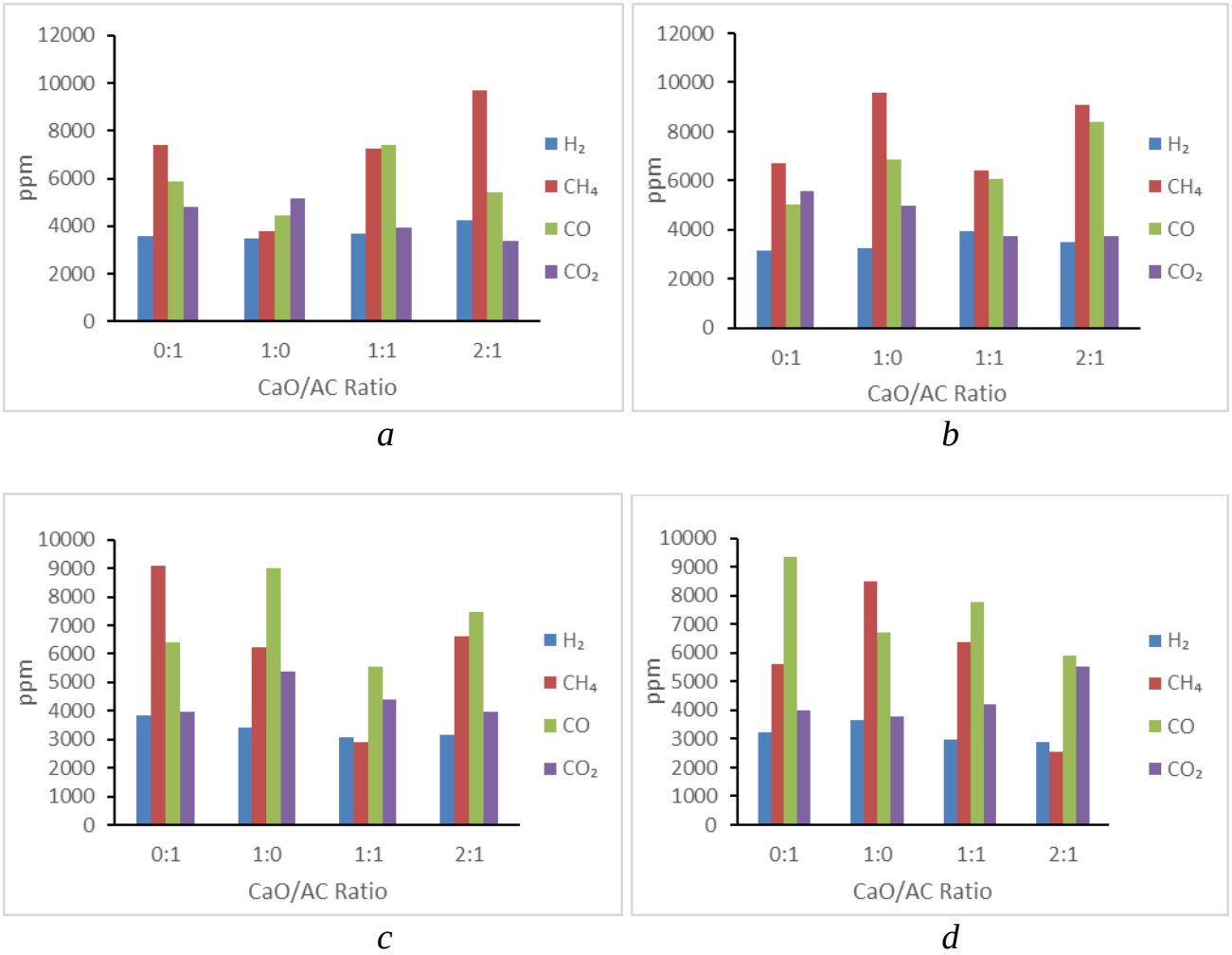


Fig. 7. Effect CaO/AC ratio with various catalyst load: *a* – 4%; *b* – 6%; *c* – 8%; *d* – 10%

At a catalyst load of 4%, the CaO/AC ratio changes the gasification reaction through differences in the dominance of tar cracking/reforming and CO_2 capture by CaO, so that the gas composition is highly dependent on the number of active sites and the effectiveness of gas-catalyst contact. At 0:1 (AC), CH_4 and CO are relatively high because AC promotes volatile/tar cracking, but CO_2 remains high because there is no

absorption. At 1:0 (CaO), CH_4 decreases but CO_2 is highest, indicating that CO_2 capture is not yet effective due to limited surface area/carbonate layer formation. The 1:1 ratio produces the highest CO with moderate CO_2, indicating CaO–AC synergy that increases the conversion of volatiles into reactive gases. Meanwhile, the 2:1 (CaO-rich) ratio provides the highest H_2 and lowest CO_2 due to the sorption-enhanced effect of CaO, but CH_4 remains high due to the smaller contribution of AC, so methane reforming/cracking is not yet optimal.

At a catalyst load of 6%, the CaO/AC ratio mainly shifts the selectivity of secondary reactions (tar cracking/reforming and CO_2 capture), where AC enhances the conversion of volatiles/light hydrocarbons, while CaO reduces CO_2 through carbonation ($CaO + CO_2 \rightarrow CaCO_3$) and changes the reaction equilibrium. At 0:1, CH_4 and CO_2 remain high because there is no CO_2 capture and methane reforming is not yet optimal, so volatiles still escape as CH_4. At 1:0, CO_2 tends to decrease, but CH_4 becomes the highest due to the absence of AC's role in cracking/reforming. The most favorable conditions occur at 1:1, with the highest H_2 and lowest CO_2, indicating CaO–AC synergy that promotes sorption-enhanced reforming and increases the conversion of hydrocarbons into syngas components. At 2:1, CO is highest and CO_2 remains low, but CH_4 rises again and H_2 is not maximized because excess CaO has the potential to rapidly carbonate/cause contact limitations, thereby reducing the contribution of AC in cracking/reforming.

At a catalyst load of 8%, the CaO/AC ratio significantly shifts the selectivity of the syngas reaction. At 0:1 (AC), CH_4 is still high because some light hydrocarbons have not been fully converted even though the tar cracking process is already active. At 1:0 (CaO), CO increases the most, but CO_2 also tends to be high, indicating that CaO in this condition is more dominant in promoting the CO formation pathway, while the CO_2 capture function is not yet optimal due to contact limitations or carbonation saturation. The 1:1 ratio produces the lowest CH_4, indicating the most effective CaO–AC synergy for cracking/reforming light hydrocarbons so that more methane is converted into reactive gas. At 2:1, CO increases again but CH_4 also rises, indicating that a smaller AC fraction reduces the intensity of methane reforming/cracking, while the decrease in CO_2 remains dependent on the effectiveness of CaO sorption.

At a catalyst load of 10%, the increase in total catalyst makes secondary reactions, reforming, solid-gas heterogeneous reactions, and equilibrium shifts very dominant, so that the CaO/AC ratio mainly determines the direction of product selectivity. At 0:1 (AC), CO formation tends to be strongest because the porous carbon surface accelerates the cracking/reforming of volatiles and the conversion of tar into reactive gases. At ratios involving CaO (1:0, 1:1, 2:1), CaO can retain CO_2 through carbonation, but at high loads the effect is often non-linear because CaO rapidly carbonates/diffusion limitations and pore blocking occur, so that under CaO-rich conditions (2:1) CH_4 can decrease, but CO_2 may increase and H_2 is not maximized due to reaction competition. Overall, at a 10% load, a trade-off is observed: AC-dominant increases CO, while CaO-

dominant suppresses light hydrocarbons but has the potential to trigger non-ideal conditions (saturation/mass transport) that reduce the benefits of H_2 and CO_2.

5. 2. 4. Syngas Low Heating Value

To calculate the LHV of syngas, it must first be converted from ppm to % volume of gas. The formula is $\%vol_i = \frac{ppmv_i}{10^4}$ to calculate the LHV, use the formula

$$LHV_{mix}\left(\frac{MJ}{Nm^3}\right) = \frac{10.8(\%H_2) + 12.63(\%CO) + 35.8(\%CH_4)}{100},$$

LHV H_2 = 10.8 MJ/Nm^3,

LHV CO = 12.63 MJ/Nm^3,

LHV CH_4 = 35.8 MJ/Nm^3.

As shown in Fig. 8, the syngas low heating value (LHV) varies with the equivalence ratio (ER) and catalyst load.

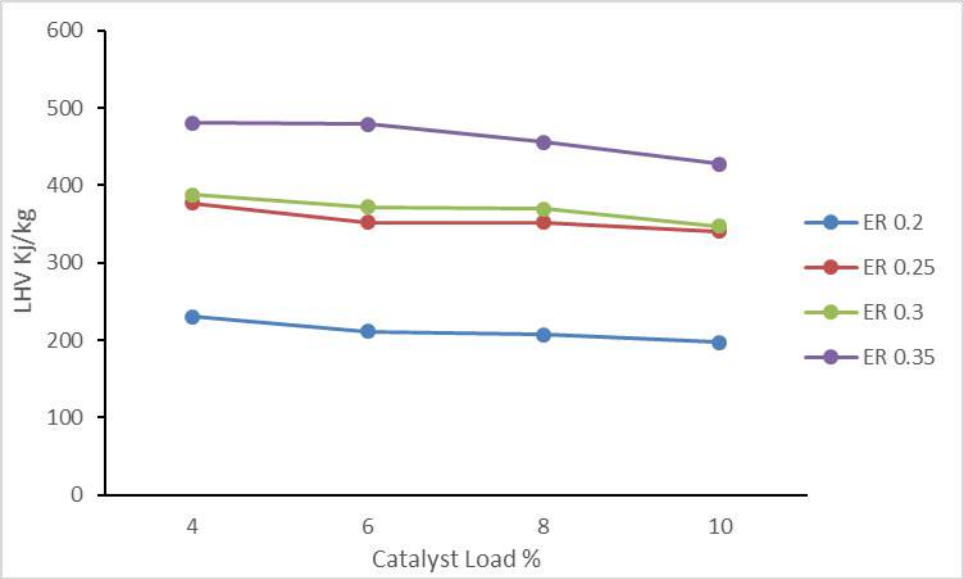


Fig. 8. Syngas low heating value with various equivalence ratio

Fig. 8 shows that the LHV value increases with the ER. At the same catalyst load of 4%, the LHV will increase in line with the increase in ER. ER 0.2 has an LHV of 230 kJ/kg and ER 0.35 has an LHV of 481 kJ/kg. Higher ER produces more intense autothermal conditions, causing the reactor temperature to rise. This increase in temperature accelerates the decomposition of volatiles and tar cracking, and promotes

more complete gasification and reforming reactions, thereby increasing the fraction of permanent gases that contribute to the calorific value, mainly CO and CH_4, as well as some H_2. In addition, the increase in temperature is also associated with more effective hydrogen formation, because H_2 formation reactions (e.g., through steam-water and reforming reactions) are generally more optimal at high temperatures, with the temperature range often reported to be most conducive to H_2 formation being 800–1000°C.

At ER 0.2, the highest LHV was obtained at a catalyst load of 4% at 230 kJ/kg and continued to decrease with increasing catalyst load to 197 kJ/kg at 10%. At ER 0.25, the highest LHV was also obtained at a catalyst load of 4% at 377 kJ/kg and also decreased to 341 kJ/kg at a catalyst load of 10%. At ER 0.3, the highest LHV was obtained at a catalyst load of 4% at 388 kJ/kg and also decreased at a catalyst load of 10% to 347 kJ/kg. At ER 0.35, the highest LHV was obtained at 481 kJ/kg and decreased at a catalyst load of 10% to 428 kJ/kg.

However, all ER values show that LHV tends to decrease when the catalyst load is increased from 4% to 10%. This decrease indicates that excessive catalyst addition under these operating conditions does not always improve gas energy quality, because the catalyst can shift the reaction selectivity towards the conversion of high calorific components especially CH_4 into CO and H_2 through reforming, while at the same time the fraction of diluent gases such as CO_2 (and steam) may increase due to reaction. Since CH_4 has a very large calorific value contribution in the syngas mixture, the decrease in its fraction is often more dominant than the increase in CO/H_2, so that the total LHV tends to decrease.

In energy system analysis, particularly in combustion, gasification, and fuel gas utilisation processes such as syngas, the LHV value is often used because it better represents the heat energy that can actually be utilised by the system. The LHV value of a fuel gas is usually influenced by the composition of combustible gases such as carbon monoxide (CO), hydrogen (H_2), and methane (CH_4). The higher the content of these gases, the greater the LHV value produced. The LHV of syngas from this study with variations in ER and CaO/AC-PF ratio can be seen in Fig. 9.

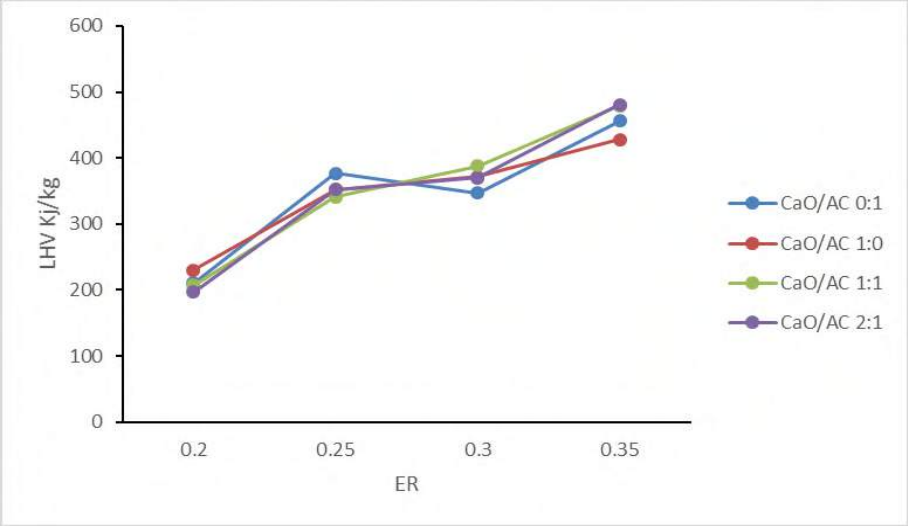


Fig. 9. Syngas Low Heating Value with Various CaO/AC Ratio

Fig. 9 shows that the LHV of syngas increases consistently with the increase in ER 0.2 to 0.35 for all CaO/AC ratios, indicating that a higher ER strengthens autothermal conditions so that the reaction temperature increases and the conversion of volatiles into syngas becomes more complete. At low ER (0.2), the difference in LHV between ratios is still small because secondary reactions such as cracking, reforming and heterogeneous reactions are not yet dominant; the system is still relatively influenced by incompletely converted volatiles. When the ER is increased to 0.25–0.30, the effect of the catalyst ratio becomes apparent: compositions involving AC tend to produce higher LHV because they accelerate tar cracking and increase the fraction of calorific gas, while the contribution of CaO can shift the reaction equilibrium through a decrease in CO_2. At the highest ER (0.35), the LHV reaches its maximum at all ratios, with CaO/AC 2:1 and 0:1 showing peak values, indicating that at high temperatures, the reactive gas formation pathway (via cracking/reforming on the carbon surface and/or CaO-rich-promoted heterogeneous reactions) becomes dominant. Overall, ER acts as the main controlling factor for LHV increase through the temperature effect, while the CaO/AC ratio modulates LHV through the balance between cracking/reforming (AC) and CO_2 control (CaO), especially at medium-high ER.

6. Discussion on the Catalytic Effect of AC-PF/CaO and Operating Conditions on Syngas Composition and LHV

The interaction of the CaO-AC-PF catalyst to improve syngas quality can be seen from the characterisation of the catalyst, the composition of the syngas and the LHV produced. From the Scanning Electron Microscopy results in Fig. 2, it can be seen that the CaO:AC-PF;2:1 catalyst (Fig. 2, *c*) appears denser than the other catalysts. With the addition of CaO, CaO particle dispersion can be seen on the white carbon surface, indicating that some micro pores are closed by CaO. With the addition of CaO, a lot of

CO_2 is absorbed and becomes $CaCO_3$. This porous structure is very important in top-flow gasification because pyrolysis gas and volatiles move through the layer, so the presence of a porous medium has the potential to strengthen secondary reactions and act as carbon capture before the gas exits to the condenser.

The interaction of the CaO-AC-PF catalyst in improving syngas quality can be observed from the catalyst characterization, syngas composition, and the resulting LHV. Based on the SEM results shown in Fig. 2, the CaO:AC-PF = 2:1 catalyst (Fig. 2, *c*) appears denser than the other catalyst formulations, indicating that CaO particles were dispersed on the carbon surface and may have partially blocked some of the smaller pores. This interpretation is reasonable because CaO-based materials are widely known to act as high-temperature CO_2 sorbents, and their carbonation proceeds through the formation of $CaCO_3$. During gasification, such sorption behaviour can reduce CO_2 concentration and influence gas quality. In addition, porous carbonaceous media are known to promote tar cracking and secondary gas-phase reactions when volatile products pass through a hot solid bed. This is particularly relevant in fixed-bed gasification, where reactor design and the interaction between volatiles, char, and catalyst strongly affect tar conversion and gasification efficiency. Therefore, the porous structure of AC-PF, together with the CO_2-capturing role of CaO, may contribute to syngas upgrading before the gas exits the reactor system.

From a surface chemistry perspective, Fourier Transform Infrared Spectroscopy (FTIR) shows the presence of –OH and calcium carbonate groups, as shown in Fig. 3. This is due to the results of KOH impregnation carried out during the manufacture of AC-PF. The presence of -OH groups functions as polar active sites capable of adsorbing polar molecules such as H_2O, CO_2, and volatile compounds. Surfaces with -OH groups tend to be hydrophilic and reactive, thereby enhancing interactions with tar compounds or heavy hydrocarbons. These tar compounds can then undergo thermal cracking or catalytic reforming into light gases such as H_2, CO, and CH_4. In addition to -OH, there are also O-H and C-O groups. The O-H group has characteristics that are almost the same as the -OH group, while the C-O group plays a role in enhancing the redox properties and chemical interactions between the carbon surface and gas molecules. In the gasification process, the C-O group can be part of the partial oxidation mechanism and carbon gasification reaction, which produces CO [25].

From a surface chemistry perspective, the Fourier Transform Infrared Spectroscopy (FTIR) results indicate the presence of O–H, C–O, and carbonate-related groups, as shown in Fig. 3. The appearance of oxygen-containing functional groups is consistent with the use of KOH during the preparation of AC-PF, since KOH activation is known to modify the surface chemistry of activated carbon and promote the formation of oxygenated groups. O–H-containing groups can act as polar active sites that enhance the interaction of the carbon surface with polar molecules such as H_2O, CO_2, and oxygenated volatile compounds. Such surface functionality may also facilitate the adsorption of tar-related species and support their further conversion through thermal cracking or reforming into lighter gases. In addition to O–H groups, the presence of C–O

groups suggests that the carbon surface retains oxygen-containing functionalities that may contribute to surface reactivity and gas–solid interactions. During gasification, these surface groups may participate indirectly in oxidation–reduction interactions at the carbon surface and support the formation of combustible gases such as CO. The carbonate-related bands may also indicate the presence of calcium-containing carbonate species, which is consistent with the CO_2-capturing function of CaO during the gasification process.

The BET data in Fig. 4 shows that the surface area decreased to 5.06 m^2/g, but the pore diameter increased to a mesopore scale of 22.87 nm, which can improve the accessibility of volatiles to active sites and improve mass transport in the reforming reaction. In Fig. 4, *b*, the BJH curve at CaO:AC-PF = 2:1 shows the highest dV/dD values of 30–40 nm, indicating a catalyst in the mesopore size range. The presence of these mesopores will further increase the active sites for CO_2 adsorption.

The BET results presented in Fig. 4 show that the specific surface area decreased to 5.06 m^2/g, while the average pore diameter increased to 22.87 nm, corresponding to the mesopore range. This change suggests that, although the surface area became lower, the larger pore structure may improve the accessibility of volatile compounds to active sites and enhance mass transport during reforming reactions. In Fig. 4, *b*, the BJH pore size distribution of the CaO:AC-PF = 2:1 catalyst shows the highest dV/dD values in the pore diameter range of 30–40 nm, confirming the dominance of mesopores in this catalyst. The presence of these mesopores may facilitate gas diffusion and improve contact between gaseous species and the catalyst surface, which can contribute to CO_2 adsorption and syngas upgrading during gasification.

From a process perspective, in Fig. 5, ER appears as the dominant variable that regulates autothermal conditions, primarily through an increase in effective temperature and secondary reaction intensity. An increase in ER from low to high levels consistently increases H_2, which can be explained by the acceleration of H_2 formation reactions such as charcoal gasification with steam ($C + H_2O \rightarrow CO + H_2$) [26], light hydrocarbon reforming, and more intense tar cracking at high temperatures. At the same time, CH_4 also increases sharply at high ER, indicating that in an autothermal upflow system, increased temperature and changes in gas composition can facilitate the formation of light gases. Meanwhile, CO tends to peak at moderate ER and then decreases at high ER, consistent with competition between CO formation and CO consumption through subsequent reactions such as methanation [27]. The decrease in CO_2 at high ER indicates the role of high temperatures in enhancing the reduction of CO_2 by charcoal (Boudouard reaction) and/or the role of CaO adsorption if available.

The effect of catalyst loading in Fig. 6 shows that adding catalyst does not always increase H_2. Increasing the catalyst loading from low to high tends to reduce H_2 and CH_4 but increase CO. Mechanistically, this condition can occur when the catalyst strengthens pathways that increase CO and/or promotes RWGS ($CO_2 + H_2 \rightarrow CO + H_2O$) [28], which consumes H_2 so that net H_2 is reduced. Furthermore, at high catalyst loadings, the possibility of diffusion/aggregation penalties increases, so that selectivity may shift and

some active sites become less effective. Therefore, the target of H_2-rich synthesis gas in this reactor is more dependent on ER adjustment and the selection of moderate/low catalyst loadings, rather than simply increasing the loading.

The CaO/AC-PF ratio in Fig. 7 shows synergistic but non-linear behaviour. AC-PF plays a major role as a porous medium that enhances the cracking/reforming process of volatile compounds, while CaO provides a basic site and CO_2 absorber to shift the equilibrium. At high CaO ratios, sorption and base effects may increase, but the risk of micro-pore closure and diffusion pathway changes also increases. This explains why certain compositions are optimal at certain catalyst loads: the best performance arises from a balance between pore accessibility (the role of AC-PF) and sorption/base strength (the role of CaO).

From an energy quality perspective, in Fig. 8, 9, the LHV value of synthetic gas is highly sensitive to changes in CH_4. Therefore, high ER conditions that increase CH_4 tend to increase LHV. H_2, CH_4 and CO are the main factors for obtaining high LHV. CO_2 has no calorific value so it must be captured. In this study, CaO was used so that CO_2 could be suppressed, meaning that the total LHV could be increased. The highest LHV in this study was 481 kJ/kg, while in another study, the highest was 550 kJ/kg using pinewood with dolomite, activated carbon, silica gel, and limestone catalysts [29]. The higher the ER, the more oxygen enters the system, thereby increasing the reforming reaction [30].

In comparison with the literature reviewed in this research, the present study demonstrates a comparable qualitative trend, particularly in showing that catalyst-assisted updraft gasification can improve syngas composition and energy quality. For example, previous studies reported that dolomite-assisted rice husk gasification increased H_2 content up to 15.4 mol% with an LHV of 5.1 MJ/Nm³, while other updraft gasification systems with catalytic enhancement also showed improved hydrogen-rich syngas production and higher heating values. In the present study, the highest syngas LHV reached 481 kJ/kg under the investigated conditions, indicating that the CaO/AC-PF catalyst system was effective in improving gas quality, although the absolute value remains influenced by the use of corncob feedstock, the small-scale reactor design, and the sensor-based gas measurement approach. Therefore, the present results support the view that the combined CaO/AC-PF catalyst is a promising low-cost alternative for syngas upgrading, particularly for agricultural biomass gasification in simple updraft systems.

In practical terms, the present study is relevant to the development of low-cost biomass gasification systems that can utilize locally available agricultural residues and catalyst materials. Corncob is an abundant agricultural by-product, while CaO and palm-fiber-derived activated carbon can be prepared from relatively inexpensive and accessible resources. Therefore, the proposed catalyst system has practical potential for application in small-scale updraft gasifiers, particularly in agricultural areas where simple and affordable waste-to-energy technologies are needed. The syngas produced from such systems may be used directly as a combustible gas for thermal applications,

such as drying, heating, or small-scale energy generation, and also has potential as an intermediate gas for further upgrading or conversion into other value-added energy and chemical products.

There are several limitations to this study. First, the gas composition was obtained from an MQ sensor based on ppm, so absolute accuracy may be affected by cross-sensitivity, humidity, sensor drift, and gas sampling temperature; this may affect the estimation of %vol and LHV, especially when changes in CO and CH_4 occur simultaneously. Second, catalyst characterisation (SEM-FTIR-BET) supports the role of surface texture and chemistry, but has not quantified changes in the active phase during operation, the degree of carbonation, and the decrease in activity due to pore closure accumulation.

The disadvantage of this research is that the CaO catalyst reacts very easily with CO_2. After the calcination process, CaO must be stored in an airtight container to prevent it from clumping into $CaCO_3$. The catalyst has a specific usage period because it is covered with tar or ash.

Based on these limitations, several future directions are recommended. Calibrate the gas composition using GC-TCD/GC-FID to convert the sensor readings into more accurate %vol and include LHV uncertainty analysis. Evaluate catalyst stability and regeneration, especially for CaO which is easily carbonated, through carbonation-calcination cycle tests and post-reaction characterisation (XRD/TGA/SEM-EDX) to assess phase changes and activity loss. Develop experimental designs towards ANOVA or RSM interactions so that interaction effects and predictive models can be obtained and verified through replication confirmation tests. Add process performance metrics such as gas yield (Nm^3/kg), cold gas efficiency, pressure drop, and air consumption so that 'syngas quality improvement' can be demonstrated based on mass-energy balance and operability, not just composition.

7. Conclusion

1. AC-PF with rich -OH group acts as a porous catalytic medium that facilitates volatile cracking and supports the reduction of condensable by-products, while CaO contributes to absorb CO_2. The BJH analysis confirms that CaO plays a dual role as a reactive sorbent and a textural promoter in palm-fiber activated carbon by enlarging mesopores (20–40 nm), thereby enhancing gas diffusion and improving access to CaO active sites, which ultimately strengthens catalytic performance.

2. Increasing ER to 0.35 enhances the combustible gas fraction H_2 and CH_4 and suppresses CO_2, whereas CO typically peaks at intermediate ER due to competing CO formation and consumption reactions along the updraft reaction zones. Increasing catalyst loading shifts syngas composition: CO increases, while H_2 and CH_4 decrease, indicating changes in dominant secondary reactions and possible diffusion or agglomeration limitations at higher loadings. Increasing ER lead to increase LHV syngas, but it can decrease at high catalyst loading. An increase in the CaO/AC ratio to 2:1 resulted in a higher syngas LHV, with a maximum value of 481 kJ/kg.

7. Conclusion

1. The present study demonstrated that the CaO/AC-PF catalyst system has potential to improve syngas quality in corncob updraft gasification. Catalyst characterization by SEM, FTIR, and BET showed that the combined catalyst possessed modified surface morphology, oxygen-containing functional groups, carbonate-related species, and mesoporous characteristics, with the CaO:AC-PF = 2:1 catalyst showing a specific surface area of 5.06 m^2/g and an average pore diameter of 22.87 nm. These characteristics indicate that the catalyst structure was altered in a way that may support gas–solid interaction during gasification.

2. The gasification experiments confirmed that equivalence ratio, catalyst loading, and CaO/AC ratio influenced syngas composition and heating value. Increasing ER from 0.20 to 0.35 increased H_2 concentration from 3150 to 3914 ppm and CH_4 concentration from 3093 to 9221 ppm, while the syngas LHV increased from 230 to 481 kJ/Nm^3. In terms of catalyst loading, increasing the loading from 4 wt.% to 10 wt.% decreased H_2 from 3742 to 3176 ppm and CH_4 from 7031 to 5746 ppm, while CO increased from 5782 to 7445 ppm. These results indicate that syngas quality was affected by the balance between catalytic activity, pore accessibility, and CO_2 sorption behaviour.

Conflict of interest

The authors declare that they have no conflict of interest in relation to this research, whether financial, personal, authorship or otherwise, that could affect the research and its results presented in this paper.

Financing

The authors sincerely thank the Ministry of Education, Culture, Research and Technology, Republic of Indonesia for fully supporting this research through the DRTPM Research Grant under Fundamental Research, Universitas Widyagama Malang, Indonesia 2025 (Grant Number:128/C3/DT.05.00/PL/2025;023/LL7/DT.05.00/PL/2025;010/ Kontrak/PT/PTS.030.7/PN/V/2025).

Data availability

Manuscript has no associated data.

Use of artificial intelligence

The authors used the AI-based language model ChatGPT (GPT-5.3) only to assist in improving the clarity of English language and grammar in several sections of the manuscript, particularly in the Introduction and Literature Review sections.

The AI tool was used solely for language editing and paraphrasing purposes. All scientific content, experimental design, data analysis, and interpretation of the results were conducted entirely by the authors.

The authors carefully reviewed and verified all AI-assisted text to ensure accuracy and consistency with the experimental results. The use of AI tools did not influence the scientific conclusions of this study.

Acknowledgements

We as the Research Team would like to thank Ministry of Education, Culture, Research and Technology, Republic of Indonesia (Kemendiktisaintek Indonesia) for financing research activities.

Authors' contributions

Purbo Suwandono: Conceptualization, Writing-original draft, Investigation, Supervision, Formal analysis, Writing – review & editing; **Widya Wijayanti**: Validation, Investigation, Data Curation, Formal analysis, Writing – original draft; **Nova Risdiyanto Ismail**: Writing – review & editing, Formal analysis; **Dzulfikar Johan Akbar:** Visualization, Writing – original draft, Data curation; **Muhammad Reza**: Project administration, Resources, Data curation.

References

1. V. K. Yadav *et al.*, "Emerging trends in the valorization of agricultural waste and their utilization in agricultural, pharmaceuticals, and environmental cleanup," *Waste and Biomass Valorization*, pp. 1–55, 2025. DOI:10.1007/s12649-025-03002-y
2. W. M. Lewandowski, M. Ryms, and W. Kosakowski, "Thermal biomass conversion: A review," *Processes*, vol. 8, no. 5, p. 516, 2020. https://doi.org/10.3390/pr8050516
3. D. Ariyanti *et al.*, "Valorization of corn cob waste for furfural production: A circular economy approach," *Biomass and Bioenergy*, vol. 194, p. 107665, 2025. DOI:10.1016/j.biombioe.2025.107665
4. J. Zhang, Z. Chu, R. Cao, X. Wu, and K. Han, "A review of resource recovery from waste plastics via pyrolysis and gasification," *Fuel*, vol. 404, p. 136319, 2026. https://doi.org/10.1016/j.fuel.2025.136319
5. Y. Tangke Tosuli, Cahyadi, H. Dafiqurrohman, R. Hermawan, and A. Surjosatyo, "Gasification of sago dreg waste in a top-lit updraft fixed bed gasifier: Syngas composition and its effect with additional Al2O3 as catalyst," *Energy Convers. Manag. X*, vol. 24, no. October, p. 100775, 2024, doi: 10.1016/j.ecmx.2024.100775. https://doi.org/10.1016/j.ecmx.2024.100775
6. P. Dinh *et al.*, "Enrichment of hydrogen in product gas from a pilot-scale rice husk updraft gasification system," *Carbon Resour. Convers.*, vol. 5, no. 3, pp. 231–239, 2025, doi: 10.1016/j.crcon.2022.07.003.
7. S. Yousef and J. Eimontas, "International Journal of Hydrogen Energy Oxygen updraft gasification-catalytic reforming of cigarettes butts for hydrogen-rich syngas production," vol. 171, no. May, 2025, https://doi.org/10.1016/j.ijhydene.2025.150650

8. D. Contreras, E. Blanco, and D. Travieso, “Experimental assessment of the energy potential of pellets produced from beekeeping wastes by updraft gasification,” vol. 343, no. January, 2025, https://doi.org/10.1016/j.enconman.2025.120206

9. N. Yesilova, O. Tezer, A. Ongen, and A. Ayol, “International Journal of Hydrogen Energy Enhancing biomass gasification : A comparative study of catalyst applications in updraft and modifiable-downdraft fixed bed reactors,” *Int. J. Hydrogen Energy*, vol. 76, no. April, pp. 290–303, 2024, https://doi.org/10.1016/j.ijhydene.2024.05.075

10. R. Skvor and A. Jan, “Experimental investigation of sorted municipal solid wastes producer gas composition in an updraft fixed bed gasifier,” vol. 289, no. August 2022, 2024, https://doi.org/10.1016/j.energy.2023.130063

11. R. Junga, M. Tańczuk, S. Sobek, M. Chabiński, and Ł. Ziółkowski, “Effect of the addition of laying hens manure to the straw on gasification efficiency in updraft gasifier under air atmosphere,” *Appl. Therm. Eng.*, vol. 226, no. February, p. 120269, 2023, https://doi.org/10.1016/j.applthermaleng.2023.120269.

12. A. Ongen and A. Ayol, “ScienceDirect Gasification performance of olive pomace in updraft and downdraft fixed bed reactors,” vol. I, 2023, https://doi.org/10.1016/j.ijhydene.2023.02.088

13. K. Ertas, “Gasification of MDF residue in an updraft fixed bed gasifier to produce heat and power via an ORC turbine,” vol. 169, no. February, pp. 43–51, 2023, https://doi.org/10.1016/j.wasman.2023.06.025

14. S. Gorthy, S. Verma, N. Sinha, S. Shetty, H. Nguyen, and M. Neurock, “Theoretical Insights into the Effects of KOH Concentration and the Role of OH–in the Electrocatalytic Reduction of CO2 on Au,” *ACS Catal.*, vol. 13, no. 19, pp. 12924–12940, 2023. DOI:10.1021/acscatal.2c06115

15. X. Wang, W. Zeng, C. Xin, X. Kong, X. Hu, and Q. Guo, “The development of activated carbon from corncob for CO2 capture,” *RSC Adv.*, vol. 12, no. 51, pp. 33069–33078, 2022, https://doi.org/10.1039/D2RA05979G

16. B. Zhou *et al.*, “Insights into effects of grain boundary engineering in composite metal oxide catalysts for improving catalytic performance,” *J. Colloid Interface Sci.*, vol. 653, pp. 1177–1187, 2024. https://doi.org/10.1016/j.jcis.2023.09.148

17. Y. Zhu *et al.*, “Preparation of hierarchically porous carbon ash composite material from fine slag of coal gasification and ash slag of biomass combustion for CO2 capture,” *Sep. Purif. Technol.*, vol. 330, p. 125452, 2024. https://doi.org/10.1016/j.seppur.2023.125452

18. M. Ilić *et al.*, “Surface functional groups and degree of carbonization of *selected* chars from different processes and feedstock,” *PLoS One*, vol. 17, no. 11, p. e0277365, 2022. https://doi.org/10.1371/journal.pone.0277365

19. R. Ali, Z. Aslam, R. A. Shawabkeh, A. Asghar, and I. A. Hussein, “BET, FTIR, and RAMAN characterizations of activated carbon from waste oil fly ash,” *Turkish J. Chem.*, vol. 44, no. 2, pp. 279–295, 2020. doi: 10.3906/kim-1909-20

20. K. J. Stanienda-Pilecki, “The importance of Fourier-Transform Infrared

Spectroscopy in the identification of carbonate phases differentiated in magnesium content," 2019.

21. F. Dai, Q. Zhuang, G. Huang, H. Deng, and X. Zhang, "Infrared spectrum characteristics and quantification of OH groups in coal," *ACS omega*, vol. 8, no. 19, pp. 17064–17076, 2023. https://doi.org/10.1021/acsomega.3c01336

22. E. M. de Salazar Martínez, M. F. Alexandre-Franco, A. J. Nieto-Sanchez, and E. M. Cuerda-Correa, "Exploring the role of surface and porosity in CO2 capture by CaO-based adsorbents through response surface methodology (RSM) and artificial neural networks (ANN)," *J. CO2 Util.*, vol. 83, p. 102773, 2024. https://doi.org/10.1016/j.jcou.2024.102773

23. J. A. Tavizón-Pozos, H. Cervantes-Cuevas, G. G. Garcia-Camacho, G. Chavez-Esquivel, and D. R. Acosta-Najarro, "Biodiesel Production Using K–Sr/CaO and CaO Catalysts Derived from Eggshells by Canola Oil Transesterification," *ACS omega*, vol. 10, no. 7, pp. 6827–6838, 2025. https://doi.org/10.1021/acsomega.4c09118

24. W. Koo-Amornpattana, P. Phadungbut, N. Kunthakudee, W. Jonglertjunya, S. Ratchahat, and M. Hunsom, "Innovative metal oxides (CaO, SrO, MgO) impregnated waste-derived activated carbon for biohydrogen purification," *Sci. Rep.*, vol. 13, no. 1, p. 4705, 2023. DOI:10.1038/s41598-023-31723-4

25. C. Quan, M. Wang, N. Gao, T. Yang, and R. Li, "In situ adsorption of CO2 to enhance biomass gasification for hydrogen production using Ca/Ni based composites," *J. Energy Inst.*, vol. 108, p. 101229, 2023, doi: https://doi.org/10.1016/j.joei.2023.101229. https://doi.org/10.1016/j.joei.2023.101229

26. F. Micheli, E. Mattucci, C. Courson, and K. Gallucci, "Bi-Functional Catalyst/Sorbent for a H2-Rich Gas from Biomass Gasification," 2021. doi: 10.3390/pr9071249. DOI:10.3390/PR9071249

27. M. Zhu, Q. Wang, and S. Wang, "Recent Advances and Future Perspectives in Catalyst Development for Efficient and Sustainable Biomass Gasification: A Comprehensive Review," 2025, https://doi.org/10.3390/su17167370

28. N. Cerone, F. Zimbardi, L. Contuzzi, J. Baleta, and D. Cerinski, "Experimental investigation of syngas composition variation along updraft fixed bed gasifier," *Energy Convers. Manag.*, vol. 221, no. July, p. 113116, 2020, https://doi.org/10.1016/j.enconman.2020.113116

29. R. Mohanty, P. Mahanta, A. Mahapatro, and R. Prakash, "Catalytic gasification of pinewood biomass in a fluidized bed reactor with dolomite , limestone , and activated carbon : An experimental study," *Energy*, vol. 325, no. April, p. 136131, 2025, doi: 10.1016/j.energy.2025.136131. https://doi.org/10.1016/j.energy.2025.136131

30. C. Liu, Y. Huang, M. Niu, and H. Pei, "ScienceDirect Influences of equivalence ratio , oxygen concentration and fluidization velocity on the characteristics of oxygen-enriched gasification products from biomass in a pilot-scale fluidized bed," *Int. J. Hydrogen Energy*, vol. 43, no. 31, pp. 14214–14225, 2018, https://doi.org/10.1016/j.ijhydene.2018.05.154

References

1. V. K. Yadav *et al.*, “Emerging trends in the valorization of agricultural waste and their utilization in agricultural, pharmaceuticals, and environmental cleanup,” *Waste and Biomass Valorization*, pp. 1–55, 2025. DOI:10.1007/s12649-025-03002-y
2. W. M. Lewandowski, M. Ryms, and W. Kosakowski, “Thermal biomass conversion: A review,” *Processes*, vol. 8, no. 5, p. 516, 2020. https://doi.org/10.3390/pr8050516
3. D. Ariyanti *et al.*, “Valorization of corn cob waste for furfural production: A circular economy approach,” *Biomass and Bioenergy*, vol. 194, p. 107665, 2025. DOI:10.1016/j.biombioe.2025.107665
4. J. Zhang, Z. Chu, R. Cao, X. Wu, and K. Han, “A review of resource recovery from waste plastics via pyrolysis and gasification,” *Fuel*, vol. 404, p. 136319, 2026. https://doi.org/10.1016/j.fuel.2025.136319
5. Y. Tangke Tosuli, Cahyadi, H. Dafiqurrohman, R. Hermawan, and A. Surjosatyo, “Gasification of sago dreg waste in a top-lit updraft fixed bed gasifier: Syngas composition and its effect with additional Al2O3 as catalyst,” *Energy Convers. Manag. X*, vol. 24, no. October, p. 100775, 2024, doi: 10.1016/j.ecmx.2024.100775. https://doi.org/10.1016/j.ecmx.2024.100775
6. P. Dinh *et al.*, “Enrichment of hydrogen in product gas from a pilot-scale rice husk updraft gasification system,” *Carbon Resour. Convers.*, vol. 5, no. 3, pp. 231–239, 2025, doi: 10.1016/j.crcon.2022.07.003.
7. S. Yousef and J. Eimontas, “International Journal of Hydrogen Energy Oxygen updraft gasification-catalytic reforming of cigarettes butts for hydrogen-rich syngas production,” vol. 171, no. May, 2025, https://doi.org/10.1016/j.ijhydene.2025.150650
8. D. Contreras, E. Blanco, and D. Travieso, “Experimental assessment of the energy potential of pellets produced from beekeeping wastes by updraft gasification,” vol. 343, no. January, 2025, https://doi.org/10.1016/j.enconman.2025.120206
9. N. Yesilova, O. Tezer, A. Ongen, and A. Ayol, “International Journal of Hydrogen Energy Enhancing biomass gasification : A comparative study of catalyst applications in updraft and modifiable-downdraft fixed bed reactors,” *Int. J. Hydrogen Energy*, vol. 76, no. April, pp. 290–303, 2024, https://doi.org/10.1016/j.ijhydene.2024.05.075
10. R. Skvor and A. Jan, “Experimental investigation of sorted municipal solid wastes producer gas composition in an updraft fixed bed gasifier,” vol. 289, no. August 2022, 2024, https://doi.org/10.1016/j.energy.2023.130063
11. R. Junga, M. Tańczuk, S. Sobek, M. Chabiński, and Ł. Ziółkowski, “Effect of the addition of laying hens manure to the straw on gasification efficiency in updraft gasifier under air atmosphere,” *Appl. Therm. Eng.*, vol. 226, no. February, p. 120269, 2023, https://doi.org/10.1016/j.applthermaleng.2023.120269.
12. A. Ongen and A. Ayol, “ScienceDirect Gasification performance of olive pomace in updraft and downdraft fixed bed reactors,” vol. I, 2023,

https://doi.org/10.1016/j.ijhydene.2023.02.088
13. K. Ertas, “Gasification of MDF residue in an updraft fixed bed gasifier to produce heat and power via an ORC turbine,” vol. 169, no. February, pp. 43–51, 2023, https://doi.org/10.1016/j.wasman.2023.06.025
14. S. Gorthy, S. Verma, N. Sinha, S. Shetty, H. Nguyen, and M. Neurock, “Theoretical Insights into the Effects of KOH Concentration and the Role of OH–in the Electrocatalytic Reduction of CO2 on Au,” *ACS Catal.*, vol. 13, no. 19, pp. 12924–12940, 2023. DOI:10.1021/acscatal.2c06115
15. X. Wang, W. Zeng, C. Xin, X. Kong, X. Hu, and Q. Guo, “The development of activated carbon from corncob for CO2 capture,” *RSC Adv.*, vol. 12, no. 51, pp. 33069–33078, 2022, https://doi.org/10.1039/D2RA05979G
16. B. Zhou *et al.*, “Insights into effects of grain boundary engineering in composite metal oxide catalysts for improving catalytic performance,” *J. Colloid Interface Sci.*, vol. 653, pp. 1177–1187, 2024. https://doi.org/10.1016/j.jcis.2023.09.148
17. Y. Zhu *et al.*, “Preparation of hierarchically porous carbon ash composite material from fine slag of coal gasification and ash slag of biomass combustion for CO2 capture,” *Sep. Purif. Technol.*, vol. 330, p. 125452, 2024. https://doi.org/10.1016/j.seppur.2023.125452
18. M. Ilić *et al.*, “Surface functional groups and degree of carbonization of *selected* chars from different processes and feedstock,” *PLoS One*, vol. 17, no. 11, p. e0277365, 2022. https://doi.org/10.1371/journal.pone.0277365
19. R. Ali, Z. Aslam, R. A. Shawabkeh, A. Asghar, and I. A. Hussein, “BET, FTIR, and RAMAN characterizations of activated carbon from waste oil fly ash,” *Turkish J. Chem.*, vol. 44, no. 2, pp. 279–295, 2020. doi: 10.3906/kim-1909-20
20. K. J. Stanienda-Pilecki, “The importance of Fourier-Transform Infrared Spectroscopy in the identification of carbonate phases differentiated in magnesium content,” 2019.
21. F. Dai, Q. Zhuang, G. Huang, H. Deng, and X. Zhang, “Infrared spectrum characteristics and quantification of OH groups in coal,” *ACS omega*, vol. 8, no. 19, pp. 17064–17076, 2023. https://doi.org/10.1021/acsomega.3c01336
22. E. M. de Salazar Martínez, M. F. Alexandre-Franco, A. J. Nieto-Sanchez, and E. M. Cuerda-Correa, “Exploring the role of surface and porosity in CO2 capture by CaO-based adsorbents through response surface methodology (RSM) and artificial neural networks (ANN),” *J. CO2 Util.*, vol. 83, p. 102773, 2024. https://doi.org/10.1016/j.jcou.2024.102773
23. J. A. Tavizón-Pozos, H. Cervantes-Cuevas, G. G. Garcia-Camacho, G. Chavez-Esquivel, and D. R. Acosta-Najarro, “Biodiesel Production Using K–Sr/CaO and CaO Catalysts Derived from Eggshells by Canola Oil Transesterification,” *ACS omega*, vol. 10, no. 7, pp. 6827–6838, 2025. https://doi.org/10.1021/acsomega.4c09118
24. W. Koo-Amornpattana, P. Phadungbut, N. Kunthakudee, W. Jonglertjunya, S. Ratchahat, and M. Hunsom, “Innovative metal oxides (CaO, SrO, MgO) impregnated waste-derived activated carbon for biohydrogen purification,” *Sci. Rep.*, vol. 13, no. 1, p.

4705, 2023. DOI:10.1038/s41598-023-31723-4
25. C. Quan, M. Wang, N. Gao, T. Yang, and R. Li, “In situ adsorption of CO2 to enhance biomass gasification for hydrogen production using Ca/Ni based composites,” *J. Energy Inst.*, vol. 108, p. 101229, 2023, doi: https://doi.org/10.1016/j.joei.2023.101229. https://doi.org/10.1016/j.joei.2023.101229
26. F. Micheli, E. Mattucci, C. Courson, and K. Gallucci, “Bi-Functional Catalyst/Sorbent for a H2-Rich Gas from Biomass Gasification,” 2021. doi: 10.3390/pr9071249. DOI:10.3390/PR9071249
27. M. Zhu, Q. Wang, and S. Wang, “Recent Advances and Future Perspectives in Catalyst Development for Efficient and Sustainable Biomass Gasification: A Comprehensive Review,” 2025, https://doi.org/10.3390/su17167370
28. N. Cerone, F. Zimbardi, L. Contuzzi, J. Baleta, and D. Cerinski, “Experimental investigation of syngas composition variation along updraft fixed bed gasifier,” *Energy Convers. Manag.*, vol. 221, no. July, p. 113116, 2020, https://doi.org/10.1016/j.enconman.2020.113116
29. R. Mohanty, P. Mahanta, A. Mahapatro, and R. Prakash, “Catalytic gasification of pinewood biomass in a fluidized bed reactor with dolomite , limestone , and activated carbon : An experimental study,” *Energy*, vol. 325, no. April, p. 136131, 2025, doi: 10.1016/j.energy.2025.136131. https://doi.org/10.1016/j.energy.2025.136131
30. C. Liu, Y. Huang, M. Niu, and H. Pei, “ScienceDirect Influences of equivalence ratio , oxygen concentration and fluidization velocity on the characteristics of oxygen-enriched gasification products from biomass in a pilot-scale fluidized bed,” *Int. J. Hydrogen Energy*, vol. 43, no. 31, pp. 14214–14225, 2018, https://doi.org/10.1016/j.ijhydene.2018.05.154

Author’s order	First Name	Middle name	Second Name
1	*Purbo*		*Suwandono*
2	*Widya*		*Wijayanti*
3	*Nova*	*Risdiyanto*	*Ismail*
4	*Dzulfikar*	*Johan*	*Akbar*
5	*Muhammad*		*Reza*

English

Purbo Suwandono
Corresponding author
Master
Department of Mechanical Engineering
Widya Gama University
Borobudur str., 35, Malang, Indonesia, 65142
E-mail: purbo@widyagama.ac.id

ORCID: https://orcid.org/0000-0003-4085-1291
Contact phone: +6282132697144
Number of publications in national journals indexed (approximate; for Ukraine citizens only): -
Number of publications in international journals indexed (approximate): 14
H-index by Scopus (if available): 4
ResearchGate: https://www.researchgate.net/profile/Purbo-Suwandono
Scopus ID: 57204187970
Researcher ID: https://researchid.co/rid80879

Widya Wijayanti
PhD
Department of Mechanical Engineering
Brawijaya University
Veteran str., 10–11, Malang, Indonesia, 65145
E-mail: widya_dinata@ub.ac.id
ORCID: https://orcid.org/0000-0003-4215-5943
Contact phone: +6285334992164
Number of publications in national journals indexed (approximate; for Ukraine citizens only): -
Number of publications in international journals indexed (approximate): 78
H-index by Scopus (if available): 12
ResearchGate: https://www.researchgate.net/profile/Widya-Wijayanti
Scopus ID: 36006672800
Researcher ID: -

Nova Risdiyanto Ismail
PhD
Department of Mechanical Engineering
Widya Gama University
Borobudur str., 35, Malang, Indonesia, 65142
E-mail: nova@widyagama.ac.id
ORCID: https://orcid.org/0000-0001-8439-6919
Contact phone:
Number of publications in national journals indexed (approximate; for Ukraine citizens only): -
Number of publications in international journals indexed (approximate): 7
H-index by Scopus (if available): 3
ResearchGate: https://www.researchgate.net/profile/Nova-Ismail-2
Scopus ID: 57204527065
Researcher ID: https://researchid.co/rid80876

Dzulfikar Johan Akbar
Master Student
Department of Mechanical Engineering
Brawijaya University
Veteran str., 10–11, Malang, Indonesia, 65145
E-mail: johanakbar@student.ub.ac.id
ORCID: https://orcid.org/0009-0002-4652-8516
Contact phone: +6282241116998
Number of publications in national journals indexed (approximate; for Ukraine citizens only): -
Number of publications in international journals indexed (approximate): -
H-index by Scopus (if available): -
ResearchGate: https://www.researchgate.net/profile/Dzulfikar-Johan-Akbar
Scopus ID: -
Researcher ID: -

Muhammad Reza
Bachelor Student
Department of Mechanical Engineering
Widya Gama University
Borobudur str., 35, Malang, Indonesia, 65142
E-mail: muhapanjangreza@gmail.com
ORCID: https://orcid.org/0009-0009-9258-0586
Contact phone: +6282139682566
Number of publications in national journals indexed (approximate; for Ukraine citizens only): -
Number of publications in international journals indexed (approximate): -
H-index by Scopus (if available): -
ResearchGate: -
Scopus ID: -
Researcher ID: -

Name of reviewer: Prof. Dr. Muji Setiyo, ST., MT.
Professor: Mechanical Engineering
Tel: +6281211020288
E-mail: muji@unimma.ac.id.
Work address: Universitas Muhammadiyah Magelang

Name of reviewer: Prof. Dr. Eng. Nurkholis Hamidi, ST., MT.
Professor: Mechanical Engineering
Tel: +62 81259293165

E-mail: hamidy@ub.ac.id
Work address: Brawijaya University

TAHAP 6

REVIEW REVIEWER TAHAP 6

6 April 2026

Purbo Suwandono <purbo@widyagama.ac.id>

from "Eastern-European Journal of Enterprise Technologies"_6th stage_No.2(140).2026

3 messages

Oksana Nikitina <0661966nauka@gmail.com> Mon, Apr 6, 2026 at 2:32 PM
To: purbo@widyagama.ac.id, "Widya Wijayanti, ST.,MT" <widya_dinata@ub.ac.id>, nova@widyagama.ac.id, johanakbar@student.ub.ac.id, muhapanjangreza@gmail.com

Good afternoon, dear authors.

The article was accepted for consideration of the possibility of publication in (No. 2(140).2026).

At the 6th stage of editing, please consider the comments of the reviews (article in the application, color notes are highlighted).

We ask you to right strictly in the option which is in the attachment (see attachment).

We ask you not to delete the comments so that we can see all your edits. Please highlight all the author's corrections in green.

Please provide an edited version of the article **by 08.04.2026.**

If you have any questions, please call or write; we will be happy to answer them.

With best regards, Manager Yu. Prylutska
TECHNOLOGY CENTER GROUP LTD
Viber/ WhatsApp/ Telegram: +380 (50) 3033801
Editorial staff of the "Eastern-European Journal of Enterprise Technologies"
Website: https://jet.com.ua/en/, http://journals.uran.ua/eejet/



Відвідати сайт



Відвідати сайт

Attention! The author (team of authors) submitting the manuscript to the editorial office of the journal **«Eastern-European Journal of Enterprise Technologies»** agrees with all requirements for registration, submission of the manuscript of the article and payment and be responsible in case of violation of these requirements.

Our company may rely on your freely given consent at the time you provided your personal data to us replying on this email then the lawfulness of such processing is based on that consent under EU GDPR 2016/679. You have the right to withdraw consent at any time.

Subscribe

Suwandono_прийнято.doc
1152K

Purbo Suwandono <purbo@widyagama.ac.id> Tue, Apr 7, 2026 at 1:32 PM
To: Oksana Nikitina <0661966nauka@gmail.com>

Good afternoon,

Thank you for your email.

We have completed the revision of the manuscript according to the editorial instructions.

Please find the revised manuscript attached. If there are any remaining mistakes or further corrections needed, we will be ready to revise it accordingly.

Best regards,
Purbo Suwandono

[Quoted text hidden]

Suwandono_прийнято - Revision.doc
1183K

Oksana Nikitina <0661966nauka@gmail.com> Tue, Apr 7, 2026 at 4:15 PM
To: Purbo Suwandono <purbo@widyagama.ac.id>

Good day!
The article has been sent to the editor for checking.
If you have any questions, please call or write. We will be happy to answer them.
We wish you a great day and a good mood!
Regards, Oksana

вт, 7 апр. 2026 г. в 09:32, Purbo Suwandono <purbo@widyagama.ac.id>:
[Quoted text hidden]

--
[Quoted text hidden]

Received date: 20.02.2026
Accepted date:

Від рецензента

№2

The article is interesting, but there are several remarks. They are inserted in the text of the article. After elimination of these remarks, the article can be publication

UDC 662.7:662.767:66.097

ПОКРАЩЕННЯ ЯКОСТІ СИНТЕЗ-ГАЗУ ПРИ ВИСХІДНІЙ ГАЗИФІКАЦІЇ КУКУРУДЗЯНИХ КАЧАНІВ З ВИКОРИСТАННЯМ КАТАЛІЗАТОРА НА ОСНОВІ CAO/АКТИВОВАНОГО ВУГІЛЛЯ НА ПАЛЬМОВОМУ ВОЛОКН

Purbo Suwandono, Widya Wijayanti, Nova Risdiyanto Ismail, Dzulfikar Johan Akbar, Muhammad Reza

SYNGAS QUALITY IMPROVEMENT IN CORNCOB UPDRAFT GASIFICATION USING CAO/ACTIVATED CARBON PALM FIBER CATALYST

Purbo Suwandono, Widya Wijayanti, Nova Risdiyanto Ismail, Dzulfikar Johan Akbar, Muhammad Reza

Об'єктом даного дослідження є поліпшення якості синтез-газу, отриманого в результаті газифікації кукурудзяних качанів за допомогою системи з подвійним каталізатором, що складається з CaO та активованого вугілля, отриманого з пальмового волокна (AC–PF). Проблема, вирішена в даному дослідженні, полягає у відносно низькій теплотворній здатності синтез-газу з кукурудзяних качанів та високій вартості традиційних каталізаторів, що використовуються для його поліпшення. Дослідження проводилося з використанням різних значень еквівалентного співвідношення (0,2; 0,25; 0,3; 0,35), навантаження каталізатора (4%; 6%; 8%; 10%) та масового співвідношення CaO/AC–PF (0:1; 1:0; 1:1; 2:1) у поєднанні з характеристикою подвійної каталітичної системи. Отримані результати показують, що збільшення ER збільшує частки H_2 і CH_4 та нижчу теплоту згоряння синтез-газу, одночасно зменшуючи CO_2, причому CO досягає оптимального значення при ER = 0,3. У той час як більш високе навантаження каталізатора має тенденцію до зменшення H_2 і CH_4, але збільшує CO, потенційно знижуючи теплоту згоряння при високих навантаженнях. Характеристика каталізатора показує, що AC-PF має пористу структуру, яка збільшує контакт

газу з твердим тілом і сприяє вторинним реакціям, тоді як додавання CaO утворює композит із модифікованою структурою пор і поверхневими видами, пов'язаними з сорбцією CO_2. З енергетичної точки зору, нижня теплота згоряння синтез-газу збільшується із зростанням ER, але зменшується при більш високих навантаженнях каталізатора через зменшення внеску CH_4. Ключовою особливістю отриманих результатів є продемонстрована функціональна синергія між пористим AC–PF і сорбцією CO_2 на основі CaO, що дозволяє одночасно здійснювати каталітичне поліпшення якості та уловлювання CO_2 в єдиній, недорогій системі з подвійним каталізатором. Ці висновки можуть стати практичною основою для проектування та експлуатації невеликих установок газифікації біомаси, зокрема реакторів з висхідним потоком для відходів кукурудзяних качанів, в межах досліджених діапазонів ER та навантаження каталізатора.

Ключові слова: газифікація, висхідний потік, кукурудзяні качани, синтез-газ, CaO, активоване вугілля.

The object of this study is the improvement of syngas quality from updraft corn cob gasification using a dual catalyst system consisting of CaO and activated carbon derived from palm fiber (AC–PF). This is an incorrect formulation of the research object. The correct version is in Section 4. It should also be as in Section 4. *The problem solved in this study is the relatively low heating value of corn cob syngas and the high cost of conventional catalysts used for its upgrading. The study was conducted using variations of equivalence ratio (0.2, 0.25, 0.3, 0.35), catalyst loading (4%, 6%, 8%, 10%), and CaO/AC–PF mass ratio (0:1, 1:0, 1:1, 2:1), combined with characterization of the dual catalyst system. The results obtained show that increasing ER increases the H_2 and CH_4 fractions and the syngas lower heating value while decreasing CO_2, with CO reaching an optimum at ER = 0.3. Whereas higher catalyst loading tends to decrease H_2 and CH_4 but increase CO, potentially reducing the heating value at high loadings Characterization of the catalyst shows that AC-PF has a porous structure that increases gas-solid contact and promotes secondary reactions, while the addition of CaO forms a composite with a modified pore texture and surface species associated with CO_2 sorption. From an energy perspective, the Lower Heating Value of syngas increases with increasing ER, but decrease at higher catalyst loadings due to the reduced contribution of CH_4. A key feature of obtained results is the demonstrated functional synergy between porous AC–PF and CaO-based CO_2 sorption, which enables simultaneous catalytic upgrading and CO_2 capture in a single, low-cost dual catalyst system. These findings could be a practical basis for designing and operating small-scale biomass gasification units, particularly updraft reactors for corn cob waste, within the studied ER and catalyst loading ranges*

Keywords: gasification, updraft, corncob, syngas, CaO, activated carbon

1. Introduction

In recent years, environmental challenges such as rising greenhouse gas emissions, fossil fuel depletion, and increasing agricultural waste have strengthened the global push toward green energy and sustainable technologies. These issues have become major concerns because they affect not only environmental quality but also long-term energy security and sustainable economic development. Green energy development is not only about reducing emissions but also about creating cleaner, more efficient ways to utilize available resources and minimize waste generation. Conversion of biomass residues into useful energy has attracted considerable attention as a practical and environmentally responsible solution. One promising approach is the thermochemical conversion of biomass through gasification, which can transform solid biomass into synthesis gas that can be used directly as a fuel or further processed as a feedstock for chemical production and other energy applications.

Indonesia is one of the largest corn producers in Southeast Asia, with national production reaching more than 18 million tons of dry kernels per year. Of this amount, about 15–20% is cobs after the kernel removal process, resulting in a very large amount of corn cob waste, estimated at 2.5–3.5 million tons annually. Until now, most corn cobs have only been used to a limited extent, for example as traditional fuel, small amounts of animal feed, or even burned directly on post-harvest land, which has the potential to cause air pollution. Most of the rest are simply piled up or left to rot on the land, posing a risk of becoming a source of plant disease [1].

Corn cobs have quite promising chemical and energy characteristics. Their composition is dominated by cellulose, hemicellulose, and lignin, with a calorific value of around 15–17 MJ/kg, making them very suitable as raw materials in various biomass-based energy conversion technologies [2]. Their hard and fibrous nature also makes them suitable for processing into biochar, activated charcoal, or direct use in pyrolysis and gasification processes. This significant potential indicates that corn cobs are not merely waste but a renewable resource that can be optimized to support energy security and reduce dependence on fossil fuels.

Biomass gasification is a promising thermochemical technology for converting renewable resources into syngas consisting of H_2, CO, CH_4, and CO_2. Of the various types of biomass, corn cobs are a potential candidate due to their abundant availability in Indonesia and lignocellulose content that supports the energy conversion process [3]. However, the biomass gasification process still faces several obstacles, particularly the low hydrogen fraction in syngas and the formation of significant amounts of tar. Tar can cause reactor clogging, reduced thermal efficiency, and increased purification costs.

To overcome these problems, the use of catalysts is an important strategy. A number of studies have proven that metal catalysts such as Ni, Ca, and K can increase hydrogen yield while suppressing tar formation. On the other hand, activated carbon is also widely used as a catalyst support because it has a high surface area, porous structure, and good chemical stability. The use of agricultural waste, particularly palm fiber, as raw material for activated carbon is not only economically valuable but also supports the concept of a circular economy in plantation waste management. In addition,

calcium oxide (CaO) is known to have a dual role, namely as a catalyst in the tar decomposition reaction and as a CO_2 absorber that promotes sorption-enhanced gasification to increase the hydrogen fraction in syngas [4].

Although various studies have examined the role of metal catalysts and activated carbon separately, research focusing on the combination of biomass bases catalyst such as palm fiber-based activated carbon with CaO in corn cob gasification is still limited. The uniqueness of this study lies in the integration of two catalyst, which is expected to provide a synergistic effect: activated carbon with high porosity increases catalyst dispersion and activity, while CaO simultaneously breaks down tar and absorbs CO_2. This approach has the potential to significantly increase hydrogen production and reduce carbon emissions.

However, there are several research gaps that remain unanswered. First, the optimal composition and ratio of activated carbon and CaO in corn cob gasification have not been extensively studied. Second, the synergistic mechanism using two catalyst in increasing syngas quality not yet fully understood. In addition, a systematic and statistically robust approach is required to disentangle the coupled effects of key operating and catalyst variables.

Based on this background and research gaps, this study aims to investigate the performance of a composite catalyst based on activated carbon from palm fiber combined with CaO in the corn cob gasification process. The main focus is on increasing hydrogen production, reducing tar, and evaluating the potential synergistic effects between materials. This research is expected to contribute to the development of low-cost, locally sourced, and sustainable catalyst systems that are relevant to supporting the clean energy transition and practical applications of biomass-to-hydrogen in the future.

This text doesn't belong in Section 1. It's a conclusion that can follow from a literature review, so it should be at the end of Section 2. However, the conclusion is already in section 2. Also, in the Introduction section did not need to annotate the article. It was necessary to justify the relevance of this **topic** in modern times. Therefore, you can remove this part of the text.

To finish this section of the article you need this text:

*Therefore, stud**ies** that are devoted….. **are** scientific relevance*

That is, it is necessary to inform not about your study, but about the relevance of this scientific topics

2. Literature review and problem statement

The paper [5] presents the result on the gasification of sago dreg waste pellets in a top-lit updraft fixed-bed gasifier. The results show that the addition of Al_2O_3 improved syngas quality, especially by increasing H_2 content up to 31.65% at 5% Al_2O_3 and enhancing CO and CH_4 production, while also increasing the H_2/CO ratio to 1.65 and

1.51 for 5% and 10% Al_2O_3, respectively, improving LHV, and reducing tar content by about 25–27.5% compared with pellets without catalyst. However, this study is limited because it was conducted only on one biomass type, within a laboratory-scale TULD fixed-bed gasifier, and only considered two catalyst loadings.

The paper [6] presents the result on hydrogen enrichment in product gas from a pilot-scale rice husk updraft gasification. The results show that dolomite-assisted air gasification gave the best performance, increasing the H_2 content up to 15.4 mol%, with an LHV of 5.1 MJ/Nm³, while steam/air gasification improved H_2 to 9.6 mol% and air alone produced only about 7.08 mol% H_2, the optimum operating condition was reported at an airflow rate of 3 m³/h and a dolomite mixing ratio of 15 wt%. However, this study is limited because it focused only on rice husk feedstock, used a pilot-scale updraft gasifier with a batch capacity of 3 kg, and evaluated only a limited range of operating conditions and catalyst type.

The paper [7] presents the result on oxygen updraft gasification coupled with catalytic steam reforming of cigarette butts for hydrogen-rich syngas production. The results show that the integrated process was effective in converting cigarette butts into syngas, with gasification producing 82.3–89.7 wt.% syngas, 6.3–8.6 wt.% soot, and 1.4–1.9 wt.% tar, while the catalytic reforming stage significantly improved the gas quality by increasing the H_2 content up to 30.27 vol.%, increasing the HHV up to 11,528 kJ/kg, and reducing tar concentration from about 18.15 g/m³ to 13.38 g/m³ under the optimum condition. However, this study is limited because it investigated only cigarette butt waste as feedstock, used a specific oxygen updraft gasifier–catalytic reformer configuration, and fixed most catalytic reforming parameters.

The paper [8] presents the result on the experimental assessment of pellets produced from beekeeping waste and slumgum–pine sawdust mixtures through updraft gasification. The results show that pure slumgum pellets exhibited very high mechanical durability (99.98%) and high HHV (27.66 MJ/kg), while during gasification the 50% slumgum–50% sawdust pellets produced the highest producer gas LHV of 7.62 MJ/Nm³, indicating that the addition of sawdust improved gas quality and energy recovery potential. However, this study is limited because the equivalence ratio remained very low (0.0125–0.0204) compared with typical gasification conditions, the experiments were conducted only in a modified laboratory-scale updraft gasifier.

The paper [9] presents the result on a comparative investigation of catalyst applications in updraft and modifiable-downdraft fixed-bed biomass gasifiers, using a biomass mixture of green waste, sewage sludge, and olive pomace together with red mud (RM) and Al–Ni alloy catalysts to improve syngas quality and hydrogen production. The results show that catalyst type and reactor configuration strongly influenced gasification performance, with the Al–Ni catalyst giving the best hydrogen enrichment, reaching up to 65 vol.% H_2 in the updraft gasifier at 900 °C, while RM increased H_2 to about 50 vol.%, the updraft gasifier produced better hydrogen-rich syngas than the modifiable-downdraft reactor. However, this study is limited because it,

used a specific mixed biomass composition and mainly focused on high temperature operation around 900 °C with limited gasifying-agent flow conditions.

The paper [10] presents the result on the experimental investigation of producer gas composition from sorted municipal solid wastes in an updraft fixed-bed gasifier. The results show that reducing the equivalence ratio from 0.21 to 0.15 increased the heating value of the combustible gases. The study indicated that the allothermal updraft fixed-bed gasifier is suitable for producing gas that can be utilized in gas engines. However, this study is limited because it used a laboratory-scale 10 kW allothermal updraft gasifier at a fixed temperature of 800 °C, and evaluated only two ER conditions.

The paper [11] presents the result on the effect of adding laying hens manure (LHM) to wheat straw on gasification efficiency in an air-blown updraft fixed-bed gasifier. The results show that increasing ER improved the gasification performance, with the producer gas LHV reaching 3.3–3.4 MJ/m³, cold gas efficiency around 60%, and carbon conversion efficiency in the range of 82–94% . However, this study is limited because it was focused on one specific co-feed system and produced a relatively low-calorific gas.

The paper [12] presents the result on the gasification performance of olive pomace in updraft and downdraft fixed-bed reactors using dry air and pure oxygen. The results show that updraft reactor achieving up to 48 vol.% H_2 with dry air and 53 vol.% H_2 with pure oxygen, while the downdraft reactor reached up to 45 vol.% H_2 with dry air and 39 vol.% H_2 with pure oxygen. However, this study is limited because only a limited range of gasifying agents, temperatures, and flow rates.

The paper [13] presents the result on the gasification of MDF residue in an industrial-scale updraft fixed-bed gasifier. The results show that MDF residue can be effectively converted into useful energy, with a syngas production rate of about 2.5 Nm³/kg, syngas LHV of around 6.0–7.0 MJ/Nm³, about 88 wt.% of MDF residue converted into syngas, and a system capable of delivering 7 MWth of thermal energy and about 955 kW net electrical power through the ORC turbine. However, this study is limited because it focused on one specific industrial waste stream (MDF residue) in one updraft gasifier configuration, mainly evaluated performance under a limited number of feed rates, and relied on direct combustion of raw hot syngas containing tar.

The paper presents the results of research on biomass gasification in updraft fixed-bed reactors aimed at improving syngas quality and thermal conversion efficiency. Shown that syngas composition and heating value are strongly influenced by feedstock properties, gasification conditions, and catalyst application. But there were unresolved issues related to the lack of effective and low-cost catalyst systems capable of simultaneously enhancing hydrogen formation and improving overall syngas quality during corncob gasification. The reason is the complexity of catalytic reactions in the gasification zone, including reforming, cracking, and CO_2 capture mechanisms, as well as the economic limitations of commercially available catalysts. A way to overcome these difficulties can be the development of composite catalysts based on CaO and activated carbon palm fiber, where CaO may promote CO_2 absorption and shift

reactions, while activated carbon palm fiber may provide a porous surface and active sites for secondary cracking reactions. This approach was used in previous studies, however, the combined use of CaO and activated carbon palm fiber in corncob updraft gasification has not been sufficiently investigated. All this suggests that it is advisable to conduct a study on syngas quality improvement in corncob updraft gasification using CaO/activated carbon palm fiber catalyst.

Previous studies have shown that biomass gasification is a promising route for converting agricultural residues into synthesis gas, and that catalytic materials such as CaO and carbon-based adsorbents can improve gas quality through tar reduction, reforming reactions, and CO_2 capture. Several researchers have also investigated different biomass feedstocks, catalyst types, and reactor configurations to enhance syngas production. However, most of these studies mainly focused on the individual performance of catalysts or on gasification systems other than corncob updraft gasification. In addition, the combined effect of CaO and activated carbon palm fiber catalyst, especially in terms of catalyst ratio, catalyst loading, and equivalence ratio, has not been systematically discussed.

Therefore, further study is needed to clarify the synergistic role of CaO as a CO_2 sorbent and activated carbon palm fiber as a porous catalytic support in improving syngas composition and heating value. Based on this research gap, the present study specifically investigates the use of combined CaO/activated carbon palm fiber catalyst in corncob updraft gasification and evaluates the influence of key operating parameters on synthesis gas quality. In this way, the study is intended to provide both a clearer scientific understanding of catalyst interaction and practical guidance for improving biomass gasification performance.

3. The aim and objectives of the study

The purpose of the study is to enhance syngas quality from corncob updraft gasification by developing a dual-synergy catalytic system based on calcium oxide (CaO) and palm-fiber-derived activated carbon (AC-PF). This will allow the production of cleaner and more energy-dense producer gas, providing practical guidance for selecting operating conditions and catalyst configurations suitable for updraft gasifiers processing agricultural residues.

To achieve these aims, the following objectives are accomplished:

– to prepare and characterize CaO and AC-PF catalysts by analyzing their morphology, surface functional groups, and pore characteristics using SEM, FTIR, and BET methods;

– to evaluate the influence of equivalence ratio, catalyst loading, and CaO/AC ratio on syngas composition and lower heating value in corncob updraft gasification, and to identify the catalyst condition that provides improved gas quality.

4. Materials and methods

4. 1. Object and hypothesis of the study

The object of the study is the updraft fixed-bed gasification process of corncob biomass using a dual catalyst system based on calcium oxide (CaO) and palm-fiber-derived activated carbon (AC-PF). The practical physical process under investigation is the catalytic upgrading of producer gas within the updraft reactor, where changes in operating parameters and catalyst configuration are expected to influence syngas composition and heating value. The results of this study are intended to be applied to improve the quality of syngas, specifically by increasing the combustible gas fraction (H_2 and CH_4) and the lower heating value (LHV), while reducing CO_2 content.

The selected methods were intended to explain both the catalyst characteristics and their effect on syngas quality. SEM, FTIR, and BET were used because they provide complementary information on catalyst morphology, surface functional groups, and pore structure, which are important for catalytic reforming, adsorption, and CO_2 capture during gasification. The investigated operating parameters, namely equivalence ratio, catalyst loading, and CaO/AC ratio, were chosen because they are the main variables governing the reaction environment, catalyst effectiveness, and synergistic interaction between CaO and activated carbon in the updraft gasification process.

The research hypothesis is that a dual-synergy CaO/AC-PF catalytic system can improve syngas quality more effectively than single-catalyst configurations in updraft corncob gasification. It is hypothesized that CaO functions as a CO_2 sorbent, shifting reaction equilibria toward enhanced hydrogen formation, while activated carbon derived from palm fiber provides high-surface-area catalytic sites that promote secondary reactions such as tar cracking and volatile reforming. The combined catalytic-sorption mechanism is expected to increase H_2 and CH_4 fractions and improve LHV under optimized equivalence ratio (ER), catalyst loading, and CaO/AC-PF ratio conditions.

It was assumed that the corncob feedstock has relatively homogeneous composition and stable proximate/ultimate characteristics during the experiments. The gasification process was assumed to operate under steady-state conditions after stabilization. It was also assumed that the CaO maintains sufficient CO_2 sorption capacity within the experimental time frame and that the activated carbon structure remains stable under the applied temperature range.

During the course of the research, several methodological simplifications were adopted in order to maintain experimental feasibility and focus on the main objective of syngas quality evaluation. Detailed kinetic modeling of individual gasification reactions was not performed; instead, the process performance was assessed based on experimentally measured syngas composition and syngas low heating value. Furthermore, although CaO carbonation-decarbonation reactions may occur during operation, microstructural evolution, sintering behavior, and long-term cyclic stability of the catalyst were not investigated in this study. The catalytic performance was evaluated within the experimental duration without conducting extended durability or regeneration-cycle analysis. This text should be at the end of the subsection 4.1.

4. 2. Catalyst Preparation

Approximately 6 grams of ground palm fiber was mixed with 60 mL of distilled water and stirred for 10 minutes. The mixture was then placed in an autoclave and heated to 200°C at a rate of 5°C per minute for 6 hours in an electric oven. After that, the reactor is allowed to cool naturally to room temperature. The resulting solid hydrocarbon product (hydrochar) is then separated using Whatman No. 42 filter paper. The filtered product is then dried at 105°C for 24 hours and stored in a glass vial. The next stage is the activation process. The hydrochar is immersed in a 3 M KOH solution with a weight ratio of 1:3 (Hydrochar:KOH) for 16 hours, then dried at 85°C for 6 hours. Spectroscopic evidence indicates that KOH preferentially reacts with oxygenated sites and can increase the relative abundance of C–OH functionalities, while higher KOH ratio and activation temperature significantly enhance porosity and BET surface area [14, 15]. To obtain the CaO/AC mixture, CaO powder and activated carbon (AC) were mixed in specific proportions using a grinder until a homogeneous mixture was obtained. Next, CaO, AC, and CaO/AC were activated using a tube furnace at a temperature of 700°C for 1 hour with a continuous flow of nitrogen during the activation process. The resulting product was then washed using distilled water until it reached a neutral pH. This stage produced activated carbon that was ready for use in research.

4. 3. Experimental Setup

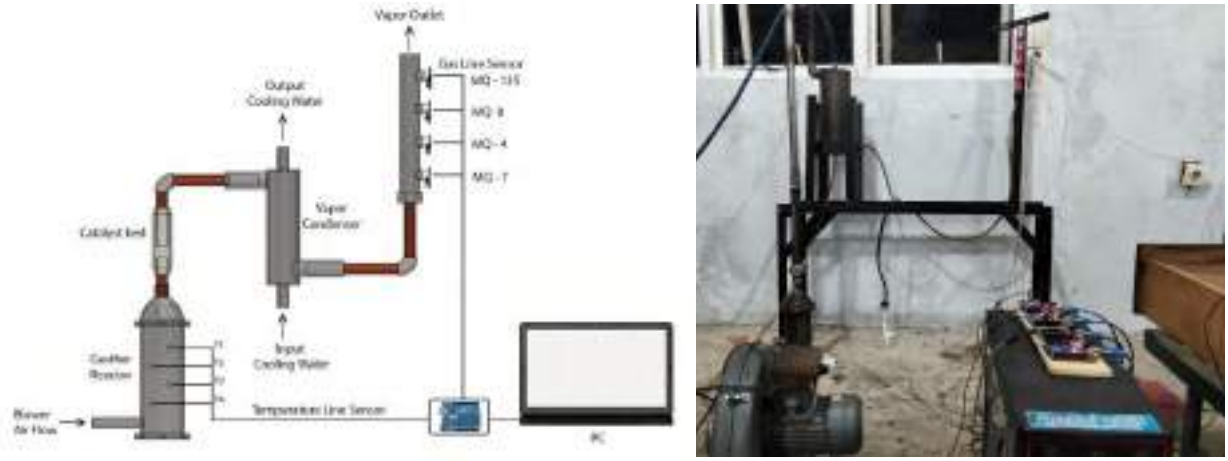
Corncob biomass was obtained from farmers in the South Malang region of East Java. Before use, the biomass was cleaned of impurities and dried in an oven for 6 hours at 100°C to remove moisture (water vapor) content. The ultimate and proximate test results are as follows.

The proximate and ultimate analyses of the corncob feedstock were conducted to determine its physicochemical characteristics prior to gasification. The results are presented in Table 1. The data indicate that corncob has high volatile matter content and relatively low ash content, which are favorable characteristics for gasification processes.

Table 1
Ultimate and Proximate Test Corn Cob

Parameter	Units	Corn cobs
Moisture	%	10
Volatile matter	%	71.38
Fixed carbon	%	12.11
Ash	%	6.51
C	%	43.6
H	%	6.3
O	%	46.8
N	%	0.22
HHV	MJ/kg	17.61

The experimental apparatus employed in this study consisted of an updraft gasifier integrated with a catalyst bed, a vapor condensation unit, gas sensors, and temperature measurement points to enable comprehensive monitoring of the gasification process. Fig. 1 shows the updraft gasifier system used in this study, including the schematic experiment (a) and the experimental setup (b).



a *b*

Fig. 1. Updraft gasifier: *a* – schematic experiment; *b* – experimental setup

This study used an updraft gasification reactor designed with a total height of 20 cm. The lower part of the reactor consisted of an ash container with a height of 5 cm, while the active reactor had a height of 15 cm and a diameter of 3 inches. The reactor was equipped with a 1-inch diameter air inlet pipe connected to a blower. The blower was modified with a potentiometer so that the air speed could be adjusted as needed. To monitor the thermal conditions inside the reactor, four 3 cm long type K thermocouples were installed at several different points so that the temperature profile in the gasification zone could be observed in more detail. Each test was conducted with a fixed biomass mass, a mixture of corn cobs weighing 80 grams. The reactor was made of iron and equipped with a gas seal to prevent leaks during the gasification process.

The gas produced by the reactor was fed into a condenser, which cooled the hot gas so that the water vapor components could be separated. The condenser was made of a copper spiral pipe with a diameter of ½ inch and a height of 30 cm. Cooling water was circulated from the bottom of the condenser and exited through the top to ensure efficient heat transfer. This cooling system was driven by a 60-watt water pump, ensuring stable water flow and optimal condensation. The catalyst was positioned downstream after the reactor, where it was supported on steel wool and wrapped with an 80-µm wire mesh to secure the catalyst and prevent particle carryover with the gas flow

To analyse the gas composition, four types of MQ gas sensors were used. The MQ-8 sensor was used to detect H_2, MQ-4 for CH_4, MQ-135 for CO_2 and MQ-7 for CO.

Each gas sensor was calibrated according to the manufacturer's datasheet, specifically by determining the Ro value, which is the sensor resistance in clean air conditions. This Ro value is used as a reference in calculating the measured gas concentration during the process.

All data from the gas sensors and thermocouples were acquired using an Arduino Uno microcontroller. Each gas sensor is connected to a separate Arduino Uno to facilitate the calibration process and reduce the possibility of interference between sensors. Arduino is also used to record temperature data from four thermocouples installed in the reactor, so that gas composition and temperature distribution data can be obtained simultaneously.

The ER range of 0.2, 0.25, 0.3 and 0.35. The catalyst load was between 4%, 6%, 8% and 10% from the mass of input feedstock. The CaO/AC-PF ratio was varied between 0:1, 1:0, 1:1, and 2:1. Design of experiment can be seen in Table 2.

Table 2
Design of Experiment using

Run	Equivalence Ratio (E.R)	Catalyst Load %	CaO/AC
1	0.2	4	1:0
2	0.2	6	0:1
3	0.2	8	1:1
4	0.2	10	2:1
5	0.25	4	0:1
6	0.25	6	1:0
7	0.25	8	2:1
8	0.25	10	1:1
9	0.3	4	1:1
10	0.3	6	2:1
11	0.3	8	1:0
12	0.3	10	0:1
13	0.35	4	2:1
14	0.35	6	1:1
15	0.35	8	0:1
16	0.35	10	1:0

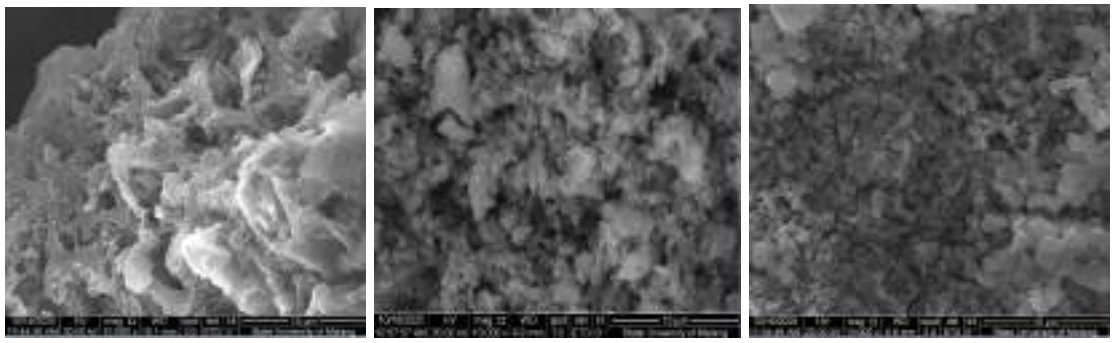
A total of 16 experimental runs were conducted systematically to enable evaluation of the main effects of each variable and the tendency of interactions between variables on the fractions of H_2, CO, CH_4, CO_2, and lower heating value (LHV). This approach enabled identification of the most effective combination of operating parameters in improving syngas quality quantitatively and measurably.

5. Results of syngas quality enhancement from corncob using calcium oxide (CaO) and palm-fiber-derived activated carbon (AC–PF).

5. 1. Characterization of Calcium Oxide (CaO) and Palm-Fiber-Derived Activated Carbon (AC–PF) Catalysts

5. 1. 1. Scanning Electron Microscopy Catalyst Result

Fig. 2, *a* shows the image obtained from a Scanning Electron Microscope (SEM) with a magnification of 10,000× shows the surface morphology of palm fiber-based activated carbon (AC-PF). The surface structure appears porous and irregular, with a combination of void areas and layered surfaces. This characteristic indicates that the activation process that using KOH has successfully formed micropores and mesopores, which play an important role in increasing the specific surface area of activated carbon.



a *b* *c*

Fig. 2. Scanning Electron Microscopy Catalyst Result: *a* – Scanning Electron Microscopy AC-PF; *b* – Scanning Electron Microscopy CaO:AC;1:1; *c* – Scanning Electron Microscopy CaO:AC-PF;2:1

The rough and textured surface indicates that most of the material has undergone lignocellulose cell wall exfoliation, resulting in numerous interparticle gaps. This porous structure greatly supports gas adsorption and diffusion capabilities when used as a catalyst in gasification or thermochemical reactions.

The presence of 1–5 μm voids indicates that most pores are in the mesopore category, supporting the adsorption of gas molecules such as H_2, CO, and tar during the gasification reaction.

The morphology of AC-PF shows the characteristics of porous activated carbon with a heterogeneous pore distribution, where the pores allow increased contact between gas reactants and active sites on the material surface, thereby increasing catalytic efficiency and the ability to absorb tar or CO_2 in biomass-based energy applications.

Fig. 2, *b* shows the surface morphology of the CaO:AC-PF catalyst with a ratio of 1:1. Visually, it can be seen that the surface of this material consists of fine particles ranging in size from microns to submicrons that stick together to form a layered and slightly agglomerated structure.

The presence of fine, light-colored grains indicates an even distribution of CaO particles impregnated on the surface of activated carbon (AC-PF). This CaO distribution fills some of the pores of the carbon, resulting in a denser surface compared to pure AC-PF. However, there are still small gaps and voids between the grains, indicating that the microporous and mesoporous structures are still formed and can support catalytic activity [16].

This morphology illustrates the success of the CaO impregnation process on activated carbon from palm fiber, where the interaction between CaO and the carbon pore walls produces a composite material that is more thermally and chemically stable. This structure is highly conducive to catalyst applications in biomass gasification processes, as CaO particles can function as CO_2 absorbers while accelerating the tar reforming reaction [17].

Fig. 2, *c* shows the surface morphology of the CaO:AC-PF (2:1) catalyst. The image shows that the surface of the material is dominated by agglomerations of fine, round, and irregular particles ranging in size from microns to submicrons. Compared to the CaO:AC-PF (1:1) sample, this structure appears denser and tighter, indicating that an increase in the CaO ratio causes partial closure of the activated carbon surface pores by CaO particles.

The distribution of CaO particles appears more uniform and covers the carbon surface, indicating the successful impregnation of a larger amount of CaO. The light color in some areas indicates the presence of a calcium oxide phase that is strongly attached to the activated carbon matrix. This structure indicates a strong interaction between CaO and AC-PF, forming a thermally stable composite.

Although some pores are covered, there are still microscopic gaps between the CaO grains that allow gas diffusion to occur, so that the catalyst retains its good adsorption capacity. The combination of the active area of CaO and the porous carbon structure makes this material very promising for biomass gasification or tar reforming applications, as CaO can act as a CO_2 absorber and increase the conversion of carbon to hydrogen gas.

5. 1. 2. Fourier Transform Infrared Spectroscopy catalyst result

The FTIR analysis results shown in the Fig. 3 reveal clear spectral differences between the AC-PF, CaO, and their mixtures (CaO:AC-PF) with ratios of 2:1 and 1:1. In the AC-PF spectrum, the absorption band at 2926 cm^{-1} is associated with the stretching vibration of the C–H group from $–CH_2$ or $–CH_3$ (methylene/methyl stretching), which indicates the presence of hydrocarbon chain residues from the lignocellulose structure. The peak at 1577 cm^{-1} indicates the presence of aromatic C=C or C=O stretching, while the band at 1056 cm^{-1} represents C–O stretching from alcohol or ether groups. In addition, the –OH group that appears in the 3500–3600 cm^{-1} region is identified as the result of AC-PF activation using a KOH solution, which causes the formation of hydroxyl groups on the activated carbon surface. This –OH group plays an important

role in increasing the surface activity and adsorption capacity of AC-PF as a catalyst support medium [18, 19].

In pure CaO, the intense band at 3639 cm^{-1} is associated with the stretching of the O–H group from $Ca(OH)_2$, which is formed due to the partial hydration of CaO when exposed to humid air. Meanwhile, the absorption bands at 1426 cm^{-1} and 876 cm^{-1} are associated with C–O stretching and CO_3^{2-} bending, respectively, indicating the formation of $CaCO_3$ due to CO_2 adsorption from the air. This shows that CaO is highly reactive to moisture and carbon dioxide in the environment.

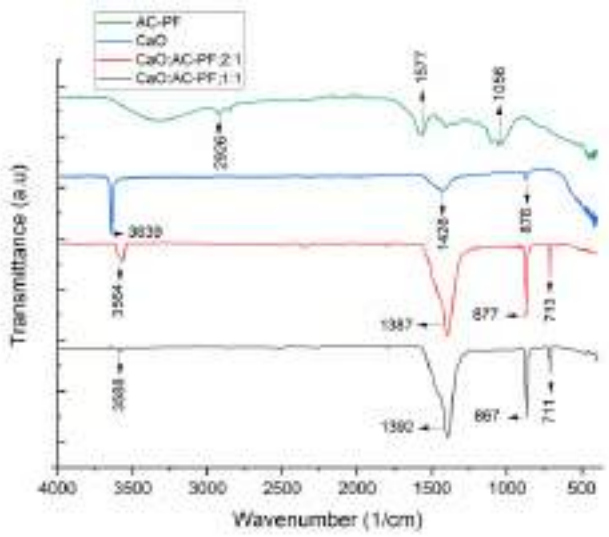


Fig. 3. Fourier Transform Infrared Spectroscopy Catalyst Result

For the CaO:AC-PF (2:1), the main absorption bands were detected at 3564 cm^{-1} (O–H stretching from $Ca(OH)_2$ and the –OH group in AC-PF), 1387 cm^{-1} (C–O stretching), and 877 cm^{-1} and 713 cm^{-1} (bending vibration of CO_3^{2-}). This combination of bands indicates the formation of carbonate compounds ($CaCO_3$) due to the interaction between CaO and the oxygen groups of activated carbon. The presence of –OH groups from KOH activation also strengthens the basic properties on the surface, which can increase the chemical interaction between CaO and AC-PF [20].

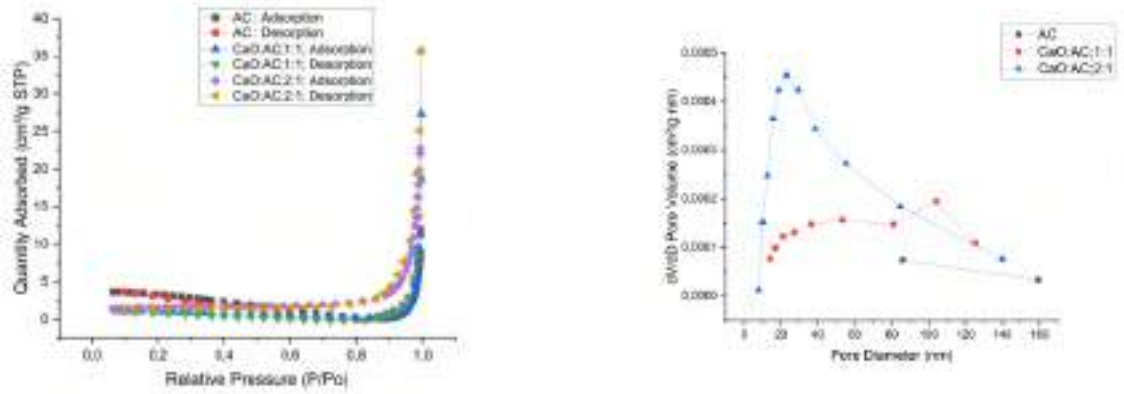
At a CaO:AC-PF ratio of 1:1, the absorption bands at 3588 cm^{-1}, 1392 cm^{-1}, 867 cm^{-1}, and 711 cm^{-1} show a similar pattern, indicating the presence of hydroxyl (O–H) and carbonate (CO_3^{2-}) groups. The difference in peak intensity compared to the 2:1 ratio indicates variations in the level of interaction between CaO and the –OH groups resulting from KOH activation on AC-PF, which affects the formation of carbonate-hydroxide complexes on the material surface [21].

5. 1. 3. Brunauer-Emmett-Teller Catalyst Result

Fig. 4 shows the adsorption-desorption isotherm curves for nitrogen for the AC, CaO:AC (1:1), and CaO:AC (2:1) samples are shown in Fig. 4. All three samples exhibit

type IV isotherms with clear hysteresis loops at relatively high pressures (P/Po > 0.9). Based on the IUPAC classification, this characteristic indicates that the material has a mesoporous structure formed through capillary condensation within the pore channels. The difference between the adsorption and desorption pathways indicates that the pore shape is not perfectly cylindrical, but rather tends to be irregular or slit-like, which is commonly found in modified activated carbon materials [22].

The pure activated carbon (AC) sample showed a relatively low nitrogen adsorption volume with a specific surface area of 24.51 m²/g and an average pore diameter of 0.74 nm, indicating a predominance of microporous structures. In the CaO:AC (1:1) composite, the surface area did not change significantly compared to pure AC, indicating that the addition of a moderate amount of CaO did not cover the carbon pores much, but only adhered to the external surface of the carbon matrix [23].



a *b*

Fig. 4. Brunauer-Emmett-Teller Result: *a* – Surface Analysis Adsorption Desorption Isotherm; *b* – Barrett-Joyner-Halenda Adsorption Pore Size Distribution

Conversely, in the CaO:AC (2:1) mixture, there was a sharp increase in adsorption volume at relatively high pressure (P/Po > 0.9) to around 35 cm³/g STP, while the BET surface area decreased dramatically to 5.06 m²/g, and the pore diameter increased to 22.87 nm.

These changes in isotherm shape and pore size increase indicate that CaO impregnation not only modifies the surface chemistry but also significantly alters the pore structure of activated carbon. This transformation is positive in the context of catalytic applications in biomass gasification processes, as the mesoporous structure can enhance gas diffusion and accessibility to active sites during the tar reforming and water-gas shift reactions. Thus, even though the specific surface area decreases, the increase in mesoporousness and pore connectivity can actually improve catalyst performance in hydrogen gas production [24].

Fig. 4, *b* shows the BJH pore size distribution curves that provide further insight into the textural evolution of the palm-fiber-based activated carbon after CaO

impregnation. The pristine AC exhibits a relatively low dV/dD value and a broad contribution only at large pore diameters (>60 nm), indicating that its pore system is dominated by macropores with a limited amount of mesopores. Such a texture is less favourable for gas-solid reactions because the accessible surface area in the mesopore range (2–50 nm) is relatively small.

After CaO loading, the shape and intensity of the BJH curves change markedly. For CaO:AC-PF = 1:1, the distribution shifts toward smaller pore diameters with a pronounced contribution in the mesopore region of approximately 15–60 nm. This behaviour shows that CaO impregnation partially reconstructs the carbon matrix, enlarging existing micropores and opening blocked pores to generate additional mesoporosity. The effect becomes even more evident at CaO:AC-PF = 2:1, where the curve displays the highest dV/dD values and a distinct maximum centred at about 30–40 nm. The strong peak in this range confirms that a higher CaO loading promotes the development of well-defined mesopores while reducing the relative fraction of very large macropores.

Overall, the BJH analysis demonstrates that CaO acts not only as a reactive sorbent but also as a textural promoter for the palm-fiber AC. The increase in mesopore volume and the shift of the dominant pore size toward 20–40 nm are expected to facilitate the diffusion of gasifying agents and tar molecules, as well as to improve the accessibility of CaO active sites for CO_2 capture and reforming reactions. These features are therefore beneficial for enhancing the catalytic performance of the CaO/AC composite in biomass gasification toward H_2-rich syngas production.

5. 2. Effect of operating parameters on syngas composition and low heating value

5. 2. 1. Effect of Equivalence Ratio on Syngas Product

The composition of syngas from updraft gasification is greatly influenced by the Equivalence Ratio (ER), which is the ratio of the mass flow rate of air compared to the mass flow rate of corncob in the experiment compared to the stoichiometry of air required for complete combustion of corncob. In this study, the ER used was 0.2–0.35 with the following formula

$$ER = \frac{(\dot{m}_a / \dot{m}_{cc})_{\exp}}{(\dot{m}_a / m_{cc})_{stc}},$$

where $\dot{m}_a$ is the air mass flow rate (kg/s), $\dot{m}_{cc}$ is the corncob mass flow rate (kg/s), exp denotes the experimental air-fuel ratio, and stc denotes the stoichiometric air-fuel ratio.

The composition of syngas produced from corncob gasification was evaluated at different equivalence ratios to determine the variation in the main combustible and non-combustible gas components. Changes in the equivalence ratio significantly affected the

concentrations of H_2, CH_4, CO, and CO_2, indicating that the air supply plays an important role in the gasification performance and gas quality. Fig. 5 shows the syngas composition obtained at different equivalence ratios.

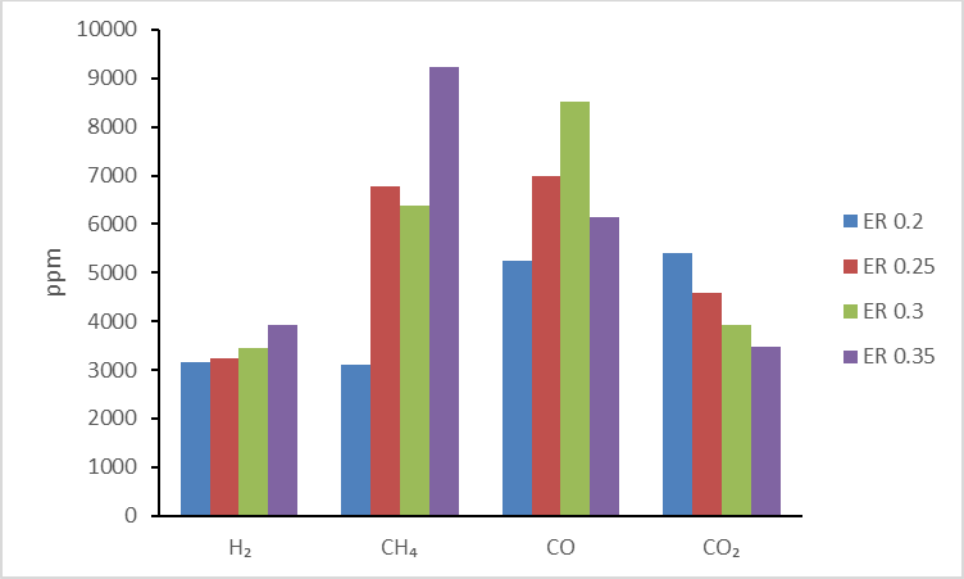


Fig. 5. Syngas composition with different equivalence ratio

The graph above shows that the higher the ER, the higher the hydrogen composition produced. At ER 0.2, the ppm is 3150 ppm, at ER 0.25 it is 3241 ppm, at ER 0.3 it is 3457 ppm, and at ER 0.35 it is 3914 ppm. A higher oxidant supply promotes the formation of more stable autothermal conditions and higher reaction temperatures due to partial oxidation. This increase in temperature accelerates hydrogen-forming reactions, particularly the gasification of active carbon catalyst interactions with steam ($C + H_2O \rightarrow CO + H_2$), the reforming of volatile compounds/light hydrocarbons ($C_xH_y + H_2O \rightarrow CO + H_2$), and the cracking of tar/volatile into lighter gas species. At low ER, some volatiles tend to be incompletely converted and still have the potential to escape as condensable components, while increasing ER increases heat availability, making the conversion of volatiles into gas fractions (including H_2) more effective.

The higher the ER, the higher the CH_4 composition produced. At ER 0.2, 3093 ppm was obtained, at ER 0.25 6767 ppm, ER 0.3 6377 ppm, and ER 0.35 9221 ppm. This trend indicates that the supply of oxidants not only increases autothermal conditions and the rate of devolatilization, but also shifts the reaction pathway towards the formation of light hydrocarbons through hydrogenation and/or methanation reactions in the reactor zone where the temperature still supports CH_4 formation. In particular, increased H_2 at higher ERs can promote the methanation reaction of CO ($CO + 3H_2 \rightleftharpoons CH_4 + H_2O$), so that CH_4 increases along with a tendency for CO to decrease at the highest ER. In addition, more intensive fragmentation of volatiles and tar at high ERs has the potential to produce light gas precursors which are then hydrogenated to CH_4.

CO formation increased up to an ER of 0.3 and decreased at an ER of 0.35. At an ER of 0.2, 5238 ppm was obtained, at an ER of 0.25, 6999 ppm, at an ER of 0.3, 8532 ppm, and decreased at an ER of 0.35 to 6145 ppm. At low ER (0.20–0.25), limited oxygen supply resulted in relatively low heat release, so that the reaction zone temperature and char reactivity were not sufficient to intensify CO formation reactions, especially the Boudouard reaction ($C + CO_2 \rightleftharpoons 2CO$) and char gasification with steam ($C + H_2O \rightleftharpoons CO + H_2$). When the ER is increased towards 0.30, the increase in autothermal heat strengthens these reduction reactions, causing CO formation to increase and reach its peak. However, at higher ERs (0.35), the CO fraction tends to decrease because some CO can be converted to CH_4.

CO_2 formation continues to decrease as ER increases. At ER 0.2, 5412 ppm is obtained; at ER 0.25, 4592 ppm; at ER 0.3, 3916 ppm; and at ER 0.35, 3479 ppm. The increase in oxidant supply at this ER does not promote complete combustion, but rather strengthens the CO_2 reduction mechanism. At higher ERs, the heat generated from partial oxidation increases the temperature of the reduction zone, thereby accelerating the Boudouard reaction ($C + CO_2 \rightleftharpoons 2CO$), in which CO_2 is reduced by char to CO. This mechanism is consistent with the increase in CO until it reaches a maximum at an ER of 0.30, while also explaining the decrease in CO_2 under the same conditions. Interestingly, at an ER of 0.35, CO_2 remains at its lowest level even though CO decreases, indicating that the CO formed is not completely accumulated at the outlet but has the potential to undergo further conversion along the gas flow path.

5. 2. 2. Effect of Catalyst Loading on Syngas Product

The catalyst load or amount of catalyst in this study was 4%, 6%, 8%, and 10% of the total biomass weight. The Fig. 6. shows that the composition of H_2 and CH_4 increases as the catalyst load decreases. The H_2 gas composition at catalyst loads of 4%, 6%, 8%, and 10% is 3742 ppm, 3471 ppm, 3372 ppm, and 3176 ppm, respectively. As the catalyst load increases, the reaction pathways that consume H_2 tend to strengthen, particularly the reverse water–gas shift ($CO_2 + H_2 \rightarrow CO + H_2O$) and H_2 interactions on the catalyst surface during the conversion of gasification compounds. As a result, even though reforming occurs, the measured net H_2 decreases because more H_2 is used for CO formation and surface reactions. The CH_4 gas composition at catalyst loads of 4%, 6%, 8%, and 10% was 7031 ppm, 6476 ppm, 6206 ppm, and 5746 ppm, respectively. An increase in catalyst load increases the number of active sites and gas-catalyst contact, so that methane/light hydrocarbon cracking and reforming occur more intensely. CH_4 then acts as a reactant that is converted into more reactive syngas components, causing the CH_4 concentration to decrease at higher catalyst loads.

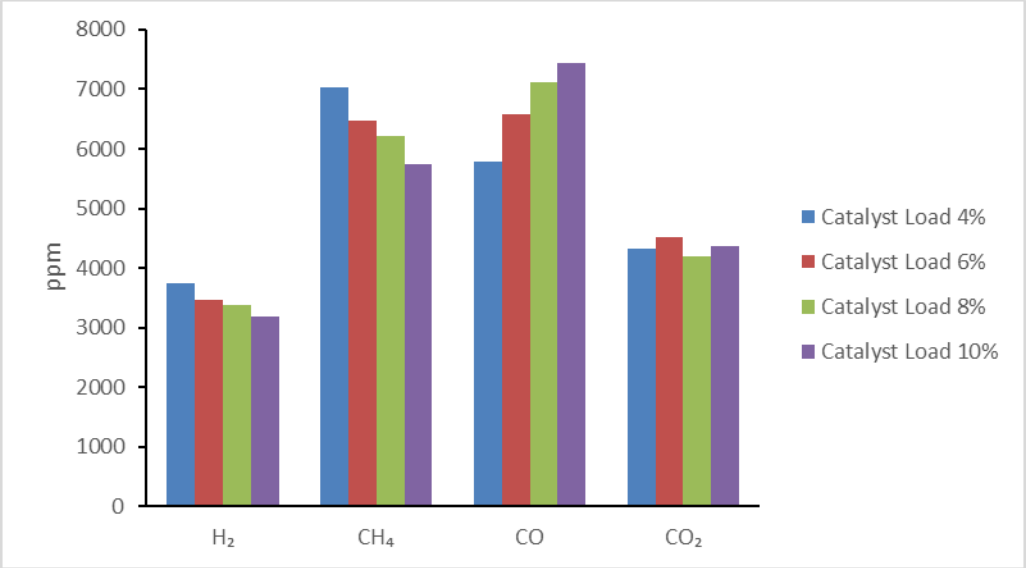


Fig. 6. Syngas Composition with Catalyst Load Variation

The CO gas composition increases with increasing catalyst load, namely for catalyst loads of 4%, 6%, 8% and 10% at 5782 ppm, 6576 ppm, 7111 ppm and 7445 ppm, respectively. The increase in catalyst loading strengthens the CO-forming reactions, particularly dry reforming ($CH_4 + CO_2 \rightarrow 2CO + 2H_2$), char–$CO_2$ reaction ($C + CO_2 \rightarrow 2CO$), and reverse water-gas shift. This combination shifts the product selectivity towards CO, so that the CO fraction increases consistently as the catalyst is increased. The CO_2 gas composition tends to stagnate with increasing catalyst loading, at catalyst loads of 4%, 6%, 8%, and 10% at 4322 ppm, 4510 ppm, 4198 ppm, and 4369 ppm, respectively. CO_2 shows minor changes because it is in a searching for a chemical equilibrium between the partial oxidation and the dry reforming. When the catalyst load increases, the rate of CO_2 consumption may rise, but this is often offset by CO_2 formation in the reaction zone, so that the CO_2 value appears stable or only fluctuates.

5. 2. 3. Effect of Catalyst Ratio on Syngas Product

At a catalyst load of 4%, the CaO/AC ratio changes the gasification reaction through differences in the dominance of tar cracking/reforming and CO_2 capture by CaO, so that the gas composition is highly dependent on the number of active sites and the effectiveness of gas-catalyst contact. At 0:1 (AC), CH_4 and CO are relatively high because AC promotes volatile/tar cracking, but CO_2 remains high because there is no absorption. At 1:0 (CaO), CH_4 decreases but CO_2 is highest, indicating that CO_2 capture is not yet effective due to limited surface area/carbonate layer formation. The 1:1 ratio produces the highest CO with moderate CO_2, indicating CaO–AC synergy that increases the conversion of volatiles into reactive gases. Meanwhile, the 2:1 (CaO-rich) ratio provides the highest H_2 and lowest CO_2 due to the sorption-enhanced effect of CaO, but

CH_4 remains high due to the smaller contribution of AC, so methane reforming/cracking is not yet optimal.

To further examine the catalytic performance, the effect of CaO/AC ratio on syngas composition was investigated under various catalyst loading conditions. This analysis was conducted to determine how the proportion of CaO and activated carbon, combined with different catalyst loads, affected the distribution of H_2, CH_4, CO, and CO_2 during corncob gasification. Fig. 7 illustrates the effect of CaO/AC ratio at catalyst loads of 4% (a), 6% (b), 8% (c), and 10% (d).

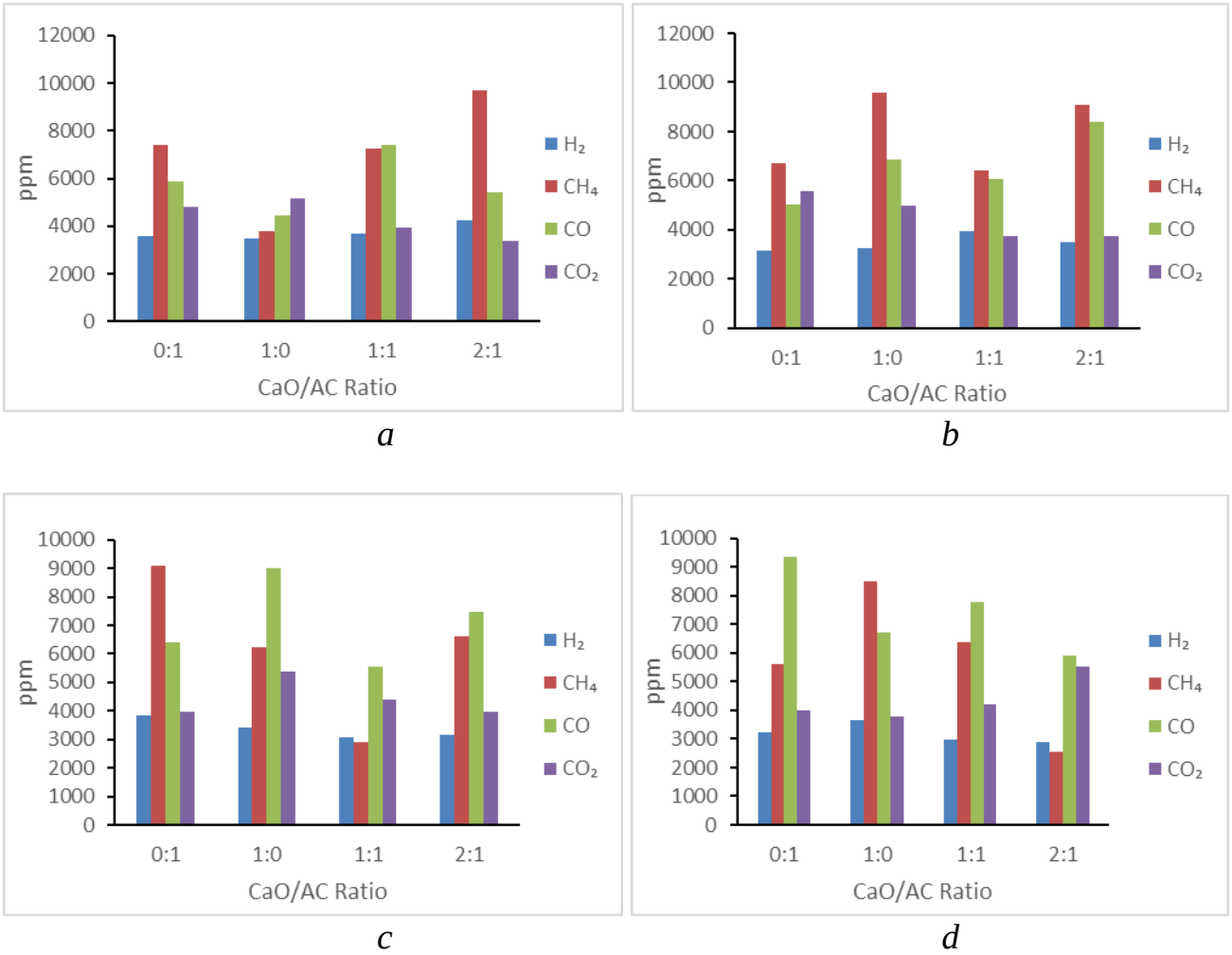


Fig. 7. Effect CaO/AC ratio with various catalyst load: *a* – 4%; *b* – 6%; *c* – 8%; *d* – 10%

At a catalyst load of 4%, the CaO/AC ratio changes the gasification reaction through differences in the dominance of tar cracking/reforming and CO_2 capture by CaO, so that the gas composition is highly dependent on the number of active sites and the effectiveness of gas-catalyst contact. At 0:1 (AC), CH_4 and CO are relatively high because AC promotes volatile/tar cracking, but CO_2 remains high because there is no

absorption. At 1:0 (CaO), CH_4 decreases but CO_2 is highest, indicating that CO_2 capture is not yet effective due to limited surface area/carbonate layer formation. The 1:1 ratio produces the highest CO with moderate CO_2, indicating CaO–AC synergy that increases the conversion of volatiles into reactive gases. Meanwhile, the 2:1 (CaO-rich) ratio provides the highest H_2 and lowest CO_2 due to the sorption-enhanced effect of CaO, but CH_4 remains high due to the smaller contribution of AC, so methane reforming/cracking is not yet optimal.

At a catalyst load of 6%, the CaO/AC ratio mainly shifts the selectivity of secondary reactions (tar cracking/reforming and CO_2 capture), where AC enhances the conversion of volatiles/light hydrocarbons, while CaO reduces CO_2 through carbonation ($CaO + CO_2 \rightarrow CaCO_3$) and changes the reaction equilibrium. At 0:1, CH_4 and CO_2 remain high because there is no CO_2 capture and methane reforming is not yet optimal, so volatiles still escape as CH_4. At 1:0, CO_2 tends to decrease, but CH_4 becomes the highest due to the absence of AC's role in cracking/reforming. The most favorable conditions occur at 1:1, with the highest H_2 and lowest CO_2, indicating CaO–AC synergy that promotes sorption-enhanced reforming and increases the conversion of hydrocarbons into syngas components. At 2:1, CO is highest and CO_2 remains low, but CH_4 rises again and H_2 is not maximized because excess CaO has the potential to rapidly carbonate/cause contact limitations, thereby reducing the contribution of AC in cracking/reforming.

At a catalyst load of 8%, the CaO/AC ratio significantly shifts the selectivity of the syngas reaction. At 0:1 (AC), CH_4 is still high because some light hydrocarbons have not been fully converted even though the tar cracking process is already active. At 1:0 (CaO), CO increases the most, but CO_2 also tends to be high, indicating that CaO in this condition is more dominant in promoting the CO formation pathway, while the CO_2 capture function is not yet optimal due to contact limitations or carbonation saturation. The 1:1 ratio produces the lowest CH_4, indicating the most effective CaO–AC synergy for cracking/reforming light hydrocarbons so that more methane is converted into reactive gas. At 2:1, CO increases again but CH_4 also rises, indicating that a smaller AC fraction reduces the intensity of methane reforming/cracking, while the decrease in CO_2 remains dependent on the effectiveness of CaO sorption.

At a catalyst load of 10%, the increase in total catalyst makes secondary reactions, reforming, solid-gas heterogeneous reactions, and equilibrium shifts very dominant, so that the CaO/AC ratio mainly determines the direction of product selectivity. At 0:1 (AC), CO formation tends to be strongest because the porous carbon surface accelerates the cracking/reforming of volatiles and the conversion of tar into reactive gases. At ratios involving CaO (1:0, 1:1, 2:1), CaO can retain CO_2 through carbonation, but at high loads the effect is often non-linear because CaO rapidly carbonates/diffusion limitations and pore blocking occur, so that under CaO-rich conditions (2:1) CH_4 can decrease, but CO_2 may increase and H_2 is not maximized due to reaction competition. Overall, at a 10% load, a trade-off is observed: AC-dominant increases CO, while CaO-

dominant suppresses light hydrocarbons but has the potential to trigger non-ideal conditions (saturation/mass transport) that reduce the benefits of H_2 and CO_2.

5. 2. 4. Syngas Low Heating Value

To calculate the LHV of syngas, it must first be converted from ppm to % volume of gas. The formula is $\%vol_i = \frac{ppmv_i}{10^4}$ to calculate the LHV, use the formula

$$LHV_{mix}\left(\frac{MJ}{Nm^3}\right) = \frac{10.8(\%H_2) + 12.63(\%CO) + 35.8(\%CH_4)}{100},$$

LHV H_2 = 10.8 MJ/Nm^3,

LHV CO = 12.63 MJ/Nm^3,

LHV CH_4 = 35.8 MJ/Nm^3.

As shown in Fig. 8, the syngas low heating value (LHV) varies with the equivalence ratio (ER) and catalyst load.

All experimental points in the figure are connected by straight lines. This is an incorrect presentation of the results because it means that there are no experimental errors. When displaying the results of experiments in the figures in the form of experimental points, it is necessary to carry out an approximation and indicate the approximating equations and the degree of accuracy of the approximation R^2 (*for example, you can use the "trend" tool in EXCEL*)

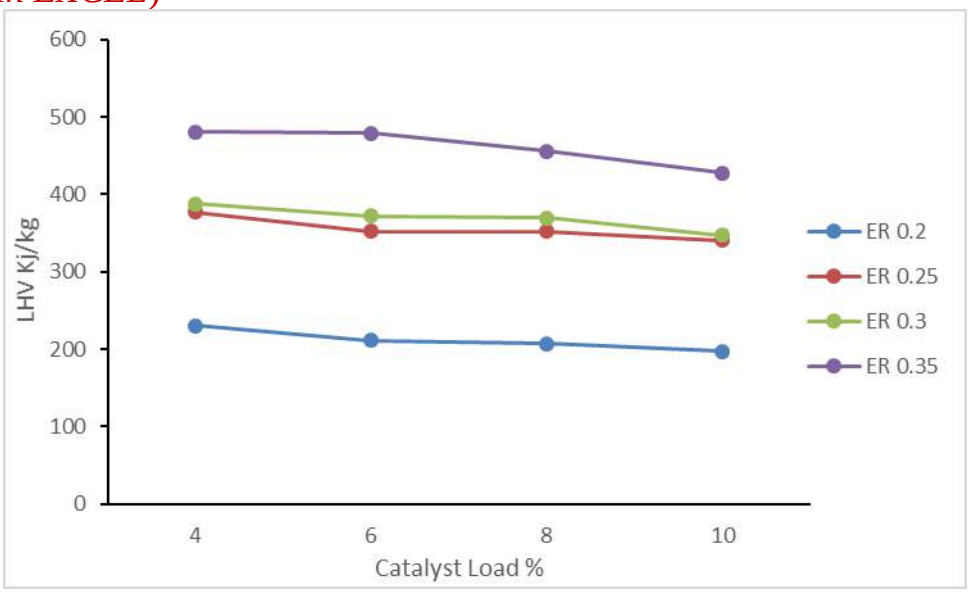


Fig. 8. Syngas low heating value with various equivalence ratio

Fig. 8 shows that the LHV value increases with the ER. At the same catalyst load of 4%, the LHV will increase in line with the increase in ER. ER 0.2 has an LHV of 230 kJ/kg and ER 0.35 has an LHV of 481 kJ/kg. Higher ER produces more intense autothermal conditions, causing the reactor temperature to rise. This increase in temperature accelerates the decomposition of volatiles and tar cracking, and promotes more complete gasification and reforming reactions, thereby increasing the fraction of permanent gases that contribute to the calorific value, mainly CO and CH_4, as well as some H_2. In addition, the increase in temperature is also associated with more effective hydrogen formation, because H_2 formation reactions (e.g., through steam-water and reforming reactions) are generally more optimal at high temperatures, with the temperature range often reported to be most conducive to H_2 formation being 800–1000°C.

At ER 0.2, the highest LHV was obtained at a catalyst load of 4% at 230 kJ/kg and continued to decrease with increasing catalyst load to 197 kJ/kg at 10%. At ER 0.25, the highest LHV was also obtained at a catalyst load of 4% at 377 kJ/kg and also decreased to 341 kJ/kg at a catalyst load of 10%. At ER 0.3, the highest LHV was obtained at a catalyst load of 4% at 388 kJ/kg and also decreased at a catalyst load of 10% to 347 kJ/kg. At ER 0.35, the highest LHV was obtained at 481 kJ/kg and decreased at a catalyst load of 10% to 428 kJ/kg.

However, all ER values show that LHV tends to decrease when the catalyst load is increased from 4% to 10%. This decrease indicates that excessive catalyst addition under these operating conditions does not always improve gas energy quality, because the catalyst can shift the reaction selectivity towards the conversion of high calorific components especially CH_4 into CO and H_2 through reforming, while at the same time the fraction of diluent gases such as CO_2 (and steam) may increase due to reaction. Since CH_4 has a very large calorific value contribution in the syngas mixture, the decrease in its fraction is often more dominant than the increase in CO/H_2, so that the total LHV tends to decrease.

In energy system analysis, particularly in combustion, gasification, and fuel gas utilisation processes such as syngas, the LHV value is often used because it better represents the heat energy that can actually be utilised by the system. The LHV value of a fuel gas is usually influenced by the composition of combustible gases such as carbon monoxide (CO), hydrogen (H_2), and methane (CH_4). The higher the content of these gases, the greater the LHV value produced. The LHV of syngas from this study with variations in ER and CaO/AC-PF ratio can be seen in Fig. 9.

Same remark

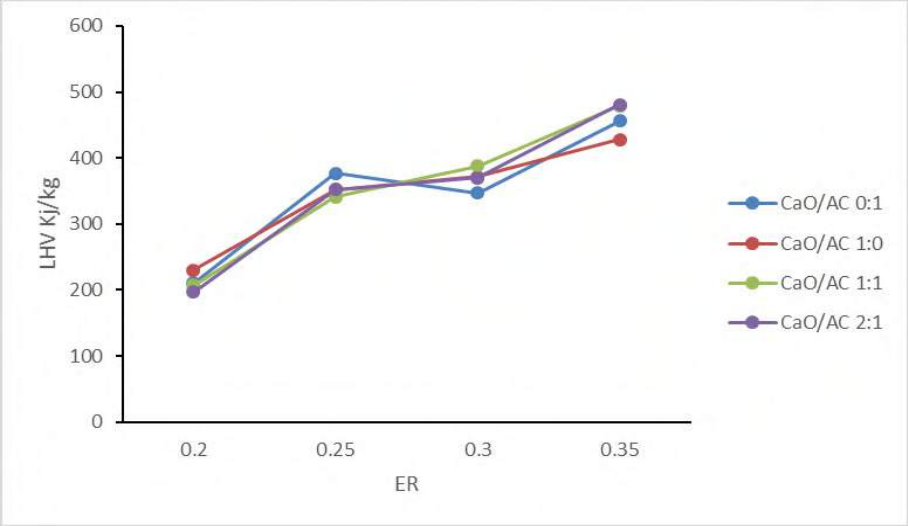


Fig. 9. Syngas Low Heating Value with Various CaO/AC Ratio

Fig. 9 shows that the LHV of syngas increases consistently with the increase in ER 0.2 to 0.35 for all CaO/AC ratios, indicating that a higher ER strengthens autothermal conditions so that the reaction temperature increases and the conversion of volatiles into syngas becomes more complete. At low ER (0.2), the difference in LHV between ratios is still small because secondary reactions such as cracking, reforming and heterogeneous reactions are not yet dominant; the system is still relatively influenced by incompletely converted volatiles. When the ER is increased to 0.25–0.30, the effect of the catalyst ratio becomes apparent: compositions involving AC tend to produce higher LHV because they accelerate tar cracking and increase the fraction of calorific gas, while the contribution of CaO can shift the reaction equilibrium through a decrease in CO_2. At the highest ER (0.35), the LHV reaches its maximum at all ratios, with CaO/AC 2:1 and 0:1 showing peak values, indicating that at high temperatures, the reactive gas formation pathway (via cracking/reforming on the carbon surface and/or CaO-rich-promoted heterogeneous reactions) becomes dominant. Overall, ER acts as the main controlling factor for LHV increase through the temperature effect, while the CaO/AC ratio modulates LHV through the balance between cracking/reforming (AC) and CO_2 control (CaO), especially at medium-high ER.

6. Discussion on the Catalytic Effect of AC-PF/CaO and Operating Conditions on Syngas Composition and LHV

The interaction of the CaO-AC-PF catalyst to improve syngas quality can be seen from the characterisation of the catalyst, the composition of the syngas and the LHV produced. From the Scanning Electron Microscopy results in Fig. 2, it can be seen that the CaO:AC-PF;2:1 catalyst (Fig. 2, *c*) appears denser than the other catalysts. With the addition of CaO, CaO particle dispersion can be seen on the white carbon surface, indicating that some micro pores are closed by CaO. With the addition of CaO, a lot of

CO_2 is absorbed and becomes $CaCO_3$. This porous structure is very important in top-flow gasification because pyrolysis gas and volatiles move through the layer, so the presence of a porous medium has the potential to strengthen secondary reactions and act as carbon capture before the gas exits to the condenser.

The interaction of the CaO-AC-PF catalyst in improving syngas quality can be observed from the catalyst characterization, syngas composition, and the resulting LHV. Based on the SEM results shown in Fig. 2, the CaO:AC-PF = 2:1 catalyst (Fig. 2, *c*) appears denser than the other catalyst formulations, indicating that CaO particles were dispersed on the carbon surface and may have partially blocked some of the smaller pores. This interpretation is reasonable because CaO-based materials are widely known to act as high-temperature CO_2 sorbents, and their carbonation proceeds through the formation of $CaCO_3$. During gasification, such sorption behaviour can reduce CO_2 concentration and influence gas quality. In addition, porous carbonaceous media are known to promote tar cracking and secondary gas-phase reactions when volatile products pass through a hot solid bed. This is particularly relevant in fixed-bed gasification, where reactor design and the interaction between volatiles, char, and catalyst strongly affect tar conversion and gasification efficiency. Therefore, the porous structure of AC-PF, together with the CO_2-capturing role of CaO, may contribute to syngas upgrading before the gas exits the reactor system.

From a surface chemistry perspective, Fourier Transform Infrared Spectroscopy (FTIR) shows the presence of –OH and calcium carbonate groups, as shown in Fig. 3. This is due to the results of KOH impregnation carried out during the manufacture of AC-PF. The presence of -OH groups functions as polar active sites capable of adsorbing polar molecules such as H_2O, CO_2, and volatile compounds. Surfaces with -OH groups tend to be hydrophilic and reactive, thereby enhancing interactions with tar compounds or heavy hydrocarbons. These tar compounds can then undergo thermal cracking or catalytic reforming into light gases such as H_2, CO, and CH_4. In addition to -OH, there are also O-H and C-O groups. The O-H group has characteristics that are almost the same as the -OH group, while the C-O group plays a role in enhancing the redox properties and chemical interactions between the carbon surface and gas molecules. In the gasification process, the C-O group can be part of the partial oxidation mechanism and carbon gasification reaction, which produces CO [25].

From a surface chemistry perspective, the Fourier Transform Infrared Spectroscopy (FTIR) results indicate the presence of O–H, C–O, and carbonate-related groups, as shown in Fig. 3. The appearance of oxygen-containing functional groups is consistent with the use of KOH during the preparation of AC-PF, since KOH activation is known to modify the surface chemistry of activated carbon and promote the formation of oxygenated groups. O–H-containing groups can act as polar active sites that enhance the interaction of the carbon surface with polar molecules such as H_2O, CO_2, and oxygenated volatile compounds. Such surface functionality may also facilitate the adsorption of tar-related species and support their further conversion through thermal cracking or reforming into lighter gases. In addition to O–H groups, the presence of C–O

groups suggests that the carbon surface retains oxygen-containing functionalities that may contribute to surface reactivity and gas–solid interactions. During gasification, these surface groups may participate indirectly in oxidation–reduction interactions at the carbon surface and support the formation of combustible gases such as CO. The carbonate-related bands may also indicate the presence of calcium-containing carbonate species, which is consistent with the CO_2-capturing function of CaO during the gasification process.

The BET data in Fig. 4 shows that the surface area decreased to 5.06 m^2/g, but the pore diameter increased to a mesopore scale of 22.87 nm, which can improve the accessibility of volatiles to active sites and improve mass transport in the reforming reaction. In Fig. 4, *b*, the BJH curve at CaO:AC-PF = 2:1 shows the highest dV/dD values of 30–40 nm, indicating a catalyst in the mesopore size range. The presence of these mesopores will further increase the active sites for CO_2 adsorption.

The BET results presented in Fig. 4 show that the specific surface area decreased to 5.06 m^2/g, while the average pore diameter increased to 22.87 nm, corresponding to the mesopore range. This change suggests that, although the surface area became lower, the larger pore structure may improve the accessibility of volatile compounds to active sites and enhance mass transport during reforming reactions. In Fig. 4, *b*, the BJH pore size distribution of the CaO:AC-PF = 2:1 catalyst shows the highest dV/dD values in the pore diameter range of 30–40 nm, confirming the dominance of mesopores in this catalyst. The presence of these mesopores may facilitate gas diffusion and improve contact between gaseous species and the catalyst surface, which can contribute to CO_2 adsorption and syngas upgrading during gasification.

From a process perspective, in Fig. 5, ER appears as the dominant variable that regulates autothermal conditions, primarily through an increase in effective temperature and secondary reaction intensity. An increase in ER from low to high levels consistently increases H_2, which can be explained by the acceleration of H_2 formation reactions such as charcoal gasification with steam ($C + H_2O \rightarrow CO + H_2$) [26], light hydrocarbon reforming, and more intense tar cracking at high temperatures. At the same time, CH_4 also increases sharply at high ER, indicating that in an autothermal upflow system, increased temperature and changes in gas composition can facilitate the formation of light gases. Meanwhile, CO tends to peak at moderate ER and then decreases at high ER, consistent with competition between CO formation and CO consumption through subsequent reactions such as methanation [27]. The decrease in CO_2 at high ER indicates the role of high temperatures in enhancing the reduction of CO_2 by charcoal (Boudouard reaction) and/or the role of CaO adsorption if available.

The effect of catalyst loading in Fig. 6 shows that adding catalyst does not always increase H_2. Increasing the catalyst loading from low to high tends to reduce H_2 and CH_4 but increase CO. Mechanistically, this condition can occur when the catalyst strengthens pathways that increase CO and/or promotes RWGS ($CO_2 + H_2 \rightarrow CO + H_2O$) [28], which consumes H_2 so that net H_2 is reduced. Furthermore, at high catalyst loadings, the possibility of diffusion/aggregation penalties increases, so that selectivity may shift and

some active sites become less effective. Therefore, the target of H_2-rich synthesis gas in this reactor is more dependent on ER adjustment and the selection of moderate/low catalyst loadings, rather than simply increasing the loading.

The CaO/AC-PF ratio in Fig. 7 shows synergistic but non-linear behaviour. AC-PF plays a major role as a porous medium that enhances the cracking/reforming process of volatile compounds, while CaO provides a basic site and CO_2 absorber to shift the equilibrium. At high CaO ratios, sorption and base effects may increase, but the risk of micro-pore closure and diffusion pathway changes also increases. This explains why certain compositions are optimal at certain catalyst loads: the best performance arises from a balance between pore accessibility (the role of AC-PF) and sorption/base strength (the role of CaO).

From an energy quality perspective, in Fig. 8, 9, the LHV value of synthetic gas is highly sensitive to changes in CH_4. Therefore, high ER conditions that increase CH_4 tend to increase LHV. H_2, CH_4 and CO are the main factors for obtaining high LHV. CO_2 has no calorific value so it must be captured. In this study, CaO was used so that CO_2 could be suppressed, meaning that the total LHV could be increased. The highest LHV in this study was 481 kJ/kg, while in another study, the highest was 550 kJ/kg using pinewood with dolomite, activated carbon, silica gel, and limestone catalysts [29]. The higher the ER, the more oxygen enters the system, thereby increasing the reforming reaction [30].

In comparison with the literature reviewed in this research, the present study demonstrates a comparable qualitative trend, particularly in showing that catalyst-assisted updraft gasification can improve syngas composition and energy quality. For example, previous studies reported that dolomite-assisted rice husk gasification increased H_2 content up to 15.4 mol% with an LHV of 5.1 MJ/Nm³, while other updraft gasification systems with catalytic enhancement also showed improved hydrogen-rich syngas production and higher heating values. In the present study, the highest syngas LHV reached 481 kJ/kg under the investigated conditions, indicating that the CaO/AC-PF catalyst system was effective in improving gas quality, although the absolute value remains influenced by the use of corncob feedstock, the small-scale reactor design, and the sensor-based gas measurement approach. Therefore, the present results support the view that the combined CaO/AC-PF catalyst is a promising low-cost alternative for syngas upgrading, particularly for agricultural biomass gasification in simple updraft systems.

In practical terms, the present study is relevant to the development of low-cost biomass gasification systems that can utilize locally available agricultural residues and catalyst materials. Corncob is an abundant agricultural by-product, while CaO and palm-fiber-derived activated carbon can be prepared from relatively inexpensive and accessible resources. Therefore, the proposed catalyst system has practical potential for application in small-scale updraft gasifiers, particularly in agricultural areas where simple and affordable waste-to-energy technologies are needed. The syngas produced from such systems may be used directly as a combustible gas for thermal applications,

such as drying, heating, or small-scale energy generation, and also has potential as an intermediate gas for further upgrading or conversion into other value-added energy and chemical products.

There are several limitations to this study. First, the gas composition was obtained from an MQ sensor based on ppm, so absolute accuracy may be affected by cross-sensitivity, humidity, sensor drift, and gas sampling temperature; this may affect the estimation of %vol and LHV, especially when changes in CO and CH_4 occur simultaneously. Second, catalyst characterisation (SEM-FTIR-BET) supports the role of surface texture and chemistry, but has not quantified changes in the active phase during operation, the degree of carbonation, and the decrease in activity due to pore closure accumulation.

The disadvantage of this research is that the CaO catalyst reacts very easily with CO_2. After the calcination process, CaO must be stored in an airtight container to prevent it from clumping into $CaCO_3$. The catalyst has a specific usage period because it is covered with tar or ash.

Based on these limitations, several future directions are recommended. Calibrate the gas composition using GC-TCD/GC-FID to convert the sensor readings into more accurate %vol and include LHV uncertainty analysis. Evaluate catalyst stability and regeneration, especially for CaO which is easily carbonated, through carbonation-calcination cycle tests and post-reaction characterisation (XRD/TGA/SEM-EDX) to assess phase changes and activity loss. Develop experimental designs towards ANOVA or RSM interactions so that interaction effects and predictive models can be obtained and verified through replication confirmation tests. Add process performance metrics such as gas yield (Nm^3/kg), cold gas efficiency, pressure drop, and air consumption so that 'syngas quality improvement' can be demonstrated based on mass-energy balance and operability, not just composition.

7. Conclusion

1. The present study demonstrated that the CaO/AC-PF catalyst system has potential to improve syngas quality in corncob updraft gasification. Catalyst characterization by SEM, FTIR, and BET showed that the combined catalyst possessed modified surface morphology, oxygen-containing functional groups, carbonate-related species, and mesoporous characteristics, with the CaO:AC-PF = 2:1 catalyst showing a specific surface area of 5.06 m^2/g and an average pore diameter of 22.87 nm. These characteristics indicate that the catalyst structure was altered in a way that may support gas–solid interaction during gasification.

2. The gasification experiments confirmed that equivalence ratio, catalyst loading, and CaO/AC ratio influenced syngas composition and heating value. Increasing ER from 0.20 to 0.35 increased H_2 concentration from 3150 to 3914 ppm and CH_4 concentration from 3093 to 9221 ppm, while the syngas LHV increased from 230 to 481 kJ/Nm^3. In terms of catalyst loading, increasing the loading from 4 wt.% to 10 wt.% decreased H_2 from 3742 to 3176 ppm and CH_4 from 7031 to 5746 ppm, while CO increased from

5782 to 7445 ppm. These results indicate that syngas quality was affected by the balance between catalytic activity, pore accessibility, and CO_2 sorption behaviour.

Conflict of interest

The authors declare that they have no conflict of interest in relation to this research, whether financial, personal, authorship or otherwise, that could affect the research and its results presented in this paper.

Financing

The authors sincerely thank the Ministry of Education, Culture, Research and Technology, Republic of Indonesia for fully supporting this research through the DRTPM Research Grant under Fundamental Research, Universitas Widyagama Malang, Indonesia 2025 (Grant Number:128/C3/DT.05.00/PL/2025;023/LL7/DT.05.00/PL/2025;010/ Kontrak/PT/PTS.030.7/PN/V/2025).

Data availability

Manuscript has no associated data.

Use of artificial intelligence

The authors used the AI-based language model ChatGPT (GPT-5.3) only to assist in improving the clarity of English language and grammar in several sections of the manuscript, particularly in the Introduction and Literature Review sections.

The AI tool was used solely for language editing and paraphrasing purposes. All scientific content, experimental design, data analysis, and interpretation of the results were conducted entirely by the authors.

The authors carefully reviewed and verified all AI-assisted text to ensure accuracy and consistency with the experimental results. The use of AI tools did not influence the scientific conclusions of this study.

Acknowledgements

We as the Research Team would like to thank Ministry of Education, Culture, Research and Technology, Republic of Indonesia (Kemendiktisaintek Indonesia) for financing research activities.

Authors' contributions

Purbo Suwandono: Conceptualization, Writing-original draft, Investigation, Supervision, Formal analysis, Writing – review & editing; **Widya Wijayanti**: Validation, Investigation, Data Curation, Formal analysis, Writing – original draft; **Nova Risdiyanto Ismail**: Writing – review & editing, Formal analysis; **Dzulfikar Johan Akbar:** Visualization, Writing – original draft, Data curation; **Muhammad Reza**: Project administration, Resources, Data curation.

References

1. V. K. Yadav *et al.*, “Emerging trends in the valorization of agricultural waste and their utilization in agricultural, pharmaceuticals, and environmental cleanup,” *Waste and Biomass Valorization*, pp. 1–55, 2025. DOI:10.1007/s12649-025-03002-y
2. W. M. Lewandowski, M. Ryms, and W. Kosakowski, “Thermal biomass conversion: A review,” *Processes*, vol. 8, no. 5, p. 516, 2020. https://doi.org/10.3390/pr8050516
3. D. Ariyanti *et al.*, “Valorization of corn cob waste for furfural production: A circular economy approach,” *Biomass and Bioenergy*, vol. 194, p. 107665, 2025. DOI:10.1016/j.biombioe.2025.107665
4. J. Zhang, Z. Chu, R. Cao, X. Wu, and K. Han, “A review of resource recovery from waste plastics via pyrolysis and gasification,” *Fuel*, vol. 404, p. 136319, 2026. https://doi.org/10.1016/j.fuel.2025.136319
5. Y. Tangke Tosuli, Cahyadi, H. Dafiqurrohman, R. Hermawan, and A. Surjosatyo, “Gasification of sago dreg waste in a top-lit updraft fixed bed gasifier: Syngas composition and its effect with additional Al2O3 as catalyst,” *Energy Convers. Manag. X*, vol. 24, no. October, p. 100775, 2024, doi: 10.1016/j.ecmx.2024.100775. https://doi.org/10.1016/j.ecmx.2024.100775
6. P. Dinh *et al.*, “Enrichment of hydrogen in product gas from a pilot-scale rice husk updraft gasification system,” *Carbon Resour. Convers.*, vol. 5, no. 3, pp. 231–239, 2025, doi: 10.1016/j.crcon.2022.07.003.
7. S. Yousef and J. Eimontas, “International Journal of Hydrogen Energy Oxygen updraft gasification-catalytic reforming of cigarettes butts for hydrogen-rich syngas production,” vol. 171, no. May, 2025, https://doi.org/10.1016/j.ijhydene.2025.150650
8. D. Contreras, E. Blanco, and D. Travieso, “Experimental assessment of the energy potential of pellets produced from beekeeping wastes by updraft gasification,” vol. 343, no. January, 2025, https://doi.org/10.1016/j.enconman.2025.120206
9. N. Yesilova, O. Tezer, A. Ongen, and A. Ayol, “International Journal of Hydrogen Energy Enhancing biomass gasification : A comparative study of catalyst applications in updraft and modifiable-downdraft fixed bed reactors,” *Int. J. Hydrogen Energy*, vol. 76, no. April, pp. 290–303, 2024, https://doi.org/10.1016/j.ijhydene.2024.05.075
10. R. Skvor and A. Jan, “Experimental investigation of sorted municipal solid wastes producer gas composition in an updraft fixed bed gasifier,” vol. 289, no. August 2022, 2024, https://doi.org/10.1016/j.energy.2023.130063
11. R. Junga, M. Tańczuk, S. Sobek, M. Chabiński, and Ł. Ziółkowski, “Effect of the addition of laying hens manure to the straw on gasification efficiency in updraft gasifier under air atmosphere,” *Appl. Therm. Eng.*, vol. 226, no. February, p. 120269, 2023, https://doi.org/10.1016/j.applthermaleng.2023.120269.
12. A. Ongen and A. Ayol, “ScienceDirect Gasification performance of olive

pomace in updraft and downdraft fixed bed reactors," vol. I, 2023, https://doi.org/10.1016/j.ijhydene.2023.02.088

13. K. Ertas, "Gasification of MDF residue in an updraft fixed bed gasifier to produce heat and power via an ORC turbine," vol. 169, no. February, pp. 43–51, 2023, https://doi.org/10.1016/j.wasman.2023.06.025

14. S. Gorthy, S. Verma, N. Sinha, S. Shetty, H. Nguyen, and M. Neurock, "Theoretical Insights into the Effects of KOH Concentration and the Role of OH–in the Electrocatalytic Reduction of CO2 on Au," *ACS Catal.*, vol. 13, no. 19, pp. 12924–12940, 2023. DOI:10.1021/acscatal.2c06115

15. X. Wang, W. Zeng, C. Xin, X. Kong, X. Hu, and Q. Guo, "The development of activated carbon from corncob for CO2 capture," *RSC Adv.*, vol. 12, no. 51, pp. 33069–33078, 2022, https://doi.org/10.1039/D2RA05979G

16. B. Zhou *et al.*, "Insights into effects of grain boundary engineering in composite metal oxide catalysts for improving catalytic performance," *J. Colloid Interface Sci.*, vol. 653, pp. 1177–1187, 2024. https://doi.org/10.1016/j.jcis.2023.09.148

17. Y. Zhu *et al.*, "Preparation of hierarchically porous carbon ash composite material from fine slag of coal gasification and ash slag of biomass combustion for CO2 capture," *Sep. Purif. Technol.*, vol. 330, p. 125452, 2024. https://doi.org/10.1016/j.seppur.2023.125452

18. M. Ilić *et al.*, "Surface functional groups and degree of carbonization of *selected* chars from different processes and feedstock," *PLoS One*, vol. 17, no. 11, p. e0277365, 2022. https://doi.org/10.1371/journal.pone.0277365

19. R. Ali, Z. Aslam, R. A. Shawabkeh, A. Asghar, and I. A. Hussein, "BET, FTIR, and RAMAN characterizations of activated carbon from waste oil fly ash," *Turkish J. Chem.*, vol. 44, no. 2, pp. 279–295, 2020. doi: 10.3906/kim-1909-20

20. K. J. Stanienda-Pilecki, "The importance of Fourier-Transform Infrared Spectroscopy in the identification of carbonate phases differentiated in magnesium content," 2019.

21. F. Dai, Q. Zhuang, G. Huang, H. Deng, and X. Zhang, "Infrared spectrum characteristics and quantification of OH groups in coal," *ACS omega*, vol. 8, no. 19, pp. 17064–17076, 2023. https://doi.org/10.1021/acsomega.3c01336

22. E. M. de Salazar Martínez, M. F. Alexandre-Franco, A. J. Nieto-Sanchez, and E. M. Cuerda-Correa, "Exploring the role of surface and porosity in CO2 capture by CaO-based adsorbents through response surface methodology (RSM) and artificial neural networks (ANN)," *J. CO2 Util.*, vol. 83, p. 102773, 2024. https://doi.org/10.1016/j.jcou.2024.102773

23. J. A. Tavizón-Pozos, H. Cervantes-Cuevas, G. G. Garcia-Camacho, G. Chavez-Esquivel, and D. R. Acosta-Najarro, "Biodiesel Production Using K–Sr/CaO and CaO Catalysts Derived from Eggshells by Canola Oil Transesterification," *ACS omega*, vol. 10, no. 7, pp. 6827–6838, 2025. https://doi.org/10.1021/acsomega.4c09118

24. W. Koo-Amornpattana, P. Phadungbut, N. Kunthakudee, W. Jonglertjunya, S. Ratchahat, and M. Hunsom, "Innovative metal oxides (CaO, SrO, MgO) impregnated

waste-derived activated carbon for biohydrogen purification," *Sci. Rep.*, vol. 13, no. 1, p. 4705, 2023. DOI:10.1038/s41598-023-31723-4

25. C. Quan, M. Wang, N. Gao, T. Yang, and R. Li, "In situ adsorption of CO2 to enhance biomass gasification for hydrogen production using Ca/Ni based composites," *J. Energy Inst.*, vol. 108, p. 101229, 2023, doi: https://doi.org/10.1016/j.joei.2023.101229. https://doi.org/10.1016/j.joei.2023.101229

26. F. Micheli, E. Mattucci, C. Courson, and K. Gallucci, "Bi-Functional Catalyst/Sorbent for a H2-Rich Gas from Biomass Gasification," 2021. doi: 10.3390/pr9071249. DOI:10.3390/PR9071249

27. M. Zhu, Q. Wang, and S. Wang, "Recent Advances and Future Perspectives in Catalyst Development for Efficient and Sustainable Biomass Gasification: A Comprehensive Review," 2025, https://doi.org/10.3390/su17167370

28. N. Cerone, F. Zimbardi, L. Contuzzi, J. Baleta, and D. Cerinski, "Experimental investigation of syngas composition variation along updraft fixed bed gasifier," *Energy Convers. Manag.*, vol. 221, no. July, p. 113116, 2020, https://doi.org/10.1016/j.enconman.2020.113116

29. R. Mohanty, P. Mahanta, A. Mahapatro, and R. Prakash, "Catalytic gasification of pinewood biomass in a fluidized bed reactor with dolomite , limestone , and activated carbon : An experimental study," *Energy*, vol. 325, no. April, p. 136131, 2025, doi: 10.1016/j.energy.2025.136131. https://doi.org/10.1016/j.energy.2025.136131

30. C. Liu, Y. Huang, M. Niu, and H. Pei, "ScienceDirect Influences of equivalence ratio , oxygen concentration and fluidization velocity on the characteristics of oxygen-enriched gasification products from biomass in a pilot-scale fluidized bed," *Int. J. Hydrogen Energy*, vol. 43, no. 31, pp. 14214–14225, 2018, https://doi.org/10.1016/j.ijhydene.2018.05.154

References

1. V. K. Yadav *et al.*, "Emerging trends in the valorization of agricultural waste and their utilization in agricultural, pharmaceuticals, and environmental cleanup," *Waste and Biomass Valorization*, pp. 1–55, 2025. DOI:10.1007/s12649-025-03002-y

2. W. M. Lewandowski, M. Ryms, and W. Kosakowski, "Thermal biomass conversion: A review," *Processes*, vol. 8, no. 5, p. 516, 2020. https://doi.org/10.3390/pr8050516

3. D. Ariyanti *et al.*, "Valorization of corn cob waste for furfural production: A circular economy approach," *Biomass and Bioenergy*, vol. 194, p. 107665, 2025. DOI:10.1016/j.biombioe.2025.107665

4. J. Zhang, Z. Chu, R. Cao, X. Wu, and K. Han, "A review of resource recovery from waste plastics via pyrolysis and gasification," *Fuel*, vol. 404, p. 136319, 2026. https://doi.org/10.1016/j.fuel.2025.136319

5. Y. Tangke Tosuli, Cahyadi, H. Dafiqurrohman, R. Hermawan, and A. Surjosatyo, "Gasification of sago dreg waste in a top-lit updraft fixed bed gasifier: Syngas composition and its effect with additional Al2O3 as catalyst," *Energy Convers.*

Manag. X, vol. 24, no. October, p. 100775, 2024, doi: 10.1016/j.ecmx.2024.100775. https://doi.org/10.1016/j.ecmx.2024.100775

6. P. Dinh *et al.*, "Enrichment of hydrogen in product gas from a pilot-scale rice husk updraft gasification system," *Carbon Resour. Convers.*, vol. 5, no. 3, pp. 231–239, 2025, doi: 10.1016/j.crcon.2022.07.003.

7. S. Yousef and J. Eimontas, "International Journal of Hydrogen Energy Oxygen updraft gasification-catalytic reforming of cigarettes butts for hydrogen-rich syngas production," vol. 171, no. May, 2025, https://doi.org/10.1016/j.ijhydene.2025.150650

8. D. Contreras, E. Blanco, and D. Travieso, "Experimental assessment of the energy potential of pellets produced from beekeeping wastes by updraft gasification," vol. 343, no. January, 2025, https://doi.org/10.1016/j.enconman.2025.120206

9. N. Yesilova, O. Tezer, A. Ongen, and A. Ayol, "International Journal of Hydrogen Energy Enhancing biomass gasification : A comparative study of catalyst applications in updraft and modifiable-downdraft fixed bed reactors," *Int. J. Hydrogen Energy*, vol. 76, no. April, pp. 290–303, 2024, https://doi.org/10.1016/j.ijhydene.2024.05.075

10. R. Skvor and A. Jan, "Experimental investigation of sorted municipal solid wastes producer gas composition in an updraft fixed bed gasifier," vol. 289, no. August 2022, 2024, https://doi.org/10.1016/j.energy.2023.130063

11. R. Junga, M. Tańczuk, S. Sobek, M. Chabiński, and Ł. Ziółkowski, "Effect of the addition of laying hens manure to the straw on gasification efficiency in updraft gasifier under air atmosphere," *Appl. Therm. Eng.*, vol. 226, no. February, p. 120269, 2023, https://doi.org/10.1016/j.applthermaleng.2023.120269.

12. A. Ongen and A. Ayol, "ScienceDirect Gasification performance of olive pomace in updraft and downdraft fixed bed reactors," vol. I, 2023, https://doi.org/10.1016/j.ijhydene.2023.02.088

13. K. Ertas, "Gasification of MDF residue in an updraft fixed bed gasifier to produce heat and power via an ORC turbine," vol. 169, no. February, pp. 43–51, 2023, https://doi.org/10.1016/j.wasman.2023.06.025

14. S. Gorthy, S. Verma, N. Sinha, S. Shetty, H. Nguyen, and M. Neurock, "Theoretical Insights into the Effects of KOH Concentration and the Role of OH–in the Electrocatalytic Reduction of CO2 on Au," *ACS Catal.*, vol. 13, no. 19, pp. 12924–12940, 2023. DOI:10.1021/acscatal.2c06115

15. X. Wang, W. Zeng, C. Xin, X. Kong, X. Hu, and Q. Guo, "The development of activated carbon from corncob for CO2 capture," *RSC Adv.*, vol. 12, no. 51, pp. 33069–33078, 2022, https://doi.org/10.1039/D2RA05979G

16. B. Zhou *et al.*, "Insights into effects of grain boundary engineering in composite metal oxide catalysts for improving catalytic performance," *J. Colloid Interface Sci.*, vol. 653, pp. 1177–1187, 2024. https://doi.org/10.1016/j.jcis.2023.09.148

17. Y. Zhu *et al.*, "Preparation of hierarchically porous carbon ash composite material from fine slag of coal gasification and ash slag of biomass combustion for CO2

capture," *Sep. Purif. Technol.*, vol. 330, p. 125452, 2024. https://doi.org/10.1016/j.seppur.2023.125452

18. M. Ilić *et al.*, "Surface functional groups and degree of carbonization of *selected* chars from different processes and feedstock," *PLoS One*, vol. 17, no. 11, p. e0277365, 2022. https://doi.org/10.1371/journal.pone.0277365

19. R. Ali, Z. Aslam, R. A. Shawabkeh, A. Asghar, and I. A. Hussein, "BET, FTIR, and RAMAN characterizations of activated carbon from waste oil fly ash," *Turkish J. Chem.*, vol. 44, no. 2, pp. 279–295, 2020. doi: 10.3906/kim-1909-20

20. K. J. Stanienda-Pilecki, "The importance of Fourier-Transform Infrared Spectroscopy in the identification of carbonate phases differentiated in magnesium content," 2019.

21. F. Dai, Q. Zhuang, G. Huang, H. Deng, and X. Zhang, "Infrared spectrum characteristics and quantification of OH groups in coal," *ACS omega*, vol. 8, no. 19, pp. 17064–17076, 2023. https://doi.org/10.1021/acsomega.3c01336

22. E. M. de Salazar Martínez, M. F. Alexandre-Franco, A. J. Nieto-Sanchez, and E. M. Cuerda-Correa, "Exploring the role of surface and porosity in CO2 capture by CaO-based adsorbents through response surface methodology (RSM) and artificial neural networks (ANN)," *J. CO2 Util.*, vol. 83, p. 102773, 2024. https://doi.org/10.1016/j.jcou.2024.102773

23. J. A. Tavizón-Pozos, H. Cervantes-Cuevas, G. G. Garcia-Camacho, G. Chavez-Esquivel, and D. R. Acosta-Najarro, "Biodiesel Production Using K–Sr/CaO and CaO Catalysts Derived from Eggshells by Canola Oil Transesterification," *ACS omega*, vol. 10, no. 7, pp. 6827–6838, 2025. https://doi.org/10.1021/acsomega.4c09118

24. W. Koo-Amornpattana, P. Phadungbut, N. Kunthakudee, W. Jonglertjunya, S. Ratchahat, and M. Hunsom, "Innovative metal oxides (CaO, SrO, MgO) impregnated waste-derived activated carbon for biohydrogen purification," *Sci. Rep.*, vol. 13, no. 1, p. 4705, 2023. DOI:10.1038/s41598-023-31723-4

25. C. Quan, M. Wang, N. Gao, T. Yang, and R. Li, "In situ adsorption of CO2 to enhance biomass gasification for hydrogen production using Ca/Ni based composites," *J. Energy Inst.*, vol. 108, p. 101229, 2023, doi: https://doi.org/10.1016/j.joei.2023.101229. https://doi.org/10.1016/j.joei.2023.101229

26. F. Micheli, E. Mattucci, C. Courson, and K. Gallucci, "Bi-Functional Catalyst/Sorbent for a H2-Rich Gas from Biomass Gasification," 2021. doi: 10.3390/pr9071249. DOI:10.3390/PR9071249

27. M. Zhu, Q. Wang, and S. Wang, "Recent Advances and Future Perspectives in Catalyst Development for Efficient and Sustainable Biomass Gasification: A Comprehensive Review," 2025, https://doi.org/10.3390/su17167370

28. N. Cerone, F. Zimbardi, L. Contuzzi, J. Baleta, and D. Cerinski, "Experimental investigation of syngas composition variation along updraft fixed bed gasifier," *Energy Convers. Manag.*, vol. 221, no. July, p. 113116, 2020, https://doi.org/10.1016/j.enconman.2020.113116

29. R. Mohanty, P. Mahanta, A. Mahapatro, and R. Prakash, "Catalytic

gasification of pinewood biomass in a fluidized bed reactor with dolomite , limestone , and activated carbon : An experimental study," *Energy*, vol. 325, no. April, p. 136131, 2025, doi: 10.1016/j.energy.2025.136131. https://doi.org/10.1016/j.energy.2025.136131

30. C. Liu, Y. Huang, M. Niu, and H. Pei, "ScienceDirect Influences of equivalence ratio , oxygen concentration and fluidization velocity on the characteristics of oxygen-enriched gasification products from biomass in a pilot-scale fluidized bed," *Int. J. Hydrogen Energy*, vol. 43, no. 31, pp. 14214–14225, 2018, https://doi.org/10.1016/j.ijhydene.2018.05.154

Author's order	First Name	Middle name	Second Name
1	*Purbo*		*Suwandono*
2	*Widya*		*Wijayanti*
3	*Nova*	*Risdiyanto*	*Ismail*
4	*Dzulfikar*	*Johan*	*Akbar*
5	*Muhammad*		*Reza*

English

Purbo Suwandono
Corresponding author
Master
Department of Mechanical Engineering
Widya Gama University
Borobudur str., 35, Malang, Indonesia, 65142
E-mail: purbo@widyagama.ac.id
ORCID: https://orcid.org/0000-0003-4085-1291
Contact phone: +6282132697144
Number of publications in national journals indexed (approximate; for Ukraine citizens only): -
Number of publications in international journals indexed (approximate): 14
H-index by Scopus (if available): 4
ResearchGate: https://www.researchgate.net/profile/Purbo-Suwandono
Scopus ID: 57204187970
Researcher ID: https://researchid.co/rid80879

Widya Wijayanti
PhD
Department of Mechanical Engineering
Brawijaya University
Veteran str., 10–11, Malang, Indonesia, 65145
E-mail: widya_dinata@ub.ac.id

ORCID: https://orcid.org/0000-0003-4215-5943
Contact phone: +6285334992164
Number of publications in national journals indexed (approximate; for Ukraine citizens only): -
Number of publications in international journals indexed (approximate): 78
H-index by Scopus (if available): 12
ResearchGate: https://www.researchgate.net/profile/Widya-Wijayanti
Scopus ID: 36006672800
Researcher ID: -

Nova Risdiyanto Ismail
PhD
Department of Mechanical Engineering
Widya Gama University
Borobudur str., 35, Malang, Indonesia, 65142
E-mail: nova@widyagama.ac.id
ORCID: https://orcid.org/0000-0001-8439-6919
Contact phone:
Number of publications in national journals indexed (approximate; for Ukraine citizens only): -
Number of publications in international journals indexed (approximate): 7
H-index by Scopus (if available): 3
ResearchGate: https://www.researchgate.net/profile/Nova-Ismail-2
Scopus ID: 57204527065
Researcher ID: https://researchid.co/rid80876

Dzulfikar Johan Akbar
Master Student
Department of Mechanical Engineering
Brawijaya University
Veteran str., 10–11, Malang, Indonesia, 65145
E-mail: johanakbar@student.ub.ac.id
ORCID: https://orcid.org/0009-0002-4652-8516
Contact phone: +6282241116998
Number of publications in national journals indexed (approximate; for Ukraine citizens only): -
Number of publications in international journals indexed (approximate): -
H-index by Scopus (if available): -
ResearchGate: https://www.researchgate.net/profile/Dzulfikar-Johan-Akbar
Scopus ID: -
Researcher ID: -

Muhammad Reza
Bachelor Student
Department of Mechanical Engineering
Widya Gama University
Borobudur str., 35, Malang, Indonesia, 65142
E-mail: muhapanjangreza@gmail.com
ORCID: https://orcid.org/0009-0009-9258-0586
Contact phone: +6282139682566
Number of publications in national journals indexed (approximate; for Ukraine citizens only): -
Number of publications in international journals indexed (approximate): -
H-index by Scopus (if available): -
ResearchGate: -
Scopus ID: -
Researcher ID: -

Name of reviewer: Prof. Dr. Muji Setiyo, ST., MT.
Professor: Mechanical Engineering
Tel: +6281211020288
E-mail: muji@unimma.ac.id.
Work address: Universitas Muhammadiyah Magelang

Name of reviewer: Prof. Dr. Eng. Nurkholis Hamidi, ST., MT.
Professor: Mechanical Engineering
Tel: +62 81259293165
E-mail: hamidy@ub.ac.id
Work address: Brawijaya University

Received date: 20.02.2026
Accepted date:

Від рецензента

№2

The article is interesting, but there are several remarks. They are inserted in the text of the article. After elimination of these remarks, the article can be publication

UDC 662.7:662.767:66.097

ПОКРАЩЕННЯ ЯКОСТІ СИНТЕЗ-ГАЗУ ПРИ ВИСХІДНІЙ ГАЗИФІКАЦІЇ КУКУРУДЗЯНИХ КАЧАНІВ З ВИКОРИСТАННЯМ КАТАЛІЗАТОРА НА ОСНОВІ CAO/АКТИВОВАНОГО ВУГІЛЛЯ НА ПАЛЬМОВОМУ ВОЛОКН

Purbo Suwandono, Widya Wijayanti, Nova Risdiyanto Ismail, Dzulfikar Johan Akbar, Muhammad Reza

SYNGAS QUALITY IMPROVEMENT IN CORNCOB UPDRAFT GASIFICATION USING CAO/ACTIVATED CARBON PALM FIBER CATALYST

Purbo Suwandono, Widya Wijayanti, Nova Risdiyanto Ismail, Dzulfikar Johan Akbar, Muhammad Reza

Об’єктом даного дослідження є поліпшення якості синтез-газу, отриманого в результаті газифікації кукурудзяних качанів за допомогою системи з подвійним каталізатором, що складається з CaO та активованого вугілля, отриманого з пальмового волокна (AC–PF). Об'єктом дослідження є процес газифікації біомаси кукурудзяних качанів у висхідному потоку з використанням подвійної каталітичної системи на основі оксиду кальцію (CaO) та активованого вугілля, отриманого з пальмового волокна (AC-PF). Проблема, вирішена в даному дослідженні, полягає у відносно низькій теплотворній здатності синтез-газу з кукурудзяних качанів та високій вартості традиційних каталізаторів, що використовуються для його поліпшення. Дослідження проводилося з використанням різних значень еквівалентного співвідношення (0,2; 0,25; 0,3; 0,35), навантаження каталізатора (4%; 6%; 8%; 10%) та масового співвідношення CaO/AC–PF (0:1; 1:0; 1:1; 2:1) у поєднанні з характеристикою подвійної каталітичної системи. Отримані результати показують, що збільшення ER збільшує частки H_2 і CH_4 та нижчу теплоту згоряння синтез-газу, одночасно зменшуючи CO_2, причому CO досягає оптимального значення при ER = 0,3. У той

час як більш високе навантаження каталізатора має тенденцію до зменшення H_2 і CH_4, але збільшує CO, потенційно знижуючи теплоту згоряння при високих навантаженнях. Характеристика каталізатора показує, що AC-PF має пористу структуру, яка збільшує контакт газу з твердим тілом і сприяє вторинним реакціям, тоді як додавання CaO утворює композит із модифікованою структурою пор і поверхневими видами, пов'язаними з сорбцією CO_2. З енергетичної точки зору, нижня теплота згоряння синтез-газу збільшується із зростанням ER, але зменшується при більш високих навантаженнях каталізатора через зменшення внеску CH_4. Ключовою особливістю отриманих результатів є продемонстрована функціональна синергія між пористим AC–PF і сорбцією CO_2 на основі CaO, що дозволяє одночасно здійснювати каталітичне поліпшення якості та уловлювання CO_2 в єдиній, недорогій системі з подвійним каталізатором. Ці висновки можуть стати практичною основою для проектування та експлуатації невеликих установок газифікації біомаси, зокрема реакторів з висхідним потоком для відходів кукурудзяних качанів, в межах досліджених діапазонів ER та навантаження каталізатора.

Ключові слова: газифікація, висхідний потік, кукурудзяні качани, синтез-газ, CaO, активоване вугілля.

The object of this study is the improvement of syngas quality from updraft corn cob gasification using a dual catalyst system consisting of CaO and activated carbon derived from palm fiber (AC–PF). This is an incorrect formulation of the research object. The correct version is in Section 4. It should also be as in Section 4.

The object of the study is the updraft fixed-bed gasification process of corncob biomass using a dual catalyst system based on calcium oxide (CaO) and palm-fiber-derived activated carbon (AC-PF). The problem solved in this study is the relatively low heating value of corn cob syngas and the high cost of conventional catalysts used for its upgrading. The study was conducted using variations of equivalence ratio (0.2, 0.25, 0.3, 0.35), catalyst loading (4%, 6%, 8%, 10%), and CaO/AC–PF mass ratio (0:1, 1:0, 1:1, 2:1), combined with characterization of the dual catalyst system. The results obtained show that increasing ER increases the H_2 and CH_4 fractions and the syngas lower heating value while decreasing CO_2, with CO reaching an optimum at ER = 0.3. Whereas higher catalyst loading tends to decrease H_2 and CH_4 but increase CO, potentially reducing the heating value at high loadings Characterization of the catalyst shows that AC-PF has a porous structure that increases gas-solid contact and promotes secondary reactions, while the addition of CaO forms a composite with a modified pore texture and surface species associated with CO_2 sorption. From an energy perspective, the Lower Heating Value of syngas increases with increasing ER, but decrease at higher catalyst loadings due to the reduced contribution of CH_4. A key feature of obtained results is the demonstrated functional synergy between porous AC–PF and CaO-based CO_2 sorption, which enables simultaneous catalytic upgrading and CO_2 capture in a single, low-cost dual catalyst system. These findings could be a practical basis for

designing and operating small-scale biomass gasification units, particularly updraft reactors for corn cob waste, within the studied ER and catalyst loading ranges

Keywords: gasification, updraft, corncob, syngas, CaO, activated carbon

1. Introduction

In recent years, environmental challenges such as rising greenhouse gas emissions, fossil fuel depletion, and increasing agricultural waste have strengthened the global push toward green energy and sustainable technologies. These issues have become major concerns because they affect not only environmental quality but also long-term energy security and sustainable economic development. Green energy development is not only about reducing emissions but also about creating cleaner, more efficient ways to utilize available resources and minimize waste generation. Conversion of biomass residues into useful energy has attracted considerable attention as a practical and environmentally responsible solution. One promising approach is the thermochemical conversion of biomass through gasification, which can transform solid biomass into synthesis gas that can be used directly as a fuel or further processed as a feedstock for chemical production and other energy applications.

Indonesia is one of the largest corn producers in Southeast Asia, with national production reaching more than 18 million tons of dry kernels per year. Of this amount, about 15–20% is cobs after the kernel removal process, resulting in a very large amount of corn cob waste, estimated at 2.5–3.5 million tons annually. Until now, most corn cobs have only been used to a limited extent, for example as traditional fuel, small amounts of animal feed, or even burned directly on post-harvest land, which has the potential to cause air pollution. Most of the rest are simply piled up or left to rot on the land, posing a risk of becoming a source of plant disease [1].

Corn cobs have quite promising chemical and energy characteristics. Their composition is dominated by cellulose, hemicellulose, and lignin, with a calorific value of around 15–17 MJ/kg, making them very suitable as raw materials in various biomass-based energy conversion technologies [2]. Their hard and fibrous nature also makes them suitable for processing into biochar, activated charcoal, or direct use in pyrolysis and gasification processes. This significant potential indicates that corn cobs are not merely waste but a renewable resource that can be optimized to support energy security and reduce dependence on fossil fuels.

Biomass gasification is a promising thermochemical technology for converting renewable resources into syngas consisting of H_2, CO, CH_4, and CO_2. Of the various types of biomass, corn cobs are a potential candidate due to their abundant availability in Indonesia and lignocellulose content that supports the energy conversion process [3]. However, the biomass gasification process still faces several obstacles, particularly the low hydrogen fraction in syngas and the formation of significant amounts of tar. Tar can cause reactor clogging, reduced thermal efficiency, and increased purification costs.

To overcome these problems, the use of catalysts is an important strategy. A number of studies have proven that metal catalysts such as Ni, Ca, and K can increase

hydrogen yield while suppressing tar formation. On the other hand, activated carbon is also widely used as a catalyst support because it has a high surface area, porous structure, and good chemical stability. The use of agricultural waste, particularly palm fiber, as raw material for activated carbon is not only economically valuable but also supports the concept of a circular economy in plantation waste management. In addition, calcium oxide (CaO) is known to have a dual role, namely as a catalyst in the tar decomposition reaction and as a CO_2 absorber that promotes sorption-enhanced gasification to increase the hydrogen fraction in syngas [4].

Although various studies have examined the role of metal catalysts and activated carbon separately, research focusing on the combination of biomass bases catalyst such as palm fiber-based activated carbon with CaO in corn cob gasification is still limited. The uniqueness of this study lies in the integration of two catalyst, which is expected to provide a synergistic effect: activated carbon with high porosity increases catalyst dispersion and activity, while CaO simultaneously breaks down tar and absorbs CO_2. This approach has the potential to significantly increase hydrogen production and reduce carbon emissions.

However, there are several research gaps that remain unanswered. First, the optimal composition and ratio of activated carbon and CaO in corn cob gasification have not been extensively studied. Second, the synergistic mechanism using two catalyst in increasing syngas quality not yet fully understood. In addition, a systematic and statistically robust approach is required to disentangle the coupled effects of key operating and catalyst variables.

Based on this background and research gaps, this study aims to investigate the performance of a composite catalyst based on activated carbon from palm fiber combined with CaO in the corn cob gasification process. The main focus is on increasing hydrogen production, reducing tar, and evaluating the potential synergistic effects between materials. This research is expected to contribute to the development of low-cost, locally sourced, and sustainable catalyst systems that are relevant to supporting the clean energy transition and practical applications of biomass-to-hydrogen in the future.

This text doesn't belong in Section 1. It's a conclusion that can follow from a literature review, so it should be at the end of Section 2. However, the conclusion is already in section 2. Also, in the Introduction section did not need to annotate the article. It was necessary to justify the relevance of this **topic** in modern times. Therefore, you can remove this part of the text.

To finish this section of the article you need this text:

*Therefore, stud**ies** that are devoted….. **are** scientific relevance*

That is, it is necessary to inform not about your study, but about the relevance of this scientific topics

Therefore, studies devoted to improving syngas quality in biomass gasification are of considerable scientific relevance in modern energy research, particularly in response to the increasing demand for clean, renewable, and sustainable energy systems. Special attention is required for strategies aimed at enhancing hydrogen production and reducing tar formation, since these remain two of the main technical barriers limiting the wider practical implementation of biomass gasification. In this context, the development and evaluation of efficient, low-cost, and sustainable catalytic materials are scientifically important for advancing biomass conversion technologies and supporting the transition toward cleaner energy utilization.

2. Literature review and problem statement

The paper [5] presents the result on the gasification of sago dreg waste pellets in a top-lit updraft fixed-bed gasifier. The results show that the addition of Al_2O_3 improved syngas quality, especially by increasing H_2 content up to 31.65% at 5% Al_2O_3 and enhancing CO and CH_4 production, while also increasing the H_2/CO ratio to 1.65 and 1.51 for 5% and 10% Al_2O_3, respectively, improving LHV, and reducing tar content by about 25–27.5% compared with pellets without catalyst. However, this study is limited because it was conducted only on one biomass type, within a laboratory-scale TULD fixed-bed gasifier, and only considered two catalyst loadings.

The paper [6] presents the result on hydrogen enrichment in product gas from a pilot-scale rice husk updraft gasification. The results show that dolomite-assisted air gasification gave the best performance, increasing the H_2 content up to 15.4 mol%, with an LHV of 5.1 MJ/Nm³, while steam/air gasification improved H_2 to 9.6 mol% and air alone produced only about 7.08 mol% H_2, the optimum operating condition was reported at an airflow rate of 3 m³/h and a dolomite mixing ratio of 15 wt%. However, this study is limited because it focused only on rice husk feedstock, used a pilot-scale updraft gasifier with a batch capacity of 3 kg, and evaluated only a limited range of operating conditions and catalyst type.

The paper [7] presents the result on oxygen updraft gasification coupled with catalytic steam reforming of cigarette butts for hydrogen-rich syngas production. The results show that the integrated process was effective in converting cigarette butts into syngas, with gasification producing 82.3–89.7 wt.% syngas, 6.3–8.6 wt.% soot, and 1.4–1.9 wt.% tar, while the catalytic reforming stage significantly improved the gas quality by increasing the H_2 content up to 30.27 vol.%, increasing the HHV up to 11,528 kJ/kg, and reducing tar concentration from about 18.15 g/m³ to 13.38 g/m³ under the optimum condition. However, this study is limited because it investigated only cigarette butt waste as feedstock, used a specific oxygen updraft gasifier–catalytic reformer configuration, and fixed most catalytic reforming parameters.

The paper [8] presents the result on the experimental assessment of pellets produced from beekeeping waste and slumgum–pine sawdust mixtures through updraft gasification. The results show that pure slumgum pellets exhibited very high mechanical durability (99.98%) and high HHV (27.66 MJ/kg), while during gasification the 50%

slumgum–50% sawdust pellets produced the highest producer gas LHV of 7.62 MJ/Nm³, indicating that the addition of sawdust improved gas quality and energy recovery potential. However, this study is limited because the equivalence ratio remained very low (0.0125–0.0204) compared with typical gasification conditions, the experiments were conducted only in a modified laboratory-scale updraft gasifier.

The paper [9] presents the result on a comparative investigation of catalyst applications in updraft and modifiable-downdraft fixed-bed biomass gasifiers, using a biomass mixture of green waste, sewage sludge, and olive pomace together with red mud (RM) and Al–Ni alloy catalysts to improve syngas quality and hydrogen production. The results show that catalyst type and reactor configuration strongly influenced gasification performance, with the Al–Ni catalyst giving the best hydrogen enrichment, reaching up to 65 vol.% H_2 in the updraft gasifier at 900 °C, while RM increased H_2 to about 50 vol.%, the updraft gasifier produced better hydrogen-rich syngas than the modifiable-downdraft reactor. However, this study is limited because it, used a specific mixed biomass composition and mainly focused on high temperature operation around 900 °C with limited gasifying-agent flow conditions.

The paper [10] presents the result on the experimental investigation of producer gas composition from sorted municipal solid wastes in an updraft fixed-bed gasifier. The results show that reducing the equivalence ratio from 0.21 to 0.15 increased the heating value of the combustible gases. The study indicated that the allothermal updraft fixed-bed gasifier is suitable for producing gas that can be utilized in gas engines. However, this study is limited because it used a laboratory-scale 10 kW allothermal updraft gasifier at a fixed temperature of 800 °C, and evaluated only two ER conditions.

The paper [11] presents the result on the effect of adding laying hens manure (LHM) to wheat straw on gasification efficiency in an air-blown updraft fixed-bed gasifier. The results show that increasing ER improved the gasification performance, with the producer gas LHV reaching 3.3–3.4 MJ/m³, cold gas efficiency around 60%, and carbon conversion efficiency in the range of 82–94% . However, this study is limited because it was focused on one specific co-feed system and produced a relatively low-calorific gas.

The paper [12] presents the result on the gasification performance of olive pomace in updraft and downdraft fixed-bed reactors using dry air and pure oxygen. The results show that updraft reactor achieving up to 48 vol.% H_2 with dry air and 53 vol.% H_2 with pure oxygen, while the downdraft reactor reached up to 45 vol.% H_2 with dry air and 39 vol.% H_2 with pure oxygen. However, this study is limited because only a limited range of gasifying agents, temperatures, and flow rates.

The paper [13] presents the result on the gasification of MDF residue in an industrial-scale updraft fixed-bed gasifier. The results show that MDF residue can be effectively converted into useful energy, with a syngas production rate of about 2.5 Nm³/kg, syngas LHV of around 6.0–7.0 MJ/Nm³, about 88 wt.% of MDF residue converted into syngas, and a system capable of delivering 7 MWth of thermal energy and about 955 kW net electrical power through the ORC turbine. However, this study is

limited because it focused on one specific industrial waste stream (MDF residue) in one updraft gasifier configuration, mainly evaluated performance under a limited number of feed rates, and relied on direct combustion of raw hot syngas containing tar.

The paper presents the results of research on biomass gasification in updraft fixed-bed reactors aimed at improving syngas quality and thermal conversion efficiency. Shown that syngas composition and heating value are strongly influenced by feedstock properties, gasification conditions, and catalyst application. But there were unresolved issues related to the lack of effective and low-cost catalyst systems capable of simultaneously enhancing hydrogen formation and improving overall syngas quality during corncob gasification. The reason is the complexity of catalytic reactions in the gasification zone, including reforming, cracking, and CO_2 capture mechanisms, as well as the economic limitations of commercially available catalysts. A way to overcome these difficulties can be the development of composite catalysts based on CaO and activated carbon palm fiber, where CaO may promote CO_2 absorption and shift reactions, while activated carbon palm fiber may provide a porous surface and active sites for secondary cracking reactions. This approach was used in previous studies, however, the combined use of CaO and activated carbon palm fiber in corncob updraft gasification has not been sufficiently investigated. All this suggests that it is advisable to conduct a study on syngas quality improvement in corncob updraft gasification using CaO/activated carbon palm fiber catalyst.

Previous studies have shown that biomass gasification is a promising route for converting agricultural residues into synthesis gas, and that catalytic materials such as CaO and carbon-based adsorbents can improve gas quality through tar reduction, reforming reactions, and CO_2 capture. Several researchers have also investigated different biomass feedstocks, catalyst types, and reactor configurations to enhance syngas production. However, most of these studies mainly focused on the individual performance of catalysts or on gasification systems other than corncob updraft gasification. In addition, the combined effect of CaO and activated carbon palm fiber catalyst, especially in terms of catalyst ratio, catalyst loading, and equivalence ratio, has not been systematically discussed.

Therefore, further study is needed to clarify the synergistic role of CaO as a CO_2 sorbent and activated carbon palm fiber as a porous catalytic support in improving syngas composition and heating value. Based on this research gap, the present study specifically investigates the use of combined CaO/activated carbon palm fiber catalyst in corncob updraft gasification and evaluates the influence of key operating parameters on synthesis gas quality. In this way, the study is intended to provide both a clearer scientific understanding of catalyst interaction and practical guidance for improving biomass gasification performance.

3. The aim and objectives of the study

The purpose of the study is to enhance syngas quality from corncob updraft gasification by developing a dual-synergy catalytic system based on calcium oxide

(CaO) and palm-fiber-derived activated carbon (AC-PF). This will allow the production of cleaner and more energy-dense producer gas, providing practical guidance for selecting operating conditions and catalyst configurations suitable for updraft gasifiers processing agricultural residues.

To achieve these aims, the following objectives are accomplished:

– to prepare and characterize CaO and AC-PF catalysts by analyzing their morphology, surface functional groups, and pore characteristics using SEM, FTIR, and BET methods;

– to evaluate the influence of equivalence ratio, catalyst loading, and CaO/AC ratio on syngas composition and lower heating value in corncob updraft gasification, and to identify the catalyst condition that provides improved gas quality.

4. Materials and methods

4. 1. Object and hypothesis of the study

The object of the study is the updraft fixed-bed gasification process of corncob biomass using a dual catalyst system based on calcium oxide (CaO) and palm-fiber-derived activated carbon (AC-PF). The practical physical process under investigation is the catalytic upgrading of producer gas within the updraft reactor, where changes in operating parameters and catalyst configuration are expected to influence syngas composition and heating value. The results of this study are intended to be applied to improve the quality of syngas, specifically by increasing the combustible gas fraction (H_2 and CH_4) and the lower heating value (LHV), while reducing CO_2 content.

The selected methods were intended to explain both the catalyst characteristics and their effect on syngas quality. SEM, FTIR, and BET were used because they provide complementary information on catalyst morphology, surface functional groups, and pore structure, which are important for catalytic reforming, adsorption, and CO_2 capture during gasification. The investigated operating parameters, namely equivalence ratio, catalyst loading, and CaO/AC ratio, were chosen because they are the main variables governing the reaction environment, catalyst effectiveness, and synergistic interaction between CaO and activated carbon in the updraft gasification process.

The research hypothesis is that a dual-synergy CaO/AC-PF catalytic system can improve syngas quality more effectively than single-catalyst configurations in updraft corncob gasification. It is hypothesized that CaO functions as a CO_2 sorbent, shifting reaction equilibria toward enhanced hydrogen formation, while activated carbon derived from palm fiber provides high-surface-area catalytic sites that promote secondary reactions such as tar cracking and volatile reforming. The combined catalytic-sorption mechanism is expected to increase H_2 and CH_4 fractions and improve LHV under optimized equivalence ratio (ER), catalyst loading, and CaO/AC-PF ratio conditions.

It was assumed that the corncob feedstock has relatively homogeneous composition and stable proximate/ultimate characteristics during the experiments. The gasification process was assumed to operate under steady-state conditions after stabilization. It was also assumed that the CaO maintains sufficient CO_2 sorption capacity within the

experimental time frame and that the activated carbon structure remains stable under the applied temperature range.

During the course of the research, several methodological simplifications were adopted in order to maintain experimental feasibility and focus on the main objective of syngas quality evaluation. Detailed kinetic modeling of individual gasification reactions was not performed; instead, the process performance was assessed based on experimentally measured syngas composition and syngas low heating value. Furthermore, although CaO carbonation-decarbonation reactions may occur during operation, microstructural evolution, sintering behavior, and long-term cyclic stability of the catalyst were not investigated in this study. The catalytic performance was evaluated within the experimental duration without conducting extended durability or regeneration-cycle analysis. This text should be at the end of the subsection 4.1.

The selected methods were intended to explain both the catalyst characteristics and their effect on syngas quality. SEM, FTIR, and BET were used because they provide complementary information on catalyst morphology, surface functional groups, and pore structure, which are important for catalytic reforming, adsorption, and CO_2 capture during gasification. The investigated operating parameters, namely equivalence ratio, catalyst loading, and CaO/AC ratio, were chosen because they are the main variables governing the reaction environment, catalyst effectiveness, and synergistic interaction between CaO and activated carbon in the updraft gasification process.

4. 2. Catalyst Preparation

Approximately 6 grams of ground palm fiber was mixed with 60 mL of distilled water and stirred for 10 minutes. The mixture was then placed in an autoclave and heated to 200°C at a rate of 5°C per minute for 6 hours in an electric oven. After that, the reactor is allowed to cool naturally to room temperature. The resulting solid hydrocarbon product (hydrochar) is then separated using Whatman No. 42 filter paper. The filtered product is then dried at 105°C for 24 hours and stored in a glass vial. The next stage is the activation process. The hydrochar is immersed in a 3 M KOH solution with a weight ratio of 1:3 (Hydrochar:KOH) for 16 hours, then dried at 85°C for 6 hours. Spectroscopic evidence indicates that KOH preferentially reacts with oxygenated sites and can increase the relative abundance of C–OH functionalities, while higher KOH ratio and activation temperature significantly enhance porosity and BET surface area [14, 15]. To obtain the CaO/AC mixture, CaO powder and activated carbon (AC) were mixed in specific proportions using a grinder until a homogeneous mixture was obtained. Next, CaO, AC, and CaO/AC were activated using a tube furnace at a temperature of 700°C for 1 hour with a continuous flow of nitrogen during the activation process. The resulting product was then washed using distilled water until it reached a neutral pH. This stage produced activated carbon that was ready for use in research.

4. 3. Experimental Setup

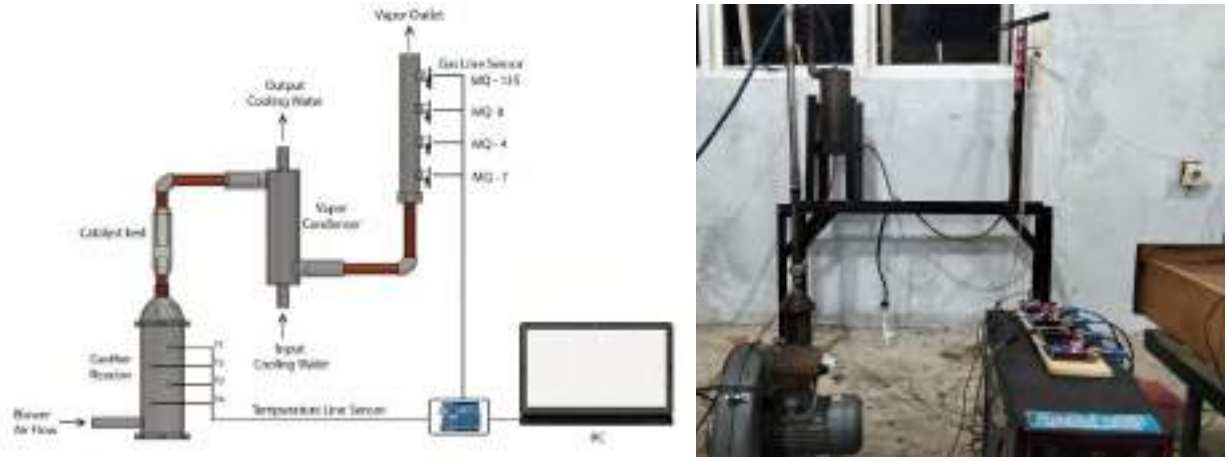
Corncob biomass was obtained from farmers in the South Malang region of East Java. Before use, the biomass was cleaned of impurities and dried in an oven for 6 hours at 100°C to remove moisture (water vapor) content. The ultimate and proximate test results are as follows.

The proximate and ultimate analyses of the corncob feedstock were conducted to determine its physicochemical characteristics prior to gasification. The results are presented in Table 1. The data indicate that corncob has high volatile matter content and relatively low ash content, which are favorable characteristics for gasification processes.

Table 1
Ultimate and Proximate Test Corn Cob

Parameter	Units	Corn cobs
Moisture	%	10
Volatile matter	%	71.38
Fixed carbon	%	12.11
Ash	%	6.51
C	%	43.6
H	%	6.3
O	%	46.8
N	%	0.22
HHV	MJ/kg	17.61

The experimental apparatus employed in this study consisted of an updraft gasifier integrated with a catalyst bed, a vapor condensation unit, gas sensors, and temperature measurement points to enable comprehensive monitoring of the gasification process. Fig. 1 shows the updraft gasifier system used in this study, including the schematic experiment (a) and the experimental setup (b).



a *b*

Fig. 1. Updraft gasifier: *a* – schematic experiment; *b* – experimental setup

This study used an updraft gasification reactor designed with a total height of 20 cm. The lower part of the reactor consisted of an ash container with a height of 5 cm, while the active reactor had a height of 15 cm and a diameter of 3 inches. The reactor was equipped with a 1-inch diameter air inlet pipe connected to a blower. The blower was modified with a potentiometer so that the air speed could be adjusted as needed. To monitor the thermal conditions inside the reactor, four 3 cm long type K thermocouples were installed at several different points so that the temperature profile in the gasification zone could be observed in more detail. Each test was conducted with a fixed biomass mass, a mixture of corn cobs weighing 80 grams. The reactor was made of iron and equipped with a gas seal to prevent leaks during the gasification process.

The gas produced by the reactor was fed into a condenser, which cooled the hot gas so that the water vapor components could be separated. The condenser was made of a copper spiral pipe with a diameter of ½ inch and a height of 30 cm. Cooling water was circulated from the bottom of the condenser and exited through the top to ensure efficient heat transfer. This cooling system was driven by a 60-watt water pump, ensuring stable water flow and optimal condensation. The catalyst was positioned downstream after the reactor, where it was supported on steel wool and wrapped with an 80-µm wire mesh to secure the catalyst and prevent particle carryover with the gas flow

To analyse the gas composition, four types of MQ gas sensors were used. The MQ-8 sensor was used to detect H_2, MQ-4 for CH_4, MQ-135 for CO_2 and MQ-7 for CO. Each gas sensor was calibrated according to the manufacturer's datasheet, specifically by determining the Ro value, which is the sensor resistance in clean air conditions. This Ro value is used as a reference in calculating the measured gas concentration during the process.

All data from the gas sensors and thermocouples were acquired using an Arduino Uno microcontroller. Each gas sensor is connected to a separate Arduino Uno to facilitate the calibration process and reduce the possibility of interference between sensors. Arduino is also used to record temperature data from four thermocouples installed in the reactor, so that gas composition and temperature distribution data can be obtained simultaneously.

The ER range of 0.2, 0.25, 0.3 and 0.35. The catalyst load was between 4%, 6%, 8% and 10% from the mass of input feedstock. The CaO/AC-PF ratio was varied between 0:1, 1:0, 1:1, and 2:1. Design of experiment can be seen in Table 2.

Table 2
Design of Experiment using

Run	Equivalence Ratio (E.R)	Catalyst Load %	CaO/AC
1	0.2	4	1:0
2	0.2	6	0:1

3	0.2	8	1:1
4	0.2	10	2:1
5	0.25	4	0:1
6	0.25	6	1:0
7	0.25	8	2:1
8	0.25	10	1:1
9	0.3	4	1:1
10	0.3	6	2:1
11	0.3	8	1:0
12	0.3	10	0:1
13	0.35	4	2:1
14	0.35	6	1:1
15	0.35	8	0:1
16	0.35	10	1:0

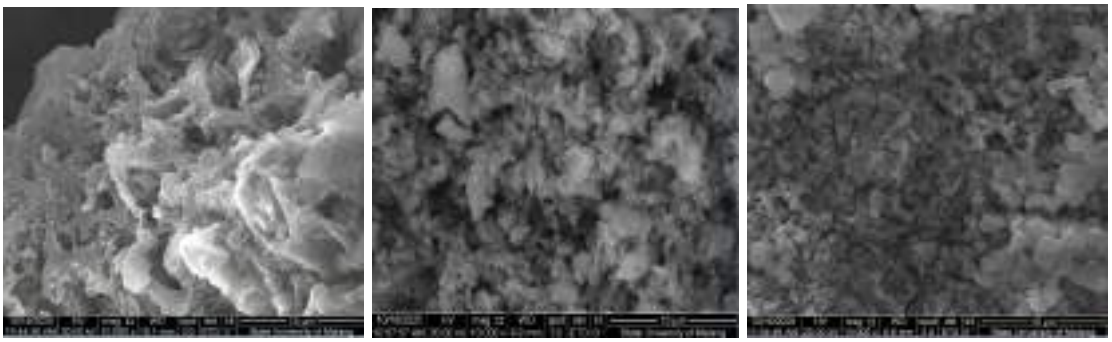
A total of 16 experimental runs were conducted systematically to enable evaluation of the main effects of each variable and the tendency of interactions between variables on the fractions of H_2, CO, CH_4, CO_2, and lower heating value (LHV). This approach enabled identification of the most effective combination of operating parameters in improving syngas quality quantitatively and measurably.

5. Results of syngas quality enhancement from corncob using calcium oxide (CaO) and palm-fiber-derived activated carbon (AC–PF).

5. 1. Characterization of Calcium Oxide (CaO) and Palm-Fiber-Derived Activated Carbon (AC–PF) Catalysts

5. 1. 1. Scanning Electron Microscopy Catalyst Result

Fig. 2, *a* shows the image obtained from a Scanning Electron Microscope (SEM) with a magnification of 10,000× shows the surface morphology of palm fiber-based activated carbon (AC-PF). The surface structure appears porous and irregular, with a combination of void areas and layered surfaces. This characteristic indicates that the activation process that using KOH has successfully formed micropores and mesopores, which play an important role in increasing the specific surface area of activated carbon.



a *b* *c*

Fig. 2. Scanning Electron Microscopy Catalyst Result: *a* – Scanning Electron Microscopy AC-PF; *b* – Scanning Electron Microscopy CaO:AC;1:1; *c* – Scanning Electron Microscopy CaO:AC-PF;2:1

The rough and textured surface indicates that most of the material has undergone lignocellulose cell wall exfoliation, resulting in numerous interparticle gaps. This porous structure greatly supports gas adsorption and diffusion capabilities when used as a catalyst in gasification or thermochemical reactions.

The presence of 1–5 μm voids indicates that most pores are in the mesopore category, supporting the adsorption of gas molecules such as H_2, CO, and tar during the gasification reaction.

The morphology of AC-PF shows the characteristics of porous activated carbon with a heterogeneous pore distribution, where the pores allow increased contact between gas reactants and active sites on the material surface, thereby increasing catalytic efficiency and the ability to absorb tar or CO_2 in biomass-based energy applications.

Fig. 2, *b* shows the surface morphology of the CaO:AC-PF catalyst with a ratio of 1:1. Visually, it can be seen that the surface of this material consists of fine particles ranging in size from microns to submicrons that stick together to form a layered and slightly agglomerated structure.

The presence of fine, light-colored grains indicates an even distribution of CaO particles impregnated on the surface of activated carbon (AC-PF). This CaO distribution fills some of the pores of the carbon, resulting in a denser surface compared to pure AC-PF. However, there are still small gaps and voids between the grains, indicating that the microporous and mesoporous structures are still formed and can support catalytic activity [16].

This morphology illustrates the success of the CaO impregnation process on activated carbon from palm fiber, where the interaction between CaO and the carbon pore walls produces a composite material that is more thermally and chemically stable. This structure is highly conducive to catalyst applications in biomass gasification processes, as CaO particles can function as CO_2 absorbers while accelerating the tar reforming reaction [17].

Fig. 2, *c* shows the surface morphology of the CaO:AC-PF (2:1) catalyst. The image shows that the surface of the material is dominated by agglomerations of fine, round, and irregular particles ranging in size from microns to submicrons. Compared to the CaO:AC-PF (1:1) sample, this structure appears denser and tighter, indicating that an increase in the CaO ratio causes partial closure of the activated carbon surface pores by CaO particles.

The distribution of CaO particles appears more uniform and covers the carbon surface, indicating the successful impregnation of a larger amount of CaO. The light

color in some areas indicates the presence of a calcium oxide phase that is strongly attached to the activated carbon matrix. This structure indicates a strong interaction between CaO and AC-PF, forming a thermally stable composite.

Although some pores are covered, there are still microscopic gaps between the CaO grains that allow gas diffusion to occur, so that the catalyst retains its good adsorption capacity. The combination of the active area of CaO and the porous carbon structure makes this material very promising for biomass gasification or tar reforming applications, as CaO can act as a CO_2 absorber and increase the conversion of carbon to hydrogen gas.

5. 1. 2. Fourier Transform Infrared Spectroscopy catalyst result

The FTIR analysis results shown in the Fig. 3 reveal clear spectral differences between the AC-PF, CaO, and their mixtures (CaO:AC-PF) with ratios of 2:1 and 1:1. In the AC-PF spectrum, the absorption band at 2926 cm^{-1} is associated with the stretching vibration of the C–H group from $–CH_2$ or $–CH_3$ (methylene/methyl stretching), which indicates the presence of hydrocarbon chain residues from the lignocellulose structure. The peak at 1577 cm^{-1} indicates the presence of aromatic C=C or C=O stretching, while the band at 1056 cm^{-1} represents C–O stretching from alcohol or ether groups. In addition, the –OH group that appears in the 3500–3600 cm^{-1} region is identified as the result of AC-PF activation using a KOH solution, which causes the formation of hydroxyl groups on the activated carbon surface. This –OH group plays an important role in increasing the surface activity and adsorption capacity of AC-PF as a catalyst support medium [18, 19].

In pure CaO, the intense band at 3639 cm^{-1} is associated with the stretching of the O–H group from $Ca(OH)_2$, which is formed due to the partial hydration of CaO when exposed to humid air. Meanwhile, the absorption bands at 1426 cm^{-1} and 876 cm^{-1} are associated with C–O stretching and CO_3^{2-} bending, respectively, indicating the formation of $CaCO_3$ due to CO_2 adsorption from the air. This shows that CaO is highly reactive to moisture and carbon dioxide in the environment.

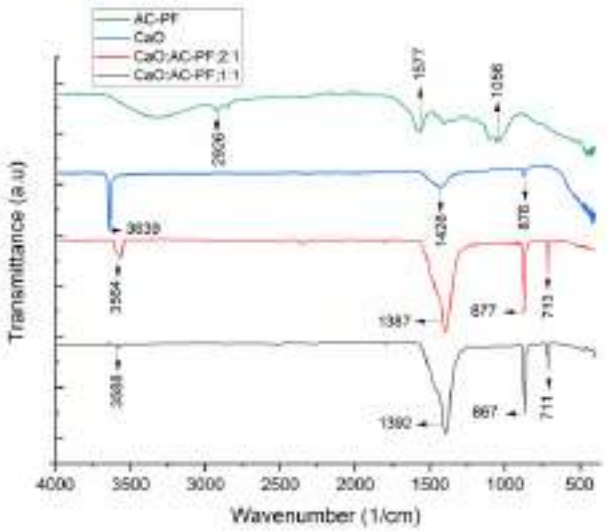


Fig. 3. Fourier Transform Infrared Spectroscopy Catalyst Result

For the CaO:AC-PF (2:1), the main absorption bands were detected at 3564 cm^{-1} (O–H stretching from $Ca(OH)_2$ and the –OH group in AC-PF), 1387 cm^{-1} (C–O stretching), and 877 cm^{-1} and 713 cm^{-1} (bending vibration of CO_3^{2-}). This combination of bands indicates the formation of carbonate compounds ($CaCO_3$) due to the interaction between CaO and the oxygen groups of activated carbon. The presence of –OH groups from KOH activation also strengthens the basic properties on the surface, which can increase the chemical interaction between CaO and AC-PF [20].

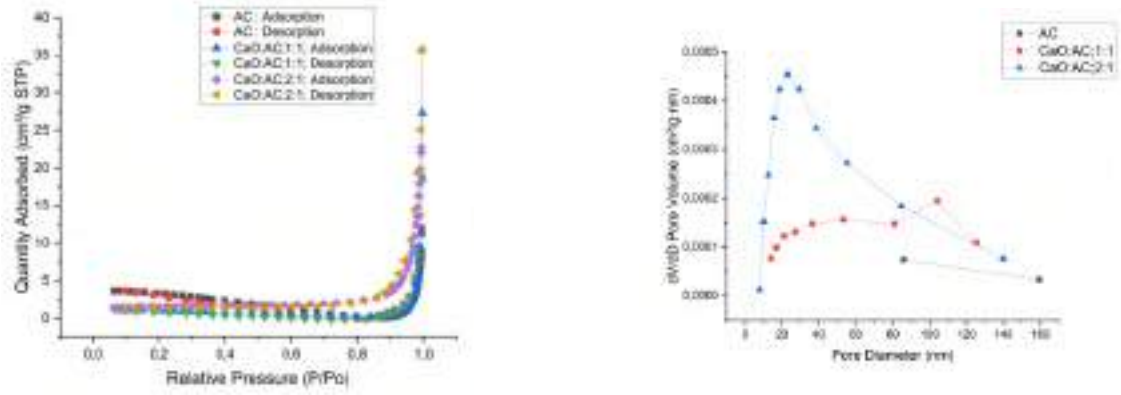
At a CaO:AC-PF ratio of 1:1, the absorption bands at 3588 cm^{-1}, 1392 cm^{-1}, 867 cm^{-1}, and 711 cm^{-1} show a similar pattern, indicating the presence of hydroxyl (O–H) and carbonate (CO_3^{2-}) groups. The difference in peak intensity compared to the 2:1 ratio indicates variations in the level of interaction between CaO and the –OH groups resulting from KOH activation on AC-PF, which affects the formation of carbonate-hydroxide complexes on the material surface [21].

5. 1. 3. Brunauer-Emmett-Teller Catalyst Result

Fig. 4 shows the adsorption-desorption isotherm curves for nitrogen for the AC, CaO:AC (1:1), and CaO:AC (2:1) samples are shown in Fig. 4. All three samples exhibit type IV isotherms with clear hysteresis loops at relatively high pressures (P/Po > 0.9). Based on the IUPAC classification, this characteristic indicates that the material has a mesoporous structure formed through capillary condensation within the pore channels. The difference between the adsorption and desorption pathways indicates that the pore shape is not perfectly cylindrical, but rather tends to be irregular or slit-like, which is commonly found in modified activated carbon materials [22].

The pure activated carbon (AC) sample showed a relatively low nitrogen adsorption volume with a specific surface area of 24.51 m^2/g and an average pore diameter of 0.74 nm, indicating a predominance of microporous structures. In the

CaO:AC (1:1) composite, the surface area did not change significantly compared to pure AC, indicating that the addition of a moderate amount of CaO did not cover the carbon pores much, but only adhered to the external surface of the carbon matrix [23].



a *b*

Fig. 4. Brunauer-Emmett-Teller Result: *a* – Surface Analysis Adsorption Desorption Isotherm; *b* – Barrett-Joyner-Halenda Adsorption Pore Size Distribution

Conversely, in the CaO:AC (2:1) mixture, there was a sharp increase in adsorption volume at relatively high pressure (P/Po > 0.9) to around 35 cm^3/g STP, while the BET surface area decreased dramatically to 5.06 m^2/g, and the pore diameter increased to 22.87 nm.

These changes in isotherm shape and pore size increase indicate that CaO impregnation not only modifies the surface chemistry but also significantly alters the pore structure of activated carbon. This transformation is positive in the context of catalytic applications in biomass gasification processes, as the mesoporous structure can enhance gas diffusion and accessibility to active sites during the tar reforming and water-gas shift reactions. Thus, even though the specific surface area decreases, the increase in mesoporousness and pore connectivity can actually improve catalyst performance in hydrogen gas production [24].

Fig. 4, *b* shows the BJH pore size distribution curves that provide further insight into the textural evolution of the palm-fiber-based activated carbon after CaO impregnation. The pristine AC exhibits a relatively low dV/dD value and a broad contribution only at large pore diameters (>60 nm), indicating that its pore system is dominated by macropores with a limited amount of mesopores. Such a texture is less favourable for gas-solid reactions because the accessible surface area in the mesopore range (2–50 nm) is relatively small.

After CaO loading, the shape and intensity of the BJH curves change markedly. For CaO:AC-PF = 1:1, the distribution shifts toward smaller pore diameters with a pronounced contribution in the mesopore region of approximately 15–60 nm. This behaviour shows that CaO impregnation partially reconstructs the carbon matrix,

enlarging existing micropores and opening blocked pores to generate additional mesoporosity. The effect becomes even more evident at CaO:AC-PF = 2:1, where the curve displays the highest dV/dD values and a distinct maximum centred at about 30–40 nm. The strong peak in this range confirms that a higher CaO loading promotes the development of well-defined mesopores while reducing the relative fraction of very large macropores.

Overall, the BJH analysis demonstrates that CaO acts not only as a reactive sorbent but also as a textural promoter for the palm-fiber AC. The increase in mesopore volume and the shift of the dominant pore size toward 20–40 nm are expected to facilitate the diffusion of gasifying agents and tar molecules, as well as to improve the accessibility of CaO active sites for CO_2 capture and reforming reactions. These features are therefore beneficial for enhancing the catalytic performance of the CaO/AC composite in biomass gasification toward H_2-rich syngas production.

5. 2. Effect of operating parameters on syngas composition and low heating value

5. 2. 1. Effect of Equivalence Ratio on Syngas Product

The composition of syngas from updraft gasification is greatly influenced by the Equivalence Ratio (ER), which is the ratio of the mass flow rate of air compared to the mass flow rate of corncob in the experiment compared to the stoichiometry of air required for complete combustion of corncob. In this study, the ER used was 0.2–0.35 with the following formula

$$ER = \frac{(\dot{m}_a / \dot{m}_{cc})_{\exp}}{(\dot{m}_a / m_{cc})_{stc}},$$

where $\dot{m}_a$ is the air mass flow rate (kg/s), $\dot{m}_{cc}$ is the corncob mass flow rate (kg/s), exp denotes the experimental air-fuel ratio, and stc denotes the stoichiometric air-fuel ratio.

The composition of syngas produced from corncob gasification was evaluated at different equivalence ratios to determine the variation in the main combustible and non-combustible gas components. Changes in the equivalence ratio significantly affected the concentrations of H_2, CH_4, CO, and CO_2, indicating that the air supply plays an important role in the gasification performance and gas quality. Fig. 5 shows the syngas composition obtained at different equivalence ratios.

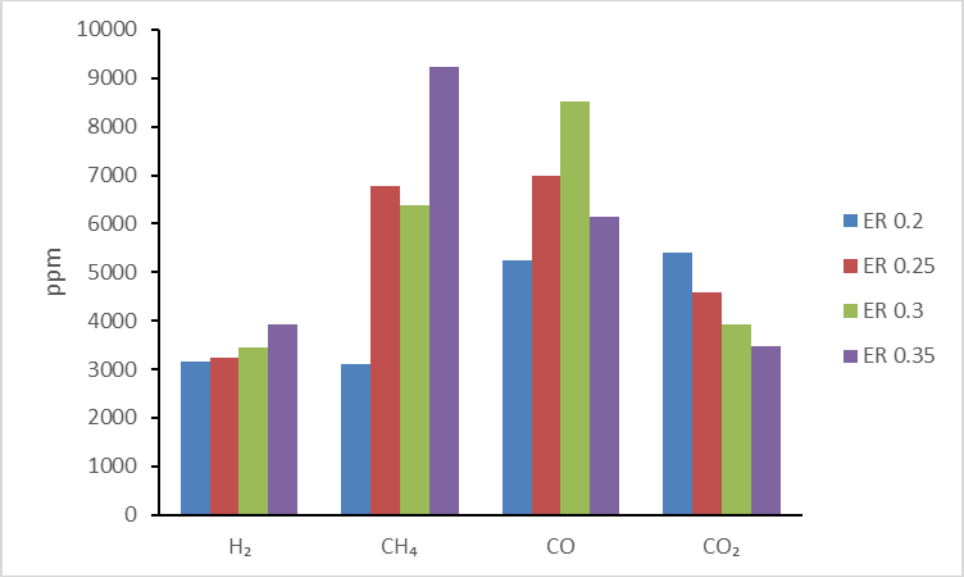


Fig. 5. Syngas composition with different equivalence ratio

The graph above shows that the higher the ER, the higher the hydrogen composition produced. At ER 0.2, the ppm is 3150 ppm, at ER 0.25 it is 3241 ppm, at ER 0.3 it is 3457 ppm, and at ER 0.35 it is 3914 ppm. A higher oxidant supply promotes the formation of more stable autothermal conditions and higher reaction temperatures due to partial oxidation. This increase in temperature accelerates hydrogen-forming reactions, particularly the gasification of active carbon catalyst interactions with steam ($C + H_2O \rightarrow CO + H_2$), the reforming of volatile compounds/light hydrocarbons ($C_xH_y + H_2O \rightarrow CO + H_2$), and the cracking of tar/volatile into lighter gas species. At low ER, some volatiles tend to be incompletely converted and still have the potential to escape as condensable components, while increasing ER increases heat availability, making the conversion of volatiles into gas fractions (including H_2) more effective.

The higher the ER, the higher the CH_4 composition produced. At ER 0.2, 3093 ppm was obtained, at ER 0.25 6767 ppm, ER 0.3 6377 ppm, and ER 0.35 9221 ppm. This trend indicates that the supply of oxidants not only increases autothermal conditions and the rate of devolatilization, but also shifts the reaction pathway towards the formation of light hydrocarbons through hydrogenation and/or methanation reactions in the reactor zone where the temperature still supports CH_4 formation. In particular, increased H_2 at higher ERs can promote the methanation reaction of CO ($CO + 3H_2 \rightleftharpoons CH_4 + H_2O$), so that CH_4 increases along with a tendency for CO to decrease at the highest ER. In addition, more intensive fragmentation of volatiles and tar at high ERs has the potential to produce light gas precursors which are then hydrogenated to CH_4.

CO formation increased up to an ER of 0.3 and decreased at an ER of 0.35. At an ER of 0.2, 5238 ppm was obtained, at an ER of 0.25, 6999 ppm, at an ER of 0.3, 8532 ppm, and decreased at an ER of 0.35 to 6145 ppm. At low ER (0.20–0.25), limited oxygen supply resulted in relatively low heat release, so that the reaction zone

temperature and char reactivity were not sufficient to intensify CO formation reactions, especially the Boudouard reaction ($C + CO_2 \rightleftharpoons 2CO$) and char gasification with steam ($C + H_2O \rightleftharpoons CO + H_2$). When the ER is increased towards 0.30, the increase in autothermal heat strengthens these reduction reactions, causing CO formation to increase and reach its peak. However, at higher ERs (0.35), the CO fraction tends to decrease because some CO can be converted to CH_4.

CO_2 formation continues to decrease as ER increases. At ER 0.2, 5412 ppm is obtained; at ER 0.25, 4592 ppm; at ER 0.3, 3916 ppm; and at ER 0.35, 3479 ppm. The increase in oxidant supply at this ER does not promote complete combustion, but rather strengthens the CO_2 reduction mechanism. At higher ERs, the heat generated from partial oxidation increases the temperature of the reduction zone, thereby accelerating the Boudouard reaction ($C + CO_2 \rightleftharpoons 2CO$), in which CO_2 is reduced by char to CO. This mechanism is consistent with the increase in CO until it reaches a maximum at an ER of 0.30, while also explaining the decrease in CO_2 under the same conditions. Interestingly, at an ER of 0.35, CO_2 remains at its lowest level even though CO decreases, indicating that the CO formed is not completely accumulated at the outlet but has the potential to undergo further conversion along the gas flow path.

5. 2. 2. Effect of Catalyst Loading on Syngas Product

The catalyst load or amount of catalyst in this study was 4%, 6%, 8%, and 10% of the total biomass weight. The Fig. 6. shows that the composition of H_2 and CH_4 increases as the catalyst load decreases. The H_2 gas composition at catalyst loads of 4%, 6%, 8%, and 10% is 3742 ppm, 3471 ppm, 3372 ppm, and 3176 ppm, respectively. As the catalyst load increases, the reaction pathways that consume H_2 tend to strengthen, particularly the reverse water–gas shift ($CO_2 + H_2 \rightarrow CO + H_2O$) and H_2 interactions on the catalyst surface during the conversion of gasification compounds. As a result, even though reforming occurs, the measured net H_2 decreases because more H_2 is used for CO formation and surface reactions. The CH_4 gas composition at catalyst loads of 4%, 6%, 8%, and 10% was 7031 ppm, 6476 ppm, 6206 ppm, and 5746 ppm, respectively. An increase in catalyst load increases the number of active sites and gas-catalyst contact, so that methane/light hydrocarbon cracking and reforming occur more intensely. CH_4 then acts as a reactant that is converted into more reactive syngas components, causing the CH_4 concentration to decrease at higher catalyst loads.

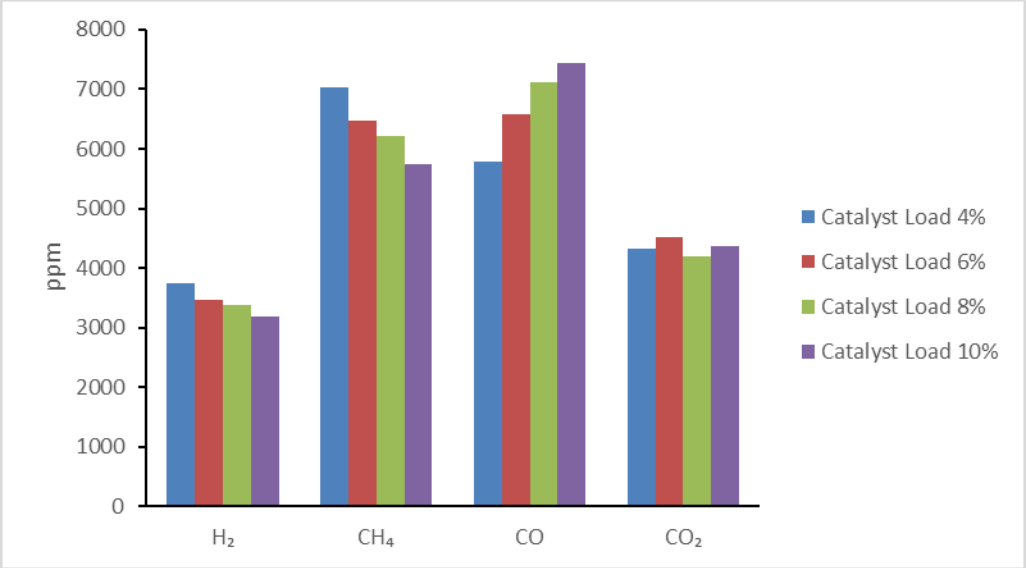


Fig. 6. Syngas Composition with Catalyst Load Variation

The CO gas composition increases with increasing catalyst load, namely for catalyst loads of 4%, 6%, 8% and 10% at 5782 ppm, 6576 ppm, 7111 ppm and 7445 ppm, respectively. The increase in catalyst loading strengthens the CO-forming reactions, particularly dry reforming ($CH_4 + CO_2 \rightarrow 2CO + 2H_2$), char–$CO_2$ reaction ($C + CO_2 \rightarrow 2CO$), and reverse water-gas shift. This combination shifts the product selectivity towards CO, so that the CO fraction increases consistently as the catalyst is increased. The CO_2 gas composition tends to stagnate with increasing catalyst loading, at catalyst loads of 4%, 6%, 8%, and 10% at 4322 ppm, 4510 ppm, 4198 ppm, and 4369 ppm, respectively. CO_2 shows minor changes because it is in a searching for a chemical equilibrium between the partial oxidation and the dry reforming. When the catalyst load increases, the rate of CO_2 consumption may rise, but this is often offset by CO_2 formation in the reaction zone, so that the CO_2 value appears stable or only fluctuates.

5. 2. 3. Effect of Catalyst Ratio on Syngas Product

At a catalyst load of 4%, the CaO/AC ratio changes the gasification reaction through differences in the dominance of tar cracking/reforming and CO_2 capture by CaO, so that the gas composition is highly dependent on the number of active sites and the effectiveness of gas-catalyst contact. At 0:1 (AC), CH_4 and CO are relatively high because AC promotes volatile/tar cracking, but CO_2 remains high because there is no absorption. At 1:0 (CaO), CH_4 decreases but CO_2 is highest, indicating that CO_2 capture is not yet effective due to limited surface area/carbonate layer formation. The 1:1 ratio produces the highest CO with moderate CO_2, indicating CaO–AC synergy that increases the conversion of volatiles into reactive gases. Meanwhile, the 2:1 (CaO-rich) ratio provides the highest H_2 and lowest CO_2 due to the sorption-enhanced effect of CaO, but

CH_4 remains high due to the smaller contribution of AC, so methane reforming/cracking is not yet optimal.

To further examine the catalytic performance, the effect of CaO/AC ratio on syngas composition was investigated under various catalyst loading conditions. This analysis was conducted to determine how the proportion of CaO and activated carbon, combined with different catalyst loads, affected the distribution of H_2, CH_4, CO, and CO_2 during corncob gasification. Fig. 7 illustrates the effect of CaO/AC ratio at catalyst loads of 4% (a), 6% (b), 8% (c), and 10% (d).

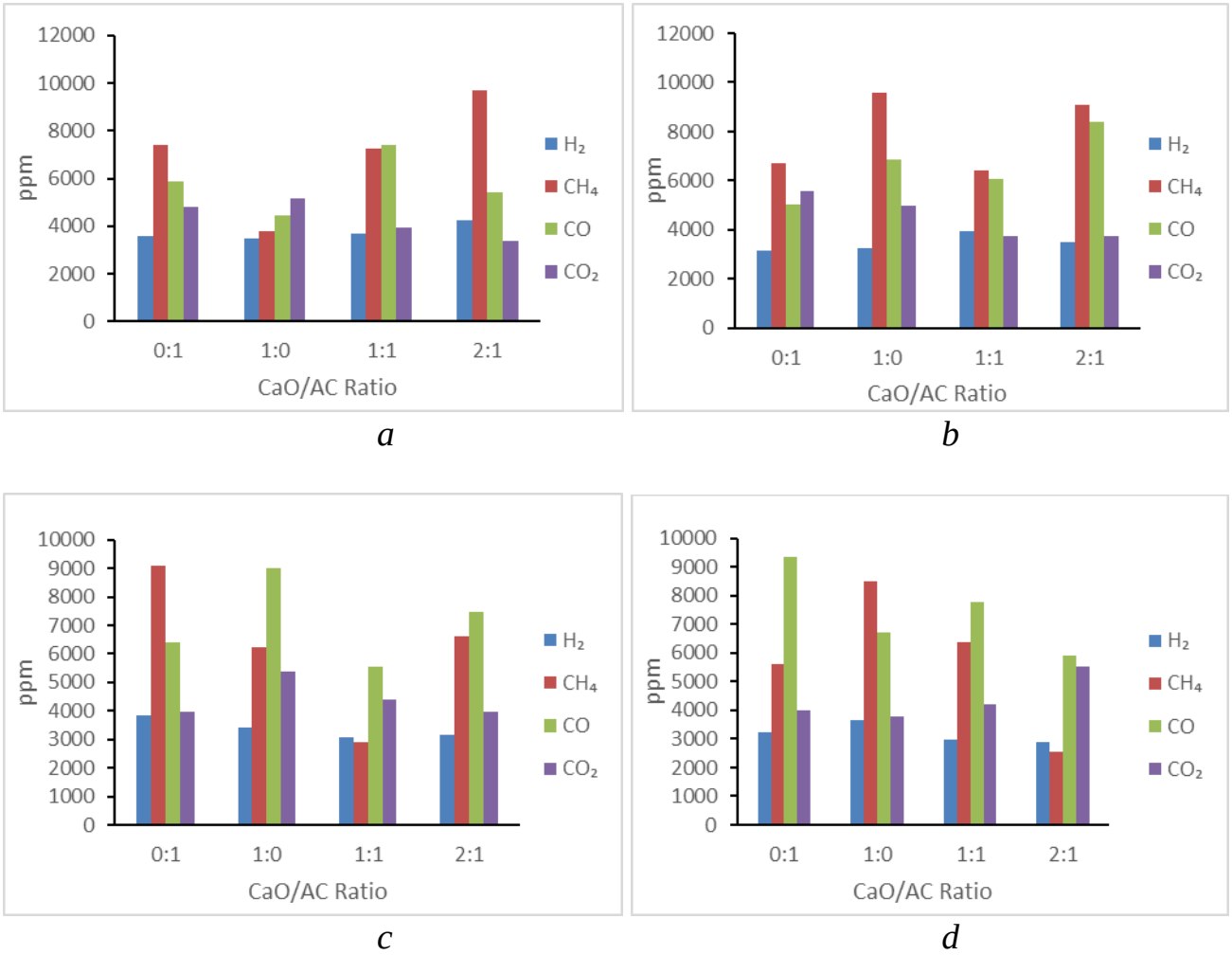


Fig. 7. Effect CaO/AC ratio with various catalyst load: *a* – 4%; *b* – 6%; *c* – 8%; *d* – 10%

At a catalyst load of 4%, the CaO/AC ratio changes the gasification reaction through differences in the dominance of tar cracking/reforming and CO_2 capture by CaO, so that the gas composition is highly dependent on the number of active sites and the effectiveness of gas-catalyst contact. At 0:1 (AC), CH_4 and CO are relatively high because AC promotes volatile/tar cracking, but CO_2 remains high because there is no

absorption. At 1:0 (CaO), CH_4 decreases but CO_2 is highest, indicating that CO_2 capture is not yet effective due to limited surface area/carbonate layer formation. The 1:1 ratio produces the highest CO with moderate CO_2, indicating CaO–AC synergy that increases the conversion of volatiles into reactive gases. Meanwhile, the 2:1 (CaO-rich) ratio provides the highest H_2 and lowest CO_2 due to the sorption-enhanced effect of CaO, but CH_4 remains high due to the smaller contribution of AC, so methane reforming/cracking is not yet optimal.

At a catalyst load of 6%, the CaO/AC ratio mainly shifts the selectivity of secondary reactions (tar cracking/reforming and CO_2 capture), where AC enhances the conversion of volatiles/light hydrocarbons, while CaO reduces CO_2 through carbonation ($CaO + CO_2 \rightarrow CaCO_3$) and changes the reaction equilibrium. At 0:1, CH_4 and CO_2 remain high because there is no CO_2 capture and methane reforming is not yet optimal, so volatiles still escape as CH_4. At 1:0, CO_2 tends to decrease, but CH_4 becomes the highest due to the absence of AC's role in cracking/reforming. The most favorable conditions occur at 1:1, with the highest H_2 and lowest CO_2, indicating CaO–AC synergy that promotes sorption-enhanced reforming and increases the conversion of hydrocarbons into syngas components. At 2:1, CO is highest and CO_2 remains low, but CH_4 rises again and H_2 is not maximized because excess CaO has the potential to rapidly carbonate/cause contact limitations, thereby reducing the contribution of AC in cracking/reforming.

At a catalyst load of 8%, the CaO/AC ratio significantly shifts the selectivity of the syngas reaction. At 0:1 (AC), CH_4 is still high because some light hydrocarbons have not been fully converted even though the tar cracking process is already active. At 1:0 (CaO), CO increases the most, but CO_2 also tends to be high, indicating that CaO in this condition is more dominant in promoting the CO formation pathway, while the CO_2 capture function is not yet optimal due to contact limitations or carbonation saturation. The 1:1 ratio produces the lowest CH_4, indicating the most effective CaO–AC synergy for cracking/reforming light hydrocarbons so that more methane is converted into reactive gas. At 2:1, CO increases again but CH_4 also rises, indicating that a smaller AC fraction reduces the intensity of methane reforming/cracking, while the decrease in CO_2 remains dependent on the effectiveness of CaO sorption.

At a catalyst load of 10%, the increase in total catalyst makes secondary reactions, reforming, solid-gas heterogeneous reactions, and equilibrium shifts very dominant, so that the CaO/AC ratio mainly determines the direction of product selectivity. At 0:1 (AC), CO formation tends to be strongest because the porous carbon surface accelerates the cracking/reforming of volatiles and the conversion of tar into reactive gases. At ratios involving CaO (1:0, 1:1, 2:1), CaO can retain CO_2 through carbonation, but at high loads the effect is often non-linear because CaO rapidly carbonates/diffusion limitations and pore blocking occur, so that under CaO-rich conditions (2:1) CH_4 can decrease, but CO_2 may increase and H_2 is not maximized due to reaction competition. Overall, at a 10% load, a trade-off is observed: AC-dominant increases CO, while CaO-

dominant suppresses light hydrocarbons but has the potential to trigger non-ideal conditions (saturation/mass transport) that reduce the benefits of H_2 and CO_2.

5. 2. 4. Syngas Low Heating Value

To calculate the LHV of syngas, it must first be converted from ppm to % volume of gas. The formula is $\%vol_i = \frac{ppmv_i}{10^4}$ to calculate the LHV, use the formula

$$LHV_{mix}\left(\frac{MJ}{Nm^3}\right) = \frac{10.8(\%H_2) + 12.63(\%CO) + 35.8(\%CH_4)}{100},$$

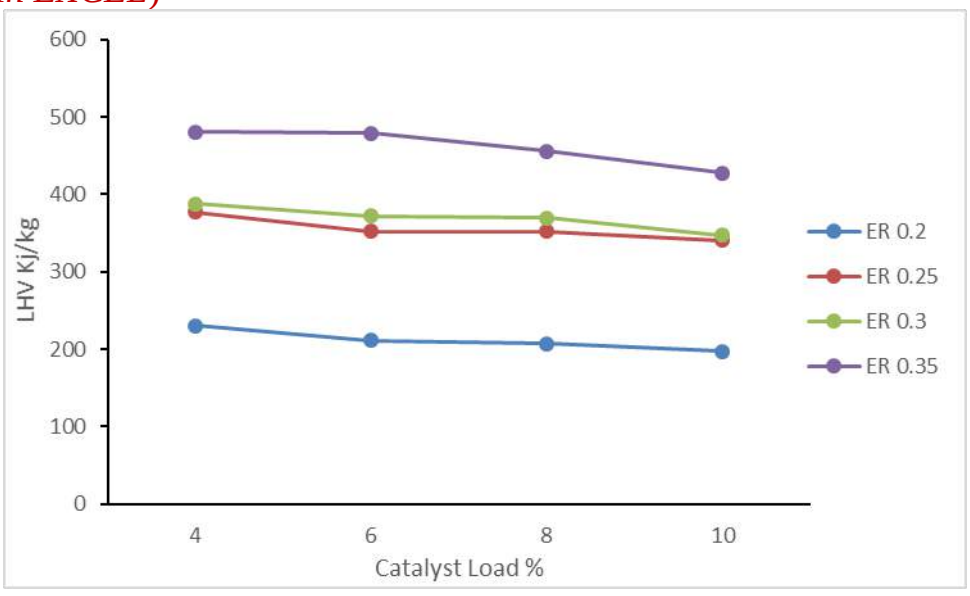
LHV H_2 = 10.8 MJ/Nm^3,

LHV CO = 12.63 MJ/Nm^3,

LHV CH_4 = 35.8 MJ/Nm^3.

As shown in Fig. 8, the syngas low heating value (LHV) varies with the equivalence ratio (ER) and catalyst load.

All experimental points in the figure are connected by straight lines. This is an incorrect presentation of the results because it means that there are no experimental errors. When displaying the results of experiments in the figures in the form of experimental points, it is necessary to carry out an approximation and indicate the approximating equations and the degree of accuracy of the approximation R^2 (*for example, you can use the "trend" tool in EXCEL*)



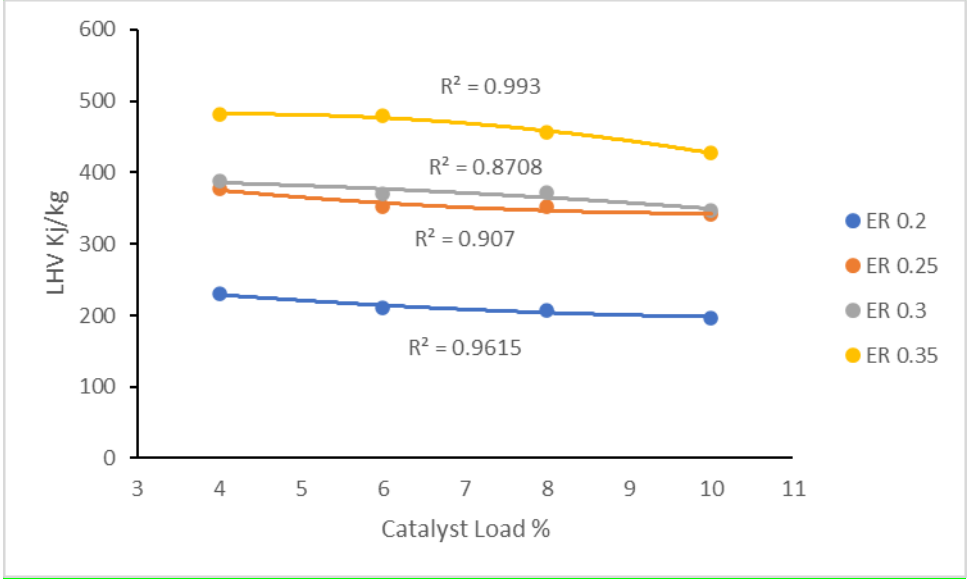


Fig. 8. Syngas low heating value with various equivalence ratio

Fig. 8 shows that the LHV value increases with the ER. At the same catalyst load of 4%, the LHV will increase in line with the increase in ER. ER 0.2 has an LHV of 230 kJ/kg and ER 0.35 has an LHV of 481 kJ/kg. Higher ER produces more intense autothermal conditions, causing the reactor temperature to rise. This increase in temperature accelerates the decomposition of volatiles and tar cracking, and promotes more complete gasification and reforming reactions, thereby increasing the fraction of permanent gases that contribute to the calorific value, mainly CO and CH_4, as well as some H_2. In addition, the increase in temperature is also associated with more effective hydrogen formation, because H_2 formation reactions (e.g., through steam-water and reforming reactions) are generally more optimal at high temperatures, with the temperature range often reported to be most conducive to H_2 formation being 800–1000°C.

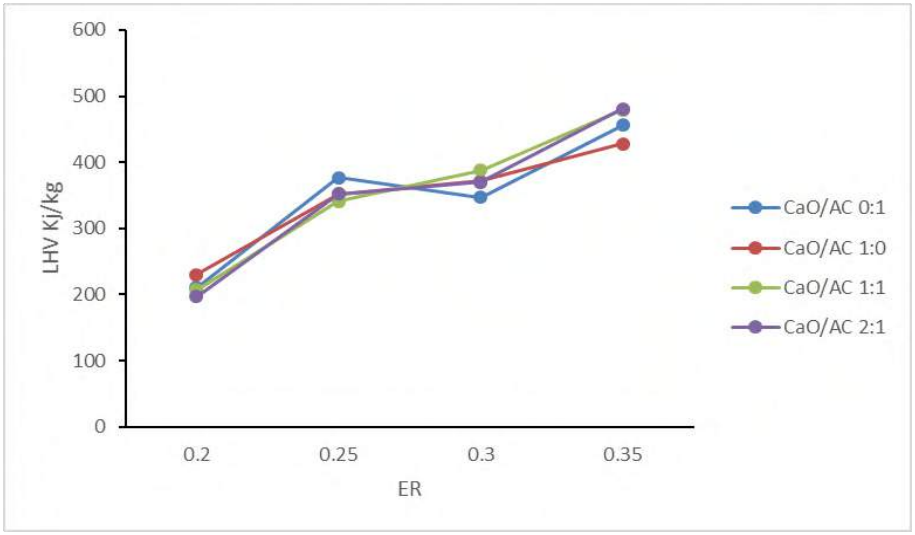
At ER 0.2, the highest LHV was obtained at a catalyst load of 4% at 230 kJ/kg and continued to decrease with increasing catalyst load to 197 kJ/kg at 10%. At ER 0.25, the highest LHV was also obtained at a catalyst load of 4% at 377 kJ/kg and also decreased to 341 kJ/kg at a catalyst load of 10%. At ER 0.3, the highest LHV was obtained at a catalyst load of 4% at 388 kJ/kg and also decreased at a catalyst load of 10% to 347 kJ/kg. At ER 0.35, the highest LHV was obtained at 481 kJ/kg and decreased at a catalyst load of 10% to 428 kJ/kg.

However, all ER values show that LHV tends to decrease when the catalyst load is increased from 4% to 10%. This decrease indicates that excessive catalyst addition under these operating conditions does not always improve gas energy quality, because the catalyst can shift the reaction selectivity towards the conversion of high calorific components especially CH_4 into CO and H_2 through reforming, while at the same time the fraction of diluent gases such as CO_2 (and steam) may increase due to reaction. Since

CH_4 has a very large calorific value contribution in the syngas mixture, the decrease in its fraction is often more dominant than the increase in CO/H_2, so that the total LHV tends to decrease.

In energy system analysis, particularly in combustion, gasification, and fuel gas utilisation processes such as syngas, the LHV value is often used because it better represents the heat energy that can actually be utilised by the system. The LHV value of a fuel gas is usually influenced by the composition of combustible gases such as carbon monoxide (CO), hydrogen (H_2), and methane (CH_4). The higher the content of these gases, the greater the LHV value produced. The LHV of syngas from this study with variations in ER and CaO/AC-PF ratio can be seen in Fig. 9.

Same remark



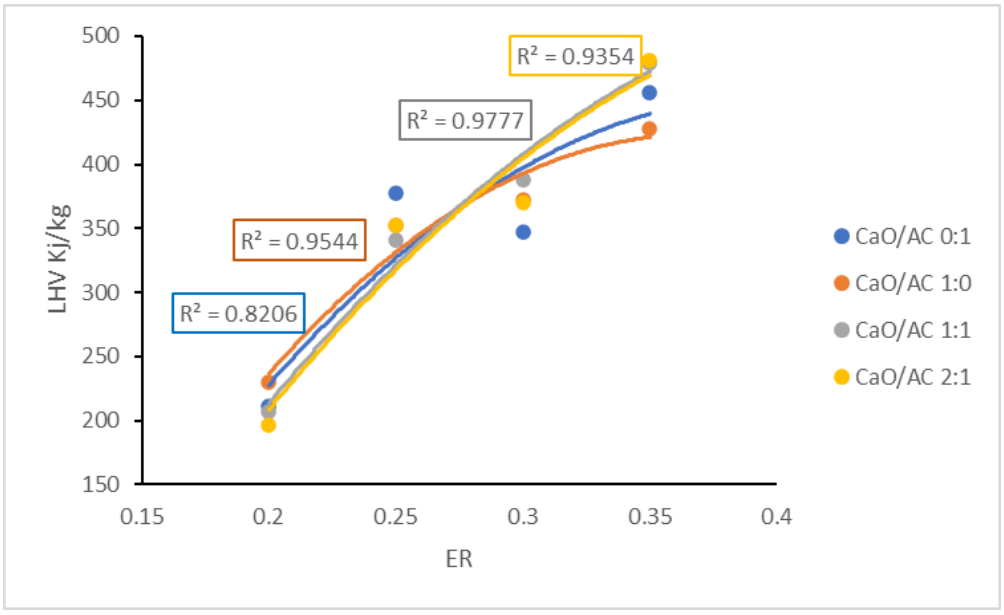


Fig. 9. Syngas Low Heating Value with Various CaO/AC Ratio

Fig. 9 shows that the LHV of syngas increases consistently with the increase in ER 0.2 to 0.35 for all CaO/AC ratios, indicating that a higher ER strengthens autothermal conditions so that the reaction temperature increases and the conversion of volatiles into syngas becomes more complete. At low ER (0.2), the difference in LHV between ratios is still small because secondary reactions such as cracking, reforming and heterogeneous reactions are not yet dominant; the system is still relatively influenced by incompletely converted volatiles. When the ER is increased to 0.25–0.30, the effect of the catalyst ratio becomes apparent: compositions involving AC tend to produce higher LHV because they accelerate tar cracking and increase the fraction of calorific gas, while the contribution of CaO can shift the reaction equilibrium through a decrease in CO_2. At the highest ER (0.35), the LHV reaches its maximum at all ratios, with CaO/AC 2:1 and 0:1 showing peak values, indicating that at high temperatures, the reactive gas formation pathway (via cracking/reforming on the carbon surface and/or CaO-rich-promoted heterogeneous reactions) becomes dominant. Overall, ER acts as the main controlling factor for LHV increase through the temperature effect, while the CaO/AC ratio modulates LHV through the balance between cracking/reforming (AC) and CO_2 control (CaO), especially at medium-high ER.

6. Discussion on the Catalytic Effect of AC-PF/CaO and Operating Conditions on Syngas Composition and LHV

The interaction of the CaO-AC-PF catalyst to improve syngas quality can be seen from the characterisation of the catalyst, the composition of the syngas and the LHV produced. From the Scanning Electron Microscopy results in Fig. 2, it can be seen that the CaO:AC-PF;2:1 catalyst (Fig. 2, *c*) appears denser than the other catalysts. With the addition of CaO, CaO particle dispersion can be seen on the white carbon surface, indicating that some micro pores are closed by CaO. With the addition of CaO, a lot of CO_2 is absorbed and becomes $CaCO_3$. This porous structure is very important in top-flow gasification because pyrolysis gas and volatiles move through the layer, so the presence of a porous medium has the potential to strengthen secondary reactions and act as carbon capture before the gas exits to the condenser.

The interaction of the CaO-AC-PF catalyst in improving syngas quality can be observed from the catalyst characterization, syngas composition, and the resulting LHV. Based on the SEM results shown in Fig. 2, the CaO:AC-PF = 2:1 catalyst (Fig. 2, *c*) appears denser than the other catalyst formulations, indicating that CaO particles were dispersed on the carbon surface and may have partially blocked some of the smaller pores. This interpretation is reasonable because CaO-based materials are widely known to act as high-temperature CO_2 sorbents, and their carbonation proceeds through the formation of $CaCO_3$. During gasification, such sorption behaviour can reduce CO_2 concentration and influence gas quality. In addition, porous carbonaceous media are known to promote tar cracking and secondary gas-phase reactions when volatile products pass through a hot solid bed. This is particularly relevant in fixed-bed gasification, where reactor design and the interaction between volatiles, char, and

catalyst strongly affect tar conversion and gasification efficiency. Therefore, the porous structure of AC-PF, together with the CO_2-capturing role of CaO, may contribute to syngas upgrading before the gas exits the reactor system.

From a surface chemistry perspective, Fourier Transform Infrared Spectroscopy (FTIR) shows the presence of –OH and calcium carbonate groups, as shown in Fig. 3. This is due to the results of KOH impregnation carried out during the manufacture of AC-PF. The presence of -OH groups functions as polar active sites capable of adsorbing polar molecules such as H_2O, CO_2, and volatile compounds. Surfaces with -OH groups tend to be hydrophilic and reactive, thereby enhancing interactions with tar compounds or heavy hydrocarbons. These tar compounds can then undergo thermal cracking or catalytic reforming into light gases such as H_2, CO, and CH_4. In addition to -OH, there are also O-H and C-O groups. The O-H group has characteristics that are almost the same as the -OH group, while the C-O group plays a role in enhancing the redox properties and chemical interactions between the carbon surface and gas molecules. In the gasification process, the C-O group can be part of the partial oxidation mechanism and carbon gasification reaction, which produces CO [25].

From a surface chemistry perspective, the Fourier Transform Infrared Spectroscopy (FTIR) results indicate the presence of O–H, C–O, and carbonate-related groups, as shown in Fig. 3. The appearance of oxygen-containing functional groups is consistent with the use of KOH during the preparation of AC-PF, since KOH activation is known to modify the surface chemistry of activated carbon and promote the formation of oxygenated groups. O–H-containing groups can act as polar active sites that enhance the interaction of the carbon surface with polar molecules such as H_2O, CO_2, and oxygenated volatile compounds. Such surface functionality may also facilitate the adsorption of tar-related species and support their further conversion through thermal cracking or reforming into lighter gases. In addition to O–H groups, the presence of C–O groups suggests that the carbon surface retains oxygen-containing functionalities that may contribute to surface reactivity and gas–solid interactions. During gasification, these surface groups may participate indirectly in oxidation–reduction interactions at the carbon surface and support the formation of combustible gases such as CO. The carbonate-related bands may also indicate the presence of calcium-containing carbonate species, which is consistent with the CO_2-capturing function of CaO during the gasification process.

The BET data in Fig. 4 shows that the surface area decreased to 5.06 m^2/g, but the pore diameter increased to a mesopore scale of 22.87 nm, which can improve the accessibility of volatiles to active sites and improve mass transport in the reforming reaction. In Fig. 4, *b*, the BJH curve at CaO:AC-PF = 2:1 shows the highest dV/dD values of 30–40 nm, indicating a catalyst in the mesopore size range. The presence of these mesopores will further increase the active sites for CO_2 adsorption.

The BET results presented in Fig. 4 show that the specific surface area decreased to 5.06 m^2/g, while the average pore diameter increased to 22.87 nm, corresponding to the mesopore range. This change suggests that, although the surface area became lower, the

larger pore structure may improve the accessibility of volatile compounds to active sites and enhance mass transport during reforming reactions. In Fig. 4, *b*, the BJH pore size distribution of the CaO:AC-PF = 2:1 catalyst shows the highest dV/dD values in the pore diameter range of 30–40 nm, confirming the dominance of mesopores in this catalyst. The presence of these mesopores may facilitate gas diffusion and improve contact between gaseous species and the catalyst surface, which can contribute to CO_2 adsorption and syngas upgrading during gasification.

From a process perspective, in Fig. 5, ER appears as the dominant variable that regulates autothermal conditions, primarily through an increase in effective temperature and secondary reaction intensity. An increase in ER from low to high levels consistently increases H_2, which can be explained by the acceleration of H_2 formation reactions such as charcoal gasification with steam ($C + H_2O \rightarrow CO + H_2$) [26], light hydrocarbon reforming, and more intense tar cracking at high temperatures. At the same time, CH_4 also increases sharply at high ER, indicating that in an autothermal upflow system, increased temperature and changes in gas composition can facilitate the formation of light gases. Meanwhile, CO tends to peak at moderate ER and then decreases at high ER, consistent with competition between CO formation and CO consumption through subsequent reactions such as methanation [27]. The decrease in CO_2 at high ER indicates the role of high temperatures in enhancing the reduction of CO_2 by charcoal (Boudouard reaction) and/or the role of CaO adsorption if available.

The effect of catalyst loading in Fig. 6 shows that adding catalyst does not always increase H_2. Increasing the catalyst loading from low to high tends to reduce H_2 and CH_4 but increase CO. Mechanistically, this condition can occur when the catalyst strengthens pathways that increase CO and/or promotes RWGS ($CO_2 + H_2 \rightarrow CO + H_2O$) [28], which consumes H_2 so that net H_2 is reduced. Furthermore, at high catalyst loadings, the possibility of diffusion/aggregation penalties increases, so that selectivity may shift and some active sites become less effective. Therefore, the target of H_2-rich synthesis gas in this reactor is more dependent on ER adjustment and the selection of moderate/low catalyst loadings, rather than simply increasing the loading.

The CaO/AC-PF ratio in Fig. 7 shows synergistic but non-linear behaviour. AC-PF plays a major role as a porous medium that enhances the cracking/reforming process of volatile compounds, while CaO provides a basic site and CO_2 absorber to shift the equilibrium. At high CaO ratios, sorption and base effects may increase, but the risk of micro-pore closure and diffusion pathway changes also increases. This explains why certain compositions are optimal at certain catalyst loads: the best performance arises from a balance between pore accessibility (the role of AC-PF) and sorption/base strength (the role of CaO).

From an energy quality perspective, in Fig. 8, 9, the LHV value of synthetic gas is highly sensitive to changes in CH_4. Therefore, high ER conditions that increase CH_4 tend to increase LHV. H_2, CH_4 and CO are the main factors for obtaining high LHV. CO_2 has no calorific value so it must be captured. In this study, CaO was used so that CO_2 could be suppressed, meaning that the total LHV could be increased. The highest

LHV in this study was 481 kJ/kg, while in another study, the highest was 550 kJ/kg using pinewood with dolomite, activated carbon, silica gel, and limestone catalysts [29]. The higher the ER, the more oxygen enters the system, thereby increasing the reforming reaction [30].

In comparison with the literature reviewed in this research, the present study demonstrates a comparable qualitative trend, particularly in showing that catalyst-assisted updraft gasification can improve syngas composition and energy quality. For example, previous studies reported that dolomite-assisted rice husk gasification increased H_2 content up to 15.4 mol% with an LHV of 5.1 MJ/Nm³, while other updraft gasification systems with catalytic enhancement also showed improved hydrogen-rich syngas production and higher heating values. In the present study, the highest syngas LHV reached 481 kJ/kg under the investigated conditions, indicating that the CaO/AC-PF catalyst system was effective in improving gas quality, although the absolute value remains influenced by the use of corncob feedstock, the small-scale reactor design, and the sensor-based gas measurement approach. Therefore, the present results support the view that the combined CaO/AC-PF catalyst is a promising low-cost alternative for syngas upgrading, particularly for agricultural biomass gasification in simple updraft systems.

In practical terms, the present study is relevant to the development of low-cost biomass gasification systems that can utilize locally available agricultural residues and catalyst materials. Corncob is an abundant agricultural by-product, while CaO and palm-fiber-derived activated carbon can be prepared from relatively inexpensive and accessible resources. Therefore, the proposed catalyst system has practical potential for application in small-scale updraft gasifiers, particularly in agricultural areas where simple and affordable waste-to-energy technologies are needed. The syngas produced from such systems may be used directly as a combustible gas for thermal applications, such as drying, heating, or small-scale energy generation, and also has potential as an intermediate gas for further upgrading or conversion into other value-added energy and chemical products.

There are several limitations to this study. First, the gas composition was obtained from an MQ sensor based on ppm, so absolute accuracy may be affected by cross-sensitivity, humidity, sensor drift, and gas sampling temperature; this may affect the estimation of %vol and LHV, especially when changes in CO and CH_4 occur simultaneously. Second, catalyst characterisation (SEM-FTIR-BET) supports the role of surface texture and chemistry, but has not quantified changes in the active phase during operation, the degree of carbonation, and the decrease in activity due to pore closure accumulation.

The disadvantage of this research is that the CaO catalyst reacts very easily with CO_2. After the calcination process, CaO must be stored in an airtight container to prevent it from clumping into $CaCO_3$. The catalyst has a specific usage period because it is covered with tar or ash.

Based on these limitations, several future directions are recommended. Calibrate the gas composition using GC-TCD/GC-FID to convert the sensor readings into more accurate %vol and include LHV uncertainty analysis. Evaluate catalyst stability and regeneration, especially for CaO which is easily carbonated, through carbonation-calcination cycle tests and post-reaction characterisation (XRD/TGA/SEM-EDX) to assess phase changes and activity loss. Develop experimental designs towards ANOVA or RSM interactions so that interaction effects and predictive models can be obtained and verified through replication confirmation tests. Add process performance metrics such as gas yield (Nm^3/kg), cold gas efficiency, pressure drop, and air consumption so that 'syngas quality improvement' can be demonstrated based on mass-energy balance and operability, not just composition.

7. Conclusion

1. The present study demonstrated that the CaO/AC-PF catalyst system has potential to improve syngas quality in corncob updraft gasification. Catalyst characterization by SEM, FTIR, and BET showed that the combined catalyst possessed modified surface morphology, oxygen-containing functional groups, carbonate-related species, and mesoporous characteristics, with the CaO:AC-PF = 2:1 catalyst showing a specific surface area of 5.06 m^2/g and an average pore diameter of 22.87 nm. These characteristics indicate that the catalyst structure was altered in a way that may support gas–solid interaction during gasification.

2. The gasification experiments confirmed that equivalence ratio, catalyst loading, and CaO/AC ratio influenced syngas composition and heating value. Increasing ER from 0.20 to 0.35 increased H_2 concentration from 3150 to 3914 ppm and CH_4 concentration from 3093 to 9221 ppm, while the syngas LHV increased from 230 to 481 kJ/Nm^3. In terms of catalyst loading, increasing the loading from 4 wt.% to 10 wt.% decreased H_2 from 3742 to 3176 ppm and CH_4 from 7031 to 5746 ppm, while CO increased from 5782 to 7445 ppm. These results indicate that syngas quality was affected by the balance between catalytic activity, pore accessibility, and CO_2 sorption behaviour.

Conflict of interest

The authors declare that they have no conflict of interest in relation to this research, whether financial, personal, authorship or otherwise, that could affect the research and its results presented in this paper.

Financing

The authors sincerely thank the Ministry of Education, Culture, Research and Technology, Republic of Indonesia for fully supporting this research through the DRTPM Research Grant under Fundamental Research, Universitas Widyagama Malang, Indonesia 2025 (Grant Number:128/C3/DT.05.00/PL/2025;023/LL7/DT.05.00/PL/2025;010/ Kontrak/PT/PTS.030.7/PN/V/2025).

Data availability

Manuscript has no associated data.

Use of artificial intelligence

The authors used the AI-based language model ChatGPT (GPT-5.3) only to assist in improving the clarity of English language and grammar in several sections of the manuscript, particularly in the Introduction and Literature Review sections.

The AI tool was used solely for language editing and paraphrasing purposes. All scientific content, experimental design, data analysis, and interpretation of the results were conducted entirely by the authors.

The authors carefully reviewed and verified all AI-assisted text to ensure accuracy and consistency with the experimental results. The use of AI tools did not influence the scientific conclusions of this study.

Acknowledgements

We as the Research Team would like to thank Ministry of Education, Culture, Research and Technology, Republic of Indonesia (Kemendiktisaintek Indonesia) for financing research activities.

Authors' contributions

Purbo Suwandono: Conceptualization, Writing-original draft, Investigation, Supervision, Formal analysis, Writing – review & editing; **Widya Wijayanti**: Validation, Investigation, Data Curation, Formal analysis, Writing – original draft; **Nova Risdiyanto Ismail**: Writing – review & editing, Formal analysis; **Dzulfikar Johan Akbar:** Visualization, Writing – original draft, Data curation; **Muhammad Reza**: Project administration, Resources, Data curation.

References

1. V. K. Yadav *et al.*, “Emerging trends in the valorization of agricultural waste and their utilization in agricultural, pharmaceuticals, and environmental cleanup,” *Waste and Biomass Valorization*, pp. 1–55, 2025. DOI:10.1007/s12649-025-03002-y
2. W. M. Lewandowski, M. Ryms, and W. Kosakowski, “Thermal biomass conversion: A review,” *Processes*, vol. 8, no. 5, p. 516, 2020. https://doi.org/10.3390/pr8050516
3. D. Ariyanti *et al.*, “Valorization of corn cob waste for furfural production: A circular economy approach,” *Biomass and Bioenergy*, vol. 194, p. 107665, 2025. DOI:10.1016/j.biombioe.2025.107665
4. J. Zhang, Z. Chu, R. Cao, X. Wu, and K. Han, “A review of resource recovery from waste plastics via pyrolysis and gasification,” *Fuel*, vol. 404, p. 136319, 2026. https://doi.org/10.1016/j.fuel.2025.136319
5. Y. Tangke Tosuli, Cahyadi, H. Dafiqurrohman, R. Hermawan, and A.

Surjosatyo, “Gasification of sago dreg waste in a top-lit updraft fixed bed gasifier: Syngas composition and its effect with additional Al2O3 as catalyst,” *Energy Convers. Manag. X*, vol. 24, no. October, p. 100775, 2024, doi: 10.1016/j.ecmx.2024.100775. https://doi.org/10.1016/j.ecmx.2024.100775

6. P. Dinh *et al.*, “Enrichment of hydrogen in product gas from a pilot-scale rice husk updraft gasification system,” *Carbon Resour. Convers.*, vol. 5, no. 3, pp. 231–239, 2025, doi: 10.1016/j.crcon.2022.07.003.

7. S. Yousef and J. Eimontas, “International Journal of Hydrogen Energy Oxygen updraft gasification-catalytic reforming of cigarettes butts for hydrogen-rich syngas production,” vol. 171, no. May, 2025, https://doi.org/10.1016/j.ijhydene.2025.150650

8. D. Contreras, E. Blanco, and D. Travieso, “Experimental assessment of the energy potential of pellets produced from beekeeping wastes by updraft gasification,” vol. 343, no. January, 2025, https://doi.org/10.1016/j.enconman.2025.120206

9. N. Yesilova, O. Tezer, A. Ongen, and A. Ayol, “International Journal of Hydrogen Energy Enhancing biomass gasification : A comparative study of catalyst applications in updraft and modifiable-downdraft fixed bed reactors,” *Int. J. Hydrogen Energy*, vol. 76, no. April, pp. 290–303, 2024, https://doi.org/10.1016/j.ijhydene.2024.05.075

10. R. Skvor and A. Jan, “Experimental investigation of sorted municipal solid wastes producer gas composition in an updraft fixed bed gasifier,” vol. 289, no. August 2022, 2024, https://doi.org/10.1016/j.energy.2023.130063

11. R. Junga, M. Tańczuk, S. Sobek, M. Chabiński, and Ł. Ziółkowski, “Effect of the addition of laying hens manure to the straw on gasification efficiency in updraft gasifier under air atmosphere,” *Appl. Therm. Eng.*, vol. 226, no. February, p. 120269, 2023, https://doi.org/10.1016/j.applthermaleng.2023.120269.

12. A. Ongen and A. Ayol, “ScienceDirect Gasification performance of olive pomace in updraft and downdraft fixed bed reactors,” vol. I, 2023, https://doi.org/10.1016/j.ijhydene.2023.02.088

13. K. Ertas, “Gasification of MDF residue in an updraft fixed bed gasifier to produce heat and power via an ORC turbine,” vol. 169, no. February, pp. 43–51, 2023, https://doi.org/10.1016/j.wasman.2023.06.025

14. S. Gorthy, S. Verma, N. Sinha, S. Shetty, H. Nguyen, and M. Neurock, “Theoretical Insights into the Effects of KOH Concentration and the Role of OH–in the Electrocatalytic Reduction of CO2 on Au,” *ACS Catal.*, vol. 13, no. 19, pp. 12924–12940, 2023. DOI:10.1021/acscatal.2c06115

15. X. Wang, W. Zeng, C. Xin, X. Kong, X. Hu, and Q. Guo, “The development of activated carbon from corncob for CO2 capture,” *RSC Adv.*, vol. 12, no. 51, pp. 33069–33078, 2022, https://doi.org/10.1039/D2RA05979G

16. B. Zhou *et al.*, “Insights into effects of grain boundary engineering in composite metal oxide catalysts for improving catalytic performance,” *J. Colloid Interface Sci.*, vol. 653, pp. 1177–1187, 2024. https://doi.org/10.1016/j.jcis.2023.09.148

17. Y. Zhu *et al.*, “Preparation of hierarchically porous carbon ash composite material from fine slag of coal gasification and ash slag of biomass combustion for CO2 capture,” *Sep. Purif. Technol.*, vol. 330, p. 125452, 2024. https://doi.org/10.1016/j.seppur.2023.125452

18. M. Ilić *et al.*, “Surface functional groups and degree of carbonization of *selected* chars from different processes and feedstock,” *PLoS One*, vol. 17, no. 11, p. e0277365, 2022. https://doi.org/10.1371/journal.pone.0277365

19. R. Ali, Z. Aslam, R. A. Shawabkeh, A. Asghar, and I. A. Hussein, “BET, FTIR, and RAMAN characterizations of activated carbon from waste oil fly ash,” *Turkish J. Chem.*, vol. 44, no. 2, pp. 279–295, 2020. doi: 10.3906/kim-1909-20

20. K. J. Stanienda-Pilecki, “The importance of Fourier-Transform Infrared Spectroscopy in the identification of carbonate phases differentiated in magnesium content,” 2019.

21. F. Dai, Q. Zhuang, G. Huang, H. Deng, and X. Zhang, “Infrared spectrum characteristics and quantification of OH groups in coal,” *ACS omega*, vol. 8, no. 19, pp. 17064–17076, 2023. https://doi.org/10.1021/acsomega.3c01336

22. E. M. de Salazar Martínez, M. F. Alexandre-Franco, A. J. Nieto-Sanchez, and E. M. Cuerda-Correa, “Exploring the role of surface and porosity in CO2 capture by CaO-based adsorbents through response surface methodology (RSM) and artificial neural networks (ANN),” *J. CO2 Util.*, vol. 83, p. 102773, 2024. https://doi.org/10.1016/j.jcou.2024.102773

23. J. A. Tavizón-Pozos, H. Cervantes-Cuevas, G. G. Garcia-Camacho, G. Chavez-Esquivel, and D. R. Acosta-Najarro, “Biodiesel Production Using K–Sr/CaO and CaO Catalysts Derived from Eggshells by Canola Oil Transesterification,” *ACS omega*, vol. 10, no. 7, pp. 6827–6838, 2025. https://doi.org/10.1021/acsomega.4c09118

24. W. Koo-Amornpattana, P. Phadungbut, N. Kunthakudee, W. Jonglertjunya, S. Ratchahat, and M. Hunsom, “Innovative metal oxides (CaO, SrO, MgO) impregnated waste-derived activated carbon for biohydrogen purification,” *Sci. Rep.*, vol. 13, no. 1, p. 4705, 2023. DOI:10.1038/s41598-023-31723-4

25. C. Quan, M. Wang, N. Gao, T. Yang, and R. Li, “In situ adsorption of CO2 to enhance biomass gasification for hydrogen production using Ca/Ni based composites,” *J. Energy Inst.*, vol. 108, p. 101229, 2023, doi: https://doi.org/10.1016/j.joei.2023.101229. https://doi.org/10.1016/j.joei.2023.101229

26. F. Micheli, E. Mattucci, C. Courson, and K. Gallucci, “Bi-Functional Catalyst/Sorbent for a H2-Rich Gas from Biomass Gasification,” 2021. doi: 10.3390/pr9071249. DOI:10.3390/PR9071249

27. M. Zhu, Q. Wang, and S. Wang, “Recent Advances and Future Perspectives in Catalyst Development for Efficient and Sustainable Biomass Gasification: A Comprehensive Review,” 2025, https://doi.org/10.3390/su17167370

28. N. Cerone, F. Zimbardi, L. Contuzzi, J. Baleta, and D. Cerinski, “Experimental investigation of syngas composition variation along updraft fixed bed gasifier,” *Energy Convers. Manag.*, vol. 221, no. July, p. 113116, 2020,

https://doi.org/10.1016/j.enconman.2020.113116
29. R. Mohanty, P. Mahanta, A. Mahapatro, and R. Prakash, "Catalytic gasification of pinewood biomass in a fluidized bed reactor with dolomite , limestone , and activated carbon : An experimental study," *Energy*, vol. 325, no. April, p. 136131, 2025, doi: 10.1016/j.energy.2025.136131. https://doi.org/10.1016/j.energy.2025.136131
30. C. Liu, Y. Huang, M. Niu, and H. Pei, "ScienceDirect Influences of equivalence ratio , oxygen concentration and fluidization velocity on the characteristics of oxygen-enriched gasification products from biomass in a pilot-scale fluidized bed," *Int. J. Hydrogen Energy*, vol. 43, no. 31, pp. 14214–14225, 2018, https://doi.org/10.1016/j.ijhydene.2018.05.154

References

1. V. K. Yadav *et al.*, "Emerging trends in the valorization of agricultural waste and their utilization in agricultural, pharmaceuticals, and environmental cleanup," *Waste and Biomass Valorization*, pp. 1–55, 2025. DOI:10.1007/s12649-025-03002-y
2. W. M. Lewandowski, M. Ryms, and W. Kosakowski, "Thermal biomass conversion: A review," *Processes*, vol. 8, no. 5, p. 516, 2020. https://doi.org/10.3390/pr8050516
3. D. Ariyanti *et al.*, "Valorization of corn cob waste for furfural production: A circular economy approach," *Biomass and Bioenergy*, vol. 194, p. 107665, 2025. DOI:10.1016/j.biombioe.2025.107665
4. J. Zhang, Z. Chu, R. Cao, X. Wu, and K. Han, "A review of resource recovery from waste plastics via pyrolysis and gasification," *Fuel*, vol. 404, p. 136319, 2026. https://doi.org/10.1016/j.fuel.2025.136319
5. Y. Tangke Tosuli, Cahyadi, H. Dafiqurrohman, R. Hermawan, and A. Surjosatyo, "Gasification of sago dreg waste in a top-lit updraft fixed bed gasifier: Syngas composition and its effect with additional Al2O3 as catalyst," *Energy Convers. Manag. X*, vol. 24, no. October, p. 100775, 2024, doi: 10.1016/j.ecmx.2024.100775. https://doi.org/10.1016/j.ecmx.2024.100775
6. P. Dinh *et al.*, "Enrichment of hydrogen in product gas from a pilot-scale rice husk updraft gasification system," *Carbon Resour. Convers.*, vol. 5, no. 3, pp. 231–239, 2025, doi: 10.1016/j.crcon.2022.07.003.
7. S. Yousef and J. Eimontas, "International Journal of Hydrogen Energy Oxygen updraft gasification-catalytic reforming of cigarettes butts for hydrogen-rich syngas production," vol. 171, no. May, 2025, https://doi.org/10.1016/j.ijhydene.2025.150650
8. D. Contreras, E. Blanco, and D. Travieso, "Experimental assessment of the energy potential of pellets produced from beekeeping wastes by updraft gasification," vol. 343, no. January, 2025, https://doi.org/10.1016/j.enconman.2025.120206
9. N. Yesilova, O. Tezer, A. Ongen, and A. Ayol, "International Journal of Hydrogen Energy Enhancing biomass gasification : A comparative study of catalyst applications in updraft and modifiable-downdraft fixed bed reactors," *Int. J. Hydrogen*

Energy, vol. 76, no. April, pp. 290–303, 2024, https://doi.org/10.1016/j.ijhydene.2024.05.075

10. R. Skvor and A. Jan, "Experimental investigation of sorted municipal solid wastes producer gas composition in an updraft fixed bed gasifier," vol. 289, no. August 2022, 2024, https://doi.org/10.1016/j.energy.2023.130063

11. R. Junga, M. Tańczuk, S. Sobek, M. Chabiński, and Ł. Ziółkowski, "Effect of the addition of laying hens manure to the straw on gasification efficiency in updraft gasifier under air atmosphere," *Appl. Therm. Eng.*, vol. 226, no. February, p. 120269, 2023, https://doi.org/10.1016/j.applthermaleng.2023.120269.

12. A. Ongen and A. Ayol, "ScienceDirect Gasification performance of olive pomace in updraft and downdraft fixed bed reactors," vol. I, 2023, https://doi.org/10.1016/j.ijhydene.2023.02.088

13. K. Ertas, "Gasification of MDF residue in an updraft fixed bed gasifier to produce heat and power via an ORC turbine," vol. 169, no. February, pp. 43–51, 2023, https://doi.org/10.1016/j.wasman.2023.06.025

14. S. Gorthy, S. Verma, N. Sinha, S. Shetty, H. Nguyen, and M. Neurock, "Theoretical Insights into the Effects of KOH Concentration and the Role of OH–in the Electrocatalytic Reduction of CO2 on Au," *ACS Catal.*, vol. 13, no. 19, pp. 12924–12940, 2023. DOI:10.1021/acscatal.2c06115

15. X. Wang, W. Zeng, C. Xin, X. Kong, X. Hu, and Q. Guo, "The development of activated carbon from corncob for CO2 capture," *RSC Adv.*, vol. 12, no. 51, pp. 33069–33078, 2022, https://doi.org/10.1039/D2RA05979G

16. B. Zhou *et al.*, "Insights into effects of grain boundary engineering in composite metal oxide catalysts for improving catalytic performance," *J. Colloid Interface Sci.*, vol. 653, pp. 1177–1187, 2024. https://doi.org/10.1016/j.jcis.2023.09.148

17. Y. Zhu *et al.*, "Preparation of hierarchically porous carbon ash composite material from fine slag of coal gasification and ash slag of biomass combustion for CO2 capture," *Sep. Purif. Technol.*, vol. 330, p. 125452, 2024. https://doi.org/10.1016/j.seppur.2023.125452

18. M. Ilić *et al.*, "Surface functional groups and degree of carbonization of *selected* chars from different processes and feedstock," *PLoS One*, vol. 17, no. 11, p. e0277365, 2022. https://doi.org/10.1371/journal.pone.0277365

19. R. Ali, Z. Aslam, R. A. Shawabkeh, A. Asghar, and I. A. Hussein, "BET, FTIR, and RAMAN characterizations of activated carbon from waste oil fly ash," *Turkish J. Chem.*, vol. 44, no. 2, pp. 279–295, 2020. doi: 10.3906/kim-1909-20

20. K. J. Stanienda-Pilecki, "The importance of Fourier-Transform Infrared Spectroscopy in the identification of carbonate phases differentiated in magnesium content," 2019.

21. F. Dai, Q. Zhuang, G. Huang, H. Deng, and X. Zhang, "Infrared spectrum characteristics and quantification of OH groups in coal," *ACS omega*, vol. 8, no. 19, pp. 17064–17076, 2023. https://doi.org/10.1021/acsomega.3c01336

22. E. M. de Salazar Martínez, M. F. Alexandre-Franco, A. J. Nieto-Sanchez,

and E. M. Cuerda-Correa, “Exploring the role of surface and porosity in CO2 capture by CaO-based adsorbents through response surface methodology (RSM) and artificial neural networks (ANN),” *J. CO2 Util.*, vol. 83, p. 102773, 2024. https://doi.org/10.1016/j.jcou.2024.102773

23. J. A. Tavizón-Pozos, H. Cervantes-Cuevas, G. G. Garcia-Camacho, G. Chavez-Esquivel, and D. R. Acosta-Najarro, “Biodiesel Production Using K–Sr/CaO and CaO Catalysts Derived from Eggshells by Canola Oil Transesterification,” *ACS omega*, vol. 10, no. 7, pp. 6827–6838, 2025. https://doi.org/10.1021/acsomega.4c09118

24. W. Koo-Amornpattana, P. Phadungbut, N. Kunthakudee, W. Jonglertjunya, S. Ratchahat, and M. Hunsom, “Innovative metal oxides (CaO, SrO, MgO) impregnated waste-derived activated carbon for biohydrogen purification,” *Sci. Rep.*, vol. 13, no. 1, p. 4705, 2023. DOI:10.1038/s41598-023-31723-4

25. C. Quan, M. Wang, N. Gao, T. Yang, and R. Li, “In situ adsorption of CO2 to enhance biomass gasification for hydrogen production using Ca/Ni based composites,” *J. Energy Inst.*, vol. 108, p. 101229, 2023, doi: https://doi.org/10.1016/j.joei.2023.101229. https://doi.org/10.1016/j.joei.2023.101229

26. F. Micheli, E. Mattucci, C. Courson, and K. Gallucci, “Bi-Functional Catalyst/Sorbent for a H2-Rich Gas from Biomass Gasification,” 2021. doi: 10.3390/pr9071249. DOI:10.3390/PR9071249

27. M. Zhu, Q. Wang, and S. Wang, “Recent Advances and Future Perspectives in Catalyst Development for Efficient and Sustainable Biomass Gasification: A Comprehensive Review,” 2025, https://doi.org/10.3390/su17167370

28. N. Cerone, F. Zimbardi, L. Contuzzi, J. Baleta, and D. Cerinski, “Experimental investigation of syngas composition variation along updraft fixed bed gasifier,” *Energy Convers. Manag.*, vol. 221, no. July, p. 113116, 2020, https://doi.org/10.1016/j.enconman.2020.113116

29. R. Mohanty, P. Mahanta, A. Mahapatro, and R. Prakash, “Catalytic gasification of pinewood biomass in a fluidized bed reactor with dolomite , limestone , and activated carbon : An experimental study,” *Energy*, vol. 325, no. April, p. 136131, 2025, doi: 10.1016/j.energy.2025.136131. https://doi.org/10.1016/j.energy.2025.136131

30. C. Liu, Y. Huang, M. Niu, and H. Pei, “ScienceDirect Influences of equivalence ratio , oxygen concentration and fluidization velocity on the characteristics of oxygen-enriched gasification products from biomass in a pilot-scale fluidized bed,” *Int. J. Hydrogen Energy*, vol. 43, no. 31, pp. 14214–14225, 2018, https://doi.org/10.1016/j.ijhydene.2018.05.154

Author’s order	First Name	Middle name	Second Name
1	*Purbo*		*Suwandono*
2	*Widya*		*Wijayanti*
3	*Nova*	*Risdiyanto*	*Ismail*
4	*Dzulfikar*	*Johan*	*Akbar*

5	*Muhammad*		*Reza*

English

Purbo Suwandono
Corresponding author
Master
Department of Mechanical Engineering
Widya Gama University
Borobudur str., 35, Malang, Indonesia, 65142
E-mail: purbo@widyagama.ac.id
ORCID: https://orcid.org/0000-0003-4085-1291
Contact phone: +6282132697144
Number of publications in national journals indexed (approximate; for Ukraine citizens only): -
Number of publications in international journals indexed (approximate): 14
H-index by Scopus (if available): 4
ResearchGate: https://www.researchgate.net/profile/Purbo-Suwandono
Scopus ID: 57204187970
Researcher ID: https://researchid.co/rid80879

Widya Wijayanti
PhD
Department of Mechanical Engineering
Brawijaya University
Veteran str., 10–11, Malang, Indonesia, 65145
E-mail: widya_dinata@ub.ac.id
ORCID: https://orcid.org/0000-0003-4215-5943
Contact phone: +6285334992164
Number of publications in national journals indexed (approximate; for Ukraine citizens only): -
Number of publications in international journals indexed (approximate): 78
H-index by Scopus (if available): 12
ResearchGate: https://www.researchgate.net/profile/Widya-Wijayanti
Scopus ID: 36006672800
Researcher ID: -

Nova Risdiyanto Ismail
PhD
Department of Mechanical Engineering
Widya Gama University
Borobudur str., 35, Malang, Indonesia, 65142

E-mail: nova@widyagama.ac.id
ORCID: https://orcid.org/0000-0001-8439-6919
Contact phone:
Number of publications in national journals indexed (approximate; for Ukraine citizens only): -
Number of publications in international journals indexed (approximate): 7
H-index by Scopus (if available): 3
ResearchGate: https://www.researchgate.net/profile/Nova-Ismail-2
Scopus ID: 57204527065
Researcher ID: https://researchid.co/rid80876

Dzulfikar Johan Akbar
Master Student
Department of Mechanical Engineering
Brawijaya University
Veteran str., 10–11, Malang, Indonesia, 65145
E-mail: johanakbar@student.ub.ac.id
ORCID: https://orcid.org/0009-0002-4652-8516
Contact phone: +6282241116998
Number of publications in national journals indexed (approximate; for Ukraine citizens only): -
Number of publications in international journals indexed (approximate): -
H-index by Scopus (if available): -
ResearchGate: https://www.researchgate.net/profile/Dzulfikar-Johan-Akbar
Scopus ID: -
Researcher ID: -

Muhammad Reza
Bachelor Student
Department of Mechanical Engineering
Widya Gama University
Borobudur str., 35, Malang, Indonesia, 65142
E-mail: muhapanjangreza@gmail.com
ORCID: https://orcid.org/0009-0009-9258-0586
Contact phone: +6282139682566
Number of publications in national journals indexed (approximate; for Ukraine citizens only): -
Number of publications in international journals indexed (approximate): -
H-index by Scopus (if available): -
ResearchGate: -
Scopus ID: -

Researcher ID: -

Name of reviewer: Prof. Dr. Muji Setiyo, ST., MT.
Professor: Mechanical Engineering
Tel: +6281211020288
E-mail: muji@unimma.ac.id.
Work address: Universitas Muhammadiyah Magelang

Name of reviewer: Prof. Dr. Eng. Nurkholis Hamidi, ST., MT.
Professor: Mechanical Engineering
Tel: +62 81259293165
E-mail: hamidy@ub.ac.id
Work address: Brawijaya University

LAST CORRECTION
LAYOUT EDITOR

8 April 2026

Purbo Suwandono <purbo@widyagama.ac.id>

from EEJET - please correct the comments from the layout editor (last correction, please execute promptly)

7 messages

Oksana Nikitina <0661966nauka@gmail.com> Wed, Apr 8, 2026 at 10:54 AM
To: Purbo Suwandono <purbo@widyagama.ac.id>

Good afternoon,

The article was accepted for consideration of the possibility of publication in (No.2(140).2026).

Please revise your comments in the article (please make changes only in the layout editor's file); the editor has highlighted all necessary edits. Additionally, please send an archive containing all source files of your illustrations, created in the original software.

Please provide an edited version of the article **by 09.04.2026.**

We work 24/7 and are ready to help you around the clock!

With best regards, Manager Yu. Prylutska
TECHNOLOGY CENTER GROUP LTD
Viber/ WhatsApp/ Telegram: +380 (50) 3033801
Editorial staff of the "Eastern-European Journal of Enterprise Technologies."
Website: https://jet.com.ua/en/, http://journals.uran.ua/eejet/



Відвідати сайт



Відвідати сайт

Attention! The author (team of authors) submitting the manuscript to the editorial office of the journal **«Eastern-European Journal of Enterprise Technologies»** agrees with all requirements for registration, submission of the manuscript of the article and payment and be responsible in case of violation of these requirements.

Our company may rely on your freely given consent at the time you provided your personal data to us replying on this email then the lawfulness of such processing is based on that consent under EU GDPR 2016/679. You have the right to withdraw consent at any time.

Subscribe

Suwandono_accepted_return figures.doc
1127K

Oksana Nikitina <0661966nauka@gmail.com> Thu, Apr 9, 2026 at 11:13 AM
To: Purbo Suwandono <purbo@widyagama.ac.id>

Good afternoon, dear authors,
This is a friendly reminder that we expect the corrected version of your article **by April 09, 2026.**
Please feel free to reach out if you need any assistance.

We are always happy to help!
Best regards, Oksana

ср, 8 апр. 2026 г. в 06:54, Oksana Nikitina <0661966nauka@gmail.com>:
[Quoted text hidden]

--
[Quoted text hidden]

Purbo Suwandono <purbo@widyagama.ac.id> Thu, Apr 9, 2026 at 7:22 PM
To: Oksana Nikitina <0661966nauka@gmail.com>

Good afternoon.

Thank you for your email. I would like to inform you that I have completed the revisions to the article according to the editor's comments in the layout editor's file.

Please also find attached the archive containing all source files of the illustrations created in the original software.

Thank you for your support. Please let me know if any further corrections are needed.

Best regards,

Purbo Suwandono

[Quoted text hidden]

Figure_Purbo_Suwandono.rar
4796K

Oksana Nikitina <0661966nauka@gmail.com> Thu, Apr 9, 2026 at 7:23 PM
To: Purbo Suwandono <purbo@widyagama.ac.id>

Good day!
The article has been sent to the editor for checking.
If you have any questions, please call or write. We will be happy to answer them.
We wish you a great day and a good mood!
Regards, Oksana

чт, 9 апр. 2026 г. в 15:22, Purbo Suwandono <purbo@widyagama.ac.id>:
[Quoted text hidden]
[Quoted text hidden]

Oksana Nikitina <0661966nauka@gmail.com> Fri, Apr 10, 2026 at 11:19 AM
To: Purbo Suwandono <purbo@widyagama.ac.id>

Good afternoon,

The article was accepted for consideration of the possibility of publication in (No.2(140).2026).

Please revise your comments in the article (please make changes only in the layout editor's file); the editor has highlighted all necessary edits. Additionally, please send an archive containing all source files of your illustrations, created in the original software.

Please provide an edited version of the article **by 11.04.2026.**

We work 24/7 and are ready to help you around the clock!
[Quoted text hidden]

Suwandono_accepted_return figures.doc
4647K

Purbo Suwandono <purbo@widyagama.ac.id> Fri, Apr 10, 2026 at 4:01 PM
To: Oksana Nikitina <0661966nauka@gmail.com>

Good afternoon.

Thank you for your email. I would like to inform you that I have completed the revisions to the article according to the editor's comments in the layout editor's file.

Please also find attached the archive containing all source files of the illustrations created in the original software (I use origin software).

Thank you for your support. Please let me know if any further corrections are needed.

Best regards,

Purbo Suwandono

[Quoted text hidden]

3 attachments

Fig.4a-BET.opju
88K

Fig.3-FTIR.opju
134K

Fig.4b-BJH.opju
53K

Oksana Nikitina <0661966nauka@gmail.com> Fri, Apr 10, 2026 at 4:03 PM
To: Purbo Suwandono <purbo@widyagama.ac.id>

Good day!
The article has been sent to the editor for checking.
If you have any questions, please call or write. We will be happy to answer them.
We wish you a great day and a good mood!
Regards, Oksana

пт, 10 апр. 2026 г. в 12:01, Purbo Suwandono <purbo@widyagama.ac.id>:
[Quoted text hidden]

--
[Quoted text hidden]

ACCEPTED

8 April 2026

Purbo Suwandono <purbo@widyagama.ac.id>

From EEJET - Please respond no later than April 09, 2026 - Suwandono P. (April issue)

3 messages

Oksana Nikitina <0661966nauka@gmail.com> Wed, Apr 8, 2026 at 11:31 AM
To: Purbo Suwandono <purbo@widyagama.ac.id>

Hello dear authors, I hope you are doing well. Your article has been accepted for publication in the April issue of the journal (No. 2(140)2026, publication date 30.04.2026). We want your article to be seen by more people and readers to increase interest in your article worldwide. So we will add your "graphic abstract" figure next to the article, an example you can see on the journal page at http://journals.uran.ua/eejet/issue/view/15935. Remember that this is important and affects the citation of your article, so please send the "graphic abstract" **no later than April 09, 2026.**
==========

For your information:
A graphical abstract is an image that appears alongside the text abstract in the contents. This is a single, concise, pictorial, and visual summary of the main findings of the article.
A graphical abstract should allow readers to quickly gain an understanding of the take-home message of the paper and is intended to encourage browsing, promote interdisciplinary scholarship, and help readers identify more quickly which papers are most relevant to their research interests.

Authors must provide an image that clearly represents the work described in the paper. It could either be the superposition of several figures from the article or a figure that is specially designed for the purpose. Any postage stamps, currency from any country, or trademarked items should not be included in it. Graphical abstracts should be submitted as a separate file.

Requirements for graphical abstract:

- *Image size: the minimum required size for the graphical abstract is 560 × 1100 pixels (height × width) with a minimum resolution of 300 dpi. If you are submitting a larger image, please use the same ratio. Please note that your image will be scaled proportionally to fit in the available window.*
- *Font: please use the font with a large enough font size as the image will be reduced in size for the table of contents to fit a window.*
- *File type: .jpg, .jpeg, .png.*
- *File size: no more than 5 Mb.*

No additional text, outline, or synopsis should be included. Any text or label must be part of the image file. Please do not use unnecessary white space or the heading “graphical abstract” within the image file.

If you have any questions, please call or write; we will be happy to answer them.

With best regards, Manager Yu. Prylutska
TECHNOLOGY CENTER GROUP LTD
Viber/ WhatsApp/ Telegram: +380 (50) 3033801
Editorial staff of the "Eastern-European Journal of Enterprise Technologies"
Website: https://jet.com.ua/en/, http://journals.uran.ua/eejet/



Відвідати сайт



Відвідати сайт

Attention! The author (team of authors) submitting the manuscript to the editorial office of the journal **«Eastern-European Journal of Enterprise Technologies»** agrees with all requirements for registration, submission of the manuscript of the article and payment and be responsible in case of violation of these requirements.

Our company may rely on your freely given consent at the time you provided your personal data to us replying on this email then the lawfulness of such processing is based on that consent under EU GDPR 2016/679. You have the right to withdraw consent at any time.

Subscribe

Purbo Suwandono <purbo@widyagama.ac.id> Thu, Apr 9, 2026 at 1:08 PM
To: Oksana Nikitina <0661966nauka@gmail.com>

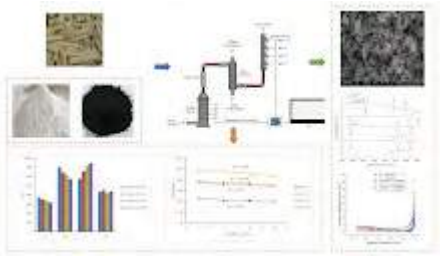
Dear editor,

I have prepared the graphical abstract in accordance with your request and the journal requirements. Please find it attached to this email.

Please let me know if there is anything that still needs to be revised or adjusted.

Best regards,
Purbo Suwandono

[Quoted text hidden]



Graphical abstract-Purbo_Suwandono.jpg
710K

Oksana Nikitina <0661966nauka@gmail.com> Thu, Apr 9, 2026 at 1:09 PM
To: Purbo Suwandono <purbo@widyagama.ac.id>



PUBLISHED

30 April 2026

Eastern-European
JOURNAL
of Enterprise Technologies

Східно-Європейський
ЖУРНАЛ
передових технологій

▪ Technology organic and inorganic substances

2/6 (140) 2026

Content

TECHNOLOGY ORGANIC AND INORGANIC SUBSTANCES

6 Determination of multi-criterion optimization features in creating systems for recomplexing anhydrous cosmetics
Tetiana Ivanishena, Zoriana Chereshnia, Anna Mahdiichuk

17 Adsorption purification of sunflower oil using acid-activated montmorilonite and quality assessment
Larisa Fialkovska, Valentyna Bandura, Marina Serdyuk, Maksym Hudzenko, Artem Antonenko, Vitalii Mihailik, Olga Vasylyshyna

27 Determining the effect of soy methyl ether additives to commercial diesel fuels on oil change interval in a 1.5 renault diesel engine, model K9K
Vasyl Melnyk, Mariia Hnyp, Ihor Zakhara, Ivan Mykytii

36 Syngas quality improvement in corncob updraft gasification using CaO/activated carbon palm fiber catalyst
Purbo Suwandono, Widya Wijayanti, Nova Risdiyanto Ismail, Dzulfikar Johan Akbar, Muhammad Reza

51 Effect of modifying the surface of cardboard with aluminum hydroxyl chloride solution on the indicators of the contact angle and surface energy
Tetiana Roik, Yevheniia Bychkar, Volodymir Oliynyk

62 Determination of the formation mechanism of zinc and nickel layered double hydroxides
Vadym Kovalenko, Anastasiia Borysenko, Dmytro Andreiev, Anton Dopira, Oleksii Demchenko, Valerii Kotok, Volodymyr Medianyk, Dnytro Sukhomlyn, German Shuklin, Volodymyr Verbitskiy

72 Identifying the operational characteristics of an ammonia synthesis column, taking into account changes in the operating parameters of the process plant
Petro Yeliseyev, Maryna Loriia, Olexii Tselishchev, Liudmyla Karpyuk, Oleksandr Duryshev, Yevgen Kobzarev

81 Abstract and References

UDC 662.7:662.767:66.097
DOI: 10.15587/1729-4061.2026.352281

SYNGAS QUALITY IMPROVEMENT IN CORNCOB UPDRAFT GASIFICATION USING CAO/ACTIVATED CARBON PALM FIBER CATALYST

Purbo Suwandono
Corresponding author
Master*
E-mail: purbo@widyagama.ac.id
ORCID: https://orcid.org/0000-0003-4085-1291
Widya Wijayanti
PhD**
ORCID: https://orcid.org/0000-0003-4215-5943
Nova Risdiyanto Ismail
PhD*
ORCID: https://orcid.org/0000-0001-8439-6919
Dzulfikar Johan Akbar
Master Student**
ORCID: https://orcid.org/0009-0002-4652-8516
Muhammad Reza
Bachelor Student*
ORCID: https://orcid.org/0009-0009-9258-0586
*Department of Mechanical Engineering
Widya Gama University
Borobudur str., 35, Malang, Indonesia, 65142
**Department of Mechanical Engineering
Brawijaya University
Veteran str., 10-11, Malang, Indonesia, 65145

The object of the study is updraft fixed-bed gasification process of corncob biomass with dual catalytic system calcium oxide (CaO) and palm-fiber-derived activated carbon (AC-PF). This study addresses the low heating value of corn cob syngas and the high cost of upgrading catalysts. This study using dual catalyst system characterization along with both equivalence ratio (0.2, 0.25, 0.3, and 0.35), catalyst loading (4%, 6%, 8% and 10%) and finally CaO/AC–PF mass ratio (0:1, 1:0, 1:1, 2:1), in addition to this the final products obtained were analyzed for dual catalyst systems further through Scanning Electron Microscope, Fourier Transform Infrared Spectroscopy and Brunauer-Emmett-Teller. These results indicate that by increasing the ER, H2 and CH4 fractions increase, whereas CO_2 decreases, and the lower heating value of syngas increases, however CO reaches an optimum at ER = 0.3. Higher catalyst loading tends to decrease H_2 and CH_4 but increase CO, which potentially lowers the heating value at high loadings. Characterization of the catalyst shows that AC-PF has a porous structure and greater gas-solid contact with enhanced secondary reactions while addition of CaO creates a composite with surface species associated with CO_2 sorption. Low Heating Value of syngas rises at high ER while decreases with the increase in catalyst loadings due to the minimal contribution of CH_4. Our obtained results feature the demonstrated functional synergetic mechanism between porous AC–PF and CaO-based CO_2 sorption, allowing simultaneous catalytic upgrading and CO_2 capture in one cheap dual catalyst system. Such empirical observations would provide an appropriate foundation for future potential designs and operation of small-scale biomass gasification units, specifically updraft reactors to convert corn cob waste at the ER and catalyst loadings investigated in this study

Keywords: gasification, updraft, corncob, syngas, CaO, activated carbon

Received 20.01.2026
Received in revised form 25.03.2026
Accepted date 03.04.2026
Published date 30.04.2026

How to Cite: *Suwandono, P., Wijayanti, W., Ismail, N. R., Akbar, D. J., Reza, M. (2026). Syngas quality improvement in corncob updraft gasification using CaO/activated carbon palm fiber catalyst. Eastern-European Journal of Enterprise Technologies, 2 (6 (140)), 36–50. https://doi.org/10.15587/1729-4061.2026.352281*

1. Introduction

In recent years, with several environmental challenges such as increased greenhouse gas emissions, depletion of fossil fuels and agricultural waste, the global movement towards green energy and sustainable technologies has taken full steam. Because these issues involve not only factors that degrade environmental quality but also ones that threaten long-term energy security and sustainable economic development, they are critical subjects of concern. This is not just about cutting emissions developing green energy means finding new, cleaner, more effective methods of using what we have and generating less waste. The conversion of biomass residues into energy seems a viable and ecologically acceptable option. Gasification of biomass to get synthesis gas is one of such potential techniques which can convert solid biomass into syngas or be further transformed as feedstock for manufacturing chemicals and other energy goods.

Indonesia is among the largest corn producers in Southeast Asia, with national production exceeding more than 18 million tons of dry seed per year. About 15–20% of this amount refers to cobs after the kernel removal process, which thus leads to an excessive volume of corn cob waste (around 2.5–3.5 million tons per year). Previously, corn cobs alone

Copyright © 2026 Authors. This is an open access article under the Creative Commons CC BY license

were largely underutilized and could be used for traditional Fuel as well as small quantities of Animal Feed or even burnt on post-harvest land that can lead to Air Pollution. Most are just left in heaps or to rot on the land, a potential source of plant disease [1].

Chemical and energy properties of corn cobs are quite promising. They are mainly composed of cellulose, hemicellulose and lignin, with a calorific value starting from approximately 15–17 MJ/kg, which makes them highly appropriate as initial feedstock for many biomass-based energy conversion technologies [2]. Their hardness and fibrous nature make them ideal candidates for production of biochar or activated charcoal process, or direct use in pyrolysis & gasification processes. This enormous potential shows that corn cobs are not waste, but rather a renewable resource that can be potentially leveraged for energy security and reduced fossil fuel dependence.

Biomass gasification is a promising thermochemical process to convert renewable resources into syngas containing H_2, CO, CH_4, and CO_2. Corn cobs are among the most abundant biomass types in Indonesia [3] and have a high content of lignocellulose that supports energy conversion. Nevertheless, the biomass gasification process still encounters various challenges, most notably the low hydrogen fraction of syngas and the generation of substantial amounts of tar. Tar formation can lead to clogging of the reactor, loss of thermal efficiency and high purification costs.

To address such issues, an important strategy is the implementation of catalysts. Several studies have shown that metal catalysts like Ni, Ca and K are able to enhance hydrogen yield but at the same time suppress tar formation. On the other side, enhanced carbon also widely used as catalyst support owing to high surface area, porous structure and good chemical stability. This type of biomass can be used to produce activated carbon from waste plantations that provide other socioeconomic benefits as an alternative source of raw material and is an economically viable process where the use of these resources in a circular economy opens up new potential such that palm fiber waste can be converted into valuable products. Furthermore, calcium oxide (CaO) acts both as a catalyst in the tar decomposition reaction and an absorber of CO_2 that triggers sorption-enhanced gasification to enhance hydrogen content in syngas [4].

While a lot of research has been done on metal catalysts and activated carbon, studies involving biomass bases catalyst like palm fiber-based activated carbon with CaO during the gasification of corn cob remain sparse. One originality of this study is on the use of a dual catalysts that gives a synergistic effect: high-pore activated carbon enhances both catalysts heterogeneous distribution and activity while the CaO helped to decompose tars as well as absorb CO_2. This strategy could lead to major increases in hydrogen production and decreases in carbon emissions.

The importance of improving syngas quality in biomass gasification systems has been the subject of significant scientific interest in contemporary energy studies, particularly as society confronts escalating expectations for clean, renewable, sustainable energy systems. Particular focus should be placed on these strategies aiming to increase hydrogen production and decrease tar generation, as they are still two of the main technology barriers preventing the broader practical application of biomass gasification. This makes the discovery and assessment of effective, low-cost and sustainable catalytic materials scientifically significant for the establishment of wide-ranging, efficient biomass conversion technologies to underpin transitioning from fossil-based fuels to cleaner energy use.

2. Literature review and problem statement

The paper [5] presents the result on the gasification of sago dreg waste pellets in a top-lit updraft fixed-bed gasifier. The results show that the addition of Al_2O_3 improved syngas quality, especially by increasing H_2 content up to 31.65% at 5% Al_2O_3 and enhancing CO and CH_4 production, while also increasing the H_2/CO ratio to 1.65 and 1.51 for 5% and 10% Al_2O_3, respectively, improving LHV, and reducing tar content by about 25–27.5% compared with pellets without catalyst. However, this study is limited because it was conducted only on one biomass type, within a laboratory-scale TULD fixed-bed gasifier, and only considered two catalyst loadings.

The paper [6] presents the result on hydrogen enrichment in product gas from a pilot-scale rice husk updraft gasification. The results show that dolomite-assisted air gasification gave the best performance, increasing the H_2 content up to 15.4 mol%, with an LHV of 5.1 MJ/Nm^3, while steam/air gasification improved H_2 to 9.6 mol% and air alone produced only about 7.08 mol% H_2, the optimum operating condition was reported at an airflow rate of 3 m^3/h and a dolomite mixing ratio of 15 wt.%. However, this study is limited because it focused only on rice husk feedstock, used a pilot-scale updraft gasifier with a batch capacity of 3 kg, and evaluated only a limited range of operating conditions and catalyst type.

The paper [7] presents the result on oxygen updraft gasification coupled with catalytic steam reforming of cigarette butts for hydrogen-rich syngas production. The results show that the integrated process was effective in converting cigarette butts into syngas, with gasification producing 82.3–89.7 wt.% syngas, 6.3–8.6 wt.% soot, and 1.4–1.9 wt.% tar, while the catalytic reforming stage significantly improved the gas quality by increasing the H_2 content up to 30.27 vol.%, increasing the HHV up to 11,528 kJ/kg, and reducing tar concentration from about 18.15 g/m^3 to 13.38 g/m^3 under the optimum condition. However, this study is limited because it investigated only cigarette butt waste as feedstock, used a specific oxygen updraft gasifier-catalytic reformer configuration, and fixed most catalytic reforming parameters.

The paper [8] presents the result on the experimental assessment of pellets produced from beekeeping waste and slumgum–pine sawdust mixtures through updraft gasification. The results show that pure slumgum pellets exhibited very high mechanical durability (99.98%) and high HHV (27.66 MJ/kg), while during gasification the 50% slumgum-50% sawdust pellets produced the highest producer gas LHV of 7.62 MJ/Nm^3, indicating that the addition of sawdust improved gas quality and energy recovery potential. However, this study is limited because the equivalence ratio remained very low (0.0125–0.0204) compared with typical gasification conditions, the experiments were conducted only in a modified laboratory-scale updraft gasifier.

The paper [9] presents the result on a comparative investigation of catalyst applications in updraft and modifiable-downdraft fixed-bed biomass gasifiers, using a biomass mixture of green waste, sewage sludge, and olive pomace together with red mud (RM) and Al-Ni alloy catalysts to im-

prove syngas quality and hydrogen production. The results show that catalyst type and reactor configuration strongly influenced gasification performance, with the Al-Ni catalyst giving the best hydrogen enrichment, reaching up to 65 vol.% H_2 in the updraft gasifier at 900°C, while RM increased H_2 to about 50 vol.%, the updraft gasifier produced better hydrogen-rich syngas than the modifiable-downdraft reactor. However, this study is limited because it, used a specific mixed biomass composition and mainly focused on high temperature operation around 900°C with limited gasifying-agent flow conditions.

The paper [10] presents the result on the experimental investigation of producer gas composition from sorted municipal solid wastes in an updraft fixed-bed gasifier. The results show that reducing the equivalence ratio from 0.21 to 0.15 increased the heating value of the combustible gases. The study indicated that the allothermal updraft fixed-bed gasifier is suitable for producing gas that can be utilized in gas engines. However, this study is limited because it used a laboratory-scale 10 kW allothermal updraft gasifier at a fixed temperature of 800°C, and evaluated only two ER conditions.

The paper [11] presents the result on the effect of adding laying hens' manure (LHM) to wheat straw on gasification efficiency in an air-blown updraft fixed-bed gasifier. The results show that increasing ER improved the gasification performance, with the producer gas LHV reaching 3.3–3.4 MJ/m^3, cold gas efficiency around 60%, and carbon conversion efficiency in the range of 82–94%. However, this study is limited because it was focused on one specific co-feed system and produced a relatively low-calorific gas.

The paper [12] presents the result on the gasification performance of olive pomace in updraft and downdraft fixed-bed reactors using dry air and pure oxygen. The results show that updraft reactor achieving up to 48 vol.% H_2 with dry air and 53 vol.% H_2 with pure oxygen, while the downdraft reactor reached up to 45 vol.% H_2 with dry air and 39 vol.% H_2 with pure oxygen. However, this study is limited because only a limited range of gasifying agents, temperatures, and flow rates.

The paper [13] presents the result on the gasification of MDF residue in an industrial-scale updraft fixed-bed gasifier. The results show that MDF residue can be effectively converted into useful energy, with a syngas production rate of about 2.5 Nm^3/kg, syngas LHV of around 6.0–7.0 MJ/Nm^3, about 88 wt.% of MDF residue converted into syngas, and a system capable of delivering 7 MWth of thermal energy and about 955 kW net electrical power through the ORC turbine. Nevertheless, this study is subject to some limitations as it investigated only a single industrial waste stream (corn cob) in a single updraft gasifier design and performance was assessed with few feed rates while direct combustion of raw hot syngas containing tar was employed.

This study shows the outcomes of researches conducted on updraft fixed-bed reactors with biomass gasification concerning improvement of syngas quality and efficiency of thermal conversion. Demonstrated that syngas composition and heating value are significantly impacted by feedstock properties, gasification conditions, and catalysts. However, problems associated with the absence of high-performance and inexpensive catalyst systems that can boost hydrogen generation in addition to optimizing syngas quality simultaneously during corncob gasification were not solved. This is due to the intricacy of catalytic processes occurring in the gasification area along with reforming, cracking and CO_2 capture pathways along with financial restrictions of promoted catalyst existing available on a market. Perhaps utilizing coupled composite catalysts consisting of CaO and activated carbon palm fiber proves to be a solution for these concerns, wherein the CaO stimulates CO_2 uptake and drives shift reactions while Coconut shell active carbon provides a porous surface and serves as an external site for secondary cracking reactions. It has been used in prior studies, but the application of CaO and activated carbon palm fiber for corncob updraft gasification is still limited. It can be concluded that a syngas quality improvement study on corncob updraft gasification using CaO/activated carbon palm fiber catalyst is recommended.

Biomass gasification represents a significant path for transforming agricultural remains into useable synthesis gas, and catalytic materials (e.g., CaO and carbonaceous adsorbents) has been shown to enhance the quality of produced gases via tar decomposition, reforming reactions, and CO_2 capture. A number of researchers have studied other biomass feedstocks, catalyst type and reactor configurations for improving syngas production. Nevertheless, most of these studies were mainly on the single performance of catalysts or gasification systems other than corncob updraft gasification. Moreover, the synergistic effect of CaO and activated carbon palm fiber catalyst with respect to catalyst dosage ratio, catalyst loading and equivalence ratios remained largely undocumented.

Thus, additional research is important for evaluating the synergism of CaO as a CO_2 sorbent and activated carbon palm fiber as a porous catalytic support in improving syngas composition and heating value. In view of this research gap, the current study aims to explore the role of combined CaO/activated carbon palm fiber catalyst in corncob updraft gasification along with the effects of different operating parameters on synthesis gas quality. Thus, this study is meant to deliver a more clear scientific angle of catalyst interaction and practical directions for performance enhancement in biomass gasification.

3. The aim and objectives of the study

The aim of this study was to improve syngas quality from corncob updraft gasification via a dual-synergy catalytic system composed of calcium oxide (CaO) and palm-fiber-derived activated carbon (AC-PF). This will enable cleaner and more energy-dense producer gas production, offering practical guidance on the utilization of operating conditions and catalyst configurations applicable to updraft gasification of agricultural residues.

To accomplish these aims, the following objectives are achieved:

– to prepare and characterize CaO and AC-PF catalysts by analyzing their morphology, surface functional groups, and pore characteristics using SEM, FTIR, and BET methods;

– to determine the effect of the equivalence ratio, catalyst loading and CaO/AC ratio on the composition of syngas and its lower heating value in updraft gasification of corncobs and to obtain the catalyst condition responsible for higher quality gas.

4. Materials and methods

4. 1. The object and hypothesis of the study

It is based on the updraft fixed-bed gasification process of corncob biomass at dual calcium oxide (CaO) and palm-fiber-derived activated carbon (AC-PF) catalyst systems, which

are used for the purpose of study. Experimental parameters adopted in the updraft reactor studying catalytic upgrading of producer gas were expected to affect syngas composition and heating value. The focus of this study is to develop a method for applying its results in order to enhance the quality syngas by increasing the flammable fraction of combustible gases (H_2 and CH_4) and lower heating value (LHV); while reducing CO_2 concentration at the same time.

This study hypothesizes that the dual-synergy CaO/AC-PF catalytic system is a more positive effect on syngas quality in comparison with single-catalytic configurations during updraft corncob gasification. The hypothesis is that CaO acts as a CO_2 sorbent, driving the equilibria of reactions to yield more hydrogen while palm fiber-derived activated carbon provides high surface area catalytic sites, facilitating secondary kinetics like tar cracking and volatile reforming. Optimized conditions of equivalence ratio (ER), catalyst loading, and CaO/AC-PF ratio are expected to not only increase H_2 and CH_4 fractions but also enhance LHV due to the effects of a combined catalytic-sorption mechanism.

It was defined that the corncob feedstock had relatively homogeneous composition and stable proximate/ultimate characteristics through the duration of experiments. It was assumed that after stabilization, the gasification process ran under steady-state conditions. It is also assumed that the CaO has enough CO_2 sorption capacity for the duration of catalytic conversion process and activated carbon structure was stable within applied temperature range.

Several methodological simplifications were applied throughout the research to enable experimental feasibility and focus on the goal of syngas quality evaluation. Detailed kinetic modeling of individual gasification reactions was not carried out but rather based the process performance on experimentally measured syngas composition and syngas low heating value. Moreover, although carbonation-decarbonation reactions of CaO can take place during operation, the microstructural evolution, sintering behavior and long-term cyclic stability of the catalyst were not studied in this work. the catalytic performance was assessed over the experimental time period with no prolonged durability or regeneration-cycle assessment.

The selected methods were intended to explain both the catalyst characteristics and their effect on syngas quality. SEM, FTIR, and BET were used because they provide complementary information on catalyst morphology, surface functional groups, and pore structure, which are important for catalytic reforming, adsorption, and CO_2 capture during gasification. The investigated operating parameters, namely equivalence ratio, catalyst loading, and CaO/AC ratio, were chosen because they are the main variables governing the reaction environment, catalyst effectiveness, and synergistic interaction between CaO and activated carbon in the updraft gasification process.

4. 2. Catalyst preparation

Approximately 6 grams of ground palm fiber was mixed with 60 mL of distilled water and stirred for 10 minutes. The mixture was then placed in an autoclave and heated to 200°C at a rate of 5°C per minute for 6 hours in an electric oven. After that, the reactor is allowed to cool naturally to room temperature. The resulting solid hydrocarbon product (hydrochar) is then separated using Whatman No. 42 filter paper. The filtered product is then dried at 105°C for 24 hours and stored in a glass vial. The next stage is the activation process. The hydrochar is immersed in a 3 M KOH solution with a weight ratio of 1:3 (Hydrochar:KOH) for 16 hours, then dried at 85°C for 6 hours. Spectroscopic evidence indicates that KOH preferentially reacts with oxygenated sites and can increase the relative abundance of C–OH functionalities, while higher KOH ratio and activation temperature significantly enhance porosity and BET surface area [14, 15]. To obtain the CaO/AC mixture, CaO powder and activated carbon (AC) were mixed in specific proportions using a grinder until a homogeneous mixture was obtained. Next, CaO, AC, and CaO/AC were activated using a tube furnace at a temperature of 700°C for 1 hour with a continuous flow of nitrogen during the activation process. The resulting product was then washed using distilled water until it reached a neutral pH. This stage produced activated carbon that was ready for use in research.

4. 3. Experimental setup

Corncob biomass was obtained from farmers in the South Malang region of East Java. Before use, the biomass was cleaned of impurities and dried in an oven for 6 hours at 100°C to remove moisture (water vapor) content. The ultimate and proximate test results are as follows.

The proximate and ultimate analyses of the corncob feedstock were conducted to determine its physicochemical characteristics prior to gasification. The results are presented in Table 1. The data indicate that corncob has high volatile matter content and relatively low ash content, which are favorable characteristics for gasification processes.

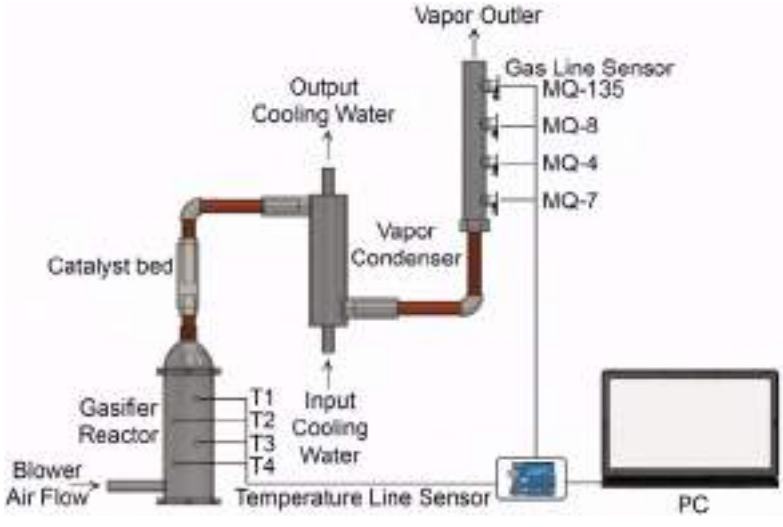
Table 1

Ultimate and proximate test corn cob

Parameter	Units	Corn cobs
Moisture	%	10
Volatile matter	%	71.38
Fixed carbon	%	12.11
Ash	%	6.51
C	%	43.6
H	%	6.3
O	%	46.8
N	%	0.22
HHV	MJ/kg	17.61

The experimental apparatus employed in this study consisted of an updraft gasifier integrated with a catalyst bed, a vapor condensation unit, gas sensors, and temperature measurement points to enable comprehensive monitoring of the gasification process. Fig. 1 shows the updraft gasifier system used in this study, including the schematic experiment (*a*) and the experimental setup (*b*).

This study used an updraft gasification reactor designed with a total height of 20 cm. The lower part of the reactor consisted of an ash container with a height of 5 cm, while the active reactor had a height of 15 cm and a diameter of 3 inches. The reactor was equipped with a 1-inch diameter air inlet pipe connected to a blower. The blower was modified with a potentiometer so that the air speed could be adjusted as needed. To monitor the thermal conditions inside the reactor, four 3 cm long type K thermocouples were installed at several different points so that the temperature profile in the gasification zone could be observed in more detail. Each test was conducted with a fixed biomass mass, a mixture of corn cobs weighing 80 grams. The reactor was made of iron and equipped with a gas seal to prevent leaks during the gasification process.



a



b

Fig. 1. Updraft gasifier: *a* — schematic experiment; *b* — experimental setup

The gas produced by the reactor was fed into a condenser, which cooled the hot gas so that the water vapor components could be separated. The condenser was made of a copper spiral pipe with a diameter of ½ inch and a height of 30 cm. Cooling water was circulated from the bottom of the condenser and exited through the top to ensure efficient heat transfer. This cooling system was driven by a 60-watt water pump, ensuring stable water flow and optimal condensation. The catalyst was positioned downstream after the reactor, where it was supported on steel wool and wrapped with an 80-μm wire mesh to secure the catalyst and prevent particle carryover with the gas flow.

To analyze the gas composition, four types of MQ gas sensors were used. The MQ-8 sensor was used to detect H_2, MQ-4 for CH_4, MQ-135 for CO_2 and MQ-7 for CO. Each gas sensor was calibrated according to the manufacturer's datasheet, specifically by determining the Ro value, which is the sensor resistance in clean air conditions. This Ro value is used as a reference in calculating the measured gas concentration during the process.

All data from the gas sensors and thermocouples were acquired using an Arduino Uno microcontroller. Each gas sensor is connected to a separate Arduino Uno to facilitate the calibration process and reduce the possibility of interference between sensors. Arduino is also used to record temperature data from four thermocouples installed in the reactor, so that gas composition and temperature distribution data can be obtained simultaneously.

The ER range of 0.2, 0.25, 0.3 and 0.35. The catalyst load was between 4%, 6%, 8% and 10% from the mass of input feedstock. The CaO/AC-PF ratio was varied between 0:1, 1:0, 1:1, and 2:1. Design of experiment can be seen in Table 2.

Table 2

Design of experiment using

Run	Equivalence ratio (E.R)	Catalyst load, %	CaO/AC
1	0.2	4	1:0
2	0.2	6	0:1
3	0.2	8	1:1
4	0.2	10	2:1
5	0.25	4	0:1
6	0.25	6	1:0
7	0.25	8	2:1
8	0.25	10	1:1
9	0.3	4	1:1
10	0.3	6	2:1
11	0.3	8	1:0
12	0.3	10	0:1
13	0.35	4	2:1
14	0.35	6	1:1
15	0.35	8	0:1
16	0.35	10	1:0

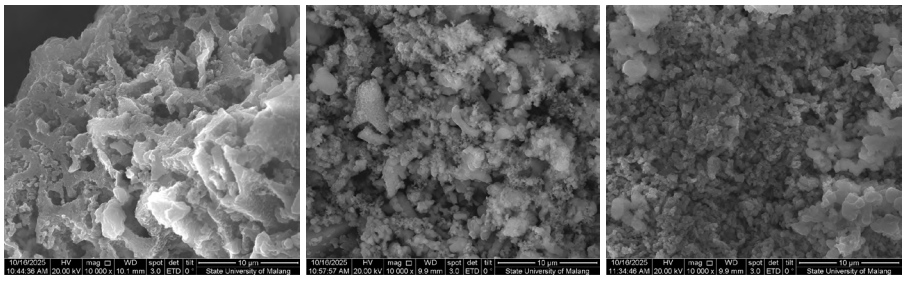
A total of 16 experimental runs were conducted systematically to enable evaluation of the main effects of each variable and the tendency of interactions between variables on the fractions of H_2, CO, CH_4, CO_2, and lower heating value (LHV). This approach enabled identification of the most effective combination of operating parameters in improving syngas quality quantitatively and measurably.

5. Results of syngas quality enhancement from corncob using calcium oxide (CaO) and palm-fiber-derived activated carbon (AC-PF).

5. 1. Characterization of calcium oxide (CaO) and palm-fiber-derived activated carbon (AC-PF) catalysts

5. 1. 1. Scanning electron microscopy catalyst result

Fig. 2, *a* indicates the surface morphology of palm fiber-based activated carbon (AC-PF). The close look at the surface reveals a porous and non-plane structure with void sections surrounded by massive stack surfaces. This property shows that the activation of KOH has successfully created micropores and mesopores, which are crucial in enhancing activated carbon specific surface area.



a *b* *c*

Fig. 2. Scanning electron microscopy catalyst result:
a — scanning electron microscopy AC-PF; *b* — scanning electron microscopy CaO:AC, 1:1;
c — scanning electron microscopy CaO:AC-PF, 2:1

This the coarse and textural surface shows that most of the material has been exposed from lignocellulose cell wall, which had many interparticle voids. When serving as a catalyst in gasification or thermochemical reactions, this porous architecture significantly promotes the ability of an adsorbed dispersed gas to diffuse on and into the structure.

The small size of the voids (1–5 μm) indicates that most of the pores belong in the mesopores category where gas molecules such as H_2, CO and tar can attach during a gasification reaction.

The porosity and aspect of AC-PF exhibit the properties of porous activated carbon materials with a heterogeneous pore structure, where pores facilitate interaction between gas phase reactants and active sites surrounding each other on the surface area of materials which increases reaction rates and improved tar or CO_2 capture targeting in biomass-derived power applications.

Fig. 2, *b* represent the surface morphology of CaO:AC-PF catalyst in 1:1. The approach of this material surface can be observed, composed of fine particles with microns and submicrons that bond together to build a layered and slightly agglomerate system.

Fine and light-colored grains suggest a well-distributed CaO particle, doped on the surface of activated carbon (AC-PF). This distribution of CaO through the pores fills some of them creating a particle with a denser surface than that observed pure AC-PF. Nevertheless, small gaps and tiny voids between the grains still point to preserved microporous and mesoporous configurations that can indeed support catalytic activity [16].

Such morphology shows the effectiveness of the CaO impregnation technique using activated carbon originated from palm fiber, where interactions between CaO and pore walls of carbon formed a composite material that provides greater thermal stability and chemical stability. This framework is particularly well-suited for catalyst applications in biomass gasification processes, because CaO particles may act as CO_2 absorbers and also facilitate the tar reforming reaction [17].

Fig. 2, *c* displays the surface appearance of CaO:AC-PF (2:1) catalyst. This implies that the exposed material is covered in agglomerations of fine, round and irregular particles between microns to submicrons. These results prove that, in comparison with CaO:AC-PF (1:1) sample, its structure becomes denser and much tighter, meaning that the increase in the ratio of CaO will lead to a partial closure effect of activated carbon surface pore by CaO particles.

In fact, the CaO particles are more evenly distributed and fill the carbon surface, which proves that there is a greater amount of CaO being successfully impregnated. Notably, the light color in certain regions suggests a calcium oxide phase that is well adhered to the activated carbon matrix. Such structure suggests the strong bonding interactions between CaO and AC-PF forming a high temperature stable composite.

While some of the pores are blocked, small voids between the CaO grains still exist where gas can diffuse, and therefore the adsorption ability of catalyst remains large. Due to the active area of CaO and porous carbon structure, this material is very competitive in biomass gasification or tar reforming applications since CaO can be CO_2 absorber and enhance conversion of carbon into H_2,

5. 1. 2. Fourier transform infrared spectroscopy catalyst result

The FTIR analysis results shown in the Fig. 3 reveal clear spectral differences between the AC-PF, CaO, and their mixtures (CaO:AC-PF) with ratios of 2:1 and 1:1. In the AC-PF spectrum, the absorption band at 2926 cm^{-1} is associated with the stretching vibration of the C–H group from $-CH_2$ or $-CH_3$ (methylene/methyl stretching), which indicates the presence of hydrocarbon chain residues from the lignocellulose structure. The peak at 1577 cm^{-1} indicates the presence of aromatic C=C or C=O stretching, while the band at 1056 cm^{-1} represents C–O stretching from alcohol or ether groups. In addition, the -OH group that appears in the 3500–3600 cm^{-1} region is identified as the result of AC-PF activation using a KOH solution, which causes the formation of hydroxyl groups on the activated carbon surface. This –OH group plays an important role in increasing the surface activity and adsorption capacity of AC-PF as a catalyst support medium [18, 19].

In pure CaO, the intense band at 3639 cm^{-1} is associated with the stretching of the O-H group from $Ca(OH)_2$, which is formed due to the partial hydration of CaO when exposed to humid air. Meanwhile, the absorption bands at 1426 cm^{-1} and 876 cm^{-1} are associated with C-O stretching and CO_3^{2-} bending, respectively, indicating the formation of $CaCO_3$ due to CO_2 adsorption from the air. This shows that CaO is highly reactive to moisture and carbon dioxide in the environment.

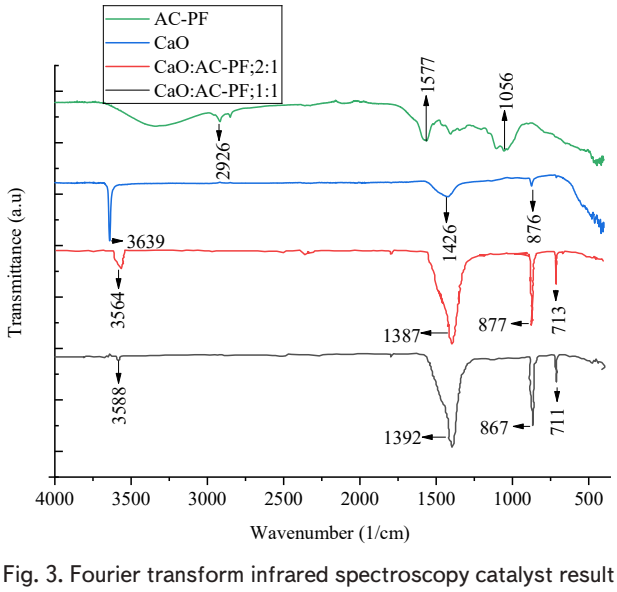


Fig. 3. Fourier transform infrared spectroscopy catalyst result

For the CaO:AC-PF (2:1), the main absorption bands were detected at 3564 cm^{-1} (O-H stretching from $Ca(OH)_2$ and the -OH group in AC-PF), 1387 cm^{-1} (C-O stretching), and 877 cm^{-1} and 713 cm^{-1} (bending vibration of CO_3^{2-}). This combination of bands indicates the formation of carbonate compounds ($CaCO_3$) due to the interaction between CaO and the oxygen groups of activated carbon. The presence of -OH groups from KOH activation also strengthens the basic properties on the surface, which can increase the chemical interaction between CaO and AC-PF [20].

At a CaO:AC-PF ratio of 1:1, the absorption bands at 3588 cm^{-1}, 1392 cm^{-1}, 867 cm^{-1}, and 711 cm^{-1} show a similar pattern, indicating the presence of hydroxyl (O-H) and carbonate $\left(CO_3^{2-}\right)$ groups. The difference in peak intensity compared to the 2:1 ratio indicates variations in the level of interaction between CaO and the –OH groups resulting from KOH activation on AC-PF, which affects the formation of carbonate-hydroxide complexes on the material surface [21].

5. 1. 3. Brunauer-Emmett-Teller catalyst result

Fig. 4 shows the adsorption-desorption isotherm curves for nitrogen for the AC, CaO:AC (1:1), and CaO:AC (2:1) samples are shown in Fig. 4. All three samples exhibit type IV isotherms with clear hysteresis loops at relatively high pressures ($P/Po > 0.9$). Based on the IUPAC classification, this characteristic indicates that the material has a mesoporous structure formed through capillary condensation within the pore channels. The difference between the adsorption and desorption pathways indicates that the pore shape is not perfectly cylindrical, but rather tends to be irregular or slit-like, which is commonly found in modified activated carbon materials [22].

The pure activated carbon (AC) sample showed a relatively low nitrogen adsorption volume with a specific surface area of 24.51 m^2/g and an average pore diameter of 0.74 nm, indicating a predominance of microporous structures. In the CaO:AC (1:1) composite, the surface area did not change significantly compared to pure AC, indicating that the addition of a moderate amount of CaO did not cover the carbon pores much, but only adhered to the external surface of the carbon matrix [23].

In contrast, the CaO:AC (2:1) mixture had a prompt sharp increase in adsorption volume at higher pressure ($P/Po > 0.9$), around about 35 cm^3/g STP, while with significantly decreased BET surface area of 5.06 m^2g and increased pore diameter to 22.87 nm

These changes in both isotherm shape and pore size increase suggest that CaO impregnation not only contributes to surface chemistry modification but also leads to substantial pore structure alteration of AC. Although this transformation is helpful, regarding catalytic applications in biomass gasification processes with respect to tar reforming and water-gas shift reactions, due to the generation of mesoporous structure that improves the diffusion of gases along with better access to active sites. Therefore, while the mesoporous catalyst has a low specific surface area, its increased mesoporosity and pore interconnection are able to enhance catalytic performance in hydrogen gas production [24].

Fig. 4, *b* presents the BJH pore size distribution curves that afford more insight into the textural evolution of palm-fiber-based activated carbon subsequent to CaO impregnation. The pristine AC shows a fairly moderate *dV/dD* value and large contribution only at the larger pore diameters (> 60 nm), suggesting its pore system is predominately macropores with very little amount of mesopores. This texture is less suitable for gas-solid reactions since the surface area available in the mesopore range (2–50 nm) is relatively small.

The BJH curves exhibit a dramatic transformation in terms of their shape and intensity after loading with CaO. In the case of CaO:AC-PF = 1:1, all other things being equal, the pore size distribution is skewed towards smaller diameters and has a larger contribution in said mesopore range (approx. 15–60 nm). This behavior indicates that CaO impregnation partially reform the carbon network, increasing volume of micropores and providing access to blocked pores, thus creating additional mesoporosity. Strengthening this effect is the CaO:AC-PF = 2:1, which shows the highest *dV/dD* in its curve and a clearly defined maximum located at ~30–40 nm. The pronounced peak within this range confirms that the greater loading of CaO favors the appearance of well-defined mesopores and suppresses the relative amount of very large macropores.

Overall, the BJH analysis demonstrates that CaO acts not only as a reactive sorbent but also as a textural promoter for the palm-fiber AC. The increase in mesopore volume and the shift of the dominant pore size toward 20–40 nm are expected to facilitate the diffusion of gasifying agents and tar molecules, as well as to improve the accessibility of CaO active sites for CO_2 capture and reforming reactions. These features are therefore beneficial for enhancing the catalytic performance of the CaO/AC composite in biomass gasification toward H_2-rich syngas production.

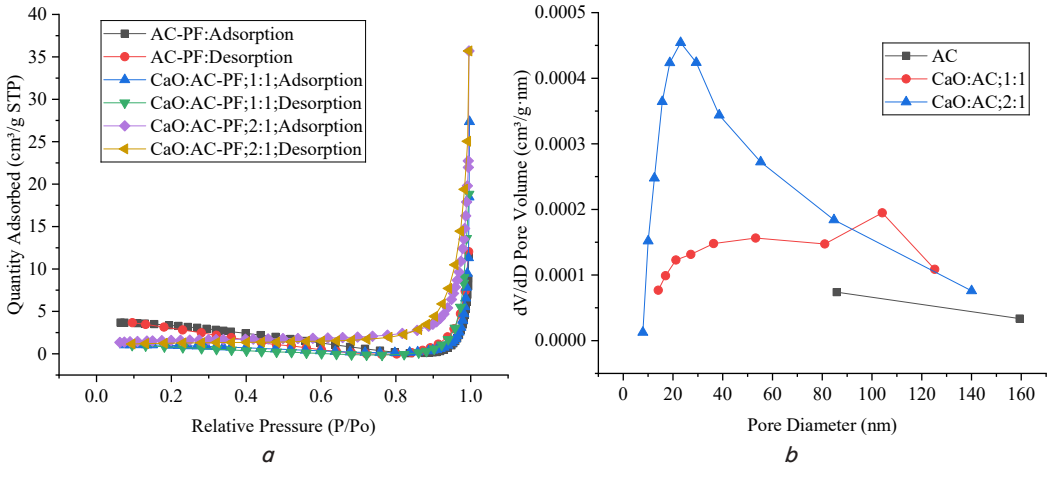


Fig. 4. Brunauer-Emmett-Teller result: *a* — surface analysis adsorption desorption isotherm; *b* — Barrett-Joyner-Halenda adsorption pore size distribution

5. 2. Effect of operating parameters on syngas composition and low heating value

5. 2. 1. Effect of equivalence ratio on syngas product

The composition of syngas from updraft gasification is greatly influenced by the equivalence ratio (ER), which is the ratio of the mass flow rate of air compared to the mass flow rate of corncob in the experiment compared to the stoichiometry of air required for complete combustion of corncob. In this study, the ER used was 0.2–0.35 with the following formula

$$ER = \frac{\left(\dot{m}_a / \dot{m}_{cc}\right)_{\exp}}{\left(\dot{m}_a / m_{cc}\right)_{stc}},$$

where $\dot{m}_a$ – the air mass flow rate (kg/s), $\dot{m}_{cc}$ – the corncob mass flow rate (kg/s), exp denotes the experimental air-fuel ratio, and *stc* denotes the stoichiometric air-fuel ratio.

The composition of syngas produced from corncob gasification was evaluated at different equivalence ratios to determine the variation in the main combustible and non-combustible gas components. Changes in the equivalence ratio significantly affected the concentrations of H_2, CH_4, CO, and CO_2, indicating that the air supply plays an important role in the gasification performance and gas quality. Fig. 5 shows the syngas composition obtained at different equivalence ratios.

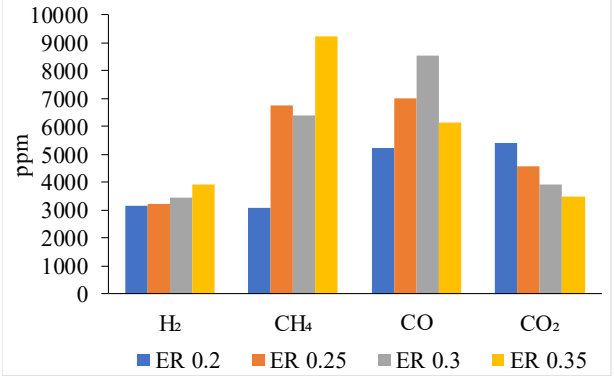


Fig. 5. Syngas composition with different equivalence ratio

The graph above shows that the higher the ER, the higher the hydrogen composition produced. At ER 0.2, the ppm is 3150 ppm, at ER 0.25 it is 3241 ppm, at ER 0.3 it is 3457 ppm, and at ER 0.35 it is 3914 ppm. A higher oxidant supply promotes the formation of more stable autothermal conditions and higher reaction temperatures due to partial oxidation. This increase in temperature accelerates hydrogen-forming reactions, particularly the gasification of active carbon catalyst interactions with steam ($C + H_2O \rightarrow CO + H_2$), the reforming of volatile compounds/light hydrocarbons ($CxHy + H_2O \rightarrow CO + H_2$), and the cracking of tar/volatile into lighter gas species. At low ER, some volatiles tend to be incompletely converted and still have the potential to escape as condensable components, while increasing ER increases heat availability, making the conversion of volatiles into gas fractions (including H_2) more effective.

The higher the ER, the higher the CH_4 composition produced. At ER 0.2, 3093 ppm was obtained, at ER 0.25 6767 ppm, ER 0.3 6377 ppm, and ER 0.35 9221 ppm. This trend indicates that the supply of oxidants not only increases autothermal conditions and the rate of devolatilization, but also shifts the reaction pathway towards the formation of light hydrocarbons through hydrogenation and/or methanation reactions in the reactor zone where the temperature still supports CH_4 formation. In particular, increased H_2 at higher ERs can promote the methanation reaction of CO ($CO + 3H_2 \rightleftharpoons CH_4 + H_2O$), so that CH_4 increases along with a tendency for CO to decrease at the highest ER. In addition, more intensive fragmentation of volatiles and tar at high ERs has the potential to produce light gas precursors which are then hydrogenated to CH_4.

CO formation increased up to an ER of 0.3 and decreased at an ER of 0.35. At an ER of 0.2, 5238 ppm was obtained, at an ER of 0.25, 6999 ppm, at an ER of 0.3, 8532 ppm, and decreased at an ER of 0.35 to 6145 ppm. At low ER (0.20–0.25), limited oxygen supply resulted in relatively low heat release, so that the reaction zone temperature and char reactivity were not sufficient to intensify CO formation reactions, especially the Boudouard reaction ($C + CO_2 \rightleftharpoons 2CO$) and char gasification with steam ($C + H_2O \rightleftharpoons CO + H_2$). When the ER is increased towards 0.30, the increase in autothermal heat strengthens these reduction reactions, causing CO formation to increase and reach its peak. However, at higher ERs (0.35), the CO fraction tends to decrease because some CO can be converted to CH_4.

CO_2 formation continues to decrease as ER increases. At ER 0.2, 5412 ppm is obtained; at ER 0.25, 4592 ppm; at ER 0.3, 3916 ppm; and at ER 0.35, 3479 ppm. The increase in oxidant supply at this ER does not promote complete combustion, but rather strengthens the CO_2 reduction mechanism. At higher ERs, the heat generated from partial oxidation increases the temperature of the reduction zone, thereby accelerating the Boudouard reaction ($C + CO_2 \rightleftharpoons 2CO$), in which CO_2 is reduced by char to CO. This mechanism is consistent with the increase in CO until it reaches a maximum at an ER of 0.30, while also explaining the decrease in CO_2 under the same conditions. Interestingly, at an ER of 0.35, CO_2 remains at its lowest level even though CO decreases, indicating that the CO formed is not completely accumulated at the outlet but has the potential to undergo further conversion along the gas flow path.

5. 2. 2. Effect of catalyst loading on syngas product

The catalyst load or amount of catalyst in this study was 4%, 6%, 8%, and 10% of the total biomass weight. Fig. 6 shows that the composition of H_2 and CH_4 increases as the catalyst load decreases. The H_2 gas composition at catalyst loads of 4%, 6%, 8%, and 10% is 3742 ppm, 3471 ppm, 3372 ppm, and 3176 ppm, respectively. As the catalyst load increases, the reaction pathways that consume H_2 tend to strengthen, particularly the reverse water–gas shift ($CO_2 + H_2 \rightarrow CO + H_2O$) and H_2 interactions on the catalyst surface during the conversion of gasification compounds. As a result, even though reforming occurs, the measured net H_2 decreases because more H_2 is used for CO formation and surface reactions. The CH_4 gas composition at catalyst loads of 4%, 6%, 8%, and 10% was 7031 ppm, 6476 ppm, 6206 ppm, and 5746 ppm, respectively. An increase in catalyst load increases the number of active sites and gas-catalyst contact, so that methane/light hydrocarbon cracking and reforming occur more intensely. CH_4 then acts as a reactant that is converted into more reactive syngas components, causing the CH_4 concentration to decrease at higher catalyst loads.

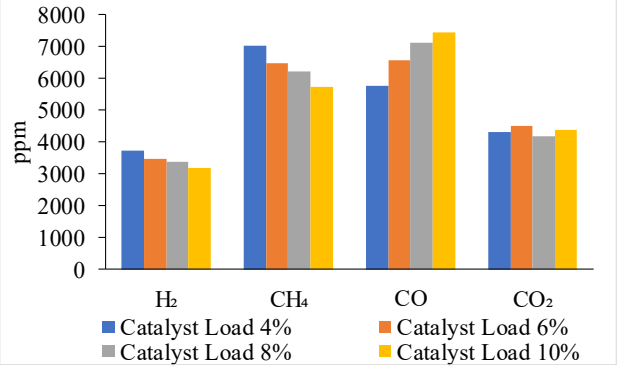


Fig. 6. Syngas composition with catalyst load variation

The CO gas composition increases with increasing catalyst load, namely for catalyst loads of 4%, 6%, 8% and 10% at 5782 ppm, 6576 ppm, 7111 ppm and 7445 ppm, respectively. The increase in catalyst loading strengthens the CO-forming reactions, particularly dry reforming ($CH_4 + CO_2 \rightarrow 2CO + 2H_2$), char – CO_2 reaction ($C + CO_2 \rightarrow 2CO$), and reverse water-gas shift. This combination shifts the product selectivity towards CO, so that the CO fraction increases consistently as the catalyst is increased. The CO_2 gas composition tends to stagnate with increasing catalyst loading, at catalyst loads of 4%, 6%, 8%, and 10% at 4322 ppm, 4510 ppm, 4198 ppm, and 4369 ppm, respectively. CO_2 shows minor changes because it is in a searching for a chemical equilibrium between the partial oxidation and the dry reforming. When the catalyst load increases, the rate of CO_2 consumption may rise, but this is often offset by CO_2 formation in the reaction zone, so that the CO_2 value appears stable or only fluctuates.

5. 2. 3. Effect of catalyst ratio on syngas product

At 4% catalyst load, the ratio of CaO/AC alters reaction thermodynamics as differences in tar cracking/reforming and CO_2 capture by CaO dominate the gasification reaction; thus, the composition of bio-gas changed significantly at mass loadings where greater amounts of active sites are available for gas diffusion to contact with the catalytic surface. At 0:1 (AC), CH_4 and CO are quite high as AC fosters volatile/tar cracking but CO_2 remains elevated due to lack of absorption. At 1:0 (CaO) CH_4 drops but the CO_2 is at its maximum, implying that there is not enough carbonate layer formation/surface area to absorb CO_2. A 1:1 ratio yields maximal CO at moderate levels of CO_2, suggesting CaO–AC synergy that enhances the conversion from volatiles to reactive gases. On the other hand, the 2:1 (CaO-rich) ratio gives the highest H_2 and lowest CO_2 due to sorption-enhanced CaO effect, but also high CH_4 because of lower contribution of AC, therefore methane reforming/cracking is still not optimal.

To explore the catalytic performance more closely, the CaO/AC ratio effects on syngas composition were carried out with multiple catalyst loading conditions. Through this study, it was aimed to investigate the effect of varying proportions of CaO and activated carbon using different catalyst loads on yield distribution of H_2, CH_4, CO and CO_2 from corncob gasification. Fig. 7 shows the influence of CaO/AC ratio at a catalyst load of 4% (*a*), 6% (*b*), 8% (*c*) and also for 10% (*d*).

Since at a catalyst loading of 4% the CaO/AC ratio alters the gasification reaction by switching between whether tar cracking/reforming is favored or CO_2 captures more CaO, it implies that under such conditions, the resultant gas composition is strongly dependent upon both number of active sites and effectiveness of contact between the gas and catalyst. Because AC promotes cracking of tar and volatile, CH_4 and CO are relatively high at 0:1 (AC); however, because no absorption occurs, the level of CO_2 remains high. By 1:0 (CaO), CH_4 is less abundant but CO_2 has reached its maximum concentration, suggesting negligible capture of CO_2 as surface area and a carbonate layer continues to grow. The high CO yield and moderate CO_2 reflect the CaO–AC synergies present in a 1:1 ratio which translate to an elevated conversion of volatiles into reactive gaseous products. On the other hand, due to the sorption-enhanced CaO effect with wider pore area presence alongside having lowest CO_2 for 2:1 (CaO-rich) ratio thus highest H_2 but CH_4 is still high alongside since lesser contribution from AC thus methane reform/cracking not ideal yet.

At a catalyst loading of 6%, CaO/AC ratio produces mainly an alteration in selectivity for secondary reactions (tar cracking/reforming and CO_2 capture) as AC favors the conversion of volatiles/light hydrocarbons, whilst CaO inhibits CO_2 via carbonate formation ($CaO + CO_2 \rightarrow CaCO_3$) and modifies reaction equilibrium. At 0:1, because there was no CO_2 capture and methane reforming is not yet optimal, volatiles escape as CH_4 while keeping high levels of CH_4 and CO_2. And so, at 1:0 CO_2 goes down most but CH_4 is lifted to highest because of the lack of AC cracking/reforming. Ideal (1:1) conditions are shown where the H_2 is maximized and CO_2 is minimized, suggesting synergies of CaO–AC leading to sorption-enhanced reforming with increasing conversion of hydrocarbons into components of a syngas. At 2:1, CO is maximized and CO_2 is minimized, but CH_4 increases again (H_2 is still not maximally usable since free circulating CaO has potential to rapidly carbonate or create contact limitations making AC a less efficient contributor for cracking/reforming).

The ratio of CaO/AC influences loss of selectivity in the syngas reaction at 8% loading. There is a high CH_4 (0:1 AC), because some light hydrocarbon are not converted even if tar cracking occurs. CO is very high at 1:0 (CaO) but CO_2 can also be very high, implying this condition favors the pathway towards CO formation along with not-so-optimal conditions for capture of increased amount of CO_2 either due to limited contact or carbonation saturation. The lowest CH_4 means that the CaO–AC synergy proved to be most effective in cracking/reforming light hydrocarbons and converting methane to reactive gas with a 1:1 rate. At 2:1, CO increases yet more but CH_4 does too; therefore, the lower AC fraction suppresses the methane reforming/cracking activity causing lower overall CO_2 concentration thus also dependent on effectiveness of CaO sorption.

At a catalyst load of 10%, the addition of total catalyst makes secondary reactions, reforming, solid-gas heterogeneous reactions and equilibrium shifts very dominant, so that product selectivity mainly depends on the ratio of CaO/AC. At 0:1 (AC), CO formation is the highest because porous carbon surfaces facilitate the cracking/reforming of volatiles and tar-to-reactive-gases conversions. The CO_2 can be retained by CaO via carbonation at ratios with CaO (1:0, 1:1, 2:1) but the effect is often encountered to be non-linear towards high loads as the CaO quickly carbonates/diffusion limits and pore blocking happen so that in conditions rich of CaO (2:1) the CH_4 arguably might decrease however CO_2 can elevate while H_2 would not be reach at full potential due reaction competition. Overall, AC-dominant promotes CO at 10% load; CaO-dominant suppresses light hydrocarbons but tempts non-ideal conditions (saturation/mass transport) that destroy the benefits of H_2 and CO_2.

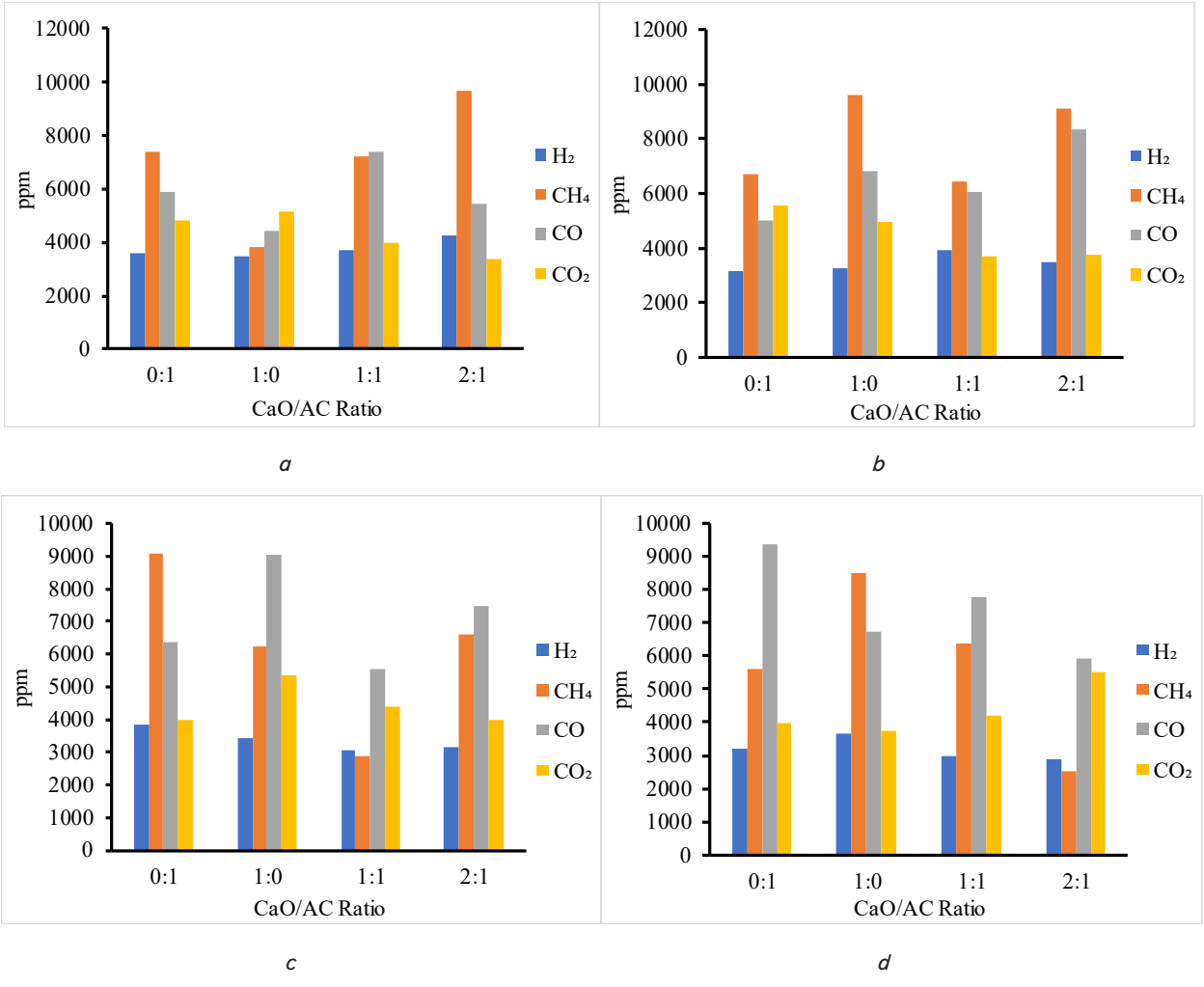


Fig. 7. Effect CaO/AC ratio with various catalyst load: *a* – 4%; *b* – 6%; *c* – 8%; *d* – 10%

5. 2. 4. Syngas low heating value

To calculate the LHV of syngas, it must first be converted from ppm to % volume of gas. The formula is $\%vol_i = \frac{ppmv_i}{10^4}$ to calculate the LHV:

$$LHV_{mix}\left(\frac{\text{MJ}}{\text{Nm}^3}\right) = \frac{10.8(\%\text{H}_2) + 12.63(\%\text{CO}) + 35.8(\%\text{CH}_4)}{100},$$

$LHV\ \text{H}_2 = 10.8\ \text{MJ/Nm}^3$,

$LHV\ \text{CO} = 12.63\ \text{MJ/Nm}^3$,

$LHV\ \text{CH}_4 = 35.8\ \text{MJ/Nm}^3$.

As shown in Fig. 8, the syngas low heating value (LHV) varies with the equivalence ratio (ER) and catalyst load.

Fig. 8 shows that the LHV value increases with the ER. At the same catalyst load of 4%, the LHV will increase in line with the increase in ER. ER 0.2 has the LHV of 230 kJ/kg and ER 0.35 has the LHV of 481 kJ/kg. Higher ER produces more intense autothermal conditions, causing the reactor temperature to rise. This increase in temperature accelerates the decomposition of volatiles and tar cracking, and promotes more complete gasification and reforming reactions, thereby increasing the fraction of permanent gases that contribute to the calorific value, mainly CO and CH_4, as well as some H_2. In addition, the increase in temperature is also associated with more effective hydrogen formation, because H_2 formation reactions (e.g., through steam-water and reforming reactions) are generally more optimal at high temperatures, with the temperature range often reported to be most conducive to H_2 formation being 800–1000°C.

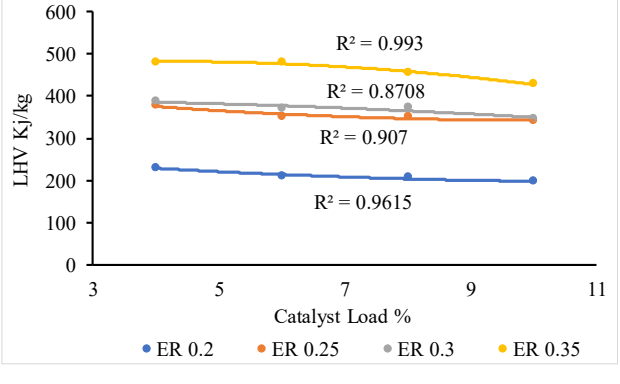


Fig. 8. Syngas low heating value with various equivalence ratio

At ER 0.2, the highest LHV was obtained at a catalyst load of 4% at 230 kJ/kg and continued to decrease with increasing catalyst load to 197 kJ/kg at 10%. At ER 0.25, the highest LHV was also obtained at a catalyst load of 4% at

377 kJ/kg and also decreased to 341 kJ/kg at a catalyst load of 10%. At ER 0.3, the highest LHV was obtained at a catalyst load of 4% at 388 kJ/kg and also decreased at a catalyst load of 10% to 347 kJ/kg. At ER 0.35, the highest LHV was obtained at 481 kJ/kg and decreased at a catalyst load of 10% to 428 kJ/kg.

However, all ER values show that LHV tends to decrease when the catalyst load is increased from 4% to 10%. This decrease indicates that excessive catalyst addition under these operating conditions does not always improve gas energy quality, because the catalyst can shift the reaction selectivity towards the conversion of high calorific components especially CH_4 into CO and H_2 through reforming, while at the same time the fraction of diluent gases such as CO_2 (and steam) may increase due to reaction. Since CH_4 has a very large calorific value contribution in the syngas mixture, the decrease in its fraction is often more dominant than the increase in CO/H_2, so that the total LHV tends to decrease.

In energy system analysis, particularly in combustion, gasification, and fuel gas utilization processes such as syngas, the LHV value is often used because it better represents the heat energy that can actually be utilized by the system. The LHV value of a fuel gas is usually influenced by the composition of combustible gases such as carbon monoxide (CO), hydrogen (H_2), and methane (CH_4). The higher the content of these gases, the greater the LHV value produced. The LHV of syngas from this study with variations in ER and CaO/AC-PF ratio can be seen in Fig. 9.

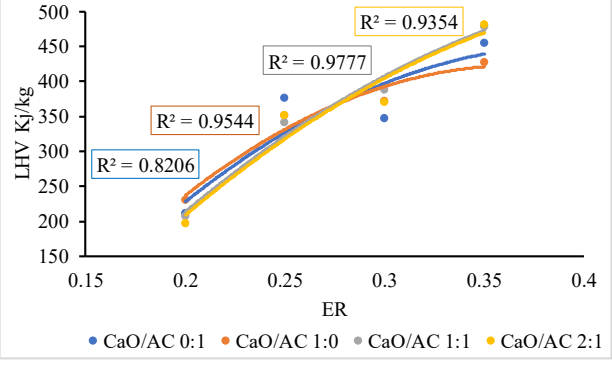


Fig. 9. Syngas low heating value with various CaO/AC ratio

Fig. 9 shows that the LHV of syngas increases consistently with the increase in ER 0.2 to 0.35 for all CaO/AC ratios, indicating that a higher ER strengthens autothermal conditions so that the reaction temperature increases and the conversion of volatiles into syngas becomes more complete. At low ER (0.2), the difference in LHV between ratios is still small because secondary reactions such as cracking, reforming and heterogeneous reactions are not yet dominant; the system is still relatively influenced by incompletely converted volatiles. When the ER is increased to 0.25–0.30, the effect of the catalyst ratio becomes apparent: compositions involving AC tend to produce higher LHV because they accelerate tar cracking and increase the fraction of calorific gas, while the contribution of CaO can shift the reaction equilibrium through a decrease in CO_2. At the highest ER (0.35), the LHV reaches its maximum at all ratios, with CaO/AC 2:1 and 0:1 showing peak values, indicating that at high temperatures, the reactive gas formation pathway (via cracking/reforming on the carbon surface and/or CaO-rich-promoted heterogeneous reactions) becomes dominant. Overall, ER acts as the main controlling factor for LHV increase through the temperature effect, while the CaO/AC ratio modulates LHV through the balance between cracking/reforming (AC) and CO_2 control (CaO), especially at medium-high ER.

6. Discussion on the catalytic effect of AC-PF/CaO and operating conditions on syngas composition and LHV

The interaction of the CaO-AC-PF catalyst to improve syngas quality can be seen from the characterization of the catalyst, the composition of the syngas and the LHV produced. From the scanning electron microscopy results in Fig. 2, it can be seen that the CaO:AC-PF;2:1 catalyst (Fig. 2, *c*) appears denser than the other catalysts. With the addition of CaO, CaO particle dispersion can be seen on the white carbon surface, indicating that some micro pores are closed by CaO. With the addition of CaO, a lot of CO_2 is absorbed and becomes $CaCO_3$. This porous structure is very important in top-flow gasification because pyrolysis gas and volatiles move through the layer, so the presence of a porous medium has the potential to strengthen secondary reactions and act as carbon capture before the gas exits to the condenser.

The interaction of the CaO-AC-PF catalyst in improving syngas quality can be observed from the catalyst characterization, syngas composition, and the resulting LHV. Based on the SEM results shown in Fig. 2, the CaO:AC-PF = 2:1 catalyst (Fig. 2, *c*) appears denser than the other catalyst formulations, indicating that CaO particles were dispersed on the carbon surface and may have partially blocked some of the smaller pores. This interpretation is reasonable because CaO-based materials are widely known to act as high-temperature CO_2 sorbents, and their carbonation proceeds through the formation of $CaCO_3$. During gasification, such sorption behavior can reduce CO_2 concentration and influence gas quality. In addition, porous carbonaceous media are known to promote tar cracking and secondary gas-phase reactions when volatile products pass through a hot solid bed. This is particularly relevant in fixed-bed gasification, where reactor design and the interaction between volatiles, char, and catalyst strongly affect tar conversion and gasification efficiency. Therefore, the porous structure of AC-PF, together with the CO_2-capturing role of CaO, may contribute to syngas upgrading before the gas exits the reactor system.

From a surface chemistry perspective, Fourier transform infrared spectroscopy (FTIR) shows the presence of -OH and calcium carbonate groups, as shown in Fig. 3. This is due to the results of KOH impregnation carried out during the manufacture of AC-PF. The presence of -OH groups functions as polar active sites capable of adsorbing polar molecules such as H_2O, CO_2, and volatile compounds. Surfaces with -OH groups tend to be hydrophilic and reactive, thereby enhancing interactions with tar compounds or heavy hydrocarbons. These tar compounds can then undergo thermal cracking or catalytic reforming into light gases such as H_2, CO, and CH_4. In addition to -OH, there are also O-H and C-O groups. The O-H group has characteristics that are almost the same as the -OH group, while the C-O group plays a role in enhancing the redox properties and chemical interactions between the carbon surface and gas molecules. In the gasification process, the C-O group can be part of the partial oxidation mechanism and carbon gasification reaction, which produces CO [25].

From a surface chemistry perspective, the Fourier transform infrared spectroscopy (FTIR) results indicate the presence of O-H, C-O, and carbonate-related groups, as shown in Fig. 3. The appearance of oxygen-containing functional groups is consistent with the use of KOH during the preparation of AC-PF, since KOH activation is known to modify the surface chemistry of activated carbon and promote the formation of oxygenated groups. O-H-containing groups can act as polar active sites that enhance the interaction of the carbon surface with polar molecules such as H_2O, CO_2, and oxygenated volatile compounds. Such surface functionality may also facilitate the adsorption of tar-related species and support their further conversion through thermal cracking or reforming into lighter gases. In addition to O-H groups, the presence of C-O groups suggests that the carbon surface retains oxygen-containing functionalities that may contribute to surface reactivity and gas-solid interactions. During gasification, these surface groups may participate indirectly in oxidation-reduction interactions at the carbon surface and support the formation of combustible gases such as CO. The carbonate-related bands may also indicate the presence of calcium-containing carbonate species, which is consistent with the CO_2-capturing function of CaO during the gasification process.

The BET data in Fig. 4 shows that the surface area decreased to 5.06 m^2/g, but the pore diameter increased to a mesopore scale of 22.87 nm, which can improve the accessibility of volatiles to active sites and improve mass transport in the reforming reaction. In Fig. 4, *b*, the BJH curve at CaO:AC-PF = 2:1 shows the highest *dV/dD* values of 30–40 nm, indicating a catalyst in the mesopore size range. The presence of these mesopores will further increase the active sites for CO_2 adsorption.

The BET results presented in Fig. 4 show that the specific surface area decreased to 5.06 m^2/g, while the average pore diameter increased to 22.87 nm, corresponding to the mesopore range. This change suggests that, although the surface area became lower, the larger pore structure may improve the accessibility of volatile compounds to active sites and enhance mass transport during reforming reactions. In Fig. 4, *b*, the BJH pore size distribution of the CaO:AC-PF = 2:1 catalyst shows the highest *dV/dD* values in the pore diameter range of 30–40 nm, confirming the dominance of mesopores in this catalyst. The presence of these mesopores may facilitate gas diffusion and improve contact between gaseous species and the catalyst surface, which can contribute to CO_2 adsorption and syngas upgrading during gasification.

From a process perspective, in Fig. 5, ER appears as the dominant variable that regulates autothermal conditions, primarily through an increase in effective temperature and secondary reaction intensity. An increase in ER from low to high levels consistently increases H_2, which can be explained by the acceleration of H_2 formation reactions such as charcoal gasification with steam ($C + H_2O \rightarrow CO + H_2$) [26], light hydrocarbon reforming, and more intense tar cracking at high temperatures. At the same time, CH_4 also increases sharply at high ER, indicating that in an autothermal upflow system, increased temperature and changes in gas composition can facilitate the formation of light gases. Meanwhile, CO tends to peak at moderate ER and then decreases at high ER, consistent with competition between CO formation and CO consumption through subsequent reactions such as methanation [27]. The decrease in CO_2 at high ER indicates the role of high temperatures in enhancing the reduction of CO_2 by charcoal (Boudouard reaction) and/or the role of CaO adsorption if available.

The effect of catalyst loading in Fig. 6 shows that adding catalyst does not always increase H_2. Increasing the catalyst loading from low to high tends to reduce H_2 and CH_4 but increase CO. Mechanistically, this condition can occur when the catalyst strengthens pathways that increase CO and/or promotes RWGS ($CO_2 + H_2 \rightarrow CO + H_2O$) [28], which consumes H_2 so that net H_2 is reduced. Furthermore, at high catalyst loadings, the possibility of diffusion/aggregation penalties increases, so that selectivity may shift and some active sites become less effective. Therefore, the target of H_2-rich synthesis gas in this reactor is more dependent on ER adjustment and the selection of moderate/low catalyst loadings, rather than simply increasing the loading.

The CaO/AC-PF ratio in Fig. 7 shows synergistic but non-linear behavior. AC-PF plays a major role as a porous medium that enhances the cracking/reforming process of volatile compounds, while CaO provides a basic site and CO_2 absorber to shift the equilibrium. At high CaO ratios, sorption and base effects may increase, but the risk of micro-pore closure and diffusion pathway changes also increases. This explains why certain compositions are optimal at certain catalyst loads: the best performance arises from a balance between pore accessibility (the role of AC-PF) and sorption/base strength (the role of CaO).

From an energy quality perspective in Fig. 8, 9, the LHV value of synthetic gas is highly sensitive to changes in CH_4. Therefore, high ER conditions that increase CH_4 tend to increase LHV. H_2, CH_4 and CO are the main factors for obtaining high LHV. CO_2 has no calorific value so it must be captured. In this study, CaO was used so that CO_2 could be suppressed, meaning that the total LHV could be increased. The highest LHV in this study was 481 kJ/kg, while in another study, the highest was 550 kJ/kg using pinewood with dolomite, activated carbon, silica gel, and limestone catalysts [29]. The higher the ER, the more oxygen enters the system, thereby increasing the reforming reaction [30].

In comparison with the literature reviewed in this study, the present study demonstrates a comparable qualitative trend, particularly in showing that catalyst-assisted updraft gasification can improve syngas composition and energy quality. For example, previous studies reported that dolomite-assisted rice husk gasification increased H_2 content up to 15.4 mol% with an LHV of 5.1 MJ/Nm^3, while other updraft gasification systems with catalytic enhancement also showed improved hydrogen-rich syngas production and higher heating values. In the present study, the highest syngas LHV reached 481 kJ/kg under the investigated conditions, indicating that the CaO/AC-PF catalyst system was effective in improving gas quality, although the absolute value remains influenced by the use of corncob feedstock, the small-scale reactor design, and the sensor-based gas measurement approach. Therefore, the present results support the view that the combined CaO/AC-PF catalyst is a promising low-cost alternative for syngas upgrading, particularly for agricultural biomass gasification in simple updraft systems.

In practical terms, the present study is relevant to the development of low-cost biomass gasification systems that can utilize locally available agricultural residues and catalyst materials. Corncob is a commonly available agricultural by-product; while CaO and activated carbon are obtained from palm-fiber waste, which can be sourced at relatively low-cost. Thus, the suggested catalyst system may have prac-

tical application in small-scale updraft gasifiers operating on agricultural residues where low-cost waste-to-energy technologies are needed. The syngas generated from that sort of systems may be used straight like a combustible gas for thermal functions, akin to drying or heating or in energy generation on a small scale; Its potential as an intermediate gas for additional upgrading/conversion into different value-added vitality and chemical substances is notable.

There are some limitations in this study. First, the gas written is based on ppm taken from an MQ sensor, thus, there could be a minor effect (relative accuracy) by cross-sensitivity and limitations of the humidity in addition to possible drift and temperature during gas capture; one entry point that can influence the %vol estimation and consequently affect LHV calculation whenever variations in CO and CH_4 occurs homogeneously. Second, the catalyst characterization (SEM-FTIR-BET) confirms the importance of surface structure and composition, but has not quantified alterations in the active phase under reaction conditions, extent of carbonation and gradual loss of activity due to pore blocking build-up.

The drawback of this study is that CaO catalyst is quite reactive with CO_2. Calcium oxide [CaO] (obtained from the calcination process) has to be kept in a closed space so that it does not form calcium carbonate $CaCO_3$. Because the catalyst is covered with tar or ash, it has a limited lifetime.

Hence, some future directions are suggested based on these limitations. It is better to use GC-TCD/GC-FID to calibrate the gas composition so that it is possible to report the sensor readings as more accurate %vol include LHV uncertainty analysis. Catalyst stability and possibility for regeneration, particularly with respect to the highly carbonatable CaO species, can be evaluated using carbonation-calcination cycle tests combined with post-reaction characterization (XRD/TGA/SEM-EDX) to assess phase alterations and loss of activity. Design experiments directed at ANOVA or RSM interactions such that interaction effects can be obtained and predictive models confirmed by replication confirmation tests. Include process performance metrics such as gas yield (Nm^3/kg), cold gas efficiency, pressure drop and air consumption so that syngas quality improvement can be shown on the basis of mass-energy balance and operability and not only composition.

7. Conclusion

1. The current study indicated that the CaO/AC-PF catalyst system can significantly enhance syngas quality for corncob updraft gasification. Characterization of the catalyst using SEM, FTIR and BET revealed that the resulting combined catalyst possessed altered surface morphology, oxygen-functional groups, carbonate counterpart species and meso-porous traits; CaO:AC-PF = 2:1 boasted a specific area of 5.06 m^2/g and pore average diameter 22.87 nm. These properties suggest that changes in the catalyst structure occurred, which might aid gas–solid interaction during gasification.

2. Equivalence ratio, catalyst loading, and CaO/AC ratio affected syngas composition and heating value in the gasification experiments. From ER 0.20 to 0.35, the H_2 concentration increased from 3150 to 3914 ppm; the CH_4 concentration increased from 3093 to 9221 ppm and the syngas LHV was elevated from 230 to 481 kJ/Nm^3. For catalyst loading, by enhancing the loading from 4 wt. % to 10 wt. With 30% for H_2, CH_4 was reduced from 3742 to 3176 ppm and 7031 to 5746 ppm, while CO increased (5783 to7445 ppm). These findings suggest that the quality of syngas was influenced by competition between catalytic activity, pore accessibility and behavior concerning sorption of CO_2.

Conflict of interest

The authors declare that they have no conflict of interest in relation to this study, whether financial, personal, authorship or otherwise, that could affect the study and its results presented in this paper.

Financing

The authors sincerely thank the Ministry of Education, Culture, Research and Technology, Republic of Indonesia for fully supporting this study through the DRTPM Research Grant under Fundamental Research, Universitas Widyagama Malang, Indonesia 2025 (Grant Number:128/C3/DT.05.00/PL/2025;023/LL7/DT.05.00/PL/2025;010/ Kontrak/PT/PTS.030.7/PN/V/2025).

Data availability

Manuscript has no associated data.

Use of artificial intelligence

The authors used the AI-based language model ChatGPT (GPT-5.3) only to assist in improving the clarity of English language and grammar in several sections of the manuscript, particularly in the Introduction and Literature Review sections.

The AI tool was used solely for language editing and paraphrasing purposes. All scientific content, experimental design, data analysis, and interpretation of the results were conducted entirely by the authors.

The authors carefully reviewed and verified all AI-assisted text to ensure accuracy and consistency with the experimental results. The use of AI tools did not influence the scientific conclusions of this study.

Acknowledgements

We as the Research Team would like to thank Ministry of Education, Culture, Research and Technology, Republic of Indonesia (Kemendiktisaintek Indonesia) for financing research activities.

Authors' contributions

Purbo Suwandono: Conceptualization, Writing-original draft, Investigation, Supervision, Formal analysis, Writing – review & editing; **Widya Wijayanti**: Validation, Investigation, Data Curation, Formal analysis, Writing – original draft; **Nova Risdiyanto Ismail**: Writing – review & editing, Formal analysis; **Dzulfikar Johan Akbar:** Visualization, Writing – original draft, Data curation; **Muhammad Reza**: Project administration, Resources, Data curation.

References

1. Yadav, V. K., Sharma, A. K., Gacem, A., Pandit, J., Wany, A., Kumar, A. et al. (2025). Emerging Trends in the Valorization of Agricultural Waste and Their Utilization in Agricultural, Pharmaceuticals, and Environmental Cleanup. Waste and Biomass Valorization, 16 (6), 2779–2833. https://doi.org/10.1007/s12649-025-03002-y
2. Lewandowski, W. M., Ryms, M., Kosakowski, W. (2020). Thermal Biomass Conversion: A Review. Processes, 8 (5), 516. https://doi.org/10.3390/pr8050516
3. Ariyanti, D., Rimantho, D., Leonardus, M., Ardyani, T., Lisnawati, Fiviyanti, S. et al. (2025). Valorization of corn cob waste for furfural production: A circular economy approach. Biomass and Bioenergy, 194, 107665. https://doi.org/10.1016/j.biombioe.2025.107665
4. Zhang, J., Chu, Z., Cao, R., Wu, X., Han, K. (2026). A review of resource recovery from waste plastics via pyrolysis and gasification. Fuel, 404, 136319. https://doi.org/10.1016/j.fuel.2025.136319
5. Tangke Tosuli, Y., Cahyadi, Dafiqurrohman, H., Hermawan, R., Surjosatyo, A. (2024). Gasification of sago dreg waste in a top-lit updraft fixed bed gasifier: Syngas composition and its effect with additional Al2O3 as catalyst. Energy Conversion and Management: X, 24, 100775. https://doi.org/10.1016/j.ecmx.2024.100775
6. Tuan, P. D., Minh Quan, L., Nhi, V. T., Huong, H. M., Phung, L. T. K., Feng, D. (2022). Enrichment of hydrogen in product gas from a pilot-scale rice husk updraft gasification system. Carbon Resources Conversion, 5 (3), 231–239. https://doi.org/10.1016/j.crcon.2022.07.003
7. Yousef, S., Eimontas, J., Zakarauskas, K., Striūgas, N. (2025). Oxygen updraft gasification-catalytic reforming of cigarettes butts for hydrogen-rich syngas production. International Journal of Hydrogen Energy, 171, 150650. https://doi.org/10.1016/j.ijhydene.2025.150650
8. Bilbao, D. C., Machin, E. B., Pedroso, D. T., Hernández, D., Aburto-Hole, J., Muñoz, L. (2025). Experimental assessment of the energy potential of pellets produced from beekeeping wastes by updraft gasification. Energy Conversion and Management, 343, 120206. https://doi.org/10.1016/j.enconman.2025.120206
9. Yesilova, N., Tezer, O., Ongen, A., Ayol, A. (2024). Enhancing biomass gasification: A comparative study of catalyst applications in updraft and modifiable-downdraft fixed bed reactors. International Journal of Hydrogen Energy, 76, 290–303. https://doi.org/10.1016/j.ijhydene.2024.05.075
10. Jančauskas, A., Striūgas, N., Zakarauskas, K., Skvorčinskienė, R., Eimontas, J., Buinevičius, K. (2024). Experimental investigation of sorted municipal solid wastes producer gas composition in an updraft fixed bed gasifier. Energy, 289, 130063. https://doi.org/10.1016/j.energy.2023.130063
11. Junga, R., Tańczuk, M., Sobek, S., Chabiński, M., Ziółkowski, Ł., Werle, S. (2023). Effect of the addition of laying hens manure to the straw on gasification efficiency in updraft gasifier under air atmosphere. Applied Thermal Engineering, 226, 120269. https://doi.org/10.1016/j.applthermaleng.2023.120269
12. Tezer, Ö., Karabağ, N., Öngen, A., Ayol, A. (2023). Gasification performance of olive pomace in updraft and downdraft fixed bed reactors. International Journal of Hydrogen Energy, 48 (60), 22909–22920. https://doi.org/10.1016/j.ijhydene.2023.02.088
13. Işık, K. E., Dogru, M., Erdem, A. (2023). Gasification of MDF residue in an updraft fixed bed gasifier to produce heat and power via an ORC turbine. Waste Management, 169, 43–51. https://doi.org/10.1016/j.wasman.2023.06.025
14. Gorthy, S., Verma, S., Sinha, N., Shetty, S., Nguyen, H., Neurock, M. (2023). Theoretical Insights into the Effects of KOH Concentration and the Role of OH– in the Electrocatalytic Reduction of CO2 on Au. ACS Catalysis, 13 (19), 12924–12940. https://doi.org/10.1021/acscatal.2c06115
15. Wang, X., Zeng, W., Xin, C., Kong, X., Hu, X., Guo, Q. (2022). The development of activated carbon from corncob for CO2 capture. RSC Advances, 12 (51), 33069–33078. https://doi.org/10.1039/d2ra05979g
16. Zhou, B., Bai, B., Zhu, X., Guo, J., Wang, Y., Chen, J. et al. (2024). Insights into effects of grain boundary engineering in composite metal oxide catalysts for improving catalytic performance. Journal of Colloid and Interface Science, 653, 1177–1187. https://doi.org/10.1016/j.jcis.2023.09.148
17. Zhu, Y., Wu, J., Zhang, Y., Miao, Z., Niu, Y., Guo, F., Xi, Y. (2024). Preparation of hierarchically porous carbon ash composite material from fine slag of coal gasification and ash slag of biomass combustion for CO2 capture. Separation and Purification Technology, 330, 125452. https://doi.org/10.1016/j.seppur.2023.125452
18. Ilić, M., Haegel, F.-H., Lolić, A., Nedić, Z., Tosti, T., Ignjatović, I. S. et al. (2022). Surface functional groups and degree of carbonization of selected chars from different processes and feedstock. PLOS ONE, 17 (11), e0277365. https://doi.org/10.1371/journal.pone.0277365
19. Ali, R., Aslam, Z., Shawabkeh, R. A., Asghar, A., Hussein, I. A. (2020). BET, FTIR, and RAMAN characterizations of activated carbon from wasteoil fly ash. Turkish Journal of Chemistry, 44 (2), 279–295. https://doi.org/10.3906/kim-1909-20
20. Stanienda-Pilecki, K. J. (2019). The importance of Fourier-Transform Infrared Spectroscopy in the identification of carbonate phases differentiated in magnesium content. Spectroscopy, 34 (6). Available at: https://www.spectroscopyonline.com/view/spec0619-pilecki
21. Dai, F., Zhuang, Q., Huang, G., Deng, H., Zhang, X. (2023). Infrared Spectrum Characteristics and Quantification of OH Groups in Coal. ACS Omega, 8 (19), 17064–17076. https://doi.org/10.1021/acsomega.3c01336
22. Martínez de Salazar Martínez, E., Alexandre-Franco, M. F., Nieto-Sánchez, A. J., Cuerda-Correa, E. M. (2024). Exploring the role of surface and porosity in CO2 capture by CaO-based adsorbents through response surface methodology (RSM) and artificial neural networks (ANN). Journal of CO2 Utilization, 83, 102773. https://doi.org/10.1016/j.jcou.2024.102773

23. Tavizón-Pozos, J. A., Cervantes-Cuevas, H., Garcia-Camacho, G. G., Chavez-Esquivel, G., Acosta-Najarro, D. R. (2025). Biodiesel Production Using K–Sr/CaO and CaO Catalysts Derived from Eggshells by Canola Oil Transesterification. ACS Omega, 10 (7), 6827–6838. https://doi.org/10.1021/acsomega.4c09118
24. Koo-amornpattana, W., Phadungbut, P., Kunthakudee, N., Jonglertjunya, W., Ratchahat, S., Hunsom, M. (2023). Innovative metal oxides (CaO, SrO, MgO) impregnated waste-derived activated carbon for biohydrogen purification. Scientific Reports, 13 (1). https://doi.org/10.1038/s41598-023-31723-4
25. Quan, C., Wang, M., Gao, N., Yang, T., Li, R. (2023). In situ adsorption of CO2 to enhance biomass gasification for hydrogen production using Ca/Ni based composites. Journal of the Energy Institute, 108, 101229. https://doi.org/10.1016/j.joei.2023.101229
26. Micheli, F., Mattucci, E., Courson, C., Gallucci, K. (2021). Bi-Functional Catalyst/Sorbent for a H2-Rich Gas from Biomass Gasification. Processes, 9 (7), 1249. https://doi.org/10.3390/pr9071249
27. Zhu, M., Wang, Q., Wang, S. (2025). Recent Advances and Future Perspectives in Catalyst Development for Efficient and Sustainable Biomass Gasification: A Comprehensive Review. Sustainability, 17 (16), 7370. https://doi.org/10.3390/su17167370
28. Cerone, N., Zimbardi, F., Contuzzi, L., Baleta, J., Cerinski, D., Skvorčinskienė, R. (2020). Experimental investigation of syngas composition variation along updraft fixed bed gasifier. Energy Conversion and Management, 221, 113116. https://doi.org/10.1016/j.enconman.2020.113116
29. Mohanty, R., Mahanta, P., Mahapatro, A., Sharma, R. P. (2025). Catalytic gasification of pinewood biomass in a fluidized bed reactor with dolomite, limestone, and activated carbon: An experimental study. Energy, 325, 136131. https://doi.org/10.1016/j.energy.2025.136131
30. Liu, C., Huang, Y., Niu, M., Pei, H., Liu, L., Wang, Y. et al. (2018). Influences of equivalence ratio, oxygen concentration and fluidization velocity on the characteristics of oxygen-enriched gasification products from biomass in a pilot-scale fluidized bed. International Journal of Hydrogen Energy, 43(31), 14214–14225. https://doi.org/10.1016/j.ijhydene.2018.05.154